

A photograph of the Hayonim Cave entrance, a large dark opening in a rocky cliff face. The surrounding landscape is arid and rocky, with sparse green shrubs and dry grass. In the background, a town and a body of water are visible under a clear blue sky.

Hayonim Cave

*From the Early to the Middle
Palaeolithic in the Levant (Israel)*

LILIANE MEIGNEN & OFER BAR-YOSEF (EDS)

Hayonim Cave

Hayonim Cave

*From the Early to the Middle
Palaeolithic in the Levant (Israel)*

LILIANE **MEIGNEN** & OFER **BAR-YOSEF** (EDS)

© 2024 Individual authors

Published by Sidestone Press, Leiden
www.sidestone.com

Lay-out & cover design: Sidestone Press
Photograph cover: Paul Goldberg

ISBN 978-94-6426-185-1 (softcover)
ISBN 978-94-6426-186-8 (hardcover)
ISBN 978-94-6426-187-5 (PDF e-book)

DOI: 10.59641/i8d53db9

Contents

Preface	9
Liliane Meignen and Ofer Bar-Yosef	
Acknowledgements	15
Introduction	17
Liliane Meignen and Ofer Bar-Yosef	
Hayonim geology and stratigraphy	27
Paul Goldberg, Liliane Meignen, Steve Weiner and Ofer Bar-Yosef	
Fire use and cave occupations by Early Middle Palaeolithic humans in Hayonim Cave	69
Liliane Meignen and Paul Goldberg	
Faunal perspectives on carbonate preservation and hearth-centred activities during the Middle Palaeolithic in Hayonim Cave	113
Mary C. Stiner	
Hayonim Cave: Lithic assemblages, from the end of the Lower Palaeolithic to the Middle Palaeolithic	139
Liliane Meignen	
Technological, cultural and behavioural changes in the Levant from the Late Lower Palaeolithic to the Mid-Middle Palaeolithic: Contribution from the Hayonim sequence	255
Liliane Meignen	
Bibliography	281

This volume is dedicated to Ofer, our colleague, but more so our friend.
Without him, this stimulating scientific and human venture could not have taken place



Photo: Ofer, in China 2005 (photograph by P. Goldberg)

Preface

Liliane Meignen and Ofer Bar-Yosef

This volume is the last in a series of previously published works (Bar-Yosef 1991b; Bar-Yosef and Meignen 2007; Bar-Yosef and Vandermeersch 1989; Bar-Yosef and Vandermeersch 1991; Meignen and Bar-Yosef 2019; Stiner 2005) reporting on the interdisciplinary research conducted in the framework of a long-term international research project on the origins of modern humans in Southwest Asia. This project was initiated in 1982 by Ofer Bar-Yosef and Bernard Vandermeersch, with completion of the fieldwork in 2000. Unfortunately, Ofer was unable to see the end of this volume, even though he was the main instigator of the project throughout the years. We hope that the publication of this report will serve as a memorial to his immense contribution to this project.

This endeavour consisted of a large interdisciplinary program involving international researchers (chiefly from Israel, the USA, and France) from many disciplines, including prehistory, geology/geoarchaeology, zooarchaeology, physical anthropology, radiometric dating, geochemistry, and phytolith studies. At the core of the project was the strategy to have all specialists present in the field during the excavations (Meignen, Goldberg, and Bar-Yosef 2017). The benefit of this innovative strategy was that it facilitated real-time, interactive daily exchanges among the researchers.

The investigations on Hayonim Cave follow on from the fieldwork and research carried out first in Kebara Cave (Bar-Yosef and Meignen 2007; Bar-Yosef et al. 1992; Meignen and Bar-Yosef 2019), and then on the long sequence at Qafzeh Cave. Fieldwork was conducted from 1992 to 2000, and the site has already been the subject of numerous publications (41 articles/books/chapters; see list below) in the various fields involved.

Some research fields, whose published results are already well known, are not included in detail in this volume, but they are, of course, implicated in the reasoning and discussions presented in this volume. This is true, in particular, for the thermoluminescence and electron spin resonance dating (Mercier et al. 2007; Rink et al. 2004) obtained in the framework of the large radiochronological dating program initiated at the beginning of our project in the early 1980s. This program allowed the establishment of a new chronological framework renewing the hypotheses on the origin of *Homo sapiens* in the region. This is also the case for the phytolith studies (Albert et al. 2003), the results of which are implicated in the interpretation of the site's modes of occupation (see chapters 3 and 6, this volume).

On another note, the numerous isolated skeletal remains, discovered mainly in the upper levels of the sequence, are unfortunately unsuitable for precise taxonomic assignment (Tillier et al. 2011). The researchers indicate that 'they lack the general robusticity that is usually claimed by scholars to distinguish late archaic humans (e.g., Neanderthals) from recent modern humans. But their overall slenderness can be explained perhaps by the early age at death of most of the individuals (adolescents

and young adults' [Tillier et al. 2011]). However, it is worth noting that this material adds to the overall Levantine sample of human remains from this crucial period (end of MIS 6–early MIS 5). Thus, it contributes to the question of the nature and origin of the human groups authoring these tools in the process of transformation (end of Early Middle Palaeolithic/early Mid-Middle Palaeolithic) (Hershkovitz et al. 2021; Hershkovitz et al. 2018).

Concerning the geochemical/mineralogical studies (a totally new field of research in the 1980s and at the beginning of this long project), many articles have already extensively documented the methodological foundations, analytical methods (Fourier transform infrared spectrometry; FTIR), and the first results obtained in the Kebara and Hayonim caves (Karkanas et al. 2000; Schiegl et al. 1996; Schiegl et al. 1994; Stiner et al. 2001b; Weiner et al. 2007; Weiner and Goldberg 1990; Weiner, Goldberg, and Bar-Yosef 1993; Weiner, Goldberg, and Bar-Yosef 2002; Weiner et al. 1995); we will not repeat them in detail here. In this volume, the results of geochemical studies are generally integrated with micromorphological data to identify the processes of deposit formation. This is the approach developed in the study of the Hayonim Cave sediments, the results of which are presented here.

Many of the results already published (41 articles; see list of publications related to research on Hayonim Cave) are included in **chapter 1**, corresponding to the general presentation of the research questions addressed and the information concerning Hayonim Cave (L. Meignen).

Following this broad introduction, **chapter 2** (P. Goldberg, L. Meignen, O. Bar-Yosef, S. Weiner) presents, for the first time, the detailed stratigraphy of the deposits based on numerous field observations throughout the excavation, as well as interpretations proposed for the site formation processes responsible for these deposits. The micromorphological and geochemical (using FTIR) studies have contributed additional information on the complex formation processes in Hayonim Cave. From a methodological perspective, the systematic combination of these two approaches in the interpretation of the deposits was initiated in the framework of the Kebara/Hayonim project in the early 1980s and is now widely used in many research programs in Israel and elsewhere in the world.

Because they are informative in terms of site formation processes (including post-depositional processes) as well as human behaviour, the numerous combustion features in Hayonim Cave have been studied in detail to enrich our knowledge of these two domains (precise field observations and mapping of the features, micromorphology, geochemistry, phytoliths, and spatial distribution). Their study has allowed us to infer the importance of the use of fire in human behaviour as early as the end of the Middle Pleistocene/beginning of the Late Pleistocene (**chapter 3**: L. Meignen, P. Goldberg, O. Bar-Yosef).

In **chapter 4**, M. Stiner first questions the taphonomic conditions that explain the uneven bone distributions within the fill (e.g., differential preservation, human activity-related distributions). She then presents the animal carcass exploitation, transport, and processing practices of the Middle Palaeolithic hunter-gatherers, particularly in relation to the use of fire, which is widely present in the Hayonim sequence. The data acquired on the practices of selection, acquisition, and processing of animal materials in the Hayonim Middle Palaeolithic occupations are then integrated into an evolutionary history of these practices from the Late Lower Palaeolithic to the Late Middle Palaeolithic in the Levant.

Chapter 5 (L. Meignen) is devoted to the lithic productions of the long Hayonim sequence, from the Late Lower Palaeolithic to the start of the Mid-Middle Palaeolithic (covering mostly the period of MIS 7, MIS 6, and early beginning of MIS 5). Detailed studies of the tools from the different units, based on the identification of technical systems, have highlighted a number of key issues. These include the important changes in the technical repertoires observed during the Late Lower Palaeolithic/Early Middle Palaeolithic transition, the long development of the Early Middle Palaeolithic over

approximately 45–50 ka (220–200/185–160 ka), and then the disappearance of this technical entity in favour of lithic assemblages constituting the start of the Mid-Middle Palaeolithic. The development of the latter in MIS 5 is associated with the presence of anatomically modern *Homo sapiens* in the region. An interpretation of the processes responsible for these major changes is proposed.

Chapter 6 summarises the main contributions of the research conducted in Hayonim Cave, focusing on two broad issues currently addressed by research on this period in the Levant region:

1. Changes in the lithic technical repertoires from the Late Lower Palaeolithic to the Mid-Middle Palaeolithic; what are the processes of these changes?
2. Subsistence strategies and site use patterns during the Middle Palaeolithic in the Levant.

As this was a French-Israeli-American project at the time of Hayonim excavations, the following colleagues joined us from the first season at Hayonim:

Prehistory:

Late Prof. **O. Bar-Yosef**, Peabody Museum, Harvard University, Cambridge, USA.

L. Meignen, CEPAM-CNRS, UMR 7264, Université Côte d'Azur, Nice, France.

A. Belfer-Cohen, Professor (emeritat), Institute of Archaeology, The Hebrew University of Jerusalem, Mt. Scopus, Israel*.

S. Kuhn, Fred A. Riecker Professor of Anthropology, University of Arizona, Tucson, USA*.

**A. B.-C. and S. K. were more specifically in charge of the excavations and study of the Epipalaeolithic site of Meged Rockshelter, in the immediate vicinity of Hayonim Cave, and integrated in our research project.*

Geology/micromorphology:

P. Goldberg, Professor Emeritus, Department of Archaeology, Boston University, Boston, MA, USA; Affiliated Professor of Geoarchaeology and Senior Researcher, Institut für Naturwissenschaftliche Archäologie (INA), Eberhard-Karls-Universität Tübingen.

Geochemistry (FTIR analysis):

S. Weiner, Professor Emeritus, Department of Structural Biology, Weizmann Institute of Science, Rehovot, Israel.

Zooarchaeology:

M. Stiner, Regents' Professor of Anthropology, University of Arizona, Tucson, USA.

Physical anthropology:

B. Arensburg, Professor Emeritus, Department of Anatomy and Anthropology, Sackler School of Medicine, Tel Aviv University, Israel.

A.-M. Tillier, UMR 5199 PACEA, CNRS, University of Bordeaux, Pessac, France.

B. Vandermeersch, Professor Emeritus, UMR 5199 PACEA, CNRS, University of Bordeaux, Pessac, France.

Dating methods:

N. Mercier, Archéosciences Bordeaux, UMR 6034 CNRS, Université Bordeaux Montaigne, Pessac, France.

H. Valladas, Laboratoire des Sciences du Climat et de l'Environnement, UMR 8212, CEA CNRS UVSQ, Université Paris-Saclay, Gif-sur-Yvette, France.

W. J. Rink, Professor Emeritus, School of Earth, Environment & Society, McMaster University, Canada.

H. P. Schwarcz, Professor Emeritus, School of Earth, Environment & Society, McMaster University, Canada.

Phytolith studies:

R. M. Albert, Research Professor, ICREA, Universitat de Barcelona, Spain.

Associated studies:

D. Bar-Yosef Mayer, the Steinhardt Museum, University of Tel-Aviv, Israel.

Mario Chech, who took care of all of the technical aspects of the excavations. We cannot imagine the success of the project without his invaluable personal skills.

Publications to date resulting from the Hayonim field project

- Albert, R.M., Bar-Yosef, O., Meignen, L., Weiner, S., 2003. Quantitative phytolith study of hearths from the Natufian and Middle Palaeolithic levels of Hayonim Cave (Galilee, Israel). *Journal of Archaeological Science* 30, pp. 461-480.
- Bar-Yosef, O., 1994. The contribution of Southwest Asia to the study of the origin of Modern Humans, in: Nitecki, M.H., Nitecki, D.V. (Eds.), *Origins of Anatomically Modern Humans*. Plenum Press, New York, pp. 23-66.
- Bar-Yosef, O., Belfer-Cohen, A., Goldberg, P., Kuhn, S., Meignen, L., Weiner, S., Vandermeersch, B., 2005. Archaeological background: Hayonim Cave and Meged Rockshelter., in: Stiner, M. (Ed.), *The Faunas of Hayonim Cave (Israel). A 200,000-Year Record of Palaeolithic Diet, Demography and Society*. American School of Prehistoric Research, Peabody Museum, Harvard University, Cambridge (US), pp. 17-38.
- Bar-Yosef, O., Meignen, L., 2001. The chronology of the Levantine Middle Palaeolithic period in retrospect. *Bulletins et Mémoires de la Société d'Anthropologie de Paris* 13, pp. 269-289.
- Berna, F., Goldberg, P., 2008. Assessing Palaeolithic pyrotechnology and associated hominin behavior in Israel. *Israel Journal of earth sciences* 56, pp. 107-121.
- Goldberg, P., 1979. Micromorphology of sediments from Hayonim Cave, Israel. *Catena* 6, pp. 167-181.
- Goldberg, P., 2003. Some observations on Middle and Upper Palaeolithic ashy cave and rockshelter deposits in the Near East, in: Goring-Morris, A.N., Belfer-Cohen, A. (Eds.), *More than Meets the Eye: Studies on Upper Palaeolithic Diversity in the Near East*. Oxbow Books, Oxford, pp. 19-32.
- Goldberg, P., Bar-Yosef, O., 1998. Site formation processes in Kebara and Hayonim Caves and their significance in Levantine prehistoric caves, in: Akazawa, T., Aoki, K., Bar-Yosef, O. (Eds.), *Neandertals and Modern Humans in Western Asia*. Plenum, New York, pp. 107-125.
- Karkanas, P., Bar-Yosef, O., Goldberg, P., Weiner, S., 2000. Diagenesis in prehistoric caves: the use of minerals that form in situ to assess the completeness of the archaeological record. *Journal of Archaeological Science* 27, pp. 915-929.
- Kuhn, S.L., Belfer-Cohen, A., Barzilai, O., Stiner, M.C., Kerry, K.W., Munro, N.D., Bar-Yosef Mayer, D.E., 2004. The Last Glacial Maximum at Meged Rockshelter, Upper Galilee, Israel. *Journal of the Israel Prehistoric Society- Mitekufat Haeven* 34, pp. 5-47.
- Meignen, L., 1994. Paléolithique moyen au Proche-Orient : le phénomène laminaire, in: Révillion, S., Tuffreau, A. (Eds.), *Les industries laminaires au Paléolithique moyen*. CNRS Editions, Paris, pp. 125-159.
- Meignen, L., 1998. Hayonim Cave lithic assemblages in the context of the Near-Eastern Middle Palaeolithic: a preliminary report, in: Akazawa, T., Aoki, K., Bar-Yosef, O. (Eds.), *Neandertals and Modern Humans in Western Asia*. Plenum Press, New York, pp. 165-180.
- Meignen, L., 2000. Early Middle Palaeolithic blade technology in Southwestern Asia. *Acta Anthropologica Sinica Supplement to Volume* 19, pp. 158-168.

- Meignen, L., 2007. Middle Palaeolithic blade assemblages in the Near East: a reassessment. *Russian Academy of Sciences, Institute of the History of material culture. Caucasus and the initial dispersals in the Old World XXI*, pp. 133-148.
- Meignen, L., 2011. Contribution of Hayonim cave assemblages to the understanding of the so-called « Early Levantine Mousterian », in: Le Tensorer, J.M., Ragher, R., Otte, M. (Eds.), *The Lower and Middle Palaeolithic in the Middle East and neighbouring regions*. ERAUL, Liège, pp. 85-100.
- Meignen, L., Bar-Yosef, O., 2020. Acheulo-Yabrudian and Early Middle Palaeolithic at Hayonim Cave (Western Galilee, Israel): Continuity or break? *Journal of Human Evolution* 139, 102733.
- Meignen, L., Bar-Yosef, O., Goldberg, P., Weiner, S., 2001a. Le feu au Paléolithique moyen : recherches sur les structures de combustion et le statut des foyers. *L'exemple du Proche-Orient*. *Paléorient* 26, pp. 9-22.
- Meignen, L., Bar-Yosef, O., Mercier, N., Valladas, H., Goldberg, P., Vandermeersch, B., 2001b. Apport des datations au problème de l'origine des Hommes modernes au Proche-Orient, in: Barrandon, J.N., Guilbert, P., Michel, V. (Eds.), *Datation. XXI° Rencontres Intern. d'archéologie et d'histoire d'Antibes*. APDCA, Antibes, pp. 295-313.
- Meignen, L., Bar-Yosef, O., Stiner, M., Kuhn, S., Goldberg, P., Weiner, S., 2010. Apport des analyses minéralogiques (en spectrométrie infrarouge à transformée de Fourier) à l'interprétation des structures anthropiques : les concentrations osseuses dans les niveaux moustériens des grottes de Kébara et Hayonim (Israël). *Paleo* 2010, 93-107.
- Meignen, L., Bar-Yosef, O., Goldberg, P., 2002. Fireplaces in the Middle Palaeolithic: case studies of Kebara and Hayonim Caves, *Journal of Human Evolution*, pp. A23.
- Meignen, L., Goldberg, P., Albert, R.M., Bar-Yosef, O., 2009. Structures de combustion, choix des combustibles et degré de mobilité des groupes dans le Paléolithique moyen du Proche-Orient: exemples des grottes de Kébara et d'Hayonim (Israël), in: Théry-Parisot, I., Costamagno, S., Henry, A. (Eds.), *Gestion des combustibles au Paléolithique et Mésolithique: nouveaux outils, nouvelles interprétations/Fuel management during the Palaeolithic and Mesolithic period: new tools, new interpretations*. Archeopress, Oxford, pp. 111-118.
- Meignen, L., Goldberg, P., Bar-Yosef, O., 2017a. Together in the field: interdisciplinary work in Kebara and Hayonim Caves (Israel). *Archaeological and Anthropological Sciences* 9, pp. 1603-1612.
- Meignen, L., Speth, J.D., Bar-Yosef, O., 2017b. Stratégies de subsistance et fonction de site au Paléolithique moyen récent : apports de la séquence de Kebara (Mt Carmel, Israël). *Paléorient* 43 (1), pp. 9-47.
- Meignen, L., Speth, J.D., Stiner, M.C., 2006. Middle Palaeolithic settlement patterns in the Levant, in: Hovers, E., Kuhn, S.L. (Eds.), *Transitions Before the Transition: Evolution and Stability in the Middle Palaeolithic and Middle Stone Age*. Kluwer, New York, pp. 149-169.
- Mercier, N., Valladas, H., Froget, L., Joron, J.L., Reyss, J.L., Weiner, S., Goldberg, P., Meignen, L., Bar-Yosef, O., Kuhn, S., Stiner, M., Belfer-Cohen, A., Tillier, A.-M., Arensburg, B., Vandermeersch, B., 2007. Hayonim Cave: a TL-based chronology of a Levantine Mousterian sequence. *Journal of Archeological Science* 34(7), pp. 1064-1077.
- Mercier, N., Valladas, H., Joron, J.L., Schiegl, S., Bar-Yosef, O., Weiner, S., 1995. Thermoluminescence dating and the problem of geochemical evolution of sediments- A case study: the Mousterian Levels at Hayonim. *Israel Journal of Chemistry* 35, pp. 137-141.
- Rink, W., Schwarcz, H., Weiner, S., Goldberg, P., Meignen, L., Bar-Yosef, O., 2004. Age of the Mousterian industry at Hayonim Cave, Northern Israel, using electron spin resonance and $^{230}\text{Th}/^{234}\text{U}$ methods. *Journal of Archaeological Science* 31, pp. 953-964.

- Schiegl, S., Goldberg, P., Bar-Yosef, O., Weiner, S., 1996. Ash Deposits in Hayonim and Kebara Caves, Israel: macroscopic, microscopic and mineralogical observations, and their archaeological implications. *Journal of Archaeological Science* 23, pp. 763-781.
- Schiegl, S., Lev-Yadun, S., Bar-Yosef, O., El Goresy, A., Weiner, S., 1994. Siliceous aggregates from prehistoric wood ash: a major component of sediments in Kebara and Hayonim Caves (Israel). *Israel Journal of earth sciences* 43, pp. 267-278.
- Shahack-Gross, R., Bar-Yosef, O., Weiner, S., 1997. Black-coloured bones in Hayonim Cave, Israel: Differentiating between burning and oxide staining. *Journal of Archaeological Science* 24, pp. 439-446.
- Stiner, M., Kuhn, S., Surovell, T., Goldberg, P., Margaritis, A., Meignen, L., Weiner, S., Bar-Yosef, O., 2005. Bone, ash, and shell preservation in Hayonim Cave, in: Stiner, M. (Ed.), *The Faunas of Hayonim Cave (Israel). A 200,000-Year Record of Palaeolithic Diet, Demography and Society*. American School of Prehistoric Research, Peabody Museum, Harvard University, Cambridge (US), pp. 59-79.
- Stiner, M.C., 2005. *The Faunas of Hayonim Cave (Israel). A 200,000-Year Record of Palaeolithic Diet, Demography and Society*. Peabody Museum, Harvard University, Cambridge (US).
- Stiner, M.C., Howell, F.C., Martínez-Navarro, B., Tchernov, E., Bar-Yosef, O., 2001a. Outside Africa: Middle Pleistocene *Lycaon* from Hayonim Cave, Israel. *Bolletino della Società Paleontologica Italiana* 40, pp. 293-302.
- Stiner, M.C., Kuhn, S.L., Surovell, T., Goldberg, P., Meignen, L., Weiner, S., Bar-Yosef, O., 2001b. Bone preservation in Hayonim Cave (Israel): a Macroscopic and Mineralogical Study. *Journal of Archaeological Science* 28, pp. 643-659.
- Stiner, M.C., Kuhn, S.L., Weiner, S., Bar-Yosef, O., 1995. Differential burning, recrystallization, and fragmentation of archaeological bone. *Journal of Archaeological Science* 22, 223-237.
- Tillier, A.-M., Arensburg, B., Belfer-Cohen, A., Vandermeersch, B., 2011. Early Hominid remains from Hayonim Cave (Israel) in the context of the Late Middle and Upper Pleistocene record from the Near East. *Paléorient* 37, pp. 47-63.
- Weiner, S., Goldberg, P., 1990. On-site Fourier Transform Infrared Spectrometry at an archaeological excavation. *Spectroscopy* 5, pp. 46-50.
- Weiner, S., Goldberg, P., Bar-Yosef, O., 1999. Overview of ash studies in two prehistoric caves in Israel: implications to field archaeology, in: Pike, S., Gitin, S. (Eds.), *The Practical Impact of Science on Near Eastern and Aegean Archaeology*. Archetype Books, London, pp. 85-90.
- Weiner, S., Goldberg, P., Bar-Yosef, O., 2002. Three-dimensional distribution of minerals in the sediments of Hayonim Cave, Israel: Diagenetic processes and archaeological implications. *Journal of Archaeological Science* 29, pp. 1289-1308.
- Weiner, S., Schiegl, S., Bar-Yosef, O., 1995a. Recognizing ash deposits in the archaeological record: a mineralogical study at Kebara and Hayonim Caves, Israel. *Acta Anthropologica Sinica* 14, pp. 340-351.
- Weiner, S., Schiegl, S., Goldberg, P., Bar-Yosef, O., 1995b. Mineral assemblages in Kebara and Hayonim, Israel: excavation strategies, bone preservation and wood ash remnants. *Israel Journal of Chemistry* 35, pp. 143-154.

Acknowledgements

By the time we finished writing and compiling this volume, Ofer was unfortunately no longer with us. Of course, the first person I would like to thank, and dedicate this volume to, is him. His personality was always enthusiastic and bursting with energy and allowed this warm collaboration for more than 20 years.

Numerous people and granting agencies were responsible for making this interdisciplinary project work.

All our thanks, of course, go to the members of our research team who, by their active participation in this project, largely contributed to the success of the research carried out in the various fields. Thanks to their deep involvement in the field, many stimulating discussions took place there that enabled the completion of this large interdisciplinary program and, along the way, gave rise to numerous publications. The present volume constitutes the last major publication of our results. And in this context, I would like to thank especially P. Goldberg for his friendly support and efficient technical help in the final phase of the preparation of this publication.

This field project and the laboratory studies could never have been accomplished without the generous funding and technical support provided by the National Science Foundation (NSF grants 9409281, 9903576, 9208163), the French Ministry of Foreign Affairs, the American School of Prehistoric Research (Peabody Museum, Harvard University), in particular for the publication of this book, the CNRS (French National Centre for Scientific Research), the Centre de Recherche Français de Jérusalem (CRFJ), and the Irene Levi Sala CARE Archaeological Foundation (London).

Without forgetting all of the research institutions who helped to conduct the different scientific programs of this interdisciplinary project, we thank the Weizmann Institute, Israel; Institute of Archaeology of Hebrew University; Centre des Faibles Radioactivités, Laboratoire Mixte CNRS-CEA; and Israel Antiquities Authority.

Special thanks to Daniel Ladiray (CRFJ, CNRS) who drew the numerous lithic artefacts presented in chapter 5, and Sabine Sorin (CEPAM-CNRS) for her help in the digitisation of the geological sections (chapter 2).

We would like to thank also all of the volunteers, who are too numerous to name here but have been highly involved in this project and were present during several campaigns; many have since become professionals in Israel, the USA, France and elsewhere. We are particularly grateful to A. Stutz for his strong participation during several field seasons, his precise mapping and descriptions of the complex combustion features in Layer E, and in the later follow-up to these efforts. Finally, we would like to thank the Israeli, French, American, Canadian, Swiss, Italian, English, Japanese, and Chinese students who participated in the fieldwork, and made it an enjoyable experience for all of us.

Introduction

Liliane Meignen and Ofer Bar-Yosef

1.1 Introduction

The question of the origin of *Homo sapiens*, and, in particular, that of their migration from Africa to Eurasia, is undoubtedly one of the most debated subjects in Palaeolithic prehistory and evolutionary biology. The general assumption that the migration route of these humans took them through Western Asia has placed this area at the centre of scientific inquiries. Due to its location at the crossroads between Africa and Eurasia, and the presence of anatomically modern human and Neanderthal remains—both in association with Mousterian industries—the Levant has always played a key role in this debate.

This has been a controversial subject since the discoveries of many important human remains in the caves of Mount Carmel and Galilee in the 1930s (Tabun, Skhul, Qafzeh [Garrod and Bate 1937; McCown and Keith 1939]), and these sites have largely contributed to the study of the origin of modern humans. While the human fossils found here have been interpreted as representing two different populations (Clark-Howell 1959; Howells 1976; Vandermeersch 1981), the phylogenetic relationships between the skeletal remains defined as Neanderthals (from Tabun and Amud) and the more modern-looking remains from Skhul and Qafzeh have been largely discussed, as has their chronological position (Clark-Howell 1959; Coon 1962; Howells 1970; Vandermeersch 1981, to cite a few). In the absence of radioactive dating methods, then practically non-existent for periods beyond the effective limits of the C14 method, the dating of these assemblages and sites was based largely on long-distance faunal correlations and palaeoclimatological interpretations inferred from the sedimentary cycles.

The 1980s ignited new interest in the Middle Palaeolithic (MP), mainly concerning the double-edged debate of modern human origins and the demise of the Neanderthals. In the early 1980s, two conflicting models were proposed to explain the relationship between these two human morphotypes. The first implies a gradual phylogenetic transformation from Neanderthal forms into modern humans that took place around 40–50 ka (continuity model) (Jelinek 1981a, b, 1982a, b; Trinkaus 1983; Wolpoff et al. 1981), while the second considers the possibility of replacement of local populations by incoming modern humans (Howells 1976). Based on their morphological attributes, the modern-looking fossils from Qafzeh and Skhul, labeled as ‘Proto-Cro-Magnons’, were then considered as the immediate predecessor to Upper Palaeolithic *Homo sapiens sapiens* populations, giving credence to the first model; an age of 40–50 ka was suggested (Jelinek 1981b; Jelinek 1982b).

It was the palaeontological analyses of microvertebrates from Levantine Mousterian sites presented by Tchernov (Tchernov 1981, 1988) that first indicated the problems with this accepted chronology. Based on the biostratigraphy proposed by Tchernov, combined with the palaeoclimatic interpretation of the Tabun Cave stratigraphy (Farrand 1979), an estimated date of 80–100 ka for the Qafzeh hominids was suggested by Bar-Yosef

and Vandermeersch (Bar-Yosef and Vandermeersch 1981). The heavy criticism of this proposition (Jelinek 1982a), convinced these researchers of the urgency of a new field project.

It was clear that unresolved chronological issues hampered fruitful discussions of the phylogeny of known Levantine human fossils. The recent availability of new dating techniques (uranium series, thermoluminescence [TL], electron spin resonance [ESR]) was expected to offer improved prospects for dating MP assemblages.

A long-term project, originally entitled ‘The Origins of Modern Humans in Southwest Asia’, was then initiated by Bar-Yosef and Vandermeersch. It included fieldwork in three sites—Kebara, Qafzeh, and Hayonim—with the hope that they would cover the entire MP sequence (Bar-Yosef and Vandermeersch 2007).

Alongside numerous questions concerning site formation processes and other aspects of palaeoanthropological and behavioural importance (lithic technology, game exploitation and subsistence strategies, fire use, site function, settlement patterns, human remains and burials), one of the main contributions of this research was the establishment of a chronological framework based on the use of radioactive dating methods (mainly TL and ESR), then recently made available (Bar-Yosef and Meignen 2007; Bar-Yosef and Vandermeersch 1991; Bar-Yosef et al. 1992). Cumulated with dating programs undertaken in other sites of the region by the same team (Tabun, Skhul, and Amud Caves), the results obtained, despite certain ambiguities, have totally renewed the hypotheses concerning the relationships between Neanderthals and anatomically modern humans in the Levant (Mercier et al. 1993; Mercier, Valladas, and Valladas 1995; Valladas et al. 1987; Valladas et al. 1988).

These new data established the idea of a succession of two human groups in the Mediterranean Levant (Bar-Yosef and Vandermeersch 1991; Vandermeersch 1995), with early anatomically modern humans (Skhul, Qafzeh) occupying the region during MIS 5 (Mercier et al. 1993; Schwarcz et al. 1988; Valladas et al. 1988), preceding the arrival of Neanderthals around 70–50 ka (Grün and Stringer 1991; Schwarcz et al. 1989; Valladas et al. 1987; Valladas et al. 1988).

These data have further fuelled the hypothesis of an arrival of these *Homo sapiens* from Africa during the MIS 5 interglacial, triggered by favourable climatic and environmental conditions (e.g., Breeze et al. 2016; Frumkin, Bar-Yosef, and Schwarcz 2011; Petraglia et al. 2010). This hypothesis is based on the presence of archaic *Homo sapiens* in Africa whose tools are considered similar to those associated with the anatomically modern humans of Skhul and Qafzeh, a hypothesis widely defended in the prehistoric community (Groucutt et al. 2015, and references therein), but which is, nevertheless, still widely debated.

The southern Levant, being the single locality worldwide where anatomical remains of both *Homo sapiens* and Neanderthals have been discovered in MP contexts (Bar-Yosef et al. 1992; Vandermeersch 1981), continues to provide a critical testing ground for assessing the possibility of alternative evolutionary scenarios (Arensburg and Belfer-Cohen 1998; Tillier and Arensburg 2017; Tillier 2006b). It is also a region in which archaeological research has been highly active for a long time, thus providing frequently renewed data.

In the two last decades, new field projects, recent discoveries, and new studies have radically changed our understanding of the origin and complex evolution of *Homo sapiens* and have emphasised their antiquity. Debates on the origin of modern humans have long focused on the MIS 5 period, considered as the time of their first appearance in the Levant at the sites of Qafzeh and Skhul. Recent data, and in particular the discovery of their presence in the Levant as early as 177–194 ka, at the site of Misliya (Hershkovitz et al. 2021; Hershkovitz et al. 2018)—earlier than previously thought—shifted the focus and questions posed by researchers in the quest for origins to the pre-MIS 5 period.

These human remains attributed to *Homo sapiens* are associated at the site of Misliya, with tools of the very Early MP (EMP), consisting of Laminar assemblages very different from those associated with the anatomically modern humans from Qafzeh and

Skhul. Moreover, the lithic tools associated with the earliest *Homo sapiens* witnessed significant technological changes (disappearance of the bifacial component and Quina-like assemblages, the emergence of full-fledged Levallois technology) when compared with the last Late Lower Palaeolithic assemblages (Acheulo-Yabrudian) that preceded them. The origins of this new technical repertoire, and especially the origins of their authors, are currently debated and have been recently argued to result from an Out-of-Africa dispersal of anatomically modern humans (Zaidner et al. 2021; Zaidner and Weinstein-Evron 2020). Whether the Levantine shift from Lower Palaeolithic to Early MP technology was an autochthonous process (arising with local populations) or triggered by demic dispersals (most probably populations from Africa) remains unclear and needs to be further explored.

As a result of these new questions, the transitional period from the Late Lower Palaeolithic (Acheulo-Yabrudian) to the Early MP (EMP) has recently received renewed attention in the Levant, as well as in other regions (Africa, Europe). This is shown, for instance, by the special issue of the *Journal of Human Evolution*, ‘The Lower to Middle Palaeolithic Boundary: Evolutionary Threshold or Continuum?’ (Kuhn et al. 2021), which follows on from the international workshop in Haifa in 2017.

Sites containing both Acheulo-Yabrudian (Late Lower Palaeolithic) and EMP levels are relatively rare in the Levant, and even more so, those excavated by modern techniques. Nevertheless, the data fuelling these debates have been renewed via projects (fieldwork and studies) concerning new sites and the resumption of studies of collections from previously excavated sites. These sites include Misliya (Weinstein-Evron et al. 2003; Weinstein-Evron and Zaidner 2017; Zaidner and Weinstein-Evron 2020), Tabun (Shimelmitz and Kuhn 2013; Shimelmitz et al. 2021; Shimelmitz et al. 2014b), Hummal and El Kowm Basin (Le Tensorer et al. 2011; Wojtczak 2011, 2015), Dederiyeh (Nishiaki, Akazawa, and Kanjou 2022; Nishiaki, Kanjou, and Akazawa 2017; Nishiaki et al. 2011), and Hayonim (Meignen and Bar-Yosef 2020).

The deep archaeological sequence at Hayonim Cave, already known for its EMP assemblages (Meignen 2011), and now extended to Acheulo-Yabrudian lithic production (Meignen and Bar-Yosef 2020), corresponds perfectly to these issues. It covers the crucial period during which *Homo sapiens* probably emerged/arrived in the region. The data recently acquired at the Neshar Ramla site (Israel), showing the presence at approximately 140–120 ka of a Middle Pleistocene archaic *Homo* (HersHKovitz et al. 2021)—thus different from the Early *Homo sapiens* present in the region around 180 ka (HersHKovitz et al. 2018)—underline the complexity of population movements in this region. They suggest a biodiversity at least as important as that often described during the MIS 5, MIS 4, and early MIS 3, probably related to numerous waves of dispersal between Africa and Eurasia, highlighted by genomic (and other) studies.

Thanks to its deep archaeological sequence, the site of Hayonim enables detailed documentation of the period concerned (MIS 8 to early MIS 5) and analyses of the changes in human behaviour (lithic production, subsistence strategies, settlement patterns) during this time, and perhaps discussions of the processes responsible for these transformations.

1.2 Hayonim Cave: context and history of the excavations

1.2.1 Site presentation

Hayonim Cave is located on the right bank of the Nahal or Wadi Meged (a tributary of the Nahal Yassaf) in western Galilee at the limit between lower and upper Galilee. It is about 250 m above sea level (asl) and about 13 km from the Mediterranean Sea. Western Galilee spans the 3–8 km wide coastal plain eastward to the foothills (200–300 m asl) and onto the hilly area of Galilee (up to 800 m asl). The major geological formations in the area are of Late Cretaceous age (the Judea Group) and are comprised mostly of limestone, dolomite, and chalk (Freund 1978). Many of these rocks contain flint nodules within 10 km of Hayonim Cave and were exploited by the prehistoric inhabitants (Delage 2001; Delage,



Figure 1.1. View of Hayonim Cave, with the Mediterranean Sea in the background.

Meignen, and Bar-Yosef 2000). The local climate comprises humid, mild winters with an annual precipitation of ~500–800 mm during the winter months; the summers (May through mid-September) are hot and humid with almost no rain.

The cave was formed by karstic activity in the hard limestone of the Yanuch Formation (Freund 1978), and originally included at least four solution chambers, but only two remain complete (Figure 1.1). The middle cave has not been excavated and is currently filled with massive modern accumulations of burned goat dung. The remnants of two other chambers contain vestiges of eroded brecciated deposits containing some Mousterian artefacts.

The excavations took place in the cave furthest to the east, which consists of two major dome-like chambers with a surface area of about 150 m² beyond the drip line. In front of the cave, there is a series of human-made terraces with olive groves extending down to the valley. The top two terraces contain the remains of a Geometric Kebaran station, a large Natufian site ('Hayonim Terrace'), and artefacts dating to the Pottery Neolithic (Henry, Leroi-Gourhan, and Davis 1981; Khalaily, Goren, and Valla 1993; Valla, Le Mort, and Plisson 1991).

1.2.2 Excavation history

1.2.2.1 Early excavations: Bar-Yosef, Tchernov, Arensburg, 1960s–70s

Initially (1965–1979), the excavations at Hayonim Cave were directed by O. Bar-Yosef (then at The Hebrew University of Jerusalem), B. Arensburg (Tel-Aviv University), and E. Tchernov (The Hebrew University of Jerusalem). These excavations focused on the deposits in the central area of the cave. There, the exposed stratigraphy consisted of historic ash deposits, Natufian sediments (Level B) with rounded/oval structures and numerous graves, and Kebaran (Level C), Aurignacian (Level D), and Mousterian levels (Level E) (Bar-Yosef 1991a; Bar-Yosef and Belfer-Cohen 1988; Bar-Yosef and Goren 1973; Belfer-Cohen 1988; Belfer-Cohen and Bar-Yosef 1981). At the time, the Mousterian deposits (Level E) were about 3 m thick, as revealed in a deep excavation near the western cave wall. Remains of brecciated deposits on the cave walls and at the entrance, as well as deposits underlying Natufian and Kebaran ones, clearly showed that the Mousterian deposits were the most widespread and covered the entire cave area.

Analysis of microfaunal assemblages from Level E suggested an early date for the Mousterian levels at the base of the sounding along the western wall (Tchernov 1981, 1988, 1989). This antiquity seemed to be confirmed by the lithic assemblages discovered in these same levels, comprising numerous tools on elongated blanks reminiscent of those then called the ‘Tabun D type’. In addition, isolated human fragments were studied and published (Arensburg et al. 1990).

In the context of our long-term research project on the origin of anatomically modern humans that followed the large field project at Kebara Cave (Bar-Yosef and Vandermeersch 2007; Bar-Yosef et al. 1992) and the dating of hominin-bearing levels at Qafzeh Cave (Valladas et al. 1988), it seemed essential to return to excavate at Hayonim Cave to complete the chronological controls of the regional cultural sequence. Thus, the excavations at Hayonim Cave were designed as the last step of this long-term project.

1.2.2.2 Recent excavations: 1992–2000

This fieldwork was organised based on the same principles as those established at the beginning of the project (Meignen, Goldberg, and Bar-Yosef 2017). The main idea was to have the entire interdisciplinary research team present in the field at the time of excavation to foster discussions among researchers from different disciplines and, interestingly, different academic traditions. The effectiveness of this daily collaboration proved to be quite productive.

1.2.2.2.1 Goals

Our later excavations at Hayonim Cave, from 1992 to 2000, were jointly conducted by O. Bar-Yosef (Harvard University), L. Meignen (CEPAM, C.N.R.S., University Côte d’Azur, France), and B. Vandermeersch (then at the University of Bordeaux, France). The main objectives were to uncover and investigate the deep MP sequence. Previous observations revealed an industry in the uppermost Mousterian deposits (so-called Upper Layer E) that, at first glance, resembled the one from Qafzeh Cave. On the other hand, the artefacts from the deep excavation next to the western wall in the central area contained numerous elongated blanks similar to those of the Tabun D assemblage. Consequently, our goal was to systematically excavate the Mousterian levels and date them by TL, ESR, and other techniques.

The discovery of Acheulo-Yabrudian assemblages at the base of the Deep Sounding at the cave entrance allowed us to broaden our initial chronological objectives. In particular, it enabled us to investigate the processes responsible for the major changes observed in the lithic technological repertoires during the Late LP/Early MP (Acheulo-Yabrudian/EMP) transition.

Furthermore, the long MP sequence, with many levels that have yielded EMP assemblages transitioning to assemblages that can be considered as the beginnings of the Mid-MP assemblages, enable us, for the first time, to assess in detail the technological changes that occurred during this period, in particular during the disappearance of the EMP Laminar toolkit.

In addition to abundant information on lithic technology, Hayonim Cave provided a unique ‘laboratory’ in which to pursue other behavioural domains. Our aim was also to collect large faunal assemblages (rarely available for this early period in the region) and to fully document the well-preserved hearth areas inside the cave. Much of this research on the details of diagenesis and site formation processes was initially stimulated by our previous excavations at Kebara Cave, where we employed the same techniques to record mineralogical and micromorphological data. The perspectives provided by the application of these scientific approaches proved especially important for understanding potential distortions in the radiometric dating results and the differential preservation of bones, mollusc shells, and wood ash in the sediments (Mercier et al. 1995).

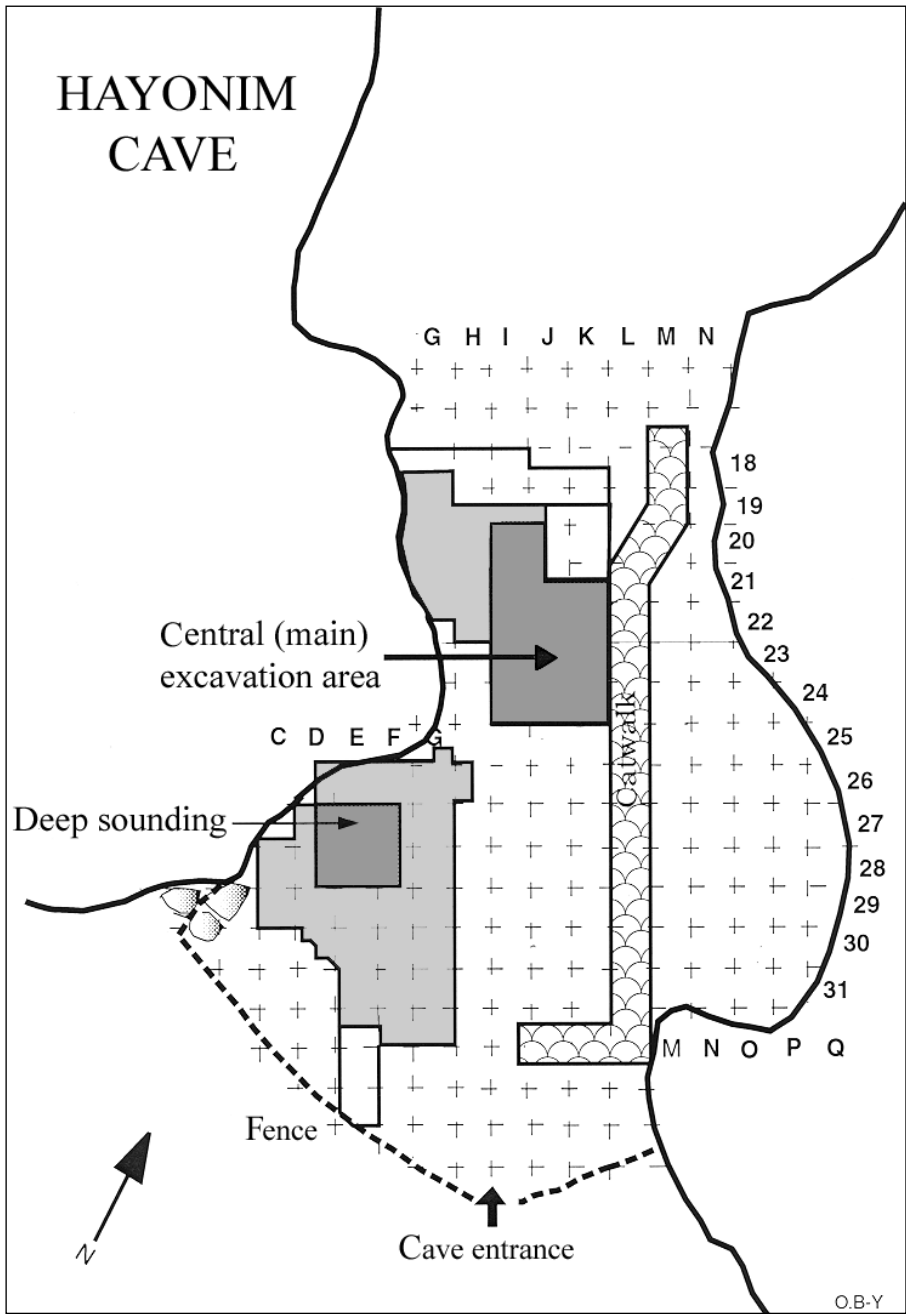


Figure 1.2. Map of excavated areas in Hayonim Cave (adapted from Stiner et al. 2001b).

1.2.2.2.2 Fieldwork approaches

1.2.2.2.2.1 Excavation techniques

Before excavating, we subdivided the entire surface of the cave into 1 × 1 m grid units (Figure 1.2), each square metre was then subdivided into four quadrants (a-b-c-d). An arbitrary, zero-point datum was fixed on the cave wall, from which the depths were measured. The excavations were conducted by *décapage* (surface stripping) in successive 5-cm volumes that followed the visible stratigraphy, paying special attention to the inclination of combustion lenses when present. All lithic pieces larger than 2.5 cm were plotted in three dimensions (north, east, and depth below datum), along with identifiable bones, teeth, and bone fragments larger than 2.5 cm. All of the sediments were



Figure 1.3. Dry and wet sieving in front of the cave.

dry- and wet-sieved (through 3-mm and 1-mm meshes) (Figure 1.3), and the small bone fragments, microfauna, fish, legless lizard scales, shells, and flint chips were retrieved by hand. Flotation techniques were applied in an effort to recover botanical remains but failed in most cases.

During the excavation, numerous observations concerning the nature of the deposits, phosphate concretions, archaeological contexts, bone and artefact concentrations, and, more specifically, the types of hearths and ash distributions, were recorded in notebooks by the excavators. For each *décapage*, a field drawing was made (scale 1/20), mapping the main combustion features, zones of phosphate concentrations, and samples collected for micromorphology, phytoliths, and Fourier transform infrared (FTIR) geochemistry. A special notebook for the precise descriptions of hearths/combustion features/large

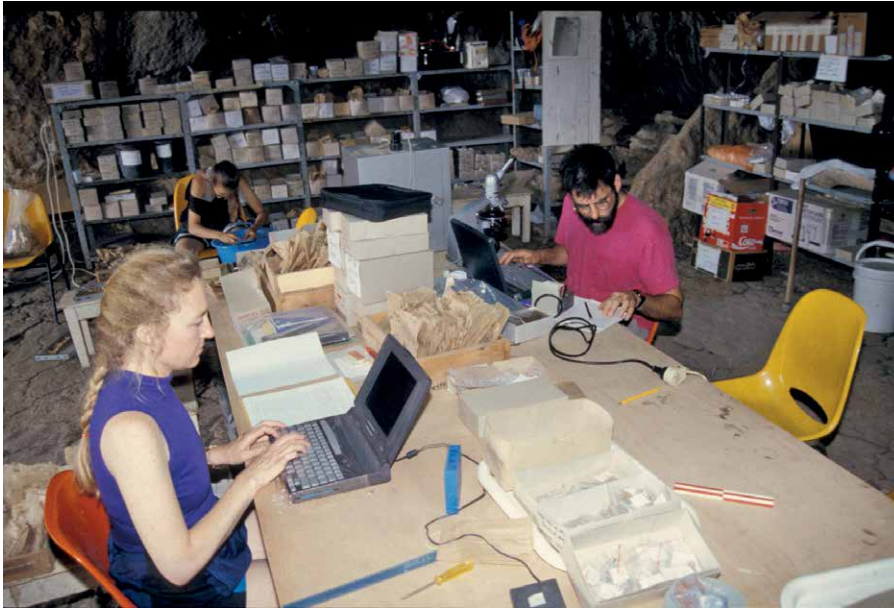


Figure 1.4. Field 'laboratory' set up in the back of the cave.

ash patches was used in the Central Area in the units in which fireplaces were more abundant. This recording allowed us to monitor the spatial and temporal differences in the combustion features during the excavation. A computerised inventory of the piece-plotted materials (lithics and bones) was constructed and updated daily.

The intensive task of deciphering the stratigraphy was carried out on the excavation site because the site formation processes were very complex (especially the post-depositional phenomena). Numerous stratigraphic section drawings and photographs were taken because the boundaries between the levels were sometimes difficult to read in the field due to the significant diagenesis phenomena that blurred them. The determination of the mineralogical components of the sediments, and, especially, of the concretions observed with the naked eye, subject to FTIR analysis as the excavation progressed thanks to the use of infrared spectrometers in the field, was of great help in interpreting the relationships between the different levels observed (especially the limit between E and F) in real time.

The deposits were monitored and described in detail during excavations. Throughout this fieldwork, we collected numerous samples of the deposits and combustion features for micromorphological analyses. Our sampling strategy consisted of removing intact blocks of sediment, which were then securely wrapped to maintain their integrity. At the same time, we collected small loose samples for other analyses, such as FTIR, and the position and context of the sample were recorded in photos and drawings.

The challenge at Hayonim Cave, as in our previous project at Kebara Cave, was to identify the anthropogenic signals in the cultural levels and to differentiate them from the multitude of independent chemical, biological, and geological processes that inevitably affect sediments.

Some of these analyses were performed in the field, in a 'laboratory' set up in the back of the cave (Figure 1.4).

1.2.2.2.2 Field analyses

We performed several analyses directly in the field in order to adjust our excavation strategies based on the results and to keep our thinking about the stratigraphy, site formation, and other aspects of the site up to date. These analyses included several field procedures.



Figure 1.5. Geochemical analysis onsite using FTIR spectrometry.

From the beginning of the excavations in Hayonim Cave, with the incorporation of computers in the field, we were able to catalogue the lithic tools and bone remains every day in the field laboratory set up at the back of the cave. This enabled us to work systematically on the differential distribution of lithic and bone elements as the excavation progressed (Stiner 2005).

Mapping of the bone distribution during the excavation helped us to focus our sampling strategy for FTIR analysis in order to test hypotheses about differential bone preservation, which turned out to be a significant issue (Meignen, Bar-Yosef, et al. 2010; Stiner et al. 2005; Stiner et al. 2001b; Weiner and Bar-Yosef 1990; Weiner, Goldberg, and Bar-Yosef 1993).

Geochemical analysis using FTIR was performed onsite from the start of the Hayonim excavation in 1991. This type of analysis was launched initially as an experiment by Steve Weiner at the Weizmann Institute (Rehovot, Israel). He had previously demonstrated the value of this technique in the laboratory and with his work in the field at Kebara

Cave. These experiments proved their effectiveness in the field and during later lab work and interpretation (Schiegl et al. 1996; Weiner, Schiegl, and Bar-Yosef 1995; Weiner et al. 1995). This analytical procedure later became a routine field technique in many other prehistoric and archaeological sites in Israel and elsewhere in the world.

We conducted onsite mineralogical analyses from the beginning of the Hayonim excavation. Over 2,100 sediment samples were collected and analysed onsite using FTIR spectrometry, providing, for the first time, a detailed three-dimensional map of mineralogical assemblages in a prehistoric cave site (Weiner, Goldberg, and Bar-Yosef 2002). The analyses were carried out during two weeks of each excavation season (Figure 1.5). The methods used in the field and in the laboratory have been described in detail (Schiegl et al. 1996; Weiner and Goldberg 1990; Weiner et al. 1995). This information is useful for understanding the ‘completeness’ of the archaeological record (Karkanas et al. 2000; Weiner et al. 2007) in terms of whether the distribution of archaeologically important materials such as bones (Meignen, Bar-Yosef, et al. 2010; Stiner et al. 2001b; Weiner, Goldberg, and Bar-Yosef 1993), ash/combustion features (Schiegl et al. 1996; Schiegl et al. 1994; Weiner, Goldberg, and Bar-Yosef 1993; Weiner, Goldberg, and Bar-Yosef 2002) (see also chapter 3, this volume), phytoliths (Albert et al. 2003), and various organic materials are intact or have been affected by diagenesis. The data are also helpful in interpreting the stratigraphy (for instance, following the erosional boundary between Layers E and F, which were not readily differentiated by the naked eye), and post-depositional site formation processes (Weiner, Goldberg, and Bar-Yosef 2002). These findings have proved to be important in understanding the age estimations of the stratigraphic levels by both ESR and TL dating of tooth enamel and burned flints, respectively (Karkanas et al. 2000; Mercier et al. 1995).

Moreover, we attempted to perform micromorphological analyses in the field, and whereas it was easy to impregnate samples with polyester resin, it proved to be much more difficult to produce a usable thin section under field conditions. In the end, we decided to bring a petrographic microscope into the field, along with thin sections and sawn block from the previous seasons, and to use these as a portable stratigraphic reference collection.

In any case, though most analyses were completed in the laboratory, the initial process of collecting samples and data in the field served to make the sampling process, sampling strategies, and overall reasoning about the site more robust and rigorous.

Hayonim geology and stratigraphy

Paul Goldberg, Liliane Meignen,
Steve Weiner and Ofer Bar-Yosef

2.1 Introduction

Excavations at Hayonim took place from 1992 to 2000, during which time the areas previously excavated by Bar-Yosef in the 60s and 70s (Bar-Yosef et al. 2005) were deepened and enlarged. Here, we present descriptions of the deposits revealed during these latest excavations and couple them with micromorphological and mineralogical analyses in order to provide a comprehensive presentation and interpretation of the geological history of the site, including both geogenic and anthropogenic depositional and post-depositional processes. The history of excavations and general information are provided in chapter 1.

Hayonim Cave (Figure 2.1) is one of several karstic caves situated in the Western Galilee part of Israel, at an elevation of about 250 m asl and about 13 km from the Mediterranean Sea (Figure 1.1). The cave is formed within the Late Cretaceous Yanuch Formation (Bar-Yosef et al. 2005).



Figure 2.1. Photo of Hayonim Cave from the south side of Wadi Meged. Other karstic cavities are visible to the left of the main entrance of the cave.

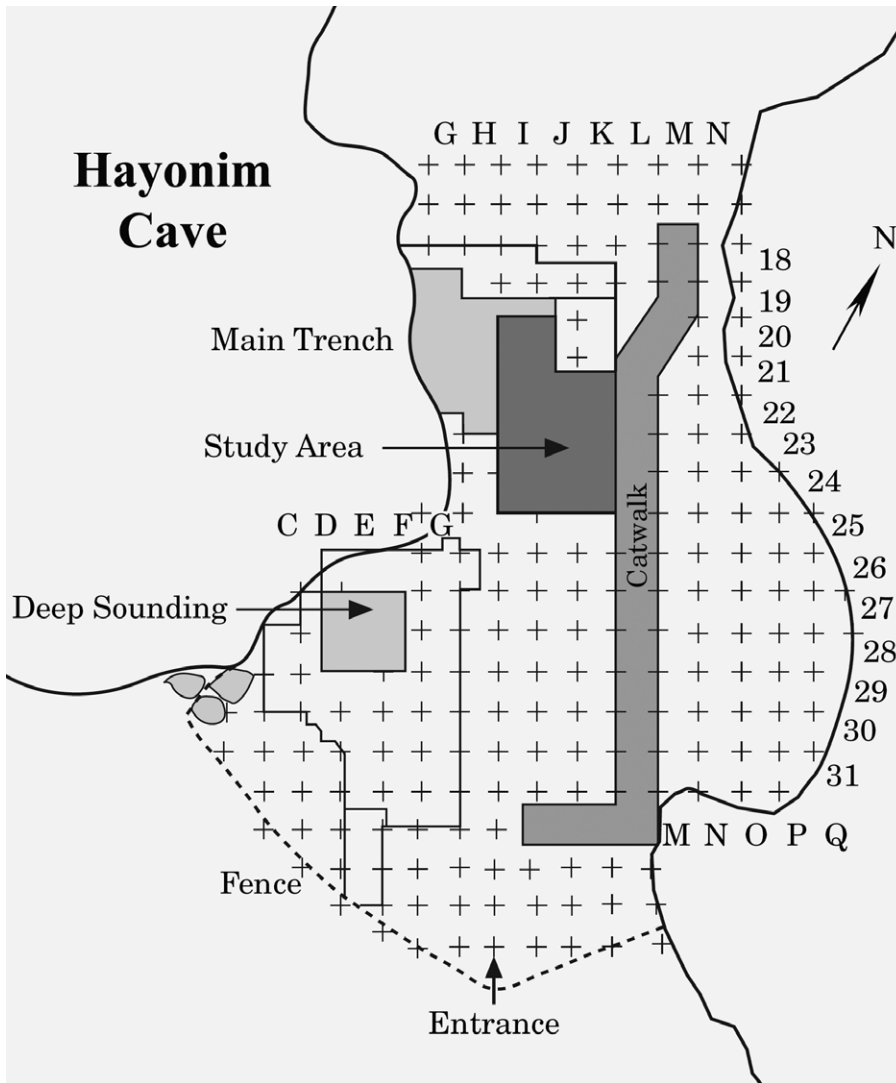


Figure 2.2. Map of excavated areas in Hayonim, with the locations of the Deep Sounding and Central Area.

Two main areas—Deep Sounding and Central Area—were the loci of excavations and the source of the stratigraphic information and interpretations presented below (Figures 2.2–2.4). Both areas revealed somewhat complementary sedimentary sequences with some stratigraphic overlap, although the two areas are not physically linked. About 4 m of deposits were exposed in both areas, but deposits in the Deep Sounding are lower in elevation (~400 to ~800 cm), in contrast to those of the Central Area, which are higher (~200 to ~600 cm) (Figure 2.4).

Previous excavations and these excavations led to the recognition of seven stratigraphic units throughout the cave sequence, Layers A–G, which were previously summarised by Bar-Yosef et al. (2005) and are briefly summarised in Table 2.1. Here, we concentrate principally on the sediments with Middle Palaeolithic and Lower Palaeolithic materials (Layers E, F, and G) and briefly include only a description of the Kebaran deposits from Layer C near the entrance.



Figure 2.3. Photos of the interior of Hayonim Cave. **a.** View toward the back of the cave in 1993, showing excavations in the Central Area. The flat area at right with the notebook and bucket are at a depth of ~-275 cm. In the background are the uppermost layers in the cave sequence (Layer A), which are composed of soft interbedded ashy and organic deposits with some limestone fragments that resemble fumier deposits. **b.** Looking south toward the excavations of the Central Area in the foreground and the cave entrance in the background. The large heap of stones next to the walkway is part of Natufian structures.

2.2 Details of Hayonim deposits by area

2.2.1 Deep Sounding

The Deep Sounding is situated close to the entrance of the cave and is bounded roughly by excavation squares D, E, F, G 26/27/28 (Figure 2.2). At the deepest part of the excavations, the area exposed was slightly larger than 2 m², but in the upper part (above ~-450 cm) the Deep Sounding area exposed is wider, slightly larger than 3 × 3 m. The modern drip line is immediately overhead, but at the time of occupation, the cave roof extended 2–3 m further south, as shown by the large, metre-sized blocks scattered at the entrance to the cave. Four stratigraphic units were visible in the Deep Sounding, from bottom to top.

2.2.1.1 Layer G

Layer G occurs only in the Deep Sounding, from about -795 to -810 cm in F28 to -855 cm in F27. Only the upper part of Layer G was exposed during excavation (Figure 2.4). Bedrock was not reached, so its true thickness is not known. The uppermost part of Layer G is comprised of hard, dark brown (7.5YR4/2), gritty silt containing numerous sand-sized opaline seed coats, but little finer interstitial material. Underlying this, seed coats are fewer and the sediments are more massive and finer grained, consisting of brown and yellow-brown silt with some phosphatic mottling. Scattered throughout are flecks of charcoal and bird gastroliths, which are semi-spherical, well-rounded, polished granules of predominantly limestone and some chert. Although poorly exposed, some rodent burrows occur, as in the overlying Layers F and E (see below). A reddish vein and void coating of crystalline material can be observed. In F27d, at ~-818 cm, the sediment becomes less bedded, with a more mottled appearance and centimetre-sized splotches

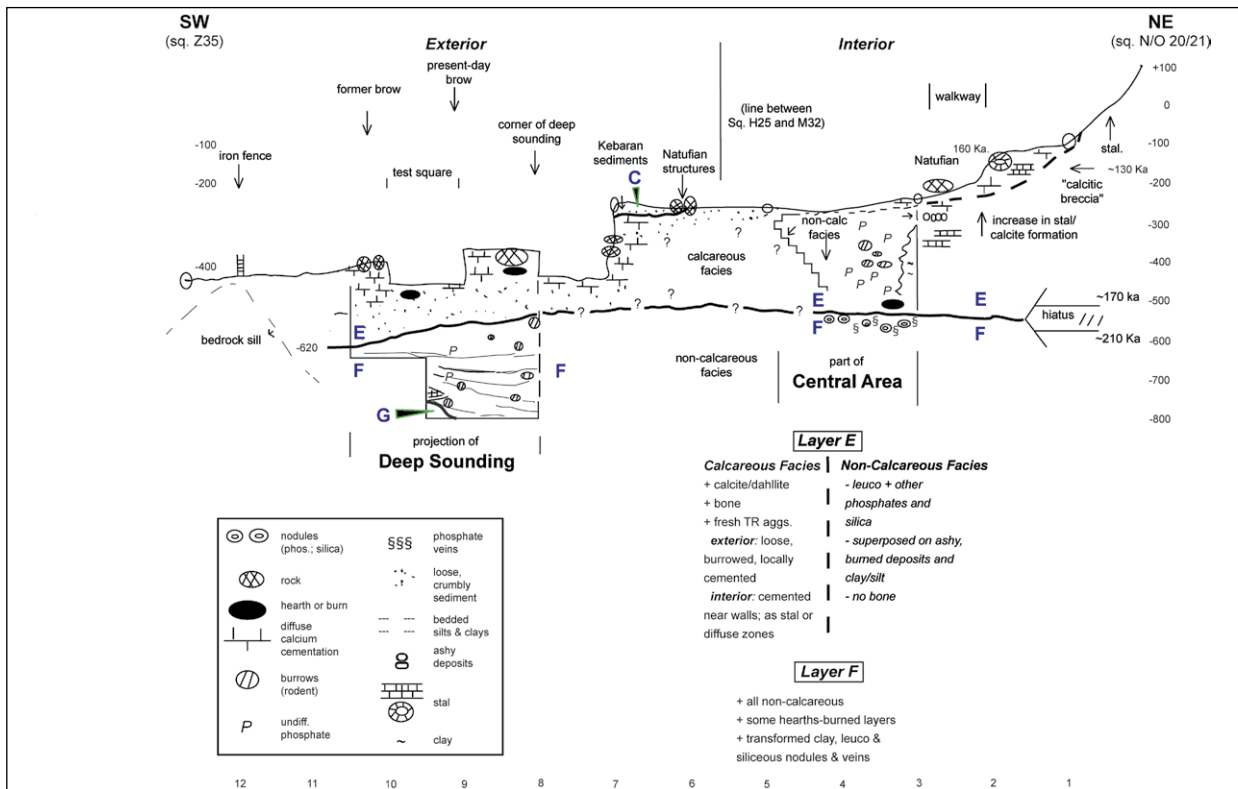


Figure 2.4. Semi-schematic cross section of the stratigraphically lower parts of the deposits exposed in the Deep Sounding and Central areas of the site; deposits of Layers A, B, C/E, and D are not illustrated here.

Layer	Description	Industry
A	The uppermost layers in the cave sequence, and up to 3 m thick. It is comprised of soft, interbedded, ashy and organic deposits with some limestone fragments, which are typical of 'fumier' deposits. A glass furnace dating to the Late Roman-Early Byzantine period was cut into the underlying Natufian deposits (Belfer-Cohen and Bar-Yosef 1981). They are not further described.	Late Roman-Early Byzantine
B	Situated primarily in the eastern third of the cave, and composed of greyish, ashy, anthropogenic deposits associated with Natufian architecture, especially rooms and graves (see chapter 1). They are not discussed here.	Natufian
C	Situated at the entrance area of the cave. It is ~2.5 m thick and comprised of calcareous, loose, reddish, crumbly silt and clay with abundant bones, which appear to have been reworked in part from the Mousterian deposits (see below). The deposits take on an elongated trough shape that parallels the location of the brow of the cave at the entrance.	Kebaran
C/E	Diffuse pocket of looser reworked sediments near Mousterian containing a mixture of Mousterian and Kebaran artefacts.	Mixed Kebaran/Mousterian
D	Was most visible in the Central Area, where it is now excavated. It ranges from 35 to 55 cm thick and is a greyish deposit with limestone fragments, imported cobbles, hearths, and numerous bones (Belfer-Cohen and Bar-Yosef 1981). During occupation, the lowermost deposits were dug into the underlying Mousterian deposits, and in turn, Natufian activities (associated with graves) removed a substantial part of these deposits (see Belfer-Cohen and Bar-Yosef 1981 for further details).	Aurignacian
E	Massive, reddish-brown, silty clay layers ~20-40 cm thick, with numerous interbedded intact and trampled hearths represented by diagenetically altered ashes, silts/clays, and organic matter. Bone fragments occur in calcareous zones in proximity to bedrock walls in the western parts of the Central Area, and in the upper part of the Deep Sounding; they are absent where diagenesis is prominent (Weiner, Goldberg, and Bar-Yosef 2002). The deposits are generally horizontal in the centre of the Central Area but dip increasing to the north and northwest toward the rear of the cave; such inclinations (as in Kebara Cave; Goldberg et al. 2007) point to subsurface subsidence into karstic depressions.	Mousterian
F	Mostly geogenic, consisting overall of diagenetically altered clay, quartz silt, and nodules of opal. Excavation of Layer F in the Deep Sounding revealed isolated (diagenetically altered) hearths and numerous pieces of charcoal; much of the layer is well bedded and becomes increasingly finely laminated with depth. Extensive diagenesis involving phosphatisation, clay transformation, and the formation of nodules of opal. Calcite is generally absent except for the Deep Sounding, where periods of calcification and decalcification can be inferred from the micromorphology (see below). Layer F in the Central Area was slightly inclined toward the rear of the cave, whereas in the Deep Sounding, deposits were generally horizontal at the base, but showed increased dips upward in the profile; these deposits were punctuated by numerous rodent holes.	Mousterian
G	Limited (~60 cm) exposure only in the Deep Sounding. Generally similar to Layer F there, with remains of a few diagenetically altered hearths.	Late Lower Palaeolithic

Table 2.1. General summary description of Hayonim deposits (modified from Bar-Yosef et al. 2005); see text below for details.

Figure 2.5. Layer G in the Deep Sounding. **a.** North profile showing Layers F and G (at base) in 2000. Note the dips toward the northeast in Layer G and the lower part of Layer F, which become more horizontal upward. These dips are tied to subsidence into an inferred depression in the bedrock below. **b.** Lower part of the Deep Sounding in 2000 showing diagenetically altered hearths within Layer G at the base, overlain by mostly geogenic deposits of Layer F that exhibit some rodent burrows. **c.** Detail of the upper part of Layer G in 1999 showing remains of apparent hearth in diagenetically altered silts. **d.** Hearth structures at the very base of Layer F/top of G. This photo was taken at the end of the excavations in 2000.



that range in color from yellow-brown to gray and brown (10YR5/3). In addition, dips become more marked and increase below -803 cm, dipping more steeply to the northeast. There appears to be a buried depression with a submerged hinge line or bedrock rise that passes diagonally across the square. The upper part of Layer G is truncated by an erosional surface that dips northeast toward the interior of the cave.

The remains of at least two combustion features were exposed in the southeast corner of E27. These structured hearths reach a maximum thickness of 10 cm and consist of diagenetically altered ashes resting on darker organic-rich substrates (Figure 2.5b; see also chapter 3). The combustion features are punctuated by several rodent burrows (*terriers*), so their true aspect, integrity, length, and thickness are difficult to assess. Nevertheless, it is evident that these burning episodes took place—and the sparse artefacts deposited—during intervals when the waterlain deposits of Layer G must have dried out and been exposed for an unknown period of time.

2.2.1.1.1 Micromorphology

The above components are also visible in the thin sections from Layer G (Figures 2.6, 2.7). The matrix is comprised of generally diagenetically altered silty clay, which is demonstrated by its isotropic nature in cross-polarised light (XPL), reflecting the transformation of crystalline clays to amorphous clays and opal, based on FTIR. These mineralogical phases are referred to as opal

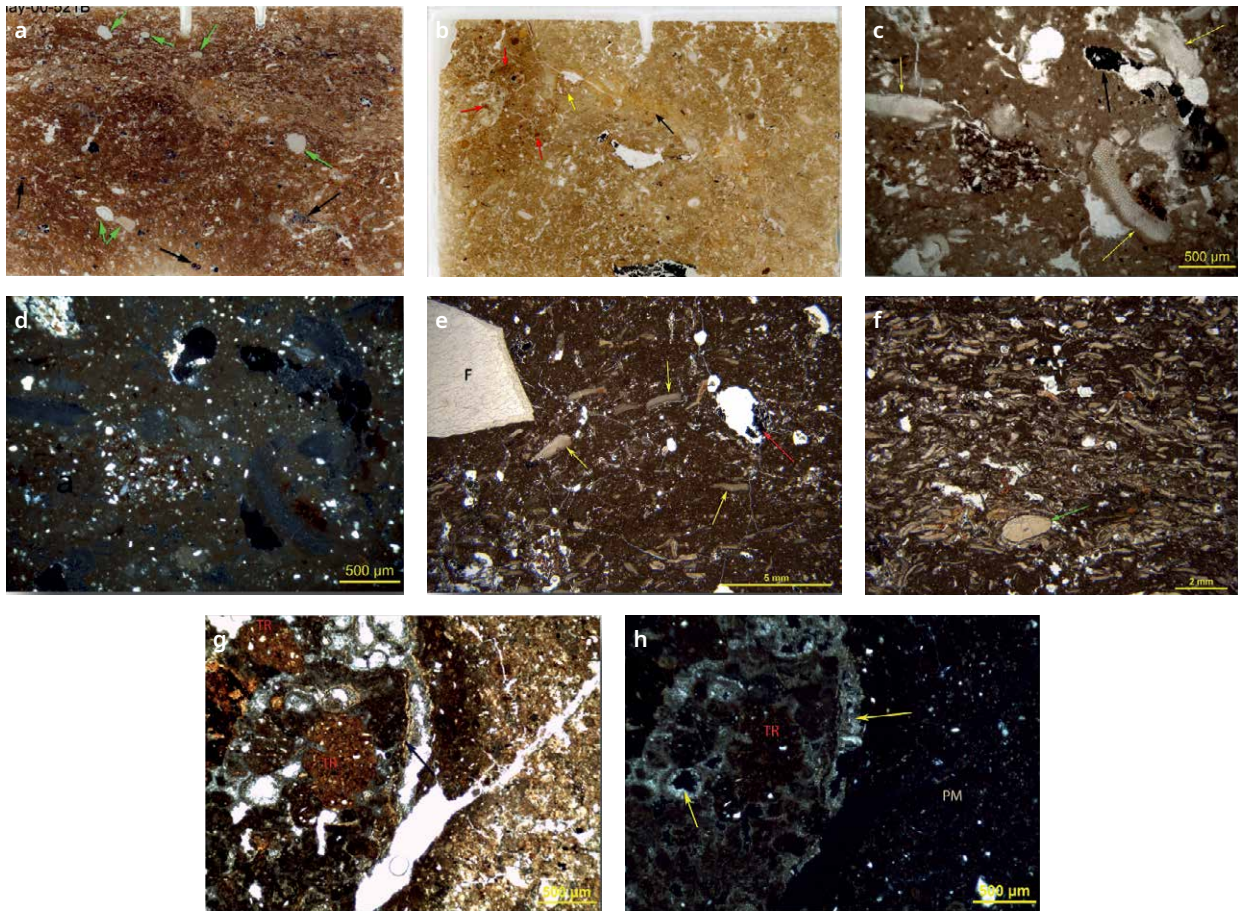


Figure 2.6. Micromorphology of Layer G sediments in the Deep Sounding. **a.** Scan of thin section of 00-521B (F27d; -806 cm) showing slightly rounded seed coats with undulating bedding that overlies with a sharp contact, brownish, silty mud with seed coats scattered throughout. Black arrows indicate both charcoal and humified organic matter; green arrows designate gastroliths. PPL; width is 75 mm. (NB: all thin section scans are 75 × 50 mm). **b.** Thin section scan of lowermost sample from the Deep Sounding (00-526; F27; -820 cm), consisting of diagenetically altered silty clay with yellowish phosphate staining of unknown specific mineralogy. Note the large grain of charcoal at base (cc) and the fine vuggy porosity due to bioturbation. A centimetre-sized grain of cave breccia is situated in the upper left; fresh terra rossa aggregates are indicated with red arrows and yellow arrow points to an area where calcite has been replaced with apatite. Adjacent to this is a domain of bedded silts (black arrow). PPL; width is 75 mm. **c.** Sample 00-521 showing a yellowish-brown, phosphatised, silty clay matrix with coarser grains of opaline seed coats (yellow arrows) and piece of crushed charcoal (black arrow). In the centre is a sand-sized grain of silty clay similar to terra rossa. Plane-polarised light (PPL), scale is 500 μm . **d.** Same as (c) but in cross-polarised light (XPL). Note the generally isotropic nature of the silty (white grains) clay matrix, which is indicative of diagenetic alteration and the formation of the phases 'opal transforming' and 'clay-transforming' (Weiner, Goldberg, and Bar-Yosef 2002). Scale is 500 μm . **e.** Sample 00-521 showing silty mud with numerous seed coats (yellow arrows), remains of a rounded grain of charcoal (red arrow), and a flint fragment (F). PPL; scale is 5 mm. **f.** A mass of bedded seed coats in sample 00-521 overlying more mud-supported sediment at the base. The arrow points to a well-rounded chert gastrolith. PPL; scale is 2 mm. **g.** Sample 00-526 (F27a; -820 cm) showing at left a compound aggregate composed of fresh and weathered terra rossa aggregates (TR) surrounded by a thin crust of apatite (black arrow), which is coated by calcite (see [f]); at right is phosphatic, isotropic, silty clay matrix (PM). PPL; scale is 500 μm . **h.** Same as (g) but in XPL. The calcite infillings and circular coatings are shown by the yellow arrows. On the right side is quartz silt within weakly isotropic matrix, signaling less diagenesis than in (b), for example. This photo shows alternating phases of calcite and phosphate precipitation.

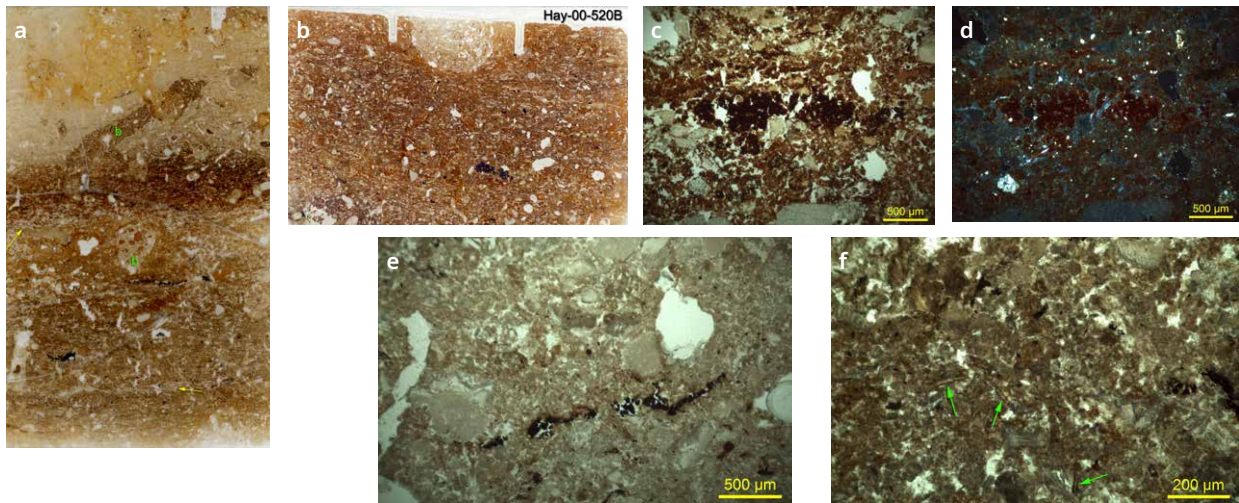


Figure 2.7. Sample 00-520 (-520A overlies -520B) from an Acheulo-Yabrudian hearth in F28d, -793 cm. **a.** Scan of thin section of -520A showing bedded seed coats (yellow arrows) at base and in the centre, where they occur within a darker organic-rich layer. Note the presence of millimetre-sized burrows (b) and yellow diagenetic staining (unknown composition) in upper part. The dark fragments are charcoal. The upper lighter part appears to be diagenetically altered ashes. PPL. **b.** Scan of underlying thin section of -520B which is mostly bedded seed coats in a dense diagenetically altered silty clay matrix with some flecks of charcoal and manganese. PPL. **c.** Photomicrograph of dark band in centre, which is comprised of unrecognisable organic matter, seed coats, and silty clay. PPL; scale is 500 μm . **d.** Same as (c) but in XPL. Except for the quartz silt (white spots), the matrix is isotropic due to diagenesis. Scale is 500 μm . **e.** Photomicrograph of the upper, lighter part with a stringer of dark organic matter. Though isotropic in XPL, these sediments appear to be diagenetically silts and ashes. PPL; scale is 500 μm . **f.** Detail of upper part of (e) with fine granular material, some of which appears to be ashes as suggested by the numerous phytoliths (green arrows). PPL; scale is 200 μm .

transforming and clay transforming (Weiner, Goldberg, and Bar-Yosef 2002; for more details also see figure 12.16 in Weiner 2010). On the other hand, some fresher reddish silty clay (*terra rossa*) aggregates were also observed, possibly less altered because of having been heated. Locally, opaline seed coats are bedded and clast supported, but elsewhere, they occur within the silty clay matrix. Gastroliths occur throughout. Although generally compact, localised irregular vughs and some channels point to bioturbation, probably by fine roots. Sample 00-526 (F27a; -820 cm), may represent a cultural layer with charcoal, some bones, and a single angular flint flake. However, it is possibly reworked from elsewhere, as it is an isolated occurrence and lacks any internal structure other than bedded seed coats, as in sample 00-520B (F28d; -793 cm). Multiple phases of diagenesis are inferred from localised calcareous hypocoatings that exhibit apatite alteration rims, which, in turn, are coated with calcite (micrite).

2.2.1.2 Layer F (-785 to -540 cm; ca. 250 cm thick) (Figure 2.8)

The sediments generally consist of brown (7.5YR5/4), soft, moist (almost greasy to the touch), laminated and bedded silts. The bottom 60 cm is more finely laminated than the upper part, with individual laminae consisting of lighter and darker silty laminae, ~4 to 10 mm thick. The laminae are between 50 and 150 cm long and are inclined with decreasing dips toward the north, namely at 16°, 9°, and horizontal. Above -640 cm, the sediments become more thickly bedded, with thicknesses increasing to ~10–25 mm near the upper limit of the unit. Colors vary from strong brown (7.5YR5/6) to dark reddish brown (5YR3/3), reddish brown (5YR4/3), and reddish brown (5YR5/3).

Scattered throughout the sediments are traces of millimetre-sized pinkish grey (5YR7/2) aggregates of what appear to be opaline silica, according to FTIR analyses (Weiner, Goldberg, and Bar-Yosef 2002); whitish opalescent seed coats are also present.



Figure 2.8. Layer F in the Deep Sounding. **a.** Base of the Deep Sounding at the end of 1999 showing the east face (F27 and F28) and the very top of Layer G and lower part of Layer F. **b.** Northeast corner of the Deep Sounding, with grey and brown diagenetically altered sediments of Layer G at the base sharply overlain by a slightly redder Layer F (see also Figure 2.5b). Note the inclined and sharp erosional contact, and the dipping beds of the base of Layer F, whose bedding becomes more horizontal and more clearly distinct upward. The continuation of these upper deposits is shown in (c) and (d). **c.** East wall in the Deep Sounding during 1999, showing finely laminated silts with intercalated dark layers, both perforated by rodent burrows. The lighter colour in the upper part of the profile represents an unconformity with the overlying sediment (see also Figure 2.12a). The yellow line is 50 cm long. **d.** Close-up view of the lower part of (c), showing the finely laminated nature of the Layer F deposits. The metre scale is 30 cm long and the top of the stake below the plumb bob is at -715 cm; sample 99-310 (E28b; -735 cm) is on the excavated surface next to the metre stick.

Abbreviation	Mineral
A	apatite
CL	clay
CLT	clay transforming
CR	crandallite
L	leucophosphate
M	montmorillonite
MA	amorphous montgomeryite
MO	montgomeryite
OC	opaline clay
OT	opal transforming
Q	quartz
V	variscite
VT	vaterite

Table 2.2. Summary of mineralogy revealed by FTIR.

Recognisable hearths are relatively few compared with the overlying units and those in the Central Area. The hearths are typically expressed as slightly darker bands that are ~4 cm thick and ~25 cm across. Because of diagenesis, calcareous ashes are not preserved.

Post-depositional changes are both physical and chemical in nature. Physical modifications are represented by common individual and compound rodent burrows that are circular and elliptical, and are generally 8 to 10 cm in diameter. They are mostly filled with softer brown (5YR4/4) sediment. Complex burrowing is more prominent on the south side of the profile (F29) and is less so on the north side, where simpler, individual burrows are more common. The presence of both soft and hard phosphatic burrow fills points to repeated burrowing and phosphatisation events.

The upper part of Layer F is sharply eroded and mirrors a similar erosional surface and relief at the E/F contact within the Central Area (see below). The contact between E and F in the Deep Sounding is clearest on the north and east faces of the Deep Sounding, but is masked by burrowing on the south face and likely on west face, which is poorly exposed. On the north face, the central part of Layer F is crumbly and burrowed. The sediments are best exposed on the east wall of FG27– 28, where they consist of bedded silts and clay that dip to the north.

Below ~-700 to -750 cm, bedding is not distinct and generally resembles the broader, diffuse lighter and darker bands, as in the upper part of the profile at -600 to -650 cm. On the other hand, at depths between roughly -600 and -700 cm, individual strata are more clearly discernible (Figure 2.8b, c). In both areas, however, several of the more prominent layers can be traced laterally for > 1 m.

Dip directions and angles change both vertically and horizontally. Near the bottom of the section (~-785 cm), apparent dips are generally uniform to the north (i.e., toward the cave interior) at about 10°. This dip angle decreases markedly from -760 to -765 cm in F27, where the sediments are close to horizontal; in F28, on the other hand, the dips increase. Above about -635 cm, bedding becomes more diffuse in F27 and effaced by burrowing in F28.

Diagenesis is similar to that in Layer G, involving transformation of the clay/silt matrix. The FTIR results of Weiner, Goldberg, and Bar-Yosef (2002) show generally OT and CLT (e.g., samples 1812, 1813, 1815, 1819–1823) (see Table 2.2; and below).

Centimetre-sized burrowing in Layer F is evident and is particularly prominent in the south wall adjoining F29 (Figure 2.8b, c). Burrowing is also widespread in the upper part of Layer F, between -540 and -600 cm, blurring the contact with Layer E. Much of the South and West profiles show extensive burrowing, but less so on the north side, where the contact between E and F occurs at -540 cm.

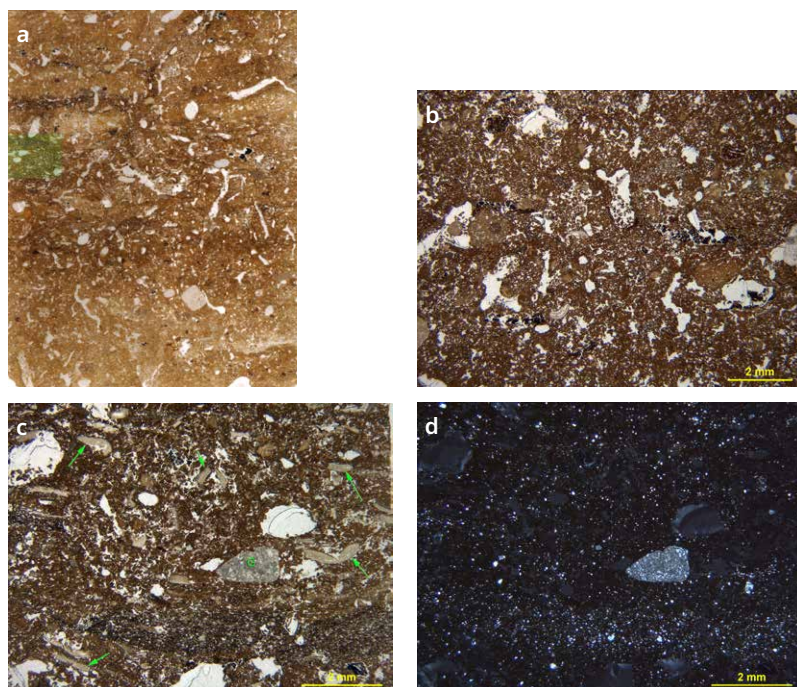


Figure 2.9. Micromorphology of Layer F sediments in the Deep Sounding, thin section of 99-310 (E28; -735 cm).

a. Thin section scan showing finely bedded grey silty clay, with dark laminae ~3 mm thick and pockets of washed silt; locally are grey silty domains. Location of (c and d) is shown by green rectangle. Note the porosity as channels and irregular vughs resulting from bioturbation.

b. Photomicrograph showing charcoal fragments dispersed within a heavily bioturbated silty matrix shown by channels, vughs, and small faecal pellets within the voids. PPL; scale is 2 mm.

c. Photomicrograph of area highlighted in (a). Note the layer of finely bedded silt underneath a rounded gastrolith grain (G) composed of chert and several siliceous seed coats (arrows). PPL; scale is 2 mm. **d.** Same as (c) but in XPL. The silty band is evident at the base of the photo; scale is 2 mm.

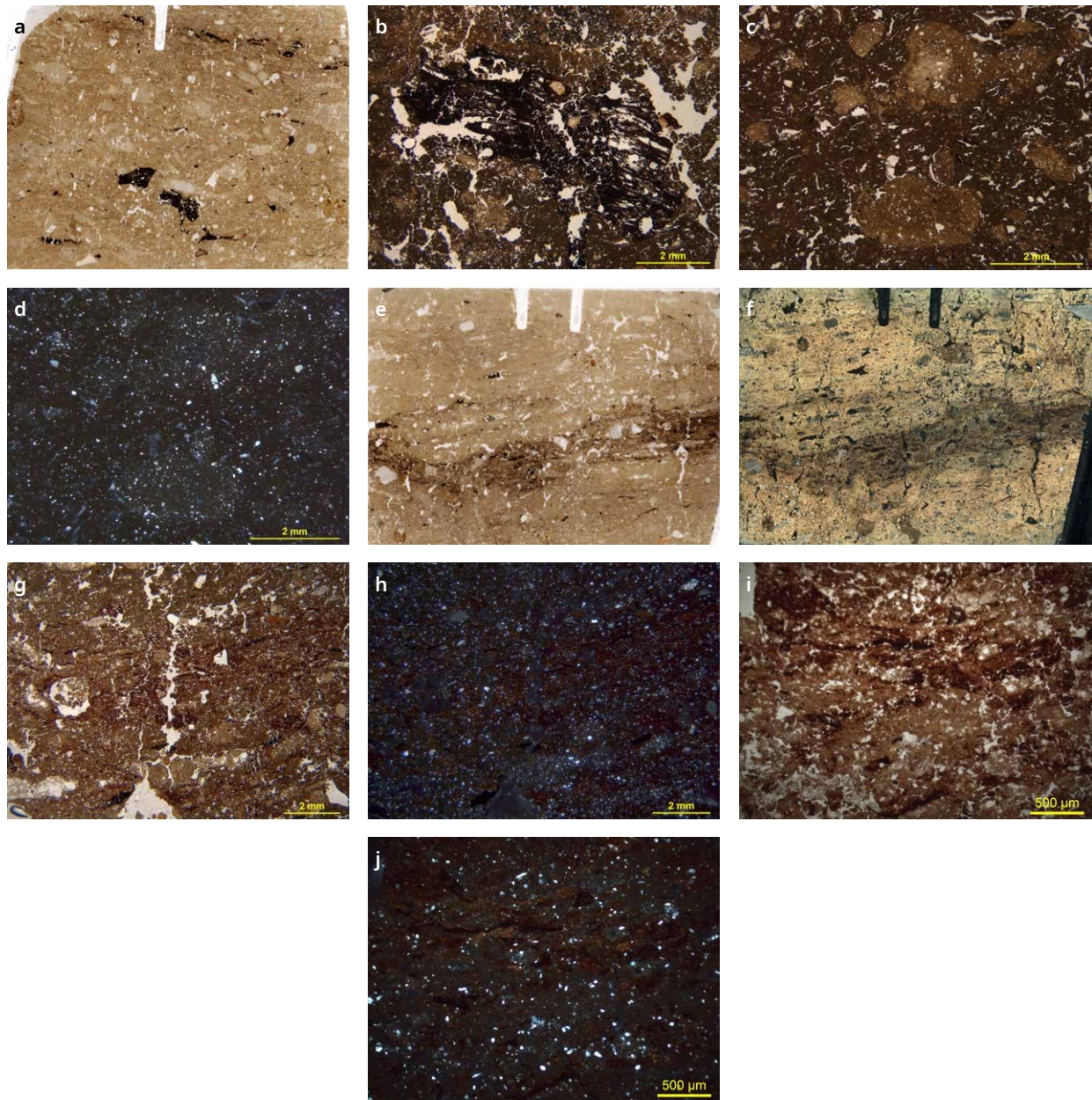


Figure 2.10. Micromorphology of Layer F sediments in the Deep Sounding, thin sections 98-252a, 98-252b (F28; -691 cm). **a.** Thin section scan of -252a showing bedded silts with organic matter fragments; at the top, the organic matter is finely laminated; there are numerous insect burrows. PPL. **b.** Photomicrograph of large organic fragment in the lower centre of (a). It has a slightly reddish colour, showing that it is more likely humified than burned. **c.** Pale yellow brown rounded silty aggregates that overall have the same general composition as the matrix but slightly richer in quartz silt. Their colour and composition suggest that they have been reworked and transported from older sediments such as those of Layer G, but this cannot be confirmed. PPL; scale is 2 mm. **d.** Same as (c) but in XPL. The slight enrichment of quartz silt within the aggregates is more apparent in this view. Scale is 2 mm. **e.** Scan of thin section of 252b (just below 252a) showing silts with organic matter fragments, some finely laminated; note the vughs and chambers produced by burrowing microfauna. **f.** Dark field scan of thin section highlighting the fine lamination and dark band in the centre. **g.** Photomicrograph of organic-rich band in the centre of -252b in (e) and (f); note the finely laminated nature of the organic material. PPL; scale is 2 mm. **h.** Same as (g) but in XPL, demonstrating the relative abundance of fine quartz silt (white dots). Scale is 2 mm. **i.** Photomicrograph of the right-hand part of the organic-rich band in the centre of -252b. Note the finely bedded brown (humified?) organic matter in a silty clay matrix. PPL. Scale is 500 μm . **j.** Same as (i) but in XPL. The quartz silt is more readily apparent in this view. Scale is 500 μm .

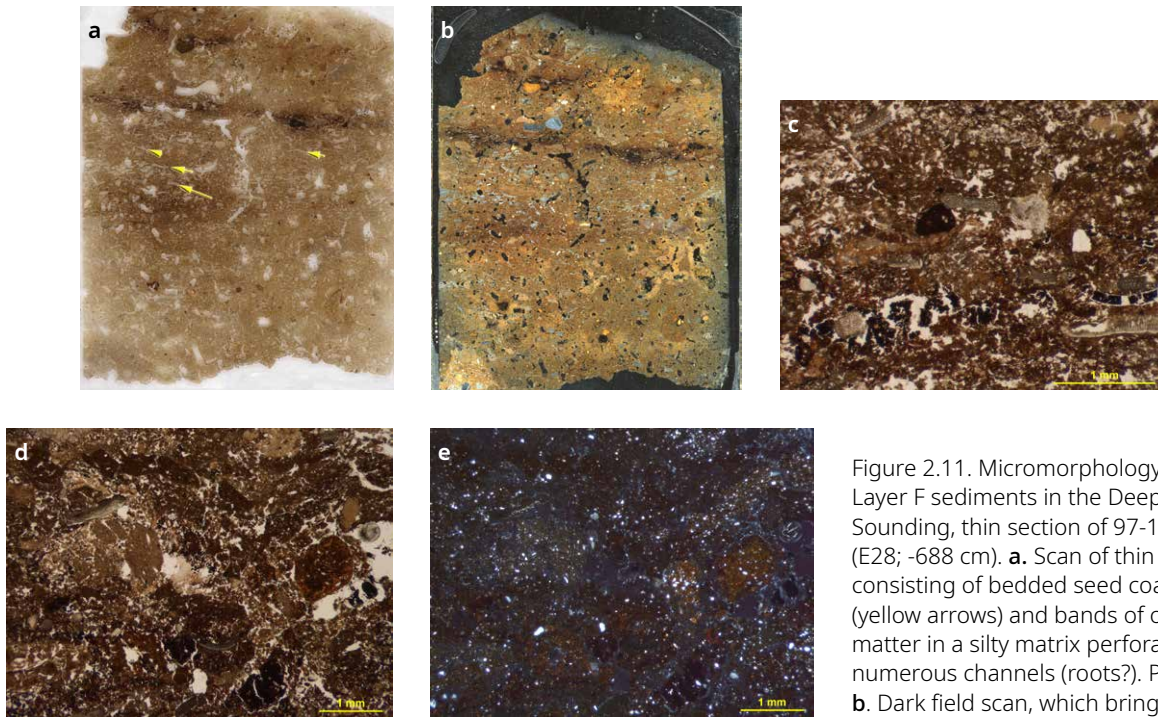


Figure 2.11. Micromorphology of Layer F sediments in the Deep Sounding, thin section of 97-143 (E28; -688 cm). **a.** Scan of thin section, consisting of bedded seed coats (yellow arrows) and bands of organic matter in a silty matrix perforated by numerous channels (roots?). PPL. **b.** Dark field scan, which brings out the lateral continuity of the bedding, both in the darker, organic-rich

layer but also the whitish grey seed coatings beneath it. **c.** Photomicrograph of crudely bedded seed coats, organic matter, and diagenetically altered silty clay. PPL; scale is 1 mm. **d.** Rounded silty clay aggregates of varying composition, including organic-rich ones. Bedding is crude but still visible, particularly in the uppermost part of the photo. PPL; scale is 1 mm. **e.** Same as (d) but in XPL; overall isotropy is due to diagenesis, likely OT and CLT (of Weiner et al. 2002). XPL; scale is 1 mm.

2.2.1.2.1 Micromorphology

Layer F in thin section is comparable to Layer G, consisting of isotropic (opaline) silty clay transforming (FTIR sample 1805; E28; -745 cm) with inclusions of seed coats, gastroliths, and generally rounded diagenetically altered (isotropic) silt-rich clasts (thin section of 98-252; F28a; -691 cm); layers of laminated silt can be observed locally (Figures 2.9 and 2.10). Charcoal and non-identifiable organic matter occur as distinct grains or are concentrated in diffuse bands. Thus, both silt and organic matter show distinct bedding.

In spite of clear bedding at all scales, bioturbation at the <1 mm scale is abundant, with vugs and channel microstructures that include micro-faunal excrements in some of the voids.

2.2.1.3 Layer E

Layer E constitutes the uppermost part of the Deep Sounding sequence, although Kebaran deposits (Layer C) fill in an elongated trough that parallels the former dripline (see below). It is best exposed below -450 cm and is typically massive, light brown (7.5YR6/4), granular, generally homogeneous calcareous silts that are locally cemented by calcite and apatite. Opaline silica components include millimetre-sized pinkish grey (5YR7/2) aggregates (confirmed by FTIR) and white seed coats, as in Layers G and F. Moreover, it contains millimetre-sized aggregates of ash, clay, and bone.

A marked unconformity with a basin-like appearance can be seen particularly in the east and north profiles of the Deep Sounding. Below this contact, the sediments are lithologically similar to those in Layers G and F, being diagenetically altered silty clays (FTIR: mostly CLT, OT, and OC) but lack the laminations visible in Layer F (Figures 2.12, 2.13).



Figure 2.12. Layers E and F in the Deep Sounding. **a.** Upper part of Layer E in the east face in 1999; blue tags are FTIR samples, of which 1602 revealed CI, Q, and A. This contrasts with sediments below this unconformable contact, which are comprised of CLT, and OT, and VT, representing a greater degree of diagenesis. The colour change at the top of Layer E is due to the drier nature of the sediment. **b.** East Profile at end of 2000 season, showing somewhat more clearly the contrast between E and F. Note the contrast in bedding between Layer F at the base and overlying Layer E. **c.** North face of the Deep Sounding, showing Layers E and F and the indistinct contact between them on the left (west) side; generally, the contact between E and F is clear. **d.** Calcareous sediments of Layer E

above the Deep Sounding in F25 (sample 00-508 is at -280 cm). Many of these are finely laminated ashes with terra rossa inclusions. **e.** View of area in H23-24 between the Central Area and Deep Sounding as shown in (d) but taken from the Central Area looking toward the southwest in the direction of the Deep Sounding. As in (d), the sediments of Layer E here are calcareous and rich in ashes; their preservation is largely a function of their proximity to the bedrock wall. The sample in the lower right is 00-517.

Several distinct circular and elliptical burrows are visible, some cemented and ash filled. Nevertheless, the massive, homogeneous nature of the deposits attests to repeated burrowing by rodents, which have obliterated most traces of the original bedding. Only at the very top of the edge of the Deep Sounding (~-450 cm and above) are there any vestiges of originally complete hearths and ashes, which typically occur as slightly darker bands ~4 cm thick and ~25 cm across. Original calcareous ashes are not preserved, only ones diagenetically altered to silica or phosphate.

At the northern part of the Deep Sounding, the upper part of Layer E is exposed between -280 and -450 cm (Figures 2.14, 2.15). Overall, the sediments represent significant anthropogenic inputs and lateral changes occur. Along the E face of G27 and G28, for example, the sediments consist of generally yellowish red (5YR4/6) silty clay with charcoal

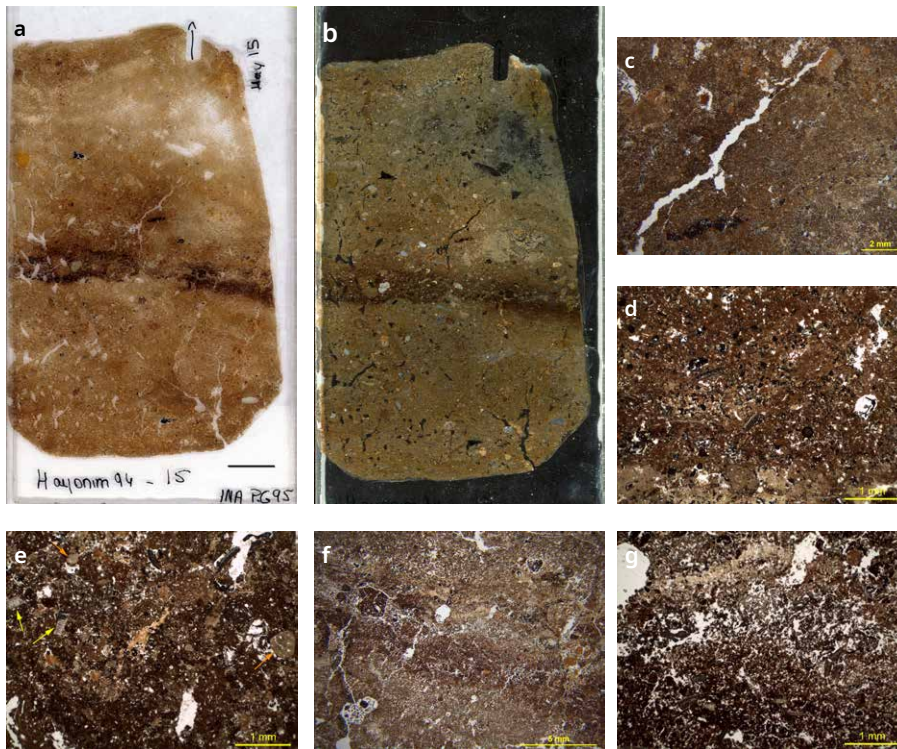


Figure 2.13. Micromorphology of Layer E sediments from the Deep Sounding below -500 cm, thin section of 94-15 (F27; -545 cm). **a.** Scan of thin section. In the field, this sediment appeared as organic clayey silt with flecks of charcoal and pieces of decayed limestone. PPL; scale is 1 cm. **b.** Dark field scan of 94-15. The bright, somewhat circular area above the band is calcite; scale is 1 cm. **c.** Photomicrograph of the upper part of the sample, showing massive phosphatic silty clay with seed coats in the middle; the dark elliptical area is organic matter stained with iron/manganese. These silty sediments are largely derived from soils and

windblown dust that have been presumably washed in place. Considerable bioturbation has blurred many depositional signatures, but some layers are preserved, such as this one, which appears to be remains of a hearth. PPL; scale is 2 mm. **d.** Crudely bedded silts, silty clay, and seed coats from the upper part of the thin section. Note the vughy porosity. PPL; scale is 1 mm. **e.** Photomicrograph of uppermost part of thin section showing chaotic mixture of compacted material of varying compositions, including seed coats (yellow arrows), rounded diagenetically altered grains of silty clay (orange arrows) that were possibly originally terra rossa. PPL; scale is 1 mm. **f.** Photomicrograph of dark area in centre of thin section. The slightly rubified nature of the centre layer on the right side occurring with charcoal and organic matter (see [a] and [b]) suggest that this may be a hearth remnant; however, reddening can be associated with oxidation of organic matter. PPL; scale is 5 mm. **g.** Detail of dark layer in the centre. The base of the photo is organic rich, whereas the upper, lighter part is rich in silica and possibly represents the insoluble fraction of ashes. PPL; scale is 1 mm.

and some bone, interspersed with cm-thick bands of pinkish grey (5YR7/2) ash. These ash bands are laterally discontinuous to the south, where they are burrowed. To the north—in the direction of the bedrock boss in F25—both the ashes and the intervening reddish clays are cemented with calcite to the extent that, locally, they are completely indurated (so-called ‘cave breccia’). In G27, these brecciated sediments reach maximum elevations of -150 cm, and are rich in flint, bone, ashes (both as ash-rich bands and dispersed ash), as well as millimetre-sized clasts (typically rounded) of terra rossa; these possibly originate as clay aggregates clinging to roots of grassy vegetation that was later burned in the fire. The ‘breccia’ also grades laterally into flowstone toward the cave wall.

To the south, the equivalent sediments of the upper part of Layer E embed metre-sized boulders of roof fall associated with roof collapse at the entrance of the cave. In addition, in EF30–31, ashes and clay are also cemented with calcite, although here, no flowstone is evident. Thus, below the cave brow, cementation appears to be tied to evaporation of carbonate-charged waters originating from the former overhang that was about 3 to 4 m further to the south. In this location, cementation is associated with evaporation of carbonate waters originating from surface runoff and water washing over the cave brow.

Figure 2.14. Micromorphology of upper Layer E sediments from the Deep Sounding above -500 cm. **a.** Scan of thin section of 99-357 (D26; -434 cm), a well-consolidated silty deposit with charcoal and calcium carbonate flecks throughout; unaltered terra rossa balls are relatively common. Note the presence of small burrows and channel microstructure. PPL.

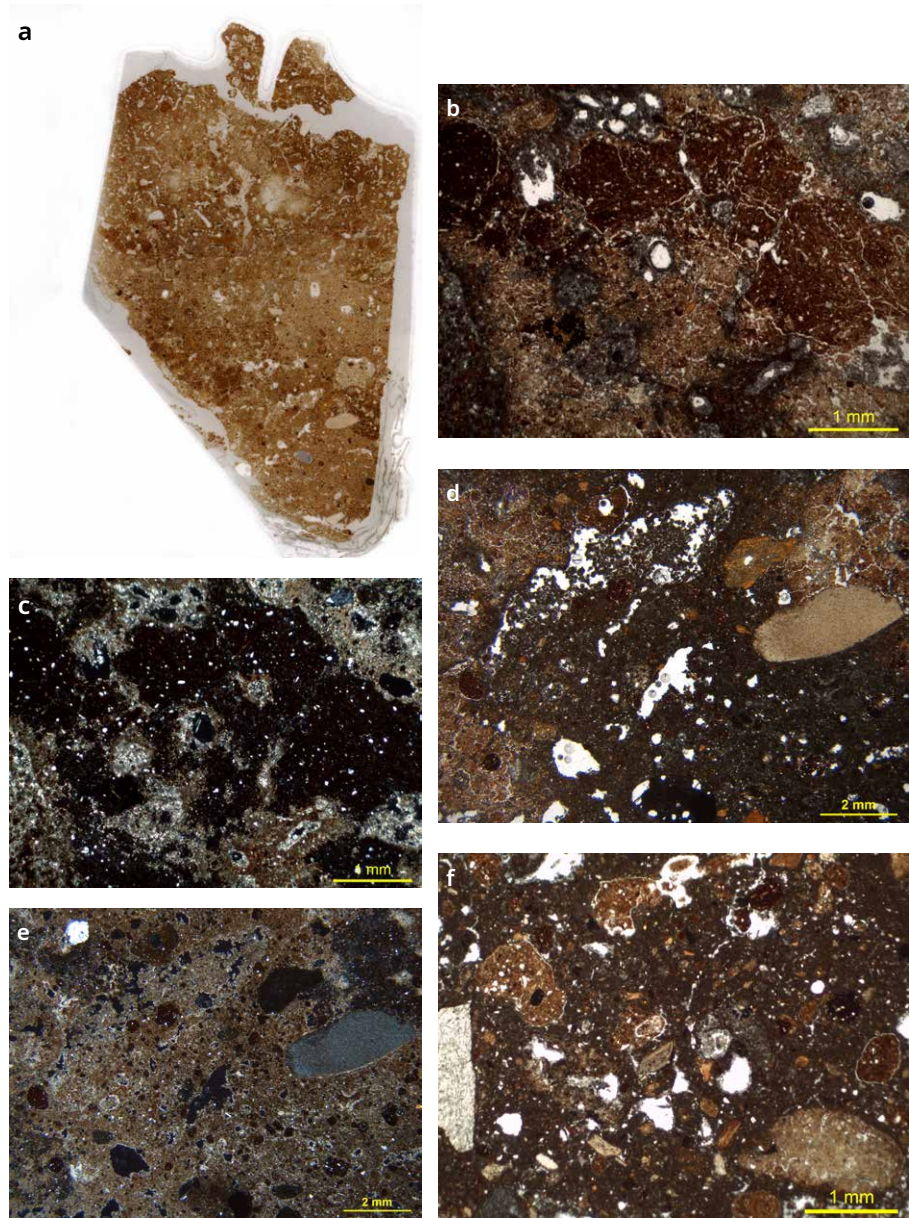
b. Photomicrograph of 99-357, displaying fractured clast of terra rossa within a cemented, silty bioturbated matrix. PPL; scale is 1 mm.

c. Same as (b) but in XPL. The bright areas are micrite and with micritic hypocoatings visible around the voids. XPL; scale is 1 mm.

d. Photomicrograph of bioturbated lower righthand part of thin section in (a), with rounded aggregate, bone, well-rounded gastroliths, vughs, and channel porosity. PPL; scale is 2 mm.

e. Same as (d) but in XPL, showing secondary calcite cement. XPL; scale is 2 mm.

f. Compact, micrite cemented mixture of rounded terra rossa clasts, bone fragments (note the large angular fragment at left), and quartz silt. PPL; scale is 1 mm.



2.2.1.3.1 Micromorphology

The micromorphology of the lower part of Layer E largely mirrors that of Layer F, although bedding is less distinct. The lower sediments consist of weakly bedded silts and silty clays with abundant seed coats and grey siliceous silty clay aggregates (Figure 2.14). Bone is absent but charcoal was observed as isolated grains, which are locally bedded or concentrated within bands as in sample 94-15 (F27; -545 cm). Hearths in the lower part of Layer E are indistinct at best, although organic-rich bands occur associated with apparent rubefication, organic matter, isolated charcoal, and what are possibly diagenetically modified ashes as in 94-15 (Figure 2.13; see chapter 3). Bioturbation is visible in the thin section by numerous passage features with fine sandy granular infillings, along with frequent vughs and channels.

The sediments in the upper part of Layer E above the unconformity described above are quite different and overall more calcareous, although in some cases, the calcite is partially dissolved and replaced by apatite (Figure 2.14). They tend to be rich in rounded grains of terra rossa and sand-sized bone fragments, commonly cemented with micritic calcite that also lines voids.

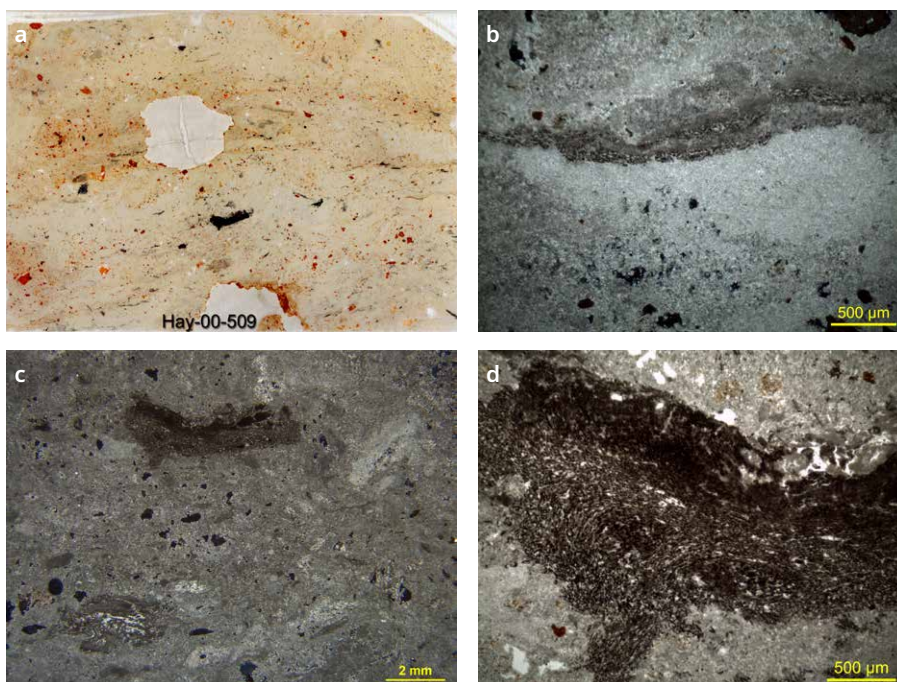


Figure 2.15. Micromorphology of Layer E sediments near the Deep Sounding; upper calcareous part in F25. **a.** Thin section scan of bedded ashes with burned terra rossa inclusions in sample 00-509 from upper calcareous part of Layer E in F25c (-315 cm); this area is situated between the Deep Sounding and the Central Area; the black bits are pieces of charcoal. Note the laminated nature of the ashes. PPL. **b.** Detail of bedded ashes from centre of the thin section, suggestive of ash accumulation in more than one depositional/fire event. XPL; scale is 500 µm. **c.** Photomicrograph of bedded ashes with partially ashed woody fragment at the top. XPL; scale is 2 mm. **d.** Detail of charred fragment in (c). PPL; scale is 2 mm.

The uppermost part of Layer E is exposed outside of the confines of the Deep Sounding itself, but nearby, in D and F25–26 (Figure 2.15). Being closer to the bedrock, the sediments are, for the most, part calcareous and generally ‘fresh’, with only localised transformation to apatite. This is particularly the case for deposits below -350 cm. Many of the thin sections are comprised of bedded calcareous ashes that contain charcoal as well as partially combusted organic matter (Figure 2.15). Most intriguing is the presence of sand-sized rounded and angular clasts of bright red (rubified) clay, whose source is not clear. They are possibly derived from soil attached to roots of vegetation (bushes and possible grasses) used in combustion (Albert et al. 2003; Meignen et al. 2009).

2.2.1.4 Layer C

Layer C contains Kebaran artefacts and occurs at the top of the profile (G27), resting on Layer E with a sharp contact (Figure 2.16). Moreover, unlike the non-calcareous underlying sediments of E and F, it is comprised of light brown (10YR6/4), loose, crumbly, calcareous silty clay that is locally indurated. Its upper part contains decimetre-sized blocks of roof fall, which decrease in abundance with stratigraphic depth; some of these blocks exhibit ~1 mm-thick apatitic (dahllite) weathering crusts. The unit displays a variable thickness since it fills in relief produced by the erosion of the underlying Mousterian sediments. The erosional surface is irregular but locally takes on a trough shape elongated along the axis of lines 27 and 28 (Figure 2.2), which corresponds to the position of the present-day dripline of the cave. Moreover, mapped elevations of the contacts between the Mousterian and Kebaran layers suggest that this depression was an open channel that possibly drained toward the cave exterior in the area of Square B30. Additionally, it is apparent that the presence of this channel-like feature relates to its location directly under the present drip line (Figure 2.2), where strong winter rains could easily produce chutes of water that would cascade down along the flat brow of the cave. Both in the field and in thin section, the sediments closely resemble those of the Mousterian, indicating that they represent local reworking of these older deposits. In addition, during excavation, we revealed a localised pocket of sediment adjacent to Layer C that contained a mixture of Middle Palaeolithic and Kebaran artefacts; we have designated the pocket Layer C/E (Figure 2.16).

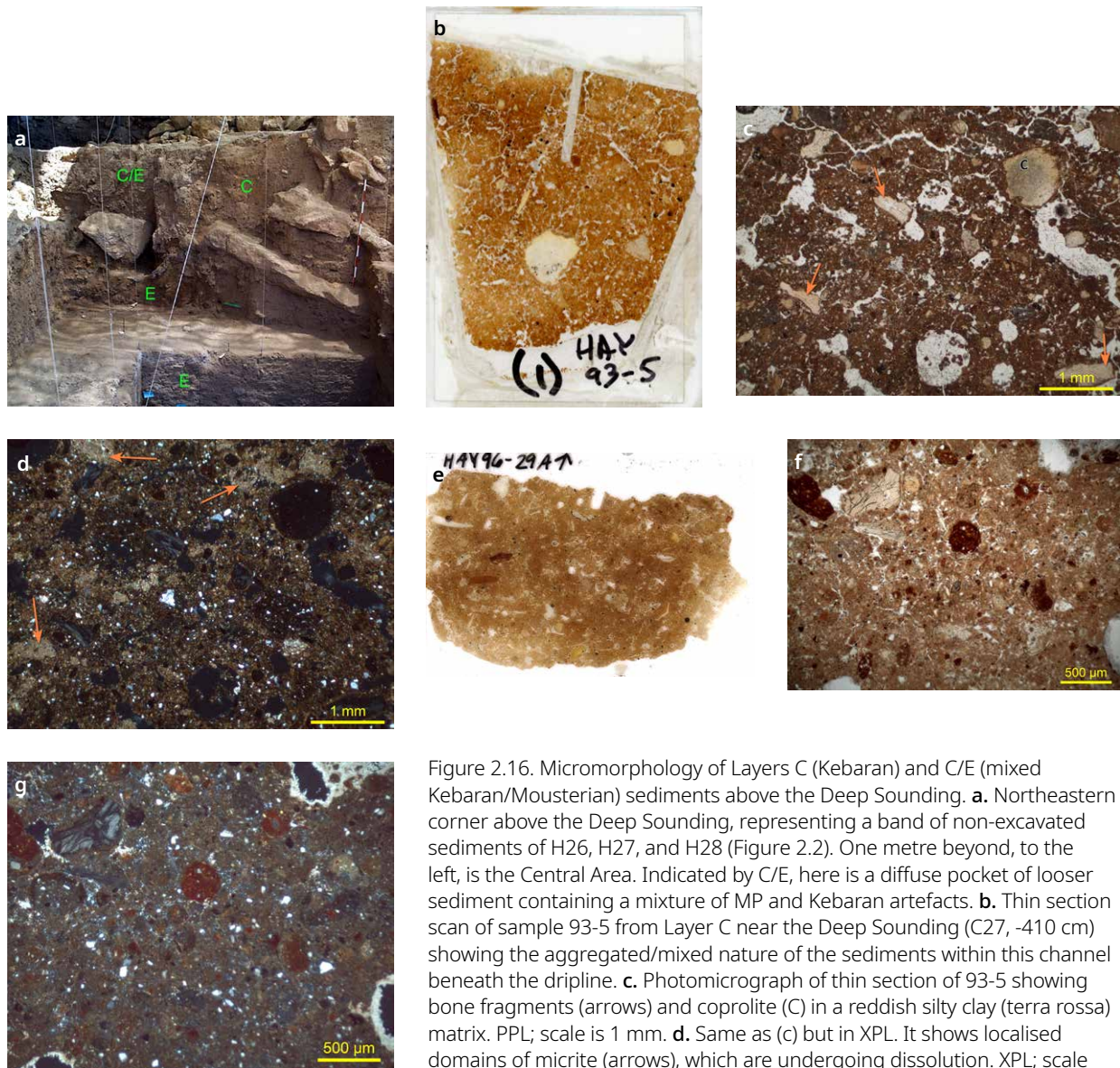


Figure 2.16. Micromorphology of Layers C (Kebaran) and C/E (mixed Kebaran/Mousterian) sediments above the Deep Sounding. **a.** Northeastern corner above the Deep Sounding, representing a band of non-excavated sediments of H26, H27, and H28 (Figure 2.2). One metre beyond, to the left, is the Central Area. Indicated by C/E, here is a diffuse pocket of looser sediment containing a mixture of MP and Kebaran artefacts. **b.** Thin section scan of sample 93-5 from Layer C near the Deep Sounding (C27, -410 cm) showing the aggregated/mixed nature of the sediments within this channel beneath the dripline. **c.** Photomicrograph of thin section of 93-5 showing bone fragments (arrows) and coprolite (C) in a reddish silty clay (terra rossa) matrix. PPL; scale is 1 mm. **d.** Same as (c) but in XPL. It shows localised domains of micrite (arrows), which are undergoing dissolution. XPL; scale is 1 mm. **e.** Thin section scan of 96-29A from Layer C/E (F31, -415 cm), consisting essentially of loose aggregates of terra rossa, bone, and pale brown silty clay. PPL. **f.** Photomicrograph of thin section of 96-29A showing fragments of bone, fresh rounded terra rossa grains, and yellow-brown isotropic apatitic silty clay. PPL; scale is 500 μm . **g.** Same as (f) but in XPL. Note the overall apatitic and isotropic nature of the matrix finer in contrast to the birefringent red terra rossa grains. The bright circular areas are calcite void coatings that are much later than the phosphatisation. XPL; scale is 500 μm .

2.2.1.5 Discussion of the Deep Sounding

The deposits in the Deep Sounding represent a significant mass of material that accumulated at the entrance of the cave, where more than 4 m were excavated in its deepest part (EF27–28) (Figures 2.2, 2.17). As a package and viewed in their entirety, the deposits of Layers G and F and the lower half of Layer E are texturally similar: phosphatised/diagenetically altered silty clays that contain various proportions of opaline seed coats, gastroliths, and bands and scatters of organic matter/charcoal; combustion features are relatively rare and, when present, appear as thin ~1 cm-thick bands).

The original detrital grains ultimately appear to be derived from the silty clay terra rossa soils above and around the site, as well as aeolian additions of silt and clay. These

sediments are thinly bedded to thickly laminated in much of Layer F on the east face of the Deep Sounding. Toward the west, however, the sediments are overall more massive. All of these sediments were deposited in a low-energy depositional environment, having been washed into a general basin-like venue, possibly in a bedrock swallow hole that mirrored the vault-like roof of the bedrock at the entrance. Possibly associated with this aqueous deposition is the siliceous diagenesis of this unit (see below). The formation of leucophosphite at least seems to be associated with the breakdown of siliceous aggregates derived from fires (oral communication of P. Karkanas to S. Weiner).

In addition, this inwashing was accompanied by inclusions of biological materials:

- Bird gastroliths possibly dropping from pigeons roosting at the cave entrance (note that 'Hayonim' in Hebrew means 'doves/pigeons', as at Tabun Cave (Goldberg 1973; Goldberg 1978).
- Woody materials (much of the wood in the entrance is humified and not burned) that were derived from decayed organic matter in the area were blown in or washed into the entrance area from the surrounding slopes.
- Siliceous seed coats falling into this depressed area, emanating from plants growing at the opening to the cave. A similar situation is present at Tabun Cave, Mt Carmel, and Kebara Cave, where tentative identification of the plant (*Podonosma orientalis* Friedman) was made by Prof. Ehud Weiss, Bar-Ilan University (personal communication, 2006).
- Archaeological inputs—artefacts, charcoal, and combustion features—can be seen in the topmost part of Layer G, and these must have accumulated at intermittent times when the sediments dried out.

However, upward in the Deep Sounding profile in Layer E, bedding becomes more muted and the sediments increasingly massive and bioturbated. This change suggests that the basin-like configuration had been filled in by Layer E time, thus sedimentation took the form of more highly concentrated flows and not sedimentation into a quiet water body, as occurred in Layer F time. This fine silty sedimentation ended during Layer C, which is comprised of unaltered terra rossa clasts, bone, and some coprolites. Layer C appears to fill in an elongated channel situated under the former dripline. At the same time, sediments adjacent to this channel of Layer C were partially reworked, perhaps by splash from dripping/cascading water emanating from the brow or trampling, resulting in the occurrence of both MP and Kebaran lithics within the same deposits (Layer 'C/E' in Figure 2.16).

Diagenetic alteration is a characteristic of the Deep Sounding sediments within the deeper 2 × 2 m trench. The sediments are predominantly non-calcareous. However, the uppermost sediments in F and G26 are calcareous and particularly ash rich; those in Layer C, just above and outside the Deep Sounding, are richer in unaltered terra rossa. Most of the sediments in Layers G, E, and Lower E exhibit neoformation and alteration of minerals including 'clay transforming' and 'opal transforming', dahllite, leucophosphite, tinsleyite, and crandallite (Weiner, Goldberg, and Bar-Yosef 2002). As shown in Figure 2.6g and h, however, micromorphological examination demonstrates that the sediments showed several cycles of decalcification, phosphatisation, recalcification, and finally, modern decalcification.

The geochemical and environmental conditions associated with this diagenesis still need to be clarified, but an abundance of water is likely, especially in light of the prominent bedding in Layer F. The profusion of gastroliths in Layer F, as elsewhere, indirectly indicates the addition of organic matter from birds (pigeons?).

The second type of diagenesis involves the phosphatic transformations described previously. The fact that these minerals are precipitated into an already transformed clay matrix suggests that their presence might be tied to phosphatic reactions in Layer E. In other words, it is possible that these phosphates formed during Layer E time and migrated down into the underlying Layer F strata. It should be noted that phosphatic transformations are probably also responsible for the dissolution of bones that might have been present in the Layer F sediments.

Figure 2.17. East side of the Deep Sounding, as exposed at the end of the 2000 excavation season, illustrating most of the stratigraphic units (although Layer G was particularly difficult to capture). Note the distinct contact between E and F. The lighter colour of the top of Layer E is due to its drier nature.



Physical diagenesis is revealed by inclined strata in Layers G and F, along with truncation of Layers G and F. The former can likely be ascribed to subsurface slumping associated with karstic activity, similar to that observed at Tabun (Jelinek et al. 1973) and at Kebara (Goldberg et al. 2007).

Layer E accumulated above the erosion surface of the predominantly geogenic Layer F. Layer E is more anthropogenic in character, as shown by the presence of several hearths and abundance of ashes, charcoal, and bone in its upper part (-360 to -370 cm), at the balk separating the Deep Sounding and Central Area (along the 25 squares; Figure 2.2). In its upper part in the Deep Sounding, Layer E is also more extensively burrowed than Layer F and noticeably less bedded, both possibly reflecting drier conditions and infilling of the basin, as stated above. In any case, initial occupation during the accumulation of Layer E took place on an irregular surface produced by the erosion of Layer F. A similar discontinuity is visible in the Central Area as well.

The areal exposure of Layer C is rather limited so it is difficult to state much about its origin. It is 'fresher' than the underlying sediments in the Deep Sounding, being a loose mixture of bone, silt, and clay, and is locally cemented with calcite, but other than that, there are essentially no mineral transformations.

2.2.2 Central Area (CA)

2.2.2.1 Field observations

The bulk of the excavation and relevant stratigraphic information comes from the Central Area, where Layers F and E are exposed over an area of about 30 m² (Figure 2.2). The two major stratigraphic units, E and F, were differentiated on the basis of their overall character/lithological differences and are comparable to the lithological units recognised in the Deep Sounding as Layers E and F, respectively. Nevertheless, there are lateral and vertical variations and facies changes within Layer E so that the stratigraphy in the south face (24/25 line) of the Central Area differs somewhat from that of the north face (17/18 and 18/19 lines); similarly, sediments exposed in the east face (K/L line) are distinctive. In this light, it is easiest to describe both layers in the different sectors of the cave and then provide a global summary at the end.

2.2.2.1.1 South Profile

The South Profile reveals both Layers E and F, although the latter was not completely exposed at the end of the excavations when it reached -585 cm. Diagenesis has extensively modified the bulk of the sediments in the South Profile, particularly in the centre, which makes it difficult to observe the nature of some of the original deposits (see also chapter 5). Nevertheless, geogenic deposition predominates, in contrast to Layer E, where anthropogenic inputs (hearths) are more common.

On the South Profile, Layer F is exposed over a thickness of 60 cm from the floor (-585 cm up to -525 cm). For the most part, it is comprised of dark brown silty clay that has been extensively altered to a variety of minerals, such as leucophosphite, variscite, montgomeryite, and the component of wood ash called siliceous aggregates. Weiner et al. (2002) refer to this assemblage as the 'LVMS mineral suite' (Weiner, Goldberg, and Bar-Yosef 2002) (Figures 2.18, 2.19; Table 2.3). The matrix is silica rich, with opaline nodules—opal, opal transforming, and siliceous aggregates; veins of leucophosphite occur near the top of the layer (Weiner, Goldberg, and Bar-Yosef 2002), which is truncated and overlain by Layer E as shown by the generally sharp contact (Figure 2.19). Scattered vestiges of hearths are visible in Layer F, especially in the eastern part, and a number of 4–5 cm-thick, dark reddish-brown (5YR3/2) charcoal-rich bands and burned features occur.

The basal sediments at the floor boundary are compact and show diffuse bedding, reminiscent of the upper part of Layer F in the Deep Sounding. The upper 10–15 cm are more homogenous and consist of compact to crumbly, massive, dark reddish-brown (5YR3/4), gritty clay silt. In the central part (i.e., J24), this upper part exhibits numerous, hard, globular leucophosphite veins ~5 mm across. The contact with overlying Layer E is sharp in the eastern part and more gradual in the western part.

In comparison to Layer E, hearths were relatively uncommon. They do occur, particularly in the upper part of Layer F (Figure 2.19), but many lack the remains of an upper ashy part, as can be seen in those from Layer E.

Layer E is exposed from ~280/300 cm down to the contact with Layer F (~510 to -525 cm). Visible in this profile are clay (diagenetically altered to varying degrees), ashes and burned features, and several rodent burrows; the burrowing is responsible for homogenising the original sediment and any primary depositional characteristics. A 15–20 cm-thick band of interbedded hearths (ashes and lighter and dark brown layers) occurs at the base, and it is particularly well preserved in the western part of the South Profile (Figures 2.18, 2.19). The remainder of the profile is comprised of ashy organic-rich bands—either representing in situ burning events or trampled or dismantled hearths—alternating with layers of red clay that vary in thickness from ~5 to 30 cm. A particularly noticeable bed of clay occurs between -370 and -430 cm (Figure 2.19a).

Nevertheless, detailed observation of the original nature of the deposits along the South Profile is hindered by diagenesis, which is expressed differently in different areas (Weiner, Goldberg, and Bar-Yosef 2002).

Along the eastern and western borders, most calcitic ashes have been transformed to apatite (dahllite).

In the middle of the South Profile a 'V'-shaped area consists of lighter-coloured sediment, which is an expression of the LVS mineral assemblage. Consequently, both anthropogenic ashy sediments and the geogenic reddish clay units have lost their initial lithological characteristics. Thus, originally light reddish-brown (5YR6/3) clay at the borders appears as pale brown (10Y6/3), gritty silt within the diagenetic zone (Figures 2.18, 2.19).

On the other hand, as noted for Layer F, along the borders of the zone, diagenesis is much less extensive and ranges from calcification of the ashy lenses near the bedrock walls to apatite (dahllite) transformation of these same sediments in a direction toward the centre of the cave (Figure 2.19f). This zone of alteration widens upward, suggesting increased diagenesis with time, or that the V-shape represents an alteration 'halo' produced during a major period of transformation. Bones are understandably absent

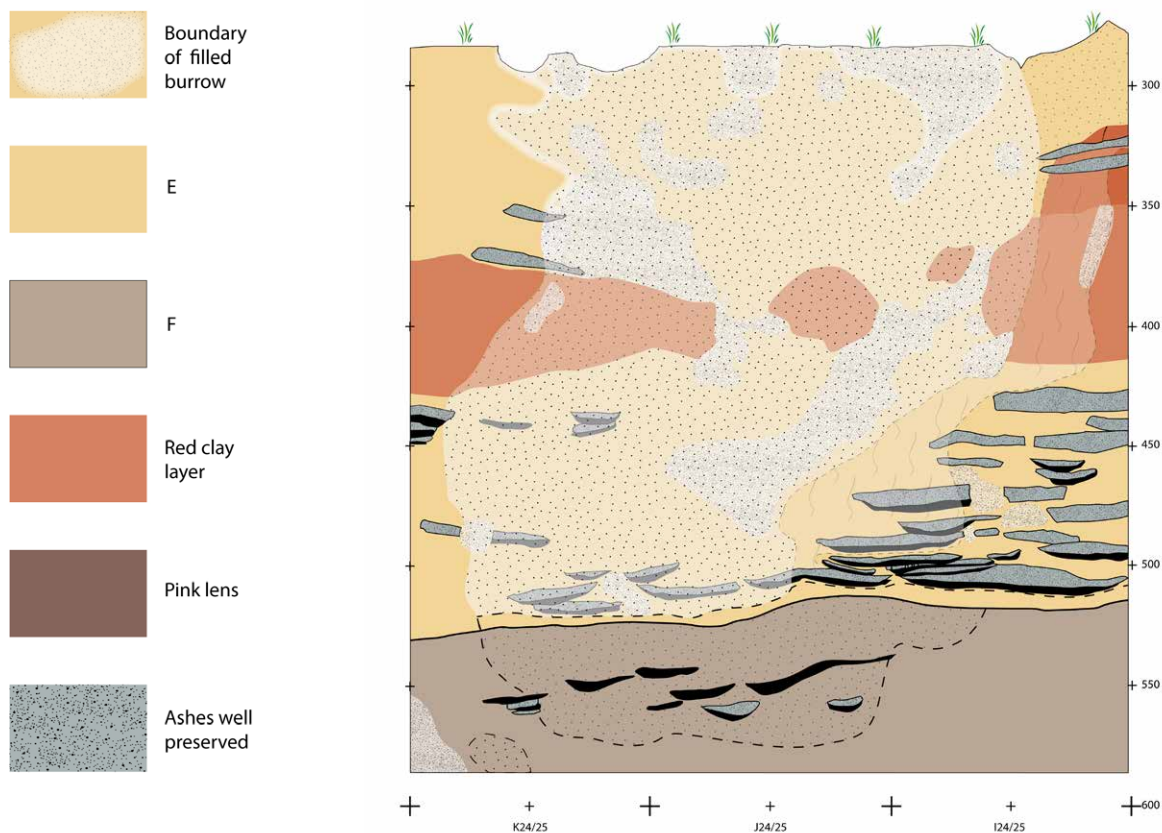


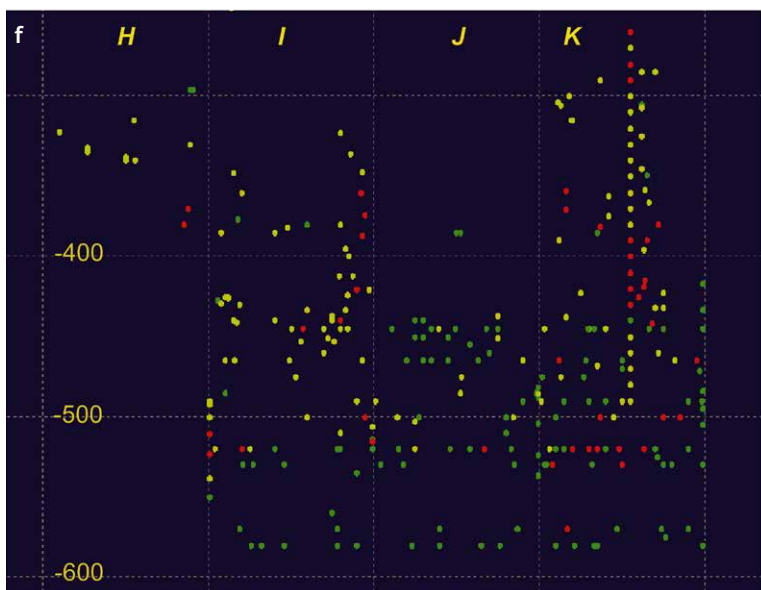
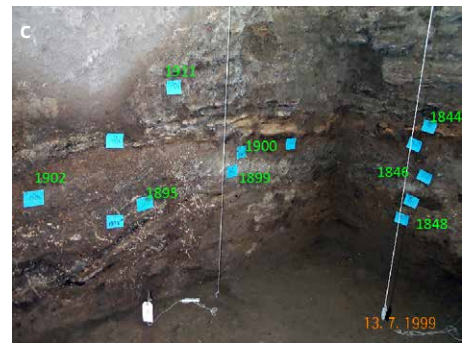
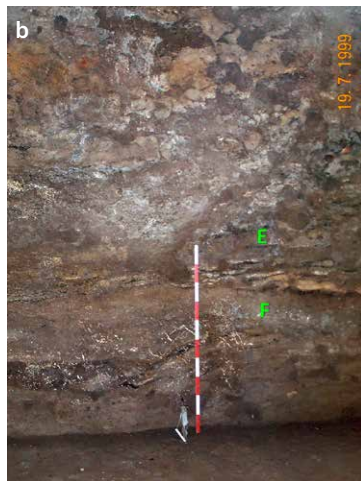
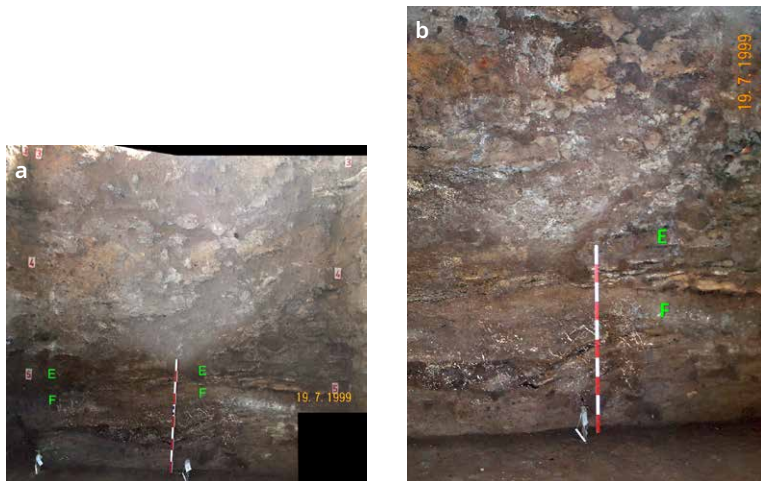
Figure 2.18. Profile drawing of South Profile in the Central Area. Although hearths can be seen in Layer F in the lower third of the drawing, they are markedly more abundant in Layer E. Note the discontinuous band of reddish clay and the extensive diagenesis in the middle part of the profile that masks the original nature of the deposits (cf. Figure 2.19).

in the ‘trough’ but, interestingly, back plots of lithic artefacts against the South Profile by S. Kuhn (Stiner 2005; see also chapter 4) show a horizontal distribution and not one that mirrors the V-shape of the diagenetic zone. This lithic distribution confirms that the ‘trough’ shape is not a result of erosion but one of overprinting by diagenesis.

Finally, a conspicuous aspect of the sediments in the South Profile is the presence of burrowing, which is characterised by either single burrows (~5–6 cm across) or areas of repeated burrowing with irregular shapes (Figures 2.18, 2.19 a, d, e). The burrows are filled generally with soft, powdery, dark reddish-brown (5YR3/3) clayey silt and were readily identified during excavation. The upper part of the profile appears to be more burrowed than the lowest part.

Table 2.3. FTIR analyses of sediment samples from South Profile, illustrated in Figure 2.19c.

Sample no.	Layer	Mineral 1	Mineral 2	Mineral 3
1844	E	A	CL	C
1845	E/F	CL	A	C
1846	F	CL	A	C
1847	F	A	C	CL
1848	F	CLT	OT	--
1895	F	L	--	--
1898	F	L	--	--
1899	F	L	CLT	--
1900	F	CLT	--	--
1902	F	OT	M	--
1906	F	M	--	--
1911	E	A	CL	--



ar
 at
 c
 cl
 clt
 i
 m
 ma
 na
 o
 oc
 ot
 lb
 vt

Figure 2.19. South Profile of the Central Area.

a. Composite photograph of the profile exposed along the line IJK24/25 in 1999. Visible are Layers E and F, and a lighter coloured diagenetic 'halo' in the centre, as emphasised in the photo by using a flash. The mineralogy in the 'halo' is composed of LVMS assemblage, whereas to the left (east) and right (west), calcite and dahllite are present (Weiner, Goldberg, and Bar-Yosef 2002). Note the presence of a few hearths within Layer F at the base of the photo. **b.** Close-up of the middle of the South Profile in 1999, photographed without a flash. Note the hearths at the base of Layer E and the more scattered ones in Layer F. In the latter, the semi-vertical veins are composed of leucophosphate, in contrast to the nodular white dots, which are comprised of opal transforming (Weiner, Goldberg, and Bar-Yosef 2002); see also (c) below. **c.** FTIR samples from Layers E and F in the South and West Profiles (see Table 2.3). Samples 1844–1848 in the West Profile are predominantly clay, apatite, and calcite, as is sample 1911 and occur in both Layers E and F. Most of the other samples, which are in the strongly diagenetic zone contain L, CLT, OT, and M. Thus, the mineralogy is dictated by the location of the sediment in the cave and not by layer. **d.** Southeast corner of the Central Area in 1999. Note the presence of the band of reddish clay (-500 cm); this layer appears to pinch out to the right (west), but continues along the East Profile to K21. **e.** Southwest corner of Central Area in 2000 at junction between South and West profiles. The mineralogy of the west face is calcite and dahllite (Weiner, Goldberg, and Bar-Yosef 2002). **f.** Vertical projection looking toward the north of different mineral types determined by FTIR within squares HJK24. Note the concentration of LVS minerals (in green) at the base and the centre, as well as the occurrence of C/D minerals (yellow) and clay (red) along the sides and upward in the profile (see also chapter 4).

2.2.2.1.2 East Profile

Sediments exposed in the East Profile are overall similar to those in the South Profile, although hearths are less prominent and there is less extensive diagenetic alteration in Layer E than in the South Profile. In general, the deposits consist of firm to cemented to crumbly, weakly bedded dark brown (10YR4/3) silt and clay. In Layer F, a few hearths are present, and as in the South Profile, the deposits have been extensively affected by diagenesis; most of the sediments are in the LVMS mineral assemblage (Weiner, Goldberg, and Bar-Yosef 2002) (Figures 2.19 f, 2.20, 2.21).

Layer E rests on Layer F with a distinct, locally sharp contact that is inclined toward the back of the cave: in K24, it is at ~-520 cm, whereas in I24 it is ~-550 cm, a trend that is visible along the North Profile (see below). In contrast to Layer F, Layer E consists of interlayered anthropogenic deposits (burned features with ash, and organic-rich silt, homogeneously distributed charcoal, ash, and silty clay mixed by trampling; see chapter 3), geogenic reddish silty clays, and some rock fall. A broad band of red clay (between ~-370 and -420 cm) can be traced across the entire East Profile from south to north (Figures 2.20, 2.21). The presence of reddish clay layers (easily identified on the surface during excavation), which are generally mixed with charcoal and bone, indicates that some occupation was coeval with their accumulation. Unlike in the South Profile, extreme (i.e., LMVS) diagenesis is less common, and instead the layer is mostly within the C/D mineral zone, with both calcite cementation and apatite transformation of calcareous elements, including ashes. Only a few pockets of sediment representing more advanced alteration were observed in the East Profile (e.g., FTIR samples 275 [I18, -280 cm]; 443 [K22, -305 cm]). Several burrows occur throughout, but the upper part appears more burrowed than the lower part, a situation similar to that in the South Profile.

2.2.2.1.3 Northeast corner (J19–21, and K21)

Sedimentary exposures in the East Profile continue to the north around a block of unexcavated sediments (within JK19–21) that are capped by a block of flowstone and travertine (Figures 2.21d, 2.22, 2.23 a, b). Layer F is similar to that in other exposures, consisting of greyish-brown, altered, silty clays, with FTIR results showing a mixture of CD and LMVS mineral assemblages. As in the Deep Sounding, siliceous seed coats are common and locally concentrated throughout (see micromorphology section). The contact with Layer E is sharp but, owing to its inclination toward the rear of the cave (see above), the E/F contact in K21 ranges from -530 to -535 cm here; thus, only ~≤30 cm of Layer F are exposed in this corner of the Central Area. Additionally, measurements in other locations in the Central Area indicate that the contact occurs at ~-555 cm in the middle of J21, -570 cm in J20, and -550 cm in J19. Such elevations point to a channel-like depression oriented in the direction of J20 (Figure 2.23c).

The deposits of Layer E—particularly toward the top—are more calcareous, as they are closer to the capping flowstone and travertine, among other possible reasons (Figures 2.22, 2.23). The lower part Layer E shows some CT and OT, but much of the mineralogy of Layer E here is apatite and clay. Nevertheless, Layer E here consists of bedded ashes, red silty clay, and mixtures of these components; some isolated, fist-sized pieces of limestone roof fall appear in the lower one-third of the layer. Continuation of the red clay from the East Profile can be observed on the south face of this block, and it can be traced around into the G excavation squares and H18. Moreover, the red clay in particular dips to the northwest; the dip angles are very slight in J21 but begin to increase more markedly in J19 (Figure 2.23b). As discussed below, these dipping strata continue toward the northwest.

Owing to the diagenesis (calcite and dahllite precipitation), details of the original nature of the deposits tend to be difficult to discern and describe. In addition, on the South Profile of this area (within J21), we observed a 15–20 cm-thick band of apatite that cuts across the deposits, demonstrating that phosphatisation does not necessarily follow the bedding; it also shows that some of the apatite formation can take place well after a deposit has been

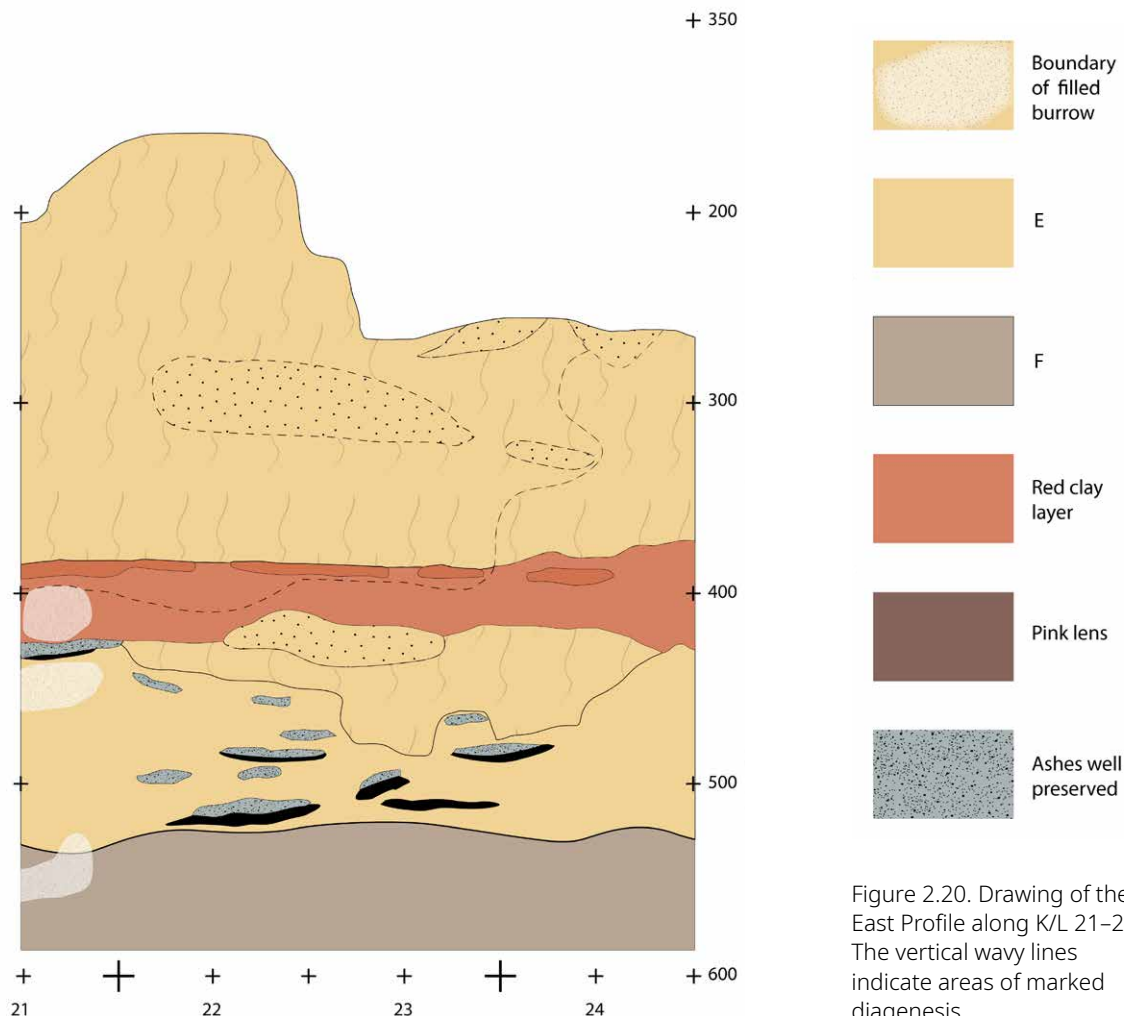


Figure 2.20. Drawing of the East Profile along K/L 21–24. The vertical wavy lines indicate areas of marked diagenesis.

buried. This latter phenomenon is also illustrated by: 1) the fact that fallen block of travertine in JK21 is partly altered to dahllite, and 2) the presence of an apatite drape underneath the fallen stalagmite (Figures 2.22, 2.23 a, b). Nevertheless, bones are relatively common in this part of the cave because of the buffering effects of the calcareous travertines.

2.2.2.1.4 North Profile (GHI17/18 and JK18 ab/cd; -360 to -600 cm)

Layers F and E continue around to the base of the North Profile along GHI17/18, and JK18ab/cd (Figures 2.24, 2.25, 2.26). Here, in Layer F, the silty clays are more finely laminated and contain darker mm to cm thick stringers and laminae (Figure 2.26 d, e), which are quite similar to the sediments in Layer F in the Deep Sounding (Figure 2.8). Moreover, as shown in Table 2.4, the FTIR results indicate mostly LMVS suite of minerals for Layer F, although some samples are clayey and apatitic.

Rodent burrows are evident in the North Profile, but are most prominent and visible in Layer F (Figure 2.26 c-f).

One of the most striking features of the North Profile is the very sharp, irregular, sculpted nature of the E-F contact, which varies considerably in height (J19, -545 cm; I19, -540 cm; H19, -530 cm; H18/19, -550 cm; G18, -550 cm). As mentioned below, these height differences point to fluted erosional channel(s) developed into Layer F and match the overall sloping trend of the E-F contact toward the rear of the cave (northeast) (see Figure 2.23 b, c). As a consequence of the dipping erosional contact, exposed thicknesses of Layer F vary between 30 and 60 cm, taking into account the height of the excavated floor in GH19 (-600 cm).

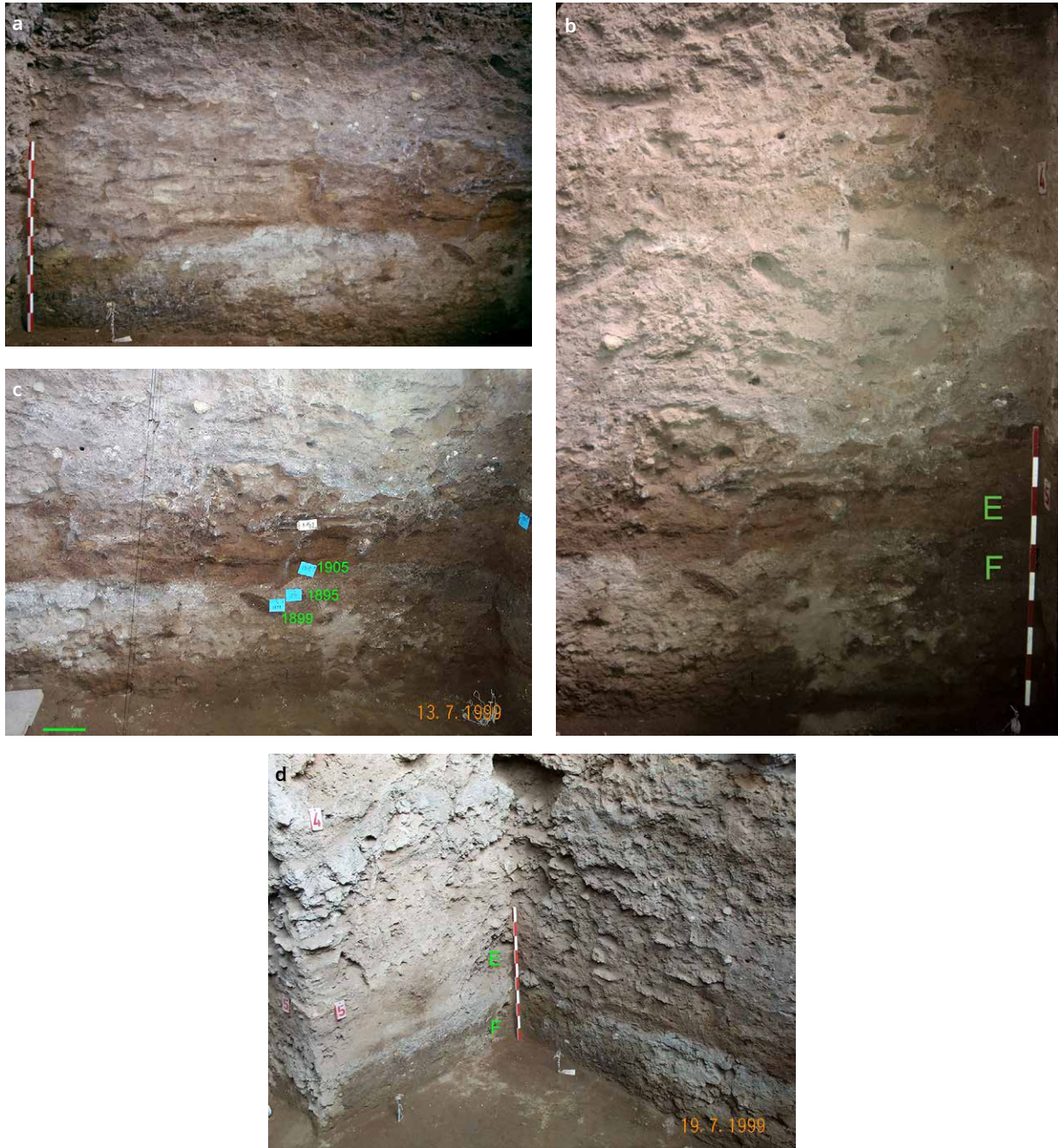


Figure 2.21. East Profile and northeast corner of Central Area. **a.** The East Profile in 1999 with floor surface at ~450 cm. Note the reddish band of silt/clay on the righthand (south) side of the photo, and the subtle expression of combustion features on the left, just above the light-coloured band in the lower third. Most of these sediments are apatitic, except for the very upper ('textured' part), which is calcareous and linked to calcite precipitation associated with flowstone in the northeast corner of the Central Area (see also [e] below). **b.** Layers E and F in K/L 23–24 in the southern part of the East Profile in 1999, with a reddish clay-rich band in the lower third of the photo. This band (composed of clay and apatite, based on FTIR) continues northward to K21, where it is overprinted by diagenetic alteration and the reddish colour is not visible as such. The top of the metre stick is at ~480 cm. (cf. Figure 2.20). **c.** Mineralogy near clay-rich layer shown in (a) (K23). Numbers refer to FTIR analyses: 1) 1905 (E), brown layer = clay and apatite; 2) 1895 (F), vein = leucophosphite; 3) 1899 (F), sediment = leucophosphite and clay transforming. Scale bar at lower left is ~15 cm long. **d.** Northeast corner of the Central Area (K21) in 1999 at junction between east wall and north face within K21. The sharp contact between the greyish-brown, altered Layer F and the overlying red clay in Layer E is particularly clear on the righthand side of the photograph.

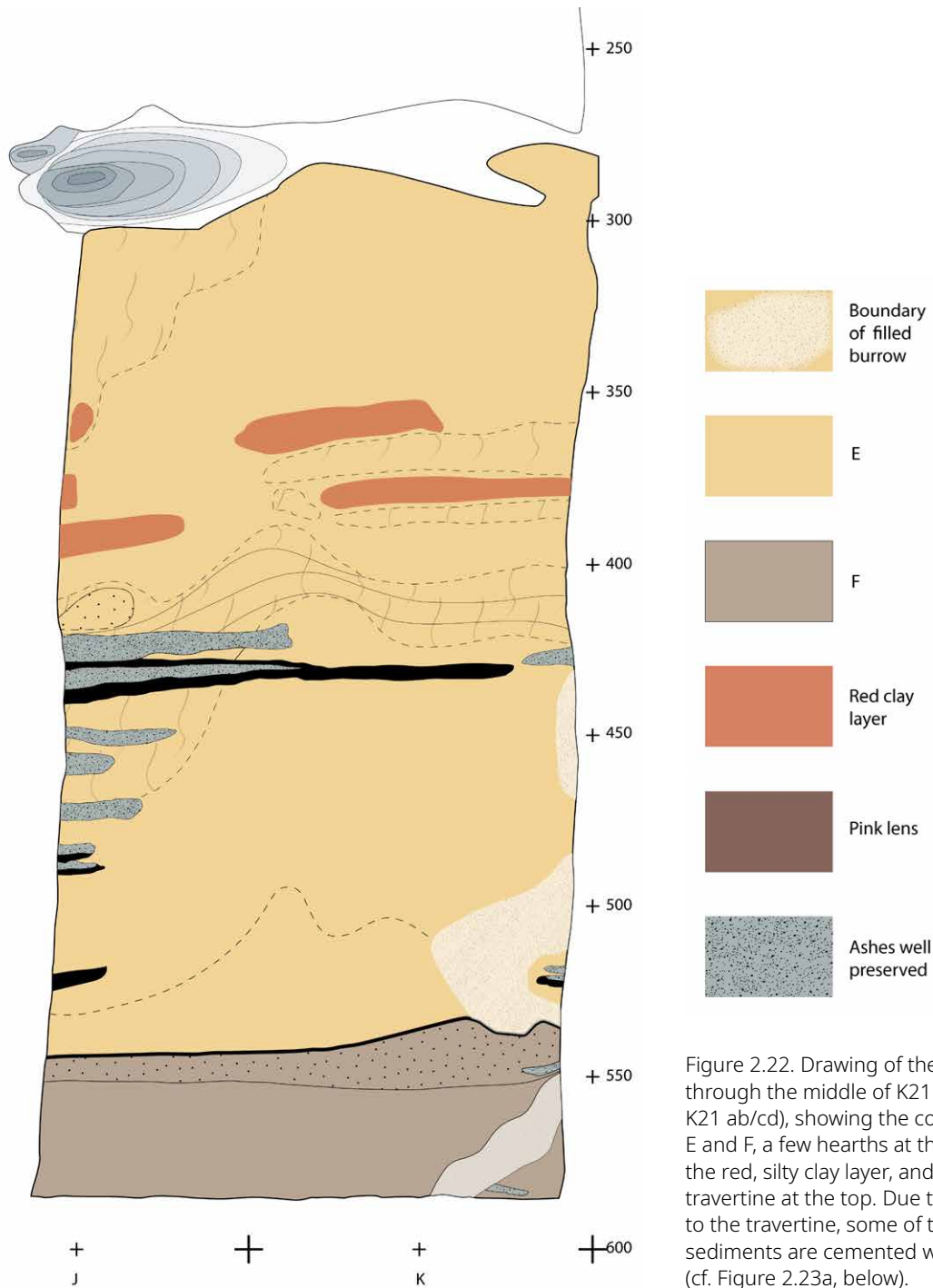


Figure 2.22. Drawing of the East-West Profile through the middle of K21 (along section K21 ab/cd), showing the contact between E and F, a few hearths at the left, traces of the red, silty clay layer, and a block of fallen travertine at the top. Due to the proximity to the travertine, some of the uppermost sediments are cemented with calcite. (cf. Figure 2.23a, below).

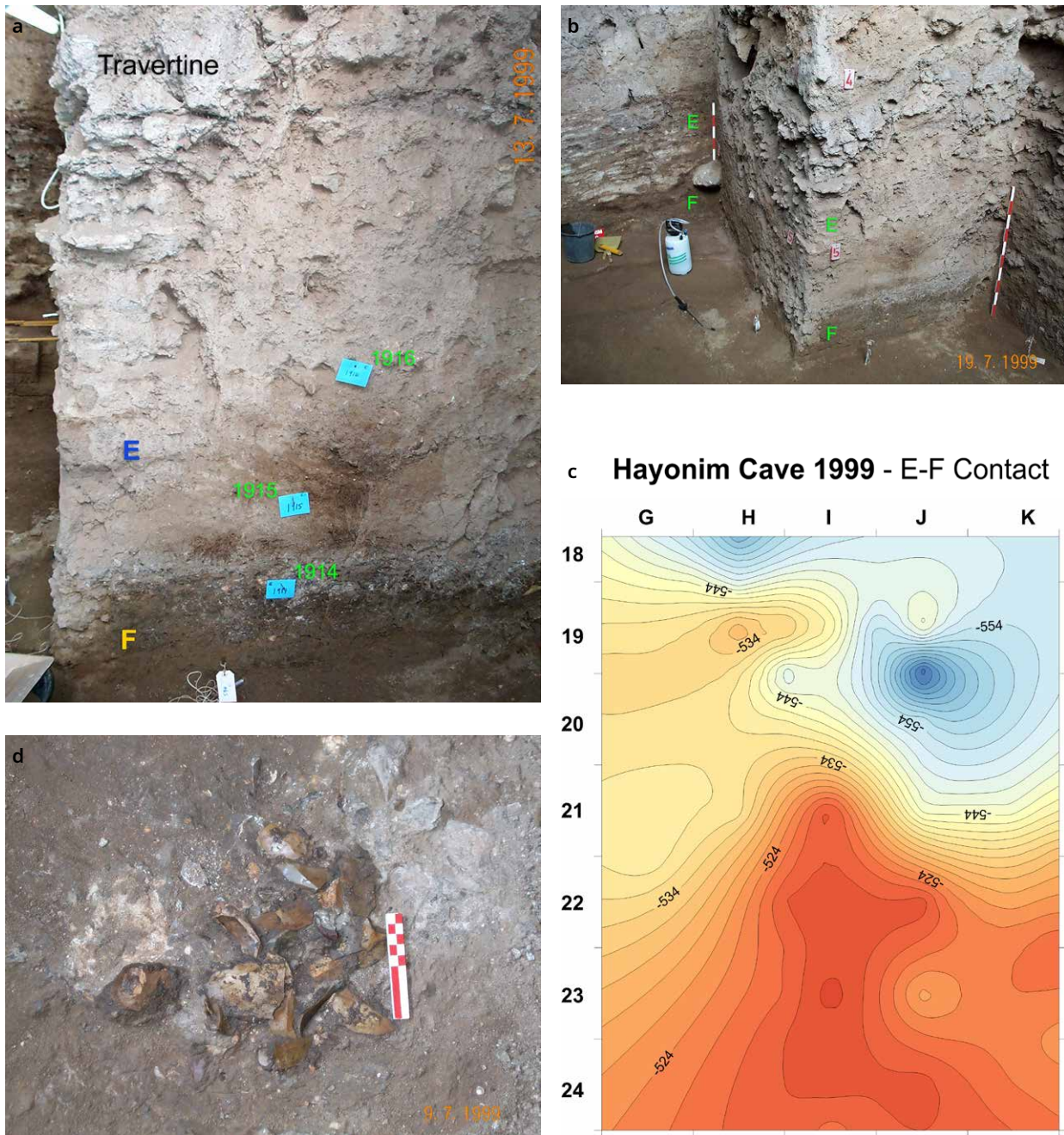


Figure 2.23. Northeast corner of the Central Area. **a.** View of the north face of section K21ab/cd in 1999 (cf. Figure 2.22), with Layer F at the base overlain by Layer E and capped with travertine/flowstone in the upper left. FTIR analyses (green numbers) show: 1914 (F) = apatite and clay 1915 (base E) = clay transforming, opal transforming 1916 (mid E) = apatite and calcite. **b.** View to the north of K21ab/cd (righthand side of photo) and part of the North Profile in K18, represented by bands of lenticular hearths to the left of the shorter metre stick. Note the slope of the E/F contact downward toward the rear of the cave (north). **c.** Interpolated contour map of the surface of the E/F contact in the Central Area. This map illustrates: 1) the overall inclination of the surface toward the rear of the cave, and 2) its undulating nature pointing to channelised flow toward the back; the 'depression' in J18 is an artefact of the computer program and, in reality, appears to have had an open, channel-like form. **d.** Accumulation of flint artefacts in J19abd in Layer F between -585 cm and ~-565 cm; see text and chapter 3 for discussion.

Layer E

The visibility of Layer E in the North Profile is better than that in the East Profile and northeast section. In HJ19, for example, the deposits are readily divisible into three segments. The lower one rests on Layer F with a sharp, irregular erosional contact; it is comprised of a series of northwest-dipping bedded, lenticular hearths totaling ~80 cm thick. These hearths are relatively thicker and lenticular at the base, and they become linear, smaller, and thinner upward in the northern section and to the west (e.g., GH18) (Figure 2.26 a-c). In the latter case, the lenses vary in width from ~5 to 35 cm and are about 5–10 cm thick; in the lower part, they are larger and 80–100 cm in width (see chapter 3). Scattered throughout many of the ashes are millimetre- to centimetre-diameter clasts of bright red burned terra rossa, similar to those observed west of the South Profile and above the West Profile.

Overlying the hearths in the second segment are more massive silty clay deposits. They consist of predominantly red silty clay, diagenetically altered clay, and trampled charcoal-rich clay. These clays are about 55 cm thick but thin dramatically to the west and northwest, where they grade into thinly bedded ashy and charcoal features (Figures 2.25, 2.26a); in GH18, the clays are only about 20 cm thick.

The third segment (visible in HJ19 below -360 cm in Figure 2.26a) consists of massive crumbly pinkish-gray (7.5YR7/2) gritty silt/clay with remains of combustion features scattered throughout. The combustion features are inclined to the northwest. Mineralogically, they are within the LVMS zone (Table 2.5). The upper part of sediments in this northern part of the Central Profile (i.e., above ~-360 cm; not shown in Figure 2.24) is difficult to observe because of diagenetic alteration.

Burrowing is clearly discernable in Layer E (Figure 2.26), particularly in the ashy units, which exhibit circular burrows as in the South Profile. They consist of larger rodent burrows, but also smaller (~1 cm diameter) insect burrows. The latter are abundant and have effectively blurred the composition, integrity, and limits of the individual ashy hearth stringers. More massive, poorly defined burrows occur in the overlying units, which makes it difficult to trace the units to the west.

Diagenesis is spatially distributed, as it was in the South Profile. FTIR analyses of sediments in G–I 18–19 (Weiner, Goldberg, and Bar-Yosef 2002: Fig. 4), reveal a wedge of superposed hearths exhibiting CD mineral assemblages; these are overlain by more altered LVMS sediments that display some hearth structures within a more massive matrix. As at Kebara Cave, bone is found in the apatitic zones.

An interesting phenomenon occurs in the main part of the North Profile. Here, near the limit between I and J, several extensional cracks occur between -360 cm and -500 cm. These are typically ~1 to 2 cm wide and are subvertical. They appear to represent extensions and cracks associated with tilting of the sediments toward the back of the

Square	FTIR sample no.	Z (cm)	Min1	Min2
G18	1465	-540	OC	T
G18	1466	-558	OC	
G18	1873	-551	OT	CLT
H18	1981	-550	OC	
H18	1982	-560	O	
I19	1711	-560	CLT	
I19	1879	-543	A	CL
I19	1880	-557	CL	A
I19	1882	-568	L	OT
J19	1885	-570	L	CLT
J19	1886	-550	CL	A

Table 2.4. Selected FTIR analyses of sediments from Layer F in the North Profile. See Table 2.2 for mineral abbreviations.

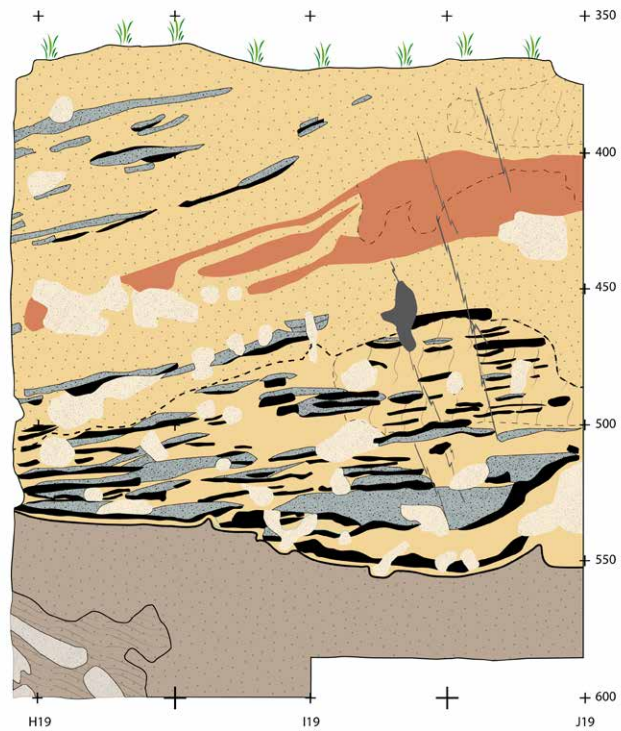
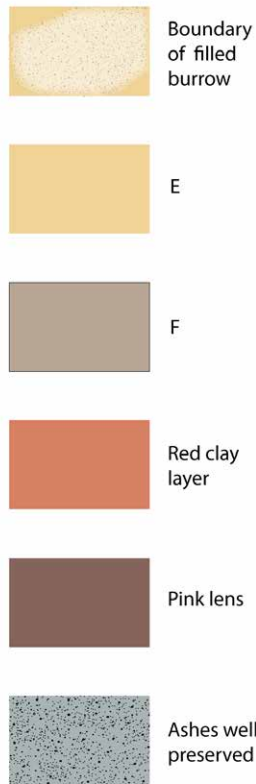
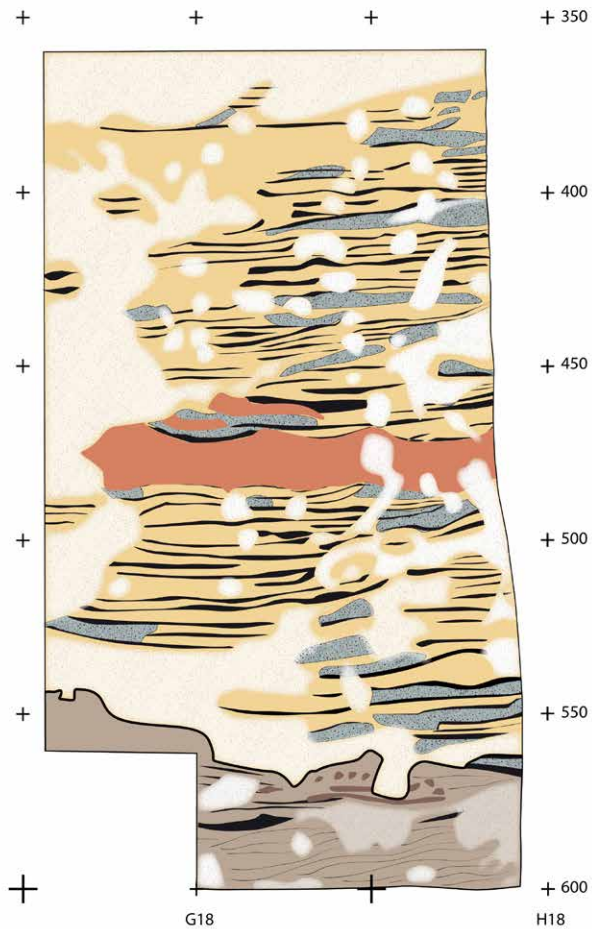


Figure 2.24. Profile of northern part of the Central Area in H19, I19, and J19 (cf. Figure 2.26 a), showing bedded lenticular hearths in the centre (Layer E) resting with a sharp, erosional contact on the altered (LMVS suite) grey-brown, silty sediments of Layer F. The sediments above the bench at -360 cm are crumbly and extensively altered by diagenesis, and are not shown here.

Figure 2.25. Profile drawing of Northern Profile in GH18. Note the abundance of thin combustion layers, the continuation of the red layer, and the sharp, erosional contact between Layers E and F. The profile is also punctuated with numerous rodent burrows, as well as small insect burrowing (see Figure 2.26d, and Figure 2.31 n, o).



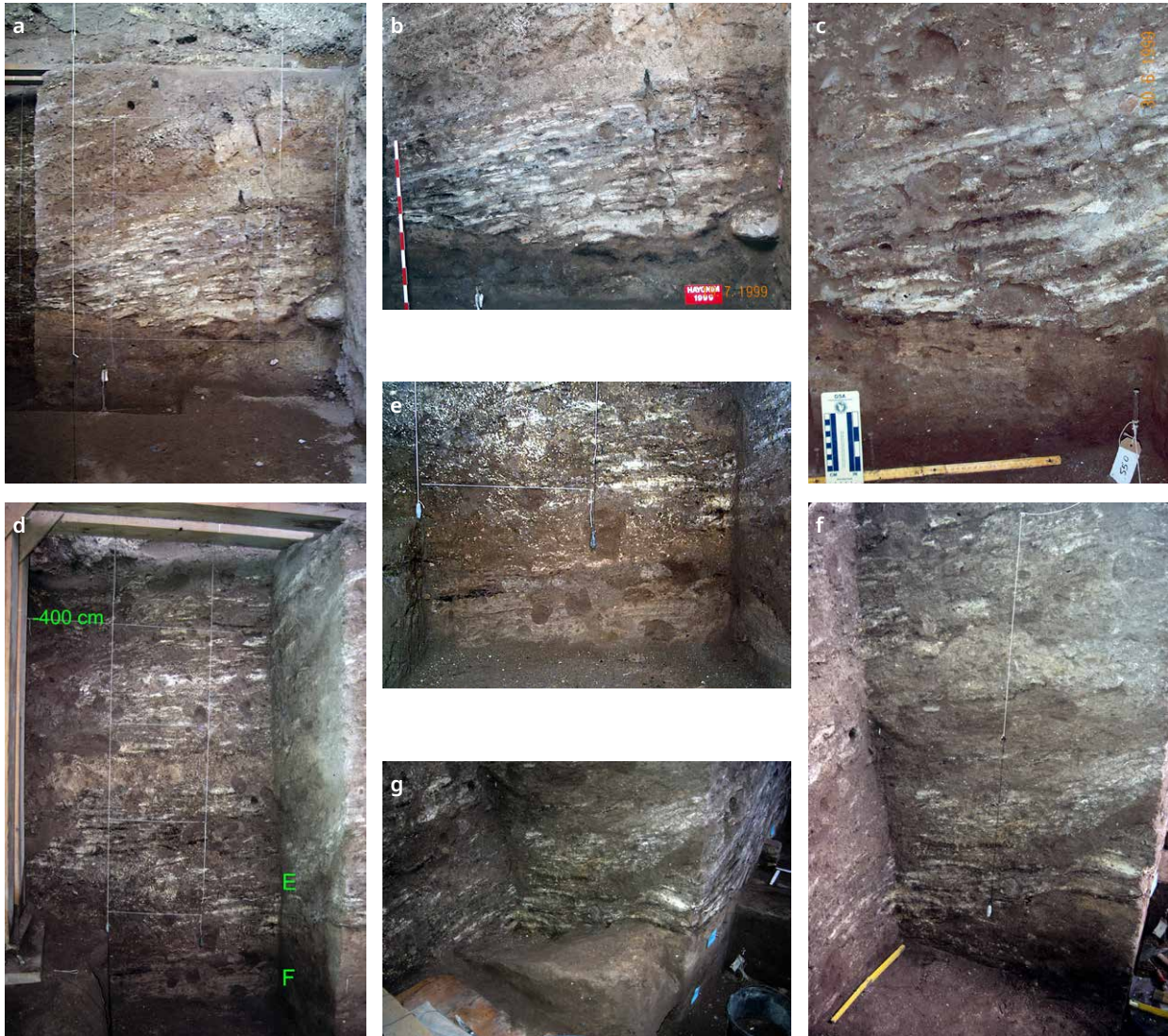


Figure 2.26. Profiles in the northern part of the Central Area. **a.** View to the north of profile in IJ18 in 2000, showing cm-thick bedded lenticular hearths in the centre (Layer E) resting with a sharp, erosional contact on the altered (LMVS) grey brown silty sediments of Layer F. The sediments above the bench at -360 cm are crumbly and diagenetically altered. **b.** Detailed view of lower part of section in (a). FTIR analyses show that most of the massive part of the profile consists of leucophosphite, montgomeryite, variscite, and siliceous aggregates (LMVS), whereas the ashy part is composed of calcite and dahllite (DA) (see Figure 4 in Weiner, Goldberg, and Bar-Yosef 2002). **c.** Close-up of sharp, erosional contact between hearths in Layer E and bedded greyish-brown sediments of Layer F; some of the hearths have been blurred by insect bioturbation. **d.** Profile of north face at H17/18 in 2000, showing in Layer E a sequence of thin lenses and stringers of hearths with whitish domains of secondary mineralisation (LVMS of Weiner et al. 2002); Layer F is visible at the base (see detail in [e]). Bioturbation is shown by insect burrowing, which blurs the limits and layering of the hearths, and by some larger (~9 cm) rodent burrows ('terriers', krotovina) that are visible, particularly in Layer F. **e.** Detail of lower part shown in (d). Layer F is visible at the bottom and here it is bedded, presenting a similar aspect to the layered deposits of Layer F in the Deep Sounding. The mineralogy and micromorphology are also similar. Rodent burrows are visible in the base. **f.** View to northeast of the west-facing section along H/I18 in 1999. Note the northward plunge of the E/F contact toward the rear of the cave; the overlying hearths of Layer E are somewhat inclined but are mostly sub-horizontal. The bedding of deposits at top of the profile is muddled by extensive diagenesis and insect burrowing (see above). The floor is at ~-570 cm. **g.** Excavated contact between Layers E and F in I18 in 1999. Here and elsewhere, the contact is sharp and dips to the north with undulating contact, indicating that Layer F was channeled prior to the deposition of Layer E.

Table 2.5. Mineralogy along the Northern Profile in I and J19.

Square	FTIR sample no.	Z (cm)	MIN1	MIN2
J19	68	-319	C	A
I19	437	-370	MA	A
J19	456	-364	A	
I19	574	-360	L	
J19	1239	-370	CL	A

cave, as revealed by their northeastern direction, which parallels the strike of the dipping hearth beds.

Finally, we note that Layer E continues upward in HIJKL17 to a depth of ~150 cm. These uppermost-accessible sediments of layer E (left by the previous excavations) are extensively altered mineralogically, and physically modified by widespread bioturbation of the silts and clays. Because of the very small scale of the excavations of these limited exposures, the uppermost deposits are not considered here in detail.

2.2.2.1.5 West Profile (within GH22–24) (Figures 2.27, 2.28)

In many ways, the West Profile exhibits characteristics similar to those observed in the South and North Profiles. These similarities include the presence of abundant calcareous ashes, burned features, and travertines in the upper 2/3 of the profile, as well as reddish clay and diagenetically altered sediments that are mostly calcite and apatite; locally, more intense diagenesis is evident by the presence of montgomeryite and OC, similar to that in Layer F.

Much of the West Profile, particularly in the southern two-thirds, is dominated by well-preserved anthropogenic deposits (Figures 2.27, 2.28). These are expressed as ash lenses, in situ burning features (hearths), homogenised ash, charcoal-rich silty clay, and bone; they are well exposed in H and I 22–24. Burning features occur at the very base (as on the South Profile), where they are preserved in soft generally dahllite-rich sediment. Above -460 to -470 cm, they become increasingly calcareous and less diagenetically modified. At -420 cm, the sediments are progressively more indurated by calcite, and cementation comprises calcareous ashy features, silts, and clays; the latter are similar to typical ‘cave breccias’. These calcite-cemented sediments continue upward to the top of profile in G23–24, where they interfinger with travertine and flowstones that are stuck onto the bedrock walls of the cave. Calcification seems to become significant above -420 to -430 cm.

In addition to calcification, other diagenetic features are particularly marked in the northern third of the profile (H/I22, Figure 2.27a). Here, a ~30 cm thick band of dahllite points to a transition zone between the generally calcareous sediments to the south and more intensively altered deposits to the north (H–J22). In the latter case, the sediments are crumbly, gritty, light brown (7.5YR6/4) silts, with a variety of nodules and veins composed of opal, opal transforming (OT), and leucophosphate (FTIR samples 1652-1659; see also Weiner, Goldberg, and Bar-Yosef 2002). Interestingly, these nodules are best developed in Layer F but continue up into the lowermost 15 cm of Layer E, suggesting the possibility that the intense diagenesis that produced them took place in Layer E and that the occurrence of nodules in Layer F results from diagenesis that took place during Layer E time. In any case, these crumbly, phosphatic sediments in H22 are situated within the ‘diagenetic trough’ that extends southeast-northwest across the site (Figure 2.19).

The red clay layer that is visible in the other profiles—particularly the East Profile—is partially visible in the West Profile. It can be traced from -380 to -410 cm in I24 to ~-390 to -420 cm in H22 and is within the C/D mineral assemblage zone. Additionally, other clay lenses occur throughout the West Profile, and these are mixed with charcoal and, locally, bone, likely representing trampled burned features.

The amount of burrowing in the Western Profile is comparable to that observed elsewhere. Numerous burrows occur, especially in the clayey, trampled inter-hearth areas.

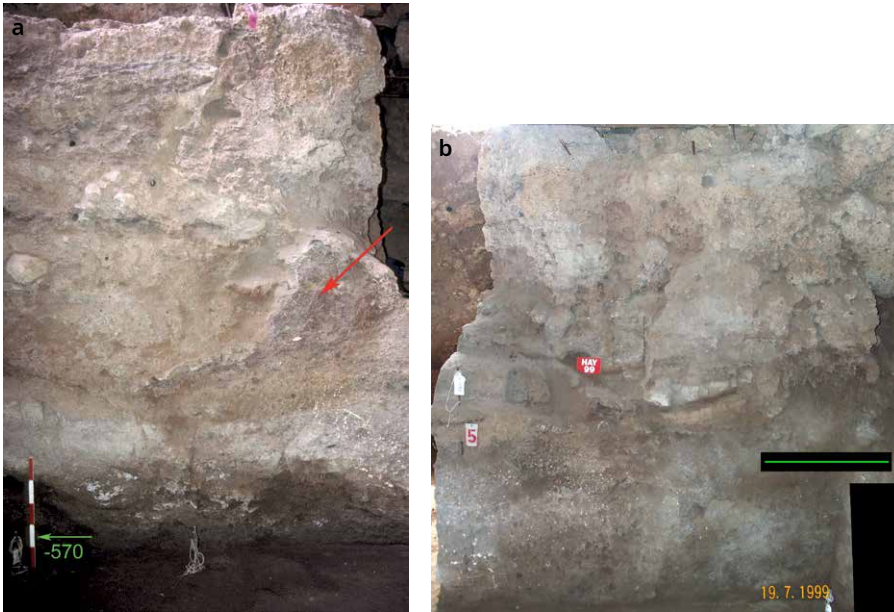


Figure 2.27. Western side of the Central Area. **a.** Part of the section between line H23 and H24 in 2000. The darker sediment along the base is Layer F and the overlying mass of calcitic deposits is Layer E, which is particularly cemented (calcite) in the upper ~40 cm. Much of these sediments consist of calcite-cemented ashes, although there is a comma-shaped band of dahllite, which cuts across the deposits (arrow). **b.** Looking south to profile along H22/23, perpendicular to the profile in (a), it shows a remnant of a partially burrowed hearth in the centre with crumbly diagenetically altered sediments; these were not studied in detail. The red '5' tag refers to depth below datum; the green line is 50 cm long. The contact between Layers F and E is at about -500 cm across the profile.

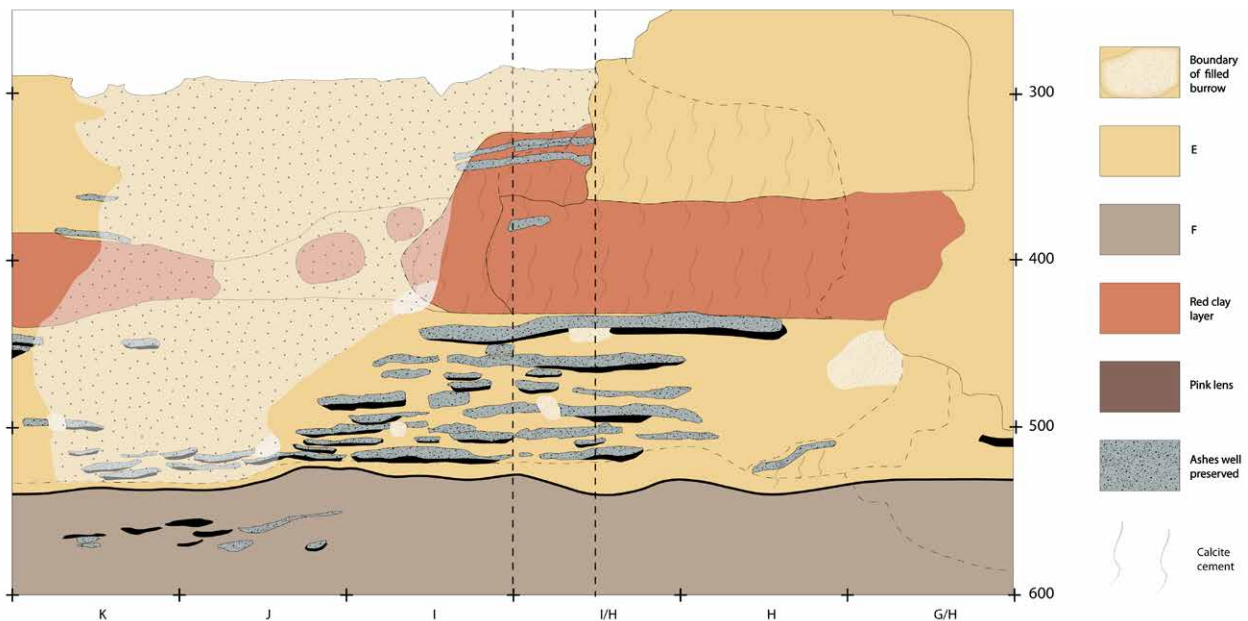


Figure 2.28. Composite of Southern (left) and Western (right) Profiles. Note the shift in location designated by the vertical dashed lines. The Western Profile, showing Layer F at the base overlain by Layer E with sharp contact. Note the lateral continuation of the hearths from the South Profile, as well as the red silty clay layer in the centre. Because the Western Profile is situated closer to the bedrock walls, the sediments are more calcareous in the upper part.

The north-facing profile along H22/23 (Figure 2.27b) was not studied in detail, mostly because the exposures were weathered, being left over from the former excavations. Stratigraphic differentiation was therefore rather general and on broad lines. Layer F is exposed below ~500 cm (Figure 2.27b) and is composed mostly of the LMVS minerals assemblage. Layer E, in contrast, is similar to the deposits exposed in the Western Profile, being generally clayey, apatitic, and calcitic (e.g., FTIR samples 615–618, 621–623). In spite of its weathered appearance, remains of a partially burrowed hearth occur just above 500 cm; it is in turn overlain by predominantly ashy sediment.

2.2.2.2 Micromorphology of the Central Area

Both Layers F and E are exposed in the Central Area and they exhibit micromorphological features that reflect their field aspects. We will discuss Layer F first, which is rather similar throughout the area. Layer E, on the other hand, displays considerably more variation in composition (geogenic versus anthropogenic) and degree of diagenesis, depending on location.

2.2.2.2.1 Layer F (Figure 2.29)

The micromorphological aspects of sediments from Layer F in the Central Area are quite similar to those from the Deep Sounding. They are overall composed of diagenetically altered silty clay (commonly as granular aggregates), and typically with coarser inclusions of siliceous seed coats, some gastroliths, and mineralogically transformed terra rossa clasts (isotropic in XPL) (Figure 2.29 b, e, m, n). The last can be massive and crumbly or bedded, particularly near the upper part (Figures 2.26 d, e, f; 2.29 d, l–n). Diagenesis is such that almost all sediments fall in the LMVS mineral association. Moreover, the sediments in the upper part, below the eroded E/F contact, commonly display millimetre- to centimetre-sized nodules or areas composed of OC, O, OT, and CLT (Figures 2.29 a–c; g–k). Veins of leucophosphate and opal/OT are prominent along the South Profile (Figure 2.29c). Interestingly, a later stage of phosphate diagenesis is demonstrated by the precipitation of apatite within veins that crosscut previously transformed matrix material (Figures 2.29 j, k), although it is not clear when this later phase took place.

2.2.2.2.2 Layer E (Figures 2.30, 2.31, 2.32)

The micromorphological aspects of sediments from Layer E in the Central Area are more variable in their original compositions, and in the styles of diagenesis. Anthropogenic additions include charcoal/organic matter, ashes, phytoliths, bone, and lithics. These occur within structured hearths (e.g., Figures 2.24, 2.25, 2.30 a–l, 2.31 a; also see section on hearths, chapter 3), or mixed materials that have been redistributed by dumping, trampling, and burrowing (rodent and insect). The latter is expressed in a number of ways. Thick red layers in the East Profile, for example (Figures 2.20, 2.21 a–c; 2.30 q–s; 2.31 i–l), are mixtures of bone, clumps of ash, phytoliths, and some charcoal.

Similarly, many of the sediments from Layer E are accumulations of finely laminated ashes (Figures 2.30, 2.31 a, q, u, z), which typically contain bright red terra rossa clasts that are most commonly burned. Depending upon location, these ashes can be calcareous (close to the bedrock walls) (Figure 31 u, v) or diagenetically transformed to apatite (Figure 2.31 a–f, q–t) (toward the centre of the Central Area). In fact, as shown previously (Weiner, Goldberg, and Bar-Yosef 2002: Fig. 4), both forms of ashes can occur in and across CD and LMVS mineral assemblage zones. Unmodified calcareous ashes can be recognised by their rhombic form with high-order interference colours, whereas apatitic ashes are isotropic in XPL, but in some cases their original rhombic shape can be discerned through close observation of the thin section.

Burrowing and biological activity is visible not only in the field, as rodent holes and centimetre-sized disruptions (e.g., Figure 2.19 a, 2.26 c), but also in thin sections. In the latter case, millimetre- to centimetre-sized passage features can be observed (e.g., Figure 2.30 g, r, q; 2.31 b, j, n, o, x)

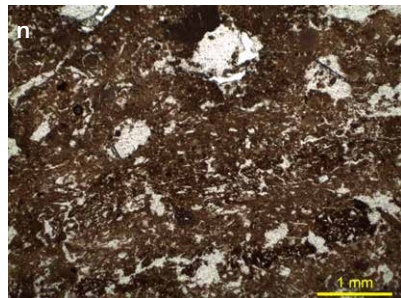
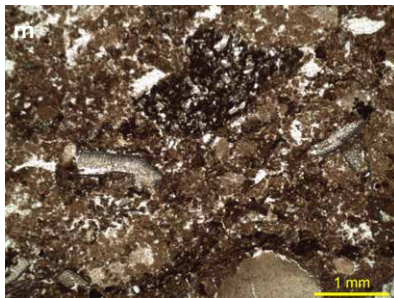
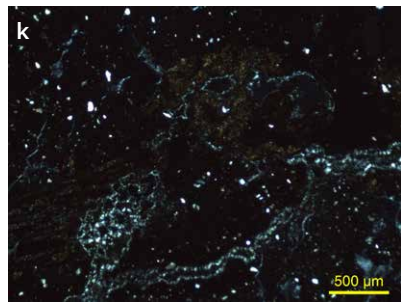
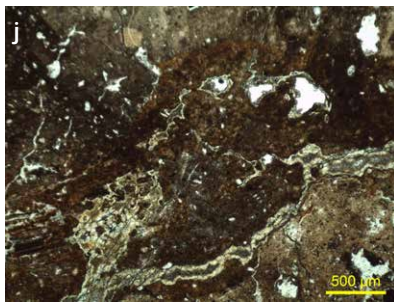
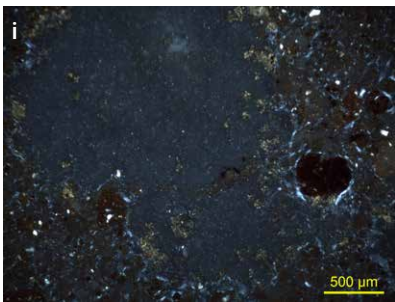
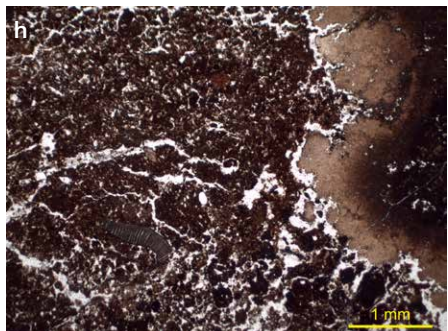
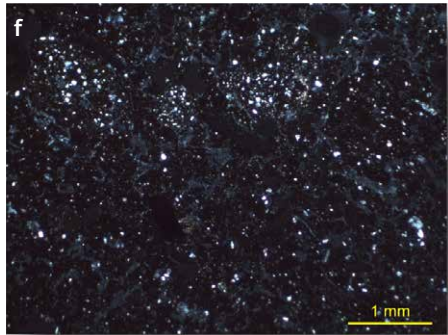
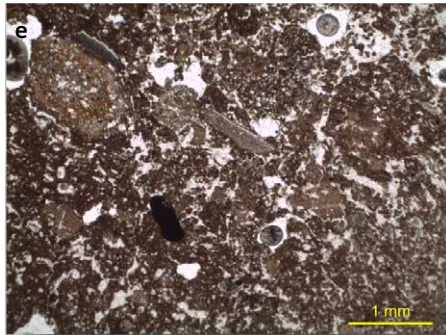
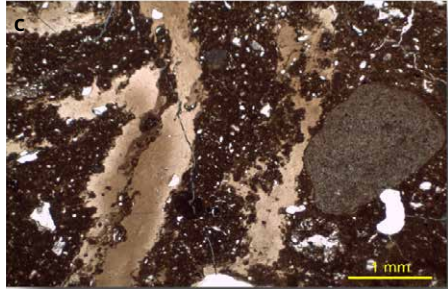
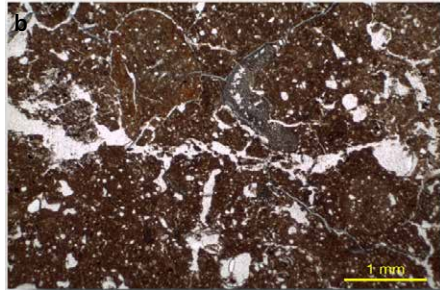


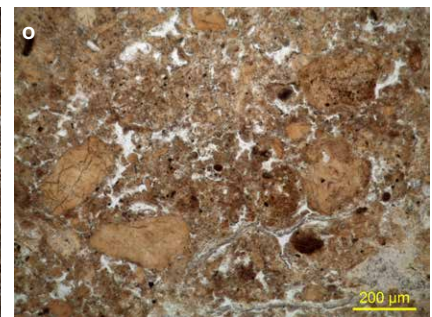
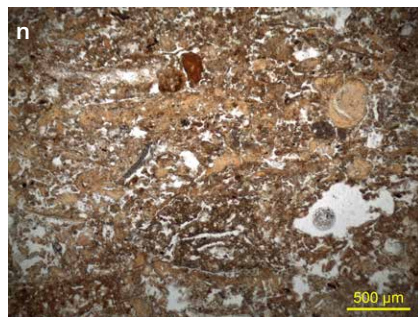
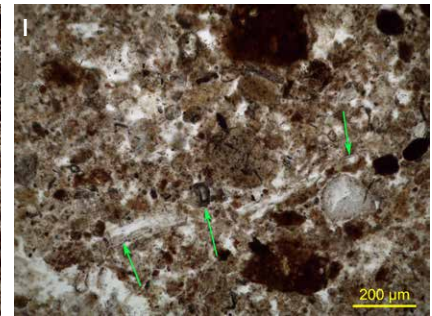
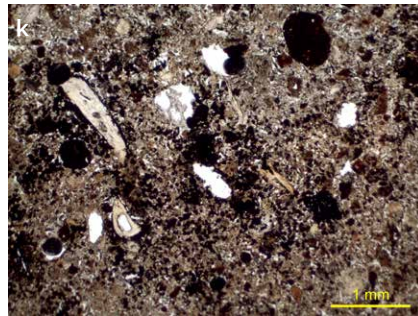
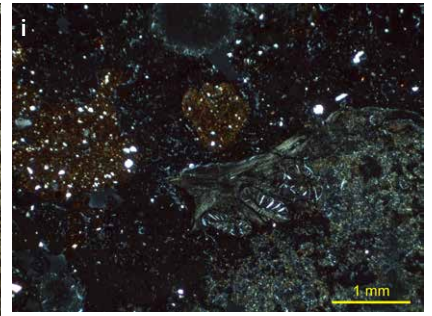
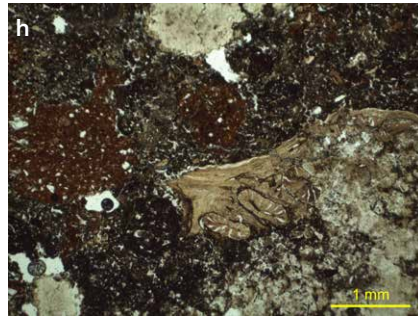
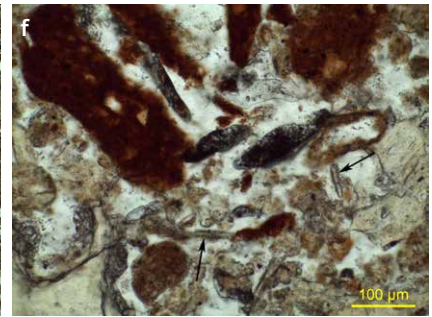
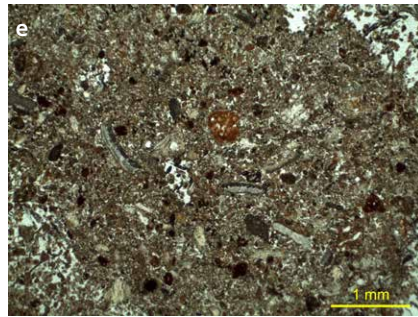
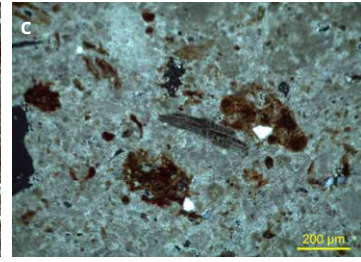
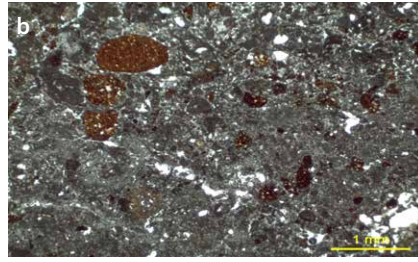
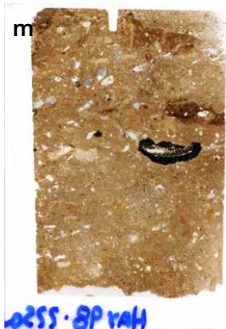
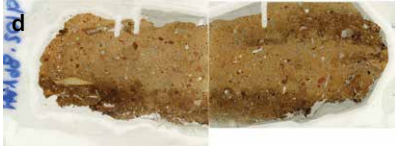
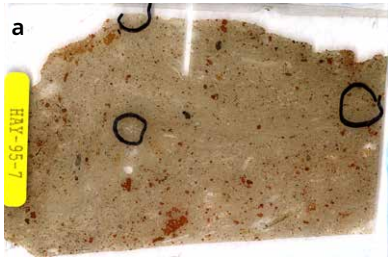
Figure 2.29. Micromorphology of Layer F from the Central Area. **a.** Thin section scan of sample 98-251 (K24d, -535 cm) showing centimetre-sized irregular nodules. These and the sediments around them yielded a number of minerals mostly in the LMVS assemblage, including L, CL, OC, O, CLT, and OT (FTIR samples 1663, 1676, 1680, 1681, 1682, 1684, 1896, 1901); these specific nodules were not analysed. PPL. **b.** Photomicrograph of 98-251, showing many of the characteristics typical to Layer F, both here and in the Deep Sounding: seed coats, altered silty clay matrix, and rounded aggregates of the same. PPL; scale is 1 mm. **c.** Photomicrograph showing displacive precipitation of OC and L in the vein; gastrolith at the right. PPL; scale is 1 mm. **d.** Thin section scan of 99-319 (K24a; -567 cm). The sediment is very similar to that in Layer F from the Deep Sounding. PPL; scale is 1 mm. **e.** Photomicrograph of 99-319 showing weak inclined bedding of seed coats and silty clay aggregates, all with an open, granular microstructure. PPL; scale is 1 mm. **f.** Same as (e) but in XPL. Note the isotropic nature of the groundmass; only the quartz silt (white dots) is visible. XPL; scale is 1 mm. **g.** Thin section scan of sample 98-253 (J24c; -535 cm) with nodules similar to those in (a) but disrupting an organic rich domain, possibly a hearth. PPL. **h.** Photomicrograph of 98-253 with nodule at right and small seed coat to the left. PPL; scale is 1 mm. **i.** Same as (h) but in XPL. Note in fact that there is an alteration phase that post-dates the opaline nodule as shown by the fine yellow crystallites that overgrow it; these are likely phosphatic. XPL; scale is 1 mm. **j.** Photomicrograph of 99-343 (K22b; -557 cm) displaying several phases of phosphatisation with a final phase of apatite vein filling. [Closest FTIR samples at -580 cm are 1965, 1966, 1967 = L, CLT, OT, CL, respectively]. PPL; scale is 500 μm . **k.** Same as (j) but in XPL. Note the veins of apatite that crosscut the matrix. XPL; scale is 500 μm . **l.** Scan of thin section of 99-351B (H18c; -590 cm) from the northern part of the Central Area. Note the bedding of organic clay and some seed coats, which are reminiscent of Layer F from the lower part of the Deep Sounding. PPL. **m.** Photomicrograph of 99-351B with bedded organic clay (slightly deformed at base) and seed coats in isotropic silty clay. PPL; scale is 1 mm. **n.** Photomicrograph of different area in 99-351B. Note the similarity to the sediments to those from the Deep Sounding (Figures 2.9, 2.10). PPL; scale is 1 mm.

2.2.2.3 Discussion and summary of the Central Area

The Central Area embodies a link and stratigraphic continuation of the deposits exposed in the Deep Sounding. Table 2.6 summarises some of the highlights of the major aspects and differences between the sediments in Layers E and F. Layer E is much more anthropogenic than Layer F and exhibits generally reddish and brownish hues (mostly 5YR), in comparison to the more yellow and brown hues of Layer F (e.g., 7.5YR

Layer E	Layer F
<ul style="list-style-type: none"> Predominantly anthropogenic, but definite geogenic units (e.g., red clay/silt at ~400 cm. <ul style="list-style-type: none"> Hearths (burned layers) and ashes Some silt/clay Burned terra rossa aggregates 	<ul style="list-style-type: none"> Predominantly geogenic <ul style="list-style-type: none"> Clay with quartz silt Some isolated burned areas and hearths (especially S. Profile of Central Area, and upper part of the Layer) and numerous pieces of scattered charcoal, but lower proportion of ash preservation
<ul style="list-style-type: none"> Generally reddish and brownish hues (e.g., 5YR) 	<ul style="list-style-type: none"> Generally more yellow and brown hues (e.g., 7.5YR and 10YR)
<ul style="list-style-type: none"> Bedded or layered 	<ul style="list-style-type: none"> Tends to be massive but clearly bedded in the upper part beneath contact with Layer E
<ul style="list-style-type: none"> Phosphatised and locally calcified Calcareous deposits and ashes in relative proximity to bedrock walls 	<ul style="list-style-type: none"> Phosphatised predominantly with LMVS assemblage No calcite Siliceous, with various forms of opal/transformed clay
<ul style="list-style-type: none"> Bone, localised 	<ul style="list-style-type: none"> No bone
<ul style="list-style-type: none"> Travertine /stalagmite along borders 	<ul style="list-style-type: none"> No apparent travertine/stalagmite
<ul style="list-style-type: none"> Generally horizontal <ul style="list-style-type: none"> Increasing dip toward interior (G19), with inclinations to north and northwest; presumed sinkhole at back Slight dip in bedding in I23 and I24 over supposed sill at depth 	<ul style="list-style-type: none"> Generally horizontal <ul style="list-style-type: none"> Some dips toward rear of cave (e.g., possible swallow hole in H18) (In entrance section, some dips toward interior)

Table 2.6. Comparison between Layers E and F.



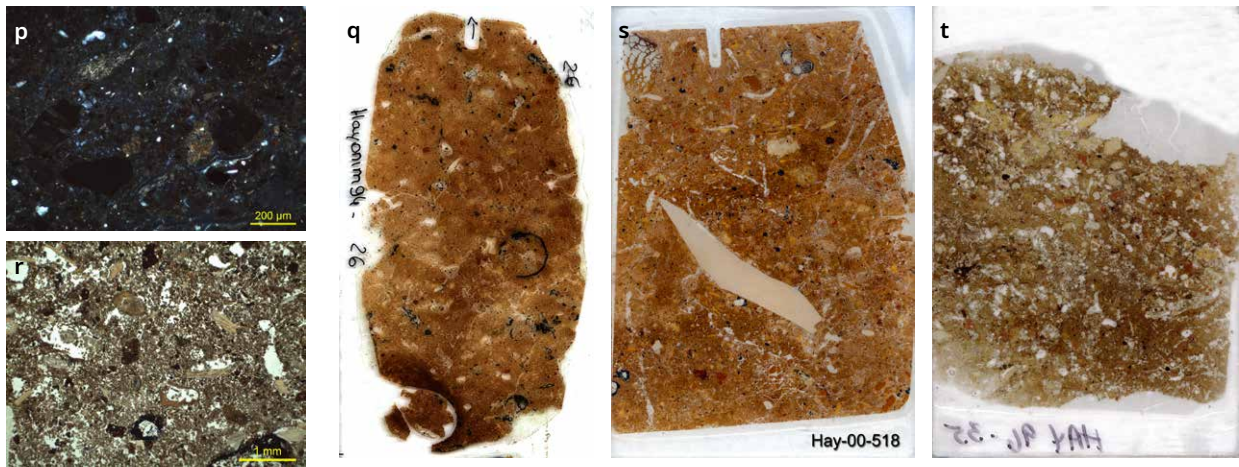


Figure 2.30. Layer E micromorphology of the South and East Profiles. **a.** Thin section scan of sample 95-7 (I24a; -430 cm) consisting of massive to bedded locally granular calcareous ashes and reddened clasts of heated terra rossa. PPL. **b.** Photomicrograph of 95-7 showing detail of terra rossa clasts (here, mostly rounded) in clumps of ashes. PPL; scale is 1 mm. **c.** Detail of 95-7 showing calcareous ashes with partially charred grey vegetal fragment in the centre. Individual ash rhombs are somewhat difficult to discern here because of the localised recrystallisation of the ashes. PPL; scale is 200 µm. **d.** Scans of two thin sections comprising sample 98-201 (I24d; -507 cm): 201b is at left, 201a at right. In the field, one side was softer and the other was harder. Reddish-yellow (5YR7/8) ashy silts overlay dark brown (7.5YR4/4) organic silts at the base of the hearth. Some red clay clasts are present as in (a) above. The right half appeared relatively fresh, and consisted of fresh clay, many phytoliths, and burned terra rossa clasts, and appeared trampled; there were some isotropic pale domains (silica?). Charcoal was dispersed and compressed. The left side (b) was similar to (a) but was richer in bone and poorer in calcite; locally, there were more abundant apatite domains, with many seed coats and other plant remains. Width is 150 mm. **e.** Photomicrograph of 98-201a, exhibiting abundant seed coats and a rounded clast of heated terra rossa in the centre. Most of the material here is non-calcareous. PPL; scale is 1 mm. **f.** Detail of 98-201a, with bright red heated terra rossa clasts and phytoliths (arrows). **g.** Scan of hearth remnant in thin section of 98-223a (J24b; -520 cm), which consists of extensive nodular phosphate but also bone and several burned terra rossa clasts with seed coats and charcoal scattered throughout. The blurry nature of this combustion feature is likely a result of bioturbation and/or trampling, but it is elusive because of diagenesis. FTIR analyses of sediments revealed a variety of minerals, including L, CLT, OT, CL, M, and A (samples: 1500, 1501, 1503, 1510, 1549, 1559). PPL. **h.** Photomicrograph of 98-223a, with large terra rossa clasts overlying a bone fragment in the lower right that exhibits unusual crystal forms and composition (not determined here). PPL; scale is 1 mm. **i.** Same as (h) but in XPL. Curious is the freshness of the terra rossa grains and the contrast with the diagenetically altered bone fragment and non-calcareous matrix. XPL; scale is 1 mm. **j.** Thin section scan of hearth sample 97-124 (K24b; -492 cm) (see below for more details). Reddish-yellow apatite occurs at the base, with overlying phosphatic ash. PPL. **k.** Photomicrograph of 97-124 with phosphatic ashes and some bones at left, along with abundant Mn staining (black 'dots'), and organic matter. PPL; scale is 1 mm. **l.** Photomicrograph of 97-124, showing phytoliths (arrows) within a matrix of apatitic ashes (isotropic in XPL). PPL; scale is 200 µm. **m.** Scan of thin section of 98-225a (K24b; -510 cm) from one of massive reddish layers on the East Profile. Note the pale brown colour, domains or reddish staining, and large Mn stain in the centre. This aspect is reflected in the FTIR analyses from this square at depths of -505 to -520 cm, which indicated L, CL, L, A, and CLT, with some Mn (samples 1509, 1516, 1522, 1523, 1542, 1546, 1547, 1550, 1551, 1560, 1561, 1903, and 1905). PPL. **n.** Photomicrograph of 98-225a, which is somewhat reminiscent of sediments from the exterior, with an isotropic, silty groundmass containing seed coats, some charcoal, and wood fragments. Yellow phosphatic lenses and rounded grains appear to be apatite. PPL; scale is 500 µm. **o.** Detailed view of (n), showing pale brown matrix and aggregates. PPL; scale is 200 µm. **p.** Same as (o) but in XPL. The birefringence and b-fabrics of some of the aggregates suggest that they are clay or clay transforming. XPL; scale is 200 µm. **q.** Scan of large thin section (140 × 90 mm) of 94-26 (K24d; -415 cm) from the red layer in the East Profile, with extensive burrowing and Mn staining. This yellowish-red, powdery silt exhibits vertical apatitic veins and matrix, Mn-stained bone, and voids (FTIR samples 646 and 647). PPL. **r.** Photomicrograph of 94-26 exhibiting a loose, granular, and bioturbated mixture of numerous, sand-sized bone fragments (some possibly burned), seed coats, and Mn impregnations. PPL; scale is 1 mm. **s.** Thin section scan of sample 00-518 (L24d; -405 cm) from the East Profile, consisting of sterile, partly phosphatised, reddish silty clay with veins of apatite and Mn. Many bone fragments. Note chert flake in the centre. PPL. **t.** Scan of thin section of 96-35 (J24a; -467 cm) from a phosphatic halo near the South Profile, comprised of silty clay and some terra rossa clasts, along with many fine phosphatic nodules. Small insect burrows provide the vughy porosity. FTIR samples of sediments at -467 cm revealed A, VT, M, CL, and OC.

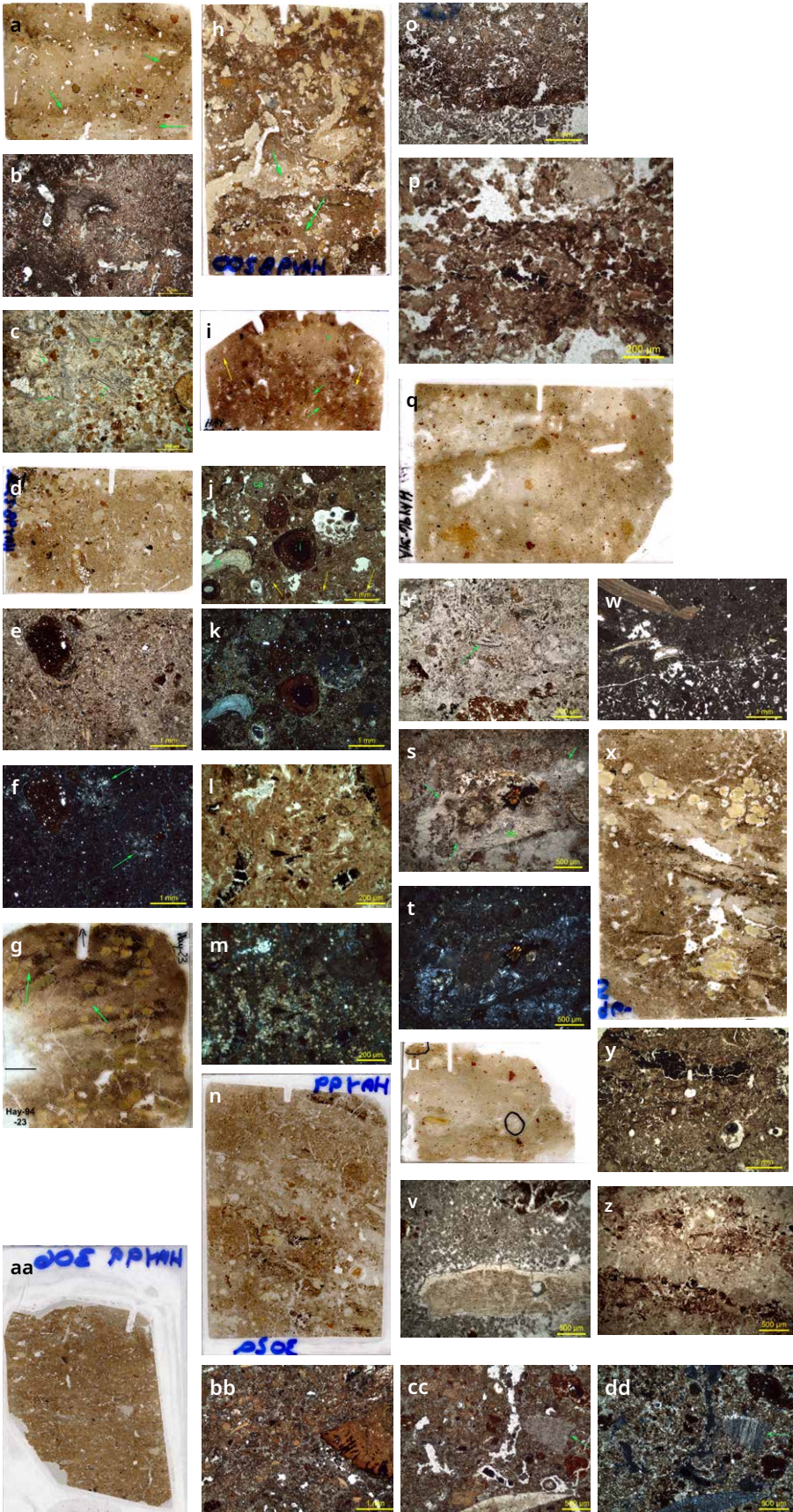


Figure 2.31. Layer E, Northeast and North Profiles. **a.** Scan of thin section of 98-228a (I20a; -520 cm), consisting of compact to cemented stratified thin hearth lenses, partly disturbed by rodent and insect burrows. Section -228a from the upper part is comprised of yellow and whitish bioturbated ashes mixed with rubified clasts of terra rossa (~1 cm-diameter passage features are shown with arrows). The ashes are replaced by apatite, with FTIR analyses at this location of A and Cl (samples 1538, 1545, and 1558). PPL. **b.** Photomicrograph of the basal, whitish zone in 98-228a (a). Much of the lighter matrix is the remains of ashy materials from a former combustion feature, including phosphatic ashes and numerous phytoliths (see a-2). PPL; scale is 1 mm. **c.** Detail of ashy portion of 98-228a, showing numerous phytoliths (arrows) in a phosphatic ash matrix. PPL; scale is 200 μm . **d.** Thin section scan of 98-230a, adjacent to 98-228, illustrating a mixture of bright red terra rossa clasts, bone fragments (note the burned spongy bone at the centre base), charcoal, and aggregates of yellow and white ash. The lack of intergranular porosity suggests that these are the remains of one or more trampled hearths. PPL. **e.** Photomicrograph of 98-230a, displaying compact phosphatic ashes with bone and a large clast of heated terra rossa in upper left. PPL. **f.** Same as (e), but in XPL. Visible here is quartz silt and some domains of concentrated apatite crystals (arrows). **g.** Scan of thin section of 94-23 from close to the North Profile (H18c, -515 cm). Visible here are the faint remains of thin hearths punctuated by yellow-brown nodules of opal and millimetre-sized insect burrows (arrows). Scale bar is 1 mm. **h.** Scan of thin section of 98-200 (I21c; -500 cm). Arrows point to passage features (burrows). Yellow nodules at the top are likely apatite (FTIR from sample 1307, yielded CL and AP). Darker domains are remains of organic-rich parts of hearths but badly modified by bioturbation. Note aggregates of bright red clay. **i.** Thin section scan of 97-129 (K21c, -497 cm) from the northeast corner of the Central Area. Reddish-brown sediment comprised of calcareous ash clumps (a), charcoal, microfauna, burned and calcined bone (green arrows), and reddish terra rossa clasts, all with fine apatite cement; FTIR (sample 1401) yielded apatite and clay. This is essentially a bone and ash mashup, likely produced by trampling. The sediment is quite porous from bioturbation, and numerous passage features are evident (yellow arrows). PPL. **j.** Photomicrograph of 97-129, with rounded grains of bone (b), iron concretion (i) in centre, and calcite-rich grain in the upper left (ca). PPL; scale is 1 mm. **k.** Same as (j) but in XPL. Note that calcite is absent in the upper right part of the photo and in other domains where decalcification has occurred. XPL; scale is 1 mm. **l.** Photomicrograph of 97-129, showing tightly packed fragments of charcoal, bone, and calcite/ash silt. PPL; scale is 200 μm . **m.** Same as (l), but in XPL. Note the scatter of calcite, which is undergoing dissolution. XPL; scale is 200 μm . **n.** Thin section scan of 99-302a (H19a; -487 cm) showing thin, ~1 mm-thick streaks of white ash punctuated many types of phosphatic concretions (grey, greenish-yellow, yellow) and 1–3 cm-diameter insect burrows filled with soft, brown, silty clay. FTIR of a white nodule (sample 373) indicated opal. PPL. **o.** Photomicrograph of darker organic-rich band in upper right part of 99-302a. This is one of many thin remnants exposed in the North Profile. Within the band are vestiges of yellow-brown organic tissues. Siliceous seed coats are visible in the whitish band at the base. PPL; scale is 1 mm. **p.** Detail of band shown in (n), with sand-sized remnants of charcoal in the middle and darker brown organic-rich silty clay. PPL; scale is 200 μm . **q.** Scan of thin section of 96-34a (I19c; -480 cm) of massive, hard, cemented, bedded phosphatic ashes containing rounded bright red terra rossa clasts with quartz silt inclusions. FTIR analysis of sediment sample in this square at -497 cm revealed apatite, which occurs in the thin section as radiating crystals. PPL. **r.** Phosphatic ashes in sample 96-34a, with phytoliths (arrow) and clasts of terra rossa. PPL; scale is 500 μm . **s.** Photomicrograph of a thin section of 96-34b, with large bone (bo) and radiating apatite crystals (arrows). PPL; scale is 500 μm . **t.** Same as (s) but in XPL. The radiating crystals of blue apatite are more evident and striking in this view. XPL; scale is 500 μm . **u.** Scan of thin section of 95-17 (J21a; -443 cm), consisting of bedded whitish and greyish cemented calcitic ash with calcined bone and numerous bright red terra rossa clasts. PPL. **v.** Photomicrograph of calcareous ashes and large bone fragment in 95-17. At the top is a terra rossa fragment. PPL; scale is 500 μm . **w.** Detailed view of bone fragments in centre, amidst calcareous ashes and terra rossa clasts. In the upper left is a well-preserved snail fragment. PPL; scale is 1 mm. **x.** Scan of thin hearth sequences in a thin section of 96-5 (H18c; -435 cm), where thin stringers of organic matter and charcoal are overlain by apatitic ashes and pierced by insect burrows and phosphatic nodules. PPL. **y.** Photomicrograph of finely bedded charcoal and ashes from middle part of a thin section of 96-5, beneath a large void. PPL. **z.** Detail of finely bedded and dispersed charcoal in diagenetically altered (apatite) ashes. PPL; scale is 500 μm . **aa.** Scan of thin section of 99-306 (K20d; -172 cm) from the area above a fallen stalagmite atop the section in the northeast corner of the Central Area. It is comprised of a homogenised mixture of cemented clay silt with many bone fragments, terra rossa clasts, and some gastroliths. It is probably trampled hearth material. PPL. **bb.** Photomicrograph of 99-306, showing a heterogeneous—and slightly bedded—compact mixture of bone, reddened terra rossa clasts, fine charcoal, possible seeds, and phosphatic ash, and cemented with microsparite, which also fills small fissures. Note the large bone at right. PPL; scale is 1 mm. **cc.** Slightly enlarged view of 99-306, with angular chert flake at the base, charcoal, a terra rossa clast, and an angular clast of flowstone (arrow). These components appear to have been mixed and compacted by trampling. PPL; scale is 500 μm . **dd.** Same as (cc) but in XPL. The fibrous nature of the flowstone clast and the microsparitic cement is clearer in this view.

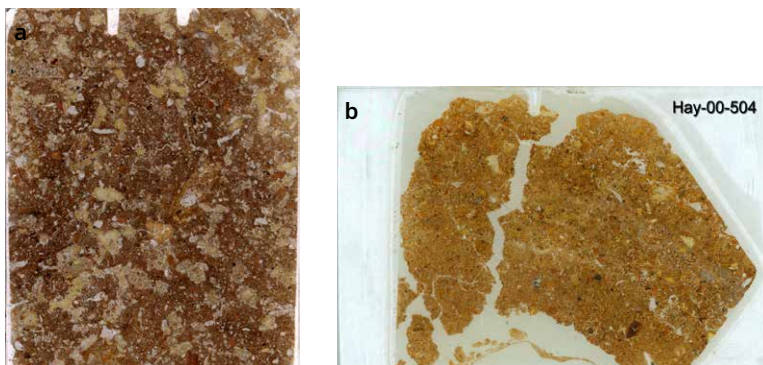


Figure 2.32. Micromorphology of the West Profile. **a.** Thin section scan of 99-333b (H22b; -485 cm, Layer F), consisting of silty clay with yellow nodules (montgomeryite?); some darker silt-sized flecks of charcoal are dispersed throughout. Note the numerous insect burrows filled with loose, lighter-coloured, silty sediment. FTIR sample 1662 from -409 cm and above revealed M and OC. PPL. **b.** Scan of thin section of 00-504 (H24a; -200 cm; Layer E) from the upper part of west section, showing compact mixture of bone, terra rossa clasts, and veins of apatite. This sample is very similar to 99-306 from above the fallen stalagmite in the East Profile. PPL.

and 10YR). As noted above and in Figures 2.18 and 2.19, only partially preserved hearths (most often black organic lenses) occur in Layer F in the Central Area, and they are particularly situated within the upper part of the Layer (see chapter 3).

In contrast, Layer E contains numerous hearths of different morphologies, ash concentrations, and, locally, areas rich in bone. It highlights the fact that the majority of the sedimentary input at Hayonim is anthropogenic, whether present as intact hearths or as those that have been modified by post-/syn-depositional factors (e.g., trampling, dumping, chemical diagenesis) (see chapter 3).

On the other hand, these anthropogenic units are also interbedded with two prominent bands of what appear to be geogenic reddish clays (Figures 2.20, 2.21). The red clay ultimately is derived from red soils outside the cave and was transported either from the entrance or from the chimney. However, the fact that the red clay does not appear to dip away from the chimney nor thicken in this direction suggests that the source is toward the entrance of the cave. The mode of accumulation and how the clay was transported into the cave is not clear (e.g., mudflow or sheetwash), since the clay is mixed with anthropogenic elements that have likely been homogenised by trampling or possibly dumping of materials. Nevertheless, the red clay constitutes a distinct layer that is between ~20 and ~50 cm, indicating that it represents a major change in depositional style, with a decrease in firemaking activities.

Ubiquitous components in the deposits, but volumetrically minor, are bright red (heated), millimetre-sized grains of terra rossa which are scattered throughout the profile but are particularly concentrated in ash lenses. This association of ash and red terra rossa clasts is not immediately obvious. However, during fieldwork, clumps of soil could be found adhering to roots of modern bushy/grassy vegetation, and when heated, these became bright red. Thus, a reasonable hypothesis is that they are linked in some way to the fuel, either with grasses possibly used to start the fire, or as material adhering to the roots of the bushes and grasses (Albert et al. 2003; Meignen et al. 2009).

Calcite is a noticeable component of Layer E and occurs in a variety of forms. These include:

- Cemented ash lenses and bedded calcareous ashes from hearths and dumps.
- Calcite/travertine, which increases from the base upward, as does the degree of phosphate diagenesis in the central axis of the Central Area. This would point to

increased wetness, and increased input of bird and/or bat guano. On the other hand, as we observed for some samples in the Central Area (Figure 2.29 j, k) some apatitic diagenesis took place later in the sequence, well after the LMVS style of diagenesis occurred. It is also notable that the upper part of the MP is situated toward the rear of the cave, which was likely damper than toward the entrance of the cave, which was drier (during Layer E), more evaporative, and more calcareous. In effect, phosphatic layers in the South Profile of the Central Area have their equivalence in the calcareous sediments in the Deep Sounding. Moreover, the phosphatic facies in the Middle Palaeolithic reaches elevations of -150 cm in GHJ17; the equivalent stratigraphic units in the middle part of the Central Area are travertines; in the south part, they are phosphatic to -300 cm and have been truncated by Natufian activities.

- Layered carbonates in flowstone and stalagmites. In J and K20, a piece of fallen stalagmite >1 metre in diameter was found on its side; however, its correlation with other Middle Palaeolithic deposits is not clear because it was not completely excavated and continues into the wall. In any case, the underlying layers pre-date the age of the travertine of $155.3 \pm 2.9 - 1.4$ ka (Mercier et al. 2007).
- Carbonate-cemented clays. These 'brecciated' deposits are found typically in proximity to the travertine (features along GH22–24, and in K20) and appear to interfinger with the travertines. We also noted a breccia deposit rich in bones outside of the present-day dripline, which is also an effectively drier setting. Nevertheless, it shows that cementation can occur quite rapidly, leading to good preservation of bone.

Peculiar to Layer F in the northeast part of the Central Area is the surprising presence, in a level otherwise poor in archaeological material, of two very dense concentrations of flint artefacts (numerous flakes and a few worn flint cobbles). These occurred between -585 cm (the floor) and ~-565 cm, and one extended into J19 (Figure 2.23 d), the other into J22. Within these localised 'pockets', lithics exhibit varying degrees of freshness, ranging from chunky pieces with alternative abrupt retouch to pieces that are completely fresh. They are piled in place and present no preferred orientation. The lack of any channel-like features and referred orientation of the flints would rule out transport within a channel. The most likely interpretation is that these concentrations correspond to flint knapping areas, locally disturbed by the effects of dripping water (edge damage), which also partially winnowed out some of the fine fraction.

In contrast to Layer F, bone is much more abundant in Layer E, but it is localised only in favoured positions, generally in proximity to the travertines and other calcareous deposits. Thus, for example, no bone was recovered from the linear, trough-like zone trending northwest-southeast from K24 to H19 (see Stiner 2005: Fig. 4-7; Meignen et al. 2010). As at Kebara, bone distribution is tied to diagenesis and similarly the distribution of calcite deposits (Weiner, Goldberg, and Bar-Yosef 1993) (see also chapter 4).

Stratification in Layer E is not uniform and is less well defined than in the finely bedded and laminated sediments of Layer F, both in the Deep Sounding and Central areas. This statement is particularly true for the ashy/burned anthropogenic deposits, which tend to be laterally discontinuous. In addition, many of the hearths have irregular boundaries and appear 'broken' into fragments. Moreover, the deposits between individual hearth structures consist of homogenised combustion products, being mixtures of clay, charcoal, and locally bone. As such, these inter-hearth deposits likely represent trampled areas/zones (see chapter 3).

For most of the Central Area, the deposits in Layer E are horizontal. However, north of 21, they can be seen to dip increasingly to the northwest, specifically toward the back of the cave (Figure 2.21 f, g). Moreover, stratigraphically upward, the dips appear to both increase and rotate slightly toward the northwest. These dips are related to subsidence in the rear of the cave into a presumed karstic depression. In a number of prehistoric caves in Israel (e.g., Kebara, Tabun), chimneys and vaults in the roof of the cave are mirrored by subterranean karstic basins in the bedrock ('swallow holes'). In the case of Hayonim, the buried, inferred depressions would be broadly situated beneath the chimney at the rear of the cave, which is in line with the dip direction of Layer E (Figure 2.2).

2.3 Final comments and synopsis of Hayonim deposits

The stratigraphy and sedimentology of the deposits in Hayonim Cave are complex, and our task to decipher and interpret them has been made difficult by a number of factors. These include lateral (localised) variations in composition, texture (e.g., between the Deep Sounding and Central Area), and the widespread presence of diagenesis, which has modified the original nature of the sediments (composition, fabric), particularly for the anthropic sediments in the Central Area.

Nevertheless, we can highlight a number of points that come from field and laboratory (micromorphology, FTIR) data. The lowermost layers at Hayonim in both the Deep Sounding and Central areas (Layers G and F, although G is poorly exposed and only in the Deep Sounding) largely consist of phosphatised silts and clays. Although direct physical connection between the two areas is not visible, it is reasonable to conclude that Layer F in both locales is the same stratigraphic unit that accumulated by the inwashing of silty clay, which is now largely modified by diagenesis. Generally wetter conditions are evident during and pene-contemporaneously with the sedimentation, in order to produce the large-scale mineralogical transformations that epitomise Layer F. Conditions changed, however, with the erosion of Layer F, which is particularly marked in the Central Area. The inclination of the erosional surface toward the interior of the cave suggests subsidence in that direction, which is needed to produce the relief necessary for this erosional episode(s).

The style of sedimentation in the cave changes with the onset of Layer E, which is characterised by the substantial increase in anthropogenic sediments, namely intact combustion features and those that have been modified or displaced by human activities, such as trampling, dumping, and rakeout. We do note, however, that some intact fireplaces do occur in the upper part of Layer F in the Central Area, but their presence—and no doubt others that are not clearly discernable—have been masked by diagenesis. In fact, as we point out here and in chapter 3, the vast majority of Layer E in the interior is anthropogenic, with relatively few contributions of geogenic sediments; the exception is the reddish layer exposed in the lower part of Layer E. It appears that the accumulation of the deposits of Layer E represent a period when overall conditions in the cave were drier, as we do not observe any reworking of sediments by flowing water. On the other hand, the concentration of diagenetically altered sediment along a northwest axis in the cave mirrors the orientation of the roof (northwest/southeast), suggesting dripping water along this alignment, which would also serve as the pathway for bats and birds (note the abundance of gastroliths). Nevertheless, an interval of wetter conditions is signalled by the formation of flowstone and a large stalagmite in the upper part of the Layer E as excavated here. Remains of similar calcareous deposits are poorly exposed on the west side of the cave at about the same elevation as that in the northeast corner of the Central Area.

Localised sedimentation is visible toward the cave entrance, where we observed an elongated trough that appears to mirror the former dripline of the cave. Here, the sediments are largely calcareous and represent a mixing of Middle Palaeolithic and Kebaran material resulting from water dripping off the former brow of the cave. As we did not study the Natufian deposits that cap much of the sequence near the cave mouth, non-systematic observation of these deposits are calcareous with little diagenesis, suggesting overall drier conditions.

There is a striking similarity in the Middle Palaeolithic sedimentary records and chronology between Tabun and Hayonim Caves. As previously pointed out by Mercier et al. 2007, both show major gaps about the same time, in the latter part of MIS 7: between Layers D and C at Tabun and Layers F and E at Hayonim. Furthermore, both lower units (Tabun D and Hayonim F) are marked by strong diagenesis that occurred under wetter conditions and are followed by erosion and deposition (both increasingly anthropogenic) associated with drier conditions.

Fire use and cave occupations by Early Middle Palaeolithic humans in Hayonim Cave

Liliane Meignen and Paul Goldberg

3.1 Introduction

It is difficult to deny the notion that fire has played a significant role in human development, and the past use of fire continues to be a very active area of research in prehistory. Its benefits and uses have been extensively discussed in numerous publications (e.g., Aldeias et al. 2016; Aldeias et al. 2012; Alperson-Afil 2008; Bellomo 1993; Karkanas 2021; Meignen, Goldberg, and Bar-Yosef 2007; Rowlett 2000) and there is no need to review these here. On the other hand, fires and the resulting hearths/combustion features and products are somewhat atypical features in the earlier part of the archaeological record, as they are short-lived (virtually instantaneous in terms of 'Palaeolithic time' goes) and thus can provide high-resolution temporal records of hominid actions/activities (Goldberg and Berna 2010).

The control of fire undoubtedly brought about a number of advantages to human groups (e.g., warmth, light, food processing, heating for technical purposes) and its advantages have been discussed elsewhere (e.g., Mentzer 2016; Roebroeks and Villa 2011; Rosell and Blasco 2019; Stahlschmidt et al. 2015). On the other hand, within human habitats, fire is largely considered the element around which all of the organised activities in the social space of the group are structured. Fire plays a pivotal role in the apparition of social interactions as evidenced by hearth-centred activities as seen as early as the Late Lower Palaeolithic in the site of Qesem (300 ka) (Blasco et al. 2016; Shahack-Gross et al. 2014). In this regard, it is considered as the emergence of true domestic spaces where food was brought in, shared and consumed (e.g., Kuhn and Stiner 2019).

Similarly, the duration of occupation of a site is reflected by a number of facets related to hearths. These include the density of combustion structures, their degree of use (permanent, repetitive, ephemeral), the location of these structures in the inhabited space, as well as the generally structured organisation of human activities around these features. The study of combustion structures is therefore an integral part of research on the behaviour of hunter-gatherers during the Middle Palaeolithic. It informs us about the nature of the human occupations, and therefore indirectly about the function of a site within its region. Over the past few decades, detailed field observations coupled with microstratigraphic and microanalytical analyses at sites in Europe and the Near East have provided significant insights into Neanderthal use of space through time (Aldeias

et al. 2012; Courty et al. 2012; Goldberg et al. 2012; Henry 2017; Henry 2012; Mallol, Cabanes, and Baena 2010; Mallol et al. 2013; Meignen et al. 2009; Meignen, Goldberg, and Bar-Yosef 2007; Vallverdú-Poch and Courty 2012).

In the Near East, the repetitive use of fire is known only in some rare Acheulean sites, as for example, Geshert Benot Ya'akov (Alperson-Afil, Richter, and Goren-Inbar 2007; Goren-Inbar et al. 2004). However, it is only from the second part of the Middle Pleistocene onwards that the systematic, repetitive use of fire is confirmed in Europe as in the Near East (Roebroeks and Villa 2011).

The earliest and most direct examples of hearths are described from Qesem Cave, where the repeated use of a central hearth was identified in a layer dated to ~300 ka (Blasco et al. 2016; Karkanas et al. 2007; Shahack-Gross et al. 2014). Evidence of heating of lithics from Tabun occurs as early as ~350–325 ka with abundant burning features occurring much later in Layer C (Jelinek et al. 1973; Shimelmitz et al. 2014a). Hearths occur at Hayonim Layer G (>250 ka), and a little bit later in the Early Middle Palaeolithic of Misliya and Hayonim Layers F/Lower E (Goldberg and Bar-Yosef 1998; Weinstein-Evron and Zaidner 2017).

Nevertheless, it is only later, from MIS 5 onward, that fire became an integral part of the technological repertoire of the human lineage, with a steady increase in MIS 4 and 3. This is illustrated in the region by a set of Middle Palaeolithic sites in which large accumulations of combustion features are visible, attesting to the use of fire over long periods (e.g., Kebara; Berna and Goldberg 2008; Goldberg and Bar-Yosef 1998; Meignen et al. 2009; Meignen, Goldberg, and Bar-Yosef 2007). These observations clearly indicate that Middle Palaeolithic hominids in the Near East had the capacity to manufacture, maintain, and transport fire. However, despite the fact that the systematic use of fire is well established and widespread in MIS 5 and later (Roebroeks and Villa 2011), we must caution that there are significant differences in the quality of the documenting of these fire-related activities from region to region, even for later periods (Murphree and Aldeias 2022).

The Mousterian deposits in the Near East are most often very anthropogenic in nature and correspond to large accumulations of sediments associated with and derived from combustion structures (e.g., Albert, Berna, and Goldberg 2012; Goldberg 2003; Goldberg and Bar-Yosef 1998; Goldberg et al. 2007; Meignen, Goldberg, and Bar-Yosef 2007); at Kebara and Tabun these are often stacked and attain thicknesses of cm to tens of cm. They commonly show good preservation of couplets consisting of lower 'organic black levels' underlying 'white ash levels'. In less favourable instances, deposits consist of large accumulations of ash, and ash-rich remains derived from the modification of combustion features (see references above). In any case, ash is a major component of the deposits.

In Southwestern Europe, on the contrary, the levels rich in combustion structures are present in few sites, and they are often interspersed with levels of geogenic sediments (e.g., Roc Marsal, Pech IV Layer 8, El Salt, Abric Romani; [Aldeias et al. 2012; Dibble et al. 2018; Mallol et al. 2013; Vallverdú et al. 2012]). Thus, combustion 'deposits' (*sensu lato*) constitute only a small part of stratigraphic record. Marked accumulations of superimposed hearths are rare and generally not very thick. At Roc de Marsal, for example, the thickness of the layers with the most hearths, Layers 9 and 7, are 5–10 cm and 5–8 cm, respectively; at Pech de l'Azé IV, Layer 8, which is ~40 cm thick in total, individual combustion features are sparse and only 1–2 cm thick. Intact fireplaces are often isolated, even in sites where they are relatively abundant (e.g., El Salt unit Xb, 10–14 cm thick, with 46 recognised combustion structures); at Abric Romani they are generally ~1–3 cm thick (Vallverdú et al. 2012). Furthermore, the ash levels are rarely preserved, and often only the organic black levels remain (Leierer et al. 2019; Mallol et al. 2013). In any case, they tend to be rather thin, a few centimetres in thickness (Roc de Marsal, El Salt, Abric Romani). Thus, within the entirety of the stratigraphic sequences of the Near East, the proportions of anthropogenic deposits are greater and the structures often better preserved than those of Western Europe, at least from the standpoint of 'black organic/white ash' couplets.

The essential questions are whether these differences result only from conditions of preservation (rapidity of burial/covering of the hearths), or the presence/absence of post-depositional phenomena of geological origin, such as dispersion by water, solifluction, or diagenesis. Alternatively, do they reflect real differences in the recurrence of combustion activities, or in the type of combustion? If so, what is the significance of these factors in terms of the type of occupation of these locations?

In the first instance, the weak presence of hearths with preserved ashes in Mousterian sites in Western Europe, for example, must have been the consequence of post-depositional phenomena (e.g., dispersion by trampling or water, diagenesis, cryoturbation, solifluction), which would have led to the disappearance of numerous hearths. The presence of numerous burned flints and bones, and scattered wood charcoal within certain deposits would be the ultimate evidence for the use of fire. However, in other sites where taphonomic conditions are more favourable (e.g., La Combette, Vaucluse, France; Texier et al. in Buisson-Catil [1994]), burning features are never as abundant as those at Kebara Cave, for example. The second case, which supposes the existence of good conditions of preservation, as well as the effects of intense and repetitive activities associated with fire, has been observed in some sites such as Kebara, for instance (Meignen, Goldberg, and Bar-Yosef 2007)

These hypotheses, and especially the meaning of such fire accumulations, should be tested through the sequence of human occupations at Hayonim. In this chapter, we concentrate on the hearths and combustion features at Hayonim and the information they can provide about human occupation of the site, their activities, and roles in site formation, and use of space at the site.

3.2 Methodology

Hearths have been the subject of ‘anthropological’ literature for some time (e.g., Binford 1981; Blasco et al. 2016; Gowlett et al. 2005; Isaac 1982; Movius 1966; Preece et al. 2006). However, studies of their components and their detailed ‘internal’ analysis and organisation have been understudied, only until the last two or three decades. Many of these investigations have been done by geoscientists and archaeologists with a scientific archaeological orientation (e.g., Albert et al. 2003; Albert and Cabanes 2007; Aldeias et al. 2012; Bellomo 1993; Courty 2017; Courty, Allue, and Henry 2020; Courty et al. 2012; Goldberg et al. 2012; Goldberg, Miller, and Mentzer 2017; Goldberg et al. 2009; Mallol and Henry 2017; Mallol et al. 2013; Mallol et al. 2007; Mallol, Mentzer, and Miller 2017; Mentzer 2002; Mentzer 2011; Mentzer 2014; Mentzer 2016; Vallverdú et al. 2012; Weiner 2010), among others too numerous to cite here. Although some of the earlier studies were aimed at evaluating the detection and early use of fire, more recent ones deal with broader issues relating to human history, such as use of space, frequency of occupation, hearth technology and function, and source and use of combustibles (see above list). They have also employed a group of analytical techniques and strategies that include micromorphology, FTIR/micro-FTIR, micro-XRD and -XRF, organic petrology, lipid biomarker analysis and compound specific isotope analysis, fire experiments (Leierer et al. 2019; Mallol, Mentzer, and Miller 2017; Mentzer 2014; Mentzer 2016; Mentzer and Quade 2013). As an ensemble, this use of such a suite of techniques has been effective in elucidating issues such as the timing and ‘intensity’ of Middle Palaeolithic occupations and importation of fuels.

In any case, the first and critical step is to start with detailed macroscale observations in the field (Goldberg, Miller, and Mentzer 2017; Mentzer 2016). It is here where one can scrutinise the composition of the sediments, such as ash, charcoal and organic content, and heated materials (e.g., bone, lithics). Other aspects can also be noted, such as dimensions and shape of a feature (if present) and its structure. Is there an internal organisation of the components? That is, can we observe a well-defined hearth consisting ideally of a sequence of substrate, charcoal-rich layer overlain by ashes (although see Mallol et al. 2013)? Or, does a deposit consist of more massive combustion products (ash, fuel, bone)

that may represent post- or syn-depositional modification of a hearth (e.g., trampling, sweeping, rakeout)? Similarly, how does a hearth articulate with surrounding sediments and features, and are its limits well defined or gradational? Such observations help insure that any further analyses are situated within a well-documented microstratigraphic context (Goldberg and Berna 2010; Goldberg, Miller, and Mentzer 2017).

Nevertheless, in order to study combustion features and their products, further analyses are needed, as field observations alone can be incomplete or misleading. The variety of analytical techniques currently employed were mentioned above and in this study, we used principally micromorphology along with FTIR and micro-FTIR (see chapter 2).

At Hayonim—as at Kebara (Goldberg et al. 2007; Meignen, Goldberg, and Bar-Yosef 2007; Schiegl et al. 1996; Schiegl et al. 1994; Weiner, Goldberg, and Bar-Yosef 1993; Weiner, Schiegl, and Bar-Yosef 1995)—study and documentation of the combustion features were part of a wider geoarchaeological study of the deposits aimed at understanding the geology of the overall site and its site formation processes (Goldberg and Bar-Yosef 1998; Weiner, Goldberg, and Bar-Yosef 2000; Weiner, Goldberg, and Bar-Yosef 2002; Weiner, Schiegl, and Bar-Yosef 1995; Weiner et al. 1995).

The deposits, including the hearths, were monitored and described during excavation as an integral portion of the geoarchaeological study. Detailed notes were also made by L. Meignen as part of the integral strategy of excavation. Finally, copious observations specifically on the hearths were carried out by one of the permanent excavators, A. Stutz, who recorded several aspects of the combustion features. These included:

- Range of depths
- Colour
- Composition, such as ash, charcoal, and bone content; both original mineralogical content and diagenetic alterations were recorded with the aid of in-field FTIR analyses carried out by S. Weiner
- Shape, size, and thickness as they pertained to entire features and patches
- Integrity of combustion features: intact versus fragmented
- Boundaries and articulation with surrounding deposits; evidence of imbrication or superposition of successive hearths were noted
- Degree of compaction: firm, loose, cemented, etc.

These observations were systematically recorded in the so-called ‘Book of Hearths’, allowing us to monitor to the spatial and temporal differences of the combustion features during the course of the excavation. They also partially served as a guide for geoarchaeological and geochemical sampling. These data were compiled for this study and presented according to depth slices (see results below), as clear spatial patterns appeared to emerge according to depth in the depositional sequence.

Over the course of the excavations numerous samples of combustion features and the deposits overall were collected for micromorphological analyses (Figure 3.1).

The sampling strategy consisted of removing intact blocks of sediment, which were securely wrapped to maintain their integrity; at the same time, small loose samples were collected for other analyses such as FTIR, and the position and context within the features and the deposits were recorded.

In the laboratory, the blocks were dried, impregnated with resin, and processed into petrographic thin sections at the University of Texas at Austin (USA), Institut National Agronomique (Plaisir-Grignon, France), and at Spectrum Petrographics (USA). Most thin sections measured 50 × 75 mm, but some made in France were 140 × 90 mm. The thin sections were scanned in reflected light at 600 and 1200 dpi (Arpin, Mallol, and Goldberg 2002) and were examined with stereo and petrographic microscopes at magnifications ranging from 6× to 200×. Plane-polarised (PPL), cross-polarised (XPL) illumination was generally used, along with oblique-incident light (OIL) and UV fluorescence (Altemüller and Van

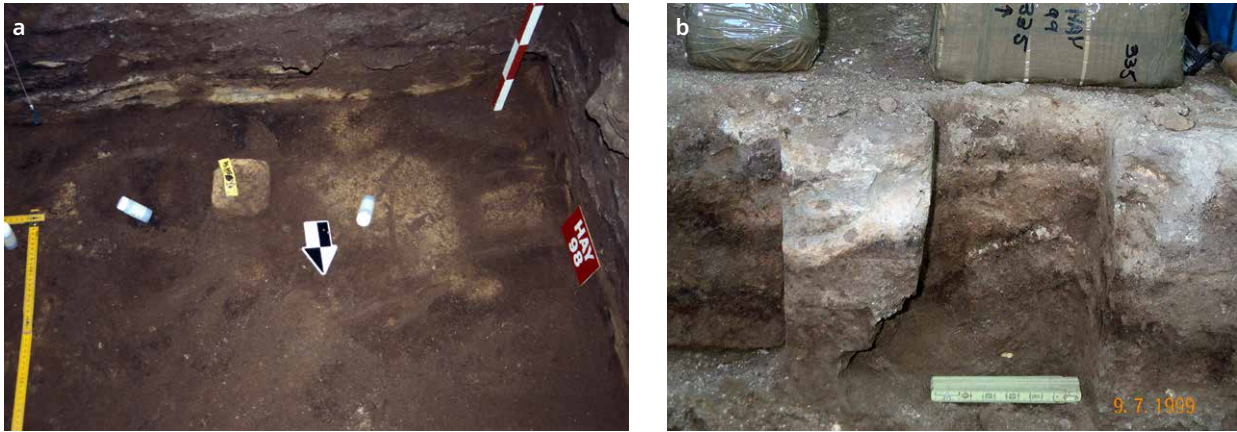


Figure 3.1. Micromorphology sampling. Because of the generally firm consistency of the sediments in the Central Area, blocks for micromorphological analysis were generally cut out from the profile, or from a free-standing sedimentary column, and then wrapped securely with tissue paper and packaging tape. **a.** Block of ashy hearth deposits under the yellow tag after surrounding sediments were excavated. The column is then removed and stabilised with tissue paper and packaging tape. Sample 98-201; I24d, -507 cm. **b.** North profile showing two sampling locales and the associated intact sample blocks, which have been wrapped securely in tissue paper and packaging tape. Sample 99-335; I19d, -540 to -560 cm.



Figure 3.2. FTIR field laboratory at Hayonim, where Steve Weiner is running a sample.

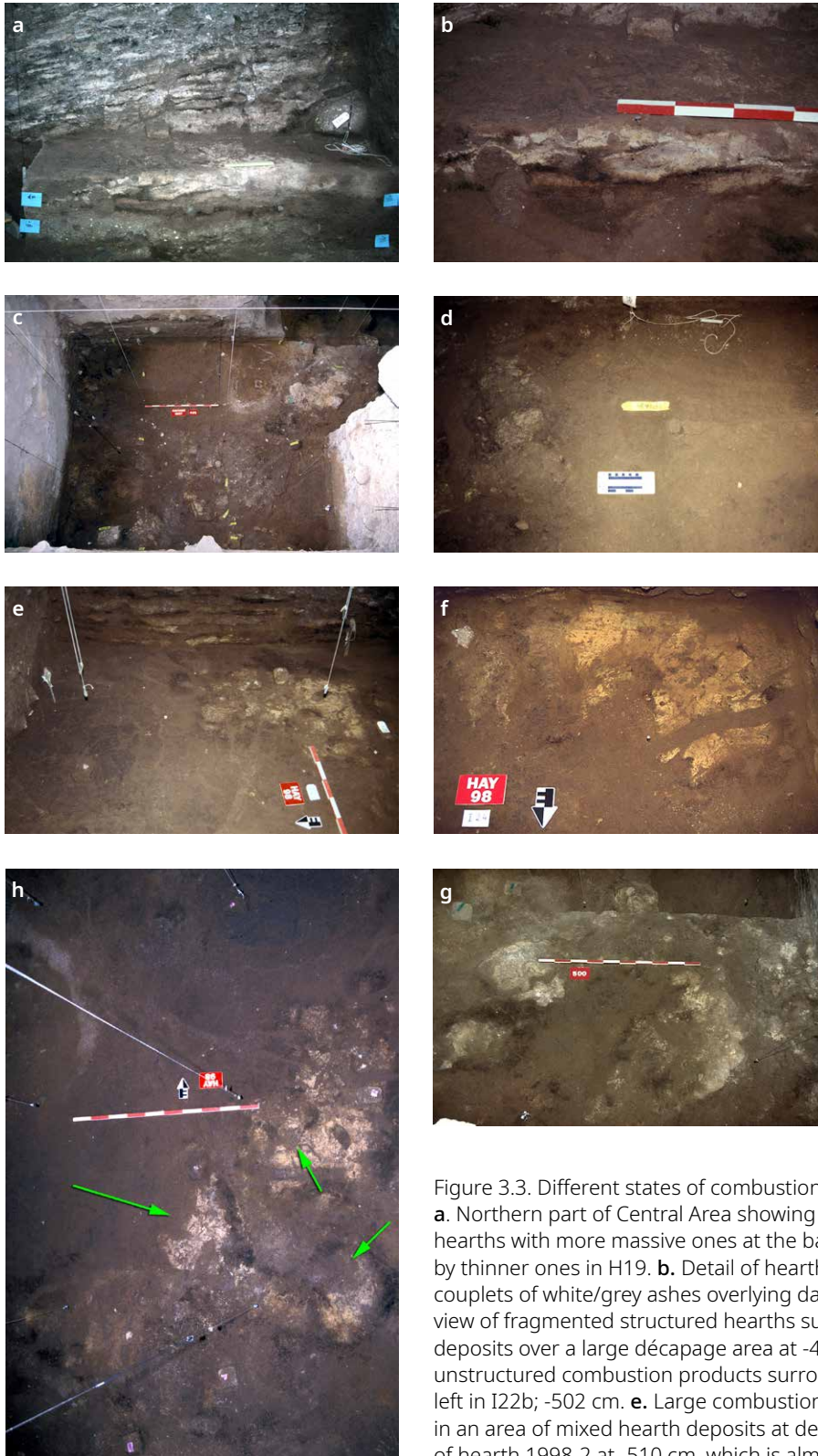


Figure 3.3. Different states of combustion features at Hayonim.
a. Northern part of Central Area showing sequence of superposed hearths with more massive ones at the base (I19 -see detail in [b]) overlain by thinner ones in H19. **b.** Detail of hearths at the base in (a) showing couplets of white/grey ashes overlying darker, organic-rich zones. **c.** Map view of fragmented structured hearths surrounded by mixed hearth deposits over a large décapage area at -495 cm. **d.** Homogenised, unstructured combustion products surrounding structured hearth at left in I22b; -502 cm. **e.** Large combustion feature (hearth 1998-12) in an area of mixed hearth deposits at depth -520 cm. **f.** Field photo of hearth 1998-2 at -510 cm, which is almost complete although the northern (lower part) is homogenised by burrowing and possibly trampling. **g.** Décapage at -500 cm, showing surface plan and detailed photo of northern part with hearths 1997-5, 1997-8, and 1997-10. **h.** Hearth complex in Central Area affected by rodent burrows (arrows).

Vliet-Lanoe 1990; Courty, Goldberg, and Macphail 1989; Goldberg and Macphail 2006; Macphail and Goldberg 2018). Descriptive criteria made use of Bullock et al. 1985; Nicosia and Stoops 2017; Stoops 2021; Stoops, Marcelino, and Mees 2018. FTIR measurements were carried out predominantly in the field by S. Weiner (Weizmann Institute, Rehovot, Israel) (Figure 3.2; see also chapter 2, this volume) on micro-bulk samples (subsamped from ~5–10 ml vials) (Weiner 2010).

These ‘real-time’ results were instrumental in providing an understanding of the nature, composition, and depositional/post-depositional history of the site as we were excavating it. It also provided clues as to the preservation of bones, ashes, and other constituents that allowed us to interpret and sample the deposits more fully, from both the geogenic (*sensu lato*) and anthropogenic points of view (Stiner et al. 2001b). Additional samples were similarly collected for other studies, such as phytoliths, and are reported by Albert et al. (2003).

3.3 Middle Palaeolithic combustion features at Hayonim

Combustion features and their remnants and residues form a prominent part of the Middle Palaeolithic sedimentary fill at Hayonim (Figure 3.3). In fact, anthropogenic deposits constitute over 50% of the present-day volume of the sedimentary fill at the cave above Layer F. Remnants of combustion occur in a variety of forms that include intact structured combustion features (i.e., hearths—organic matter/ash couplets [e.g., Meignen, Goldberg, and Bar-Yosef 2007]), fragmented structured hearths, accumulations of homogenised unstructured combustion products (ash, organic matter, bone), and bedded buildups of ashes (see details below).

Differences are observed according to the spatial and chronological positions of the combustion features inside the cave: in the Deep Sounding, combustion features/products are relatively rare, and most of the deposits are geogenic. Nevertheless, hearths relatively recognisable as such first occur at the top of Layer G at ~795 cm in an Acheulo-Yabrudian context (Figure 2.5c), as shown by the presence of a biface close to the combustion feature. They are rare in Layer F, although traces of a few centimetre-thick hearths do occur (e.g., sample 99-328; F27b, -747 cm).

Layer E within the Deep Sounding itself shows few, if any, intact features (in part due to bioturbation). However, just to the north, bedded accumulations of calcareous ashes are relatively abundant (e.g., samples 97-109, F26c, -450 cm; 00-509, E25b, -315 cm).

In the Central Area, in contrast, combustion remains are much more abundant. Layer F includes a series of hearths, most often isolated lenses spread over the Central Area (JK24, JK23, IJ22) and at different depths (e.g., 99-321, J21c, -567 cm). Generally, ashes are not preserved and only the basal black organic layer was observed. These hearth lenses are thin (most often 3–5 cm) and their maximum diameter is only ~40/50 cm. Some of them are visible along the South Profile (Figures 2.18 and 2.19a, b, c; Figure 3.4). However, in this layer, the sediments are overall diagenetically altered silty clays.

Layer E, on the other hand, exhibits abundant hearths and sediment accumulations derived from them. These are clearly visible at the base of the layer, which varies in elevation from north to south, at elevations from ~510–515 cm along the South Profile to ~530 cm in the North Profile (e.g., J18) (see Figures 2.18, 2.19b, 2.24–2.26). They occur in different forms: intact, well-preserved hearth structures, and those where the combustion components (ash, burned bone, etc.) are preserved as what we call, ‘mixed hearth sediments’ and ‘homogeneous ash derived sediments’ (see definitions below).

Many of the hearth features and deposits are difficult to recognise in their entirety or in their initial state for a number of reasons (see above and chapter 2, this volume). First is chemical diagenesis, which principally involves mineralogical transformations, particularly of silicates (clay minerals) and carbonates (e.g., calcitic ashes). In addition, precipitation of phosphatic nodules—evident in both North and South Profiles (Figures 2.18, 2.26)—has the effect of blurring/erasing the original form of the hearths as seen in the field. Moreover, substantial transformation of calcitic ashes into apatite in



Figure 3.4. Scan of thin section of 99-321, showing thin intact hearth. Size of all thin section scans is 50 × 75 mm, except where noted.

many areas of the Central Area (Figure 2.30 and mineral plots below; see also chapter 4, this volume) makes their identification in the field and in thin section a challenge.

In addition to chemical diagenesis, physical modification of original hearths is common in Layer E. Insect bioturbation, for example, takes place on the order of cm and can result in the partial or total obliteration of smaller hearth features, such as those in the North Profile in H18 (Figures 2.25, 2.26). Larger bioturbation features that tend to be more readily recognisable are rodent burrows (~9 cm in diameter [krotovina]), which are common in prehistoric sites and were documented at Kebara (Goldberg et al. 2007). At Hayonim, they are widespread, and isolated ones can be observed breaching hearths in the North Profile (again in H18). On the South Profile, individual burrows also occur, but more striking is a complex of repeated burrowing that has homogenised some of the sediment of the upper, diagenetic part of Layer E (Figures 2.18, 2.19).

In the Deep Sounding, a similar situation exists for Layer E (Figures 2.5, 2.8), as well as several burrows in Layer F. Remarkable in the South Profile is that the rodent burrows post-date the phosphatisation of sediments in the central part of the section. Burrows can also be seen in *décapage* views of larger hearths (e.g., Figure 3.3), but they can be readily recognised and do not destroy the integrity of the hearths as do the small insect burrows in the North Profile. In thin section, burrowed sediments are readily recognisable and characteristically comprised of loose/porous, fine, granular material with heterogeneous compositions.

Trampling is also responsible for homogenisation of hearth sediments but it is more difficult to recognise this process unequivocally in the field. In general, trampled layers (also at Kebara) are comprised of the remnants of combustion, including ash, organic matter/charcoal, and bone. Trampled sediment tends to be compact and is unlike burrowed material, which is granular with compositions that commonly differ from the surrounding intact, non-burrowed sediment. Thus, at Hayonim, homogenised anthropogenic material situated between and surrounding hearths that lack sharp boundaries and a circular/elliptical shape are interpreted as having been trampled (Figure 3.3). This is borne out in thin sections where trampled deposits are non-granular compacted material, with few intergranular voids (Figure 3.4); void space is typified by vughs, channels, and fissures, for example.

In spite of issues of post-depositional modifications discussed above, we were able to recognise in Layer E in the Central Area numerous, essentially complete, centimetre- to

decimetre-thick structures of combustion/hearths. This allowed us to document diachronic and spatial changes of fire activity throughout the sequence of Layer E, which we present here in this chapter. Hearths in Layer F in the Central and Deep Sounding areas were so few (and where present, diagenetically altered) that we decided to concentrate solely on those from Layer E in the Central Area.

3.4 Combustion features in the Central Area (Layer E)

3.4.1 General characteristics and nomenclature

Hearth features in Layer E typically are readily identifiable by their clear shapes, which delimit them from the surrounding sediments that are largely anthropogenic, as revealed in thin sections. The latter are comprised of mixtures of ashes, charcoal, bone, grains of rubified terra rossa, which have been derived and modified from the original hearth sediments by actions such as trampling and burrowing.

Hearth characteristics are variable within the Central Area and differ spatially and diachronically (i.e., with depth). Therefore, at a particular depth/décapage slice, combustion features and products are more or less abundant, have irregular contours, and are more or less identifiable in the form of multilayered hearths, partially preserved hearths, hearth lenses, ashy lenses, and black organic remnant sediments.

As discussed above, in addition to clearly recognisable hearth structures (i.e., defined outlines, general sequence of couplets with black/dark base overlain by ashes (either calcitic or apatitic), we recognised modified hearths and contents that enclosed obvious hearth features. Field descriptions of the hearths and associated deposits in the Central Area are presented in ‘Descriptions of the principal ‘décapages’.

In this chapter, the terms ‘hearth’ and ‘combustion structure’ are employed in a similar sense, while the term ‘combustion feature’ signifies a more general category that includes hearths and burned materials in secondary position due to human activities or natural processes (Mentzer 2014). Features that appear to have a lower degree of integrity may be termed ‘hearth areas’ or ‘combustion areas’ to distinguish them from those of well-preserved and structured hearths.

In addition to these terms, we employed two additional descriptors for the modified hearth deposits.

‘Mixed hearth deposits’

These represent patchy, partially preserved, partially stratified, and heavily burrowed/trampled concentrations of hearths. Mixed hearth deposits represent zones of recurrent hearth construction and fire production, but they are preserved—where the hearths have not been burrowed or trampled—as homogenous grey brown ashy masses.

‘Homogenous ash-derived sediment’

This kind of sediment includes rare patches of cemented calcitic ash and apatite crusts and veins, but that is otherwise compact to soft silt and clayey silt.

Both of the above, as well as the hearths themselves, contain rubified/burned terra rossa clasts that are commonly rounded.

3.4.2 Methods of excavation and drawing of combustion structures

Décapage excavations were carried out in successive 5-cm slices that followed the inclination of combustion lenses. These were most often horizontal, except very locally in the northwest area. Spatial coordinates for archaeological material (lithic, bones) and all samples were recorded systematically (Paleo 3 software) with a theodolite and saved on the field computer in the cave laboratory. For each décapage, a field drawing was made. In addition, we compiled a set of field photos and noted any samples taken (e.g., micromorphology, phytoliths, and FTIR geochemistry); the latter included analyses made in the field. Associated sediments were sieved and sorted.

Drawings on millimetre paper at a scale of 1:20 were made as soon as we reached levels where the structures became quite large and legible. In the case of complex combustion structures, detailed plans and small sections were successively drawn as and when excavated to record their evolution (e.g., hearth 1998-16). Furthermore, we recorded:

- The contours of the combustion features.
- Information about the deposits around the hearths.
- ‘Geochemical’ information and mineralogy (phosphatic and calcitic concretions and cementation); this information was macroscopically visible in the field and evaluated continually with field-based FTIR analyses. The location of the FTIR samples was noted on the plans.

Such consecutive field drawing made it possible to follow the evolution of the features and their distribution through the stratigraphic sequence. In parallel, the ‘Book of Hearths’ was kept by Aaron Stutz (1997, 1998, 1999), which allowed a more detailed description of the observations made during the excavation of the combustion structures. These descriptions allowed for dynamic monitoring of complex/multilayered structures from one *décapage* to another, an essential complement to plans drawn at systematic depths.

Having noted this, we should mention that, as in many other sites of the Middle Palaeolithic, the identification of the limits of the structures was not easy. This is particularly the case of the combustion structures made up of small levels of thin, lenticular hearths that are frequently superposed and often overlap (e.g., Kebara, Pech de l’Azé IV; Goldberg et al. 2018; Meignen, Goldberg, and Bar-Yosef 2007). In the instance of Hayonim, however, the generally systematic presence of these black/white couplets allowed for the recognition in the field of small, superposed hearths, even though they were often difficult to follow in their lateral extent. Specifically, Stutz noted in the field that:

- It is often difficult to follow a distinct single hearth because the black organic/charcoal component is preserved under grey ash in only small, random patches.
- Because the features are often as thin as 2 or 3 cm, including two or more hearths bedded within a 5 cm level, it is difficult to follow layers during excavation.
- In general, we have tried to describe well-preserved, relatively large portions of hearths in this book, although the actual number of hearth features is at least 3 times greater than what is counted as a hearth feature here.

Similar issues were documented for the combustion features at the sites of Roc de Marsal and Pech de l’Azé IV (see Aldeias et al. 2012; Dibble et al. 2018; Sandgathe et al. 2011).

Additionally, the nesting of many combustion structures at the same depth makes it very difficult to attribute archaeological objects (lithic, bone remains) to one structure rather than another. This problem was also crucially encountered at Kebara (Meignen, Goldberg, and Bar-Yosef 2007), and in fact it occurs in all sites where combustion structures are abundant at the same level (see also Goldberg et al. 2009).

Consequently, we have not been able to undertake a detailed study of the spatial distribution of the lithic and bone material in relation to each combustion feature. Although the material is spatially recorded on plans and profiles, the links between combustion structures/anthropogenic activities can only be discussed in a global sense. Our experience at Kebara led us to comparable conclusions (Meignen, Goldberg, and Bar-Yosef 2007). Attempts at more sophisticated spatial research carried out at Roc de Marsal by Aldeias et al. (2012) highlight this same difficulty and led to this same observation.

3.4.3 Descriptions of principal ‘*décapages*’

For this presentation of the results, we have chosen to select only part of the numerous *décapages* carried out, those that seemed to us to be the most representative of the changes observed in the sequence. For each *décapage*, the most obvious structures were

drawn. Numerous small fragments of structures were identified during the excavation, but were not all reported on the plans (in particular those scattered in the mixed hearth deposits). The combustion structures are therefore undoubtedly more numerous than those documented here.

In the following descriptions, for each *décapage*, we first present a brief description of the overall composition of the *décapage* surface (e.g., mixed hearth deposits, combustion features, hearths, etc.), as well as its mineralogical characteristics (e.g., phosphates/calcite concretions). These geochemical and mineralogical data are based on observations made during the excavation and supported by FTIR analyses carried out simultaneously in the field. Such mineralogical data are grouped by *décapage* and shown as comments to the mineralogical maps (see below); additional discussion can be found in chapter 2, this volume.

Additionally, the main structures are described based on the systematic observations made during the excavation by A. Stutz, who was in charge of this work during the entire project. The use of a single viewer responsible for centralising all of the observations guarantees the consistency of the descriptive criteria and vocabulary employed to define the different structures. Some thick structures persisted throughout several *décapages*. They are therefore represented on several successive planes. We have chosen to describe them where they are best expressed.

Many of the accompanying illustrations that follow comprise a variety of data that vary from figure to figure but generally include a mineral map based on FTIR analyses of S. Weiner, a plan of the *décapage*, photographs of the *décapage* at various scales, and thin section scans.

3.4.3.1 Décapage -530 cm and below

3.4.3.1.1 Mineralogical map (Figure 3.5)

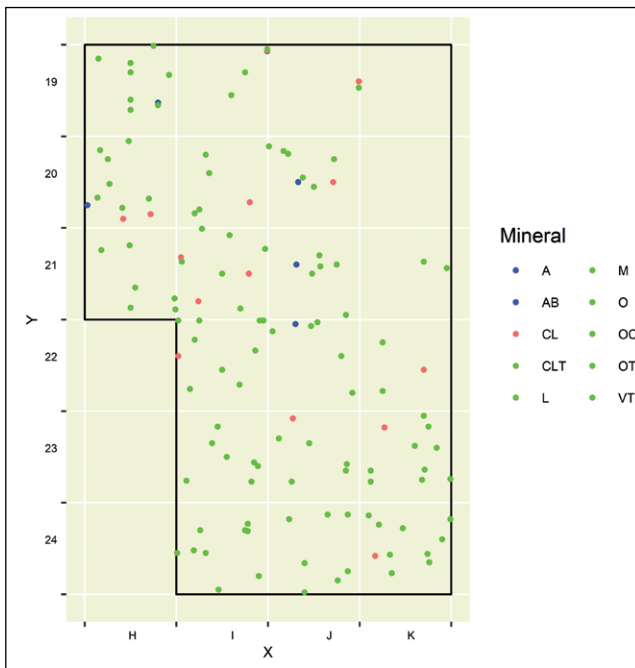


Figure 3.5. Mineral distribution map of FTIR analyses from a combined depth below -540 cm. (This and all mineral maps were compiled by Shannon P. McPherron, MPI, Leipzig). Some calcite/apatite (CD suite of minerals) occur in the northern part of Central Area and grey compact diagenetically altered silty clay + phosphates over the rest of the area, which corresponds to Layer F.

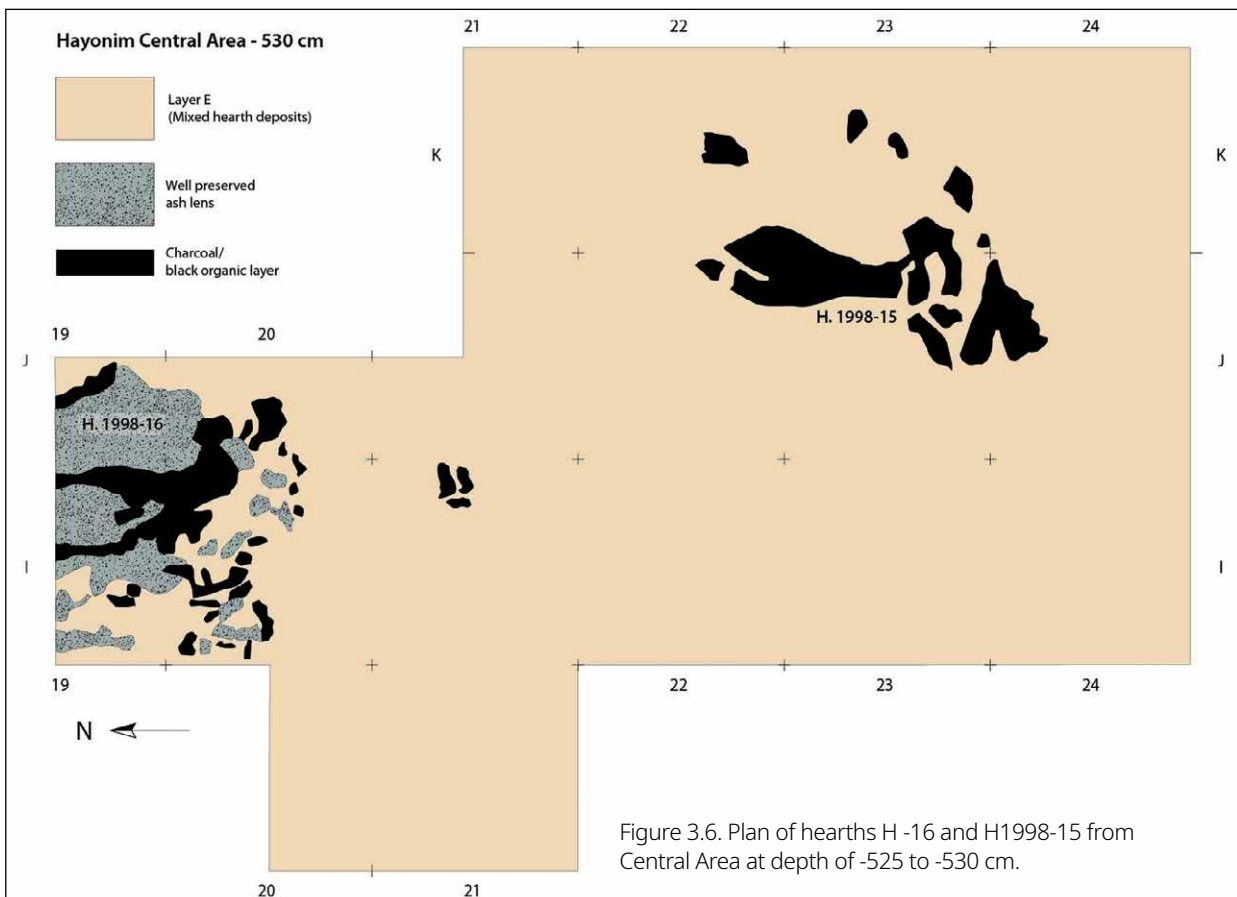
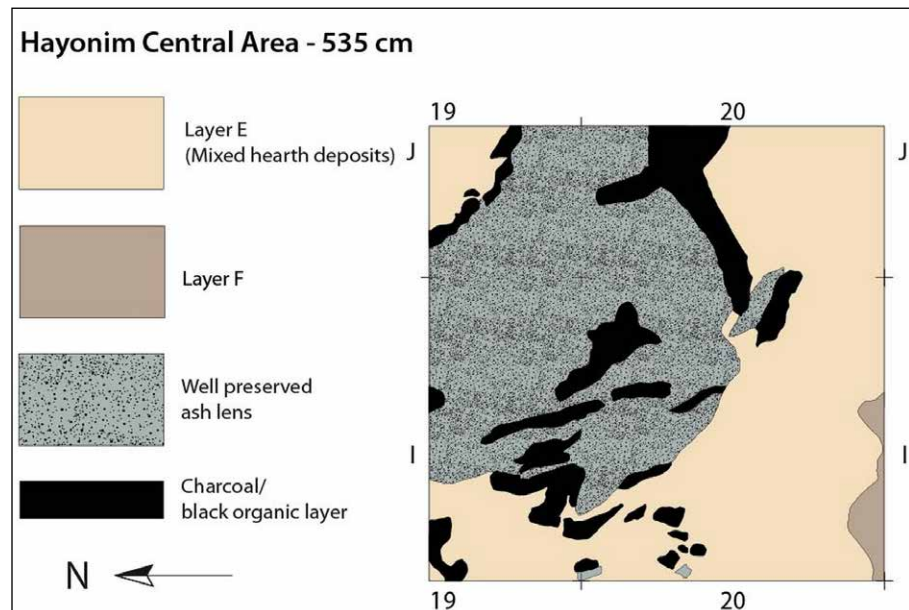


Figure 3.6. Plan of hearths H -16 and H1998-15 from Central Area at depth of -525 to -530 cm.

Figure 3.7. Detailed plan of hearth 1998-16 in IJ19–20 at depth of -535 cm.



3.4.3.1.2 Description of the *décapage* (Figures 3.6 to 3.12)

This *décapage* (-525 to -530 cm) is at the limit between Layers E and F. Most of the surface is still within Layer E, especially, the zone IJ19-20 and JK22-24 where hearths 1998-16 and 1998-15 are located. Layer F, characterised by compact, grey silty clay with scattered charcoal and burned red clay terra rossa, starts in some areas at a depth of -530/-535 cm, just below.

This area includes one large hearth feature (hearth 1998-16) and the remnants of the dark organic sediment corresponding to the base of a medium-sized shallow basin-shaped hearth developed between -532 and -525 cm.

Main features (Figure 3.6)

Hearth 1998-16: I19d, J19c, I20a–c, J20a. Begins at -520 and ends at -555/-560 cm (>30 cm thick)

- Between -520 and -530 cm, it appears mostly as a thick accumulation of ash. However, its upper boundary (see *décapage* at -520 cm) was difficult to define, since the thick ash accumulation is truncated or overlain in places by smaller hearth lenses, some visible in the I-J19 section. It became evident that this is possibly one large hearth only when the black organic layer was reached at about -530 cm.
- The thickness of the ash lenses is surprising, reaching almost 10 cm in places. It most probably represents reuse in the same location. The estimated diameter is 80–100 cm, and is essentially circular.

At -535 (Figure 3.7), the outline of this hearth is more coherent. After removing the top portion of the feature—which included at least 4 or 5 smaller hearths within the larger feature, possibly adding to its thickness—black organic sediment was observed almost completely around the subcircular area of ash.

A small section through the feature between -535 and -540 cm showed that the western edge of hearth 1998-16 was cut by at least two, possibly three smaller hearths (~3 to 5 cm thick, 20–40 cm in diameter) between -535 and -540 cm in I19c. Thus, the feature was spread or cut by additional overlying fireplaces. This effectively enlarged the diameter of the feature apparent at its maximum extension at -535 cm.

After intact hearth sediments were removed at -555 cm, only few patches of black organic material rested on the diagenetic clay of Layer F.

It is clear that the multiple hearths that predate and also those that post-date the main hearth (depth -535 cm) were built one on top of the other, producing a series of hearths difficult to distinguish during excavation because of the small amount of sedimentary matrix between the lenses (around 10 or so separate lenses were identifiable in hearth 1998-16).

This thick complex of hearths sits on the top of Layer F with a sharp, clear contact, at a maximum depth of around -560 cm. It fills a depression of the very irregular undulating erosional surface between Layers F and E (chapter 2, this volume). Thus, the complex encompasses the beginning of the transition from the geogenic regime of Layer F to the heavily anthropogenic one of Layer E.

Illustrations

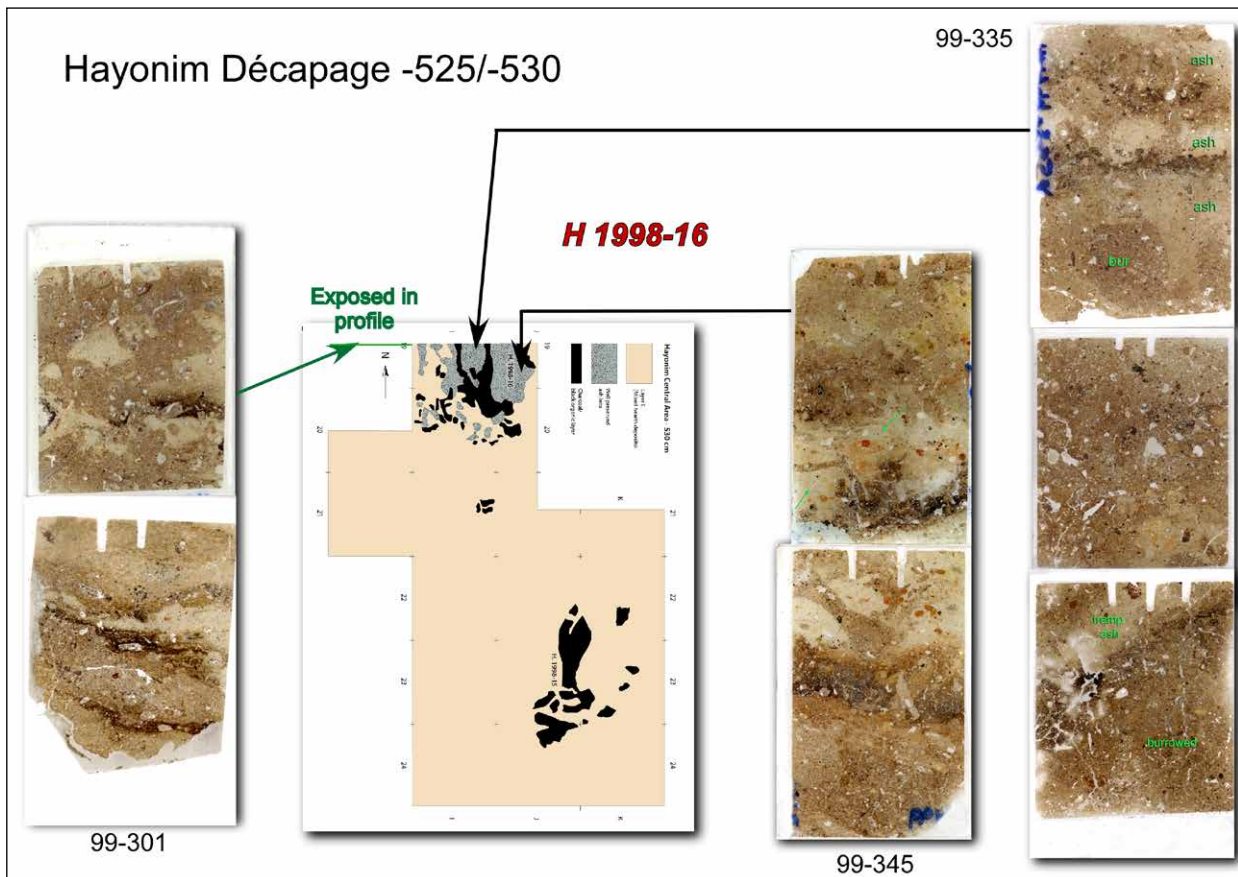


Figure 3.8. Décapage plan at -525/-530 cm, showing location of hearth 1998-16 and hearth area within the section at upper left.

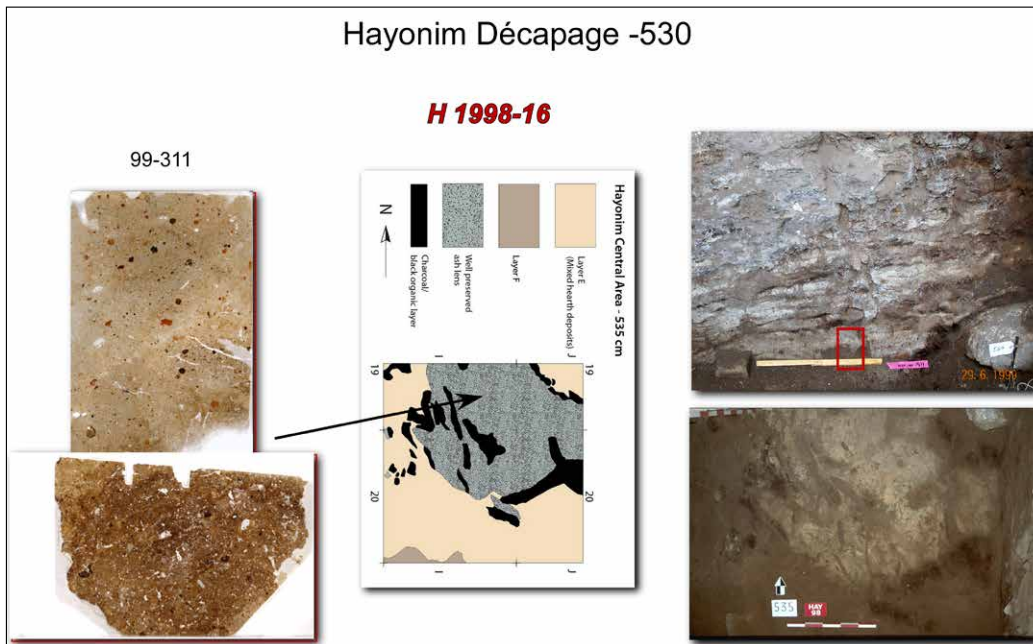


Figure 3.9. Plan, detailed field photo, and thin section scans of hearth 1998-16. Two thin sections of sample 99-311 reveal in the upper one, massive apatitic ash with scatters of terra rossa clasts, abundant phytoliths, and black Mn impregnations; the lower one is finely burrowed with remnants of mixed organic matter, fine bone, and phytoliths. Both show vein fillings of well-crystallised apatite.

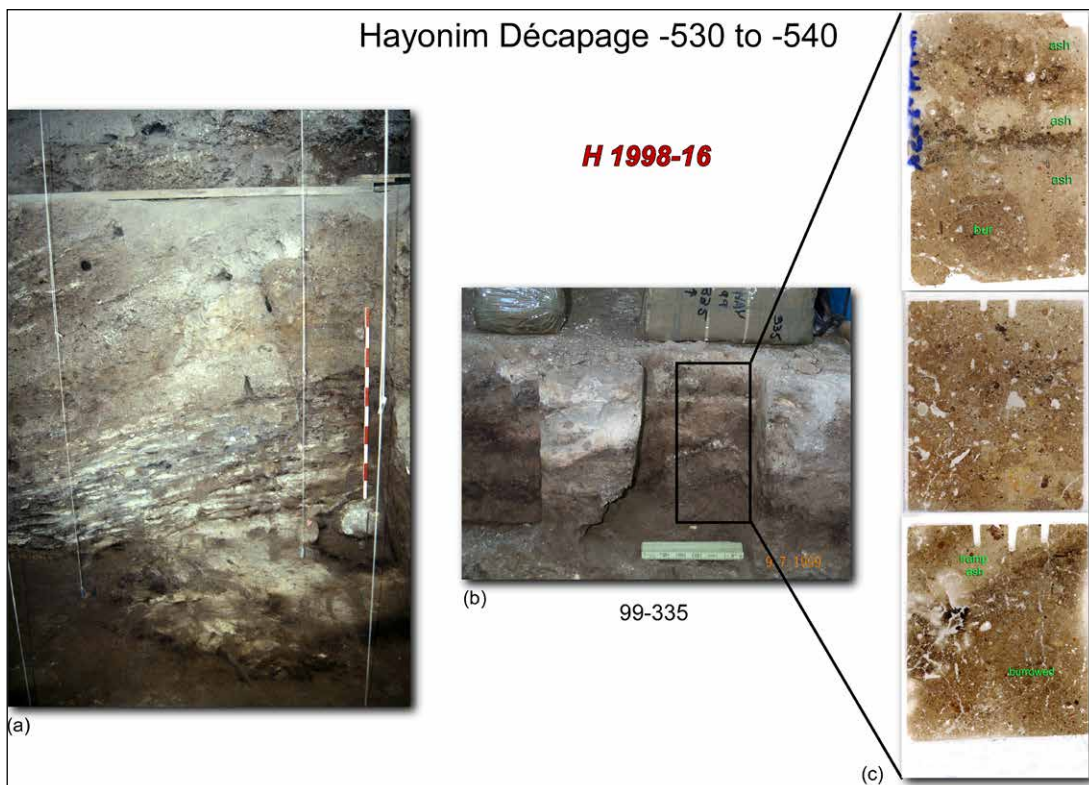


Figure 3.10. Hearth 1998-16, as revealed in the profile (a) and after sampling (b). Thin section scans (c) are from sample 99-335 (I19d; -550 cm), which show predominantly phosphatic ashes that are burrowed and trampled, but the remains of two features are visible in the uppermost and lowermost thin sections.

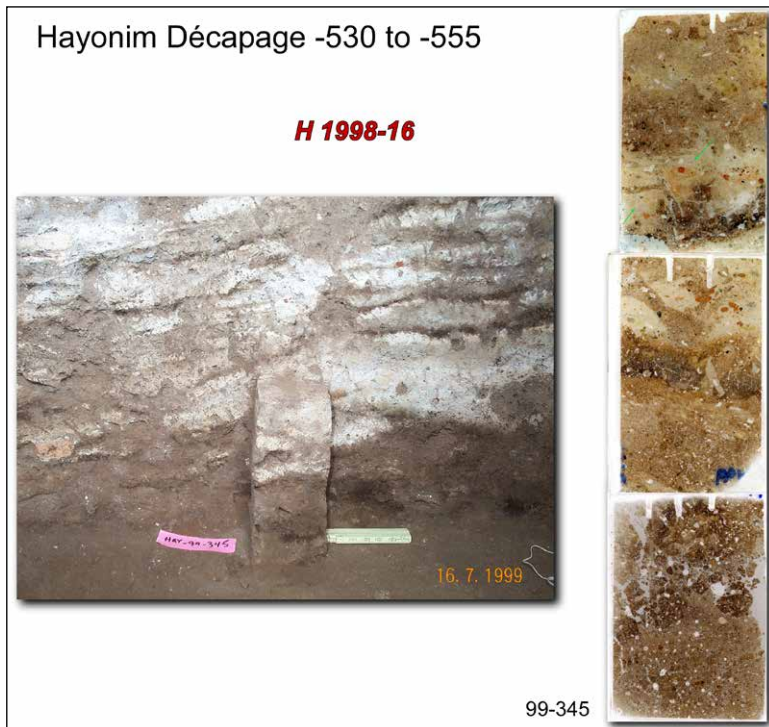


Figure 3.11. Thin section column of sample 99-345 (I19c; -545 cm) from the North Profile with thin section scans at right, revealing a sequence of hearths with interspersed organic-rich hearth bases overlain by phosphatic ashes (scale is 20 cm). Both layers are punctuated and homogenised by insect burrows. In 99-345A (top), the lighter-coloured ashes (arrows) are intact whereas the remaining ashes have been subjected to bioturbation.

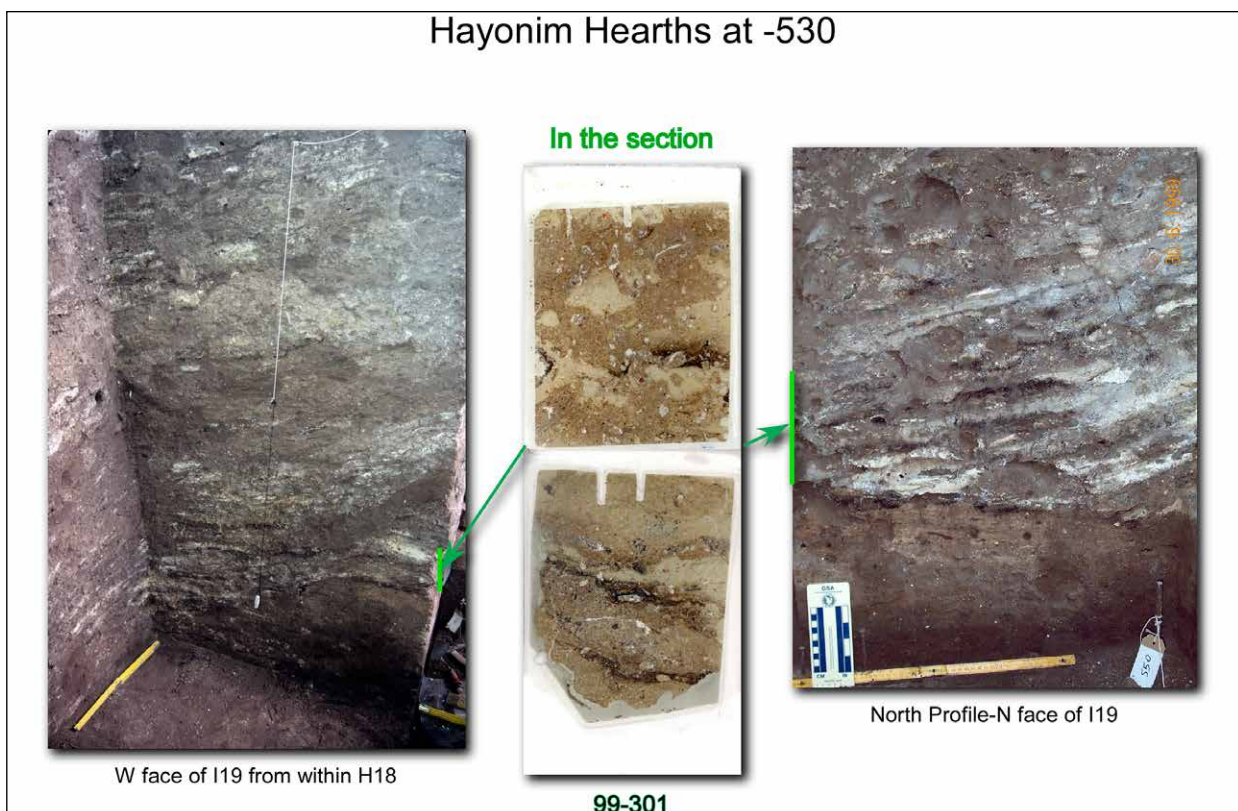
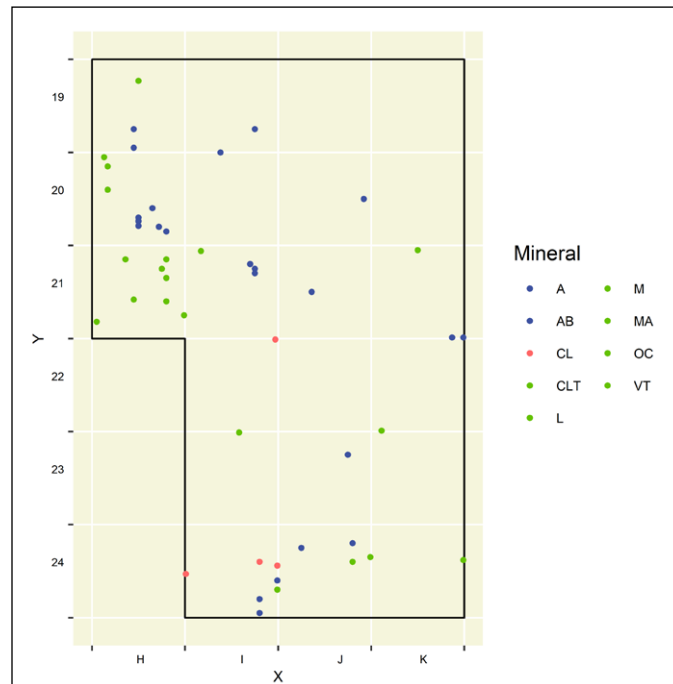


Figure 3.12. Hearths near the E/F contact in the northern part of the Central Area. The locations of thin sections from sample 99-301 (H19a; -530 cm) are indicated by arrows. The dark bands are composed of thinly bedded humified organic matter interbedded with ashes. These bands are over and underlain by phosphatic ashes; insect-scale bioturbation is common.

3.4.3.2 Décapages -520 to -500 cm

3.4.3.2.1 Mineralogical map (Figure 3.13)

Figure 3.13. Mineral distribution map of FTIR analyses of sediments between -500 and -520 cm. Exhibited here is a mosaic of widespread CD minerals (calcite-apatite), with LMVS minerals concentrated along a northwest/southeast linear axis in the centre, but with some locations in the CD zone.



3.4.3.2.2 Description of the main décapages

3.4.3.2.2.1 Décapage -520 cm (Figures 3.14, 3.15, 3.16)

Hearths 1998-16, 1998-12 (K22-23), 1998-13 (limit between K23-24), and broken hearths (JK24)

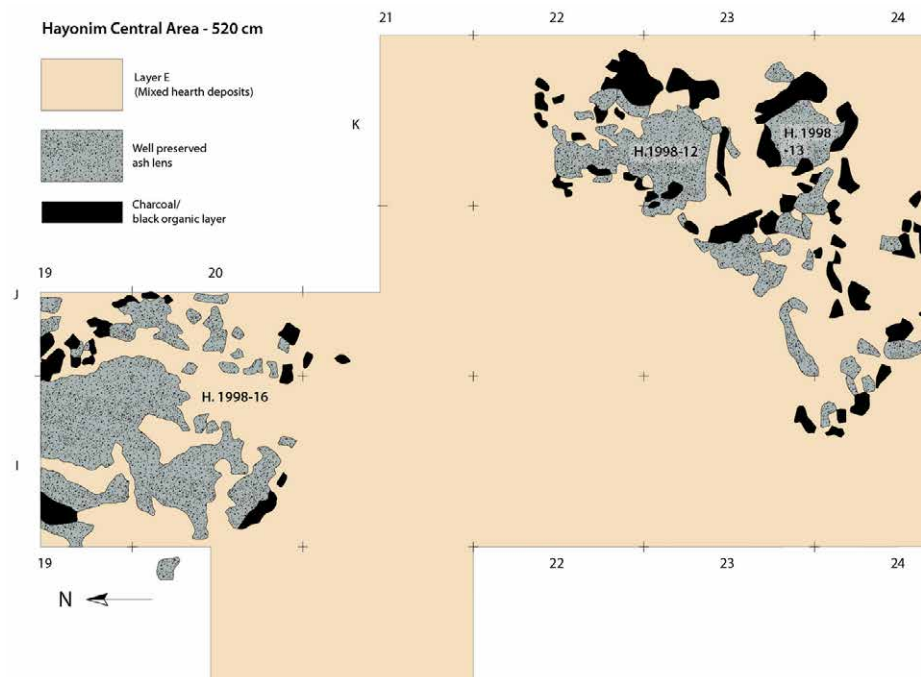


Figure 3.14. Plan of hearths 1998-12, 1998-13, and 1998-16 at -520 cm.

At -520 cm, grey phosphatised (mostly apatitic) sediments are spread over a large surface, and the areas of mixed hearth deposits are largely in the central part (IJ21–22, K21, I23) as well as in H20–21. Hearths/combustion features seem to be spatially localised and to show repeated use in a patterned way. At this depth, the mixed hearth deposits include at least three large hearths: 1998-12, 1998-13, and the upper part of hearth 1998-16 (the latter previously described in *décapage* of -530 cm).

Main features (Figure 3.14)

Hearth 1998-12: K22cd, K23ab, J23bd; between -516 and -525 cm (~9 cm thick)

- At -520 cm, this large oval feature contains a lens of light orange grey ash ~4–8 cm thick, underlain by black (remnant charcoal) silty sediment.
- Excavation through the top of the feature between -515 and -520 cm showed that at least four or five smaller overlapping thin shallow-basin hearth lenses (~30 cm in diameter) overlie it; in some cases, the lenses also interfinger with each other and with hearth 1998-12.
- At most, the diameter of 1998-12 is ~150 cm, but its shape in plan at -520 cm likely reflects two or three adjacent, slightly overlapping hearths. The maximum thickness of the feature is about 7 cm with ~2–5 cm of ash and ~1–3 cm of remnant charcoal.
- Overlying hearth 1998-12 (or its adjacent hearths) are partially preserved thin hearth lenses that have smaller diameters. The overall feature is part of a zone of mixed hearth deposits that continued upward to about -500 cm.

Hearth 1998-13ab: K23cd, K24ab, I23d (?), J24b (?); between -518 and -527 cm

This feature is adjacent to and may overlie hearth 1998-12 in its southern edge. Hearth 1998-13 is subcircular, with a shallow lens of light, orange-grey ash surrounded by black remnant charcoal, which at least partially underlies it. Close inspection of the section between K23–24 (-520 to -525 cm) reveals a fine 1–2 cm-thick lens of remnant charcoal within the ash accumulation of 1998-13. Therefore, the feature in fact consists at least of two stratified hearths in its southern extent. The upper one comprises an ash lens 5–6 cm thick and 1–2 cm of black organic sediment; it is underlain by 1–2 cm of only ash, and another 1–2 cm-thick layer of organic sediment under that. Neither hearth can be followed very far to the north, largely because of extensive burrowing, which produces a homogenised medium-grey/medium-brown-grey sediment.

Both 1998-12/13 are in the zone of mixed hearth deposits, surrounded, overlain and perhaps underlain by partially preserved shallow basin-shaped hearth lenses. These two features probably represent relatively complete hearth lenses in an area of dense hearth deposits. Hearths 1998-13 and 12 represent two features whose outlines are determined by 1 or 2 relatively thick, well-preserved ash lenses, but the distribution of charcoal all around them reflects many smaller additional thin overlapping and finely bedded hearth lenses.

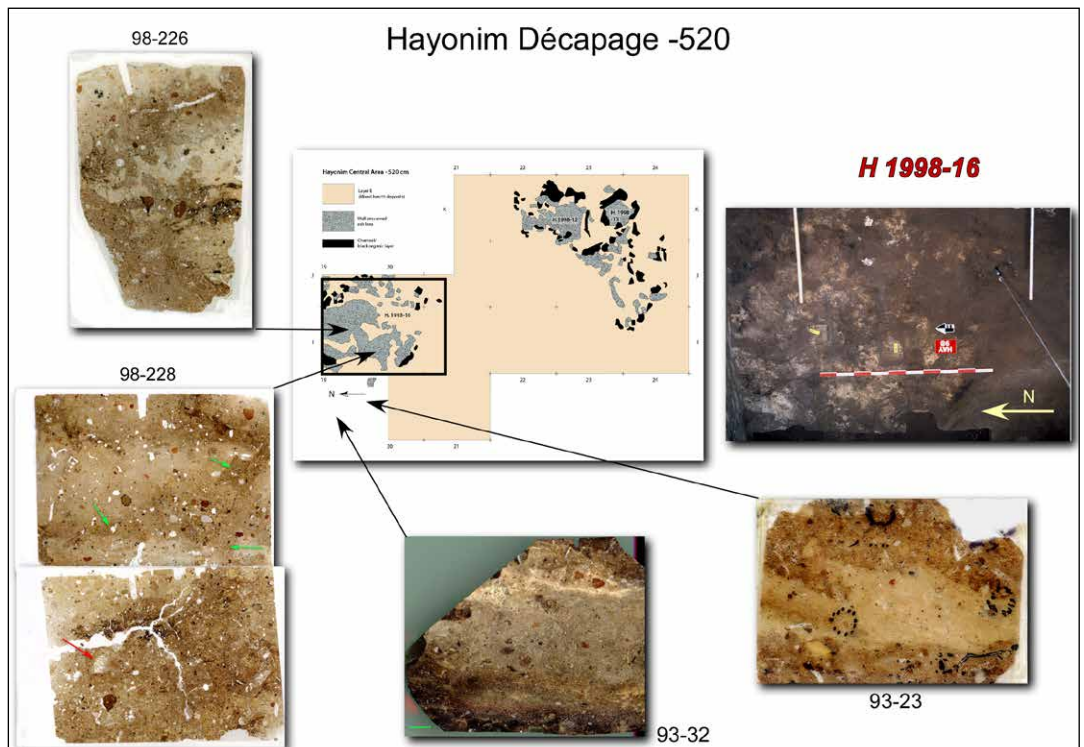
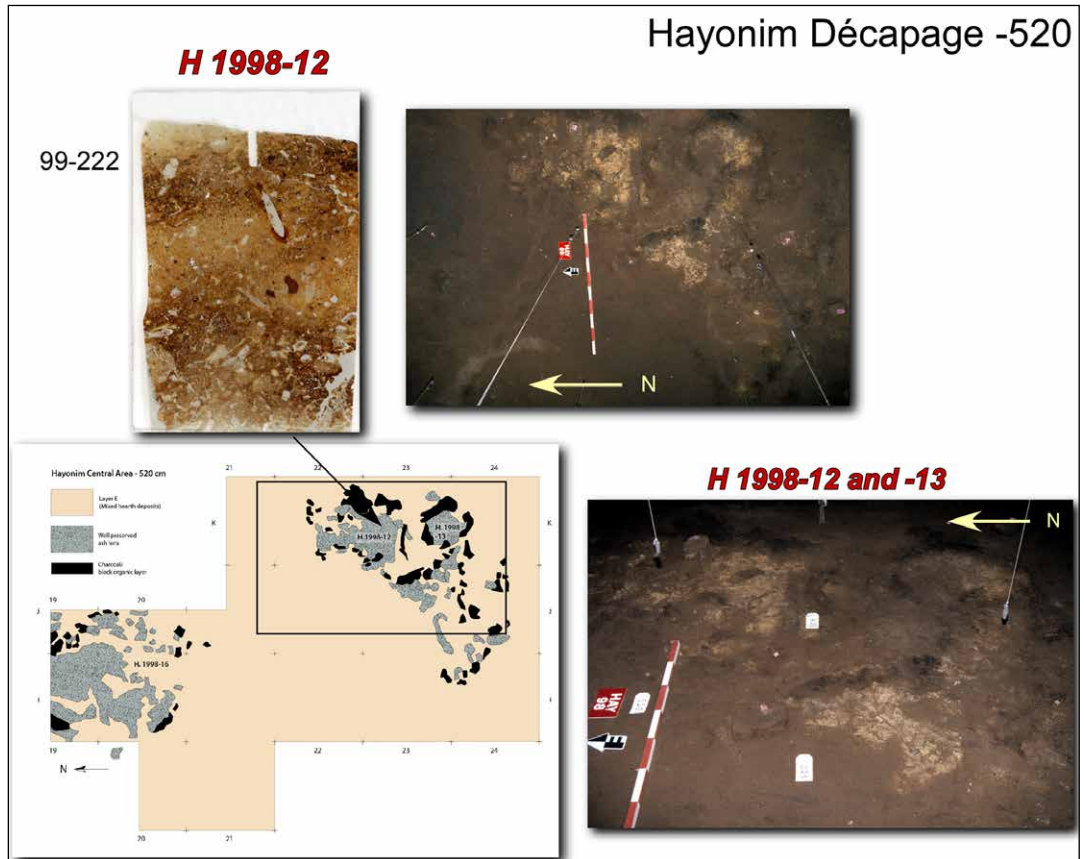
Hearth 1998-16:

At this depth, only the upper part of this thick combustion feature is observed. It appears as a large ashy zone spread over IJ19–20 and is truncated or overlain in places by smaller hearth lenses, some of which are evident in the IJ19 section (see Figure 2.26).

Figure 3.15 (following page above). *Décapage* at -520 cm, showing plan and photos of hearths 1998-12 and -13, and scan of thin section (99-222). These two large adjacent, probably partially superposed combustion structures are surrounded by smaller hearth lenses; they represent relatively well-preserved hearths in an area of high-density combustion features. The thin section scan shows two relatively thick diffuse hearths composed of an organic-rich base overlain by phosphatic ashes.

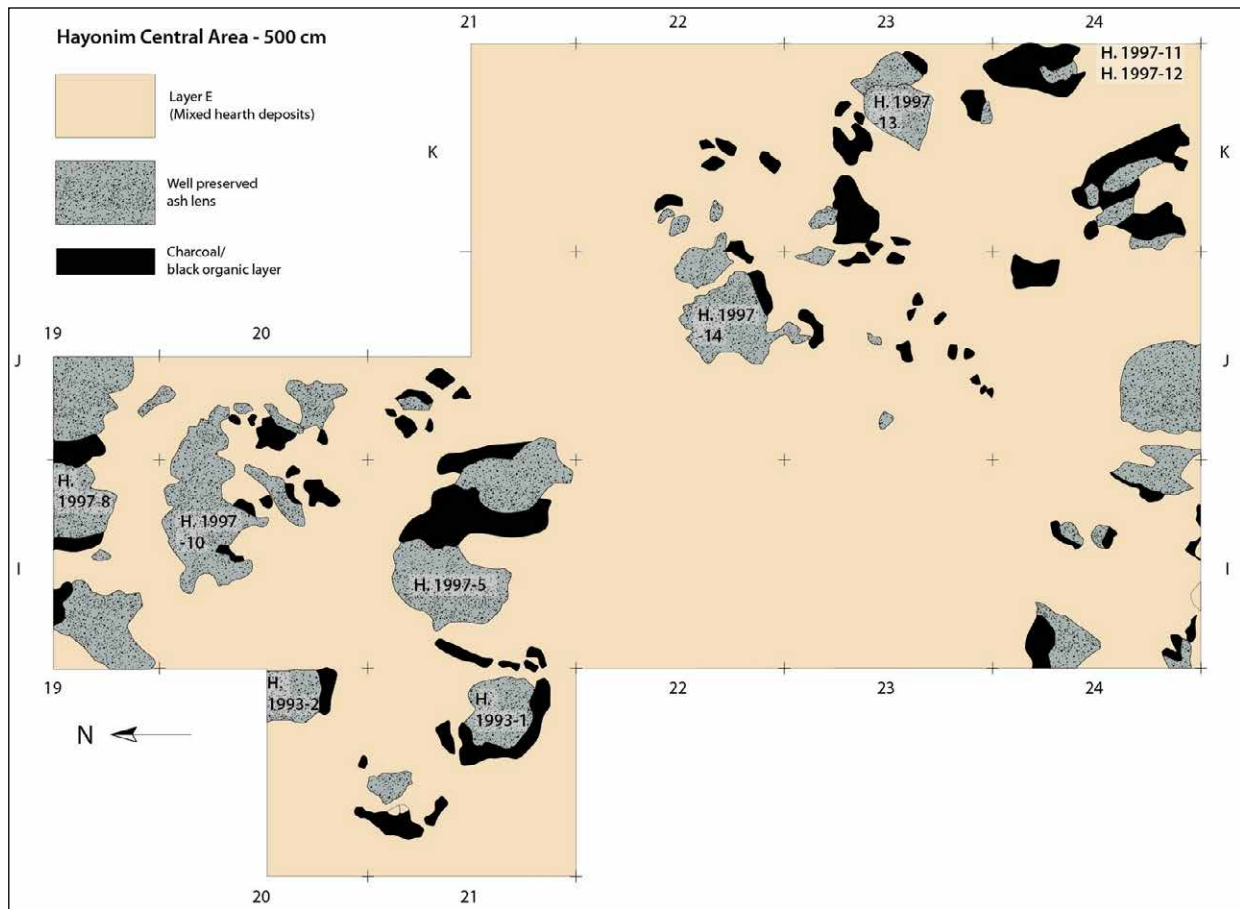
Figure 3.16 (following page below). *Décapage* at -520 cm, displaying plan, detailed field view of hearth 1998-16, and thin section scans and locations of samples 93-23, 93-32, 98-226, and 98-228. Intact features are only locally preserved (e.g., 93-32, 98-226), and the surrounding sediments tend to be comprised of apatitic ashes with terra rossa clasts and some diffuse bands richer in organic matter (e.g., 98-226).

Illustrations



3.4.3.2.2.2 Décapage -500 cm (Figures 3.17, 3.18)

Hearths 1997-8, 1997-10, 1993-1, 1993-2, 1997-5, 1997-14, 1997-13, 1997-11 and 12, fragmented hearth (K24 south).



The central part is comprised of mostly anthropogenic ashes (mixed homogeneous hearth deposits), as well as some better-preserved hearth features. These include: 1) the base of several large and thick multiple-hearth features that can be followed into the upper décapages (1997-5; 1997-8; 1993-1; 1997-10; 1997-11 and 12), and 2) thin lenses spread over the surface. The main importance of this décapage is to illustrate the coexistence of thick features (represented here by their basal part) and the numerous patchy remnants of ash and/or black charcoal that correspond to thin combustion features (1997-13; 1997-14, for example).

Main features (Figure 3.17)

Hearth 1997-5:

The lower part of this large and thick feature (already present at -480 cm, and mainly described at -495 cm), was identified in its full extent when the cemented ash was removed at -495 cm, which revealed the black, charcoal-rich (clayey) silt remnant below. The black organic sediment appeared to continue under the thick ash lens covered by an apatitic crust in I21bd.

Figure 3.17. Plan of hearths 1993-1, 1993-2, 1997-5, 1997-8, 1997-10, 1997-11 and 12, 1997-13, 1997-14, and fragmented hearth at -500 cm.

Hearth 1993-1:

At -500 cm, these two hearth (1997-5 and 1993-1) proved to be essentially adjacent features. Field observations showed that hearth 1993-1 rested just on top of the charcoal circle of 1997-5, and thus post-dates 1997-5. The black organic sediment (remnant charcoals) underlaid and surrounded the feature, which is 60 cm in diameter.

Hearth 1997-10: I20bd, J20ac

From -495 to -505 cm (~10 cm thick), this broad feature may be multiple hearths or a single, large, shallow basin feature. It is about 100 cm in diameter and comprised of mostly soft light brownish grey calcitic ash, with an apatitic crust often associated with the base of the ash at -500/-502 cm. It is mostly rimmed by black silty sediment and is surrounded by loose silty or cemented material that is simply mixed hearth sediment.

Hearth 1997-8: I19cd, J19c

From -495 to -500 cm (~5–10 cm thick), the poorly preserved hearths (patches of imbricated ashes and black organic sediment, extensively disturbed by burrowing observed at -490 cm) gave way to these better-preserved parts of hearths. These appeared at around -495 cm; the ashes are ~5–10 cm thick. As observed at -500 cm, there were at least two generally contemporaneous and adjacent hearths, preserved as compact calcitic/apatitic ash associated with thin (1–3 cm) black organic layers.

Hearths 1997-11 and 12: K23d, K24bd

Only the black organic layer (basal part of the hearths) was identified at a depth of -495 cm. The black organic sediment that ringed and underlay the ash was always preserved as a blocky silty clay with bluish grey fine veins of apatite.

'Hearth' 1997-13: K23bd

This is a large centimetre-thick cemented calcitic ash occurring at -497 cm. It is about 40 cm in diameter, with patches of black organic sediment occurring to the west.

Hearth 1997-14: J22d, K22c

This feature is best defined as a zone of imbricated thin horizontal bedded hearths that cut one another from -495 to -500 cm. The ash is generally calcitic with apatite precipitation on top and below the ash.

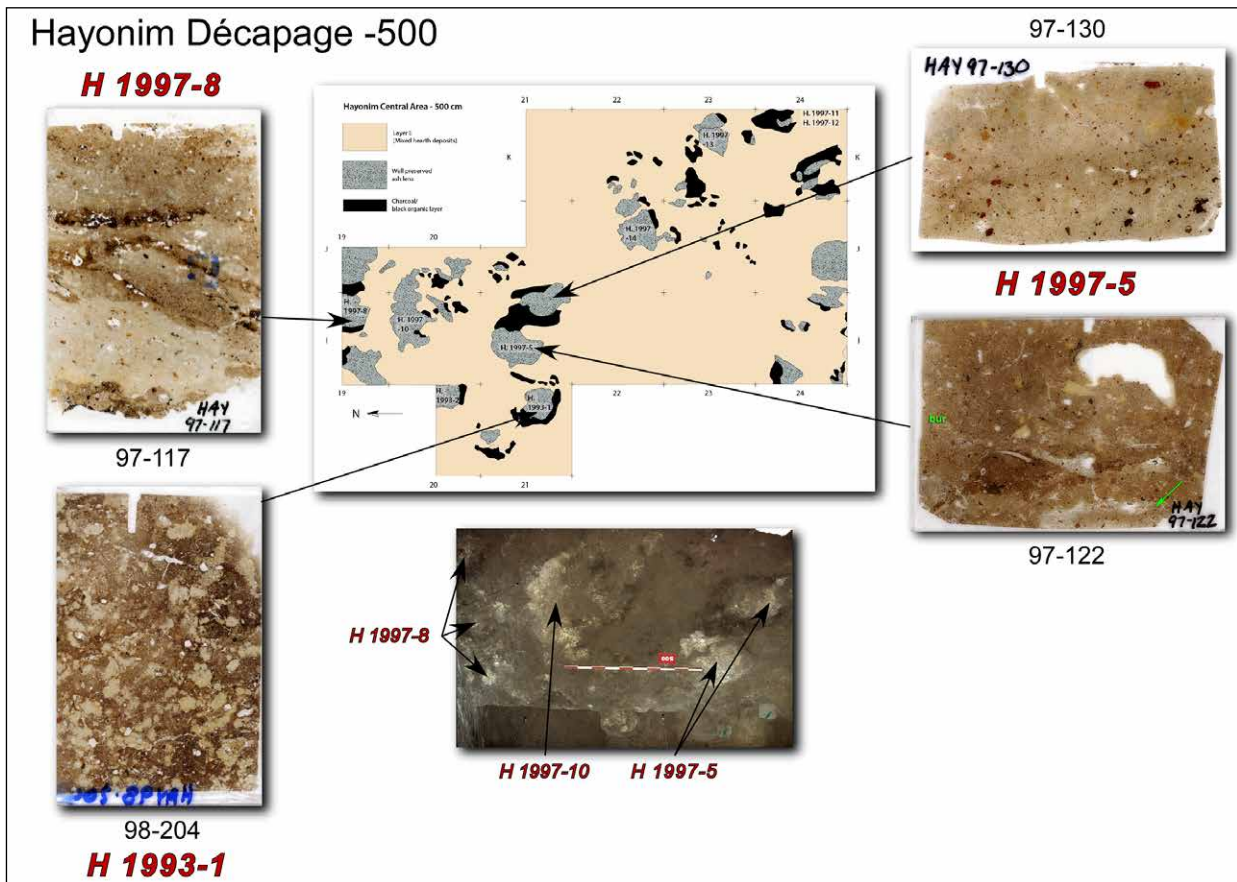


Figure 3.18. Décapage at -500 cm, with surface plan and detailed field photo of area with hearths 1993-1, 1997-5, and 1997-8. These features include the thin section scans of samples 97-117, 97-122, 97-130, and 98-204. Most of the samples are within the CD mineral zone and the ashes are typically apatitic. On the other hand, sample 98-204 displays two darker domains in the upper right and at the base, along with a matrix that is punctuated with numerous phosphatic LMVS nodules; the latter have muddled the appearance of the original features. Thin section of 97-117 is mostly composed of phosphatised ashes and organic-rich bands representing the base of hearths; the bottommost dark band has been bioturbated by insects.

3.4.3.3 Décapages -495 to -480 cm

3.4.3.3.1 Mineralogical map (Figure 3.19)

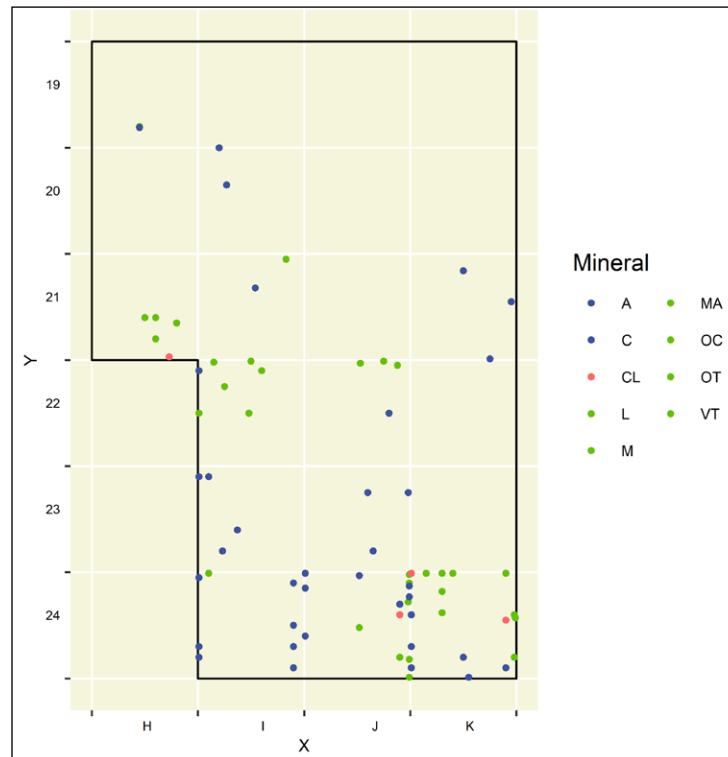


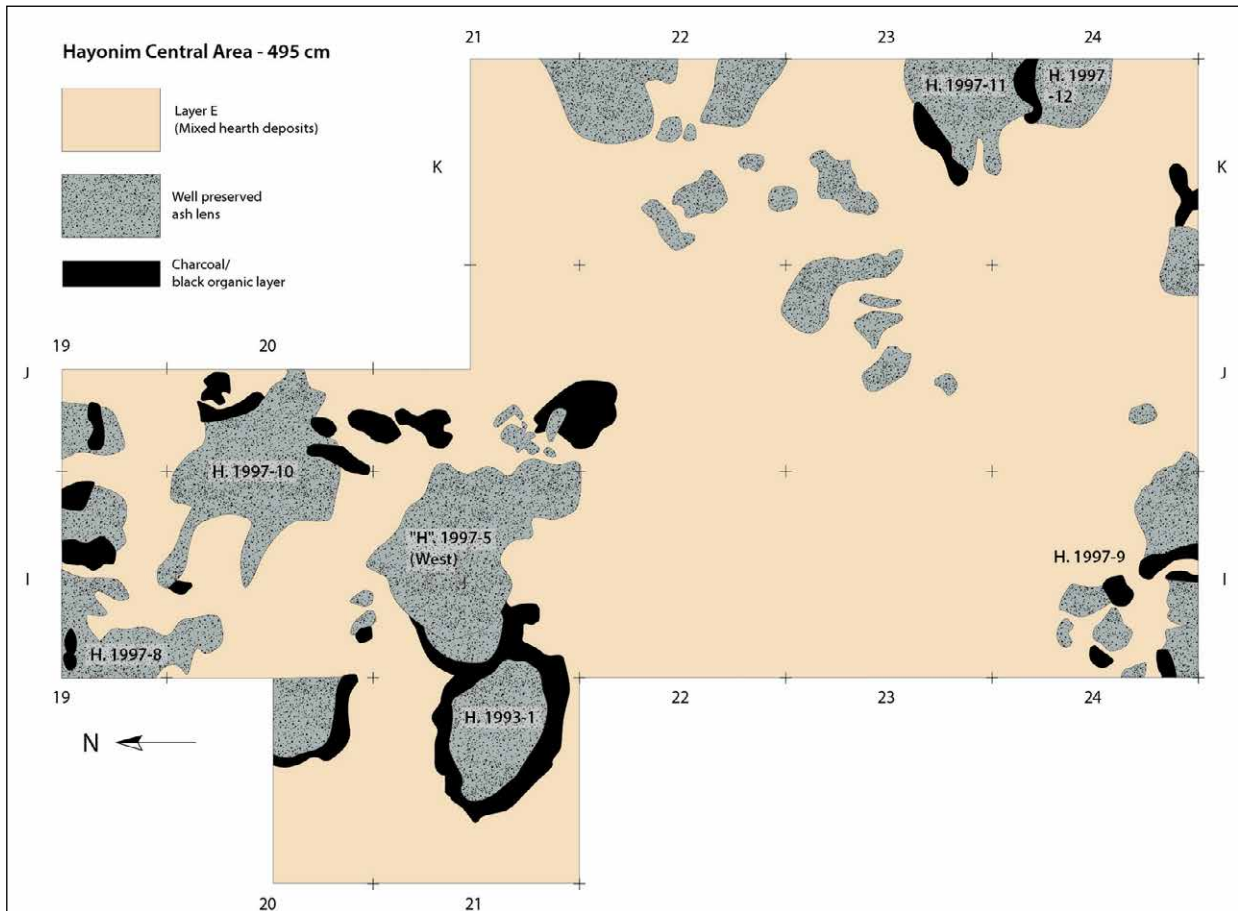
Figure 3.19. Mineral distribution map between -495 and -480 cm. Here, calcite/apatite (CD) covers much of the area, and LMVS minerals are at the fringe, particularly in JK24, and somewhat in H21 and IJ22.

3.4.3.3.2 Description of the main décapages

3.4.3.3.2.1 Décapage -495 cm (Figures 3.20 to 3.23)

Hearths 1997-5, 1993-1, 1997-10, 1997-11 and 12, 1997-8, 1997-9.

At this depth, mixed hearth deposits are spread over a large area in the central part, often phosphatised (mostly apatitic/calcitic, but also locally zones of leucophosphite/taranakite). Numerous large and thick hearths/combustion features are present, some of them already recognised at the depth of -500 cm (e.g., 1997-5; 1997-8; 1997-10). The most important feature here is 1997-5, which appears as a vast ash accumulation.



Main features (Figure 3.20)

Hearth 1997-5: I21ad, J21ac, J22ab (approximate thickness in the eastern part from -478 to -490 cm and from -490 to -505 cm in the western part).

- The base of this feature is undulating and higher in its eastern part; it exhibits a deep patch of cemented ash at its base. Overall, the ash layers are 5–15 cm thick, with the remnant charcoal lens underlying (at least intermittently) much thinner (2–5 cm).
- At the basal depth in the western part of this feature, a remnant of a relatively deep basin of ash is exposed in I21a, surrounded by black remnant charcoal sediment (see map at -500 cm).
- Thus, overall, the feature has at its surface an east-west extent of ~130 cm and north-south length of 50 to 60 cm. Its eastern extent is more or less horizontally higher in J21ac, a bit of J22ab, and I21bd, with ash, mostly cemented in this zone, varying in thickness of 10–18 cm, underlain in patches by ~2–3 cm of very dark grey brown sediment that is likely charcoal remnant.
- It is also important to note that at its western extent the hearth slightly overlaid the ash and charcoal lenses of hearth 1993-1 further to the west, mostly in H21bcd.

Hearth 1993-1: H21. Mainly between -500 and -515 cm.

This well-defined feature occurs on a slope inclined northwest because of an inferred ‘sinkhole’. The light grey ashes are likely siliceous aggregates. The black organic sediments underlie and surround the feature, which is 60 cm in diameter.

Figure 3.20. Plan of hearths 1997-5, 1993-1, 1997-10, 1997-11 and 12, 1997-8, 1997-9 at -495 cm.

Hearth 1997-10: I20bd, J20ac. Present between -495 and -505 cm, previously described at depth -500.

This broad feature appears at this depth as a large continuous ashy zone ~1 m in diameter that corresponds most probably to a single large shallow basin feature. Few thin patches of dark sediment (remnant charcoal) are found nearby.

Hearths 1997-11 and 1997-12: K23d, K24bd. From -490 to -500 cm (~10 cm thick).

- Two well-preserved hearths occur, with the southernmost one lying on top of the northern one.
- In section, hearth 1997-12 showed multiple fine layers of charcoal and ash, both phases exhibiting laminations 1–2 cm thick.
- Thus, hearth 1997-12 is composed of at least three combustion features within one larger hearth feature. In places, the cemented ash in these hearths form a 10 cm thick accumulation.
- The black organic layer is clearly observed at -500 cm.

Hearth 1997-9: I24ac (at -490 cm) and I24acd (at -495 cm).

Between -495 and -500 cm, 1 to 3 hearths were identified, even if the patchy distribution of charcoal and terriers make it impossible to distinguish overlying hearths. The same area is occupied by a large ashy feature at -490 cm.

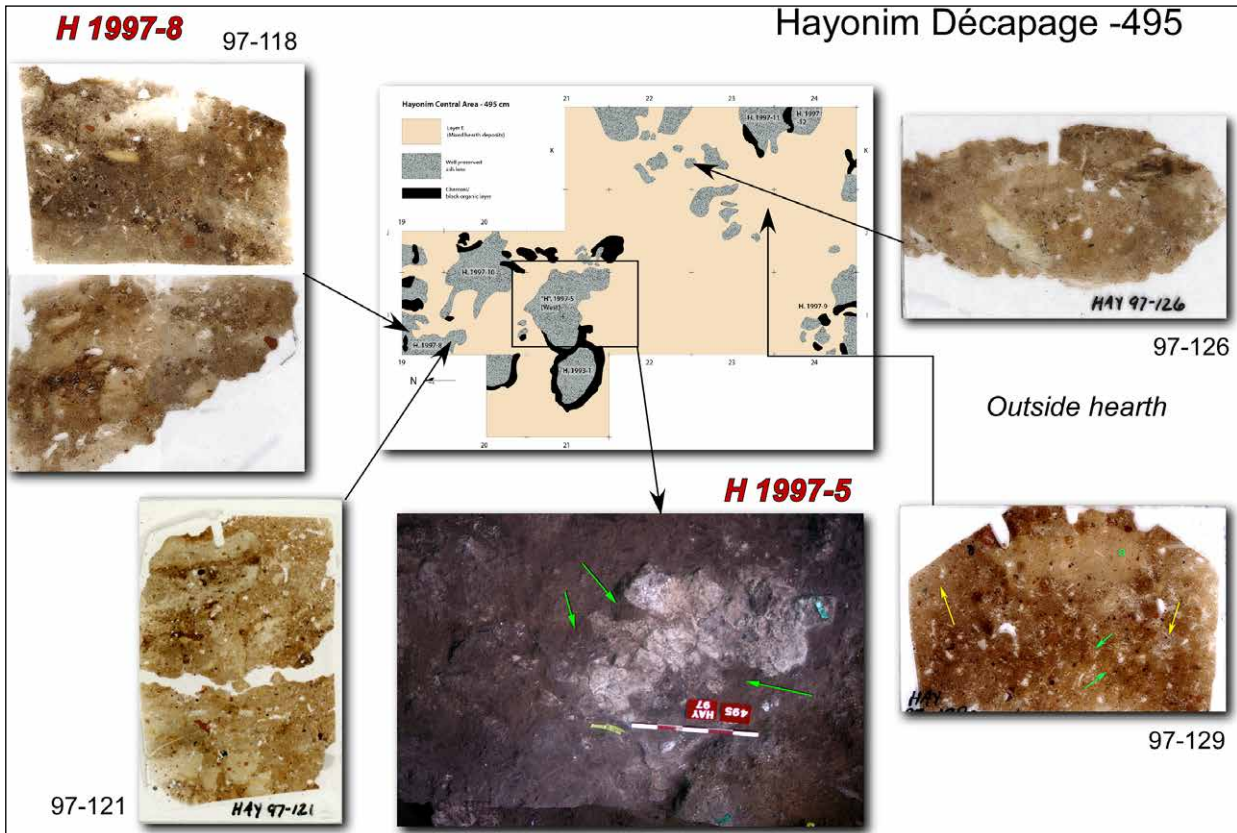


Figure 3.21. Décapage at -495 cm, showing surface plan and detailed field photo of area with hearths 1997-5 and 1997-8 (arrows indicate rodent burrows) in photo. Thin section scans are from samples within hearth 1997-8 (samples 97-118 and 97-121 at left) and from outside hearth areas (samples 97-126 and 97-129 at right). Sample 97-129 from outside the hearth is comprised of massive calcareous ash at the top surrounded by decalcifying heterogeneous mixture of sand-sized bone fragments and terra rossa grains. The other thin sections reveal trampled and burrowed phosphatic ashes with remnants of hearth structures shown by organic-rich zones.

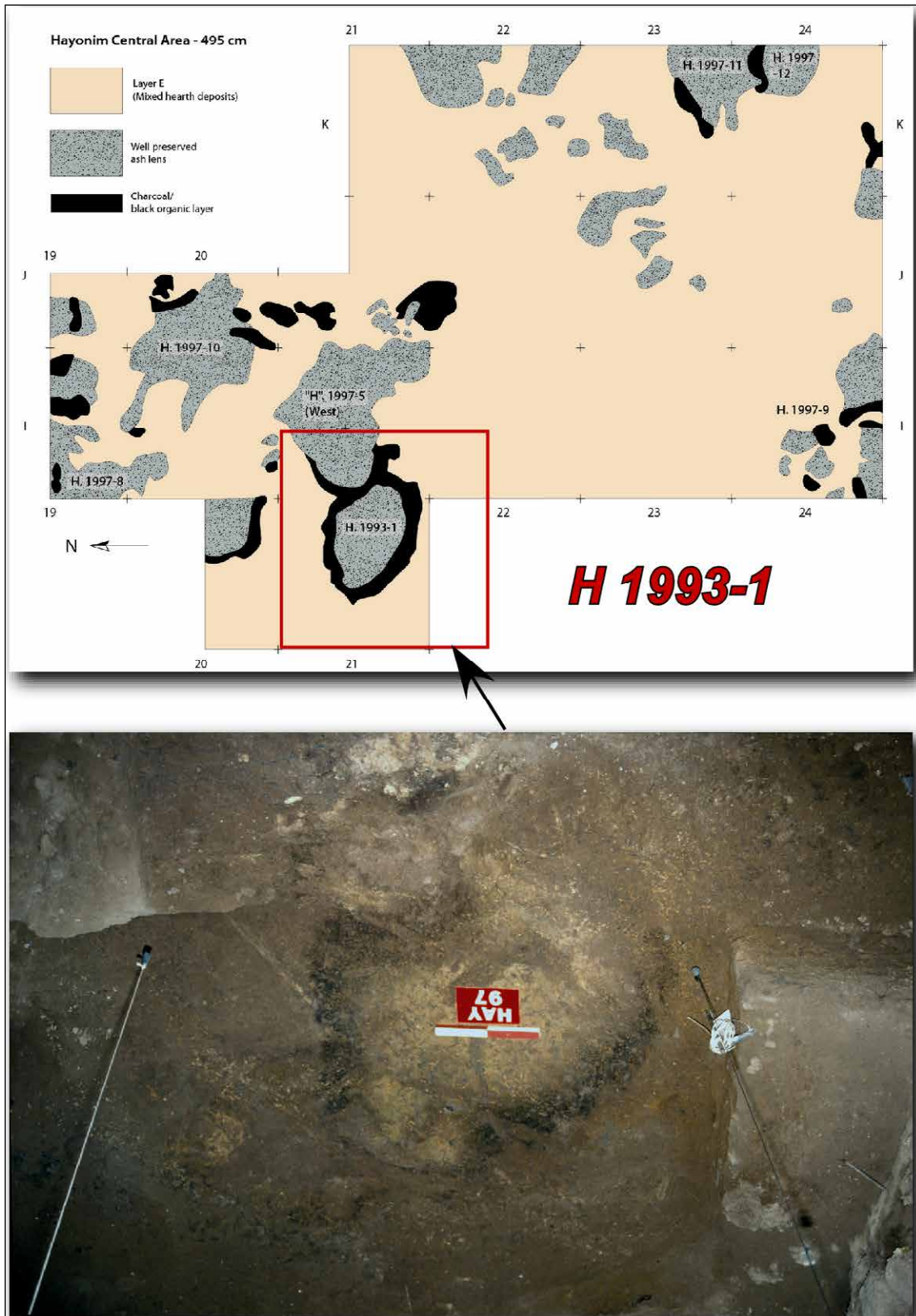


Figure 3.22. Décapage at -495 cm, showing overall surface and detailed plan views of hearth 1993-1; field photo is below. This is one of the rare instances at Hayonim where a hearth exhibits a black organic aureole surrounding white ashes.

Hayonim Décapage -485 to -490

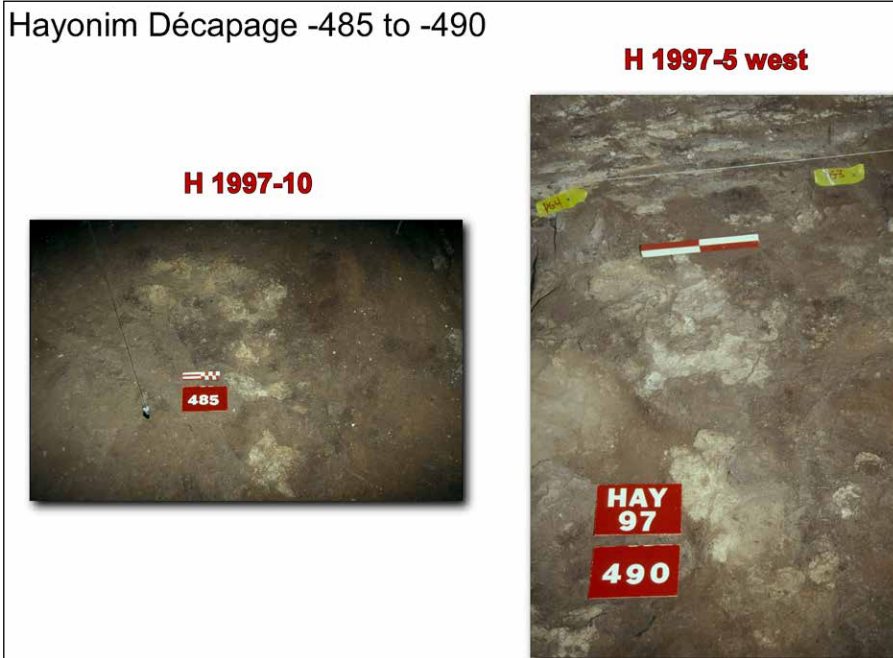


Figure 3.23. Décapage -485 to -490 cm, showing detailed photos of hearths 1997-10 and 1997-5.

3.4.3.3.2.2 Décapage -480 cm (Figures 3.24, 3.25)

Combustion features: Large lenses of white/grey ashes and patches of black organic sediment in K22-23 ('hearth' 1997-6), in J21-22 (higher part of hearth 1997-5?), in I24 ('hearth' 1997-4).

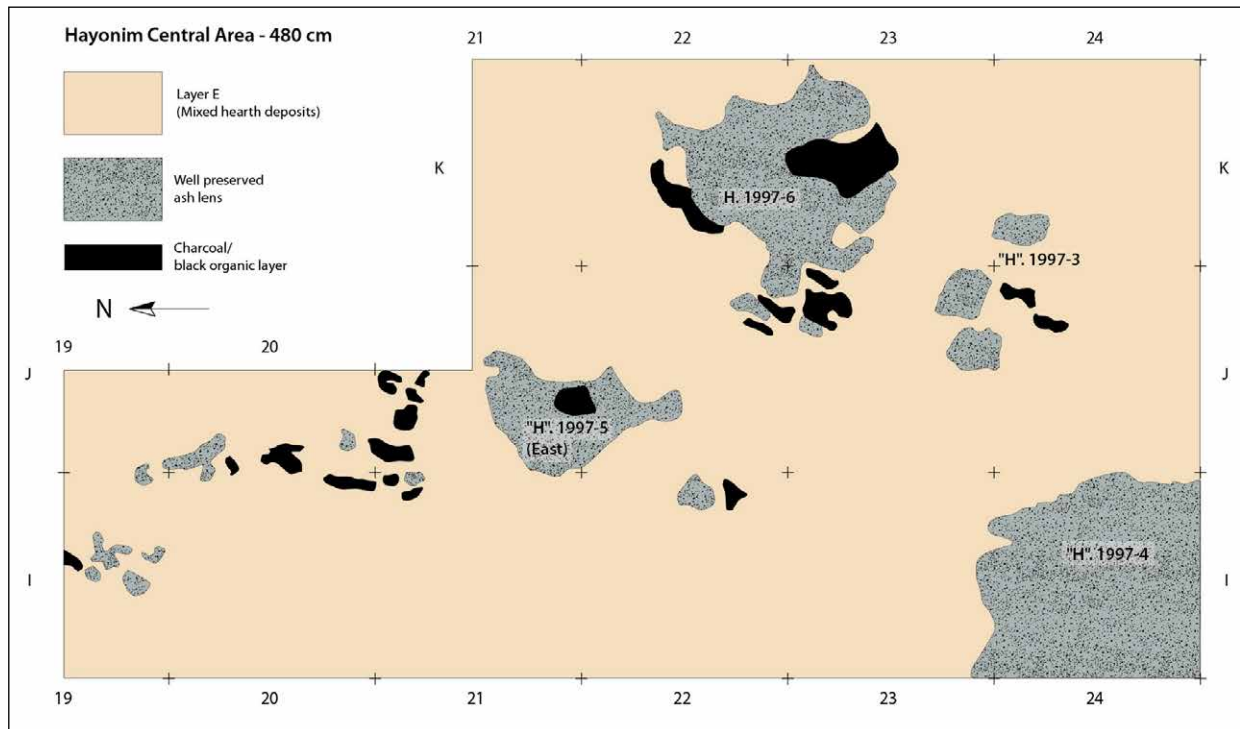


Figure 3.24. Décapage at -480 cm showing 'hearth' 1997-4, 1997-5(?), and 'hearth' 1997-3 and 'hearth' 1997-6.

The surface is composed mostly of mixed homogeneous hearth deposits, as well as some better preserved 'hearth' features in the form of large patches of 'mixed ashes and charcoal' to 'well preserved lenses of calcitic ashes'. Often no discrete hearth boundaries are visible, but this situation may (most probably) reflect trampling and/or superposed, somewhat imbricated hearths.

Main features (Figure 3.24)

'Hearth' 1997-4: I24. Between -478 and -485 cm (~5–7 cm thick).

It is comprised of a well-preserved, thin lens of grey calcitic ash, locally cemented and with a clayey consistency (diameter around 1 m). The ash is 2–4 cm thick and is underlain in spots by black clayey silt, ~2 cm thick, likely representing an incompletely preserved black organic layer. In the field, it is not clear how many hearths originally comprised this ash lens.

Hearth 1997-6: K22cd, K23ab. From -477 to -490 cm (although the lower part is patchy).

It is a large, irregular, rather thin (5 to 10 cm thick) accumulation of ashes (~100 cm in diameter), lying more or less horizontally. It is comprised of apatitic white/light grey ashes with burned terra rossa clasts, burned flint and bones, and is underlain by patches of black organic sediment (charcoal remnants).

'Hearth' 1997-5 (eastern part): J21–22. Between -478 and -490 cm.

This is a thick accumulation of ash, lying more or less flat, and corresponding to the eastern extension of hearth 1997-5, mostly developed at -495 cm. It is variably preserved as calcite and apatite with only patchy preservation of underlying charcoal.

'Hearth' 1997-3: K24, J24.

This is composed of patches of ashes corresponding to the bottom of a series of 'imbricated small to medium shallow basin hearth features', 15–60 cm diameter. These have an irregular shape because they have been likely trampled, burrowed, and cut by other hearths. Ashes are recognisable by the inclusion of small balls of burned terra rossa clay (0.5–1.5 cm in diameter).

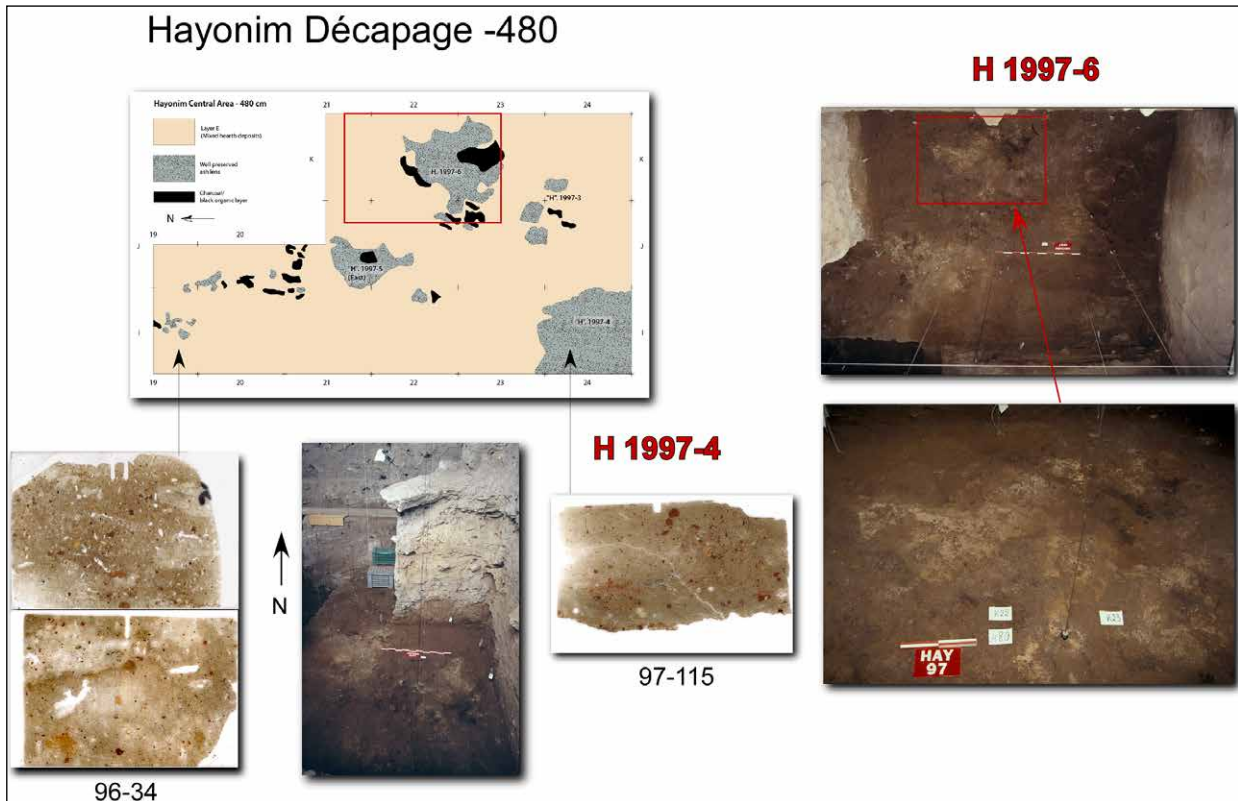


Figure 3.25. Décapage -480 cm, with plan view and field view of the surface. On the left, thin section scans of sample 96-34 come from mixed hearth sediments in I19, whereas on the right, a thin section of 97-115 is from hearth 1997-4 in I24 at the lower-right in the plan. Both samples show layers of compact combustion products comprised of phosphatised ashes, phytoliths, and terra rossa clasts.

3.4.3.4 Décapages -475 to -460 cm

3.4.3.4.1 Mineralogical map (Figure 3.26)

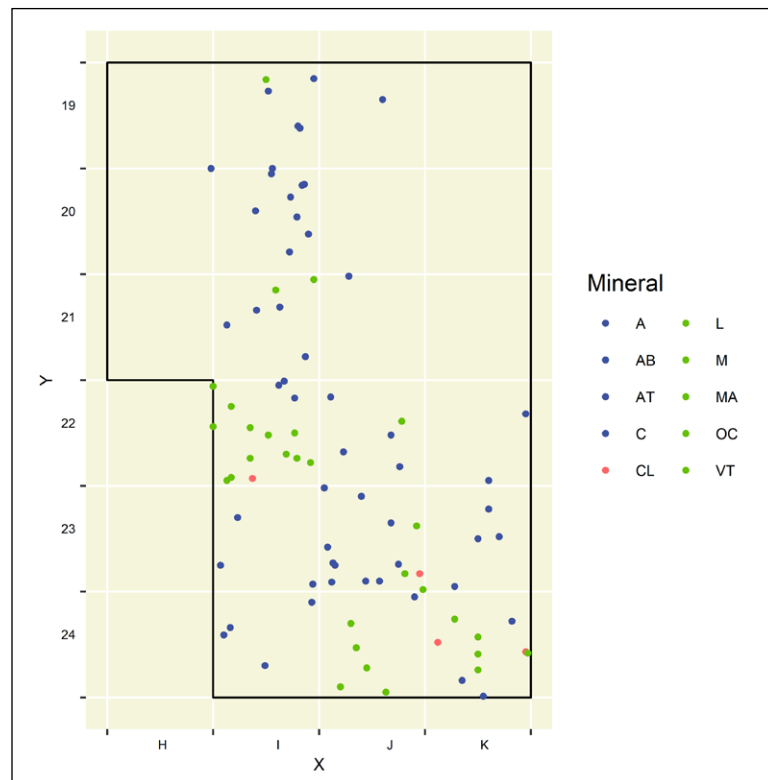


Figure 3.26. Mineral distribution map between -475 and -460 cm. Here, calcite/apatite (CD) covers much of the area, and LMVS minerals are mostly concentrated along a northwest/southeast axis.

3.4.3.4.2 Description of décapage -460 cm (Figures 3.27, 3.28)

Most of the Central Area surface at this level is 'mixed ashy sediment' with localised small areas of grey ashes and black organic sediment (JK22–23, J20, J21) (Figure 3.27). In addition, there are larger patches of white/grey ashes and/or black organic sediment (e.g., large white ash lens [>100 cm] along a western slope in I20), and large patches of light grey ash, locally cemented in I24ac and I23c (they already occur at -465 cm and are ≥ 5 –7 cm thick). They all may correspond to thin lenses of ashes and black organic sediment largely disturbed by trampling and burrowing.

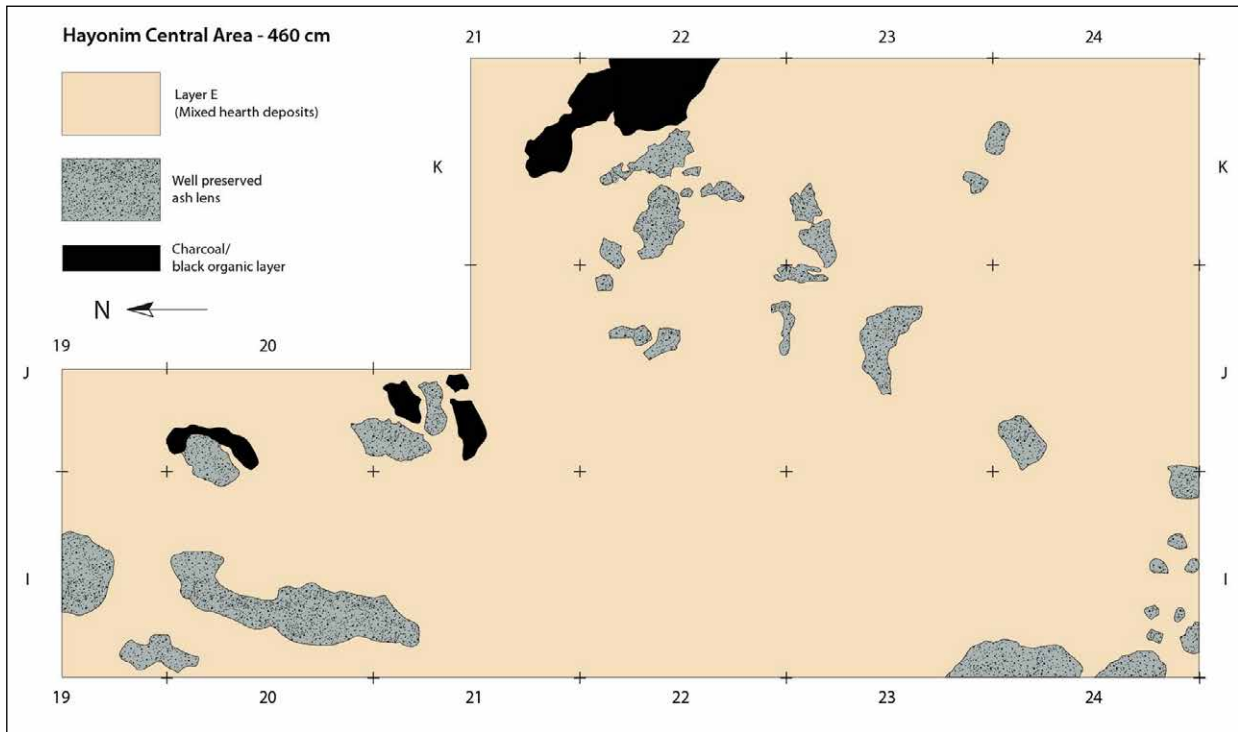


Figure 3.27. Plan of décapage at -460 cm.

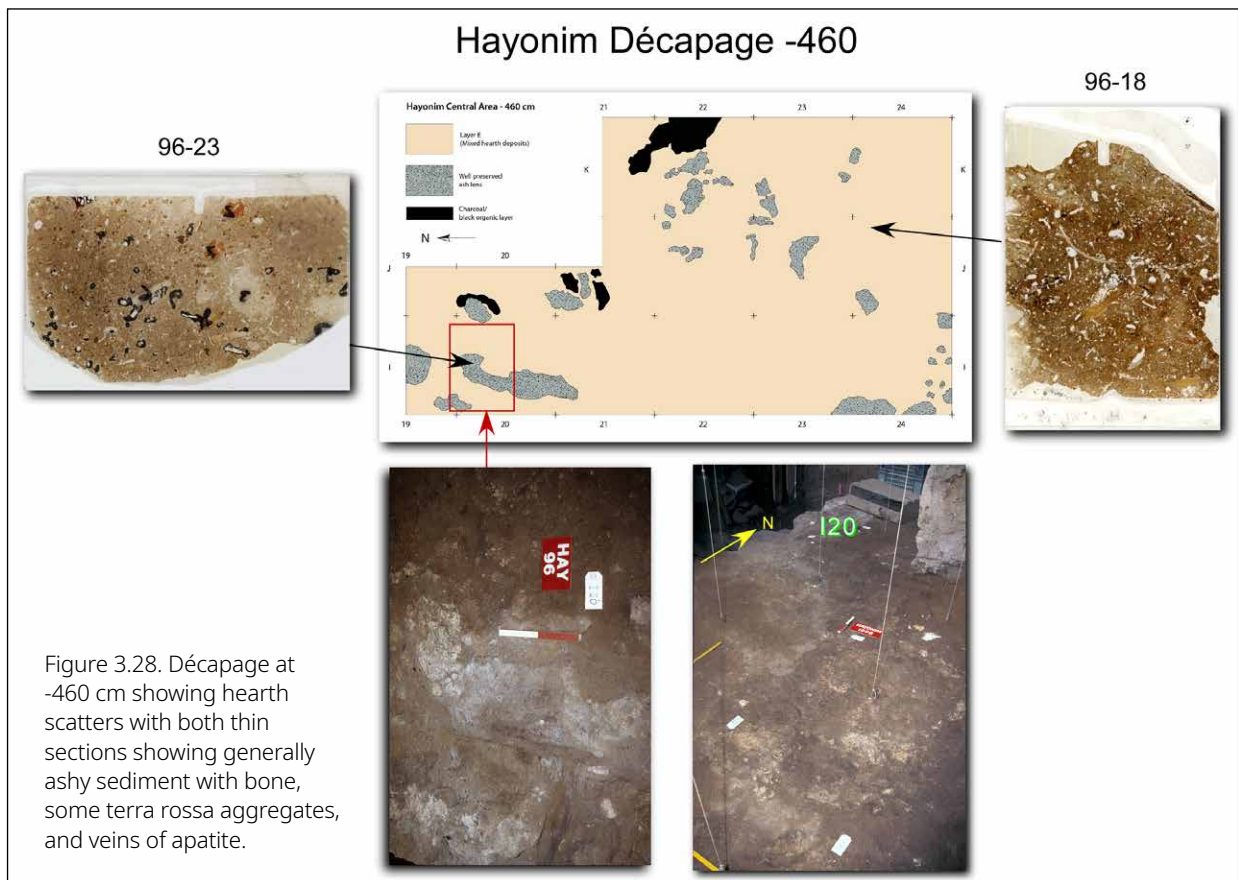
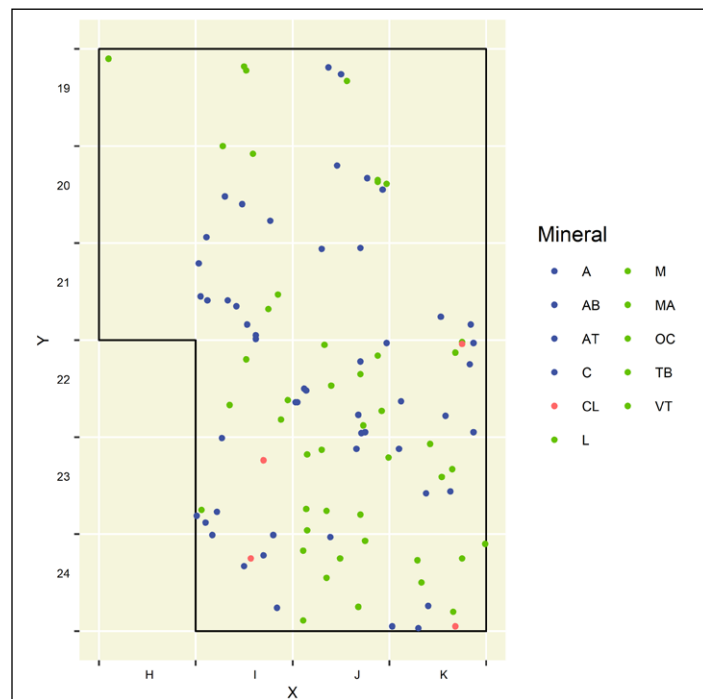


Figure 3.28. Décapage at -460 cm showing hearth scatters with both thin sections showing generally ashy sediment with bone, some terra rossa aggregates, and veins of apatite.

3.4.3.5 Décapages -450 to -440 cm

3.4.3.5.1 Mineralogical map (Figure 3.29)

Figure 3.29. Mineral distribution map of FTIR analyses from between -440 and -450 cm. Here, the calcite/apatite (CD) zone is rather widespread, but the LMVS still occupies a band oriented northwest-southeast that includes I21-22, J22-24, K22-24; it corresponds to field observations for the décapage at -445 cm.



3.4.3.5.2 Description of décapage -445 cm (Figures 3.30, 3.31)

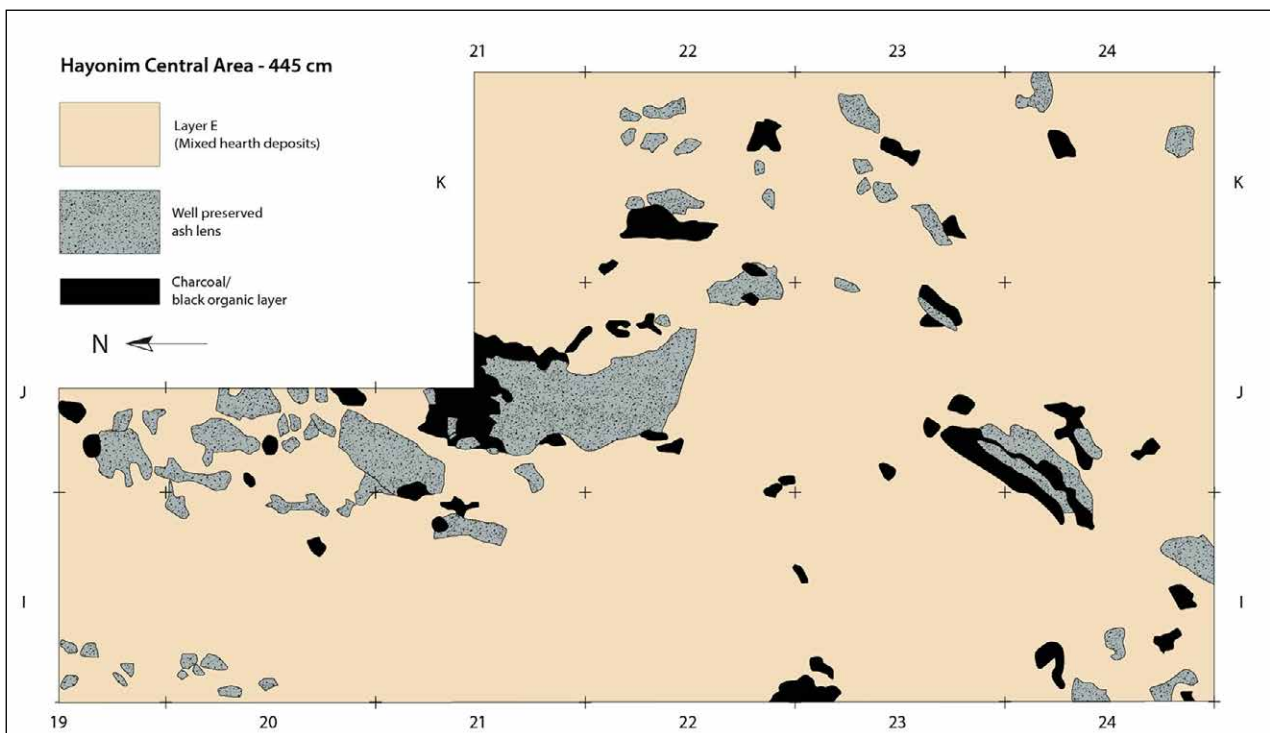


Figure 3.30. Décapage plan at -445 cm.

Main features (Figure 3.30)

This décapage is comprised of locally cemented mixed hearth deposits, with apatitic/calcitic zones and only some low solubility phosphate nodules. Numerous patches of locally cemented whitish/grey ashes occur together with localised dark organic zones. Terra rossa clasts are always present.

The entire surface of the Central Area is occupied by a series of small patches of white or light grey ashes including more continuous/larger ones that are described below:

- I24-J24a-J23cd: numerous patches of locally hard and cemented white or light grey ashes occur with large remnants of black dark silty clay (organic sediment) that underly them (basal hearth deposits).
- J22ab-J21acd: large continuous but irregular lens of white ashes (100 × 50 cm), 5–10 cm thick, are underlain and partially surrounded by large patches of black organic sediment (remnants of charcoal).
- J19a-J20ac-J21a: more or less poorly preserved hearth lenses are stratigraphically contemporaneous with the large main lens in J22 (possibly the same feature).
- All the hearth lenses are quite thin (5–10 cm) and are not present in the sediments above -450 cm.

Illustrations

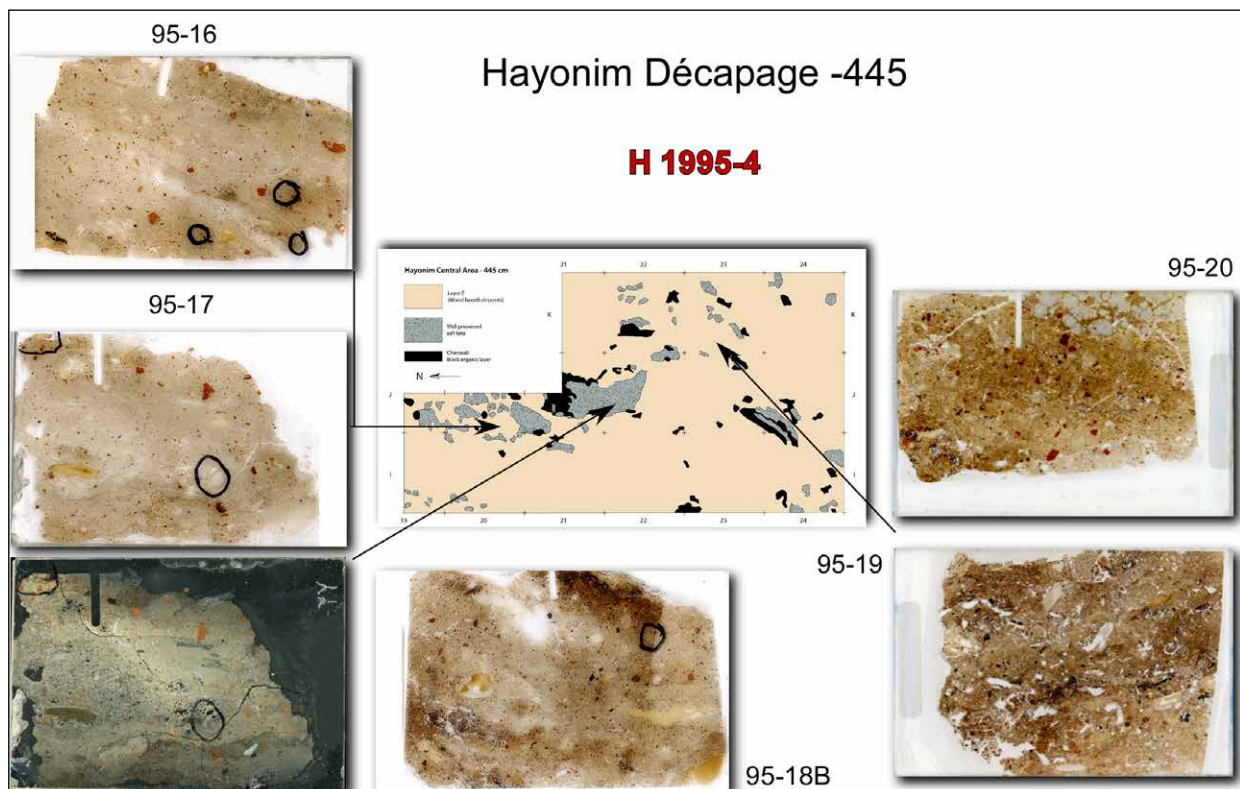
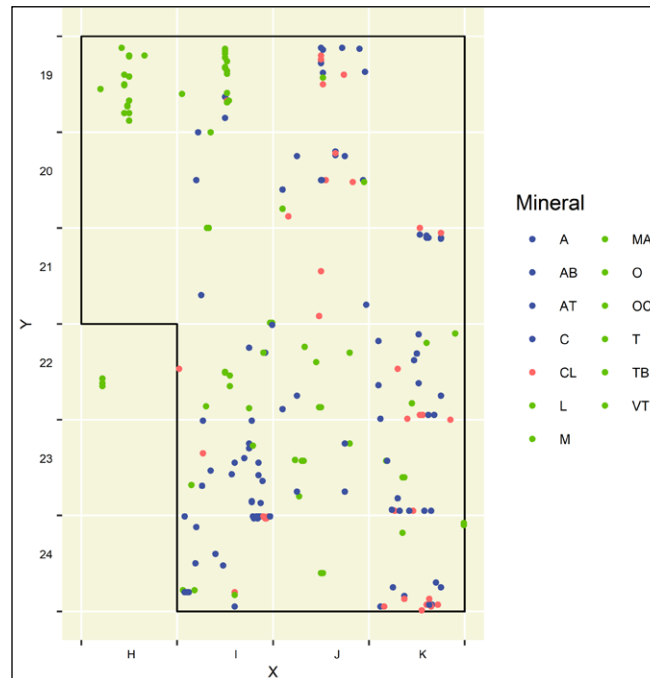


Figure 3.31. Décapage at -445 cm with plan showing hearth 1995-4, which is surrounded by essentially mixed ashy sediment. The latter is illustrated in the accompanying thin section scans of samples 95-16, 95-17, 95-18, 95-19, and 95-20, which show unstructured bedded ashes and organic-rich ashes, which are generally apatitic or calcitic, with no LMVS minerals. At lower left is dark field scan whose brightness emphasises the calcitic nature of the ashes in 95-17.

3.4.3.6 Décapages -425 cm and above (Figures 3.32, 3.33)

3.4.3.6.1 Mineralogical map (Figure 3.32)

Figure 3.32. Map showing mineral distributions from -350 to -435 cm. Since this slice is ~100 cm thick, it is difficult to provide a precise summary. However, the LMVS assemblage is quite prominent in the northern part (H18-19) and spotty along the northwest/southeast axis described above. On the other hand, the less altered CD minerals and clay (CL) are much more widespread over the entire area, particularly in the southern half and toward the edges of the Central Area.



3.4.3.6.2 General description (Figure 3.33)

In the levels -445 cm and above, few or no combustion features were observed in the Central Area, with some exceptions in the upper part of the southwest corner of the South Profile (e.g., I24, -330 to -340 cm) as well as the upper northwest part of the North Profile (HI19, -380 to -430 cm).

Hayonim Décapage -425 and above



Figure 3.33. Décapage at -425 cm. Combustion features are poorly represented and instead, sediments consist of crumbly brown to dark brown silt with abundant pale yellow phosphate (LMVS) nodules (95-4); yellowish red powdery silt with vertical apatitic veins, and Mn-stained bone and voids (94-25; note that this thin section measures ~50 × 50 mm); and crumbly, altered clay with yellow phosphatic (LMVS) concretions in reddish silty clay (00-517).

3.4.4. Major changes in combustion features observed through sequence

Here, we summarise the overall changes in the aspects of the combustion features throughout the excavated sequence in the Central Area of Hayonim.

-540 to -520 cm Within this interval are localised, large, thick hearth features (e.g., H 1998-16 in IJ19, IJ20: 80–100 cm in diameter [Ø], 30 cm thick; H 1998-12 in K22–23, J23: at most, ~150 cm Ø, 12 cm thick) resulting from the accumulation of numerous superimposed/overlapping shallow hearth lenses. The combustion features seem to be spatially localised, and they illustrate repeated use in a patterned way. These features probably represent relatively complete hearth lenses in an area of dense hearth deposits, and their outlines are determined by one or two relatively thick, well-preserved ash lenses. However, the distribution of charcoal that surrounds them reflects many smaller additional overlapping and finely bedded thin hearth lenses.

-515 to -505 cm This interval consists of mostly mixed hearth deposits with a high density of partial hearth lenses in some areas, such as in K22–23, J23. Here, a large concentration of partially preserved, overlapping, or superimposed hearths is preserved; a similar situation exists in IJ24 and IJ19–20. In all of these areas, multiple, thin, partially preserved hearth lenses are observed. Typically, a lens—or rather, a partial lens—comprised of stratified ash and remnant charcoal, is only about 3–5 cm thick and is partially underlain or overlain by other imbricated hearths.

It is clear, though, that the Central Area from -505 to at least -515 cm was repeatedly used as a place to make hearths. However, it is not known whether this zone extended beyond its current visible limits, having been obliterated or truncated by trampling, burrowing, or chemical diagenesis.

-500 to -490 cm The hearths in this slice are characterised by the co-occurrence of large (>100 cm), thick features (e.g., hearths 1997-5 in J21–22; 1997-8 in I19–20 and J19) and numerous patches of ash and/or black organic remains corresponding to thin (a few centimetres) combustion features (e.g., 1997-13, 1997-14 in the zone J22–23, K22–23). Hearths 1997-8 and 1997-5 reflect examples of multiple hearths being locally preserved in the same position and representing a thickness of over 10–15 cm.

-485 to -480 cm Hearths in this interval are represented by only a few large (~100 cm in diameter and 5–7 cm thick), continuous, well-preserved, thin patches of white/light grey ash. In some cases, they are locally underlain by black (organic) clayey silt. For the most part, these patches are surrounded by homogenised mixed hearth deposits, which occupy most of the surface of the excavated area.

-470 to -440 cm In contrast to the underlying *décapages*, this block of deposits is mainly composed of ‘mixed ashy sediment’ with numerous small patches of grey ash and black organic sediment (JK22-23, J20–21). Locally, some larger, more continuous patches of white/light grey ashes and/or black organic sediment are observed, especially at -445 cm. Nevertheless, all of these combustion ‘features’ are quite thin and probably correspond to thin hearth lenses that have been disturbed and made less discernable largely by trampling, insect burrowing, and possibly diagenetic alteration, which is visible in Figure 2.19 of the South Profile.

-430 cm and above (up to -270 to -300 cm depending on the specific location; these latter depths represent the beginning of our excavations). There are practically very few visible traces of combustion features above these levels in the successive *décapages* of the Central Area. Field observations reveal that traces of fire are represented locally by small clusters

and lenses of white ashes, which may be consolidated or not. They are thin and contain small concentrations of burned bones and flints. Some small hearth lenses are observed.

We note, however, that there are some exceptions:

- Some small, partial hearths were observed in the southwest corner of the Central Area and visible in I24, at around -320 to -330 cm.
- Also in HIJ19 along the North Profile, we recognised fine remnants of hearths and ash lenses dipping northwest, at -370, -400, -405, and -410 cm, including a ‘partial black hearth, yellow/white phosphates, and locally cemented ashes’. These lenses pass laterally into a number of small, thin superposed hearths visible in G/H18–19 that have been highly bioturbated by insects (see Figures 2.25, 2.26).
- Thus, in contrast to what we observe in the main part of the Central Area (i.e., HIJK20–24), it appears that combustion features—even some that are badly preserved and found within the LVMS zone—are present throughout in the area north of the décapage.

3.5 Discussion: interpretation of observed changes

3.5.1 Impact of diagenesis on combustion features

The observations presented above highlight fairly clearly the variation in different spatial and temporal aspects of the combustion features as they occur throughout the sequence. These facets include the types of combustion structures (isolated hearths and superposed ones in the same place resulting in thick combustion structures, etc.), the intensity of combustion, and the degree of preservation. Before interpreting their significance in terms of traces of human activity, it is necessary to evaluate the impact of chemical diagenesis, which may affect the morphology of the hearths, their degree of preservation, and their possible disappearance. Understanding diagenesis ensures that the hearths we observe are not mainly the consequence of differential preservation (Berna and Goldberg 2008; Karkanas et al. 2000; Weiner et al. 2007).

The mapping of combustion structures, as well as that of phosphate zones (corroborated by FTIR analyses mostly undertaken in the field during excavation), highlight mineralogical transformations that can be seen to vary spatially (within the same level) and temporally (vertically through the sequence). These variations are illustrated in plots of minerals from the Central Area within different décapage slices (see mineralogical plans for each décapage). Although there are some local mineralogical variations in the point-plotted data, some global trends are evident (see also Weiner, Goldberg, and Bar-Yosef 2002).

Sediments in proximity to the bedrock walls are understandably calcareous for the most part due to the abundance of calcite. On the other hand, away from the walls and areas with travertine accumulations, these calcareous areas exhibit markedly increased degrees of diagenesis. Sediments closest to these calcitic zones are apatitic and in a direction toward the central axis of the cave are transformed into a number of different Ca, Al, and K phosphates, including degraded clays and the formation of opal. This overall distribution is exhibited by a roughly linear zone of extensively phosphatised deposits along an axis from ~H19 to ~J24. This horizontal mineral distribution remained virtually in the same location in all excavated areas. However, the exact position of the boundary between phosphate types and less altered calcite/dahllite zones change through time, as can be seen both in profile and in map slices made at different levels (see also chapter 4). Consequently, the size of the diagenetic band appears to shrink or grow through time. The reason for this shifting is not clear but it may be related to changes in water availability and flow rates over time.

Nevertheless, examination of the different plans showing the distribution of the combustion structures throughout the sequence shows that, in the levels above -485 cm, the (well) preserved ash zones are distributed over the entire surface except for the zones marked by the presence of strong diagenesis (the LMVS mineral assemblage of Weiner,

Goldberg, and Bar-Yosef (2002): leucophosphite, montgomeryite, variscite, siliceous aggregates). Likewise, in the levels below -495 cm (i.e., where the LMVS phosphate zones are much more restricted), the state of preservation of the combustion structures is better. They are distributed over a larger area and are more or less related to the widening of the calcite/apatite zone (the CD mineral assemblage of Weiner, Goldberg, and Bar-Yosef [2002]: calcite-dahllite) in these levels.

At first glance, therefore, a link seems to exist between soil geochemistry and state of preservation of the hearths. These trends have already been underlined by Weiner, Goldberg, and Bar-Yosef (2002: 1300), who reported, 'The best preserved hearths are the calcitic ones...[and] the large majority contain as their second most abundant mineral, dahllite...In fact very few hearths were analysed which contain these minerals (i.e., LMVS) as their most abundant phase' (see also chapter 4, this volume).

However, as briefly noted above, a more detailed observation of the data adds certain nuances to these findings and highlights frequent exceptions to this general pattern. Field data show that the link between mineralogical/geochemical environment and state of preservation of structures is not systematic. In particular, numerous examples demonstrate that there is no total disappearance of the structures in the LMVS zones:

- Weiner, Goldberg, and Bar-Yosef (2002:1294) indicate that '...visible hearth-like features extend from the CD assemblage zone into the LMVS zone (Figure 4)'.
- The combustion structures present in the upper part of the northern profile of HI19 (~-400 to -420 cm) are in the LMVS area (see figure 13 profile D, in Weiner, Goldberg, and Bar-Yosef 2002:1302).
- In the décapage of -520 cm, hearth 1998-13 maintains its morphology across the apatite/leucophosphite boundary.
- In the décapage of -510 to -515 cm, thin, partially overlapping, clearly stratified hearth lenses are found in both apatitic areas and those with taranakite and other less soluble phosphates.
- In décapage -445 cm (-440 to -449 cm) (also Stiner et al. 2005: Figures 4-7), we observe an area of well-preserved hearths not only in J21cd and J22ab (calcite/dahllite area), but also, in J24-23, an LMVS area with a significant number of hearth remains. Conversely, in this same level, in I24-23, the structures are very fragmented and poorly preserved in a calcite/apatite zone, one that theoretically should be rather favourable for preservation.
- In the North Profile (HI19), the base of these exposures show thinly bedded burned zones that closely resemble those in G18. In the latter case, FTIR analysis revealed mostly siliceous aggregates. Those in H19 and I19, however, are apatitic, which suggests that these thinly bedded hearths/burned areas do not owe their morphology to diagenesis; rather they maintain the form associated with the original human activities that produced them.

Chemical diagenesis, and in particular, the formation of phosphates, very probably make the visibility and 'reading' of combustion features more difficult by blurring the picture. However, they do not ultimately eradicate their main characteristics. They can modify the contours, the initial shape of the combustion structures (probably less than do physical phenomena such as trampling/burrowing), but they do not change their 'construction' and the organisation of the hearths (i.e., stacking of hearths versus thin, isolated, non-stacked ones). The structures are probably easier to read in a CD mineralogical environment, but it is very likely that they are not totally destroyed by the formation of phosphates, as we can see in the hearths around H18 (Figure 2.26) in which, despite insect burrowing and LMVS diagenesis, traces of the original fine hearths can still be observed. The same is true at Kebara (Meignen, Goldberg, and Bar-Yosef 2007). In sum, the main destructive post-depositional phenomena are physical factors (e.g., precipitation, wind, erosion), or ones of biological/human origin (e.g., trampling, rakeout, insect and rodent burrowing) rather than chemical ones.

3.5.2 Interpretation of human activities: types of hearths, 'intensity of occupation'

The reflections above tend to show that the processes of chemical diagenesis do not make the organisation of combustion levels or their composition disappear. Their presence—or remains even if modified—allow us to assess their significance in terms of human activities. Thus, we are in a position to address and interpret the differences through the sequence that we described above.

When viewed as a whole, the diachronic changes of the combustion structures highlight a break within the sequence that makes it possible to identify two major groups of features.

3.5.2.1 The Lower Levels (décapages -540 to -490 cm)

These lower levels encompass large combustion structures, which are generally quite thick (~5–12 cm) and correspond to the stacking/superposition of several fireplaces of smaller size. These different features are most often composed of well-preserved white/gray ash levels superimposed on organic black ones; the latter are often not very thick and are discontinuous (with some exceptions). In fact, it is the good state of preservation in the field—at least locally—of these 'black organic/white ash' couplets that made it possible to identify the stacking of these fairly fine combustion levels (ash levels: 5 to 10 cm; organic levels: 1–2 cm), even if they are sometimes difficult to follow over a large area. It should similarly be noted that on the microstratigraphic scale of the thin sections, we also observe the superposition of several small combustion episodes (e.g., Figure 3.12). These can commonly be imperceptible in the field (Aldeias et al. 2012).

The conditions of formation of these large structures as observed in the field therefore correspond to the accumulation of numerous combustion episodes that, individually, were probably quite brief. In fact, it is only the repetition of fires occurring more or less in the same place that provides the morphological aspect of large hearths (both in thickness and in area; cf. hearth 1998-16, for example).

The contours of these large structures are irregular and very sharp (a consequence of mainly trampling and burrowing), and their dimensions are considerable:

- Thicknesses vary generally from 10 to 20 cm, and up to >30 cm for hearth 1998-16, for example.
- Maximum diameters are most commonly from ~100 to 150 cm.

These hearths, however, are different from the few large combustion structures described in Kebara (e.g., the hearths in unit XIII in the Deep Sounding), which are also comprised of the superposition of several hearths (Meignen, Goldberg, and Bar-Yosef 2007). Nevertheless, in Kebara, these hearths are thicker, particularly the white ashes, whereas in Hayonim, as noted above, these large structures consist of brief, superimposed combustion episodes. It should also be noted here that these large structures are very largely surrounded by mixed hearth deposits.

Hearths in the Central Area are thus represented by repetitive combustion activities with many thin, superposed, and overlapping hearths that are more or less in the same place. These observations seem to indicate that the combustion zones occur or are preserved in a rather distinct location, and therefore point to a concentration of fire activities in certain places. This situation would therefore point to continuity in the localisation of some combustion activities over a significant interval of time. In turn, this suggests a structuring of the domestic space within the central area of the cave.

The occurrence of the 'dark organic matter/white ash' couplets in the field demonstrates a relatively good state of preservation of the combustion episodes. The presence of well-preserved ash levels here is most likely the consequence of the relatively rapid superposition of the hearths, which in turn allows for at least partial protection

of the thin hearths during successive occupations over time. It is widely known in the literature that under certain circumstances, combustion structures can be preserved by the protective effects of overlying hearths, provided that the time interval between events is relatively short (Aldeias et al. 2012; Karkanas 2021; Mallol et al. 2013; Mallol et al. 2007; Meignen et al. 2009; Meignen, Goldberg, and Bar-Yosef 2007; Mentzer 2014; Weiner, Goldberg, and Bar-Yosef 2002). These observations therefore suggest that combustion episodes are rather closely spaced in time.

3.5.2.2 The Upper Levels (décapages above -490 cm)

The upper layers contain combustion features that are much less 'legible'. They are most often identified during excavation in the form of large areas of ash (white/light gray ashes) that are more or less consolidated.

Between -485/-480 cm, combustion features are mainly represented by large areas of ash, in addition to a few visible remains of hearths (e.g., hearth 1997-6). However, generally these 'structures' are not very thick (~5-7 cm) and the charcoal zones are very discontinuous, in the form of patches. Thin section observations show that these ash zones result from intense trampling, even if sometimes small episodes of in situ combustion are still visible, although difficult to identify.

In the overlying levels (-470 to -440 cm), the remains of combustion are mainly comprised of mixed hearth deposits within which are observed numerous patches with variable dimensions of white/light gray ashes or black organic sediment. These areas of ash are not very thick, but more or less continuous, and very irregular in shape. In thin section, they show very strong traces of trampling and burrowing, but again, in some cases we observe traces of several intact combustion episodes.

What is observed therefore suggests areas of thin hearths represented mainly by ashes. Despite not having clear limits, they are not stacked, and therefore are different from the structures observed in the lower levels. They would appear to have been largely modified or obliterated by trampling or burrowing. In short, these combustion features probably correspond to small, poorly delimited, successive localised fires.

These large areas of white ash (white/light gray ashes)—which are not very thick—most likely correspond to periods of combustion of shorter duration than those in the lower levels. The examination in thin sections sometimes indicates the presence of still locally identifiable couplets of small white ash/organic black sediment, which testify to very short combustion episodes (see experiments in Karkanas 2021).

They probably correspond to large combustion areas that are not very thick, and made up of small, more or less adjacent/contiguous hearths that are not systematically superposed (i.e., not stacked). Their thinness makes them sensitive to homogenisation by processes such as trampling and insect bioturbation. Furthermore, these observations most likely indicate a lower degree of spatial organisation of combustion activities. In fact, during successive human occupations, the installation of new fireplaces does not take into account the spatial organisation of previous ones.

Moreover, ethnological data show that long-term human occupations tend to perpetuate the structuring of the space occupied by activities. Conversely, the lack of permanence of activities in the same place could suggest short-term occupations separated by significant gaps between periods of occupation.

Finally, as we described above, the levels corresponding to the upper units (above -430 cm) provided evidence of combustion (e.g., small ash lenses, small concentrations of burned bone, as well as burned lithics and bones dispersed in the deposits). These all attest to the use of fire. On the other hand, these remains are very difficult to interpret given their state of preservation, and we therefore do not include them in this summary.

3.6 Conclusions

In concluding, we highlight some fundamental elements characteristic of the combustion phenomena in Hayonim Layer E.

Firstly, the large volume occupied by deposits directly linked to combustion activities in the Central Area in Layer E is remarkable and striking, especially in light of the fact that each hearth undoubtedly represents numerous burning episodes (see experiments in Karkanas 2021). We note, however, that similar phenomena have been already described in other cave sites from the region (e.g., Amud, Kebara; Madella et al. 2002; Meignen, Goldberg, and Bar-Yosef 2007, respectively). This remark is applicable only to Layer E, since during the deposition of Layer E, only a low density of combustion structures are visible in the Central Area, which goes hand in hand with a low density of lithic material.

In Layer E, not only are many structures present (more or less legible depending on the level, as described above), but the deposits surrounding these structures are made up of what has been called ‘mixed hearth deposits’. These correspond to the destruction/homogenisation of a large part of the combustion elements by processes such as trampling and burrowing. As such, it is nevertheless clear that the former inhabitants lived consistently in an ‘ashy environment’, which was associated with intense fire-related activities. In this regard, Weiner, Goldberg, and Bar-Yosef (2002: 1303–4) noted,

The sediment separating these hearths also contain abundant ash-derived components and micromorphologically appear to be hearths modified by trampling... This raises the question of why hearths are preserved as well defined entities even though they are essentially buried in ash of the same or similar composition.

The answer to this question is first physical, as we mentioned earlier. Where a combustion/hearth structure is quickly covered (by sediment, or other combustion structures), it is protected and better preserved. The rapidity of burial is an important factor for the preservation of hearths, as it mitigates against, at least partially, the effects of trampling, which seem to be so destructive at Hayonim (cf. Mallol et al. 2007). On the other hand, Weiner, Goldberg, and Bar-Yosef (2002: 1304) posit that ‘...the repeated action of making a fire in the same location stabilises some of the ash calcite that remains in the hearth... [and] that the practice of making a fire in the same place accounts for the preservation of hearth ash in the Mousterian’. The re-formation of calcite associated with burning stabilises the hearth ash versus the surrounding dispersed ash. These comments are confirmed by the experiments of Karkanas, which show that ‘Continuous relighting of ashes radically changes their physical characteristics by producing a sintered, compacted and, thus, more stable formation’ (Karkanas 2021: 34).

Overall, the evidence shows that the majority of the identified combustion features represent features in which the fire activity took at that locale, but which, in some cases, have been syn- or post-depositionally modified by trampling, burrowing, and diagenesis. Moreover, throughout the Hayonim sequence, the combustion structures show preservation of the ashes, which are generally significantly thicker than the organic black levels. The latter are often not very thick, discontinuous, and different from what is observed at Kebara, where the black levels are clearly visible in plan and in section (halo); only a few examples of a ‘halo’ occur at Hayonim (e.g., hearths 1993-1; 1998-16). The thinness of the black/organic levels compared with the overlying ash levels suggests almost complete combustion (Mentzer 2014).

These black levels are characterised by the presence of organic matter, but very little char or charcoal. Charcoal is very rarely preserved, and very few macroscopic pieces of charcoal were recovered, despite numerous attempts at flotation in the field; it is also infrequent in thin sections. The notable absence of charcoal raises the question of the types of combustion responsible for this situation. The role of fuels is also very likely to be taken into account. The study of phytoliths shows a strong representation of phytoliths of dicotyledonous leaves alongside those from wood or bark, a particular combination

most likely corresponding to the use of bushes and branches as fuel (Albert et al. 2003); ashes visible in thin sections suggest wood or woody vegetation like bushes or shrubs. The combustion of such materials, especially if they represent complete combustion, results in a significant production of ash and a very low production of charcoal. The fuels used together with complete combustion are therefore likely responsible for the very low presence of charcoal.

Short-term fireplaces seem to be the rule in combustion activities in Hayonim. In all cases, it seems that the fires/combustion structures observed in the Hayonim sequence correspond to thin fireplaces. They therefore most probably relate to short-term combustions episodes, separated by more or less important intervals of time depending on the levels. These successive small combustion episodes can also be observed on the scale of the thin section (see also Aldeias et al. 2012).

Depending upon the level, thin hearths are either:

- Superposed more or less in the same place, thus resulting in large combustion structures that are often thick (up to $\sim >30$ cm for hearth 1998-16); they correspond to repetitive occupations of the Central Area, which follow one another fairly quickly within the framework of a 'structured' activity space. This situation was observed in the lower levels.
- Or unorganised, not superposed, and their original structure has been more or less destroyed (homogenised by trampling). They therefore constitute combustion areas identified mainly by the presence of ash zones. The time between the different occupations would be longer than in the above case. These circumstances (destruction of structures) was seen in the upper levels.

In an initial study of the hearths (Meignen et al. 2009), the second scenario seemed to us the most representative of the types of combustion in Hayonim, in contrast to the very thick combustion structures observed in Kebara (Meignen, Goldberg, and Bar-Yosef 2007). More recently, an in-depth study of the lower levels of Hayonim, where the combustion structures are more impressive, has highlighted the intensity and continuity of the hearths, which are superimposed on them. However, it seems that, taken individually, the combustion levels that make up these large structures also correspond to relatively short combustion episodes. Throughout the entire Hayonim sequence, we never were able to elucidate the lengths of occupation that we were able to infer from the study of the Kebara hearths. In any case, as we described in this previous article on Hayonim, our conclusions that combustion activities suggest short-term occupations are in agreement with the other contextual data (lithic, fauna, phytoliths).

The study of phytoliths in the absence of well-preserved charcoal made it possible to tackle the question of fuels. It shows that the assemblages are very different from those described in other Mousterian sites of the Near East (Albert et al. 1999; Albert et al. 2000; Madella et al. 2002). In Hayonim Layer E, in most of the hearths sampled, phytoliths from dicotyledonous leaves are widely represented alongside those from wood or bark. This particular combination is said to be the result of the use of bushes and branches as fuel (Albert et al. 2003). It would correspond to a non-selective collection of any available plants in the immediate environment of the cave. This hypothesis is confirmed by the presence of heated red clay clasts, whose almost ubiquitous presence in the ashes (see above and chapter 2) could be explained by the uprooting of bushes that grow on the terra rossa soils distributed around the cave. This non-selective behaviour would reflect a low requirement related to the quality/efficiency of the fuels collected.

The large amount of contextual data we have allows us to integrate these behavioural data into a larger context (Meignen et al. 2009). In the Mousterian levels of Hayonim Layer E, the occupancy densities are low, as suggested by the low quantities of tools (an average of ~ 300 pieces >2.5 cm per m^3 [see chapter 5, Table 5.8] in sediment deposited over 10,000–15,000 years). On the other hand, the production and use of lithic tools

were carried out onsite within the cave (Meignen et al. 2006 and chapter 5, this volume). Wildlife studies (Stiner et al. 2005 and chapter 4, this volume) indicate a hunt focused on a few ungulates (gazelle, Mesopotamian fallow deer) and low numbers of animals killed. All of these data converge on the hypothesis of short occupations and/or groups with small numbers. The opportunistic acquisition of fuels, as we have described previously, seems to go hand in hand with short-term occupations, which entail lower requirements in terms of energy needs (Théry-Parisot and Costamagno 2005).

Hayonim Cave thus appears to be a residential encampment where all production and consumption activities took place, but it was visited only for rather short episodes of time. These repetitive occupations were probably separated by long periods of absence, as shown by the abundance of rodent remains in this infill. Such breaks in anthropogenic sedimentation have no doubt contributed, in part, to the partial destruction of the combustion structures described above by weathering/chemical diagenesis during periods of cave abandonment (Weiner, Goldberg, and Bar-Yosef 2002).

Faunal perspectives on carbonate preservation and hearth-centred activities during the Middle Palaeolithic in Hayonim Cave

Mary C. Stiner

4.1 Introduction

When the Hayonim field project began in 1992, information on early Middle Palaeolithic (MP) subsistence was rare in the Levant and across Eurasia more generally. The technological record was somewhat better known, but deeply stratified sites that preserved bones alongside stone artefacts, such as Hayonim Cave (Figure 4.1), were almost unheard of. Later MP sites in the region were already yielding rich combinations of faunal remains and artefacts (e.g., Kebara Cave on Mount Carmel; Bar-Yosef and Meignen 2007; Bar-Yosef et al. 1992; Meignen and Bar-Yosef 2019). Having worked previously on MP cave faunas along the northern Mediterranean Rim, I had a taste of what the earlier MP might hold. Important hypotheses of the day concerned small prey use, fire-centred base camps, and hominins already expert in taking down large hoofed animals. However, working with an international team at Hayonim Cave offered me much more than this. It was a collaborative experience that set me on a novel path of scientific and personal growth, thanks especially to the vision and generosity of Ofer Bar-Yosef. My work at Hayonim spanned 1992–2000 and culminated in a monograph with Peabody Museum Press (Stiner 2005). That monograph and related publications (Stiner, Howell, et al. 2001; Stiner, Kuhn, et al. 2001; Stiner et al. 1995) are the primary sources on the depositional contexts, faunal assemblage formation, biogeography, and hominin diet at Hayonim Cave.

The present chapter is limited to two themes, which complement the technology and geoarchaeology studies in this volume. The first theme uses the faunal record to learn about site formation processes, such as why bones had much patchier distributions than lithic artefacts in Layer E of Hayonim Cave. The main (but not exclusive) answer is uneven preservation conditions for bones, because the calcium phosphate minerals underwent chemical diagenesis as organic inputs temporarily lowered the pH of the sediments (Weiner et al. 2002; Stiner et al. 2001b; Stiner et al. 1995; Surovell and Stiner 2001).

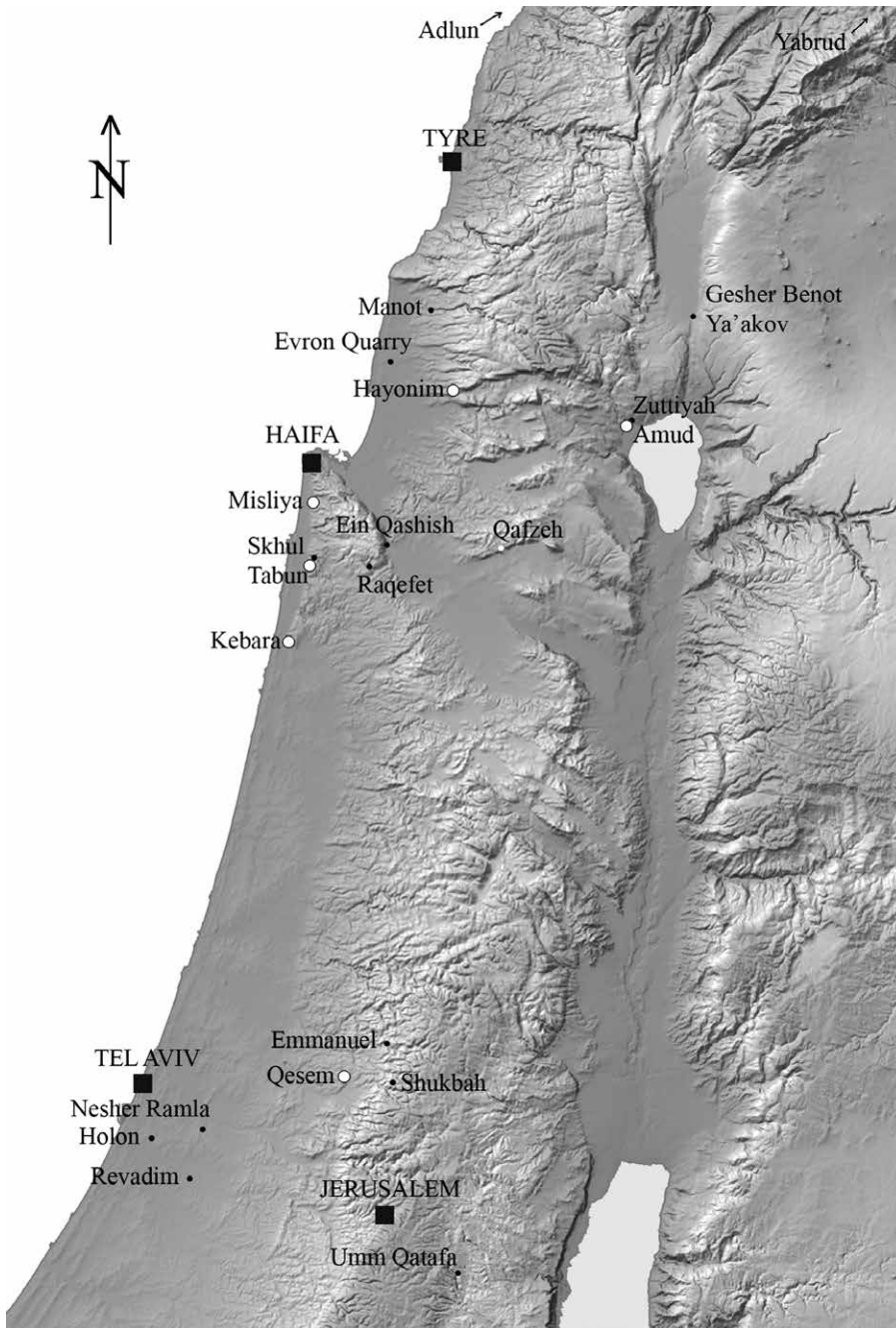


Figure 4.1. Locations of selected Middle and Lower Palaeolithic cave and open sites in the southern Levant. Open circles represent sites important to this chapter. Base map credit: Eric Gaba, Wikipedia Commons.

But our collaborative investigations of carbonate mineral preservation were more far-reaching this—they affected our understanding of combustion phenomena (chapter 3, this volume), differential density of plant phytoliths, and variation in sediment radiation doses that are essential to ESR and TL dating. Because fire records can be fugitive, microarchaeology perspectives proved to be game-changers for interpreting MP fire use in the site (Mercier et al. 2007; Mercier et al. 1995; Rink et al. 2004; Schiegl et al. 1996; Schiegl et al. 1994; Shahack-Gross, Bar-Yosef, and Weiner 1997; Weiner, Goldberg, and Bar-Yosef 1993; Weiner, Goldberg, and Bar-Yosef 2002; Weiner et al. 1995).

The second theme presents, with updated information, the spatial and functional connections between animal carcass processing and fire use inside the cave during the MP. Intensive mapping and analysis of combustion features in Layer E revealed a rich

record of fire use (chapter 3, this volume). Behavioural connections between carnivory and fire were drawn by cross-referencing taphonomic signatures of food processing, animal body part representation, and spatial variation in burning and other types of bone damage (Stiner 2005: 81-112). The results illustrate the integral nature of fire in MP existence during the Middle Pleistocene, both as an element of technology and a focal point of domestic life in residential camps. Bones tell a critical part of this story.

The two themes illustrate the conceptual power of processual archaeology, a long-standing and, at times, underappreciated agenda in the service of new questions. An abiding interest of mine is the evolution and functionality of human domestic spaces (Stiner 2021). The concept holds the interest of many palaeoanthropologists, but the devil remains in the details. Simply put, it is impossible to infer human activity patterns in sites without a thorough consideration of site formation processes. Archaeologists have proposed behavioural transitions during the Palaeolithic mainly from shifts in stone technologies and diagnostic artefacts. While strong connections exist between technology and subsistence in general, the characteristics we commonly measure may not change in lockstep with one another. There is also the question of how 'crisp' certain behavioural shifts were over the course of the Middle Pleistocene, and to what extent they related to broad environmental changes, if at all. Gaps in the Levantine archaeological record have posed significant obstacles to answering these questions. The Hayonim Cave archaeological sequence fills one of these gaps to an unprecedented degree. This chapter closes with a comparison of continuity and change in 'hearth-side economics' and animal community structures from the late Lower Palaeolithic through MP in the study area.

4.2 Stratigraphic units, faunal samples, and analytical methods

Layer E in Hayonim Cave (chapter 2, this volume) contains MP artefacts throughout its depth. This layer may reach a thickness of 8 m in the rear of the cave but thins to 3–4 m in its centre, where we placed the main excavation trench (Central Area). A coherent chronostratigraphic series was identified in squares G18–K24, and the zooarchaeological study focused on material from an area of ca. 8–10 m² within the trench. Here, Layer E is directly overlain by later cultural deposits that are also rich in bones and artefacts, including remnants of Aurignacian Layer D, Kebaran Layer C, and Natufian Layer B (Bar-Yosef 1991a; Belfer-Cohen and Bar-Yosef 1981; Tchernov 1994). The possibility of vertical mixing between the MP and later layers had to be considered for this reason (see below).

No clear stratigraphic divisions were found within Layer E, but it represents a general time series based on technological and dating evidence. Most of the sediments accumulated horizontally under the cave roof and were protected from direct sunlight (Goldberg 1979; Goldberg and Bar-Yosef 1998; Goldberg and Laville 1988); indeed, weathered bone specimens are very rare. Layer E was subdivided into six vertical units (units 1 through 6) based on variation sediment microstructure and artefact densities (exemplified for the J-row in the Central Area in Figure 4.2). Technological analyses indicate differences between the MP lithic assemblages in units 1–3, which display centripetal Levallois flaking methods, and those in units 4–6, which retain properties of the Levantine Early MP (termed EMP, Meignen, this volume). This trend is an important point of reference for variation in the faunal assemblages discussed below. Because faunal remains were abundant in some but not all squares, variation in faunal abundance was not used to subdivide the sediment column in Layer E in the Central Area. Unit 4 was exceptionally rich in faunal material and so was further subdivided into units 4a and 4b for some of the faunal analyses (Stiner 2005).

Layer F is also subdivided into semi-arbitrary units 7 through 10. This layer was exposed mainly in the Deep Sounding at the front of the cave, but the top of it (unit 7) was also encountered in the Central Area. The technology of Layer F is attributed to the EMP (Meignen 2011; Meignen and Bar-Yosef 2020) and these materials occur throughout the layer. Unfortunately, bones were not preserved in the Deep Sounding, and only a small amount of bone was encountered in unit 7 (NISP 270) in the Central Area. Layer G

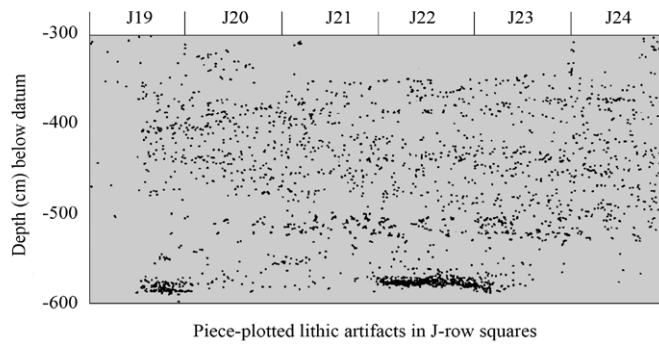


Figure 4.2. Distribution of piece-plotted lithic artefacts in the J-row section of Middle Palaeolithic Layers E and F, in the Central Area. Mild variation in artefact density is apparent on the vertical plane. Two very dense lithic concentrations, interpreted as possible knapping areas, are visible at the base of the section, corresponding to the top of Layer F. Plot provided by S. Kuhn. Image adapted from Stiner 2005: Fig. 4.16.

Layer	Depth range (cm bd)	Total NISP	Ungulate MNI
E, unit 1	250–299	161	3
E, unit 2	300–349	352	4
E, unit 3	350–419	1,870	7
E, unit 4a	420–444	4,854	17
E, unit 4b	445–464	4,054	⋮
E, unit 5	465–494	3,176	8
E, unit 6	495–529	2,351	6
F, unit 7	>530	270	3

Table 4.1. Faunal sample sizes (NISP) for MP assemblages from Layers E and uppermost F in the central excavation trench of Hayonim Cave. MNI calculations are based on skull parts, for which there is good correspondence between tooth- and bone-based estimates.

(unit 11), which is known only from the Deep Sounding, contains Acheulo-Yabrudian artefacts (Meignen and Bar-Yosef 2020) and is almost entirely lacking in bone.

The discussion to follow will focus on MP materials from Layer E. The faunal sample from the Central Area exceeded 17,000 identified specimens (Table 4.1), and these materials were studied in their entirety (Stiner 2005). Fine dry-screening was employed systematically during the excavations, and sediment chemistry relevant to faunal preservation conditions was tested throughout the Central Area in collaboration with Steve Weiner, Ruty Shahack-Gross, Paul Goldberg, Todd Surovell, and others. Unidentified bone fragments were many more in number, and these were sampled systematically for burning damage, tool marks and related characteristics. Burning damage criteria were developed experimentally during the field project (Stiner et al. 1995) and applied throughout the zooarchaeological work at Hayonim Cave. Faunal samples from units of unclear origin, or representing mixed cultural entities, were removed consideration. The main quantitative units used for this chapter are the number of identified specimens (NISP), the minimum number of skeletal elements (MNE), and the number of unidentified specimens (NUSP).

Diagenetic alterations were examined using a portable Fourier transform infrared (FTIR) spectrometer, (Weiner and Bar-Yosef 1990; Weiner and Goldberg 1990) in the cave and later in my laboratory at the University of Arizona (Stiner et al. 2001b; Stiner et al. 1995; Surovell and Stiner 2001). FTIR data served as a proxy for the chemical volatility of the preservation environment in the cave sediments. We also investigated mechanical disturbances of the sediments and the extent of macroscale bone attrition caused by mechanical destruction. The latter process tends to destroy spongy (trabecular) bone tissues more rapidly than compact bone tissues (see reviews by Lyman 1994; Stiner 2002, 2004), resulting in biases such as greater loss of proximal versus distal fragments of an ungulate humerus. The analyses compare the relative abundance of different skeletal portions with predictions of their resistance to mechanical destruction based on inherent bulk bone densities of modern control samples.

Figure 4.3. Top view of the spatial distributions of piece-plotted lithics (top) and bones (bottom) in the Middle Palaeolithic sediments from 300 to 540 cm bd in the Central Area. Horizontal spatial units are square metres. The most notable clustering in the lithic distribution is due highly localised concentrations of artefacts around the boundary of Layers E and F. Plots provided by S. Kuhn. Image adapted from Stiner et al. 2001b: Fig. 3.

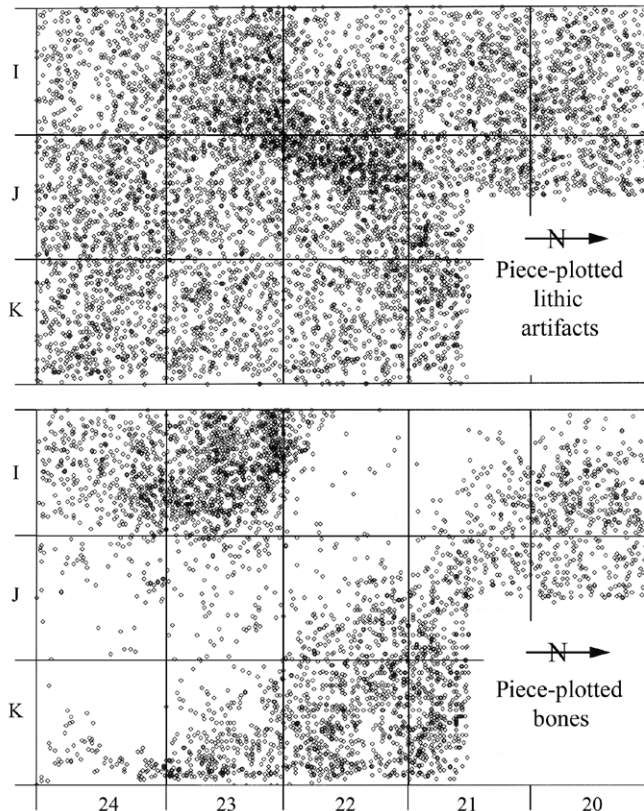
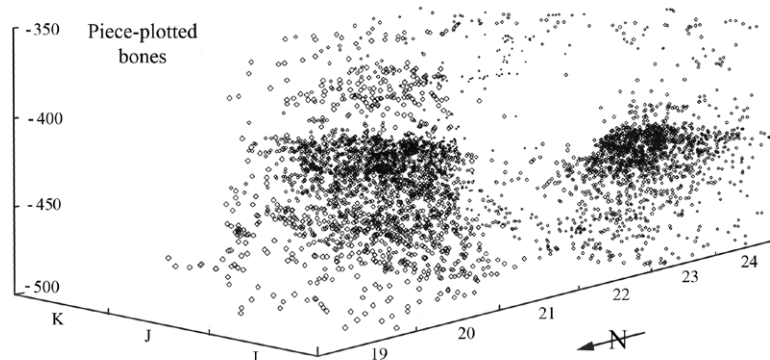


Figure 4.4. Three-dimensional view of the distribution of piece-plotted bones from Middle Palaeolithic Layers E and upper F, in the Central Area. Horizontal spatial units are square metres; vertical increments are centimetres. Plot provided by S. Kuhn. Image adapted from Stiner et al. 2001b: Fig. 4.



4.3 Faunal distributions and the impact of mineral diagenesis

This section examines the relationship between the spatial distributions of the faunal remains in the sediments and preservation of osseous and other carbonate-rich materials. Bones and flint artefacts were most abundant in the sediment column between 400 and 470 cm below datum (bd) (Figure 4.2). They co-occur in smaller numbers between 300 and 400 cm bd, and between 470 and 520 cm bd. A horizontal map (Figure 4.3) representing the entire depth of Layer E in the Central Area reveals stark contrasts in the distributions of lithic artefacts and faunal remains. A three-dimensional map of piece-plotted bones (Figure 4.4) provides another view of the large diagonal gap in the faunal distributions, which bisects the Central Area from top to bottom (i.e., spanning all of Layer E and the top of Layer F). The boundaries of this diagonal feature are relatively sharp. This phenomenon was not encountered in the overlying Upper Palaeolithic and later archaeological deposits. We found no evidence of hydrological sorting or erosion in Layer E.

Given the distinct chemical compositions of flint (silica) and skeletal materials (biogenic carbonates), it seemed likely that localised dissolution of primary carbonates could explain the patchy distributions of faunal materials and carbonate-rich wood ash. 'Hearth areas' rich in charcoal and recognisable ash lenses were common where bones were abundant in Layer E and generally absent where bones were rare. Faunal specimens were particularly abundant under calcareous breccia shelves near the cave walls, where flowstones and localised calcium saturation shunted seeping water toward the centre of the cave (chapter 2, this volume).

Mineral diagenesis can cause dissolution and low-temperature recrystallisation of the primary biocarbonate minerals (Weiner and Price 1986). These chemical transformations result from interactions of the material with waterborne organic compounds, which tend to lower the pH of the surrounding sediments (Bernier 1971; Hedges and Millard 1995; Hedges, Millard, and Pike 1995; Karkanas et al. 2000; Shahack-Gross et al. 2004; Weiner and Bar-Yosef 1990). A major concern for us was the possibility of subtractive dissolution; faunal remains may become completely unrecognisable as dissolution advances. Also of interest was the extent of recrystallisation in the bone mineral (Hedges and Millard 1995; Shipman, Foster, and Schoeninger 1984; Stiner et al. 1995), a process by which the crystals become larger and the crystal lattice more orderly. Recrystallisation does not necessarily destroy the macrostructure of the skeletal specimens but does indicate a dynamic chemical environment.

Vertebrate bone, ostrich eggshell, and mollusc shell contain carbonate minerals of one kind or another. The biogenic minerals in fresh bones and teeth are dominated by calcium phosphates, mainly dahllite (McConnell 1952). Bird eggshell and wood ash instead are rich in calcite and related compounds (e.g., fairchildite, bütschliite; Karkanas 2021). Mollusc shells (land snails in our case) are rich in aragonite and/or calcite. All of these minerals tend to break down in acidic sedimentary conditions, such as when organics from animal waste and decomposed plants are introduced by percolating water (Nielsen-Marsh and Hedges 2000a; Nielsen-Marsh and Hedges 2000b). Derivative (secondary) minerals may then precipitate from the water in the same location or elsewhere in the sediment column (Weiner et al. 1995).

Naturally abundant calcite in sediments tends to stabilise pH at around 8.0, conditions that minimise or halt dissolution. Once set in motion, however, a dissolution cascade can proceed rapidly (Hedges, Millard, and Pike 1995; Karkanas et al. 2000; Weiner and Bar-Yosef 1990; Weiner, Goldberg, and Bar-Yosef 1993), obliterating skeletal specimens within a blink of geological time. This is a common outcome in many Palaeolithic caves and open sites. Bone dissolution therefore depends upon acid concentration and the degree of solution recharge relative to the mass of the sediments and their constituent materials.

Fortunately, carbonate dissolution processes can leave characteristic secondary minerals in their wake (e.g., Schiegl et al. 1996; Weiner et al. 1995). The presence of calcite and/or dahllite in sediments is taken to indicate chemical conditions conducive to good preservation of bones and wood ash (Schiegl et al. 1996; Weiner, Goldberg, and Bar-Yosef 1993), regardless of whether these minerals originated from biological or geological sources. Sediments that lack calcite or dahllite but contain less soluble phosphate minerals (Schiegl et al. 1996) would suggest that whatever bones may have been present in the past have largely decomposed (Weiner, Goldberg, and Bar-Yosef 1993; Weiner et al. 1995). This appears to have been the situation in most of Layer F and, especially, in Layer G in Hayonim Cave (Weiner, Goldberg, and Bar-Yosef 2002). Similar arguments apply to mollusc shells because aragonite is even less stable than calcite. The mineral component of fresh ostrich eggshell is calcite but fares somewhat better than other calcite materials because of its very high mineral density (>95% mineral). The calcite in wood ash is more fragile because of its powdery structure (see Karkanas 2021; Schiegl et al. 1996).

To understand the formation history of Layer E and its faunal assemblages, we mapped FTIR results on the condition of wood ash residues and other minerals in the

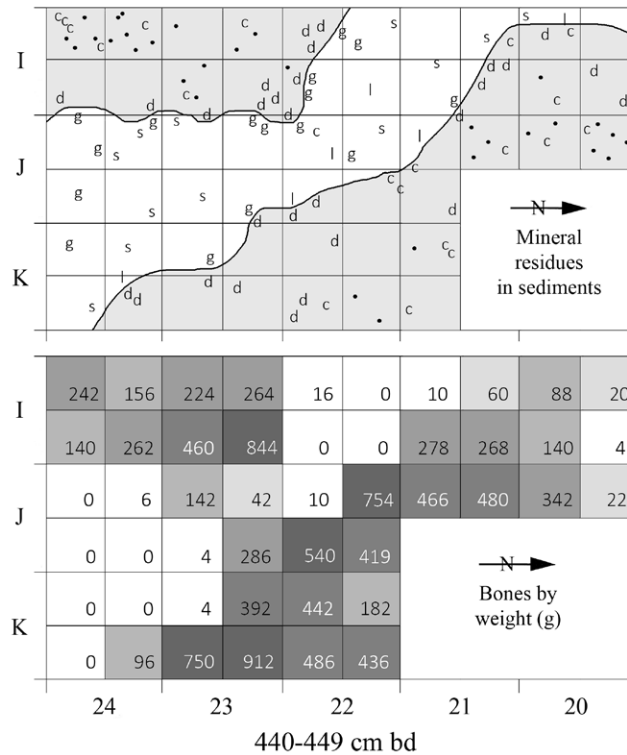


Figure 4.5. Distribution of dominant minerals in sediments (top) relative to screen-recovered bones by weight in grams (bottom) between 440 and 449 cm bd in Middle Palaeolithic Layer E, in the Central Area. Mineral in sediment samples dominated by (c) calcite and (d) dahllite indicate favourable preservation conditions for faunal remains. Sediments containing poorly preserved wood ash and/or bone residues are indicated by the presence of montgomeryite (g), leucophosphate (l), and siliceous aggregates (s) as their major components. The actual bone distributions are consistent with the mineral assemblage that predicts favourable preservation conditions. Black dots represent preserved land snail shells. Mapped dissolution fronts appear as solid lines and were determined onsite from visible colour changes and point-specific FTIR sediment analysis. The total number of sediment samples was 84. Note that data on bone weights are missing for three sub-squares in J-K 21. Adapted from Stiner et al. 2001b: Fig. 9.

sediments (Weiner, Goldberg, and Bar-Yosef 2002). We then compared these findings with data on bone mineral condition (Stiner et al. 2001b; Stiner et al. 1995), bone abundance, and bone macro-damage patterns (fragmentation, the relative representation of porous to compact tissue types, and abrasion; (see Stiner 2005). Figures 4.5 and 4.6 show selected 10 cm-thick horizontal cuts within Layer E in the Central Area. The sediments in the bone-poor zone consistently lacked calcite or dahllite minerals but did contain highly decomposed secondary mineral phases (see also chapter 2, this volume). Yet calcite and dahllite were well preserved in sediments on either side of this diagonal feature. Bone abundance by bulk weight (g) corresponded well to the distribution of intact dahllite and calcite in the sediments, as did the distribution of preserved terrestrial gastropod shells (*Levantina spiruplana*). FTIR analysis of 38 land snail shell specimens confirmed that all of the unburned shells were composed mainly of aragonite, a particularly soluble carbonate mineral. Snail shells were virtually absent in the bone-poor zone.

A significant positive spatial relation was found between mineral compositions conducive to ash and bone preservation and the quantities of recovered bone throughout the central area of Layer E (300–470 cm bd; $n = 521$, Spearman's $\rho = 0.54$, $p < 0.001$).

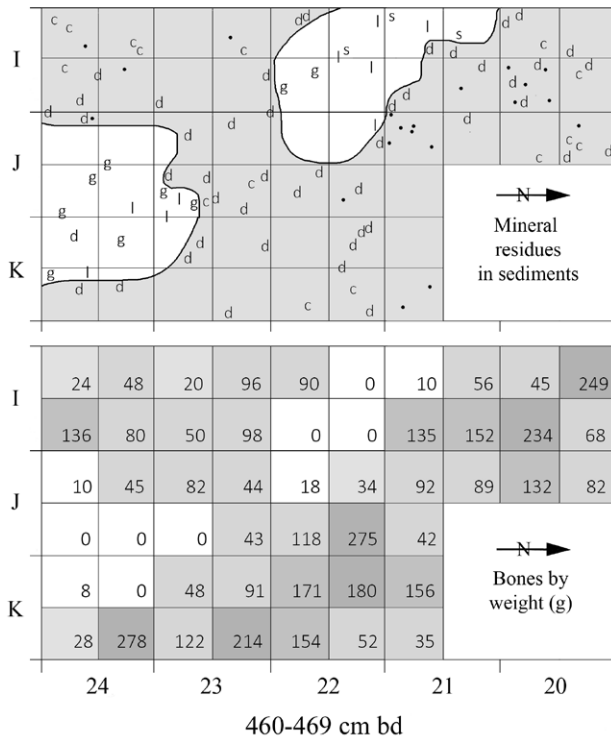


Figure 4.6. Distribution of dominant minerals in sediments (top) relative to screen-recovered bones by weight in grams (bottom) between 460 and 469 cm bd in Middle Palaeolithic Layer E, in the Central Area. Symbols are as in Figure 5. The number of sediment samples was 83. Adapted from Stiner et al. 2001b: Fig.10.

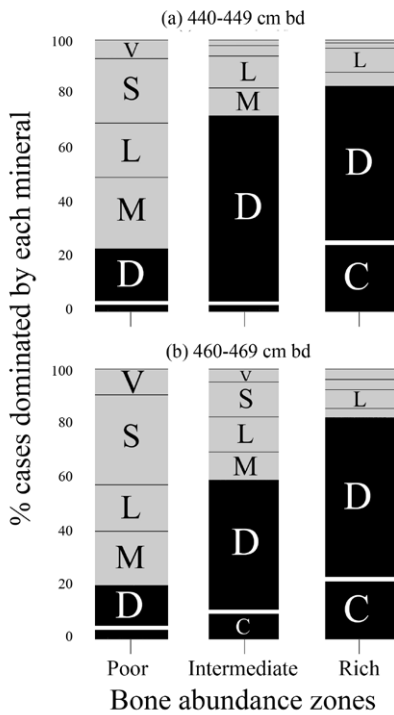
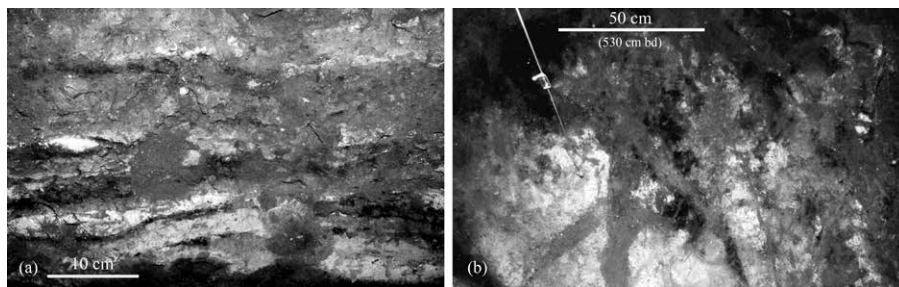


Figure 4.7. Percent of the total number of sediment samples dominated by each of the following minerals, organised according to bone abundance zone by weight. Examples are shown for (a) the 440-449 cm depth interval and (b) the 460-469 cm depth interval. (V) variscite, (S) siliceous aggregates, (L) leucophosphate, (M) montgomeryite, (D) dahllite, (C) calcite. Black shading indicates relatively unaltered carbonates and phosphates, light shading the consecutive stages of diagenetic alteration of the parent minerals, from bad to worse. Adapted from Stiner et al. 2001b: Fig. 11).

This strong relation exists even though the point-plotted sediment results had to be compared with bone NISP by gross 50 × 50 × 5 cm excavation units (Figure 4.7). Calcite was the first compound to decline as bone abundance declined, followed by dahllite. The other minerals in the diagenetic cascade, representing conditions unfavourable to bone and wood ash preservation, predominate where bones are least abundant. The crisp

Figure 4.8. Intrusive rodent burrows in relatively well-preserved hearth area features in Middle Palaeolithic Layer E: (a) burrow holes in vertically stacked hearth lenses, exposed in section; (b) burrow tracks through one large hearth area viewed from above. Adapted from Stiner 2005: Fig. 4.14.



boundaries between favourable and unfavourable preservation environments for calcite and dahllite—and thus for wood ash and bones—in Layer E represent major dissolution fronts. We sought evidence for chemically transitional specimens along the edges of the dissolution fronts, but these proved to be exceedingly rare. The changes in mineral composition seem to have been rapid and thorough (see Karkanas et al. 2000 on chemical stability fields and equilibria).

We concluded that the uneven distribution of two types of anthropogenic materials in the Central Area—faunal remains and wood ash—is best explained by geochemical dissolution, not by patchy deposition by MP humans. But the story of preservation in Layer E is more complicated than this. The ‘bone-poor’ zone did not lack bone entirely—bones were just conspicuously few in comparison with nearby units. One might wonder why bones occurred there at all, given the sediment chemistry results described above. The few bones that occur in the bone-poor zone were somewhat abraded but otherwise in surprisingly good condition. This observation suggested that they represent more recent material that was introduced into older layers via bioturbation in combination with gravity. In fact, small rodent burrows were commonly encountered during excavation, in the section walls and cutting through intact hearth areas (Figure 4.8). Other geoarchaeological observations indicated that the sediments were subject to minor remixing over short vertical intervals due to burrowing insects and small vertebrates (chapter 2, this volume).

The scale of mechanical disturbance was evaluated by quantifying the downward migration of post-MP stone artefacts into Layer E (Stiner 2005). Post-MP artefacts constituted about 3% of all diagnostic tools in the upper part of Layer E (300–419 cm bd), near the contact with the overlying cultural deposits. Post-MP artefacts declined to about 2% in the middle section of Layer E (420–469 cm bd), and to 0% in the lowest section (470–539 cm bd). It is important to note in this comparison that time-diagnostic artefacts generally make up higher proportions of later Palaeolithic and Natufian industries than is true of MP industries. This technological disparity should amplify rather than suppress signals of potential stratigraphic mixing downward through the deposits. In the lower units of Layer E, downward mixing is also likely to have taken place but cannot be detected from stone tool types because all are MP.

Using the demonstrable mixing rate in the top of Layer E as a guide, we estimated that (a) downward movement of younger material could account for $\leq 3\%$ of the total assemblage, and (b) vertical migration usually occurred over relatively short distances based on the rapid decline in the frequency of post-MP tools with depth (see Stiner 2005: Tab. 4.6). An average of $\leq 3\%$ downward migration of bones is not a great deal of mixing for zones wherein MP faunal remains were very abundant. The situation in the bone-poor zone of the Central Area is another story. Here, the bones were more abraded on average and fewer were in anatomical articulation, indicating greater movement within the sediments (Stiner 2005: 69-75).

The chronological integrity of the Hayonim cultural sequence in the Central Area was essentially intact, even though mild time averaging likely occurred throughout the MP series. The quantitative visibility of these mixing effects for the zooarchaeological

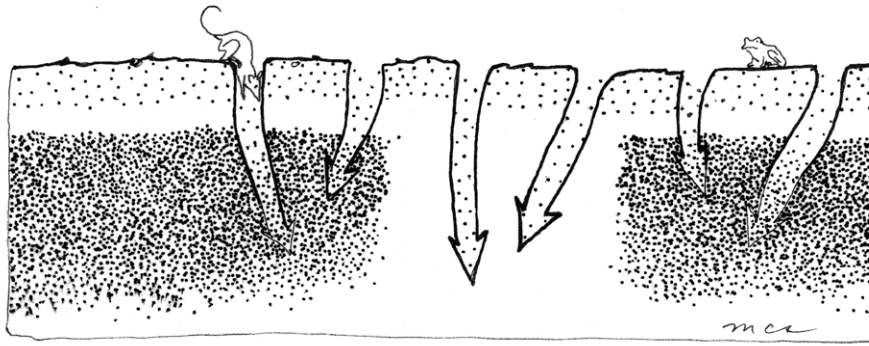


Figure 4.9. Scenario of the differential visibility of bioturbation effects in excavation units that preserve large quantities of original bone versus units from which original bone was lost by dissolution. Gravity can move younger material downward into older, bone-rich, and bone-depleted units as animals make and modify burrows. A hypothetical faunal assemblage taken from the central area would be most affected proportionally by intrusive material, whereas the bone-rich units on either side would be minimally affected due to the high density of original material preserved in them. Adapted from Stiner et al. 2001b: Fig. 16.

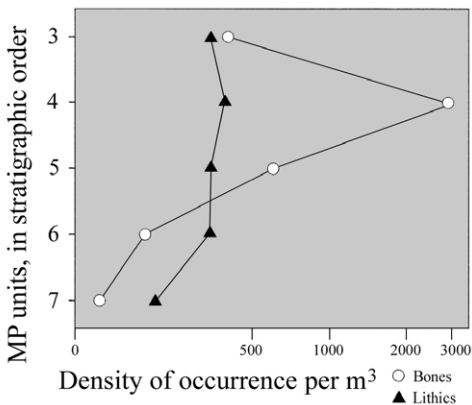


Figure 4.10. The density of occurrence of identified bones (NISP) and lithic artefacts per cubic metre of sediment in the Middle Palaeolithic units in Layer E and uppermost Layer F in the Central Area.

analyses is proportionately greatest in the units where the initially deposited bone was already lost by dissolution (Figure 4.9). That said, the quantities of bone are very small in relation to the total faunal assemblage from each vertical unit.

To explore other (non-diagenic) causes of variation in bone distributions, total bone abundance was compared with lithic abundance in units 3 through 7 (units 1–2 were too sparse), but only for areas in which sediment chemistry indicated a favourable preservation environment for bones. Figure 4.10 plots the density of bones (NISP) and diagnostic lithic artefacts (large blanks, retouched pieces, etc.) per m³ of sediment. The scale of variation is greater for bones than for lithic artefacts in units 3–5. A different relation is apparent in units 6–7, where bone abundance is lower than lithic abundance. This difference could indicate relatively more dissolution in the lower units but it could also reflect, at least in unit 6, somewhat different circumstances of site use by the hominins. Unit 7 represents the top of Layer F, where preservation conditions were relatively poor overall; some of the material could have down-mixed from unit 6. Almost no bones were preserved below unit 7 in the Central Area or in the Deep Sounding at the front of the cave.

In summary, variation in faunal versus lithic distributions in Layers E–F in the central excavation area is largely explained by differential preservation of carbonate minerals—bones, eggshell, mollusc shell, and wood ash—in the sediments. Macroscopic bone preservation was quite good in many zones of MP units 1–5, perhaps less good in unit 6,

and poor in unit 7. Due to poor preservation conditions in units 8 and below (Layers F–G), the faunal record of Hayonim begins with MP units 6–7 dated ca. 200–170 ka.

4.4 Animal carcass processing and fire use

Prehistoric combustion features tend to be fugitive because they are dominated by carbonate compounds (Goldberg, Miller, and Mentzer 2017; Karkanas 2021). Dissolution and minor mechanical disturbances easily destroy the visible integrity of combustion features. The powdery quality of wood ash in particular allows for quick chemical reactions under acidic conditions, and admixing of ash particles with the surrounding sediments may erase the contours of combustion features even in favourable chemical environments (Karkanas 2021). Chemical microsignatures may persist better than structural features (Albert, Berna, and Goldberg 2012; Schiegl et al. 1996; Schiegl et al. 1994), although even these chemical traces can elude archaeologists where dissolution was severe.

Burned bones are somewhat more durable than wood ash because of their larger particle sizes, chemistry, and higher mineral density. Burned bones and other faunal remains thus have a potentially critical role to play in studies of cyclical fire use wherever preservation conditions are suboptimal (e.g., Stiner, Gopher, and Barkai 2011; Stiner et al. 1995). Burned lithic artefacts also can serve this purpose if their tendency to shatter at high temperatures is compensated for by quantifying only the diagnostic technical elements in the assemblages (Shimelmitz et al. 2016).

4.4.1 Burning and tool damage patterns

The MP faunas in Hayonim Cave are overwhelmingly anthropogenic, and they are dominated by large mammal remains (Table 4.2). The exceptions are microfaunal remains that were accumulated mainly by owls, which inhabited high ceiling niches of the main chamber. Weathering damage from atmospheric exposure, and gnawing damage from carnivores and rodents, are exceptionally rare in the MP macrofaunal assemblages (generally <1% of total NISP), whereas traces of human-caused damage are common (Stiner 2005: 91–112). Human modifications of the faunal materials include distinctive fracture forms, tool marks, and burning damage. Cut marks could not be recorded very systematically due to the prevalence of light concretions on bone surfaces. The cut mark data discussed below therefore represent minimum abundance estimates, but they are still quite informative about the modes of carcass processing. Other kinds of bone modification could be recorded systematically (Table 4.3).

Tortoises (*Testudo graeca terrestris*) are the most common small prey animal in the MP assemblages based on NISP (Table 4.2). The high frequencies of burning damage (22%, Table 4.4) and abundant impact fractures (cones, dents, depressions, and spiral breaks) on carapace and plastron parts of these animals are attributable to humans. The tortoises were roasted on open coals and then cracked open with stone hammers, usually along the carapace-plastron bridge. Damage to the proximal ends of humeri indicates that the front legs were torn away from the body, probably after cooking. Tortoise shell fragments were frequently deposited near or within active hearth areas (e.g., Figure 4.11). While blackening from carbonisation is common, very few of these specimens were burned to the point of calcination. Legless lizards (*Ophisaurus apodus*) were also hunted and about 23% of their bones were burned, on a par with the rate for tortoises. Ostrich eggshell is uncommon in the MP deposits, but about 60% of them are also burned. No ostrich bones were found, only eggshell fragments. We do not know if the contents of these huge eggs were eaten and/or the shells used as water containers, although both uses seem likely. Unfortunately, none of the ostrich egg fragments could not refitted. Such high rates of burning damage, roughly double that seen on other faunal materials, indicate an intimate connection between ostrich eggs and reptile remains and hearth areas.

Apart from microfauna, very few small mammal species are represented in Layers E–F. At least some of the few present appear to have been humans' prey, based on an

Taxon Unit:	1	2	3	4a	4b	5	6	7	All
<i>Gazella gazella</i>	30	71	244	422	370	468	278	29	1,912
<i>Capreolus capreolus</i>	-	1	7	2	-	-	1	-	11
Small ungulate (SU)	46	59	268	664	342	310	279	28	1,996
<i>Sus scrofa</i>	1	4	20	45	39	50	17	-	176
<i>Capra aegagrus</i>	-	1	4	1	-	1	-	1	8
<i>Equus cf. hemionus</i>	-	-	3	3	-	5	1	-	12
<i>Dama mesopotamica</i>	14	20	156	438	300	159	75	16	1,178
Medium ungulate (MU)	21	33	335	959	735	358	192	48	2,681
Large cervid	4	3	44	94	89	46	37	4	321
<i>Cervus elaphus</i>	4	7	24	55	37	9	17	2	155
<i>Bos primigenius</i>	5	12	29	60	67	55	50	3	281
<i>Equus caballus</i>	-	-	2	5	3	-	-	-	10
Large ungulate (LU)	6	22	69	95	97	103	63	5	460
<i>Dicerorhinus hemitoechus</i>	-	-	1	1	-	-	-	-	2
<i>Testudo graeca</i>	14	48	426	1,469	1,686	1,417	1,184	113	6,358
<i>Coluber</i> sp.	-	10	81	262	101	38	53	2	548
<i>Ophisaurus apodus</i>	-	2	22	112	49	27	12	3	227
Indet. lizard	-	1	-	3	-	-	-	-	4
Indet. bird	-	1	-	5	-	-	-	-	6
Small bird (songbird)	-	-	4	5	11	8	1	-	29
Medium bird (partridge/dove)	-	4	15	13	8	14	3	2	59
Large bird (predator)	1	1	9	4	3	3	5	1	27
Huge bird (predator)	-	2	9	-	7	-	-	-	18
<i>Struthio camelus</i> eggshell	-	2	1	22	21	28	16	1	91
<i>Lepus capensis</i>	1	1	3	-	-	-	-	-	5
<i>Sciurus anomalus</i>	-	-	1	2	9	-	-	-	12
Indet. small mammal	1	7	20	37	14	11	3	1	94
Hyaenidae	-	1	-	-	-	-	-	2	3
<i>Vulpes vulpes</i>	2	1	7	4	4	-	-	-	18
<i>Canis</i> sp.	-	-	-	4	-	-	1	-	5
<i>Lycaon</i> sp.	-	-	-	-	-	4	-	-	4
<i>Panthera pardus</i>	-	-	-	5	3	-	1	-	9
<i>Ursus arctos</i>	-	1	3	3	-	1	13	-	21
<i>Felis cf. sylvestris</i>	1	1	-	1	-	4	1	-	8
<i>Felis chaus?</i>	-	-	-	-	1	-	-	-	1
<i>Martes foina</i>	-	-	1	-	2	-	-	-	3
Small carnivore	1	-	-	-	5	-	1	2	9
Large carnivore	-	-	3	1	1	-	3	-	8
Indet. carnivore	-	-	3	2	-	-	-	-	5
<i>Erinaceus</i> sp.	-	-	-	-	-	2	-	-	2
Indet. large mammal	9	36	54	56	50	54	44	7	305
Total NISP	161	352	1,870	4,854	4,054	3,176	2,351	270	17,097

Table 4.2. Taxonomic abundances (NISP) for Middle Palaeolithic units of the Central Trench in Hayonim Cave (from Stiner 2005, Appendix 11).

Assemblage	Total bone-based MNE	NISP	Completeness index (MNE/NISP)	% All types impact damage	% Tool-marked (NISP)	% NISP Split	% NISP Transverse	% NISP Burned
Small Ungulates:								
Unit 1	35	76	0.46	4	4	26	30	21
Unit 2	49	130	0.38	5	2	38	21	12
Unit 3	135	512	0.26	6	2	27	26	12
Unit 4	450	1,798	0.25	4	1	27	27	14
Unit 5	239	778	0.31	3	1	40	23	15
Unit 6	150	557	0.27	13	2	35	19	19
Unit 7	23	57	*0.40	14	3	47	19	26
Medium Ungulates:								
Unit 1	13	43	*0.30	7	2	23	12	16
Unit 2	16	64	*0.25	9	0	30	12	*8
Unit 3	98	566	0.17	8	2	22	12	16
Unit 4	474	2,709	0.17	9	1	27	18	14
Unit 5	109	572	0.19	6	1	27	12	13
Unit 6	69	322	0.21	17	2	33	14	10
Unit 7	26	70	*0.37	9	0	33	19	13
Large Ungulates:								
Unit 1	2	11	*0.18	9	0	9	0	*9
Unit 2	7	34	*0.21	6	3	15	6	*12
Unit 3	17	98	0.17	8	3	14	3	16
Unit 4	61	319	0.19	13	1	25	9	18
Unit 5	33	158	0.21	11	0	30	9	17
Unit 6	20	113	0.18	22	1	21	3	8
Unit 7	1	8	*0.12	*	*	*	*	*

Table 4.3. Element completeness index and frequencies (% of NISP) of human modifications by ungulate body size class and MP unit in Hayonim Cave. Calculations for small samples are noted by an asterisk.

overall burning rate of 12% (Table 4.4). Hare (*Lepus capensis*) remains are rare and confined to the uppermost units, but two of the five specimens are burned. While it seems likely that at least some of these small mammals were consumed by humans, they contributed very little to the overall diet. Carnivore remains are also rare in the MP units (92 NISP total) and are mostly from fox (*Vulpes vulpes*) and brown bear (*Ursus arctos*). Transverse fractures occur on about 30% of the carnivore remains, and many of these fractures were caused by stone tools. Cut marks were found on one fox scapula and on one first phalanx of brown bear. Burning damage is less common on carnivore remains (4% of NISP overall) than on other animal remains and in fact is confined mainly to fox (17%). While the prevalence of human-caused damage is generally lower for carnivores as a group, the patterns of bone modification point to human predatory activities.

Ungulate bones dominate the MP assemblages (Table 4.2), mainly Mesopotamian fallow deer (*Dama mesopotamica*) and mountain gazelle (*Gazella gazella*), along with smaller amounts of wild boar (*Sus scrofa*), red deer (*Cervus elaphus*), and rare occurrences of rhinoceros (*Dicerorhinus*), horse (*Equus caballus*), onager (*E. hemionus*), goat (*Capra aegagrus*), and roe deer (*Capreolus capreolus*). The frequencies of tool marks, distinctive fracture forms, and burning damage on the ungulate bones are summarised in Table 4.3 by body size class. A simple measure of element completeness (MNE/NISP) reveals much consistency in the extent of fragmentation within and between body size classes in units 1 through 7. The only notable deviation is found for the largest species (aurochs, red deer), whose bones were less complete. Burning damage ranges between 12–22% of ungulate NISP in most of the assemblages, irrespective of ungulate body size. Impact damage from stone hammers and/or anvils is widespread (3–17% of ungulate NISP) and occurs in the forms of Hertzian cone (compression) fractures, impact notches, transverse or circular dents, localised crushing, and large semi-detached cracks (Table 4.3). The impact damage reflects a combination of through-bone dismemberment techniques

Taxon	Observed NISP	% Burn code 0	% Burn code 1	% Burn code 2	% Burn code 3	% Burn code 4	% Burn code 5	% Burn code 6	Total % burned
Ungulates:									
<i>Gazella gazella</i>	1912	84	4	5	6	<1	<1	<1	16
<i>Sus scrofa</i>	176	87	2	3	6	0	2	0	13
<i>Dama mesopotamica</i>	1178	86	2	5	6	<1	<1	0	14
<i>Cervus elaphus</i>	476	85	3	3	9	1	0	0	16
<i>Bos primigenius</i>	281	84	4	4	7	0	0	0	16
Reptiles:									
<i>Testudo graeca</i>	5212	78	7	9	5	<1	<1	<1	22
<i>Coluber</i> sp.	325	86	2	5	6	0	0	0	14
<i>Ophisaurus apodus</i>	227	77	2	10	10	0	0	0	23
Aves:									
Small-medium bird	98	93	1	3	2	1	0	0	7
Large bird (predator)	45	91	0	2	6	0	0	0	9
<i>Struthio</i> eggshell	91	40	4	21	26	9	0	0	60
Small mammals:									
<i>Sciurus anomalous</i>	12	92	0	0	8	0	0	0	8
Indet. small mammal	94	88	3	2	6	0	0	0	12
Carnivores:									
<i>Vulpes vulpes</i>	18	83	6	11	0	0	0	0	17
<i>Ursus arctos</i>	21	100	0	0	0	0	0	0	0



Table 4.4. Incidence and degree of burning damage (following Stiner et al. 1995) on common taxa in MP Layer E of Hayonim Cave.

Figure 4.11. A crushed, burned tortoise carapace in cemented wood ash lens in Layer E.

and extraction of medullary marrow from the larger limb elements and mandible. It is interesting that impact damage and split fractures are considerably more common in the earliest of the MP assemblages, especially in unit 6, for all ungulate size classes. The situation for the small assemblage from unit 7 (uppermost Layer F) appears similar.

4.4.2 On the question of how bones came to be burned

Traces of fire occur in one form or another throughout Layer E (chapter 3, this volume), but the features identified during excavation were at least partly disturbed. Because wood ash traces are fragile and burned bones somewhat more durable, the distribution of burned bones was used to explore the importance of fire as a regular element of MP technology. The incidence of burning damage on bones and teeth in units 1–7 ranges between ca. 8–30% of total NISP among the common prey taxa (Table 4.4, Figure 4.12).

While the higher burning rates for small prey (tortoise, legless lizard, ostrich eggshell) suggest a particularly strong spatial association with hearth-centred activities, burning damage varies little in its distribution or intensity among other taxa. There are few if any biases to body part among the ungulate remains as well (Table 4.5). In other words, the distribution of burning damage for most of the species verges on random. However, burning damage is more common on unidentified specimens (Figure 4.13). Increased brittleness from advanced carbonisation may have amplified the fragments counts based

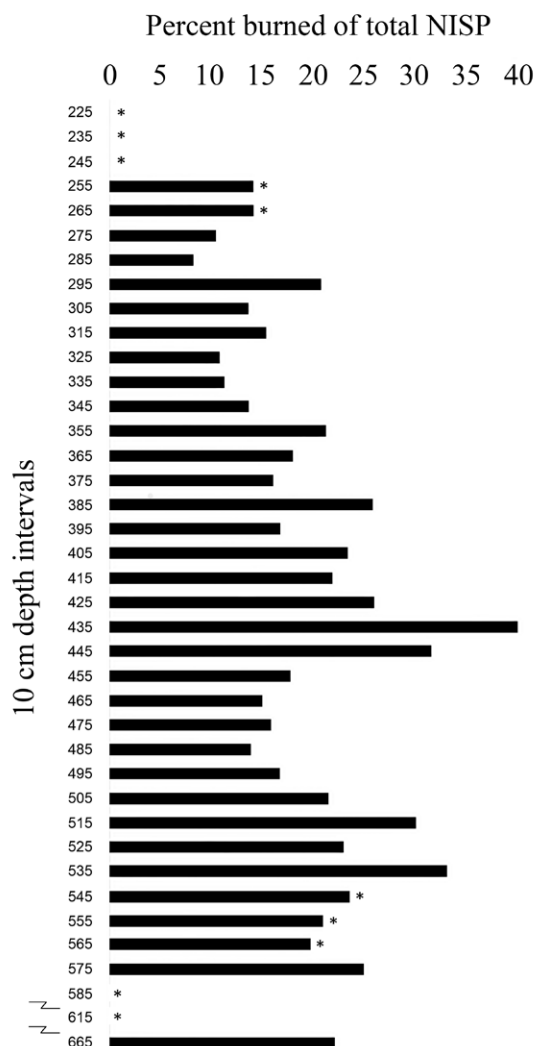


Figure 4.12. Vertical distribution of burned bones (as percent of total NISP) in Layers E–F in the main excavation trench by 10 cm depth increments. (*) Small sample makes calculation suspect. Note that intervals below 600 cm bd are compressed on graph due to small number of bones in cut.

on experimental evidence (see Stiner et al. 1995), but the smallest fragments also would have been the least likely to be swept or pushed away from activity areas before new fires were built.

These facts raise questions about the dominant mechanism(s) by which faunal specimens were exposed to heat. Most of the burning damage on bones falls well short of calcination (whitening), implying that few were exposed to very high temperatures typical of the red heat zone of a fire bed. Experimental work shows that small campfires fuelled by Mediterranean hardwoods can easily reach temperatures up to 900°C, more than enough to calcine bones (Stiner et al. 1995). Heat from the same fires only partly or wholly carbonised bones buried to 5–6 cm below the live coal bed. The extent of burning damage to buried bones declined with depth and never surpassed a state of carbonisation. Calcination of bones thus seems to occur only by direct exposure to red heat, a restricted and generally short-lived zone within a hearth area.

The prevalence of burned bones throughout Layer E confirms that combustion features were once prevalent in many areas of the cave. There were many firebuilding and fire maintenance cycles during the MP occupations—highly repetitive activities that meant that most surfaces and surface debris in the cave would be heated by fire at some point or another. While it is reasonable to assume that fire was used by MP people to cook food, much of the burning damage to bones occurred after they were discarded. This pattern testifies to a close but generalised spatial association between fire maintenance,

Element(s)	SU Total NISP	SU % burned	MU Total NISP	MU % burned	LU Total NISP	LU % burned
Cranium-mandible	344	13.1	291	10.7	122	13.1
Cervical vertebrae	259	16.2	211	14.7	27	18.5
Ribs-axial vertebrae	982	12.3	799	12.0	52	9.6
Innominate	73	26.0	68	10.3	19	26.3
Scapula	136	20.6	129	9.3	37	8.1
Humerus	93	19.4	76	14.5	50	22.0
Radius-ulna	134	17.9	108	15.7	48	18.8
Carpals	50	8.0	83	16.9	15	20.0
Femur	103	13.6	55	3.6	28	7.1
Tibia	138	18.1	139	8.6	70	7.1
Patella	25	12.0	5	20.0	-	-
Tarsals	142	14.1	99	16.2	38	15.8
Metapodials	226	20.8	219	18.7	131	16.0
Phalanges-sesamoids	391	19.2	395	15.9	112	14.3

Table 4.5. Percent of NISP burned by skeletal element or element group for small ungulates (SU), medium ungulates (MU) and large ungulates (LU) in Layers E and uppermost F in Hayonim Cave.

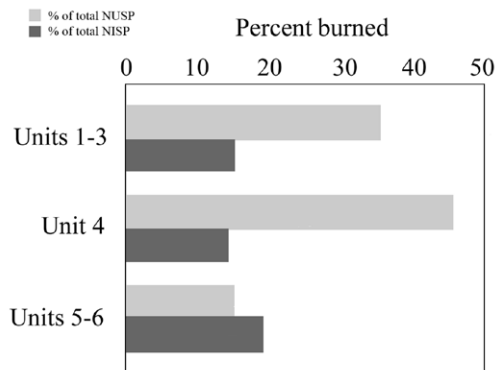


Figure 4.13. Comparison of the proportion burned among the identified specimens (NISP) and the unidentified specimens (NUSP) in the faunal assemblages from Layer E.

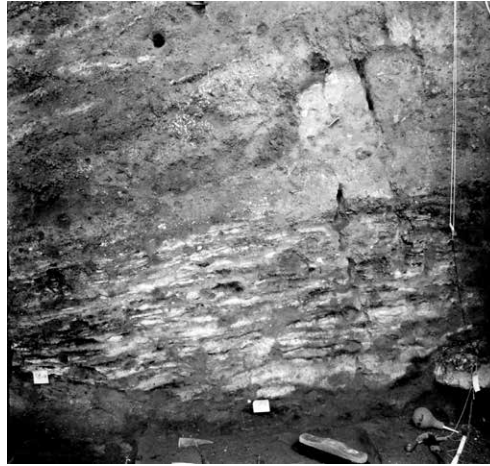
food preparation and food consumption day after day. Sedimentation rates were slow enough during the formation of Layer E that substantial amounts of surface debris were charred before being fully buried by sediment. The paucity of calcination damage, on the other hand, suggests that the probability of bone debris being exposed to red heat from the fireplace core was low. It is also important to note that the MP inhabitants seem not to have been burning bones as supplementary fuel.

In summary, the cave interior was used rather intensively in the sense that many fires were made and maintained. However, the size and duration of the hearth constructions was not sufficient to expose debris to red heat very often. The results on bone burning suggest that each fire was small and relatively short-lived (see also review by Karkanas 2021).

4.5 Comparisons of LP and MP bone damage patterns

The MP occupations in Hayonim Cave were likely small-scale residential encampments, and hominin mobility within the larger territory was high (Meignen et al. 2010; Stiner 2005). Frequent firebuilding and maintenance inside the cave nonetheless led to the formation of deeply stacked lenses of charcoal and wood ash, which are reasonably well preserved in certain parts of Layer E (e.g., Figures 4.8 and 4.14). Limited fire traces were found in Layer F as well (chapter 3, this volume; Meignen and Bar-Yosef 2020) and some of the bones in unit 7 of Layer F (down to 665 cm bd) were also burned.

Figure 4.14. Stacked hearth lenses in Layer E, exposed in the north wall of the Central Area, and lying just west of travertine deposits.



Clearly, fire was a focal point of the MP residential camps. Micromorphological evidence indicates, for example, considerable trampling of the sediments around and within the hearth areas (chapter 2, this volume; see also Albert et al. 2003; Albert et al. 2000; Goldberg and Bar-Yosef 1998; Meignen et al. 2010; Weiner, Goldberg, and Bar-Yosef 2002). These camps represented predictable hubs for food processing and shelter due to the cooperative maintenance of fire. MP hunters frequently deferred consumption of prey carcasses until many of the valuable parts could be carried to the cave. While we assume that the proximate goals of food transport were to prepare foods with the aid and comfort of fire, these situations would also have made sharing with other members of the group difficult to avoid.

The lack of highly defined activity spaces in Layers E–F is regrettable, but there are strong connections between carcass processing, bone waste disposal, and hearth-centred activities. The evolutionary significance of these observations is made clearer by comparison to Late LP cave records in the southern Levant. Qesem Cave (Gopher et al. 2010; Gopher et al. 2005) is an important example on account of its time range, deep stratigraphy, abundant faunal remains, and the availability of quantitative data on burning rates (Stiner, Gopher, and Barkai 2011). Other Late LP and/or MP comparators in the study area include Misliya Cave (Weinstein-Evron and Zaidner 2017; Yeshurun, Bar-Oz, and Weinstein-Evron 2007), Tabun Cave (Jelinek et al. 1973; Rink et al. 2004), and the late MP sequence in Kebara Cave (Bar-Yosef and Meignen 2007; Meignen and Bar-Yosef 2020). While important new cases have come to light, few of these so far have yielded faunal series of the same magnitude as Hayonim and Qesem.

Burned bone concentrations in the Late LP faunal series in Qesem Cave provide strong, if indirect, evidence of sequential combustion events (Stiner, Gopher, and Barkai 2011: Tab. 2). One large, semi-intact combustion feature that preserves wood ash traces was identified roughly midway through the sedimentary sequence (Karkanas et al. 2007; Shahack-Gross et al. 2014), but intact combustion features are quite rare overall. Rather, it is the distribution of unidentified burned bone splinters, which occur throughout the 8 m of deposits, that demonstrates the periodicity of fire use starting around or shortly after 400 ka. Most of the burned specimens are merely carbonised, but calcined bone specimens constitute up to 16% of the total number of unidentified bone specimens (NUSP) and testify to intense heating in some locations. The relative frequency of burned bones is notably higher mid-sequence and upward through the stratigraphic sequence (Stiner, Gopher, and Barkai 2011: Tab. 2). A similar scale of firemaking is documented in Tabun Cave. Hearth areas in this cave were inferred from clusters of burned diagnostic lithic artefacts because bone preservation was generally poor (Shimelmitz et al. 2014a). The Tabun and Qesem records indicate that serial firebuilding was already a regular feature of encampments during the Late LP in the southern Levant. Such practices

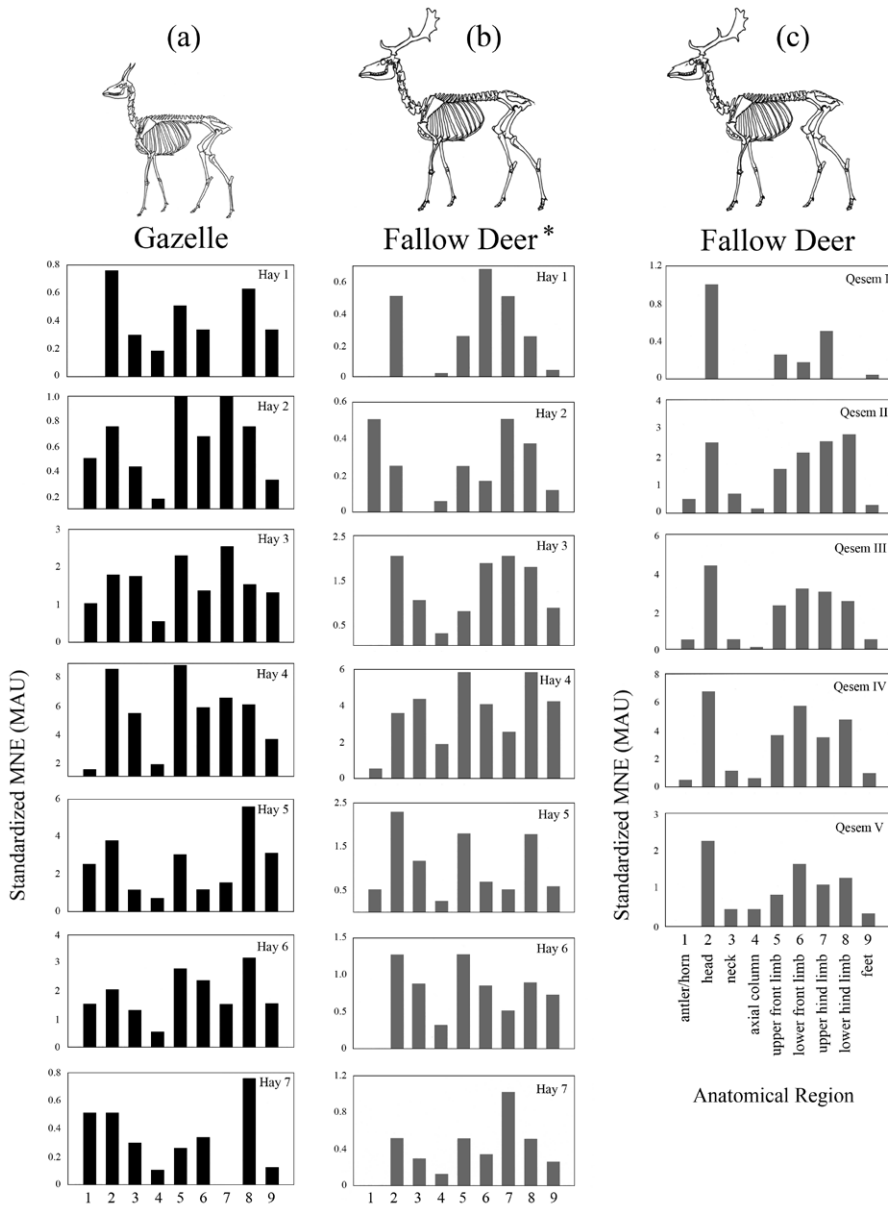


Figure 4.15. Body part profiles based on standardised MNE (observed MNE/expected MNE, a.k.a. MAU) for (a) Hayonim gazelles, (b) Hayonim medium-sized ungulates, - (*nearly all specimens are fallow deer), and (c) Qesem fallow deer.

continued and apparently intensified in some cave sites through the Middle Palaeolithic. Examples include the MP series in Hayonim Cave and the later MP series in Kebara Cave (chapter 3, this volume; Meignen, Speth, and Stiner 2006) and Amud Cave (Alpers-Afil and Hovers 2005).

Other commonalities between the Late LP and the MP cave records are seen in the general patterns of large game hunting, specifically prey age selection and the range of ungulate body parts that hunters transported from kill sites to caves. Modern foragers' transport decisions normally depend upon some combination of potential food value, weight, and travel times between kill sites and safe havens. Greater travel distances may discourage people from transporting many low-utility or very heavy body parts. Another mitigating factor is the technological system itself, especially the methods and infrastructure for extracting nutrients from carcasses. MP and Late LP implements used for processing the bodies of prey were mainly hammer stones and/or anvils, cutting and scraping tools, and fire. Marrow removal in these periods relied on 'cold' extraction

methods, which targeted nutrient concentrations within the main cavities (medullae) of limb and mandible bones.

Body part representation for the common ungulate species in Hayonim and Qesem caves is illustrated in Figure 4.15. The data are presented as standardised MNE values, which corrects for differential fragmentation and the fact that some elements naturally occur in greater number than others in the live animal. Perfectly complete body part representation therefore would be indicated by bars of equal height across the different anatomical regions; disparities among body regions reflect divergences from the complete body model. The body part profiles of mountain gazelle and fallow deer for the Hayonim MP units show generally balanced representation of head and limb parts, but lower-than-expected frequencies of axial elements (including the neck) and some foot bones (Figure 4.15ab). Head counts are based on boney features of the skull, not teeth, to be consistent with the preservation conditions for post-cranial elements. The anatomical pattern is widely repeated for small and medium-sized ungulates across vertical units. Carcasses of aurochs, a much larger species, are somewhat less complete but the sample sizes are small (see Stiner 2005). Tests for density-mediated attrition indicate that the biases against vertebrae and ribs are due mainly to the transport decisions of prehistoric humans (Stiner 2005: 177-184); they are not biased significantly by in situ mechanical destruction. These items were often left behind at kill sites or elsewhere on the landscape. Similar patterns of body part representation are found in the Late LP of Qesem Cave (Figure 4.15c), the Early MP of Misliya (Yeshurun, Bar-Oz, and Weinstein-Evron 2007: 665), and the Late MP of Kebara Cave (Speth and Tchernov 1998, 2001). Hominins' basic formula for deciding which body parts to transport back to caves seems to have changed little from the Late LP through Late MP in the study area.

Gaining the full value from ungulate bone marrow was a high priority for the MP occupants at Hayonim Cave (Stiner 2005: 83-91). The uniform interest in marrow implies that prey tended to be in good nutritional condition. Figure 4.16 illustrates the thoroughness of medullary marrow extraction at the cave. The skeletal elements (MNE) of small gazelles and medium-sized fallow deer are rank-ordered according to medullary cavity volume, from largest to smallest. It is clear from this comparison that cold marrow extraction was pushed nearly to its maximum caloric potential (reviewed in Stiner 1994: 225-230). Very little was wasted; marrow extraction stopped short only of the second and third phalanges and calcanei of gazelles and the third phalanges of fallow deer, which contain very small marrow reserves. Large ungulates are not plotted, because every medullary cavity of their skeletons was opened for marrow. It is interesting that ungulate heads were consistently transported to the cave along with limb parts. They are less easily taken apart with tools, but the problem can be solved by slow roasting.

The patterns of body part representation for fallow deer, the dominant prey item during the Late LP in Qesem Cave (Figure 4.15c), resemble those observed for the MP at Hayonim. Again, heads and major limb bones dominate, but the relative abundance of head parts tends to exceed limbs by a small margin. Very little of the variation in body part representation can be explained by density-mediated attrition (Stiner, Gopher, and Barkai 2011). The array of deer body parts correlates positively to marrow utility but not significantly to other nutritional value indexes. Many of the transported limb elements also associate with large muscle masses in life, but some of the meat may have been removed from the bones prior to transport to the cave. It seems that high marrow content was the leading precondition for transport in this case, too. Head parts, which include significant within-bone nutrients such as the brain, were also a priority for transport.

Much of the burning damage to bones in Qesem Cave occurred following deposition. The fact that the ends and shafts of the limb bones were burned at similar rates, for example, points to a randomising process. Tortoise remains pose a notable exception in Qesem, just as they do in Hayonim, in that burning damage occurs mainly on carapace and plastron parts (roasting damage). Unlike in the Hayonim fauna, however, the frequency of burning damage on fallow deer remains in Qesem is biased to certain skeletal elements

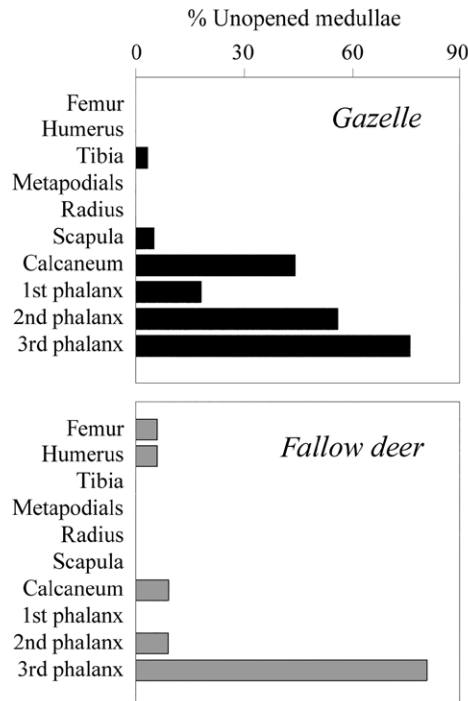


Figure 4.16. Proxy data for the 'thoroughness' with which the major limb element medullary cavities of mountain gazelles and fallow deer were opened by MP humans at Hayonim Cave. Elements are rank-ordered according to medullary cavity size, from largest to smallest.

(Stiner, Barkai, and Gopher 2009; Stiner, Gopher, and Barkai 2011). Specifically, the bones of the skull, axial column (spine, ribs, pelvis), scapula, and ulna are less often burned than large limb bones that possess exploitable medullary cavities. The fact that cranium and mandible fragments were less often burned does not negate the roasting hypothesis noted above, because the cranium is encased in connective tissues that would have cooled the mass during roasting. Carbonisation damage would be limited to small, unprotected areas of bone that were directly exposed to heat. The difference in the case of limb bones is that most of the adhering tissue had been removed prior to heating the bones for cooking and removing the marrow (see also Blasco et al. 2016).

At the later MP site of Kebara Cave, Speth and Clark (2006: 20–24) link some of the burning damage on deer and gazelle leg bones to marrow heating as well. Lower limb elements were most often burned, and the outer surfaces of the shafts sustained greater heat damage than the inner surfaces or the epiphyses. This practice is not unlike those reported among recent foraging peoples such as the Nunamiut (Binford 1978). If this practice also took place during the MP in Hayonim Cave, evidence of it was erased by the more powerful influence of post-depositional burning.

4.5.1 Anomalous cut marks

The domestic spaces of the Late LP versus the MP in the Levantine caves were not equivalent. Tool-mark patterns suggest an interesting trend during the Middle Pleistocene, ambiguities of dating notwithstanding. At Qesem, cone fractures occur at rates of 19–31% of total ungulate NISP (Table 4.6). Cone fractures are present but less common in units 5 and above in Hayonim (Table 4.3) and similarly so in a variety of later MP and UP comparison assemblages studied by the author (4–18%). The lowest units in Hayonim show values intermediate, or more similar, to those observed at Qesem (Table 4.6). Given that few hammer strikes were sufficient to open the medullary cavity of a given limb bone during the MP and UP periods, the patterns seen in Qesem and the earliest MP units in Hayonim imply a less efficient, or less discriminating, use of force.

The cut mark data from Qesem show a similarly 'heavy-handed' approach, especially on ungulate limb shaft surfaces (Stiner, Barkai, and Gopher 2009). Cut marks in the Qesem faunas occur at roughly 3 times the rate observed for the later periods (Stiner, Gopher,

Table 4.6. Percentage of medium ungulate specimens, primarily from fallow deer, with cone fractures by vertical excavation units in Hayonim Cave and Qesem Cave.

Site	Unit	Medium ungulate NISP	% cone fractured
Hayonim	1-2	107	7
	3	566	7
	4	2709	8
	5	572	6
	6	322	16
	7	70	9
	Qesem	I-II	887
III		1009	19
IV		1449	31
V		435	25

and Barkai 2011). Moreover, mean cut mark angle variation on multiply marked shaft specimens is much greater in the Qesem faunas than it is for the same and similar prey from the northern Levantine MP and early UP sites of Üçağızlı Caves II and I in Levantine Turkey (Stiner, Gopher, and Barkai 2011).¹ Direct comparison of these data to cut mark orientations on the Hayonim material was limited by surface encrustations, although non-encrusted samples are consistent with the later MP datasets.

The greater variation or ‘chaos’ in cut mark orientations during the Late LP at Qesem suggests a wider range of butchering postures, or ways of holding a body part while cutting the connective tissue. The Qesem tool users seemed to have been less concerned with precision in their efforts to separate soft tissue from bones. We cannot assume, however, that Late LP hominins were less dexterous. Skillful stone working is widely apparent in the Late LP in the Levant and elsewhere. Rather, there may have been differences between the periods in the carcass processing agendas and techniques used, and possibly the extent of collaborative efficiency within the group (i.e., leaving some tasks to more skillful individuals in advance of consumption). A subtle difference may also exist between the carcass processing goals with time. It could be that more consumption of soft tissues occurred prior to moving ungulate body parts to the cave encampment during the Qesem occupations, rather than postponing most of the consumption until after carcasses could be carried to and processed in the cave. While fire was a central need throughout the periods considered here, the function of cave sites seems to have become more complex early in the MP period. We cannot be certain when, or how rapidly, the observed shifts in butchering practices occurred in the study area. More cases and appropriate quantitative data are needed to resolve these questions.

4.6 Biogeographic background to the hominin behavioural trends

We still know little about the taxonomic identities of the Middle Pleistocene hominin populations that inhabited the study area. Diagnostic fossils are rare, and the differences once thought to separate accepted hominin species increasingly are blurred as ancient DNA results become available. The ways in which these hominin populations interacted with their environments and biotic communities reveals considerably more about their evolution.

1 The faunal analyses of Kebara Cave by J.D. Speth and colleagues involved a very different sampling strategy and concentrated to a large extent on certain taxonomic groups and body parts with high identifiability. Their results on relative variation in damage frequencies among taxa and excavation units are important but difficult to compare directly with the more holistic data collection strategy used at Hayonim Cave, wherein all of the material was studied and reported.

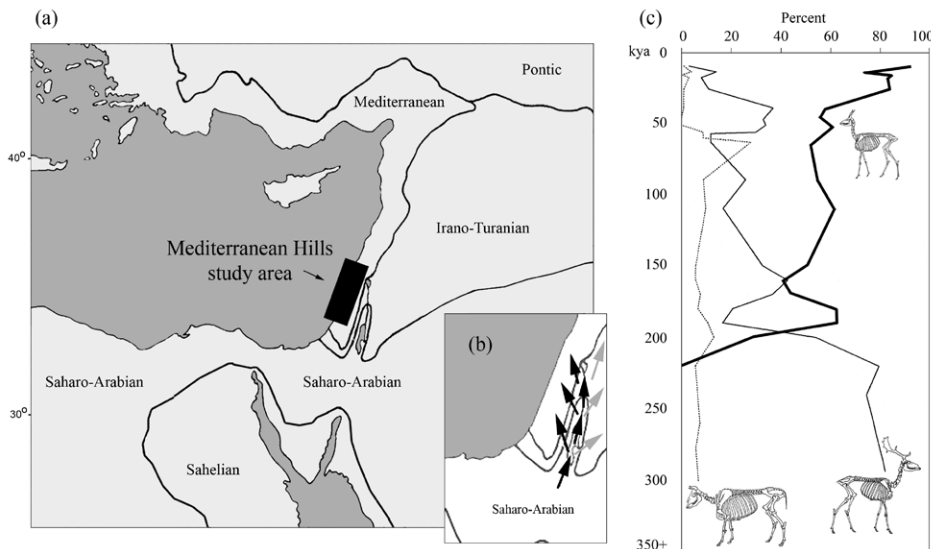


Figure 4.17. The inter-digitation of (a) suture zones between biogeographic provinces in the Levant, and (b) the inferred route (arrows in inset image) of influx of Afro-Arabian large mammals ca. 200 ka into Mediterranean Hills study area (base map adapted from Blondel and Aronson, 1999). The filled square denotes the study region. (c) Frequency variation in three important ungulate species in the Mediterranean Hills region from the late Lower Palaeolithic through Epipalaeolithic, based on the archaeofaunal series from Qesem Cave, Hayonim Cave, Kebara Cave, and Meged Rockshelter. Adapted from Stiner, Gopher, and Barkai 2011: Figs. 4 and 5.

The ecological conditions in the southern Levant were dynamic during the Middle Pleistocene, and the composition of biotic communities experienced intermittent turnover. Eitan Tchernov championed a biogeographical approach to thinking about hominin population history and ecology in this region of the world (Tchernov 1992b, 1994, 1998a, b). A longstanding question was whether shifts in hominin populations and economic behaviours could be linked to broader animal community turnover events, including periodic incursions of Afro-Arabian taxa into the region via the Jordan Rift valley (e.g., Tchernov 1992a, b). The southern Levant straddles complexly folded 'suture zones' between biogeographic provinces (Figure 4.17a). Under conditions of greater biogeographic isolation, one might expect hominin adaptive efficiency to become strongly tied to a specific zoogeographic province. As the boundaries of these provinces shifted within the Levant, the geography of an endemic hominin population might become more fluid as well. The question has been whether periodic endemism in hominin populations obtained in the southern Levant prior to roughly 50,000 years ago.

The Hayonim faunal record spans a poorly known segment of human evolutionary history in the Mediterranean Hill zone. Its total cultural sequence may represent up to 400,000 years, but the preserved faunal record begins only around 170–200 ka. Subsequent archaeological discoveries in the region, particularly Qesem Cave, extend the faunal chronology deeper into the past. The Qesem record spans roughly the last 200,000 years of the Lower Palaeolithic (Barkai et al. 2003; Gopher et al. 2010; Gopher et al. 2005; Stiner, Barkai, and Gopher 2009). Some temporal gaps likely exist within and between each of the cave series, but together, they offer much more information on biotic communities than archaeologists had before. Several open-site faunas are also available for consideration, though these assemblages tend to include proboscideans and hippopotamus on account of their lowland settings, such as at Holon, Revadim, and Evron Quarry (Chazan and Kolska-Horwitz 2001; Marder et al. 1999; Monchot and Horwitz 2007; Tchernov 1994).

An environmental transition is suggested in the cave records by shifting prey composition around 200 ka. The Qesem faunas are exclusively Eurasian—mountain gazelles are absent or extremely rare. Thereafter, we see progressive increases in gazelles in the Mediterranean Hills area (Figure 4.17c), which is taken to signal a shift toward more dry steppe conditions (Bate 1937; Stiner 2005; Yeshurun 2016). The northward projection of arid grassland habitats through the Jordan Valley would have been the closest pathway by which Afro-Arabian mammals could infiltrate Eurasia (Figure 4.17b). A unique occurrence of wild dog (*Lycaon* sp.) in the lower part of Hayonim Layer E (unit 5 at 489 cm bd), the only specimen known for all of Eurasia in the Middle Pleistocene, dates to early OIS 6 or late OIS 7 (Stiner et al. 2001a). The appearance the gazelles, a single wild dog, and ostriches (indicated by eggshell fragments) may associate with considerable fragmentation of Mediterranean forests in the EMP and grassland expansion.

This shift in animal community composition only roughly coincides with the LP-MP palaeoculture transition in the study area. Some 30 ka may separate the end of the Qesem faunal record (or at least the bulk of it) and the onset of the Hayonim faunal record. Moreover, carcass processing practices indicated in EMP units 6–7 of Hayonim show greater affinity to those of the Late LP in Qesem Cave. The observed changes in carcass processing therefore may not correspond simply to the traditional boundary of the LP and MP.

4.7 Concluding discussion

Two separate phenomena—site occupation intensity and evolving complexities in the function of residential camps—were important questions for our work at Hayonim Cave. Information about the intensity of the MP occupations relates to land use patterns, whereas site function relates more closely to how people utilised certain places within their territory. Comparisons of the Hayonim MP to earlier and later cave series in the Mediterranean Hills help to set the results in broader evolutionary perspective and to isolate some important similarities and differences.

The MP occupations in Hayonim Cave were repetitive and light, yet anthropogenic sources of sediment buildup in the form of wood ash were comparatively high. A low density of artefacts in other circumstances might be explained by rapid sedimentation in some sites, but this is not the case for the MP in Hayonim. Thermoluminescence dates suggest that sediments accumulated at a rate of about 1 m per 10,000–15,000 years (Stiner 2005), in stark contrast to estimates for the later MP in Kebara Cave, where 1 m of depth accumulated in roughly 3,000 years (units XI–IX, ca. 60–57 ka, Bar-Yosef 1998b). Kebara also appears to have been occupied somewhat more intensively based on piled bone waste in the rear of the cave (Meignen, Speth, and Stiner 2006; Speth 2007), and higher accumulation rates for lithic artefacts and animal remains. At Hayonim, MP humans repeatedly exploited ungulates and tortoises but never in great quantities at once. The number of individual animals (MNI) per vertical unit is quite low (Table 4.1), and the inhabitants maintained narrow diets dominated by high-yield prey types (Stiner 2005). These and other observations point to low human population densities in the study area during the earlier MP. The later MP occupations in Kebara Cave instead associate with significantly denser faunal accumulations (Meignen, Speth, and Stiner 2006) but the overall diet was similar. The number of known cave sites with dense accumulations is also greater for the later MP.

Occupation intensity is less easily compared between the MP in Hayonim and the Late LP in Qesem due to ambiguities in stratigraphy and dating, but the total MNI values for ungulates (mostly fallow deer) and other prey are similarly low in the Qesem series (see Stiner, Barkai, and Gopher 2009). Large amounts of material have been excavated from Qesem, but the overall timespan is great and the Late LP occupations appear to have been light from a subsistence point of view. Patterns of ungulate body part representation and the importance of medullary marrow content in determining transport decisions were similar to patterns observed at Hayonim, although the Qesem pattern may have

emphasised marrow and head parts somewhat more, with more defleshing taking place out in the open. Hearth-focused activities are evidenced through most, if not all, of the Qesem sequence (see also Gopher et al. 2016). The prevalence of post-depositional burning of bones links these butchering activities to areas in the cave where fires were made repeatedly.

Differences between the two sites are found in the incidence of impact and other tool damage on bones, which decreases significantly with time, while cut mark alignments become more orderly. The great diversity of cut mark orientations at Qesem suggests the formation of sequential overlays of marks from distinct cutting actions and postures by multiple individuals. This pattern implies, at least to this author, a simpler or less evolutionarily derived pattern of meat consumption around hearths (Stiner, Gopher, and Barkai 2011). The Late LP may have lacked some of the complexity in staging of carcass butchering and consumption that became commonplace during the MP. It seems that the formalised ‘apportioning’ of meat that is so typical of later foragers was quite limited at Qesem—perhaps more feeding from carcasses took place at acquisition sites and hominins reserved less of the edible soft tissue for processing and consumption in the cave. The evidence suggests significant reorganisation in patterns of food sharing within the timeframe of the late Middle Pleistocene. The contrasts described here do not divide conveniently between the two sites. The tool damage patterns on ungulate remains from the earliest EMP units in Hayonim better resemble those in Qesem Cave. The shift seems to have occurred gradually within Layer E, to the extent that available samples and dating allow us to determine.

A related theme in this research is the role of fire as a magnet for multiple onsite activities. Many archaeologists have proposed that hearth-anchored base camps became a novel theater for social and diet evolution during the Middle Pleistocene (Gowlett 2006; Kuhn and Stiner 2019; Roebroeks and Villa 2011; Rolland 2004; Stiner 2018; Stiner, Gopher, and Barkai 2011; Wrangham and Carmody 2010). In the Levant, early if somewhat controversial evidence for fire use is reported at the open site of Geshert Benot Ya’akov in the upper Jordan Valley at ca. 780 ka (Alperson-Afil 2008; Goren-Inbar et al. 2004). This case is separated from later occurrences by nearly 400,000 years, after which the fire record picks up unequivocally in cave sites such as Qesem and Tabun (Karkanas et al. 2007; Shahack-Gross et al. 2014; Shimelmitz et al. 2014a). This is followed by Early MP fire records in Hayonim (chapter 3, this volume) and Misliya (Schiegl et al. 1996; Shahack-Gross et al. 2014; Weinstein-Evron and Zaidner 2017). And hearth features are equally or more abundant in later MP cave sites such as Kebara (Bar-Yosef and Meignen 2007; Bar-Yosef et al. 1992; Meignen and Bar-Yosef 2019; Speth 2007) and Amud caves (Alperson-Afil and Hovers 2005; Hovers 1998). Collectively speaking, the southern Levant preserves a continuous record of fire use from at least 320 ka to the present, and probably back to 400 ka.

Suffice it to say, there is indisputable evidence for hearth-centred human activities throughout the MP sequence in Hayonim Cave. The human occupations may not have been as intensive as those in some later MP sites, but fire was already a central fixture in cave encampments. The structure and abundance of these combustion features shows us that fires were built repeatedly in certain parts of the cave, and that wood ash was an important component in sediment buildup. Incidental burning of small items, such as bone detritus, was also commonplace, consistent with the large quantity of wood ash residues. While there is direct evidence for cooking animal prey during the MP (e.g., roasting of tortoises) in Hayonim Cave, most other bones were burned after they had been discarded by humans. The dominance of accidental (post-depositional) burning underscores the core importance of fire facilities in MP everyday social and economic life. This may also have been true during the Late LP, but the earlier record does not display the same complexity of hearth-associated activities.

While basic firemaking and maintenance practices clearly had developed sometime in the Lower Palaeolithic, the suite of activities conducted around hearth areas is a separate

consideration. Generally speaking, the types and overall diversity of hominin activities that transpire at a site should constrain the cumulative structure of the archaeological record produced. All the Palaeolithic cave records discussed in this chapter represent palimpsests of debris from an abundance of relatively short-lived activities. The earliest cave records nonetheless seem to repeat a narrower range, or less complex set, of socioeconomic activities than do most of the MP occupations. The Late LP layers in Tabun Cave, for example, indicate a comparatively narrow scope of technological repetition within the Acheulo-Yabrudian industries, in contrast to typical MP patterns in the same site (Kuhn and Clark 2015). A similar situation for stone tool functions is suggested, at least by some authors, in the Late LP in Qesem Cave (Lemorini et al. 2006), and by the complexity in Levallois technology from the LP to the MP in Tabun Cave (Shimelmitz et al. 2016). The faunal and lithic assemblages of the MP in Hayonim suggest a trend within the early part of the MP toward more diverse patterns of activity variation and along with greater formalisation in Levallois blank production (Meignen, this volume).

The evolution of hearth-centred residential camps and the diversity of activities performed at them also have implications for the evolution of hominin social relations. Residential camps were part of the heritable niche of hominin groups, and as such, they ultimately may have shifted the opportunities for, and constraints on, social interaction and cooperation. The archaeological results from Hayonim point to a subtle but important trend toward greater complexity in camp function in caves that transpired during the late Middle Pleistocene. The trend involved shifts in the staging and dissemination of animal resources, some of the most shareable classes of food in Palaeolithic societies, and use of hearths to process these carcasses. Fire bestowed multiple benefits for hominins from the inception of the technology, but the multifunctionality of this class of facility clearly expanded with time, probably because of the new possibilities that it created within the habitable space.

The information gained on these topics could not have been realised without working analytically through the filter of site formation processes. Collaborations between zooarchaeological and geoarchaeological studies of how archaeological sites come into being in Levantine caves has elevated our knowledge to a level that could not be achieved by either discipline alone. The contents of this edited volume illustrate important inroads in our quest to master this learning curve.

Acknowledgements

I am indebted to Ofer Bar-Yosef in more ways than I can describe—not least for including me in one of the most stimulating research contexts of my career, and also for his generous advice and his ingenious way of making complex projects peopled by strong-minded folk function fruitfully. I also owe much thanks to Liliane Meignen, Bernard Vandermeersch, Eitan Tchernov, Stephen Weiner, Ruth Shahack-Gross, Rivka Rabinovich, Paul Goldberg, Natalie Munro, Steven Kuhn, Mario Chech, Anna Belfer-Cohen, John Speth, Todd Surovell, and many others. This zooarchaeological research was supported from 1995 through 2004 by CAREER and Creativity Extension Grants from the National Science Foundation (SBR-9511894), and by a 1997–2000 Israel-United States Binational Science Foundation grant.

Hayonim Cave: Lithic assemblages, from the end of the Lower Palaeolithic to the Middle Palaeolithic

Liliane Meignen

5.1 Introduction

Following recent excavations at Hayonim Cave, the long archaeological sequence (>7 m thick), long known for its Early Middle Palaeolithic (EMP) assemblages (Meignen 1998, 2000, 2011), now covers a broad period from the Late Lower Palaeolithic (LP) to the beginning of the Mid-MP. The available dates (Mercier et al. 2007) indicate a chronology extending at least from the MIS 7 to the end of the MIS 6/beginning of MIS 5 (no dates available for the Layer G/Acheulo-Yabrudian level). At its base, this archaeological sequence consists of thin levels containing Acheulo-Yabrudian (Late Lower Palaeolithic) artefacts, followed by a sequence of superimposed levels approximately 7 m deep, containing Early MP assemblages dated to between 220 ka and 130 ka (Mercier et al. 2007).

This archaeological sequence thus provides new information on the major changes observed in the technical repertoires during the Late LP/Early MP transition, which are still the subject of numerous debates, particularly concerning the processes responsible for it (see Haifa Workshop 2017, ‘The Lower to Middle Palaeolithic boundary: A view from the Near East,’ published in a special volume of *JHE* 2022 entitled ‘The Lower to Middle Palaeolithic Boundary: Evolutionary Threshold or Continuum?’; EAA session September 2019, ‘Process of change from Late Acheulean to Early Middle Stone Age/Early MP in Africa and Eurasia’). One of the most original contributions of this sequence, however, is the record provided by the numerous Early MP levels, which inform us about the development, expansion, and end of the Early MP. This is a technical entity that recent discoveries and studies—even if still few in number (sites of Misliya, Hummal, Tabun IX, Emanuel, Hayonim, Abou Sif, Dederiyeh) (Figure 5.1)—have now enabled us to identify, date, and widely document (Goder-Goldberger et al. 2012; Meignen 2011; Nishiaki, Kanjou, and Akazawa 2022; Shimelmitz and Kuhn 2013; Wojtczak 2011; Wojtczak and Malinsky-Buller 2022; Zaidner and Weinstein-Evron 2020). Few currently published sites permit us to discuss the processes involved in the disappearance of the Early MP Laminar technology and the development of assemblages close to the Mid-MP. At present, only the data from the upper levels of the Hayonim sequence, covering the 160 ka–135 ka period, document this process of change from the Early MP to a yet undefined MP, which will



Figure 5.1. Map showing Levantine sites cited in this chapter.

need, therefore, to be confirmed by future discoveries and/or artefact studies. Let us recall that the lower levels of Neshar Ramla (unit V–VI), which cover approximately the same period (140 ka–120 ka), have yielded assemblages already belonging to the Mid-MP (Zaidner et al. 2021).

While the results concerning the Hayonim Early MP assemblages have thus far been the subject of numerous exploratory publications (Meignen 1998, 2000, 2007, 2011; Meignen and Bar-Yosef 2020), in this chapter we present, for the first time, an exhaustive study of the assemblages contained throughout the sequence (Acheulo-Yabrudian, Early MP, MP called the Tabun C type in the first excavations).

5.2 Methodology

5.2.1 Technological approach

In recent decades, research in prehistory has largely focused on understanding the behaviours and technical knowledge of Palaeolithic humans. Based on new concepts sometimes borrowed from other fields, along with experimentation, prehistoric

lithic technology specialists have developed methods that address issues such as the identification of technical knowledge and skills, raw material procurement strategies within a region, mineral, animal, and plant resource management, and mobility patterns.

The technological approach that we used in this study is based on an analytical tool first defined by ethnologists: the *chaîne opératoire* (operational sequence) (Inizan, Roche, and Tixier 1992; Sellet 1993; Soressi and Geneste 2011; Tostevin 2011). This concept was largely formulated by a group of French ethnologists studying material culture (Balfet 1991; Cresswell 1976; Lemonnier 1976, 1983, 1992; Leroi-Gourhan 1964; Mauss 1947).

As a tool for the description and analysis of technical processes, it allows one to address ‘the ensemble of operations organised and realised by a human group according to their available means, including their technical know-how, in order to attain a result, which is the satisfaction of a socially accepted need’ (Balfet 1991).

In these studies, the underlying assumption is that technological artefacts bear socio-economic implications, as they are physical manifestations of a society’s cultural pool expressed as technological behaviours (considered ‘social production’ [Lemonnier 1992]).

Due to the limited nature of archaeological data, it is not easy to adapt this concept, nor its interpretative potential, to prehistoric research. It has been applied mostly to lithic artefacts, since these are the objects most frequently found at sites and those which best preserve the stigmata related to the different phases of the technical process.

In lithic studies, the technological approach, now largely adopted by lithic specialists, is grounded in the use of the *chaîne opératoire*. This logical tool permits the identification of the final result of the reduction process (tools) and the options chosen (the preferred solutions/technical choices) among the available possibilities (other options that could have been used to attain the same result) at each stage of the operational sequence; the latter includes raw material procurement and tool production and management (Karlin, Bodu, and Pelegrin 1991; Pelegrin 1990; Pelegrin, Karlin, and Bodu 1988). It thus enables a reconstruction of the time/order organisation of the different phases involved in producing an artefact (Geneste 1991), as well as the concept(s) that govern the technical lithic system(s) adopted.

Conceived as such, the technological approach allows us to address two broad aspects that contribute to our understanding of Palaeolithic groups:

- The techno-economic domain, such as the technological organisation of lithic production across a prehistoric landscape (for more details, see Meignen 2019).

The tool-making process is often ‘discontinuous’ in the sense that the different phases of the *chaîne opératoire* can be realised at different times and locations (Geneste 1985, 1988). *Chaîne opératoire* analysis enables us to replace the objects studied within a temporal sequence corresponding to the different economic phases commonly recognised in technical production: raw material procurement, production (core shaping and blank production), and consumption (tool manufacturing, use and maintenance, and possible recycling), followed by their discard. Depending on the situation, these different phases, identified by the presence or absence of their significant products, can be realised in the same location or locations distant from each other, thus representing diverse economic strategies, mobility patterns, and so on.

Based on these same archaeological foundations, S. Kuhn (1992, 1995) proposed interpretive models such as the notion of ‘technological provisioning’, for which he identifies different provisioning strategies for technical activities (provisioning of individuals, provisioning of place). These strategies can be identified in the archaeological record via the types of techno-economic studies described above.

The relative importance of these two provisioning strategies depends on the degree of residential mobility of a group (Kuhn 1995) and thus in part on the occupation durations. The identification of these strategies in the archaeological record thus contributes to our understanding of regional occupation patterns.

- The cognitive aspects

Alongside *chaîne opératoire* analysis, which allows us to identify the logical succession of technical acts in time and space, the technological approach also enables us to identify the technical knowledge underlying these acts.

This technical knowledge is transmitted from generation to generation mostly via enculturation (primarily by apprenticeship via imitation after observation of technical gestures and repetitive experimentation/replication of these same actions [Karlin, Bodu, and Pelegrin 1991; Pelegrin 1995]), which, according to some authors, can be accompanied by oral explanations in the more complex cases (Roux 2007).

This knowledge remains stable over long periods, and it is this stability that permits us to identify it archaeologically because it is repetitive and shared by the majority of the members of the group. Because they are infrequent and not repeated, individual variants are ‘drowned out’ among the abundant objects corresponding to the shared norm and thus appear only very sporadically in archaeological studies, and then only at a detailed level of analysis (cf. refitting/high-resolution studies).

At the scale at which we work (except for specific analyses, such as refitting, which permit the identification of individual variants; see, for example, Bar-Yosef and Van Peer 2009; Ploux 1991), our studies mostly concern the dominant elements, including their internal variability, meaning those that are most often repeated.

Due to the palimpsests represented by the units that we study, it is difficult to claim that we can identify anything more than strong general tendencies, or dominant methods, through an evaluation of the most frequently adopted variants (Bar-Yosef and Meignen 1992). Based on the total assemblage of lithic artefacts (tools and by-products), it is thus possible to identify the objective(s) of a production and the means used to attain these objective(s) (*schéma opératoire*/methods and techniques used to achieve it).

Meanwhile, one of the essential goals of our work is to identify the concept(s) that govern the lithic system(s) adopted; that is, the geometric construction of the volume to be exploited and the rules followed during the flaking process to maintain this structure in order to produce the intended products (defined by Boëda as the ‘volumetric conception’ [Boëda 1994, 1995]).

This type of analysis thus opens new directions for the study of lithic production systems, independent of that involving only the morphology of the objects studied, meaning their ‘typology’. Since the morphology of a core can change during the flaking process without changing the internal organisation (Boëda 1997: 11), a morphological (typological) identification of the core alone is not sufficient. For each lithic production system, it is necessary to identify the technical criteria (formation of the convexities on flaking surfaces, relationships between the striking platform surface and the flaking surface, percussion technique, etc.) that are common among all of the morphologies belonging to this technical production system.

To achieve this objective, we must consider not only the core and the end-products, but all of the characteristic pieces associated with the preparation and maintenance of the core, which permit the production of the intended products (also called ‘technologically diagnostic artefacts’ [Monigal 2002] or ‘core management pieces’ [Hovers 2009]). This latter category of objects includes shaping, maintenance, and core trimming elements, which are often very informative. All of these elements are significant because they allow us to identify the options chosen by the knappers to create, on the core, the technical criteria necessary to detach products according to the flaking conception adopted (‘ways of doing’).

In order to explore the diachronic technological variation of these assemblages throughout the sequence, we used this technological/*chaîne opératoire* analytical approach at Hayonim (Boëda, Geneste, and Meignen 1990; Soressi and Geneste 2011) in combination with an attribute analysis of selected criteria (Bar-Yosef and Goren-Inbar 1993; Goren-Inbar 1990; Hovers 2009; Meignen 2019; Soressi and Geneste 2011; Tostevin 2000). We reconstructed the lithic operational sequences (i.e., lithic production systems) involved in

the different technical entities, as well as the tool manufacture/maintenance processes. Throughout the archaeological sequence, we attempted to reconstruct the dynamics of change in the economic strategies. However, we have, unfortunately, not been able to conduct a detailed study of the raw material procurement strategies as our team lacks a researcher in this field. In the late 1990s, C. Delage, as part of his Ph.D., mapped and characterised siliceous material sources in the region concerned (Delage 2001). A first exploratory study of the raw material procurement strategies in unit 10 was then carried out and a summary of the promising results was presented at a conference (Delage, Meignen, and Bar-Yosef 2000). Unfortunately, this work could not be continued. Therefore, our interpretations of site function in the territory are based on the identification and quantification of the characteristic products of the sequences of the *chaîne opératoire* in the different production systems. We are not able, however, to include the distances of raw material origins, and therefore to discuss the associated procurement zones.

5.2.2 Analytical procedures

The study presented here was conducted by combining the *chaîne opératoire* approach with an attribute analysis. Throughout the stratigraphic sequence, our main goals were to identify the strategies adopted at different stages in the reduction sequences, as well as the concept(s) underlying the productions in the technical system(s) adopted. In practice, for the study of each assemblage, our analysis protocol is organised in the following phases.

First, a global analysis of the lithic assemblage, permitting us to identify its main characteristics and evaluate the production system(s) employed based on the identification of significant features (Inizan, Roche, and Tixier 1992; Soressi and Geneste 2011).

Then, we sorted the objects according to significant technological categories (corresponding to production phases), thus preparing the assemblage for more precise inventories. We then systematically counted all of the objects according to broad categories (cores, cortical flakes, ordinary flakes, CTEs, Levallois products, Laminar products, and retouched tools), allowing us to inventory the tool assemblage composition in order to identify the *chaîne opératoire* phases represented in each assemblage and thereby document the role of the site within the territory.

Finally, we conducted a detailed techno-morphometric analysis (attribute analysis) of large samples of objects from the main technological categories (Levallois products, Laminar products, retouched tools, cores). The use of quantifiable, precisely defined attributes favoured replicable observations and comparisons. The attributes considered are based on the cumulative experience of previous researchers, as well as the particular questions raised by the assemblages we are studying. These attributes were selected for their capacity to aid in the identification of the flaking method, the morphometric characterisation of the products, and the selection of tool blanks, to test and further analyse the results obtained during the first stage of analyses. The observations and attribute combinations considered relevant during this first stage were quantified to allow their use for descriptive and comparative tests.

This quantitative analysis allows us to better characterise the goals of the production process, as well as the methods and modalities employed.

This analysis thus concerns not only the core reduction sequence (which is an obvious essential element), but also blank selection, the transformation (or not) of blanks by retouching, and the functional characteristics of the tools.

Considering the conditions of this study (the collections being located at the Hebrew University of Jerusalem, and the relatively short study period of around 2.5 months per year), we decided not to undertake systematic recording numerous attributes for each lithic object with no precise question in mind. Rather, we chose to focus our work on large samples and precise questions arising from our first observations of the complete assemblages. This choice has its risks, of course, but also has the advantage of being based on selected criteria that are adapted to our research questions (see also Soressi and Geneste 2011).

5.3 Preliminary information on the Hayonim lithic samples

During the first excavations at Hayonim (1965–1979), a deep sounding along the west wall of the cave revealed, at its base, the presence of levels containing MP assemblages characterised by elongated products (elongated points and retouched blades), overlain by levels mostly containing assemblages rich in Levallois flakes. This initial work thus clearly highlighted the stratigraphic succession of Mousterian assemblages of the Tabun D type (thus equivalent to Early MP), and assemblages with predominantly Levallois flakes (known as the Tabun C type Mousterian) (Bar-Yosef 1998a; Bar-Yosef et al. 2005). These assemblages had never been previously studied in detail. The collections are kept at the Institute of Archaeology, Hebrew University of Jerusalem.

5.3.1 Locations of the excavated areas

Our excavations (1992–2000) focused mainly on the MP levels and older ones discovered during our work. To excavate large areas continuously, we selected two zones: the Central Area, inside the cave, where the MP levels had been identified during previous excavations, and the area under the porch at the entrance to the cave (Entrance Area) (Figure 5.2). However, the presence of later ‘disturbances’ of anthropogenic (Natufian features, Aurignacian levels that intersect the MP deposits) or natural (Kebaran erosion in the Mousterian deposits) origin made continuous stripping difficult over large areas. In addition, the large areas with strongly brecciated sediments and metre-sized roof collapse boulders encountered in the entrance area limited the exploitable excavation surface in this sector, thus restricting our work to a large ‘sondage’ whose surface decreases with depth (the Deep Sounding). Consequently, it was not possible to establish direct stratigraphic continuity in the field between the levels of these two areas, which nevertheless revealed complementary sedimentary sequences with some stratigraphic overlap.

Our fieldwork between 1991 and 2000 revealed a sequence that was longer than that previously excavated, including Acheulo-Yabrudian levels discovered and excavated only during the last two years of the project. The deep MP sequence (Layers F and E) has been dated by TL to between 220 ka/130 ka (second half MIS 7 and MIS 6) (Mercier et al. 2007). The Acheulo-Yabrudian level (Layer G) could not be dated. Tests using the TL method were impeded by an excessively high external dose.

5.3.2 Reminder of the stratigraphic and chronological data

(see also chapter 2, this volume)

Layer G

Layer G was reached only at the base of the sondage at the cave entrance (Deep Sounding); it was excavated across 2 m² (squares F27–28) and to a depth of approximately 60 cm.

The artefacts collected correspond to the Acheulo-Yabrudian (Meignen and Bar-Yosef 2020). No dating is available.

Layer F

Layer F was excavated mainly in the Deep Sounding at the entrance of the cave, near the porch, across an area of approximately ten square metres for the upper part, and less in the lower part, and to a depth of approximately 2.5 m. In these levels, the abundant archaeological artefacts correspond to the Early MP.

Layer F was also identified in the Central Area, across the entire excavated surface. This layer is generally thin, varying between 30 and 60 cm depending on the square, because its upper limit is determined by erosive contact with the overlying layer (Layer E). The base of Layer F was not reached in this area during our excavations. In the Central Area, archaeological artefacts are generally scarce, being limited to a few large flaking concentrations. It corresponds to an Early MP.

TL dates: approximately 210 ka–220 ka (Mercier et al. 2007).

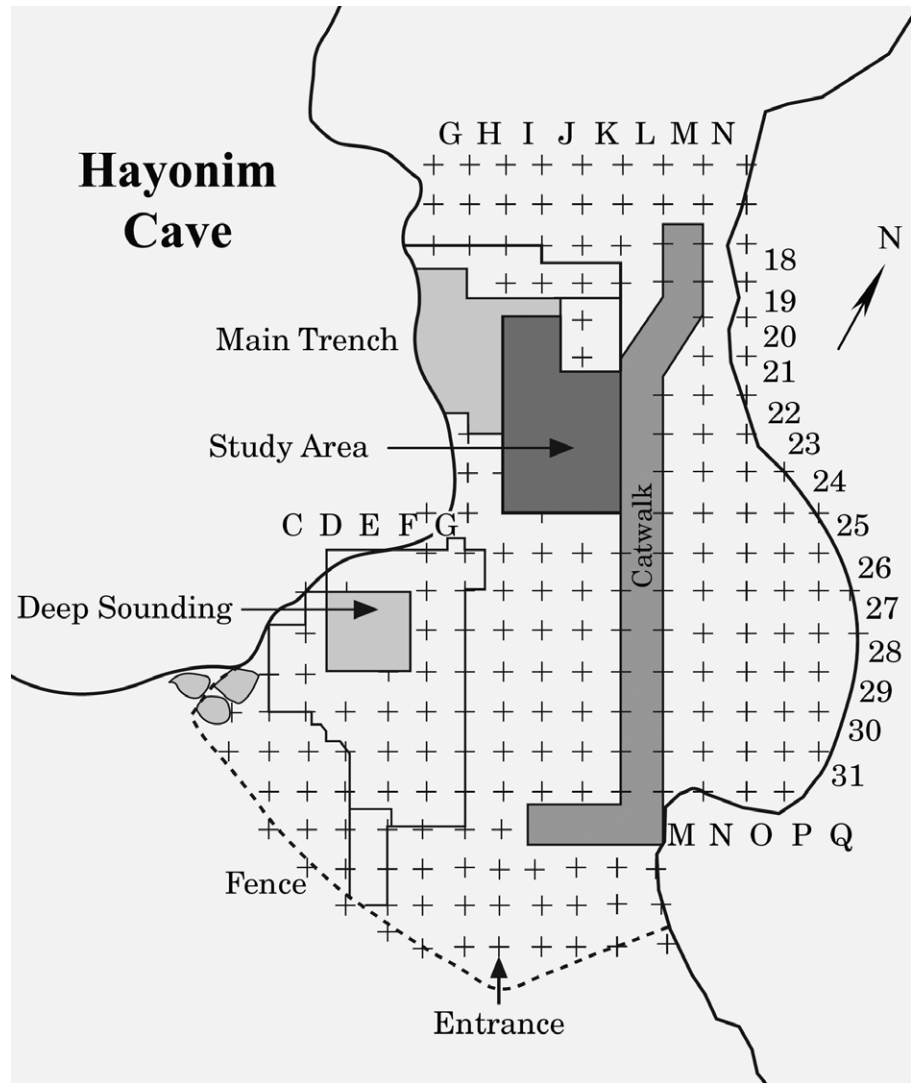


Figure 5.2. Hayonim excavation plan. Adapted from Stiner 2005: Fig. 1.2.

Layer E

Layer E was excavated to a depth of approximately 2.30–2.50 m, mainly in the Central Area, thus constituting the greatest proportion of our work. This layer is also present in deeper deposits (more than 3 m deep) at the cave entrance. However, due to the complex formation processes in this area (accumulation of Layer E deposits above the erosion surface of Layer F in a basin-like setting and locally disturbed by a later Kebarian channel), the study of the Layer E artefacts in this area proved difficult. We thus focused our analyses on the artefacts from the Central Area, where the stratigraphic context is much clearer (see chapter 2).

Depending on the levels, the archaeological artefacts identified correspond to Early MP in the Lower E Layer and MP dominated by Levallois flake production in the Upper E Layer.

TL dates: 185 ka–130 ka (Mercier et al. 2007).

5.3.3 Division of the archaeological sequence into units

We subdivided this long archaeological sequence (Layers G, F, E) into 11 units whose limits were determined either by changes in the nature of the deposits (layers) or more often by changes in the density of lithic artefacts (units). The boundary between Layers

E and F, most clear in the Central Area, corresponds to an erosion phenomenon with a large chronological gap between the two (Mercier et al. 2007). The upper limit of Layer G was defined based on changes observed in the geology, as well as in the tools (easily identifiable Acheulo-Yabrudian bifaces and scrapers). In addition, locally, it corresponds to a hearth level that constitutes a useful reference point.

The two main stratigraphic entities (Layers E and F), whose sediments are relatively homogeneous, were further subdivided into units (Layer F: units 10 to 7; Layer E: units 6 to 1) based on lithic material density profiles (analysis by S. Kuhn).

5.3.4 Artefact collection procedures

All lithic artefacts with a maximum length greater than 2.5 cm were collected and recorded in three dimensions. All of the sediments were sieved first with 3–4 mm mesh screens and then with water through 1 mm mesh screens. The numerous small flakes were collected in 50 × 50 × 5 cm subsquare units. All objects associated with the lithic production are thus available for study. A computerised inventory of the piece-plotted material was updated daily in the field.

5.3.5 Selection of study samples

The abundant lithic artefacts greater than 2.5 cm long comprise more than 19,960 of the plotted pieces recorded in the database.

However, considering the deposit formation processes in certain areas, we chose to focus our study on sectors in which the stratigraphy was easily decipherable. Moreover, the lithic artefact analysis was organised according to the subdivisions (units) defined after the excavation. Therefore, the large samples studied were chosen mainly in sectors in which the stratigraphic context is clear, and from squares in which the sedimentary levels are horizontal to enable the collection of samples that correspond to the units defined based on density profiles.

Therefore, the study of the Layer E assemblages was conducted with artefacts from the Central Area, where the units are easy to distinguish, whereas the very complex formation processes of the Layer E sediments in the sondage did not enable us to subdivide Layer E for correlation with those of the Central Area. Conversely, the lithic assemblages from Layer F were studied in the Deep Sounding area where the lithic densities are higher and the deposits much thicker (ca 250 cm) than in the Central Area.

However, due to the lack of stratigraphic continuity in the field, a precise correlation between the sequences of the two zones remains problematic. While the base of Layer E (corresponding to erosion between Layers E and F) is indeed synchronous in the two areas and thus constitutes a good stratigraphic reference, the upper layers of Layer E, intersected by erosion in these two areas, are probably not strictly equivalent. Because the erosional boundary is deeper in the entrance area (see chapter 2, Figure 2.4), it is likely that a greater thickness of the upper portion of Layer F was washed away at the entrance. Although the two sequences partially overlap, it is thus impossible to precisely correlate the subdivisions of Layer F in the two areas.

In our study, it was sometimes necessary to group units together, either because the available samples were too small (units 7–8 in the Deep Sounding) or because it was impossible to distinguish units based only on data from the former excavations (units 1–2, in the Central Area).

5.3.6 Taphonomic features

The surface condition of the objects varies depending on the location of the deposits. The condition is generally good, showing few, marked post-depositional irregular retouch, except in a few sectors. The Layer E deposits, mostly anthropogenic (corresponding to combustion areas), are in a good state of preservation, even if some trampling damage altered the edges of some of the thinnest artefacts. Geological analyses show that the Layer F deposits are associated with a 'low energy depositional environment', suggesting that

the formation processes probably had little effect on the artefacts. This is especially true because the occupations likely occurred when the sediment was 'dried out' (chapter 2, this volume). However, two specific examples illustrate the presence of pieces modified by post-depositional phenomena:

- In Upper Layer F, in the Central Area, two large lithic concentrations correspond to artefacts disturbed in situ by dripping (see description in chapter 2);
- In Layer G, the local presence of pieces with modified edges (alternating retouch) is probably related to the formation of the deposits (or burrows?). The small volume excavated makes it difficult to identify the phenomenon responsible.

Frequent concretions (calcite and especially phosphates) in the brecciated sediment zones are also significant. These consist of crusts that are often difficult to dissolve, thus preventing the analysis of certain pieces. This problem is also noted by Stiner (chapter 4, this volume) for the bones, whose cleaning was difficult.

Field observations and geological/micromorphological studies have highlighted several types of syn- and post-depositional phenomena, the impact of which is important to assess.

First, bioturbations (burrows), on a deci- to centimetric scale, but mostly bioturbations on a micrometric scale (insects), as frequently observed in the ashy anthropogenic sediments characteristic of this filling (Goldberg and Bar-Yosef 1998), were spotted during the excavation and in the laboratory (micromorphological study). The easy identification of the former in the field (loose sediment, well-defined burrows intersecting areas of combustion or bedding) allowed the elimination of disturbed elements. As for the smaller-scale disturbances, their effect on the artefact locations is negligible due to the degree of precision adopted in our studies. Tests to evaluate mechanical disturbance in Layer E (chapter 4, this volume) confirmed the limited impact on the representativeness of the artefacts studied.

As we previously discussed in chapter 3, the effects of diagenesis, sometimes locally significant, do not seem to have strongly disturbed the artefact distributions.

Micromorphological analyses also identified anthropogenic disturbances (mainly trampling), frequently identified in poorly consolidated sediments corresponding to combustion features. These phenomena do not occur at great depths, and we adapted the depth of our units accordingly. However, taking into account such post-depositional disturbances, we did not look in detail at the spatial organisation of the artefacts.

Finally, it is important to emphasise the high proportion of objects displaying varying degrees of fire-related modifications. These modifications range from simple colour changes to cracks and cupules, to the total destruction of the piece. In the latter case, the object is broken into multiple small thermal flakes that are found in 'connection' in the sediment. This phenomenon is clearly linked to the abundance and superposition of combustion features, as these modifications result from contact with them, and their nature depends on the distance of the object from the fire. Among all of the pieces spatially recorded during the excavation, 43.5% display heating modifications. More specifically, 53% were recovered in Layer E, where the hearths are most numerous, and 34.1% in Layer F, where their remains are less obvious, indicating that combustion features were present even if they are no longer detectable. These high proportions of accidentally heated pieces are a logical consequence of the high accumulation of successive combustion features that we describe in our study (chapter 3, this volume).

The presence of these very numerous heated artefacts is likely related to the low rate of sedimentation between the different periods of occupation (predominantly anthropogenic deposits in Layer E). The artefacts, abandoned on the surface or at a shallow depth, were impacted by the broad spread of combustion features during the following occupations (see chapter 3, this volume). When hearths were superposed in the same place (as described in unit 6, for instance), the size and duration of the fireplaces

increased, which in turn deepened the heating impact (see experiments described by Sorensen and Scherjon 2018), thus resulting in more heated flints. The high occurrence of burning damage on bones (between ca. 8–30% of total NISP for common prey taxa), results from the same phenomenon (chapter 4, this volume).

The high proportions of heated artefacts, therefore, reflects the repetition of combustion activities even during low-density occupations, as long as the sedimentation rate was low between these successive occupations.

5.4 The end of Lower Palaeolithic/unit 11

5.4.1 Introduction

Layer G, in which Lower Palaeolithic artefacts were discovered during the final excavation seasons at the base of the large sondage at the cave entrance, was excavated over just a small area. The highly brecciated sediments prevented us from enlarging this excavation area. Only a large excavation more than 3 m deep could allow future researchers to reach Layer G, and thus to enlarge the sample. The artefacts were thus collected from a 2 m² surface approximately 0.55 m deep, a small volume that obviously warrants interpretative caution. This small sample size did not allow us to address subjects such as techno-economic behaviours, tool circulation, and the techno-economic organisation of the production, in contrast to the approaches currently frequently applied to this period (Tabun [Shimelmitz 2015; Shimelmitz, Kuhn, and Weinstein-Evron 2020]; Misliya [Zaidner and Weinstein-Evron 2016]; Qesem [Assaf et al. 2015; Barkai et al. 2009; Lemorini et al. 2015; Lemorini et al. 2006]). Although this sample size is small (225 pieces), the assemblage is characteristic of the Acheulo-Yabrudian (Meignen and Bar-Yosef 2020), or more precisely of the ‘Acheulean facies of Mugharan tradition’ defined by Jelinek (1982b). This tradition comprises two distinct components: a flake tool-dominated assemblage (broad thick flakes used as scraper blanks, with Quina/semi-Quina retouch), and a bifacial component.

Brief reminder of the Acheulo-Yabrudian complex

At the end of the LP, generally occurring between 400 ka and 250 ka (Malinsky-Buller 2016, and references therein), the assemblages assigned to the Acheulo-Yabrudian technocomplex (Bar-Yosef 1994; Copeland 2000; Garrod 1956; Rust 1950)—also known as the ‘Mugharan tradition’ (Jelinek 1982a, b)—are characterised by the production of non-Levallois blades and broad, thick flakes for Quina scrapers, along with bifaces in some facies. This technocomplex, identified only in the northern and Central Levant (Jagher et al. 2016; Le Tensorer 2005/2006), is composed of three facies: the Acheulean (also known as the Acheulo-Yabrudian [Rust 1950]), Yabrudian, and Amudian.

The Acheulean/Acheulo-Yabrudian is characterised by bifacial tools and flake production, with some scrapers shaped by the Quina or semi-Quina retouch, while the Yabrudian is mainly characterised by scrapers on thick flake blanks, often transformed with a Quina-type retouch. The Amudian is characterised by a significant increase in blade production (Barkai and Gopher 2013; Copeland 2000; Garrod 1956; Jelinek 1982a, b, 1990).

These characteristic elements—handaxes, Quina scrapers, and Amudian blades—tend to exist in most assemblages of the Acheulo-Yabrudian technocomplex, albeit in very different proportions (Copeland 2000; Jelinek 1982a, b, 1990), resulting in a remarkable technological diversity during this period. The three facies are generally considered different variants of a single cultural complex (Copeland 1975; Jelinek 1982a, b, 1990) that may have represented different activities (Barkai et al. 2009; Copeland 1975; Jelinek 1990; Parush, Gopher, and Barkai 2016). In all of these variants, Levallois technology is absent, or considered intrusive when it is marginally present.

New excavation projects and numerous technological studies, mainly in the last decade, have highlighted a more complex situation in terms of core reduction strategies and tool production. This research has contributed to a more complete documentation and recognition of the technological variability of this Acheulo-Yabrudian complex. This variability includes a

Table 5.1. Hayonim unit 11 – General breakdown of lithic artefacts. Percentages in column 3 are of ‘total debitage’; and in column 4, of ‘total assemblage’.

Category	N	%	%
Cortical flakes	54		
Cortical blades	5		
Cortical broken/debris	9		
Total cortical items	68	53.5	
Non-cortical flakes	30		
Non-cortical blades	3		
Non-cortical broken/debris	26		
Total non-cortical items	59	46.5	
Total debitage	127		56.4
Cores	23		10.2
Retouched tools	41		18.2
Bifaces	27 + 7 fragments		15.1
Total shaped pieces	75		33.3
Total	225		

specific blade core reduction method (often producing cortical-backed blades) in the Amudian (Barkai et al. 2009; Shimelmitz 2009; Shimelmitz, Barkai, and Gopher 2011; Shimelmitz et al. 2016), the intentional production of thick flakes in the Yabrudian and Acheulo-Yabrudian assemblages (Malinsky-Buller 2016; Nishiaki, Kanjou, and Akazawa 2017; Nishiaki et al. 2011; Shimelmitz et al. 2014b; Shimelmitz et al. 2016; Weinstein-Evron and Zaidner 2017; Zaidner and Weinstein-Evron 2016), a bifacial technology (Shimelmitz et al. 2017; Shimelmitz et al. 2021; Zaidner, Druck, and Weinstein-Evron 2006), and, in some cases, the remarkable presence of cores-on-flakes (Parush et al. 2015).

All of these industries are now frequently grouped under the term ‘Acheulo-Yabrudian cultural complex’ (AYCC: Barkai and Gopher 2013; Parush, Gopher, and Barkai 2016; Shimelmitz et al. 2014b) or sometimes the ‘Acheulo-Yabrudian technocomplex’ (Zaidner and Weinstein-Evron 2016).

The composition of the unit 11 assemblage is similar to the facies defined as the ‘Acheulean facies’ by Jelinek (1982a, b), also called the ‘Acheulo-Yabrudian’ (Rust 1950). We have adopted this simplified name because the composition of the Hayonim assemblage includes a high representation of both components (handaxes and flake production for scrapers), the latter having clear affinities with the Yabrudian.

As recently reported by Shimelmitz et al. (2021), the assemblages most often referred to as Acheulo-Yabrudian and that correspond to this ‘Acheulean facies in the Acheulo-Yabrudian cultural complex’ are relatively rare. Above all, they have not been the subject of recent technological studies. The publication of the Tabun unit X (Shimelmitz et al. 2021) is an exception and will constitute the main point of comparison in our work. We will also place the unit 11 assemblage in the context of the technological data currently available for the Yabrudian facies assemblages to identify the relationships between these different facies.

Despite the small sample size, it is thus important to thoroughly record the unit 11 assemblage at Hayonim to enrich our data on the variability identifiable within the Acheulo-Yabrudian technocomplex.

5.4.2 Study of the unit 11 lithic artefacts

The basic composition of the Layer G assemblage is presented in Table 5.1. This inventory is clearly dominated by flakes and flake tools. Secondarily modified pieces (retouched tools on flakes and bifaces) are numerous (n = 75) and comprise about 33.3% of the assemblage, while debitage and cores represent 56.4% and 10.2%, respectively (Table 5.1). Cores are thus proportionally abundant.

Category		N	N	%
Plain	Wide <i>incliné</i>	15		
	Straight	27		
	Convex, <i>à pans</i>	1		
	Total plain		43	55.13
Dihedral	Symmetrical	1		
	Asymmetrical	3		
Faceted		24		28.91
Cortical		5		
Punctiform		2		
Total	78			

Table 5.2. Hayonim unit 11 – Butt categories of the debitage products. Percentages are of ‘total number of identifiable striking platforms’. For definitions, see text.

5.4.2.1 Flake tool-dominated assemblage

5.4.2.1.1 Blanks

The blank production method in this unit emphasises large, thick, and often cortical flakes. Flakes dominate the assemblage and blades are scarce (n = 8). Cortical products, almost exclusively flakes, are abundant, constituting 53.5% of the assemblage, thus in higher proportion than ordinary products (Table 5.1). These flakes are short or elongated in roughly equivalent proportions; they are generally thick or very thick (68.5%).

The flakes usually have a prominent bulb of percussion, giving them a highly convex ventral curvature. They are often largely cortical, with a cortical back sometimes associated with a cortical overshoot, representing 16.5% of the assemblage.

The flaking was conducted with a hard hammer, using an internal percussion gesture (i.e., striking well back from the edge of the striking platform toward the centre of the core volume; *percussion rentrante* in French). This most often results in flakes with wide, thick, plain striking platforms (observed on 54.2% of the flaking products [Table 5.2]), often oriented at an obtuse angle (ca 100–110°) to the ventral face (19.2%) (*talon lisse large incliné*). The latter (resulting from the ‘high-angle technique’ described by Skinner [1970]), as well as the presence of a few asymmetrical dihedral platforms, evoke the reduction system already identified in the French Quina assemblages (Bourguignon 1997, 1998).

In addition to the low frequency of thin flakes often identified in the Acheulo-Yabrudian assemblages (here, 31.5% of the flaking products, some of them with the characteristic plain platform oriented at an obtuse angle, as described above), a series of thin flakes with a more elaborate striking platform (often faceted), which we identified as Levallois (n = 18), is present. However, a careful examination of the general state of preservation of the entire assemblage shows that their edges are often more abraded than those of the other flakes. We thus concluded that they are most likely intrusive, probably resulting from post-depositional processes (burrowing).

5.4.2.1.2 Cores

Cores are abundant in this assemblage (n = 23; 10.2% of the assemblage; Table 5.1) and have diverse atypical morphologies; they can be described as globular, ‘informal’, and sometimes discoid, and it is difficult to decipher their reduction patterns and volumetric structure. These cores are often discarded at various stages of reduction. In the case of relatively unstandardised production systems as observed here, it is important to consider the final morphology of the core, as well as to understand the sequence of technical gestures that created the morphotechnological characteristics of the intended products (i.e., to decipher the algorithm on which the structure is based and the volumetric conception applied). In other words: the ‘repeated set of procedures aimed at producing blanks with specific morphological features’ (Shimelmitz et al. 2014b).

Table 5.3. Hayonim unit 11 – Core types. For definitions, see text.

Core types	N
'Debitage facial/hierarchical surface' (Shimelmitz et al. 2014b)	4
Non hierarchical surface cores (Quina type)	3
Hierarchical surface cores/deep scars	7
Discoid	1
Isolated non-organised deep removals	8
Total	23

All of these variable cores share the following features: small dimensions (mean length = 46.50 [s.d. 9.55]; mean width = 44.29 [s.d. 11.60]; mean thickness = 24.21 [s.d. 8.40]); a low number of removals and therefore a low productivity; the use of direct, hard hammer and internal percussion, shown by the deep concave scars created by the detachment of thick flakes, often with very pronounced percussion bulbs. However, the most striking feature is the absence of an obvious core-shaping phase.

The blanks on which these cores are made are most often difficult to identify: 9 possible blocks, 4 flakes, and 3 corresponding to the reduction of nodules. Some of them (n = 12) show evidence of the production of thick blanks (deep, concave scars). The small number of pieces and their poorly prepared volumetric structures (often with only one or two flake scars) make it difficult to systematically attribute them to one of the volumetric structures already known.

Meanwhile, in addition to an assemblage of cores with only a few flake scars (n = 13), other, more informative, cores have enabled us to detect regularities in the reduction sequences, thus facilitating the identification of algorithms that we believe are significant in terms of the volumetric concept (Table 5.3).

Our analysis of the removals on the few most informative cores allowed us to distinguish the following:

- A small core assemblage (n = 4) on which we can identify a reduction sequence organised on the widest face of the volume (facial flaking), and the presence of two hierarchical surfaces (one for the striking platform preparation, the other for flake production). The few removals present on the flaking surface are roughly parallel (sometimes slightly oblique) to the intersection plane between the two surfaces (exploitation of a preferential surface), and are unidirectional, bidirectional, or multidirectional in equal proportions.
- The flake scars indicate often-thick flakes (as well as thin flakes) that remove a large part of the core surface and edge. These observations recall the reduction sequence for scraper blank production described by Shimelmitz et al. (2014b) in three Yabrudian assemblages at Tabun that they called 'debitage facial/hierarchical surfaces' (Shimelmitz et al. 2014b). However, the small number of these core assemblages makes this diagnosis difficult.
- Another core assemblage (n = 3) might correspond to the Quina flaking system defined by L. Bourguignon (1996, 1997) based on European assemblages. These cores show an alternating exploitation (here, with few removals) of two adjacent and secant surfaces (Figure 5.3). These surfaces are non-hierarchical (each one is used alternately as a striking platform surface and a flaking surface): surface A is relatively flat and surface B is inclined with respect to surface A.

In this reduction sequence, the first step is the construction of surface A, which is relatively flat and parallel to the intersection plane between the two surfaces, corresponding to the exploitation of a preferential surface via deep removals (producing thick flakes with large cortical surfaces). These flake scars then served as a striking platform for the local installation of the secant surface B: this new surface is composed of a small series of removals on an inclined plane (angle <90°) relative to the intersection plane of the

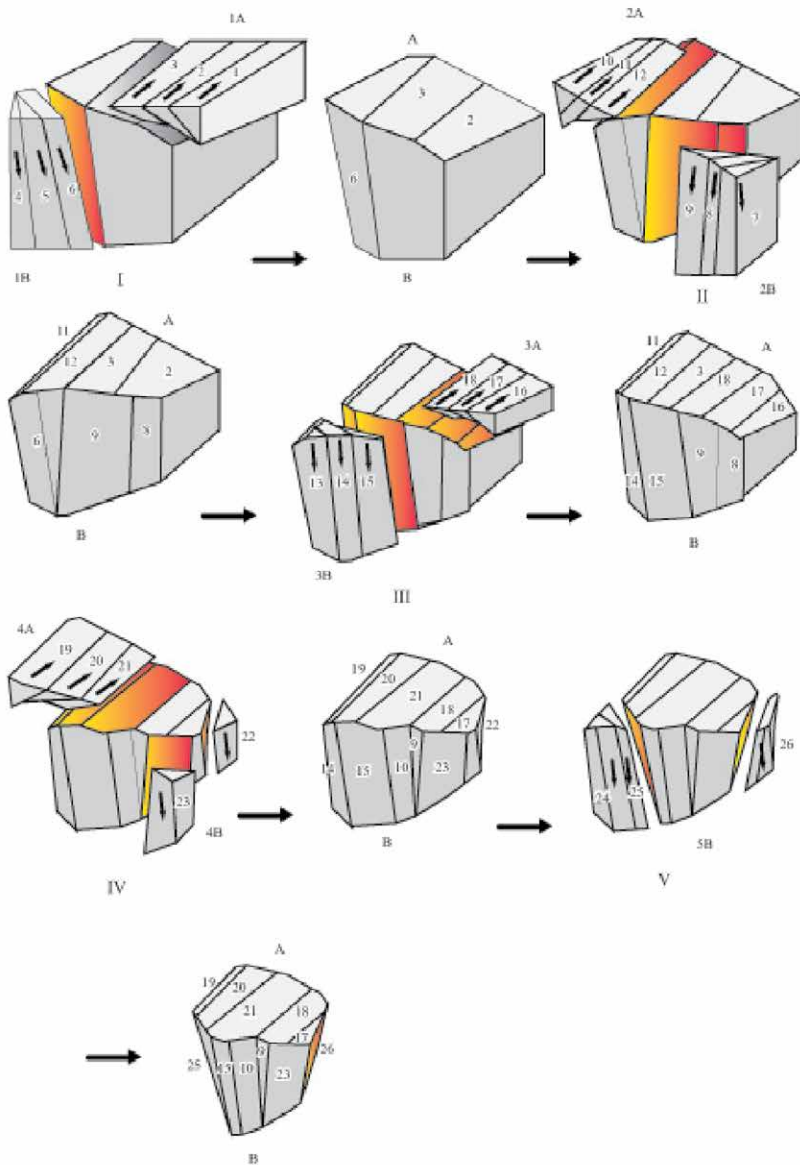
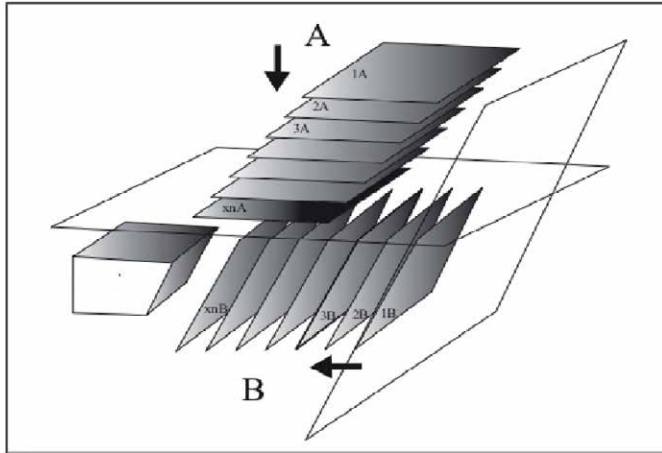


Figure 5.3. Schematic reduction sequence of the Quina flaking system. Alternating exploitation of two adjacent and secant non-hierarchical surfaces. The first surface (surface A), relatively flat, is subparallel to the intersection plane between the two surfaces. This surface A served as a striking platform for the local installation of the secant surface B, with an inclined angle relative to the intersection plane. The reduction sequence continues with a return to surface A and the all sequence is repeated several times in different places of the volume. Adapted from Bourguignon 1997.

two faces. These removals produced the characteristic flake with *talon lisse large incliné* (high-angle >90–100° between the bulbar surface and the butt) known in the European Quina and considered typical of the Yabrudian. These blanks are present in Hayonim unit 11. This pattern of blank production was clearly anticipated by Skinner (1970:157) in the Yabrudian assemblages from Maslouk. There, he identified ‘Clactonian cores’, for which he described the ‘manipulation of a piece of raw material to obtain successively high-angle striking platform for flake removals...often a scar will serve as the striking platform for successive flake removal operations’.

The creation of convexities on both surfaces is integrated into the production sequence via the use of *débordant* flakes with a cortical back or unworked. On both surfaces, each series of removals is unidirectional.

The core reduction sequence continues with a return to surface A, and the sequence previously described is repeated several times, the exploitation of surface B being located at different places of the volume to continually maintain the desired striking angle until the core is exhausted (Figure 5.3). In the final stage, a cortical residue is often present on the core.

The flaking sequences are generally short because, to produce thick flakes, this method consumes a large quantity of the raw material at the beginning of the reduction sequence. Then, on the following flaking surfaces, non- or slightly cortical flakes are detached, along with cortical-backed flakes that often have an open angle in the case of ‘wide plain inclined butts’.

The result, in the final reduction phase, is cores that are morphologically diverse but have the characteristic silhouette displaying the asymmetrical dihedral (*dièdre d'angle fermé*; Bourguignon 1996, 1997) between a more or less flat surface and an inclined surface (Figure 5.3). In the case of Hayonim, the number of scars in the final stage is low.

It is likely that these two options often coexist in assemblages. Our observations show that this is the case in the unit 11 assemblage, even if the numbers in each of the two categories are very low.

The presence of the two core types described above, as well as the corresponding desired blanks, confirms this. While the two proposed reduction concepts enable the production of thick cortical, broadly cortical, and, especially, cortical-backed blanks, the specific blanks (thick flakes with wide plain inclined butts often reported in the literature [Copeland 2000; Skinner 1970]), sometimes identified at Hayonim, cannot result from the first production concept (facial flaking/hierarchical surfaces). The cores with the low-angle dihedral morphology (*dièdre d'angle fermé*), described in our second option, are the only structures capable of producing these typical flakes (with a wide plain inclined butt), which do not seem to be present in some Acheulean-Yabrudian assemblages (as at Tabun, for instance). Moreover, in her preliminary study of the Yabrudian levels of Yabrud, Bourguignon (1997: 646 and fig. 415) describes the characteristic butts of this flaking mode: the *talons à pans* which correspond to the use of the previous scars of surface A as a striking platform for the exploitation of surface B. This type of butt has been observed in the Hayonim unit 11 assemblage, although in small quantities. Shimelmitz et al. (2014b: 10 and table 3) describe ‘multi-scarred platforms’, ‘which differ from faceted ones in that they lack negatives of the bulbs of percussion, meaning that the removal scars were not necessarily directed toward shaping the specific platform’. This kind of butt, which is quite numerous in Beds J82BS, J83B1, and R63 at Tabun, could be an indication of the presence in the Tabun Yabrudian levels of the flaking system described by Bourguignon.

It is difficult to generalise the observations made on the cores from Hayonim unit 11, given their small numbers. However, published descriptions of other assemblages from Yabrudian or Acheulo-Yabrudian assemblages show that these two exploitation patterns are most likely present at different sites, either individual or coexisting, often identified under different names. It would be therefore interesting to test the presence/absence of these two concepts, dominant or exclusive. The observations available in recent publications provide some clues.

In their study of the Acheulo-Yabrudian assemblage from Misliya, Zaidner and Weinstein-Evron (2016) report that ‘evidence for alternate knapping which is often reported for Quina flaking in European Middle Palaeolithic is rare’. However, at the same time, these authors report the presence of ‘flakes with wide thick plain striking platforms, often oriented at an obtuse angle (ca 100–110°) to the ventral face’. According to the authors, the cores corresponding to these large flakes are not present at the site because they would have been produced off-site and then imported. However, the presence of these particular flakes indicates that this flaking system, considered typical of the European Quina, was probably known to the Yabrudians of Misliya, even if the corresponding cores are not present.

The blanks described in the Yabrudian assemblages from Maslouk, for example, indicate a predominance of the ‘Quina’ production system (Skinner 1970), while the cores described in unit X at Tabun suggest the majority (exclusive?) implementation of the ‘facial flaking’ system as recognised by Shimelmitz et al. (2014b). However, the description of the organisation of the exploitation surfaces of the cores in unit X provided by Shimelmitz et al. (2021: 10), ‘the other cores show a mixture of orientations, with some parallel and some oblique to the face of removals’, suggests a flaking sequence close to the system described in our second concept (*dièdre d’angle fermé*), at least on some of the cores.

Shimelmitz et al. (2014b) highlight in the Tabun Yabrudian levels (Beds J82BS and J83BI/Layer R63), the dominance of the ‘facial flaking/hierarchical surfaces system’. However, as previously mentioned, it is important to keep in mind the presence of specific butts that are very well described (‘multi-scarred platforms’) and could correspond to the roughly faceted butts identified in the Quina Mousterian as a result of using anterior detachments as a striking platform.

In the Dederiyeh assemblages (Nishiaki, Kanjou, and Akazawa 2017), the descriptions of ‘different kinds of cores with one or two working surface(s)’, and the published drawings of the cores (fig.3) suggest the presence of both production systems.

The characteristics of the blanks produced (more or less thick) and the possibilities of producing scalar/stepped retouch (Quina), preferentially on thick blanks, depend on the role played by these different reduction sequences in the assemblages. It is possible that the flaking system described by Shimelmitz et al. (2014b) at Tabun (facial flaking/hierarchical surfaces) results in thinner blanks, which are themselves not conducive to the widespread development of Quina retouch.

All of these observations, which are only avenues for consideration, reflect the difficulties encountered in identifying flaking systems that do not display strong constraints in the management of the volume to be flaked. It seems that the exploitation of these cores corresponds rather to a permanent adaptation to the morphology of their volume—with the knapper looking for the technical conditions and choosing the percussion location that would allow them to obtain the characteristics of the desired blank (in this case, thick flakes with a wide butt) (Bourguignon 1997). Interestingly, this is an element already well perceived by Skinner (1970) when he points out in Maslouk’s assemblages ‘a preoccupation with high-angle flake removal technique in which the core is constantly shifted to make use of high-angle striking platforms’.

Relatively few thin flakes were produced at Hayonim. Moreover, the thin blanks that are present are frequently broken. Therefore, this small sample does not allow for a detailed study. However, we can note the almost equivalent proportions of faceted and plain butts, among which some are plain inclined butts, typical of the flaking mode described for the production of thick blanks. These thin products are, moreover, rarely cortical, most often being only slightly cortical (<25% cortex). In this respect, they differ from the thick blanks described above. However, as observed in the Quina system in European assemblages, it is possible that the production of these blanks was integrated into the reduction sequence or occurred at the end of the sequence in the two ‘core reduction strategies’ previously described. In particular, the production of these

blanks may occur during the exploitation of a hierarchical surface, system described by Shimelmitz et al (2014b) who envisage a ‘reconversion’ of cores initially producing thick blanks. The production of these thin blanks would intervene at the end of the sequence, when the exploitation of the preferential surface is no longer possible. The presence of the ‘multiplatform cores’ described in the Tabun Yabrudian, for example, would be the result of this reconversion process.

The production of thin flakes can also occur during the exploitation of surface A in the case of the second flaking system (Bourguignon 1997). She describes, in Layers 21, 22, and 25 of Yabrud, an occasional production of thin blanks during the exploitation of surface A via a series of detachments parallel to the intersection plane.

The presence of thin flakes alongside the characteristic thick blanks is identified in many European Quina assemblages and is also regularly reported in Yabrudian assemblages (Copeland 2000; Shimelmitz et al. 2014b; Zaidner and Weinstein-Evron 2016). In most cases, it does not seem necessary to consider a specific *chaîne opératoire* for their production, except when this production is quantitatively important and presents particular features (as at Misliya, where the abundant thin blanks are clearly the shortest [Zaidner and Weinstein-Evron 2016]).

5.4.2.1.3 Retouched tools

The retouched tools on flake blanks (n = 41; 18.2% of the lithic assemblage, including cores; Tables 5.1, 5.4), especially scrapers, are preferentially made on largely cortical flakes (cortex greater than 50%). Short and elongated blanks are present in the same proportions.

Scrapers of various types (Figure 5.4) and, in particular, simple ones (single side, n = 8), dominate the retouched tool assemblage (58.5%). Skewed (*déjeté*) scrapers (n = 6, most often transformed by Quina or ½ Quina retouch) and transverse scrapers (n = 3), both often considered typical of the Yabrudian (Bordes 1955; Copeland and Hours 1983), were also recorded. Because it is generally the longest edge that is retouched, depending on the blank morphology, the scraper is lateral or transverse. The retouched edge is most often convex or straight.

Most of the tool blanks have plain butts and it is worth noting the presence of the ‘plain wide inclined’ butts described above, corresponding to what Skinner called a ‘high-angle striking platform for flake removals’. More than half of the scrapers (14 of 24) show the ‘Quina’ or ‘semi-Quina’ retouch (scalar/stepped) considered typical of the Yabrudian/

Tool category	N	Quina retouched only	Semi-Quina retouched only
Retouched blade/one edge	3	1	1
Retouched point	1		
Single scraper	8	1	3
Double scraper	1		1
Convergent scraper	1		1
<i>Déjeté</i> scraper	6	2	3
Transverse scraper	3	1	
Scraper on ventral face	1		
Endscraper	1		
Truncated flake	1		
Notch	3		
Denticulate	2		
Miscellaneous/retouched flake	10		
Total	41	5	9

Table 5.4. Hayonim unit 11 – Typological breakdown of the assemblage.

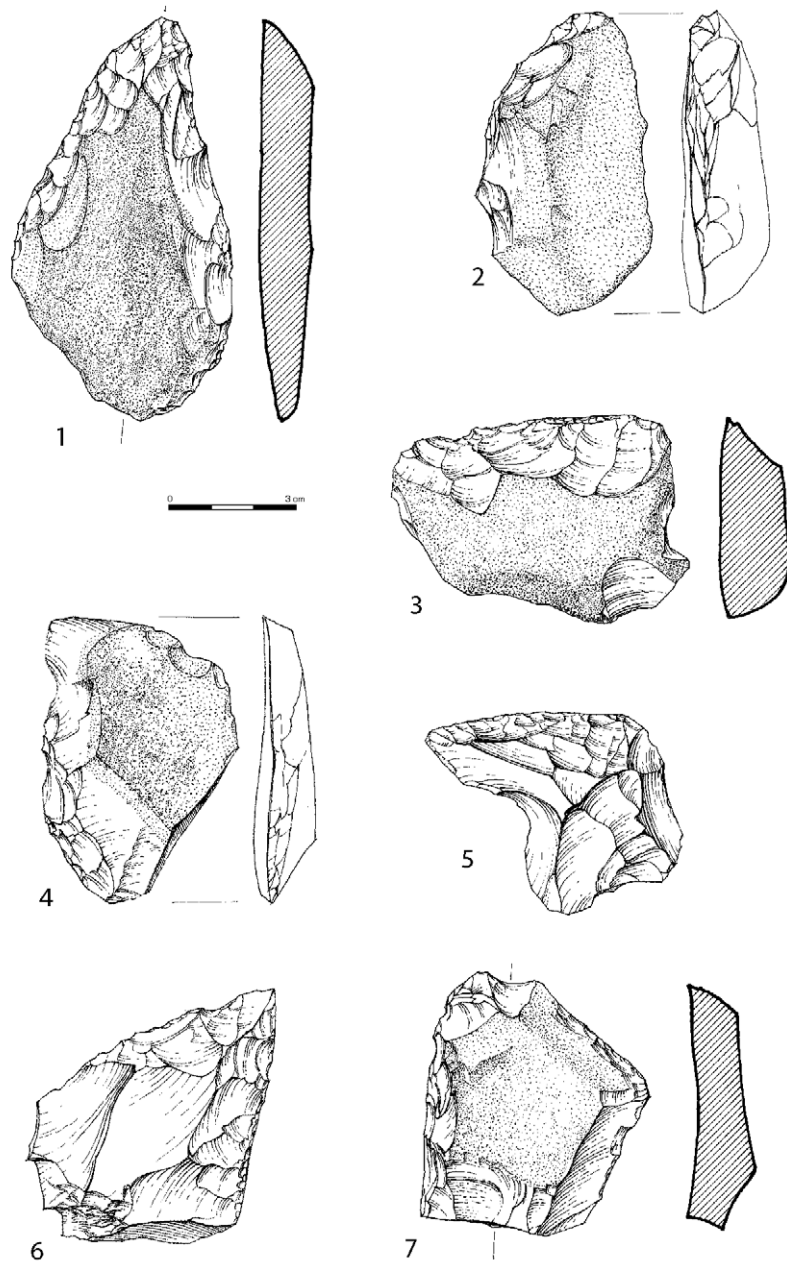


Figure 5.4. Hayonim Layer G (unit 11), Acheulo-Yabrudian – Retouched tools on flake. Adapted from Meignen and Bar-Yosef 2020.

1. Convergent scraper. 2, 4. Simple convex scrapers. 3, 5. Transverse scrapers. 6. Déjeté scraper. 7 Simple scraper + endscraper. (1–3, 5, 7 with Quina or semi-Quina retouch; 1, 2, 7 are double patinated).

Acheulo-Yabrudian assemblages (Figure 5.4: 1–3, 5, 7). The latter is more frequent than the Quina retouch, in relation to the production of more or less thick supports according to the flaking methods.

Although the sample size is small, it is obvious that largely cortical blanks were frequently selected as blanks for these Yabrudian/Quina scrapers (7 out of 14). On the other hand, there does not seem to be a systematic desire to create a back opposite the retouched edge, a feature observed in other Yabrudian assemblages (Nishiaki, Kanjou, and Akazawa 2017).

The dimensions (length-L, width-W, thickness-T) of the retouched tools are significantly larger than those of the debitage products, thus indicating a selection of the larger, wider blanks for tool making (Table 5.5). The differences are significant for length and width (respectively, $p = 0.038$ and $p = 0.041$ at an alpha [significance] level of 0.05) but not so for the thickness, L/W, and W/T ratios. The butts of these tool blanks are also thicker. From

T-test for debitage products versus retouched tools

p values at an alpha [significance] level of 0.05	
Length	0.038
Width	0.041
Thickness	0.058
Platform width	0.639
Platform thickness	0.581

Table 5.5. Hayonim unit 11 – Metrical attributes (in mm) of debitage products and retouched tools. Complete artefacts only. Standard deviations are given in parentheses.

	Debitage products (N = 78)					Retouched tools (N = 30)				
	Length	Width	Thickness	Platform width	Platform thickness	Length	Width	Thickness	Platform width	Platform thickness
Mean	51.76	38.53	11.65	20.25	7.04	59.32	44.60	13.68	26.00	10.00
	(13.85)	(13.10)	(4.73)	(10.60)	(3.73)	(18.11)	(10.20)	(3.69)	(9.22)	(4.17)

these data, we can thus conclude that large, often thick/very thick cortical blanks with plain wide butts were selected as scraper blanks and frequently transformed by scalar/stepped retouch (Quina and ½ Quina retouch).

The quantity of scalar/stepped retouch (Quina and ½ Quina) in this assemblage should also be noted, as it plays a more distinct role than in the Acheulean facies assemblages of Tabun unit X (Shimelmitz et al. 2021). The use of Quina retouch is undoubtedly linked to the blank thickness. As previously described by Bourguignon (1996, 2001), the process of blank transformation by scalar/stepped retouch is aimed at obtaining a particular type of tool—scrapers with a sharp cutting-edge—while the blank obtained via flaking is thick (Bourguignon 1997; Lemorini et al. 2015). In the case of the Quina Mousterian, the transformation of the active edge of the scraper is based on the detachment of successive rows of different types of retouch flakes, the first row comprising flakes often with a convex profile and largely invasive on the dorsal face. The next removals are shorter, with a concave profile and hinged termination (Bourguignon 1996). This specific transformation concept creates a balance between the low angle required for the scraper’s sharp edge and the thickness of the blank (Boëda 2013: 79-82). The semi-Quina scrapers, often made on thinner blanks, show a sequence of lightly stepped retouch made on thinner blanks or do not exhibit Quina retouch on the entire working edge but only over the thicker portions of the blank (Lemorini et al. 2015).

As we have already noted for the Quina Mousterian in Western Europe (Meignen, Delagnes, and Bourguignon 2009), we must stress here, in the case of the Yabrudian and Acheulo-Yabrudian tools, there is less emphasis on pre-shaping blanks and more use of supplementary retouch to achieve the tool shape (low investment in core shaping). Similar observations have been made by Shimelmitz et al. (2014b) concerning the Yabrudian assemblages from Tabun.

However, it is worth noting the absence of resharpening flakes in the unit 11 assemblage, whereas these by-products of the transformation/resharpening phase are frequently found in Acheulo-Yabrudian assemblages. However, this may be due to the small and very localised area excavated in Hayonim Cave.

In addition to this Yabrudian component, the Hayonim unit 11 assemblage contains a relatively large biface assemblage.

5.4.2.2 Bifacial component

Twenty-seven bifaces (24 handaxes and 3 bifacial pieces) and seven fragments (most often proximal) were recovered in unit 11, comprising 15.1% of the total assemblage (including cores) (Table 5.1; Figures 5.5 to 5.9), which is significant compared with other Acheulo-Yabrudian assemblages. No bifacial shaping flake was found. All of the bifaces but one are made on flint. Among them, one is obtained in a flint rich in Foraminifera coming from the Zor’a Formation (lower Eocene)(Ekshtain, personal communication) whose outcrops in primary position are located at about 30 km from the cave.

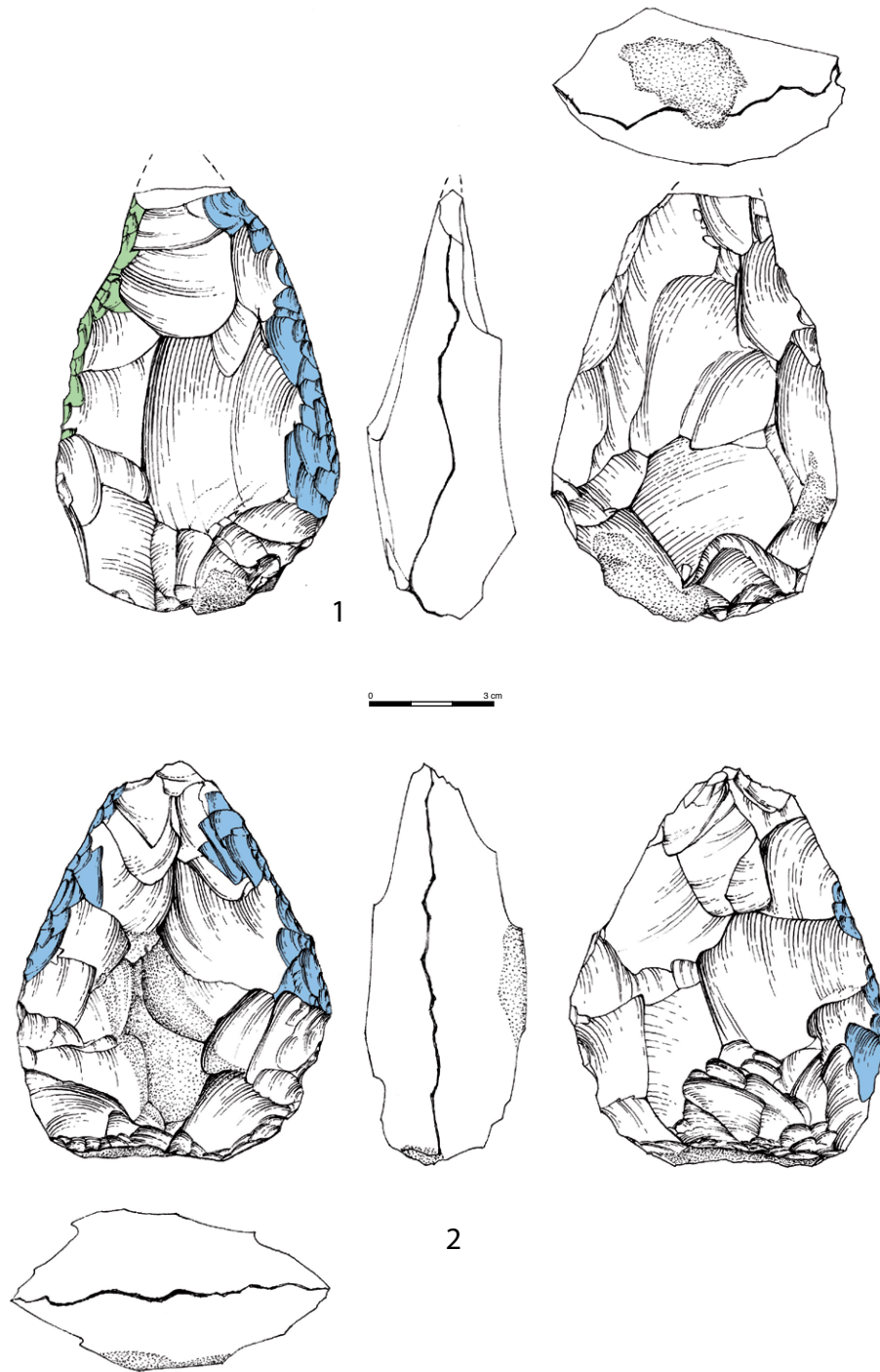


Figure 5.5. Hayonim Layer G (unit 11), Acheulo-Yabrudian – Bifaces used as blanks for tools (*biface support d'outil*). 1, 2. 'Scraper-type' modification (1- associated with intentional crushing on the opposed edge).

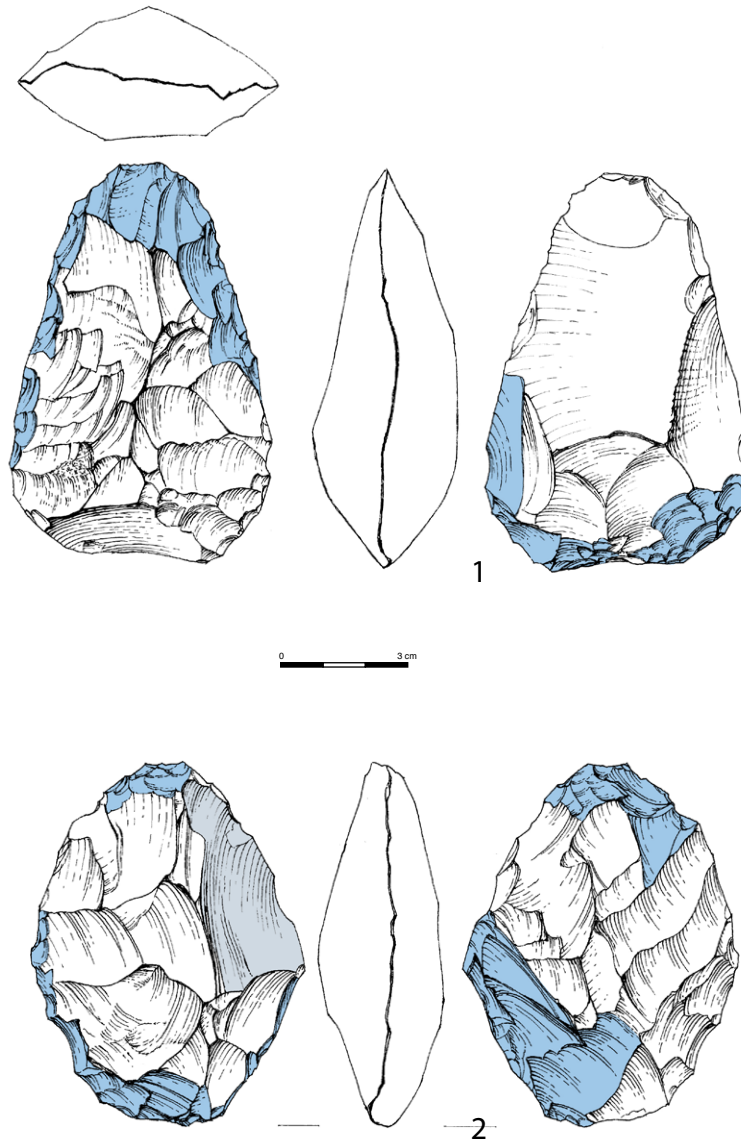


Figure 5.6. Hayonim Layer G (unit 11), Acheulo-Yabrudian – Bifaces used as blanks for tools (*biface support d'outil*)/'Scrapper-type' modification. 1. Biface made on a large flake; only partially transformed on one face; careful distal modification. 2. *limande*; careful distal modification; one large concave flake removal.

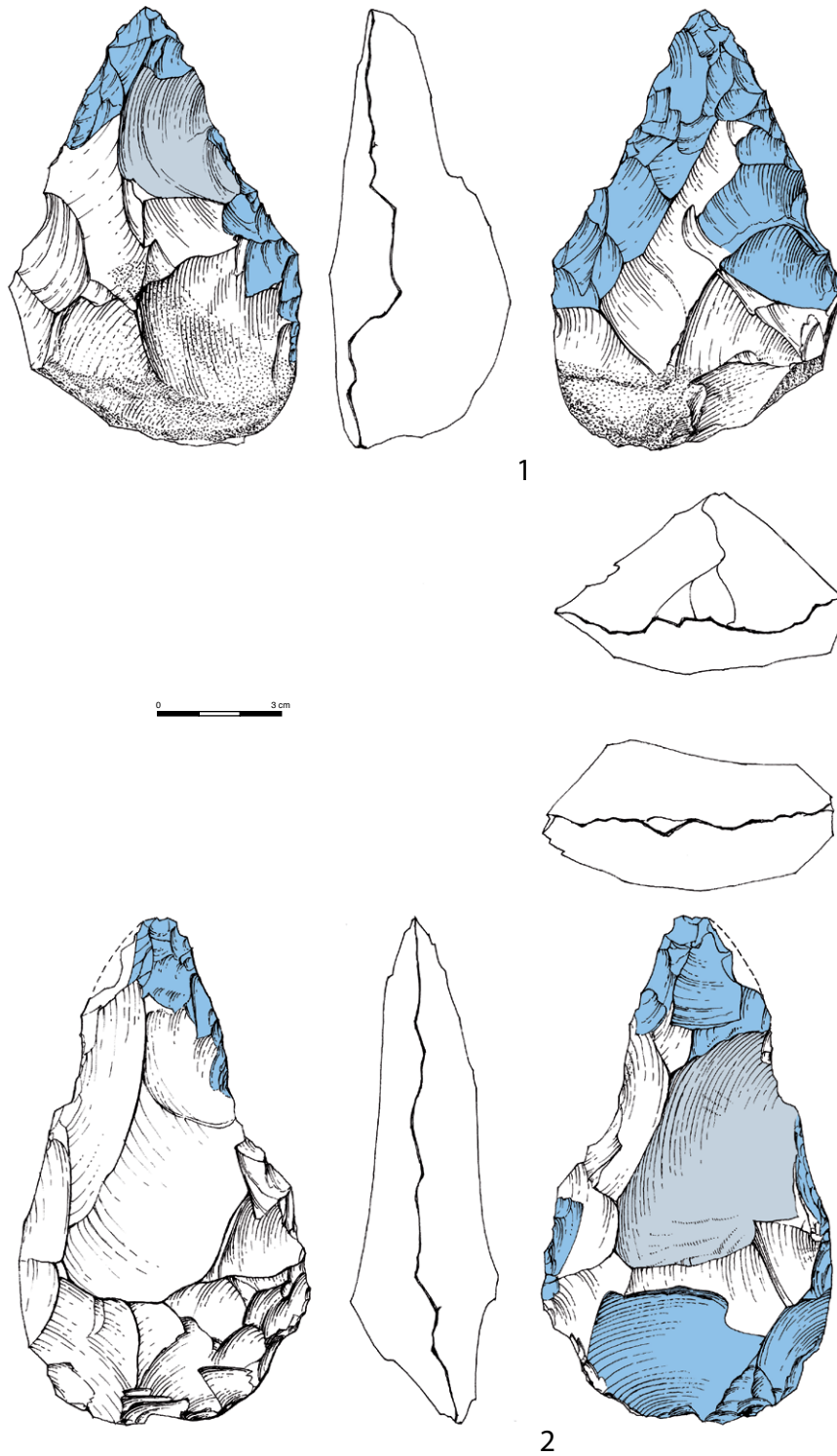


Figure 5.7. Hayonim Layer G (unit 11), Acheulo-Yabrudian – Bifaces used as blanks for tools (*biface support d'outil*). 1, 2. *Modification of point and contiguous edge(s); apical zones carefully transformed; large deep concave flake removal.*

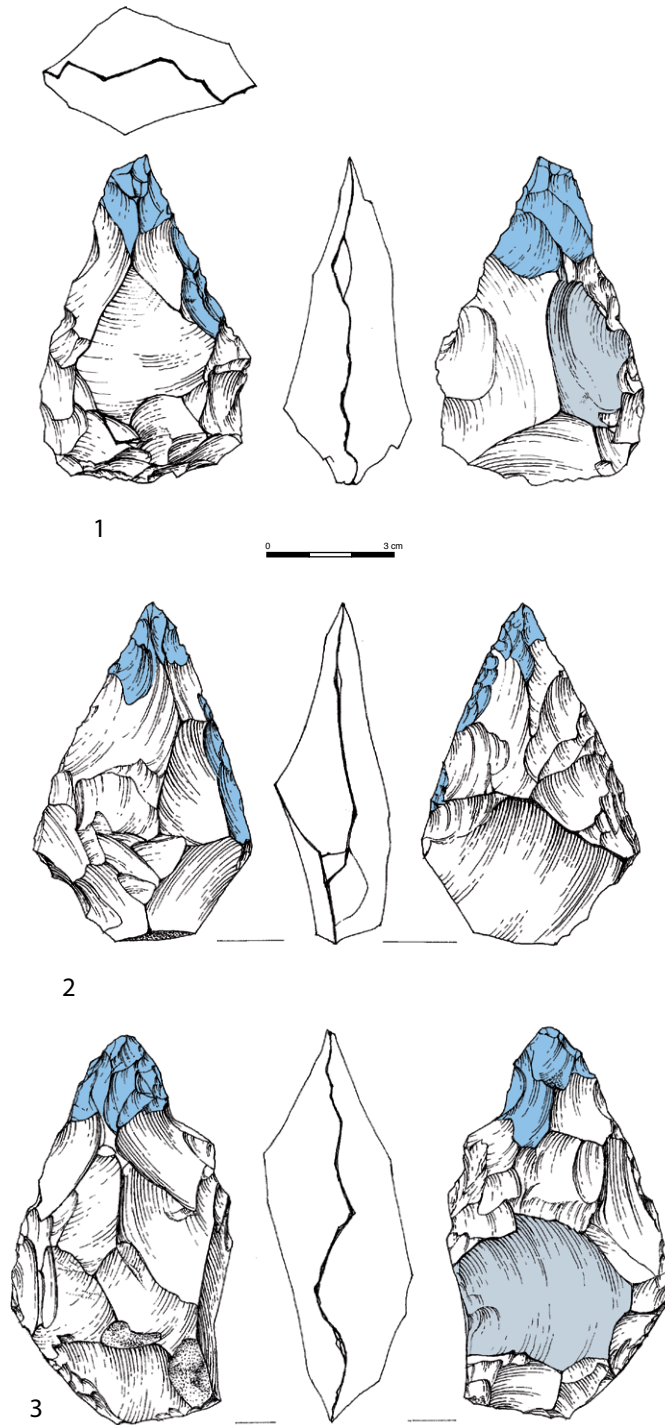


Figure 5.8. Hayonim Layer G (unit 11), Acheulo-Yabrudian – Bifaces used as blanks for tools (*biface support d'outil*). 1, 2. Modification of point and contiguous edge(s); careful thinning of the apical part (1-with one deep concave flake removal). 3. Modification of point only; careful thinning of the apical part; one large deep concave flake removal.

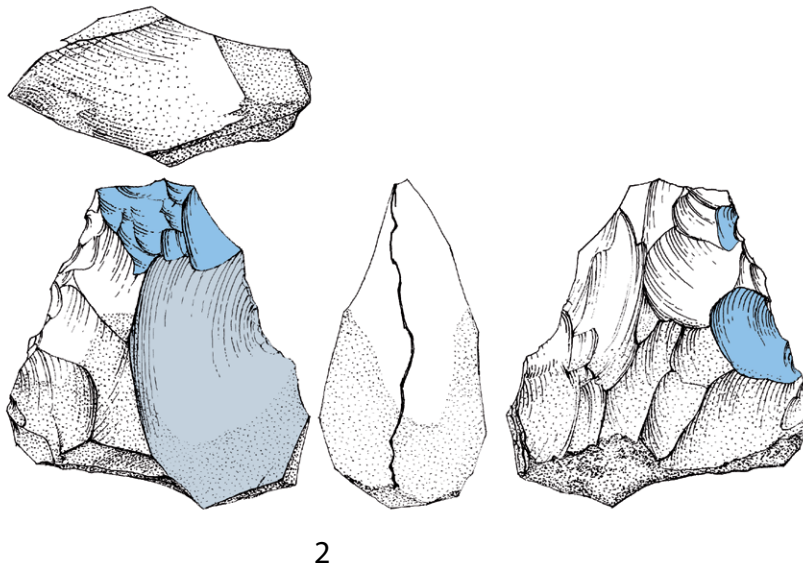
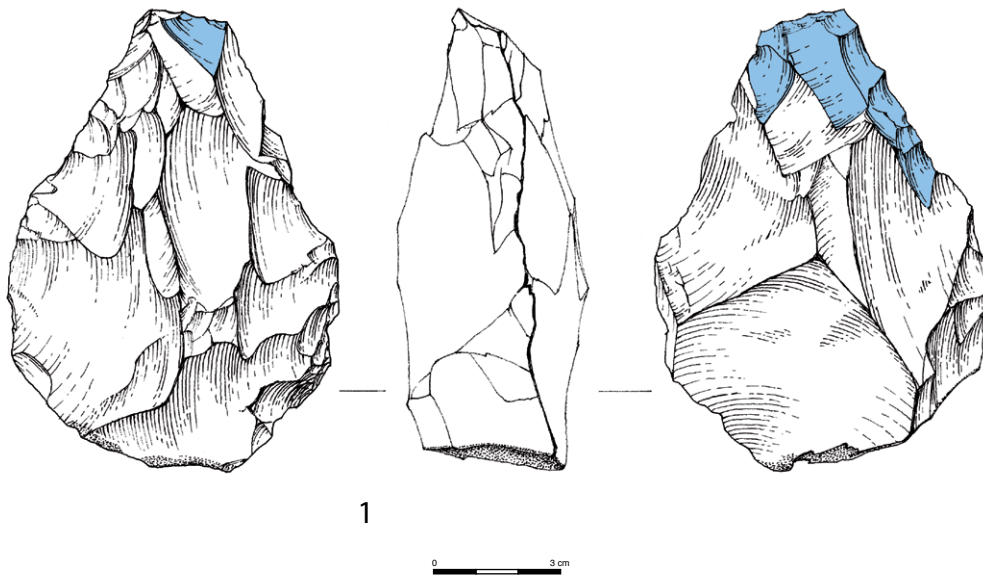


Figure 5.9. Hayonim Layer G (unit 11), Acheulo-Yabrudian. 1. Thick biface; one face shaped by hard hammer percussion; careful distal modification ('beveled tip'). 2. Recycled biface (double patinated); one large concave removal; and later, careful distal modification ('beveled tip').

Many of them are patinated, but only one bears clear traces of abrasion on the edges. They are most often pointed or globally triangular, except for one *limande* morphology (Figure 5.6: 2). A few of them display a transverse flaking tip that is usually carefully shaped (Figure 5.9: 1, 2).

They are not standardised in shape and size but do tend to be relatively short and thick (flatness ratio mean $W/T = 1.88$, s.d. 0.30). Their lengths range from 67 to 121 mm, with a mean length of 90.13 mm (s.d. 14.87). Their widths vary from 47 to 85 mm ($\bar{x} = 64.3$; s.d. 10.56), and their thickness ranges from 21 to 54 mm ($\bar{x} = 35.13$ mm; s.d. 8.52). Seventeen (out of 24 complete) bifaces are less than 100 mm long. They fall within the upper range of the Acheulo-Yabrudian bifacial pieces (as observed in Tabun E, Zuttiyeh, and Misliya assemblages for example; Malinsky-Buller 2016; Shimelmitz et al. 2017; Zaidner, Druck, and Weinstein-Evron 2006). They are also very similar to the recently published Tabun unit X sample (Acheulean facies) (Shimelmitz et al. 2021) (Table 5. 6) and are generally smaller than the Late Acheulean ones. Whether this characteristic can be considered a

Table 5.6. Hayonim unit 11 – Comparison of biface metrics (in mm) from selected Acheulo-Yabrudian assemblages. Data from Shimelmitz et al 2021; Zaidner, Druck, and Weinstein-Evron 2006 ; Malinsky-Buller 2016 ; Shimelmitz et al. 2017. Data not available are noted by an asterisk. Standard deviations are given in parentheses.

	Length	Width	Thickness	W/T
Hayonim unit 11	90.13	64.30	35.13	1.88
N = 23	(14.87)	(10.56)	(8.52)	(0.30)
Tabun unit X	84.5	53	26	*
N = 40	(15)	(11)	*	
Misiya	84.24	62.49	23.38	2.74
N = 47	(19.02)	(21.77)	(7.06)	(0.72)
Zuttiyeh	91.1	60.6	33.4	*
N = 40	(15.9)	(14.2)	(8.7)	
Tabun				
Ea, b	87.6	*	*	*
Ec	84.3	*	*	*
Ed	85	*	*	*

cultural marker for the Acheulo-Yabrudian is still open to debate (Weinstein-Evron and Zaidner 2017).

These bifaces are generally made on nodules (n = 12), and less often on large flakes (n = 4) (Figure 5.6: 1). One, double-patinated, is made on an ancient biface, and is thus recycled (Figure 5.9: 2). It was often difficult to identify the blank type (11 ‘indeterminate’) due to the intensive shaping, which masks the initial morphology. Many of the bifaces lack cortex on both faces (n = 15), but when residual cortex is present (on 11 of them), it is generally concentrated on the proximal part, especially on the butt (cortex or natural surface) (n = 11), a characteristic that might have been advantageous for gripping.

These pieces are often bifacially shaped by large invasive removals from more or less the entire periphery (except the butt for some of them; Figures 5.5: 1; 5.7: 1; 5.9: 2). The shaping flakes are detached by hard hammer percussion (deep to lightly concave scars) and soft hammer percussion in the final stages (slightly convex scars). This process results in pieces with thick (or somewhat thick) biconvex or plano-convex sections in their proximal part, often more roughly shaped, contrasting with thinner distal parts resulting from a careful transformation of the tip (for instance, Figures 5.6: 1; 5.7: 1; 5.8: 1, 2, 3; 5.9: 1).

A few bifaces made on a large flake are carefully transformed on one side, while the other side is only slightly transformed (Figure 5.6: 1).

Interestingly, many bifaces show evidence of their use as blank for a retouched tool (*biface-support d’outil*, Boëda 1997) (19 out of 27), which means that the bifacial shaping should be considered as the preparation of a blank for additional retouch. In the final stage, the bifacial volume, roughly almond- or oval-shaped, is locally retouched to create a special localised ‘working edge’ (Figures 5.5 to 5.9) and several of these retouched units may coexist on the same piece. These bifaces thus seem to be designed as blanks for multifunctional tools. These secondary modifications may concern the lateral and proximal edges: ‘scraper type’ modification with a long bifacially or uniaxially retouched edge on one or two sides (n = 5) (Figure 5.5: 1, 2; 5.6: 1, 2). In some cases, the opposite edge was intentionally crushed (thus creating a ‘back’) (Figure 5.5: 1), probably for gripping purposes, suggesting the creation of an active zone opposite the prehensile zone. But most often, these modifications concern the apical/distal part (tip area: n = 14) in different combinations: only the point (Figure 5.8: 3), or a point and a contiguous

edge(s) (e.g., Figures 5.7: 1, 2; 5.8: 1, 2); the tip may also correspond to a transverse flaking edge (n = 4) ('beveled' tip; Figure 5.9: 1, 2) sometimes shaped by a burin-like 'tranchet' blow (n = 2). This apical/distal zone was carefully transformed, resulting in a thinned tip, contrasting with the otherwise thick morphology of the piece. For the sake of efficiency, the tip seems to be thin not only on the periphery of the piece but also over its entire width. This careful thinning of the apical part by invasive removals has also been reported in the Yabrudian tools from Zuttiyeh (Malinsky-Buller 2016) and Misliya (Zaidner and Weinstein-Evron 2016). Malinsky-Buller (2016) defines it as a characteristic that distinguishes Acheulo-Yabrudian bifaces from those of the Upper Acheulean, whose apical part is mostly transformed by retouch.

In contrast to this carefully worked apical area, which may be considered the active area of the biface, the less carefully worked proximal part that is often partially cortical may have been used for gripping.

Zaidner, Druck, and Weinstein-Evron (2006) describe, in the Acheulo-Yabrudian assemblages from Misliya, a gradual transition from 'true' bifaces, through artefacts fully worked on one face and only partially on another, to real unifaces and scrapers. Copeland (1983: 109) made a similar observation in her analysis of the Bezez Cave assemblage, in which she describes pieces that seemed to be intermediate between bifaces and scrapers. And the work of Malinsky-Buller at Zuttiyeh (2016) again shows the difficulty 'of distinguishing between heavily shaped scrapers and handaxes'. These observations do not seem to apply to the bifacial component of Hayonim. Although there are a few rare artefacts fully worked on one face and only partially on another, there is no morphological gradation between bifaces, unifaces, and heavily shaped bifacial scrapers, the latter two categories being absent from the assemblage.

A remarkable feature in this assemblage is the rather large set of bifaces characterised by the detachment of large, deep, concave flakes (Figures 5.6: 2; 5.7: 1, 2; 5.8: 1, 3; 5.9: 2), which interrupt, or sometimes end, the final phase of the transformation of these pieces generally executed with the soft hammer (shallow invasive removals). There is thus a break in the sequence of the last exploitation phases of these bifaces, which seems to 'destroy' the regularity of the biface. Such a phenomenon has already been reported in the literature but is generally identified in the final phase of the reduction sequence ('bifaces assemblages exhibit the scar of a last removal that often seems to destroy their general shape' [Zaidner, Druck, and Weinstein-Evron 2006]). In such cases it is then described as the recycling of a biface into a core (Rollefson, Quintero, and Wilke 2006; Shimelmitz 2015; Shimelmitz et al. 2017; Zaidner, Druck, and Weinstein-Evron 2006). Such pieces have been observed in Acheulean and Acheulo-Yabrudian assemblages and interpreted as bifaces recycled into cores 'in a way that mimics the Levallois technology' (DeBono and Goren-Inbar 2001). In the case of Hayonim, the large concave scar(s) do not cover the entire surface of the biface (described as 'handaxes with peripheral flake removals' in Shimelmitz 2015: 38). Furthermore, the phenomenon does not occur exclusively in the final phase: in many cases, after this broad deep removal, a final localised transformation is carried out on the biface, either by retouch or thinning the apical part (creating a bevel, for example; Figure 5.9: 2). In these cases, the final phase consists of creating a 'tool'. However, the large, thick flakes produced by these large deep detachments are undoubtedly potential blanks and it seems possible to interpret this phenomenon as a sign of very short production sequences during the final phases.

5.4.3 Discussion and conclusion for unit 11

A larger and more representative corpus of artefacts would be undoubtedly necessary to observe regular recurrences in tool making in unit 11. Nevertheless, these preliminary results already show that Hayonim Cave should be considered as one of the rare sites that document a classic Acheulo-Yabrudian (here, of the Acheulean facies) assemblage in the Central Levant.

In unit 11, a prevalent bifacial shaping strategy was associated with flake production and a complex tool management system that seems to be based on two core exploitation modalities. One is similar in many respects to the Quina Mousterian system (Bourguignon 1996), which produces very thick, frequently cortical blanks (totally cortical or cortical-backed), with plain or sometimes wide and plain inclined butts resulting from a 'high-angle striking technique'. The second is mainly based on the exploitation of the wide face of the core with hierarchical surfaces and produces blanks that often present a cortical back or a cortical back and butt (Shimelmitz et al. 2014b). The unit 11 assemblage displays the distinct features of the Late Lower Palaeolithic in the Levant in its variant known as the Acheulo-Yabrudian, here with a significant bifacial component (45.3% of the shaped pieces) relative to other sites in the region. Based on the recently published data, among the Acheulo-Yabrudian assemblages, only the unit X assemblage at Tabun shows similar biface proportions. In Hayonim unit 11, bifaces seem to have often been used as blanks for specific tools, and the careful shaping and thinning of the apical part is especially noteworthy. This characteristic was previously noted on bifaces from Zuttiyeh (Malinsky-Buller 2016) and Misliya (Zaidner, Druck, and Weinstein-Evron 2006). In this latter case, however, the proximal parts remain fully cortical, while in Hayonim unit 11, they are most often roughly shaped.

These results enrich our knowledge of the internal variability of the Acheulo-Yabrudian cultural complex (AYCC) through the acquisition of new data on an otherwise poorly represented and little-studied facies.

A rapid review of the data currently available shows that, although three facies have been identified in published studies, the Acheulo-Yabrudian assemblages, characterised by the production of thick flake blanks for scrapers, associated with an often poorly represented bifacial production (with quite low proportions of bifaces), are the most frequent. Few sites have yielded numerous Amudian levels (Tabun, Bezez, Yabrud [pre-Aurignacian]), except for the Qesem site, which contains a remarkable sequence of this facies (Barkai and Gopher 2011).

Among these Acheulo-Yabrudian assemblages, the two extremes (Acheulean facies rich in bifaces and Yabrudian facies *sensu stricto* for Jelinek/absence of bifaces) are quite rare and not well documented in recent studies based on the same technological criteria. The assemblages of unit X at Tabun correspond to the first facies (Shimelmitz et al. 2021), while those of unit F at Dederiyeh (recent excavations; Nishiaki, Kanjou, and Akazawa 2017) to the second. In fact, the term Acheulo-Yabrudian is now often used to designate all of the assemblages of this technocomplex, whether they have many or few bifaces.

To examine the status of the Hayonim unit 11 assemblages among this group, we compared our results with recently published data, and specifically with the Tabun unit X assemblage, which is considered one of the rare examples of Acheulean facies in the Acheulo-Yabrudian technocomplex (Shimelmitz et al. 2021). In addition, we used a small group of assemblages representative of the Yabrudian facies, for which data are at least partially available. These include Misliya (Zaidner and Weinstein-Evron 2016); Dederiyeh (Nishiaki, Kanjou, and Akazawa 2017); Qesem (Parush, Gopher, and Barkai 2016); Tabun Yabrudian layers J82BS, J83B1, R63 (Shimelmitz et al. 2014b); and Maslouk (Skinner 1970) (Table 5.7).

The criteria we considered are those generally used to define the variations within this assemblage (shaped artefacts %; bifaces %; scrapers %; Q + 1/2Q retouch %; % of cortical blanks among scrapers). On this basis, Hayonim unit 11 is unquestionably similar to the material described in Tabun unit X, thus representative of what Jelinek called the Acheulean facies. In these two assemblages, bifaces are well represented in proportions similar to those of scrapers (Hayonim unit 11: bifaces 45.3% of the modified pieces/scrapers 32%; Tabun unit X: bifaces 35.5%/scrapers 39.5%), and they are clearly distinguishable from the other assemblages in which bifaces are scarce (0 to 14.6%).

	Hayonim unit 11	Tabun unit X	Misliya	Dederiyeh	Qesem	Tabun (Yabrudian)			Maslouk
	AchY	AchY	AchY/ Yabrudian	Yabrudian	Yabrudian	J82BS	J83B1	R63	Yabrudian
		(Shimelmitz et al. 2021)	(Zaidner Weinstein 2016)	(Nishiaki et al. 2017)	(Parush et al. 2016)	(Shimelmitz et al. 2014)			(Skinner 1970)
% shaped pieces (out of total assemblage)	33.3	32.0	7.3	44.1	20.5	*	*	*	*
% retouched pieces (out of total assemblage)	18.2	20.6	6.2	44.1	20.4	*	*	*	*
% bifaces (out of shaped pieces)	45.3	35.5	14.6	0	0.3	3.6	8.4	4.3	4.2
% scrapers (out of shaped pieces)	32.0	39.5	54.2	48.2	21.5 (+ ret blades)	76.8	59.3	43.6	84.8
% Q and 1/2Q retouch (among scrapers)	14 of 24	few	46.2	63.6	65.8	*	*	*	60.0
	(½Q > Q)	mainly 1/2Q and scalar	(Q = ½Q)	(½Q > Q)					
% cortical blanks (among scrapers)	18 of 25	63.2	92.3	*	*	*	*	*	*

However, two elements distinguish the Hayonim assemblages from those of Tabun unit X:

- The absence of intentional/systematic blade production in the Hayonim Acheulo-Yabrudian, whereas it is present in Tabun.
- And, especially, the more frequent use of scalar/stepped retouch at Hayonim, while scrapers are more frequently transformed by scalar or ½ Quina retouch at Tabun unit X. Shimelmitz et al. (2021) report that, ‘while Quina retouch is observed, many edges are better defined as modified by ½ Quina or scalar retouch’ (statistics not available).

Insofar as the development of scalar/stepped retouch is a criterion often put forward in previous studies to define the Yabrudian (Copeland 1975; Jelinek 1982b; Skinner 1970), it is important to verify whether this characteristic is indeed specific to the Yabrudian facies alone. We should remember that the importance of Quina retouch is a criterion generally advanced in the definition of the Yabrudian facies, whereas the Acheulean facies is simply defined by the abundance of scrapers, possibly on thick flakes (Copeland 2000; Nishiaki, Kanjou, and Akazawa 2017; Shimelmitz et al. 2021; Shimelmitz et al. 2016; Zaidner and Weinstein-Evron 2016).

If we refer to the quantitative data available (Table 5.7), Quina and ½ Quina retouch seem to be widely represented in the Yabrudian assemblages of Qesem, Misliya, Dederiyeh, and Maslouk. However, these modes of retouch are also abundant in the Hayonim unit 11 assemblage (considered as an Acheulo-Yabrudian of Acheulean facies), in a percentage similar to those observed in the Yabrudian sites. This type of retouch, therefore, cannot be considered specific to the Yabrudian.

On the other hand, the unit X Tabun assemblage (Acheulean facies, similar to Hayonim unit 11) shows little use of this retouch method. The same is true for the other assemblages in this sequence, whether Acheulean (Beds 72, 76, 79) or Yabrudian facies (Beds 75, 82, 83) (about 12%; Jelinek 1982a: Table III; 1982b). The low proportions of this retouch type may be specific to the Tabun sequence, in association with the identified *chaînes opératoires* (facial flaking defined by Shimelmitz et al. 2014b) resulting in blanks that are most likely less thick than those of the Quina exploitation modality.

Table 5.7. Hayonim unit 11 – Comparison of the toolkits from selected Acheulo-Yabrudian and Yabrudian assemblages. Data not available are noted by an asterisk. AchY = Acheulo-Yabrudian; Q and ½Q = Quina and semi-Quina.

Based on these observations, it is clear that the prominence of Quina and ½ Quina retouch cannot be considered as a criterion for distinguishing assemblages rich or poor in bifaces (Yabrudian facies versus Acheulean facies). The two criteria seem to be independent, as already suggested by Jelinek (1982a: 64), although obtained from different criteria.

On the other hand, recent technological studies, including the Hayonim study presented here, clearly highlight, in all of these Acheulo-Yabrudian assemblages, the same objectives for the production sequence of flake blanks for scrapers, the dominant tools in these assemblages, and this regardless of the biface proportions. This technological data completes the remarks made earlier on the typological homogeneity of the ‘tools on flakes’ component of these different assemblages (dominant side-scrapers, remarkable presence of transverse and skewed scrapers) (Copeland 1983; Copeland and Hours 1983; Jelinek 1981a; Jelinek 1982a).

The Hayonim data thus confirm the continuity of technical traditions within the AYCC, between Acheulean and Yabrudian facies (Mugharan tradition, Jelinek 1982a). Only the presence of bifaces versus side-scrapers constitutes a relevant criterion for evaluating the internal changes within this Acheulo-Yabrudian ensemble. On the other hand, the production of tools on flakes, and especially the side-scrapers that always dominate the retouched tools, seems to belong to the same core reduction strategies, possibly in different proportions (‘Quina-type flaking’ versus ‘facial flaking/hierarchical surfaces’), thus resulting in internal variability that has already been recognised.

5.5 The Middle Palaeolithic assemblages/units 10 to 1

5.5.1 The dominant core reduction strategies

As previously mentioned, the Hayonim assemblages (especially those of Layer F and Lower E) have already been the subject of several exploratory papers mainly focused on identifying the core reduction strategies used and characterising the lithic productions (debitage and retouched tools), without any detailed inventories having been published thus far (Meignen 1998, 2000, 2007, 2011; Meignen and Bar-Yosef 2020).

These publications highlighted an essential technological feature of the assemblage of these levels, which is the presence, alongside a Levallois production system producing flakes and elongated blanks (blades and points), of a specific production system, known as ‘Laminar’ (Meignen 2000, 2007). This identification of a Laminar system based on technological criteria was then widely adopted in more recent studies, and the presence of this production type has been identified in the assemblages of the same period identified as Early MP (Hummal [Wojtczak 2011], Misliya [Zaidner and Weinstein-Evron 2014; Zaidner and Weinstein-Evron 2020], Emmanuel [Goder-Goldberger et al. 2012], Abou Sif [Wojtczak and Malinsky-Buller 2022], Dederiyeh [Nishiaki, Kanjou, and Akazawa 2022]). Results that have documented the main characteristics of the Early MP are thus available, such as the core structures (‘volumetric concept’), the characteristics of the resulting products, and the specific tool types.

In a broad introduction, we will recall here the main current knowledge on Hayonim Cave lithics, before presenting detailed results concerning the assemblages of the different units of the sequence, including this time the upper levels (Layer Upper E), never before published. Finally, we will discuss the contributions of this long MP sequence in the Levantine context.

In our previous work (Meignen 2000, 2007, 2011), we identified several simultaneously used core reduction strategies. Depending on the unit, these production systems are more or less represented and are also oriented toward obtaining different types of products (flakes, blades and points), which are also present in varying proportions.

Here, we will thus first present the production systems identified, which will then be illustrated by the study of the different units.

These production systems include:

- a. The Levallois method for the ‘mixed’ production of short (flakes and points) and elongated Levallois blanks (Boëda 1994, 1995; Boëda, Geneste, and Meignen 1990; Meignen 1995; Shimelmitz and Kuhn 2017b).

- b. The Laminar method (as defined by Boëda 2013; Meignen 2000) for the almost exclusive production of blades, ranging in size from large blades to small blades/bladelets.
- c. And much less frequently represented, a flake-oriented reduction strategy that we call a 'preferential surface exploitation', which it is necessary to specify here (Meignen 2019; Meignen and Bar-Yosef 2020).

In the case of the latter, which does not play a significant role in the Hayonim toolkit, the ventral face of a flake was most often used as a flaking surface for the organised detachment of a few blanks (more than 3). These flakes are located in the same plane, more or less parallel to the plane of intersection between the flaking surface and the striking platform surface, the roles of which are not interchangeable. This flaking system is quite similar to the Levallois system, with the same hierarchical treatment of the surfaces. It is, however, a less formal and less productive technology involving only short exploitation sequences without maintaining the lateral and distal convexities, and with only a slight preparation of the striking platform. This core reduction method is often called 'core-on-flake' (Goren-Inbar 1988; Hovers 2007; McPherron 2007), a term that we avoid as it is too imprecise and gives no information on the flaking system, as it describes only the blank (Meignen 2019; Meignen and Bar-Yosef 2020). We can consider this flaking system here as a special category among the cores-on-flakes. It has been easily distinguished and counted separately from cores-on-flakes with a few (<3) isolated, non-organised scars (non-contiguous, not in the same plane), often grouped under the term 'isolated removals' (Hovers 2009; Malinsky-Buller 2016).


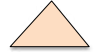


In addition to the specific production of flakes on the ventral surface of other flakes mentioned above, two different major volumetric concepts were identified in our previous publications based on the characteristics of the total production (cores/products/by-products): the Levallois system and the Laminar system (Meignen 1998, 2000, 2011; Meignen and Bar-Yosef 2020). While flake production is undoubtedly the major objective of the Levallois flaking system within the sequence, the question arises for the production of elongated products (blades and points). For this type of production, which is widely present in the lower units, in particular, the characteristics of the products and cores have led us to identify two production modalities for these blades, which differ in their volumetric concept, and whose relationships are not always easy to identify.

The currently available data show that these two flaking systems coexist systematically in the same assemblage, at Hayonim and in other Early MP assemblages (Goder-Goldberger et al. 2012; Malinsky-Buller 2016; Meignen 2007; Shimelmitz and Kuhn 2013; Wojtczak 2011; Zaidner and Weinstein-Evron 2014; Zaidner and Weinstein-Evron 2020). However, the question arises as to whether they are carried out successively on the same block (thus constituting a single system with high variability in its procedure) or whether, on the contrary, they are carried out on different blocks (independent systems).

The hypothesis of the succession of these two exploitation systems has been defended by various authors, such as E. Boëda, based on his experience as a flintknapper and his observations of Hummalian industries (Boëda 1995). For these assemblages, he mentions a system of blade flaking (Laminar of the 'D2-type volumetric concept') in which the core can have, at certain stages of its exploitation, morphologies simulating the Levallois concept, even if it does not belong to the latter (Boëda 2013: 181). In this case, during the reduction sequence, the core has successive volumetric morphologies/structures, of the 'volumetric exploitation' type (e.g., Laminar) or the Levallois type (Levallois-like). Later, Wojtczak (2015) and Malinsky-Buller (2016) also defended this interpretation but without a demonstration based on archaeological artefacts (e.g., identification of artefacts showing the change in orientation of the striking platforms during the transition from one system to the other).

In her study of Hummal Layer 6b and alpha h, Wojtczak (2015: 642), referring to the work of Boëda, considered that both Levallois-like and Laminar systems participate

Figure 5.10. Hayonim (Early MP) – Comparison of Levallois versus Laminar blade diagnostic features. Adapted from Meignen and Bar-Yosef 2020.

Diagnostic features	Levallois blades	Laminar blades
Cross sections	 Wide thin/ triangular	 Narrow thick/ triangular
	 Wide thin/ trapezoidal	 Narrow thick/ trapezoidal
Lateral sides	Removals slightly oblique Acute edge angles	Removals highly oblique More obtuse edge angles
	Faceted or dihedral	Plain or roughly faceted
Striking platforms	Faceted or dihedral	Plain or roughly faceted

in the same production sequence, thus identifying an original core reduction strategy whose different steps are described in Wojtczak, Le Tensorer, and Demidenko (2014: 27). This process was called a ‘reduction order’, in which non-Levallois blades were removed during the first reduction stage, followed by the production of more Levallois-like elongated products. As they are usually removed at a later stage of the reduction process, these morphologically Levallois blades are shorter. However, the data from Hummal Layer 6c2 (an assemblage studied by the same author) do not confirm this reduction model. The morphometric study of blades from Hayonim Layer F seemingly shows no significant difference in length for the Laminar and Levallois categories (see below). These controversial results highlight the variability/flexibility of the reduction process for blade production in these Early MP assemblages. The case of the Laminar production at Hayonim is, in my opinion, more complex—we will return to this subject later—but these two patterns must be kept in mind during the analyses.

The study of the production of elongated blanks at Hayonim allowed us to highlight the existence of two blade groups with different morphotechnical characteristics (thickness, width/thickness, sections, and thus edge angles) (Figure 5.10) that we were able to relate to the two production systems previously described (Levallois and Laminar) (Meignen and Bar-Yosef 2020). The differences observed in these morphotechnical characteristics—particularly the cross sections and angles of the working edges—suggest probable different functionalities that must be considered. Whatever the hypothesis adopted (succession of two operating systems on the same core or independence of the two systems), the hypothesis of an intentional search for different blade morphologies, possibly for different functions, must be taken into consideration (see experimental results and discussion in Hoggard [2017], and references therein). Use-wear analysis of the elongated products from Hayonim is in progress (D. Wojtczak) to test the relevance of this idea to the Hayonim case. However, we must keep in mind the existence of a large group of so-called ‘undifferentiated’ blades which, based on their characteristics, could not be integrated into the two previously defined groups and which, therefore, make the suggested questions (relationship between morphofunctional characteristics of the blades and the flaking system) complex (see also Shimelmitz and Kuhn 2013, 2017b; Wojtczak 2011).

Therefore, we chose in our study to distinguish and characterise the different blade morphologies and considered that they most likely resulted from two different exploitation systems (Levallois and Laminar type D2, i.e., for the latter, an alternation of Levallois and Laminar volumetric-type core morphologies). Contrary to the observations

made by E. Boëda for the Hummalian industries, where Laminar production seems to be exclusive (corresponding to the flaking method called the D2 type [Boëda 2013]), the substantial presence of Levallois production system among the Hayonim assemblages, leads us to consider that the blades with a Levallois morphology could also originate from Levallois cores. Blades morphologically identified as Levallois may thus originate from:

- The Levallois production system, which would integrate the entire range of products (including blades), as is typically the case in Levallois industries.
- The Laminar type D2 system (in its various expressions as identified in the Hummalian [Boëda 2013]).
- Or perhaps (probably) from both.

Our previous studies showed significant flexibility in the flake and blade productions at Hayonim Cave, with variations that our analysis of the cores and associated products (CTEs, end products) enables us to evaluate; we will see this more in detail in our analyses of the various units.

At Hayonim, these two major lithic production systems can be characterised as follows.

- The Levallois (and related) system

This system corresponds to an exclusive exploitation of the widest surface of the core (= facial débitage). The core corresponds to an entirely configured raw material volume with a substantial initialisation/preparation phase (called 'F type' in Boëda 2013: 142). It is characterised by the production of diverse artefacts (here, mainly flakes, but also points and blades).

At Hayonim, the Levallois reduction system is mainly oriented toward the production of flakes (more or less prominently throughout the sequence), but also, depending on the units, toward the production of short points, and even more so, blades and elongated points. This reduction system, carried out on the widest face of the volume, is identified based on the criteria defined by E. Boëda (Boëda 1986, 1995). All of these criteria must be present to identify the Levallois concept.

In all units at Hayonim, the preferential and recurrent flaking methods have been identified. 'Predetermining' flakes ensure the creation and maintenance of the predetermination features (i.e., convexities and/or ridges on the flaking surface) necessary for the detachment of Levallois 'predetermined' products.

In the case of unidirectional parallel and bidirectional flaking, the creation and maintenance of the lateral convexities necessary to detach flakes/blades is mainly achieved by detaching elongated *débordants* flakes, most often with a cortical back, as the lower face of the core often remains largely cortical.

In the case of unidirectional convergent pattern, as we have identified at Kebara (Meignen 1995, 2019), the cortical *débordants* flakes are also often intentionally overshot and have a slightly twisted profile. The corresponding cores thus have steep lateral edges, especially in the distal part, giving a characteristic morphology to the core section, which is different from the classic Levallois section (Meignen 1995: Fig. 25.10). This obliqueness is necessary if the knapper wishes to create both a distal and a lateral convexity via the detachment of a large, elongated, often slightly twisted *débordant* flake.

The products resulting from the Levallois system are relatively thin (mainly flakes and points), with long regular edges and acute edge angles (Boëda 1997; Delagnes and Meignen 2006). The significant variability in the overall contour and size of the intended products results from the numerous methods of initialisation and production. At the same time, however, a high degree of standardisation of their proximal part (similar narrow butts) is recognised in association with the carefully prepared striking platform. Faceting increases the precision of the percussion gesture and the control of the blank detachment, resulting in the regularised morphofunctional features of the proximal end of the blank (Boëda 1997, 2013; Bonilauri 2010, 2015).

Moreover, in the Hayonim Lower E and F layers, few characteristic Levallois cores for blades have been identified that demonstrate the henceforth-classic Levallois structure, as defined by Boëda (1986, 1995). The use of the Levallois recurrent core reduction method on relatively flat or slightly convex, broad flaking surfaces (the widest surface of the core) results in wide, thin, and elongated products, often with faceted platforms and thin, trapezoidal, or sometimes triangular, sections (Meignen and Bar-Yosef 2020).

- The Laminar system (Meignen 2000)

The Laminar system, on the contrary, corresponds to a volumetric reduction concept. This flaking system, organised along the longitudinal axis of the raw material volume and oriented toward the production of elongated blanks (blades and points), displays variants that have in common the exploitation of the core according to a mostly semi-rotating flaking sequence (volumetric concept).

The core-shaping phase is succinct and localised, concerning only the exploited part (flaking surface and striking platform preparation) of the core. The raw material volume is thus not completely shaped, as it is in the Levallois system. On the contrary, only the so-called ‘useful’ volume is prepared, a volumetric concept that E. Boëda defines as the ‘D2 type’ (Boëda 2013: 112). In particular, the ‘back’ (posterior part of the core), opposite the flaking surface, often remains in its natural state, which is most often cortical (no crested back). The flaking is then ‘recurrent’ (i.e., continual detachment of blades without a major reorganisation of the flaking surface).

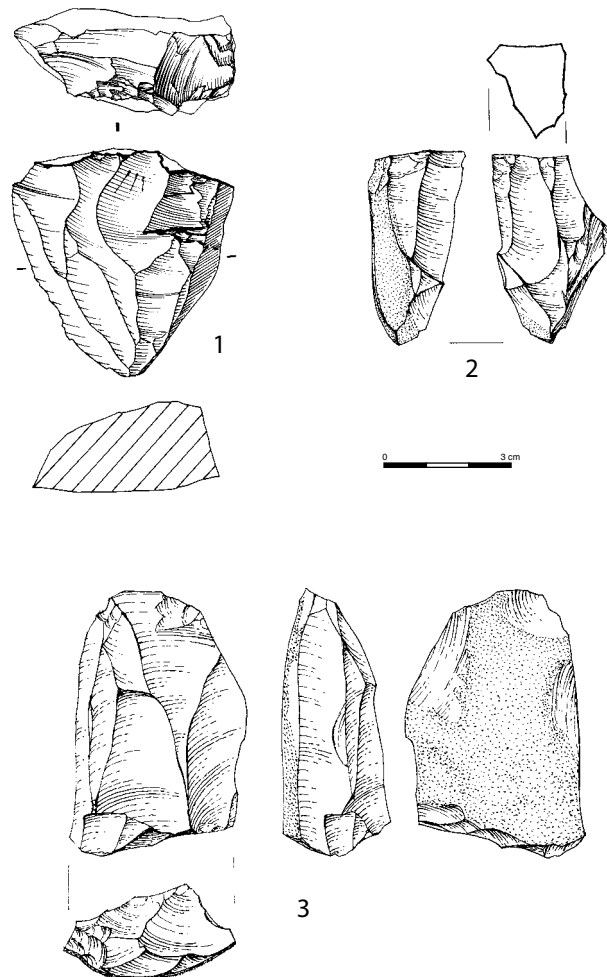


Figure 5.11. Hayonim (Early MP) – Diagnostic artefacts illustrating the variability inside Laminar reduction strategies (unidirectional exploitation). 1–3. Cores (unit 7).

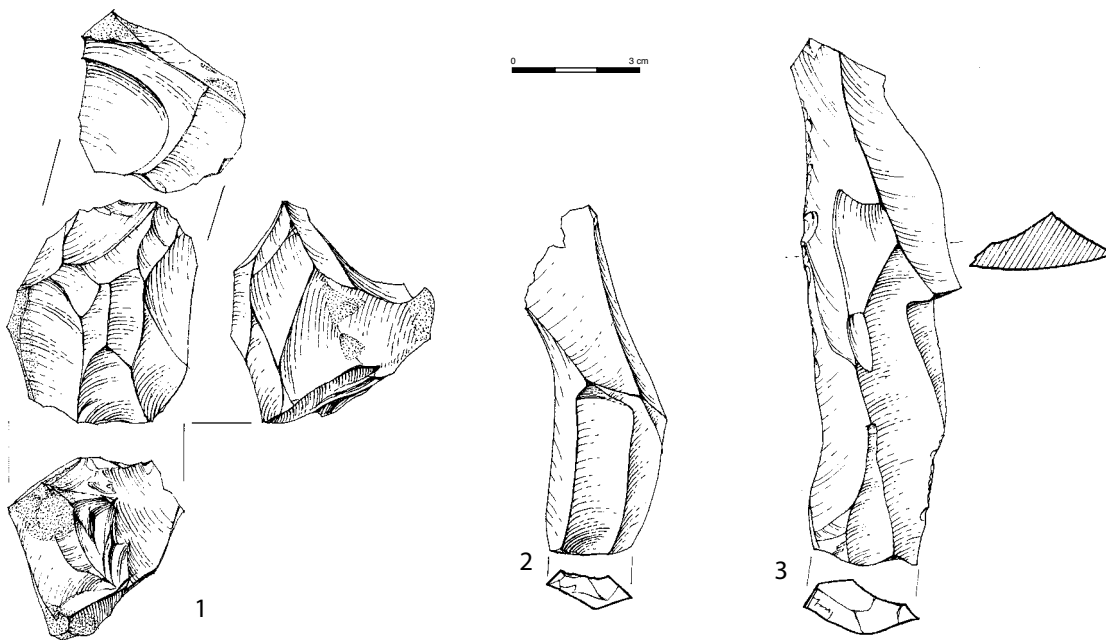


Figure 5.12. Hayonim (Early MP) – Diagnostic artefacts illustrating the variability inside Laminar reduction strategies (bidirectional exploitation from slightly offset striking platforms). 1. Core (unit 4). 2, 3. Blades with the characteristic scar pattern resulting from this exploitation (units 10 and 7).

On the Laminar cores at Hayonim, the exploitation usually occurred on the broad face, or on the broad face combined with the narrow face, or more rarely on the narrow face only (frontal débitage) (Meignen 2007, 2011; Meignen and Bar-Yosef 2020). The resulting products are narrow or wide thick blades (depending on the exploited surface of the core), with triangular or trapezoidal sections, and frequently plain or roughly faceted butts.

These ‘volumetric’ cores generally have a markedly convex flaking surface (contrary to Levallois cores) from which elongated blanks were struck in series from one or two striking platform(s).

The unidirectional cores (Figure 5.11: 1, 2), the most frequent, have a very convex section and a flaking surface extending to the lateral edges around a large part of the core periphery (‘débitage semi-tournant’ in French, semi-rotating in English). This was enabled by a specific preparation of the striking platform achieved by removals that created the angle necessary to exploit the lateral edges of the core (greater than 50°, often close to 80–90°) (Figure 5.11: 1). Their morphology is most often semi-pyramidal and they are of different sizes (including small) and geared toward the production of large to small blades, or even microblades (Figure 5.11: 2).

We identified bidirectional core exploitation in the form of cores with two opposed twisted platforms (slightly or largely offset). From these two striking platforms, two reduction surfaces, slightly or largely intersecting (one along the widest face, the other along the narrow face of the core) were exploited, and the intersection created the necessary convexities for flake detachment. The resulting flaking surface is, as in the previous case, highly convex, and the morphology of the core is semi-prismatic (Meignen 2011). These cores with two opposite, offset striking platforms correspond to true bidirectional exploitation. The blades extracted from the second striking platform invade a large part of the flaking surface, as do those from the first striking platform.

In addition to these characteristic cores, it is important to point out variants that demonstrate flexibility within these production concepts.

In the case of bidirectional cores, the two opposing striking platforms may be only slightly offset (Figure 5.12: 1). The exploitation then occurs mainly on the wide face, resulting in a slightly convex flaking surface similar to that of some Levallois bidirectional

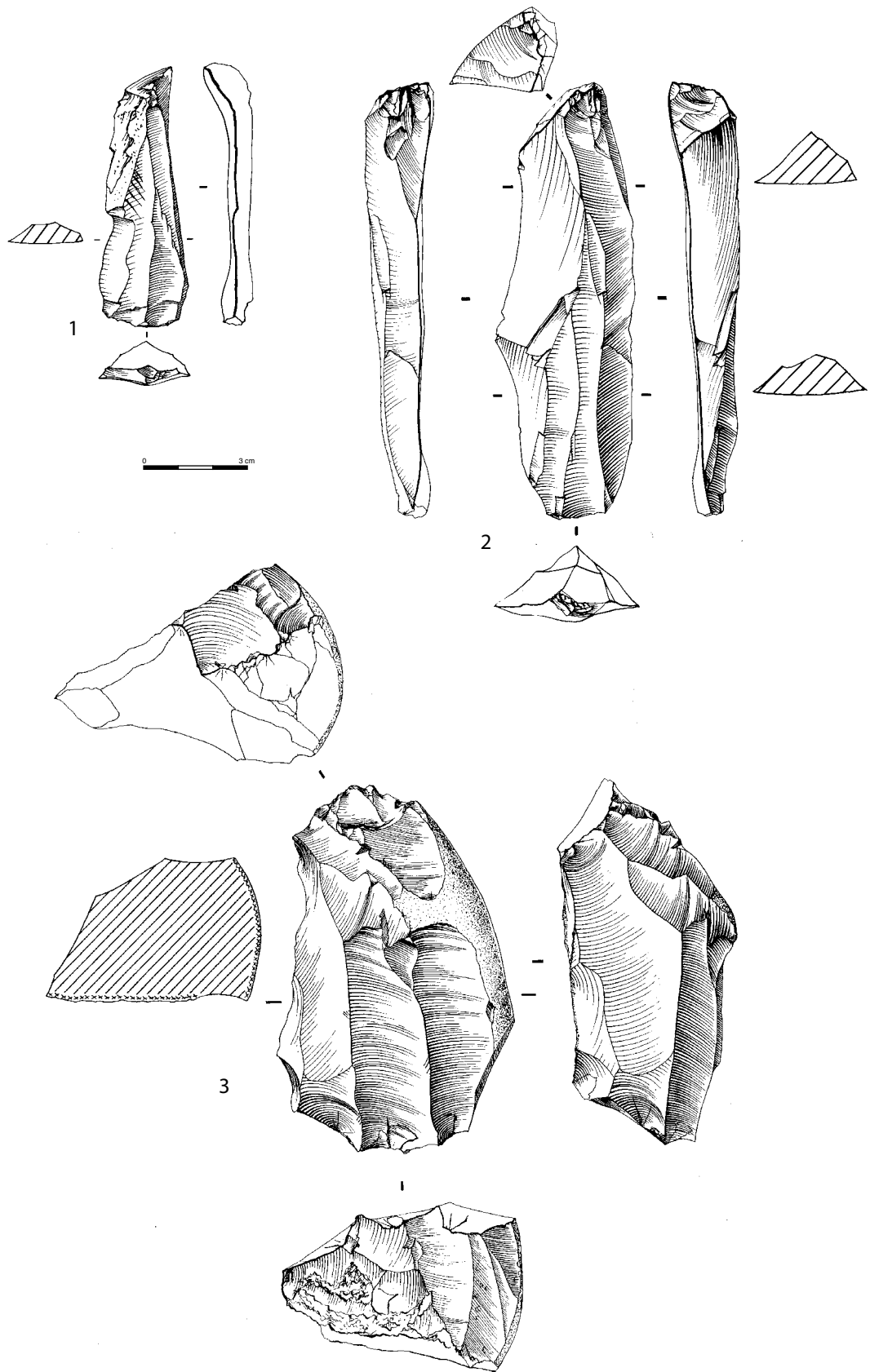


Figure 5.13. Hayonim (Early MP) – Diagnostic artefacts illustrating the variability inside the Laminar reduction strategies (bidirectional exploitation from highly 'offset' striking platforms). 1, 2. Overshoot blades that remove the opposite 'offset' striking platform (units 7-8). 3. Core with 2 highly 'offset' striking platform (unit 4).

cores. In the case of this Laminar option, however, the removals follow clearly different intersecting axes, thus resulting in characteristic pieces whose profile presents a slight break (Figure 5.12: 2, 3) and are therefore different from the blades obtained by the Levallois method.

In summary, the volumetric exploitation of the Laminar cores seems to have been organised in different ways depending on how the removals were organised.

In the case of unidirectional cores, the exploitation of the volume was made possible by the enlargement of the flaking surface initially located on the wide face. The reorientation of the striking platform removals enabled the lateral edges to be exploited in the thickness of the core (either without a break in the sequence, in the case of subpyramidal cores (Figure 5.11: 1, 2), or with a break, in the case of the exploitation of two intersecting surfaces (Figure 5.11: 3). When the striking platform was not reoriented, the removals were hinged, and the core was then often discarded.

In the case of bidirectional cores, the volume was exploited by opening a second (opposite) striking platform. This was either strongly offset (resulting in two intersecting flaking surfaces, one mainly on the wide face, the other on the narrow face, in the thickness of the core (Figure 5.13), or slightly offset (resulting in two different flaking axes, but remaining mainly on the wide face). This arrangement resulted in a flaking surface with a convex cross section and a slightly 'broken' longitudinal profile (Figure 5.12: 1).

The cores resulting from these different options thus have different morphologies, while still corresponding to the same flaking concept.

In the Laminar volumetric concept, the shaping and maintenance of the flaking surface are represented by the presence of a few, often partial, crested blades (central and lateral). The role of the central crests was mainly to elongate the flaking surface and maintain the distal convexities (longitudinal curvature/carination). The lateral crests (one side only), which enabled maintenance of the curvature (lateral enlargement of the flaking surface/maintenance of the transverse convexity of the flaking surface), are even less frequent.

Most often, the maintenance of lateral convexities and the widening of the flaking surface were achieved by detaching large *débordantes* blades (which are often cortical because the 'back' of the core was generally not prepared), or *débordantes-and-overshot* blades in the case of unidirectional convergent flaking. The core was continuously exploited (with no break between the flaking surface and the sides of the core) via the removal of these large blades.

The resulting products of this Laminar system are mostly narrow thick blades of different sizes, associated with highly oblique lateral removals. However, in the case of the Laminar method at Hayonim, the flaking was often partially performed on the widest face of the core. Consequently, numerous wide, thick blades with a high trapezoidal section were also produced.

On the Laminar products, the characteristics of the striking platform (plain or roughly faceted), the bulb of percussion (prominent), and the ventral surface suggest direct internal percussion by hard hammer. In previous articles (Meignen 1998: 175; 2000: 63), some characteristics observed on a few elongated pieces led us to suggest the possible use of direct percussion with a soft-stone hammer. After the completion of the final study, our observations were too few to definitively confirm the use of this technique.

The presence of these different options in relation to the flexibility of the Laminar and Levallois concepts, particularly in the case of bidirectional cores, could suggest that the two blade production systems are not really independent, thus supporting the hypothesis defended by Boëda of the passage from one type of structure to the other on the same core.

Therefore, in the case of bidirectional exploitation, it seems relatively simple for the knapper to go from cores with strictly opposed striking platforms (as in the Levallois system) to cores with two slightly offset striking platforms, whose flaking remains on the wide face. The reorganisation of one of the striking platforms, allowing the flaking of

the volume in its thickness, results in cores with two very offset striking platforms. This process could thus be carried out gradually and without the detachment of characteristic technical pieces that would reflect the passage from Levallois to Laminar flaking (or vice versa).

Concerning the exploitation of cores by unidirectional convergent removals, several overshoot blades, wide in their proximal part, with highly inclined sides in their mesial/distal part, may correspond either to an accidental overshoot in the final phase of semi-rotating cores on the wide face of the volume, or to an overshoot removal in the final phase of a unidirectional convergent Levallois core with strongly inclined sides, as those described at Kebara (Meignen 1995) or Misliya (Zaidner and Weinstein-Evron 2020). The use of highly oblique lateral removals in unidirectional convergent flaking could have ‘initiated’ the creation of semi-prismatic core structures on a wide face—subject to the creation of a correctly oriented striking platform allowing the lateral flaking of the volume in its thickness.

These observations could then indicate that the core reduction strategies identified based on core morphologies (as well as blade products) might not be completely independent. Rather, they may represent different moments in a production sequence carried out on the same volume (Boëda 2013). If these remarks by no mean demonstrate a continuous reduction process, they clearly show the high flexibility observed in this process. The results published on Hummal 6C2 by Wojtczak, Le Tensorer, and Demidenko (2014), as well as our observations, suggest more an ad hoc adjustment of core exploitation to the successive core morphologies. This is in contrast to a rigid/fixed sequence of reduction, with the Levallois systematically succeeding the Laminar system on the same block (as initially proposed by Wojtczak, Le Tensorer, and Demidenko [2014]). The hypothesis proposed by Boëda (2013) of a specific D2 Laminar flexible production system different from the Levallois should be taken into consideration to explain the different core morphologies observed.

5.5.2 General features of the sequence

The long MP sequence in Hayonim Cave, extending from 220 ka to 130 ka (Mercier et al. 2007), covers a long period (last half of MIS 6) that encompasses many levels associated with the Early MP, along with those corresponding to the transition from Early MP to the Middle MP. Few sites document this latter period, leading some authors even to consider the possibility of an occupation hiatus in the Levant (Bar-Yosef 1998a; Hovers 2009). Consequently, little precise information on the corresponding technological changes is available, except for the recent well-documented study of the Neshar Ramla site (Centi and Zaidner 2021; Prevost and Zaidner 2020; Zaidner et al. 2021; Zaidner et al. 2018).

In the Hayonim sequence, above the lower units (Layer F, assemblages considered as Early MP; Meignen and Bar-Yosef 2020), Layer Lower E (units 6–4/dated to 185 ka–160 ka), and Layer Upper E (units 3–1/145 ka–130 ka) cover this period. They thus enable us to assess the changes in technological practices, and perhaps the processes involved, particularly at the time of the disappearance of Early MP Laminar technologies during the MIS 6.

A review of our results on the study of all the lithic assemblages enables us to identify some of the main elements that indicate significant changes within the sequence.

After a general presentation of the main characteristics of the sequence, based on these new data, we propose a grouping of units considered to be very close, which will serve as a foundation for the structure of this study.

Main characteristics

- First, we observe strong variations in the sample sizes, partly due to differences in the area/volume excavated (Table 5.8), as well as (and probably mainly) due to differences in the occupation densities. Between the Layer F (10 to 7–8) and Layer E (6 to 1) units,

Unit	Excavated volume (m3)	Quantity	Density (per m3)
Units 1-2	3.92	4033	212
Unit 3	9.45	2209	230
Unit 4	5.94	2383	383
Unit 5	3.92	786	252
Unit 6	3.38	978	267
Units 7-8	4.05	1357	335
Unit 9	3.26	1820	663
Unit 10	1.63	1681	1065

Table 5.8. Hayonim – Estimated lithic densities in units 10 to 1.

Category	Unit 10		Unit 9		Units 7-8		Unit 6		Unit 5		Unit 4		Unit 3		Units 1-2 (total)	
	N	%	N	%	N	%	N	%	N	%	N	%	N	%	N	%
Flakes (ordinary + cortical)	750	44.62	761	41.81	268	31.72	619	63.29	519	66.03	1625	68.19	1426	64.55	2391	59.29
Laminar blades	121	7.20	178	9.78	78	9.23	40	4.09	59	7.51	152	6.38	54	2.44	316	7.84
Undifferentiated blades	135	8.03	145	7.98	86	10.18	51	5.21	53	6.74	152	6.38	140	6.34	*	*
Laminar elongated points	16	0.95	12	0.66	5	0.58	2	0.21	14	1.78	4	0.17	3	0.14	*	*
Undifferentiated elongated points	2	0.11	1	0.05	2	0.23	0	0.00	3	0.38	0	0.00	0	0.00	*	*
Levallois blades	45	2.68	85	4.67	31	3.67	51	5.21	20	2.54	44	1.85	39	1.77	100	2.48
Levallois elongated points	24	1.43	10	0.55	9	1.07	4	0.42	5	0.64	4	0.17	6	0.27	35	0.87
Levallois flakes	171	10.17	140	7.69	63	7.46	113	11.55	54	6.87	171	7.17	222	10.05	632	15.66
Short Levallois points	25	1.49	15	0.82	15	1.78	19	1.94	5	0.64	17	0.71	12	0.54	66	1.64
Cores	65	3.87	60	3.30	35	4.14	41	4.19	34	4.33	84	3.52	85	3.85	153	3.79
Retouched tools	327	19.45	413	22.69	253	29.94	38	3.89	20	2.54	130	5.46	222	10.05	340	8.43
Total	1681	100.00	1820	100.00	845	100.00	978	100.00	786	100.00	2383	100.00	2209	100.00	4033	100.00

Table 5.9. Hayonim – General breakdown of the lithic artefacts from the Middle Palaeolithic assemblages (units 10 to 1). Data not available are noted by an asterisk. Percentages are of 'total assemblage'.

Unit	Total assemblage	Without cores	Cortical products		Short Levallois		Elongated Levallois		All blades (including Levallois)		Retouched tools		Cores	
	N	N	N	%	N	%	N	%	N	%	N	%	N	%
Units 1-2	4033	3880	1357	34.97	788	20.31	158	4.07	527	13.58	340	8.76	153	3.79
Unit 3	2209	2124	806	37.95	324	15.25	54	2.54	283	12.81	222	10.45	86	3.89
Unit 4	2383	2299	1002	43.58	204	8.87	65	2.83	398	17.31	130	5.65	85	3.57
Unit 5	786	752	298	39.63	60	7.98	27	3.59	159	21.14	20	2.66	34	4.33
Unit 6	978	937	399	42.58	138	14.73	57	5.98	157	16.76	38	4.06	41	4.19
Units 7-8	845	810	317	39.13	107	13.21	83	10.25	365	45.06	253	31.23	35	4.14
Unit 9	1819	1760	700	39.77	215	12.22	161	9.15	657	37.33	413	23.47	60	3.30
Unit 10	1681	1616	615	38.06	271	16.77	102	6.31	472	29.21	327	20.24	65	3.87

Table 5.10. Hayonim unit 10 to 1 – Frequencies of the main technological categories. Blanks of retouched tools included. Percentages are of 'total assemblage without cores', except for cores (out of 'total assemblage').

Unit	Total assemblage		Without cores		Total Levallois		Levallois blades		Elongated Levallois points		Total elongated Levallois		Levallois flakes		Short Levallois points		Total short Levallois	
	N	N	N	%	N	%	N	%	N	%	N	%	N	%	N	%	N	%
Units 1–2	4033	3880	946	24.38	120	12.68	38	4.02	158	16.70	714	75.48	74	7.82	788	83.30		
Unit 3	2209	2124	378	17.80	45	11.90	9	2.38	54	14.28	305	80.69	19	5.03	324	85.72		
Unit 4	2383	2299	269	11.70	60	22.30	5	1.86	65	24.16	184	68.40	20	7.44	204	75.84		
Unit 5	786	752	87	11.57	21	24.14	6	6.90	27	31.03	55	63.22	5	5.75	60	68.97		
Unit 6	978	937	195	20.81	53	27.18	4	2.05	57	29.23	117	60.00	21	10.77	138	70.77		
Units 7–8	845	810	190	23.46	56	29.47	27	14.21	83	43.68	79	41.58	28	14.74	107	56.32		
Unit 9	1819	1760	376	21.36	139	36.97	22	5.85	161	42.82	186	49.47	29	7.71	215	57.18		
Unit 10	1681	1616	373	23.08	64	17.16	38	10.19	102	27.35	209	56.03	62	16.62	271	72.65		

Table 5.11. Hayonim units 10 to 1 – Frequencies of the Levallois product categories. Blanks of retouched tools included. Percentages of ‘total Levallois’ are of ‘total assemblage without cores’, those of other columns are of ‘total Levallois’.

in particular, there are significant differences that could be interpreted as changes in the site occupation patterns, a point that we will discuss later. However, we must also consider the location of the samples in the cave, such as the cave entrance for the lower units (Layer F) versus the Central Area of the cave for units 6 to 1, Layer E). These different locations could account for some of the technological features observed (e.g., the proportions of retouched products), and thus signify a spatial organisation of some activities. Given the available data (no precise stratigraphic correlations possible between the units of the Central Area and Deep Sounding), it is not easy to address this question, but this hypothesis deserves to be kept in mind.

- Throughout the sequence, high proportions of cortical products, ordinary products, and CTEs, as well as cores (Tables 5.9, 5.10) suggest flaking operations carried out onsite, inside the cave. This point will be discussed further below.
- All of the assemblages of the MP sequence contrast greatly with the Acheulo-Yabrudian assemblages of the underlying unit 11. The most striking element is the total absence of bifacial productions in any of the MP levels and the disappearance of the systematic production of thick blanks to be used as side-scrapers, often with Quina retouch (Meignen and Bar-Yosef 2020), a crucial point that we will discuss in our conclusions.
- In all of the MP units, Levallois production plays a significant role (Table 5.11)—a common feature of the Levantine Mousterian industries as a whole (Bar-Yosef 2006). At Hayonim, nevertheless, there are significant variations in the composition of the Levallois blanks in the sequence, along with the presence, especially in the lower units, of another production system for blade production.
- We should also note that the Levallois presence begins in the lower units (Layer F), and thus from the very beginning of the MP (Table 5.11) at around 210 ka/220 ka, in sharp contrast with the underlying unit 11, containing Acheulo-Yabrudian toolkits (Meignen and Bar-Yosef 2020).
- A large portion of the sequence is also characterised by significant blade production (Table 5.10), especially in the lower units, while blades tend to disappear in the upper portion.

Based on these elements, three main groups emerge:

First, the lower units (10 to 7–8/Layer F) are distinguished by:

- A remarkable production of elongated blanks (blades and points, Levallois and Laminar) more prevalent in Layer F (units 10, 9, 7–8) than in the other units (Table 5.12).
- A high proportion of retouched tools (Table 5.10) and, among them, a very high proportion of retouched blades and elongated points (Table 5.13).
- And more generally, a higher proportion of tools on elongated blanks (Table 5.14).

Unit	Total assemblage	Without cores	Total elongated		Laminar		Undifferentiated		Levallois	
	N	N	N	%	N	%	N	%	N	%
Units 1-2	4033	3880	527	13.58	*		*		*	
Unit 3	2209	2124	283	12.81	66	23.32	163	57.60	54	19.08
Unit 4	2383	2299	398	17.31	164	41.21	169	42.46	65	16.33
Unit 5	786	752	159	21.14	75	47.17	57	35.85	27	16.98
Unit 6	978	937	157	16.76	43	27.38	57	36.31	57	36.31
Units 7-8	845	810	365	45.06	137	37.53	145	39.73	83	22.74
Unit 9	1819	1760	657	37.33	239	36.38	257	39.11	161	24.51
Unit 10	1681	1616	472	29.21	171	36.23	199	42.16	102	21.61

Table 5.12. Hayonim units 10 to 1 – Frequencies of the elongated product categories. Data not available are noted by an asterisk. Blanks of retouched tools included except for the sample from units 1-2.

Frequencies of the elongated product categories based on the units 1-2 analysed sample.								
	Total elongated		Laminar		Undifferentiated		Levallois	
	N	%	N	%	N	%	N	%
Units 1-2	281	16.72	47	16.72	119	42.35	115	40.92

Unit	Retouched tools		Total retouched elongated blanks		Retouched blades		Elongated retouched points		Short retouched points		Scrapers		Scrapers on ventral face		UP tools		Burins		Notches+denticulates	
	N	%	N	%	N	%	N	%	N	%	N	%	N	%	N	%	N	%	N	%
Units 1-2	276	13.41	37	13.41	29	10.51	8	2.90	5	1.81	141	51.09	3	1.09	16	5.80	8	2.90	23	8.33
Unit 3	222	9.91	22	9.91	15	6.76	7	3.15	6	2.70	98	44.14	7	3.15	19	8.56	15	6.76	25	11.26
Unit 4	130	22.31	29	22.31	24	18.46	5	3.85	1	0.77	37	28.46	1	0.77	20	15.38	16	12.31	16	12.31
Unit 5	20	15.00	3	15.00	1	5.00	2	10.00	0	0.00	5	25.00	0	0.00	6	30.00	6	30.00	1	5.00
Unit 6	38	7.89	3	7.89	1	2.63	2	5.26	2	5.26	12	31.58	2	5.26	8	21.05	7	18.42	5	13.16
Units 7-8	253	63.64	161	63.64	99	39.13	62	24.51	17	6.72	30	11.86	2	0.79	16	6.32	10	3.95	4	1.58
Unit 9	413	51.82	214	51.82	151	36.56	63	15.25	27	6.54	97	23.49	42	10.17	10	2.42	4	0.97	18	4.36
Unit 10	327	34.25	112	34.25	70	21.41	42	12.84	39	11.93	91	27.83	60	18.35	18	5.50	13	3.97	10	3.06

Table 5.13. Hayonim units 10 to 1 – Frequencies of retouched tool categories. Percentages are of 'total number of retouched items'.

Unit	Identifiable blanks	On elongated blanks		On short Levallois blanks		On short non-Levallois flakes	
	N	N	%	N	%	N	%
Units 1-2	221	45	20.36	90	40.72	86	38.91
Unit 3	130	22	16.92	66	50.77	42	32.31
Unit 4	111	39	35.14	15	13.51	57	51.35
Unit 5	17	4	*	1	*	12	*
Unit 6	32	9	28.13	6	18.75	17	53.13
Units 7-8	237	186	78.48	28	11.81	23	9.70
Unit 9	355	229	64.50	57	16.05	69	19.44
Unit 10	287	127	44.25	72	25.09	88	30.66

Table 5.14. Hayonim units 10 to 1 – Blank types of the retouched tools. Data not available are noted by an asterisk. Percentages are of 'total number of identifiable blanks'.

The situation is more complex for the Layer E assemblages (units 6 to 1), which show variations in blade proportions (elongated blanks), retouched products (Table 5.10), and blade tools (Table 5.14), all of which are prevalent in the lower units. However, at this stage of the presentation, it is important to note the appearance in the higher units (unit 3 and especially units 1-2) of characteristic elements that contrast sharply with those in the

underlying units (Table 5.10). The upper units (3 to 1) show a sharp decrease in blade production (Table 5.12), an increase in Levallois flakes (Table 5.11), and, above all, few tools on blades (Table 5.14), which seem to distinguish them from the underlying assemblages.

Following these initial observations, it now seems necessary to specify the characteristics of the assemblages recovered in the various units and to consider their relationships (continuity/discontinuity in the technologies from one level to another), and to explore the processes of change at play throughout the sequence. In particular, it is important to test whether the Lower E assemblages (units 6 to 4) belong to the Early MP technical entity clearly identified in the lower units (Layer F). Another question that arises is that of the processes operating during the changes observed within the Levallois throughout the entire MP sequence.

5.5.3 Detailed study of the unit groups.

Preliminary note

Because we encountered difficulties in organising the presentation of our results, it is important to explain the choices that we made. As previously explained, the Levallois morphology blades can originate either from the Levallois production system integrating the whole range of products (thus including blades), or from a D2 type Laminar system, thus including episodes of 'typo-Levallois' blade production in its reduction sequence (as observed in the Hummalian [Boëda 2013], and supra).

To account for these two possibilities, which are most probably present in the assemblages described, we felt it necessary to characterise these assemblages both in terms of the role played by the production of elongated blanks (one of their main characteristics) and in terms of the Levallois production present throughout the sequence.

In the following study, we therefore decided to describe:

- On one hand, the production of elongated blanks (blades and points) by including all of the blades, regardless of flaking system from which they originate,
- On the other hand, the Levallois production by focusing our descriptions on the short blanks and including the information (previously described) concerning the elongated Levallois products, in order to obtain a global vision of the Levallois.

The data concerning the blades with Levallois morphology are thus present in both studies (particularly, in the tables).

It should be noted that in the majority of studies concerning Laminar Early MP assemblages, the problem we have just mentioned is not posed because the authors have often decided not to separate these categories of blades and flaking systems, even if they recognise their existence. This position is generally justified by the difficulties encountered in classifying the blades in one type of production or another and thus in counting them (Shimelmitz and Kuhn 2013; Wojtczak 2015; Zaidner and Weinstein-Evron 2020).

5.5.3.1 Lithic production from units 10 to 7–8

5.5.3.1.1 Preliminary techno-economic considerations

The lower units are characterised by average debitage proportions (ordinary and cortical flakes including CTE) (31.7 to 44.6%), and cores (3.3 to 4.1%, with a more marked presence in 7–8) (Table 5.15). The proportion of retouched tools is high (19.4 to 29.9%; Table 5.9).

The lithic artefact densities are also relatively high, especially in units 9–10, at least in comparison with those observed in the other units (Table 5.8).

5.5.3.1.2 Elongated blank production

The lower units are characterised by an abundant production of elongated blanks (blades and points), the highest in the entire sequence (Table 5.10), but this production is

Unit	Total assemblage		Non-cortical flakes		Cortical flakes		Total cortical+ non-cortical		Cores	
	N		N	%	N	%	N	%	N	%
Units 1-2	4033		1341	33.25	1050	26.04	2391	59.29	153	3.79
Unit 3	2209		814	36.85	612	27.70	1426	64.55	86	3.89
Unit 4	2383		862	36.17	763	32.02	1625	68.19	85	3.57
Unit 5	786		303	38.55	216	27.48	519	66.03	34	4.33
Unit 6	978		313	32.00	306	31.29	619	63.29	41	4.19
Units 7-8	845		120	14.20	148	17.51	268	31.72	35	4.14
Unit 9	1820		366	20.11	395	21.70	761	41.81	60	3.30
Unit 10	1681		368	21.89	382	22.72	750	44.62	65	3.87

Table 5.15. Hayonim units 10 to 1 – Debitage products: cortical versus non-cortical flakes. Percentages are of ‘total assemblages’.

Unit	Total assemblage		Without cores		Total elongated		Laminar		Undifferentiated		Levallois	
	N		N	%	N	%	N	%	N	%	N	%
Units 7-8	845		810	95.86	365	43.08	137	37.53	145	39.73	83	22.74
Unit 9	1819		1760	96.76	657	36.23	239	36.38	257	39.12	161	24.51
Unit 10	1681		1616	95.84	472	28.01	171	36.23	199	42.16	102	21.61

Table 5.16. Hayonim units 10 to 7-8 – Frequencies of the elongated product categories. Blanks of retouched tools included. Percentages of ‘total elongated’ are of ‘total assemblage without cores’, those of other columns are of ‘total elongated’.

Unit	Total elongated products					Elongated Levallois					Laminar				
	blades		elongated points		total elongated	blades		elongated points		total elongated	blades		elongated points		total elongated
	N	%	N	%	N	N	%	N	%	N	N	%	N	%	N
Units 7-8	195	92.42	7.58	77.50	211	31	77.5	9	22.50	40	78	93.97	5	6.03	83
Unit 9	408	94.66	23	5.34	431	85	89.47	10	10.53	95	178	93.68	12	6.32	190
Unit 10	301	87.76	42	12.24	343	45	65.22	24	34.78	69	121	88.32	16	11.68	137

Table 5.17. Hayonim units 10 to 7-8 – Frequencies of blades versus elongated points. Excluding blanks of retouched tools.

associated with an equally ample production of short Levallois blanks (flakes and points). All of the blanks have a frequently prominent impact point and bulb of percussion, thus testifying to direct percussion with a hard hammer and internal percussion gesture (i.e., struck toward the interior of the core on the striking platform surface, rather than on the edge of the core).

Based on the previously defined criteria (Figure 5.10), the blades were thus attributed to one of the two identified systems: Levallois and Laminar. However, we were unable to attribute a significant proportion of so-called ‘undifferentiated’ blades, whose characteristics are often intermediate between these two systems.

In units 10 to 7-8, elongated blanks of the Laminar system are always more abundant than those of the Levallois system (Table 5.16). The Laminar production thus dominates. It is important to keep in mind, however, the substantial number of blades that we were not able to attribute to either of these systems.

Blades are always much more abundant than elongated points among the flaking products (between 87.8% and 94.7%; Table 5.17). This observation is valid for the blanks in both the Laminar (between 88.3% and 94%) and Levallois (between 65.2% and 89.5%) systems, even if elongated points are often much more numerous in the Levallois production, probably because they are more frequently left unworked. This remark is particularly valid in unit 10, in which elongated Levallois points are proportionally more numerous than in the other units (34.8%).

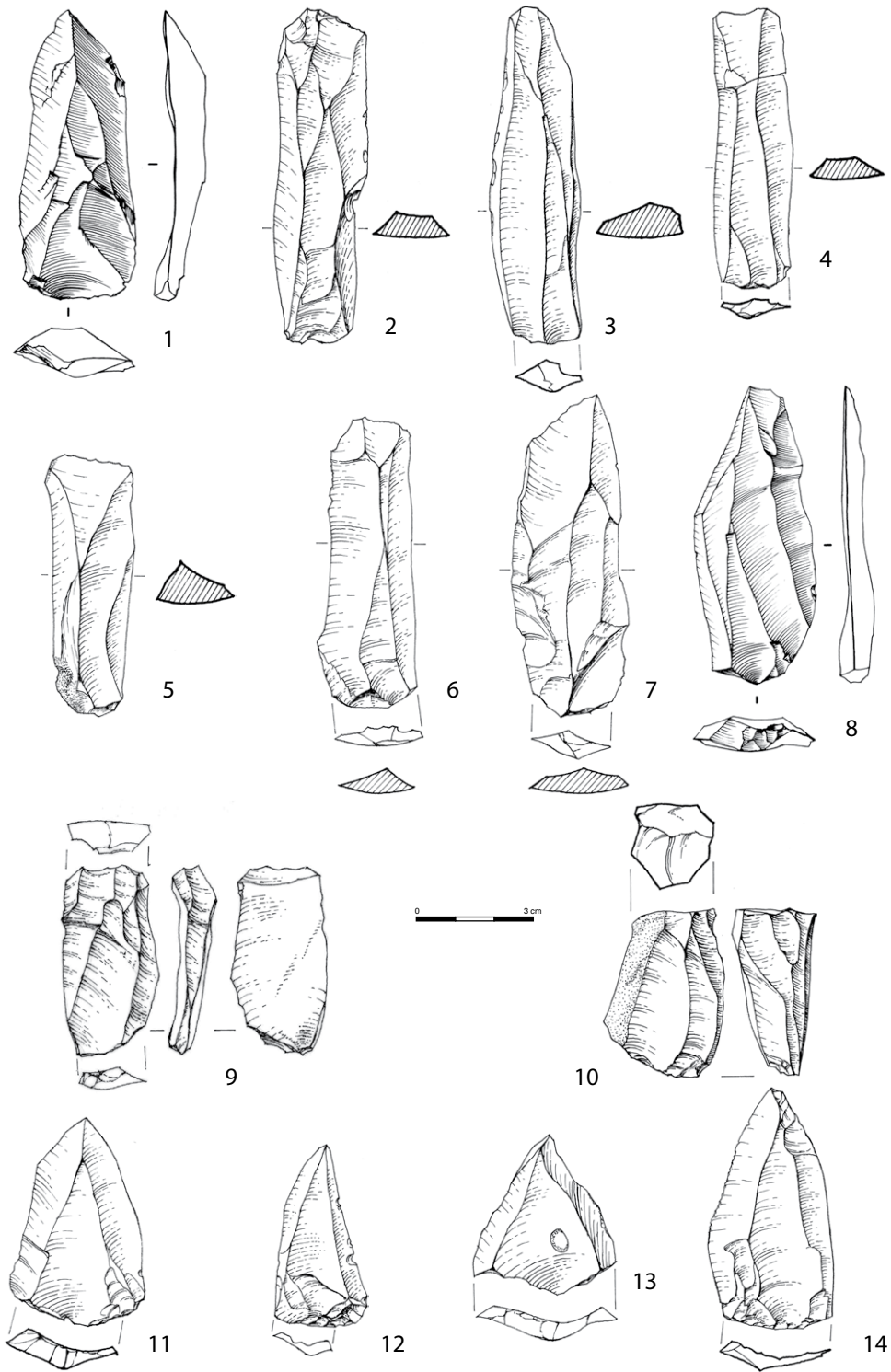


Figure 5.14. Hayonim Layer F (units 10 to 7-8), Early MP. 1-6. Laminar blades. 7-8. Levallois blades. 9. CTE from bladelet core. 10. Bladelet core. 11-14. Levallois points.

Small lamellar production is present in these lower units (n = 28 in unit 10; n = 16 in unit 9; n = 2 in units 7–8), not only as final products (small blades and microblades) but also as CTEs and small cores that are typical of microblade productions originating from flaking systems similar to those identified for blade production (mostly unidirectional) (Figure 5.14: 9, 10). For this reason, we included these small assemblages of small blades/bladelets in our analysis of blades. A large proportion of these small blades/microblades could represent the final stages of blade production.

These small blades/microblades have morphotechnological features that distinguish them from the intrusive Upper Palaeolithic and Kebarian bladelet productions that we were able to easily eliminate. The small blades and bladelets of the MP are often quite wide and not very thin, with irregular, non-parallel edges. Variably pronounced bulbs of percussion are most often present. Overhang abrasion marks, not very developed, are rare; small lips are sometimes present, but in low proportion. The small microblade cores, reduced by semi-rotating removals, most often show an exploitation of the wide face to obtain small, elongated products in association with the exploitation of the narrow part of the core to produce microblades.

Although this lamellar production is a very small component of assemblage, it seems to be present in the levels where Laminar production is well represented. We should also note that some of the microblades identified most likely originate from the core-burins present in these assemblages, or even from the more typical burins (with only a few microblade scars) described below.

The presence of small microblade production, such as the one observed at Hayonim, is also reported in other Laminar-related assemblages (Hummal [Copeland 1985; Wojtczak 2011, 2015]; Misliya [Zaidner and Weinstein-Evron 2020]). However, in contrast to what is observed at Hayonim and Hummal, at Misliya, the small blades/bladelets seem to come exclusively from the blade production sequence at the end of the core exploitation sequence. The burin-cores reported at the other two sites are absent.

5.5.3.1.2.1 Morphology of the blades and elongated points (Figure 5.14: 1–8)

All the blades (including the ‘undifferentiated’ ones) are morphologically quite variable, as are their dimensions.

They are generally thick (but this criterion is variable depending on the production system) (Table 5.18), and morphologically irregular. Their ridges are usually not parallel and sometimes convergent, with a notable percentage of pieces whose edges are generally convergent (44 to 60%) (Table 5.19). The distal extremities are most often quadrangular, but subtriangular and sub-oval morphologies are also frequent (Table 5.19). Among the latter, there are morphologies that we can qualify as ogival, corresponding to blades with mostly subparallel edges that become convergent and non-rectilinear in their distal portion. On the contrary, the true triangular morphologies (products that are widest at the base and truly pointed) are not very numerous.

The dorsal scar pattern of the blades is dominated by a unidirectional parallel organisation, followed by a unidirectional convergent one (Table 5.20).

If we now look more precisely at the elongated production associated with the Levallois system (Figure 5.14: 7–8), the blades/points are mostly wide and thin, but narrow, thin blanks are also well represented (Table 5.18). Proximally, flat trapezoidal sections dominate in association with distal ends that have a flat triangular section (Figure 5.10). The distal ends are most often subtriangular (Table 5.19), which is related to the greater frequency of elongated points among the Levallois pieces, especially in unit 10.

Most of the ridges and edges are convergent (Table 5.19), mainly due to the presence of elongated Levallois points, but this convergence is also observed on some of the blades. This is thus a clear trend in this production. The dorsal scar pattern is most often unidirectional convergent, followed by unidirectional parallel (Table 5.20), a pattern that again dominates in association with the greater number of points in the Levallois category.

	Levallois blades/elongated points						Laminar blades /elongated points						Total blades /elongated points					
	Unit 10		Unit 9		Units 7-8		Unit 10		Unit 9		Units 7-8		Unit 10		Unit 9		Units 7-8	
	N	%	N	%	N	%	N	%	N	%	N	%	N	%	N	%	N	%
wide thin	49	72.06	47	67.14	15	37.50	0	0.00	0	0.00	0	0.00	57	16.71	63	14.89	19	8.96
wide thick	5	7.35	9	12.86	7	17.50	57	41.61	66	35.68	29	35.37	128	37.54	119	28.13	71	33.49
narrow thin	14	20.59	14	20.00	17	42.50	7	5.11	6	3.24	0	0.00	42	12.32	79	18.68	36	16.98
narrow thick	0	0.00	0	0.00	1	2.50	73	53.28	113	61.08	53	64.63	114	33.43	162	38.30	86	40.57
Total	68	100.00	70	100.00	40	100.00	137	100.00	185	100.00	82	100.00	341	100.00	423	100.00	212	100.00

Table 5.18. Hayonim units 10 to 7-8 – Morphologies of the elongated products. Excluding blanks of retouched tools.

	Total blades/elongated points			Levallois blades/elongated points			Laminar blades/points		
	Unit 10	Unit 9	Units 7-8	Unit 10	Unit 9	Units 7-8	Unit 10	Unit 9	Units 7-8
Ridges	N = 156	N = 203	N = 129	N = 42	N = 53	N = 31	N = 56	N = 99	N = 59
	%	%	%	%	%	%	%	%	%
more or less parallel	2.56	13.79	8.53	2.38	16.98	12.90	5.36	14.14	10.17
non parallel	40.38	36.95	49.61	35.72	32.08	38.71	50.00	37.38	45.77
one ridge	19.88	12.31	3.88	9.52	3.77	0.00	12.50	10.10	1.69
convergent	37.18	36.95	37.98	52.38	47.17	48.39	32.14	38.38	42.37
Edges	N = 129	N = 190	N = 141	N = 31	N = 44	N = 30	N = 47	N = 94	N = 57
	%	%	%	%	%	%	%	%	%
parallel	3.10	0.00	0.71	6.45	0.00	0.00	4.26	0.00	1.75
more or less parallel	19.38	26.32	43.26	16.13	25.00	50.00	25.53	27.66	43.86
convergent	59.69	55.79	43.97	74.19	59.09	46.67	46.81	56.38	42.11
divergent	17.83	17.89	12.06	3.23	15.91	3.33	23.40	15.96	12.28
Distal ends	N = 250	N = 313	N = 165	N = 60	N = 73	N = 34	N = 90	N = 139	N = 62
	%	%	%	%	%	%	%	%	%
subovalar	21.60	27.16	27.27	13.33	26.03	20.59	16.67	26.62	25.81
subtriangular	31.60	29.39	30.31	50.00	35.61	47.06	26.67	29.50	32.26
subquadrangular	46.80	43.45	42.42	36.67	38.36	32.35	56.66	43.88	41.93

Table 5.19. Hayonim units 10 to 7-8 – General characteristics of blades and elongated points. Percentages calculated from the number of artefacts on which the characteristics are identifiable.

Table 5.20. Hayonim units 10 to 7-8 – Dominant dorsal scar patterns of elongated products. Excluding indeterminate patterns. KEY: unid par = unidirectional parallel; unid conv = unidirectional convergent; bidir = bidirectional; centr = centripetal.

	Total elongated		Levallois		Laminar	
	N	%	N	%	N	%
Units 7-8			N = 38	%	N = 64	%
	unid par	45.66	unid conv	36.84	unid par	35.94
	unid conv	27.75	unid par	34.21	unid conv	34.38
Unit 9			N = 80	%	N = 144	%
	unid par	47.43	unid conv	45.00	unid par	45.14
	unid conv	37.46	unid par	36.25	unid conv	40.97
Unit 10			N = 64	%	N = 88	%
	unid par	42.91	unid conv	45.31	unid conv	35.23
	unid conv	31.91	unid par	34.38	bidir	29.55
					unid par	28.41

Unit	Total elongated			Levallois blades			Elongated Levallois points			Total Laminar		
	identifiable butts	faceted	plain	identifiable butts	faceted	plain	identifiable butts	faceted	plain	identifiable butts	faceted	plain
	N	%	%	N	%	%	N	%	%	N	%	%
Units 7-8	101	53.47	38.61	26	69.23	30.77	7	*	*	68	44.12	44.12
Unit 9	213	49.30	43.66	64	59.38	31.25	10	*	*	139	45.32	48.92
Unit 10	142	61.27	33.80	34	64.71	23.53	16	93.75	6.25	92	54.35	42.39

On the other hand, the elongated production linked to the Laminar system (Figure 5.14: 1–6) comprises thick narrow blades, as well as a significant proportion of thick wide blades that probably originate from the broad face of the cores (Table 5.18). This is reflected in the trapezoidal sections of these blades. This Laminar production also has more frequent subquadrangular morphologies and non-parallel ridges, but here again, a tendency toward convergent morphologies is demonstrated by the often-convergent edges (Table 5.19).

The flaking organisations are roughly balanced between unidirectional parallel and unidirectional convergent, with bidirectional flaking developing in unit 10 (Table 5.20).

The trend toward convergent morphologies is therefore global for all elongated blanks, even when the flaking organisations are unidirectional parallel. We should note, however, that the unidirectional parallel/unidirectional convergent distinction is not always easy to make, since the degree of convergence of the products is generally not very pronounced in the case of elongated blanks. Moreover, as previously mentioned, true triangular morphologies (with a wide base) are not frequent, and the convergence of the edges usually becomes perceptible only in the distal third of the piece.

5.5.3.1.2.2 Striking platforms (Table 5.21)

Faceted butts dominate all of the elongated production (Levallois and Laminar). Careful faceting is much more prevalent in the Levallois system (>60%), however, especially on the elongated points.

In the Laminar system, on the other hand, the proportions of plain and faceted butts are more or less equal. The significant proportion of faceted butts may seem surprising, as we often consider that faceting is typical of Levallois, and not of Laminar. These results show that this is not the case. However, it is important to point out that the faceted butts on the Laminar products are often sketchy, with only two or three more or less well-defined facets. This suggests that the striking platform is less carefully prepared on Laminar cores.

5.5.3.1.2.3 Morphometry (Table 5.22ab)

The blades are of all sizes, with fairly high variability in their length and width, and even higher variability in thickness, as shown by the fairly high coefficients of variation (Table 5.22a). These variations in thickness are partly due to the coexistence of Levallois and Laminar productions, whose products are differentiated based on this criterion (see below). But these variations are probably also linked to the frequency of in situ flaking activities, which tend to produce cortical blanks (backed and overshot blanks) that are generally thicker. Throughout the assemblage, the blades lengths are fairly average (63–68 mm), with a L/W ratio of approximately 2.50–2.70 (Table 5.22a). In addition, the butts are relatively thick (Table 5.22b).

The Laminar blades/points are significantly longer than those of the Levallois system (but not to a statistically significant degree). On the other hand, they are clearly distinguished by greater thicknesses, which is reflected in clear differences in the L/W and W/T ratios (based on T-tests, significant differences for W, W/T, and L/W for units 7–8, 9, 10) (Table 5.22a). Clear differences also appear in the butt thicknesses, which are clearly greater on the elongated blanks from the Laminar production system than on those

Table 5.21. Hayonim units 10 to 7–8 – Faceted versus plain butts for the elongated products. Small samples are noted by an asterisk. Percentages are of 'total number of identifiable striking platforms'.

Unit	Total blades/elongated points					Levallois blades/elongated points					Laminar blades/points							
	N	Length	Width	Thickness	L/W	W/T	N	Length	Width	Thickness	L/W	W/T	N	Length	Width	Thickness	L/W	W/T
Units 7-8	157	68.12 (12.81)	27.56 (6.48)	9.07 (2.93)	2.54 (0.54)	3.27 (1.06)	31	66.45 (16.46)	26.81 (5.47)	6.84 (2.46)	2.48 (0.32)	4.26 (1.24)	64	72.67 (17.04)	25.48 (6.80)	10.72 (3.73)	2.95 (0.66)	2.51 (0.61)
Unit 9	265	63.77 (15.08)	24.40 (6.35)	8.17 (3.46)	2.69 (0.59)	3.36 (1.39)	57	61.32 (15.08)	25.09 (6.19)	5.77 (1.80)	2.49 (0.49)	4.51 (0.96)	119	68.05 (16.44)	24.70 (6.79)	9.27 (3.02)	2.85 (0.65)	2.81 (0.74)
Unit 10	180	62.97 (14.08)	25.34 (6.48)	8.84 (3.72)	2.56 (0.58)	3.23 (1.21)	42	61.45 (11.92)	26.12 (4.52)	6.05 (1.72)	2.37 (0.38)	4.53 (0.97)	63	66.40 (15.40)	25.22 (6.06)	10.13 (3.76)	2.73 (0.73)	2.67 (0.70)
T-test for Laminar versus Levallois elongated products																		
p values at an alpha [significance] level of 0.05																		
	Unit 10	Unit 9	Units 7-8															
Length	0.082	0.010	0.095															
Width	0.415	0.714	0.348															
Thickness	<0.0001	<0.0001	<0.0001															
L/W	0.004	0.000	0.000															
W/T	<0.0001	<0.0001	<0.0001															
Coefficient of variation for elongated products																		
	Unit 10	Unit 9	Units 7-8															
Length CV	0.22	0.24	0.23															
Width CV	0.26	0.26	0.26															
Thickness CV	0.38	0.42	0.39															

Table 5.22a. Hayonim units 10 to 7-8 – Metrical attributes (in mm) of the elongated products. Complete artefacts only. Standard deviations are given in parentheses.

Unit	Total blades/elongated points			Levallois elongated			Laminar blades/points		
	N	Width	Thickness	N	Width	Thickness	N	Width	Thickness
Units 7-8	146	15.59 (5.99)	5.90 (2.37)	30	18.03 (5.86)	5.57 (1.83)	60	16.10 (6.62)	6.27 (2.60)
Unit 9	236	15.76 (5.78)	6.14 (2.52)	54	16.31 (5.51)	5.19 (2.12)	109	16.60 (6.35)	6.63 (2.68)
Unit 10	170	15.69 (5.81)	6.12 (2.87)	41	17.63 (5.80)	5.05 (2.07)	61	15.70 (5.97)	6.56 (2.78)
T-test for Laminar versus Levallois elongated product butts									
p values at an alpha [significance] level of 0.05									
	Unit 10	Unit 9	Units 7-8						
Butt width	0.109	0.782	0.179						
Butt thickness	0.004	0.001	0.190						
Butt W/T	0.000	0.000	0.008						

Table 5.22b. Hayonim units 10 to 7-8 – Metrical attributes (in mm) of the elongated product butts. Complete artefacts only. Standard deviations are given in parentheses.

Unit	Total elongated blanks		Cortical elongated blanks		including cortical back	
	N		N	%	N	%
Units 7-8	213		86	40.38	31	14.55
Unit 9	431		143	33.18	59	13.69
Unit 10	343		119	34.69	52	15.16

Table 5.23. Hayonim units 10 to 7-8 – Cortical elongated blanks (blades and elongated points).

from the Levallois system (significant differences based on T-tests, except for units 7-8) (Table 5.22b).

These data, combined with the more frequent faceting of Levallois blades and the higher representation of slightly prepared butts in the Laminar system (plain or roughly faceted butts) (Table 5.21), suggest different knapping gestures.

In the case of the Levallois system, the carefully prepared butts, often with a convex delineation (sometimes of the *chapeau de gendarme* type), allow a precise localisation of the strike on the prominent part of the butt, and the strike is aimed only slightly toward the centre of the core's striking platform. On the contrary, in the Laminar system, the strike is aimed more toward the interior/centre of the core, away from the striking platform edge, and a larger part of the striking platform is thus taken when the blade is detached. This results not only in a thicker butt but also in a thicker blade.

5.5.3.1.2.4 Elongated cortical blanks

A considerable proportion of the elongated blanks (33-41%; Table 5.23) have cortex on their dorsal surface or in the form of a back or a back + an overshot blank. However, the cortical area on the upper surface is generally not largely developed and the proportions of pieces with cortical backs are not very high (13-15%; Table 5.23). A large proportion of these cortical backed or backed + overshot pieces can be considered as CTEs to prepare or maintain the convexities necessary to detach blanks from the core. A more detailed description of these CTEs is provided below, following that of the cores.

5.5.3.1.3 The Levallois production

Preliminary remark:

The features of the blades identified as Levallois have already been presented in the 'Elongated production' section of which they are obviously a part. We recall their characteristics in the following analysis because they are also part of this Levallois production.

The general table (Table 5.16) gives the total number of blades, as well as the numbers of blanks for each production system.

The Levallois system is prevalent in the lower units, (21 to 23.5%; Table 5.24), starting from the beginning of the sequence, and the entire range of Levallois products is present from the beginning of the Early MP. In particular, we should emphasise the already clear presence of Levallois points (short and elongated) (Figure 5.14: 11-14), and this for the first time in the Middle Palaeolithic sequences of the Near East; they will later become one of the markers of the Middle Palaeolithic in this region.

Alongside the elongated Levallois blanks (blades and points) described above, which are prominent in the Levallois production, the proportions of short blanks (flakes and points) are notable (Table 5.24); they are always in the majority (sometimes by a small margin: 56 to 73% of the Levallois products), even in these lower units.

Among these short products, the flakes, quite elongated (L/W 1.60 to 1.64) most often have a subquadangular morphology, followed by sub-oval or subtriangular depending on the units (Table 5.25). The presence of short Levallois points is remarkable, especially in units 10 and 7-8 (respectively, 16.6% and 14.7% of Levallois products; Table 5.24). These short points are often even more abundant than elongated points (especially in

Unit	Total assemblage	Without cores	Total Levallois		Levallois blades		Elongated Levallois points		Total elongated Levallois		Levallois flakes		Short Levallois points		Total short Levallois	
	N	N	N	%	N	%	N	%	N	%	N	%	N	%	N	%
Units 7–8	845	810	190	23.46	56	29.47	27	14.21	83	43.68	79	42.00	28	14.74	107	56.32
Unit 9	1819	1760	376	21.36	139	36.97	22	5.85	161	42.82	186	49.47	29	7.71	215	57.18
Unit 10	1681	1616	373	23.08	64	17.16	38	10.19	102	27.35	209	56.03	62	16.62	271	72.65

Table 5.24. Hayonim units 10 to 7–8 – Frequencies of the Levallois product categories. Blanks of retouched tools included. Percentages of ‘total Levallois’ are of ‘total assemblage without cores’, those of other columns are of ‘total Levallois’.

Units 7–8	Levallois flakes		Levallois short points		Levallois blades		Levallois elongated points		Total elongated Levallois		Total Levallois	
	N = 49		N = 15		N = 25		N = 9		N = 34		N = 98	
	n	%	n	%	n	%	n	%	n	%	n	%
subcirc/ovalar	16	32.65	0	0.00	7	28.00	0	0.00	7	20.59	23	23.47
subtriangular	12	24.49	15	100.00	7	28.00	9	100.00	16	47.06	44	44.90
subquadrangular	21	42.86	0	0.00	11	44.00	0	0.00	11	32.35	31	31.63

Unit 9	Levallois flakes		Levallois short points		Levallois blades		Levallois elongated points		Total elongated Levallois		Total Levallois	
	N = 106		N = 15		N = 63		N = 10		N = 73		N = 194	
	n	%	n	%	n	%	n	%	n	%	n	%
subcirc/ovalar	31	29.24	0	0.00	19	30.16	0	0.00	19	26.03	50	25.77
subtriangular	32	30.19	15	100.00	16	25.40	10	100.00	26	35.61	73	37.63
subquadrangular	43	40.57	0	0.00	28	44.44	0	0.00	28	38.36	71	36.60

Unit 10	Levallois flakes		Levallois short points		Levallois blades		Levallois elongated points		Total elongated Levallois		Total Levallois	
	N = 112		N = 25		N = 36		N = 24		N = 60		N = 197	
	n	%	n	%	n	%	n	%	n	%	n	%
subcirc/ovalar	38	33.93	0	0.00	8	22.22	0	0.00	8	13.33	46	23.35
subtriangular	17	15.18	25	100.00	6	16.67	24	100.00	30	50.00	72	36.55
subquadrangular	57	50.89	0	0.00	22	61.11	0	0.00	22	36.67	79	40.10

Table 5.25. Hayonim units 10 to 7–8 – Morphologies of the Levallois blanks. Percentages are of ‘total number of identifiable morphologies’.

unit 10; Table 5.24), in contradiction with the typical image of Early MP assemblages (the development of elongated Levallois points is considered a characteristic feature of the Early MP, the so-called Tabun D type [Bar-Yosef 1998a; Copeland 1975; Garrod and Bate 1937]).

In the entire Levallois production, these two tendencies—subtriangular and subquadrangular morphologies—are more or less equal in frequency (Table 5.25); the subtriangular dominance being determined by the more or less frequent presence of the points depending on the levels: the blades and flakes are usually subquadrangular, while the points (short and elongated) are 100% subtriangular. We should also recall the strong tendency for converging edges in this entire production, even if the morphologies of the distal parts are predominantly subquadrangular.

Unit	Levallois flakes			Levallois short points			Levallois blades			Levallois elongated points			Total Levallois		
	identifiable butts	faceted	plain	identifiable butts	faceted	plain	identifiable butts	faceted	plain	identifiable butts	faceted	plain	identifiable butts	faceted	plain
	N	%	%	N	%	%	N	%	%	N	%	%	N	%	%
Units 7-8	57	73.68	21.05	11	*		26	69.23	30.77	7	*		101	76.24	20.79
														(1.98)	
Unit 9	117	61.54	35.04	15	86.67	13.33	64	59.38	31.25	10	*		206	61.65	33.01
		(3.41)			(13.33)									(2.91)	
Unit 10	166	82.53	14.46	22	81.82	18.18	34	64.71	23.53	16	93.75	6.25	238	80.67	15.55
		(3.00)			(27.27)			(2.94)						(5.04)	

Table 5.26. Hayonim units 10 to 7-8 – Faceted versus plain butts for the Levallois blanks. Small samples are noted by an asterisk. Percentages are of ‘total number of identifiable striking platforms’. The percentage of *chapeau de gendarme* butts is shown italicised in parentheses.

Unit	Levallois flakes						Short Levallois points					
	N	Length	Width	Thickness	L/W	W/T	N	Length	Width	Thickness	L/W	W/T
Units 7-8	46	50.61	31.78	6.17	1.64	5.45	11	53.30	32.30	5.40	1.66	6.37
		(10.56)	(7.92)	(2.12)	(0.32)	(1.39)		(11.46)	(6.72)	(1.78)	(0.22)	(1.67)
Unit 9	93	50.59	32.47	6.82	1.63	5.24	14	50.79	30.07	6.14	1.70	5.02
		(9.35)	(7.38)	(2.82)	(0.55)	(1.72)		(11.72)	(7.00)	(1.41)	(0.21)	(1.15)
Unit 10	101	49.93	31.69	6.72	1.60	4.95	21	51.67	34.48	6.62	1.52	5.45
		(9.64)	(6.49)	(1.90)	(0.27)	(1.26)		(11.09)	(7.54)	(1.96)	(0.22)	(1.29)

Table 5.27. Hayonim units 10 to 7-8 – Metrical attributes (in mm) of the short Levallois blanks. Complete artefacts only. Standard deviations are given in parentheses.

5.5.3.1.3.1 Striking platforms

The striking platforms of all of the Levallois products are carefully prepared, with faceted butts (especially convex faceted) clearly dominating (Table 5.26). *Chapeau de gendarme* butts are present (especially on the short points) without being as remarkable as in the Late Middle Palaeolithic assemblages at Kebara (Meignen 1995, 2019). The short, broad-based Levallois points that go hand in hand with this specific striking platform in the Kebara assemblages (Meignen 1995) are not widely represented here (depending on the units: 5 of 11 in units 7-8; 5 of 14 in unit 9; 5 of 21 in unit 10).

5.5.3.1.3.2 Morphometry

The Levallois flakes are rather elongated (L/W ratio around 1.6; Table 5.27), as are the points (L/W ratio generally between 1.5 to 1.7; Table 5.27). These values are thus higher than at Kebara, for example, in the units where abundant short Levallois points often have a wide base (L/W mean: 1.3 for unit IX-X) or at Tor Faraj (L/W mean: 1.4, [Henry 2003]). The degree of convergence of the point preparation removals is much lower here (in relation to the lower proportion of *chapeau de gendarme* butts; see Meignen 2019: fig.1-14).

5.5.3.1.3.3 Dorsal scar patterns

The organisation of the removals on the upper face shows, for the entire Levallois production (flakes, blades, points), a unidirectional convergent preparation/flaking pattern, followed very closely (even equally in some units), by a unidirectional parallel organisation (Table 5.28). This is observed for flakes and blades, whereas the majority of points (short and elongated) are prepared by unidirectional convergent removals (especially for short points, for which this organisation is always greater than 72%; Table 5.28).

But the remarkable feature in all of these units is the very low representation of centripetal patterns (1.8 to 2.9% for the entire Levallois system, even for the Levallois flakes (2.3 to 5.6%; Table 5.28). On the other hand, units 7-8 shows a clearer development of bidirectional patterns.

These features on the unworked Levallois products are similar for retouched Levallois products (the dominant features remain the same).

Table 5.28. Hayonim units 10 to 7-8 – Dominant dorsal scar patterns of the Levallois blanks. Excluding indeterminate patterns. KEY: unid par = unidirectional parallel; unid conv = unidirectional convergent; bidir = bidirectional; centr = centripetal.

Unit	Total Levallois		Levallois flakes		Short Levallois points		Levallois blades		Elongated Levallois points	
	N	%	N	%	N	%	N	%	N	%
Units 7-8	N = 105	%	N = 54	%	N = 18	%	N = 30	%	N = 8	%
	unid conv	35.24	unid par	29.63	unid conv	76.92	unid par	43.33	unid conv	100.00
	unid par	27.62	bidir	29.63	bidir	15.38	bidir	26.67		0.00
	% centr	2.86	% centr	5.56	% centr	0.00	% centr	0.00	% centr	0.00
Unit 9	N = 216	%	N = 121	%	N = 15	%	N = 70	%	N = 10	%
	unid conv	43.98	unid conv	39.67	unid conv	73.33	unid conv	40.00	unid conv	80.00
	unid par	34.72	unid par	35.54	unid par	20.00	unid par	40.00	unid par	10.00
	% centr	1.85	% centr	3.31	% centr	0.00	% centr	0.00	% centr	0.00
Unit 10	N = 218	%	N = 132	%	N = 22	%	N = 41	%	N = 23	%
	unid conv	38.99	unid par	45.45	unid conv	72.73	unid par	43.90	unid conv	65.22
	unid par	38.99	unid conv	30.30	unid par	13.64	unid conv	34.15	unid par	17.39
	% centr	1.83	% centr	2.27	% centr	0.00	% centr	2.44	% centr	0.00

Table 5.29. Hayonim units 10 to 7-8 – Typological breakdown.

Tool category	Unit 10	Unit 9	Units 7-8
	N	N	N
Retouched blade (one edge)	56	115	61
Retouched blade (two edges)	14	36	38
Short retouched point	39	27	17
Elongated retouched point	42	63	62
Simple scraper	46	50	21
Double scraper	2	12	1
Convergent scraper	5	9	3
Déjeté scraper	4	3	3
Transverse scraper	0	1	1
Scraper on ventral face	31	19	1
Abrupt ret scraper	3		
Bifacial ret scraper		1	
Alternate ret scraper		2	
Endscraper	1	1	4
Burin	13	4	10
Awl	2	1	1
Truncation	2	4	1
Notch	9	6	3
Denticulate	1	12	1
Retouches on ventral face	4	8	1
Retouched flake/blade	30	19	9
Miscellaneous	3	13	10
Nahr Ibrahim piece	18	6	4
Notch+Nahr Ibrahim technique	2	1	1
Total	327	413	253

Unit	Total assemblage		Without cores		Retouched products		Total retouched elongated blanks		Retouched blades		Elongated retouched points		Short retouched points		Scrapers		Scrapers on ventral face		UP tools		Burins		Notches + denticulates	
	N	%	N	%	N	%	N	%	N	%	N	%	N	%	N	%	N	%	N	%	N	%	N	%
Units 7-8	845		810		253	31.23	161	49.24	99	39.13	62	24.51	17	6.72	30	11.86	2	0.79	16	6.32	10	3.95	4	1.58
Unit 9	1819		1760		413	23.47	214	51.82	151	36.56	63	15.25	27	6.54	97	23.49	42	10.17	10	2.42	4	0.97	18	4.36
Unit 10	1681		1616		327	20.24	112	44.27	70	21.41	42	12.84	39	11.93	91	27.83	60	18.35	18	5.50	13	3.97	10	3.06

5.5.3.1.4 Retouched tools

5.5.3.1.4.1. Tool assemblage composition (Tables 5.29, 5.30)

Units 10 to 7-8 have a high proportion of retouched tools (20.2 to 31.2%; Table 5.30). These are mainly retouched blades and elongated points, the former always being more abundant than the latter (Tables 5.29, 5.30). It is worth noting the high proportion of blades used as tool blanks in the assemblages.

The tool assemblages also include a large component made on short blanks (Tables 5.29, 5.30). These are mainly Mousterian-type tools, especially side-scrapers, most often with one retouched edge (simple scrapers). Convergent scrapers are not very common, whereas short, retouched points are quite frequent. It thus appears that elongated convergent blanks were used to manufacture convergent tools, whose active part is the point (retouched elongated points).

Units 10 and 9 have a remarkable proportion of tools retouched on the ventral face, whether side-scrapers, short points, or retouched blades and elongated points (Tables 5.29, 5.30). Different types of retouch on the ventral face have been observed (see detailed description, *infra*).

Upper Palaeolithic-type tools, on the other hand, are poorly represented, contrary to the prevailing idea for Early MP assemblages (Bar-Yosef 1994; Marks 1981, 1992; Shea 2003). These tools consist mainly of burins (Tables 5.29, 5.30), even if the main function of some of them seems to have been as cores for production of microblades, rather than as tools.

Notches and denticulates are rare.

We should also note the presence, in each unit, of a small number of pieces typically encountered in the Middle Palaeolithic of the Levant, but here proportionally rare. The Nahr Ibrahim technique pieces (Table 5.29), also called 'truncated-faceted pieces', generally have an inverse truncation (on the lower face), either on the distal end (most frequently), the proximal end, or both, from which small flakes are detached on the upper surface. Their function as a tool or core for the production of very small flakes is highly debated (Meignen 2019: 27, and references therein). In units 10 to 7-8, these pieces are generally infrequent (1.7 to 6.1%; Table 5.29), usually made on thick blades or elongated flakes, often originating from the Laminar system. Some of these pieces could be interpreted as cores for the production of small blanks.

5.5.3.1.4.2. Tool blanks (Table 5.31)

The tools are frequently made on elongated blanks (blades and points originating from the Laminar and Levallois systems). However, it is the non-Levallois blanks (i.e., Laminar and indistinguishable categories) that were most often transformed. This probably means that the elongated Levallois blanks, less often retouched, had directly obtained the desired morphofunctional characteristics during the flaking process.

These are followed by the non-Levallois and Levallois flake blanks, for which there does not seem to have been any particular search for cortical-backed blanks (cortical backs are infrequent).

Table 5.30. Hayonim units 10 to 7-8 – Frequencies of retouched tool categories. Percentage of retouched products is of 'total assemblage without cores'. Percentages for each category of retouched pieces are of 'total number of retouched products'.

Table 5.31. Hayonim units 10 to 7–8 – Blank types of the retouched tools. Percentages are of ‘total number of identifiable blanks’.

Unit	Identifiable blanks	On elongated blank		including				On short Levallois blank		On short non-Levallois blank	
				Levallois		non-Levallois					
	N	N	%	N	%	N	%	N	%	N	%
Units 7–8	237	186	78.48	44	18.56	142	59.92	28	11.81	23	9.70
Unit 9	355	229	64.50	68	19.15	161	45.35	57	16.05	69	19.44
Unit 10	287	127	44.25	35	12.19	92	32.06	72	25.09	88	30.66

Unit	Total retouched			Tools on Levallois blank			Tools on blade			Tools on non-Levallois blade		
	identifiable butts	faceted	plain	identifiable butts	faceted	plain	identifiable butts	faceted	plain	identifiable butts	faceted	plain
	N	%	%	N	%	%	N	%	%	N	%	%
Units 7–8	186	66.67	26.34	65	83.08	10.77	145	65.52	28.97	106	60.38	33.96
Unit 9	314	56.69	39.49	118	66.95	33.05	48	60.42	39.58	131	51.15	44.27
Unit 10	217	68.20	29.03	107	82.24	14.95	89	65.17	31.46	59	57.63	38.98

Table 5.32. Hayonim units 10 to 7–8 – Faceted versus plain butts for the retouched tools. Percentages are of ‘total number of identifiable butts’.

5.5.3.1.4.3 Striking platforms

The tool blanks often have carefully shaped butts. In all units, faceted butts are always more numerous than plain butts. This is especially true for tools on Levallois blanks, of course, and less clear for tools on blades, and especially non-Levallois blades (Table 5.32).

5.5.3.1.4.4 Description of the main tool groups

As noted above, tools made on elongated blanks (mainly blades) are highly dominant in the lower units, alongside flake tools. A substantial morphological and technical variability characterises the production of these unworked blades by various methods. The high proportions of retouched elongated blanks suggest that retouching (for the active part of the tool or the prehensile area) was frequently necessary to obtain the desired silhouette of the future tools.

The blades were thus used as blanks to make various tool types, among which we have identified two main trends:

retouched artefacts of the scraper type: these are blades retouched on one or two edges. The retouch observed on these blades corresponds either to the shaping of the working edge or, in some cases, to the shaping of the prehensile zone (to facilitate gripping, as shown by functional studies).

a range of convergent tools: the great diversity of edge modifications (symmetrical, skewed, backed knives, etc.) creating the convergent parts suggests the existence of tool types with different functions. These modified areas are more or less localised in a ‘point + edge’ pattern.

Table 5.33. Hayonim units 10 to 7–8 – Blank types of the retouched blades, retouched points and scrapers. Blanks of the elongated retouched points includes blades and elongated points. Percentages of elongated points are shown italicised in parentheses. The number of short Levallois points used as blanks for short retouched points are also shown italicised in parentheses.

Unit	Retouched blades				Elongated retouched points				Scrapers				Short retouched points							
	N total		Non-Levallois		Levallois		N total		Elongated non-Levallois		Elongated Levallois		N total		Non-Levallois		Levallois			
	N	%	N	%	N	%	N	%	N	%	N	%	N	%	N	%	N	%		
Units 7–8	99	83	83.84	16	16.16	62	40	64.51	21	33.87	30	8	26.66	16	53.33	17	3	*	14	*
							(11)		(16)										(10)	
Unit 9	151	110	72.85	37	24.50	63	37	58.73	23	36.51	97	53	54.64	35	36.08	27	5	18.52	22	81.48
							(15)		(12)										(12)	
Unit 10	70	55	78.57	14	20.00	42	19	45.24	17	40.47	91	46	50.55	43	47.25	39	6	15.38	33	84.62
							(4)		(13)										(24)	

Unit	Total retouched blades			Cortical		including cortical back		Total unretouched blades			Cortical		including cortical back	
	N	N	%	N	%	N	%	N	N	%	N	%		
Units 7-8	99	31	31.31	4	4.04	195	86	44.10	31	15.90				
Unit 9	151	54	35.76	18	11.92	408	143	35.05	59	14.46				
Unit 10	70	24	34.29	9	12.86	301	117	38.87	51	16.94				

Table 5.34. Hayonim units 10 to 7-8 – Cortical retouched blades. Counts concerning the unretouched blades are given for comparison.

Retouched blades (Figure 5.15)

Retouched blades are very abundant and most often made on non-Levallois blades (Table 5.33), frequently with cortex (Table 5.34), even if there does not seem to be a particular selection of these blank types. There does not seem to be a particular desire for a cortical back either (Table 5.34).

Retouch location/intensity

There is great variability in the location and intensity of the retouch: some blanks are widely and deeply retouched, others are retouched locally and in a regular manner, and others locally with slight marginal retouch (Figure 5.15).

These tools usually have only one retouched edge (Table 5.29), which is most often extensively retouched. This is a general feature of these blades, which have at least one edge totally retouched, sometimes in association with a second edge that is totally or extensively retouched. They differ in this respect from the retouched elongated points which, as we will see later, are more often locally retouched.

The size and invasiveness of the retouch is also variable, ranging from light, more or less localised retouch to what we have called ‘superimposed scalar’ retouch, consisting of several rows of retouch.

The blades are most often transformed by relatively short scalar retouch (Table 5.35) (Figure 5.15: 1-3), only slightly modifying the blank morphology. The retouched edge often has a semi-abrupt angle because the retouch follows the obliqueness of the often-thick sides of the blank, with a slight modification of the edge. This is followed by ‘superimposed scalar’ retouch comprising several superimposed rows of scars, often with step terminations. This retouch significantly transforms the blank and especially the angle of the retouched edge (semi-abrupt to abrupt) (Figure 5.15: 4-7). It is carried out on thick blanks originating from the Laminar system. However, this retouch is different from the scalar/stepped type we described for the Yabrudian, for which the sequence of retouching actions is more complex (Bourguignon 1997).

Finally, lightly retouched, non-invasive modifications are infrequent and often localised.

It is also important to note the significant number of blades with retouch on ventral face, which we will describe in more detail below (Figure 5.15: 8, 9).

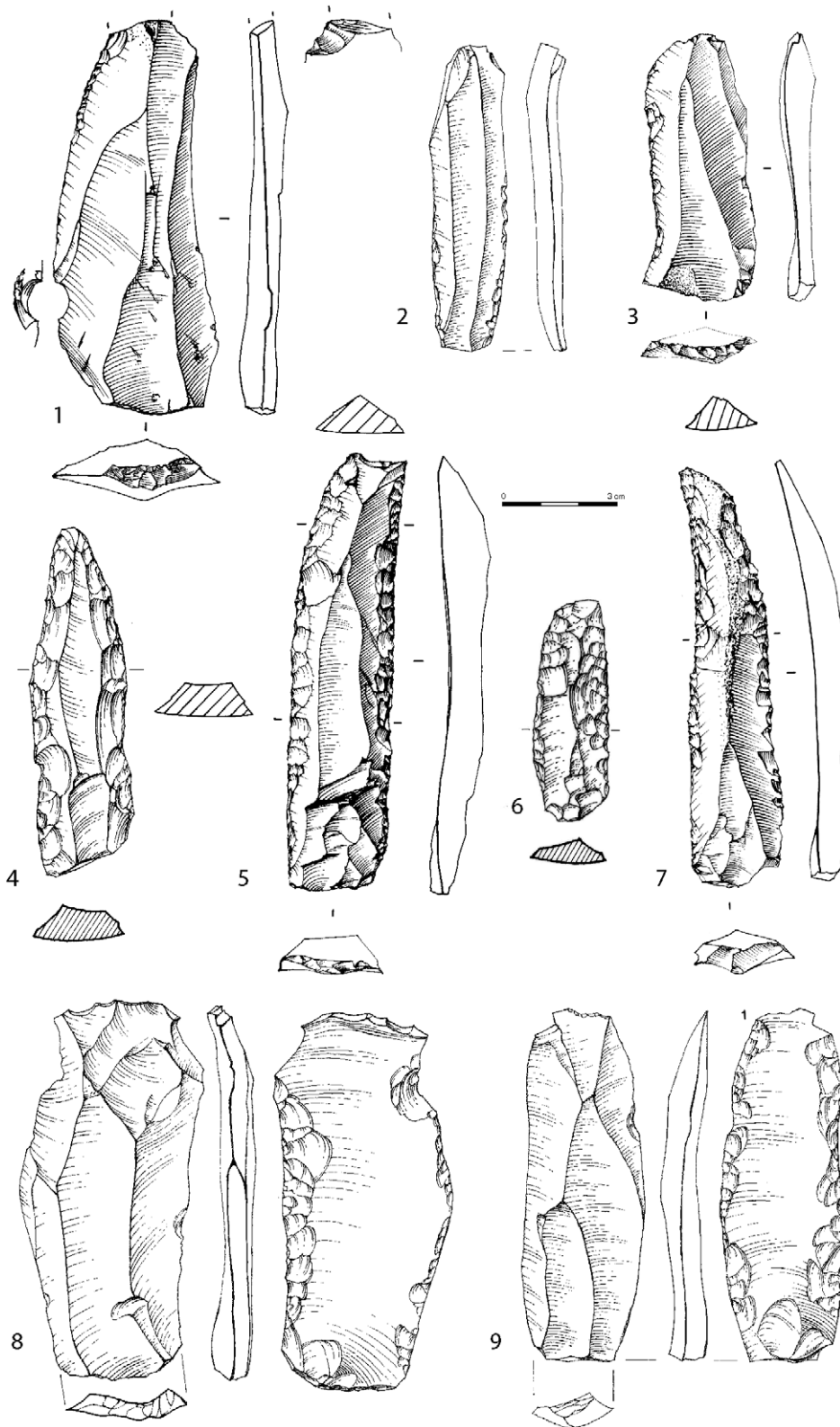


Figure 5.15. Hayonim Layer F (units 10 to 7/8), Early MP – Retouched blades. 1–3. *With short scalar retouch.* 4–7. *With 'superimposed scalar' retouch.* 8, 9. *Retouched on ventral face.*

Categories	Unit 10				Unit 9				Units 7-8		
	Retouched blades	Elongated retouched points	Scrapers	Short retouched points	Retouched blades	Elongated retouched points	Scrapers	Short retouched points	Retouched blades	Elongated retouched points	Scrapers
	N = 70	N = 42	N = 91	N = 39	N = 151	N = 63	N = 97	N = 27	N = 99	N = 62	N = 30
	%	%	%	%	%	%	%	%	%	%	%
marginal/light	14.29	21.43	19.78	5.13	7.95	7.94	4.12	7.41	13.13	16.13	16.67
scalar	57.14	45.24	57.14	51.28	78.81	53.97	79.38	44.44	72.73	54.84	70.00
superimposed scalar	20.00	21.43	14.29	15.38	9.27	17.46	5.15	18.52	11.11	12.90	0.00

Table 5.35. Hayonim units 10 to 7-8 – Main retouch categories. In units 7-8, small sample for short retouched points makes percentage calculation suspect.

A-Metrical attributes of the retouched blades and elongated points.												
Unit	Retouched blades						Retouched elongated points					
	N	Length	Width	Thickness	L/W	W/T	N	Length	Width	Thickness	L/W	W/T
Units 7-8	65	78.77 (13.84)	28.40 (6.31)	9.12 (3.12)	2.85 (0.57)	3.33 (0.91)	52	70.77 (17.17)	25.12 (5.33)	7.42 (2.30)	2.87 (0.66)	3.60 (1.02)
Unit 9	104	73.90 (15.90)	28.30 (5.43)	8.77 (3.32)	2.66 (0.53)	3.51 (1.06)	49	68.10 (17.06)	26.43 (5.44)	7.29 (1.97)	2.62 (0.60)	3.76 (0.84)
Unit 10	51	71.29 (11.90)	29.35 (5.43)	8.43 (2.05)	2.47 (0.39)	3.66 (1.02)	22	68.50 (8.84)	29.41 (5.32)	7.95 (2.55)	2.37 (0.32)	3.98 (1.22)

B- Metrical attributes of the unretouched blades.						
Unit	Unretouched blades					
	N	Length	Width	Thickness	L/W	W/T
Units 7-8	125	68.12 (12.81)	27.56 (6.48)	9.07 (2.93)	2.54 (0.54)	3.27 (1.06)
Unit 9	265	63.77 (15.08)	24.40 (6.35)	8.17 (3.46)	2.69 (0.59)	3.36 (1.39)
Unit 10	180	62.97 (14.08)	25.34 (6.48)	8.84 (3.72)	2.56 (0.58)	3.23 (1.21)

T-tests for unretouched versus retouched blades
p values at an alpha [significance] level of 0.05

	Unit 10	Unit 9	Units 7-8
Length	0.000	<0.0001	<0.0001
Width	<0.0001	<0.0001	0.001
Thickness	0.454	0.131	0.746
L/W	0.255	0.595	0.493
W/T	0.022	0.325	0.109

Coefficients of variation			
	Unit 10	Unit 9	Units 7-8
Retouched blades			
Length CV	0.17	0.22	0.18
Width CV	0.18	0.21	0.22
Thickness CV	0.24	0.38	0.34
Unretouched blades			
Length CV	0.22	0.24	0.23
Width CV	0.26	0.26	0.26
Thickness CV	0.42	0.42	0.39

Table 5.36 Hayonim units 10 to 7-8 – Metrical attributes (in mm) of retouched elongated products. Complete artefacts only. Standard deviations are given in parentheses.

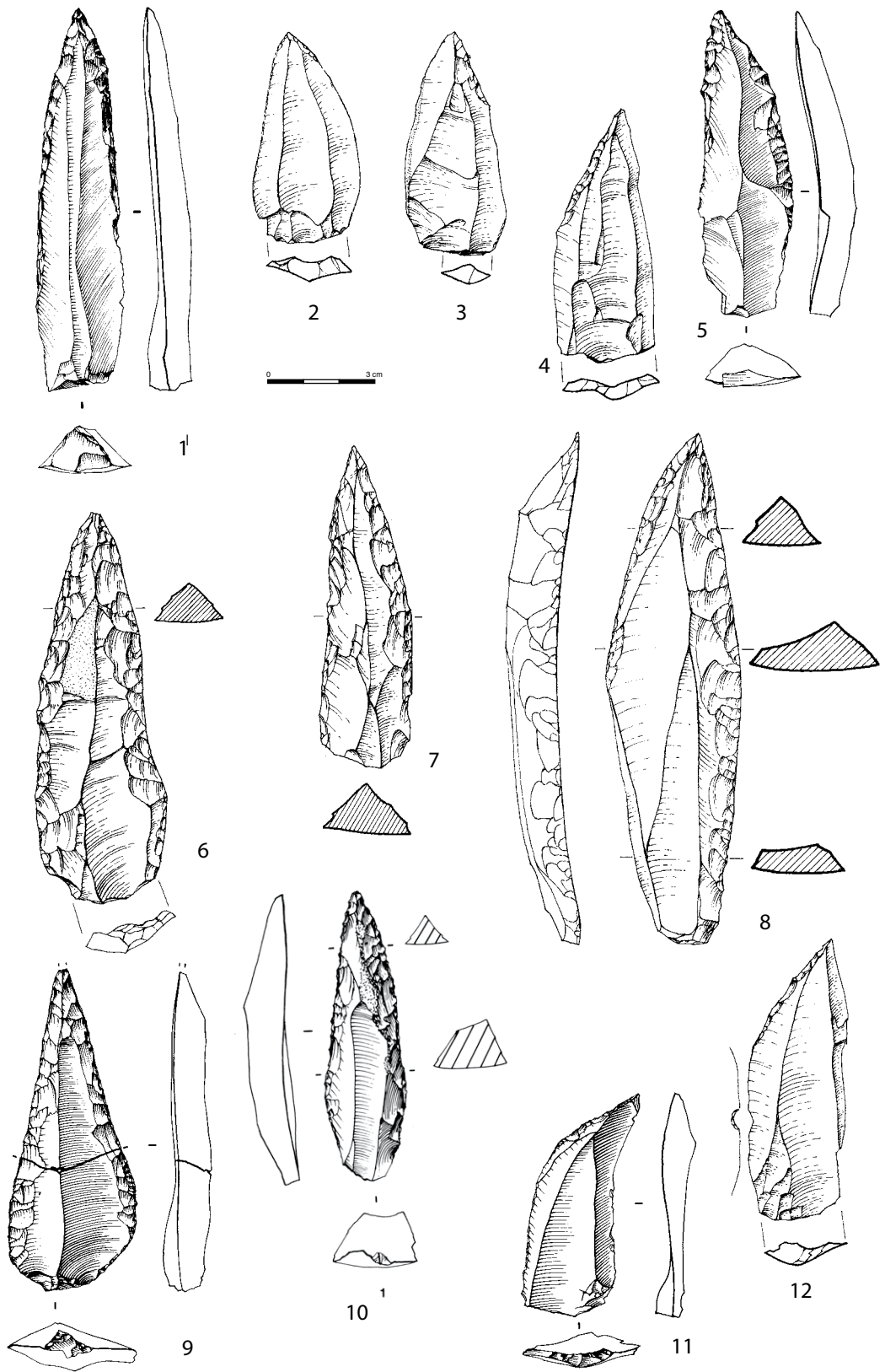


Figure 5.16. Hayonim Layer F (units 10 to 7/8), Early MP – Retouched elongated points. 1–3, 5. *Locally retouched*. 6–10. *Extensively retouched* (6–8, 10 with *superimposed scalar retouch*). 4, 11, 12. *Asymmetrical points*.

Morphometry (Table 5.36)

The largest (longest and widest) elongated blanks were selected to manufacture retouched blades. The differences between lengths and widths of retouched versus unretouched blades from all units are statistically significant (Table 5.36). It also seems that retouched blades are more regular than the blades left unworked (the coefficients of variation are slightly lower for retouched pieces; Table 5.36). Retouching thus regularised the products, creating a feature that is easily perceptible when studying the material.

Elongated retouched points (Figure 5.16)

We observed high variability in the transformation of the apical part of the blank, formed by the convergence of two edges (natural or retouched), most likely corresponding to different functions, whereas the mesio-proximal parts (likely corresponding to the prehensile zone) are less frequently retouched. The overall morphology of these tools varies as well. We can generally distinguish between symmetrical and skewed points, relative to the morphological axis of the blade blank, a difference that probably also implies different functions.

Blanks

The points are most often made on non-Levallois blanks (Table 5.33) (Figure 5.16: 1, 6–10). Those on Levallois blanks frequently display very localised retouch, often in the distal part (marginal retouch or small abrupt retouch), which seems to indicate that the blank obtained during flaking was already as close as possible to the desired morphology (Figure 5.16: 2, 3).

When the retouched elongated points are highly transformed, it is often difficult to identify the initial blank (blade or point). However, examination of the identifiable blanks shows that retouched points were frequently made on points already obtained during flaking (about 40–45%; Table 5.37). These results thus indicate that additional transformation (retouch) was sometimes necessary to obtain the desired functional characteristics, which is probably the consequence of a production that was not very standardised during flaking.

Location/intensity/retouch type

Symmetrical points are the most frequent. The retouch is generally localised, most often on the distal part; it modifies the apical part (point) as well as sometimes one or two adjacent edges ('point + edge(s)' transformation). The proximal part of these retouched points is less often modified. In most cases, the two edges of the point are only partially retouched with localised retouch, either distally or mesio-distally. They are made on different blank types (thin Levallois blanks or thick narrow Laminar blanks) (Figure 5.16: 1, 5). These tools are called 'Hummal points' by Copeland (1985) and Zaidner and Weinstein-Evron (2014).

Less often, the point is formed by two entirely retouched edges. These tools are extensively retouched, often by 'superimposed scalar' retouch. These points are most often made on thick narrow Laminar blanks (Figure 5.16: 6, 7, 9), but sometimes, less often, on elongated Levallois blanks. They are referred to as 'elongated Mousterian point' by Copeland (1985), and as 'Abou Sif point' by Zaidner and Weinstein-Evron (2014).

Less frequently, the point is nearly completely formed directly during the flaking process, but a series of thin retouch flakes, or some abrupt retouch, was necessary to

Unit	N identifiable blanks	Non- Levallois points	Levallois points	Total pointed blanks	
		N	N	N	%
Units 7–8	61	11	16	27	44.26
Unit 9	63	15	12	27	42.86
Unit 10	42	4	13	17	40.48

Table 5.37. Hayonim units 10 to 7–8 – Frequencies of pointed blank for retouched elongated points. Percentages are of 'total number of identifiable blanks'.

obtain the final morphology of the point (regularisation of the distal part) (Figure 5.16: 2, 3), or to regularise the edges (via light retouch). This light retouch is most often applied to Levallois blanks, showing once again that the desired morphology is, in this production system, mostly obtained during the flaking process.

In the case of asymmetrical points, the selected blank is usually a blade that has been truncated by abrupt or semi-abrupt retouch to form the point. The retouched part, straight or slightly convex, is oblique to the longitudinal axis of the point. In some cases, the elongated blank is itself already skewed (*déjété*), and the abrupt retouch only accentuates this feature (Figure 5.16: 4, 11, 12).

The points are most often transformed by scalar retouch (Table 5.35), which only slightly transforms the blank, but also by marginal retouch, which is frequent in the case of a localised transformation (distal, near the point, or lateral) on the pointed blanks obtained directly from the flaking process (Figure 5.16: 2, 3). These two retouch types are usually only slightly invasive.

Less frequent, but particularly remarkable, is the scalar retouch superimposed in several rows ('superimposed scalar retouch'), which significantly transforms the blank, and more specifically, the angle of the retouched edge (semi-abrupt to abrupt). This technique was often used to make the intensively retouched points (on one or two edges) previously described (continuous intensive retouch) which are made on thick Laminar blanks (Figure 5.16: 6–8, 10).

However, there is a great deal of variability within the major groups described here, which is difficult to explain. We have thus not established well-defined types, as Zaidner and Weinstein-Evron (2014) did, and Copeland (1985) before them. In these earlier attempts, a high degree of variability exists within the defined types that partially overlap. It is likely that the retouch only creates the morphofunctional characteristics sought (active part/gripping part) based on the characteristics obtained during flaking, which are themselves very diverse, as we have seen in the blade production. The blank production is not very standardised, and the same seems true for the overall morphology of the retouched points. In effect, the main aim seems to have been to obtain a point (and partially the adjacent edges). But it is likely that the variability observed among these points also corresponds to different tools with differentiated morphofunctional characteristics (the functional angle of the edges, for example, is very different between points with heavily retouched edges by superimposed scalar retouch and thin Levallois points transformed by a few localised retouches). These different degrees of retouch intensity probably do not correspond to differences in resharpening intensity, as shown by Zaidner and Weinstein-Evron (2014) in the Misliya assemblages. Rather, they represent a desire to create active parts with different characteristics via the choice of the blank (from different flaking systems) and their transformation by retouching to make tools for different functions.

Among these retouched elongated points, we must point out the presence of some that are retouched on ventral surface, which we will discuss later along with the other tools displaying the same transformations.

Morphometry (Table 5.36)

In each assemblage, the dimensions of the retouched elongated points are similar to those of the retouched blades and have a similar modulus. Given the small number of unworked elongated points, it is impossible to determine if a selection was made for pieces to be transformed into tools.

Side-scrapers (Figure 5.17: 1-9)

Still constituting the second largest group (Tables 5.29, 5.30), the number of side-scrapers also indicates a significant production of tools on short blanks (flakes and points). Relatively numerous in unit 10 (27.8% of retouched tools) and unit 9 (23.5%), they are less abundant in units 7–8 (11.9%).

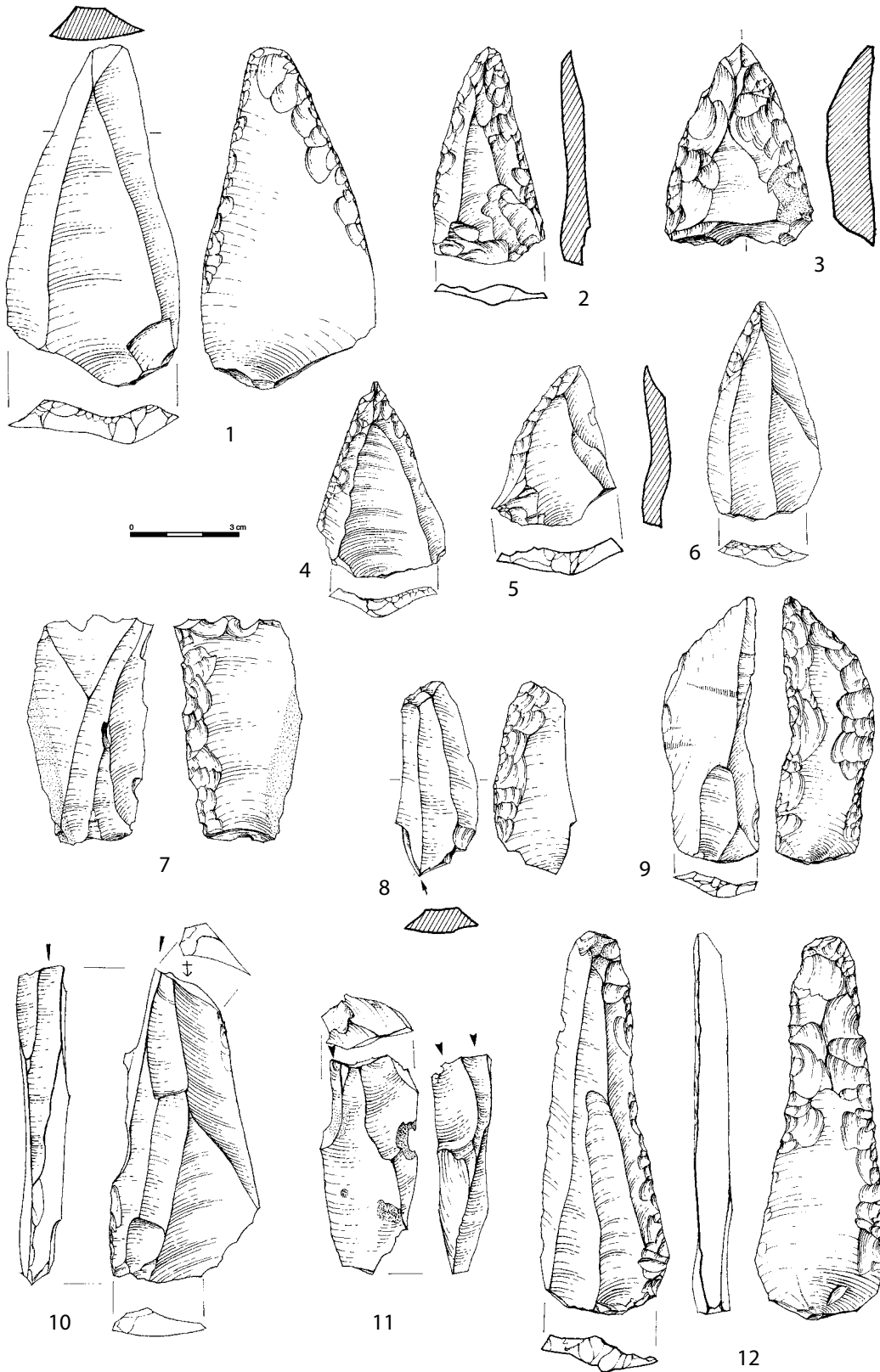


Figure 5.17. Hayonim Layer F (units 10 to 7/8), Early MP – Other retouched tools. 1, 7-9, 12. Tools retouched on ventral face (9. dissymmetrical piece, due to intensive resharpening on the left edge by 'laminated' retouch [several rows of invasive retouch]). 2. Convergent scraper. 3-6. Retouched short points (4-6. on Levallois blanks). 10, 11. Burins.

Blanks

Side-scrapers were made on Levallois blanks (most often elongated flakes) or non-Levallois blanks, one or the other category dominating depending on the units (Table 5.33). There does not seem to be a systematic selection of Levallois blanks for retouching. The blanks have little cortex (especially the Levallois ones, of course). A notable point is the manufacturing in units 9 and 10 of side-scrapers on ventral face, a point to which we will return later.

Location/intensity/retouch type

Simple scrapers (one retouched edge) dominate the side-scrapers (Table 5.29). The retouch on these tools is often partial and localised. While convergent (Figure 5.17: 2) and skewed (*déjété*) scrapers are remarkably scarce, the presence of short, retouched points should be noted as they are sometimes abundant. We should note the presence of a single bifacial retouch scraper, intensively and invasively retouched, an isolated element of this type in the entire sequence.

The scrapers are most often slightly transformed with lightly invasive scalar retouch, and more or less often with light retouch. Superimposed scalar retouch, frequently observed on retouched elongated blades and points, is rare in this case (Table 5.35).

Short retouched points (Figure 5.17: 3-6)

Relatively abundant in unit 10 (11.9% of retouched tools; Table 5.30), and to a lesser extent in units 7–8 and 9 (6.7% and 6.5%, respectively), their transformation by retouch displays characteristics similar to those described above for retouched elongated points.

Blanks (Table 5.33)

Most of the blanks are Levallois points (Figure 5.17: 4–6), while non-Levallois blanks are rare (Figure 5.17: 3). The Levallois blanks are frequently of the ‘broad-based’ type, with convex faceted butts (but few *chapeau de gendarme* butts). We should note, however, that thick blanks with rather obtuse functional angles (rare) are grouped under this same name, ‘short retouched points’, as well as thin blanks with very acute angles (the most frequent). This group thus includes tools with diverse techno-morphofunctional characteristics.

Location/intensity/retouch type

These points are generally largely retouched (depending on the unit, the pattern of 1 or 2 retouched edges dominates).

The different manners of obtaining the point part are similar to what we described earlier for elongated points. Frequently, the point (apical part) is created by two edges retouched over a varying length of the flaking edge (‘point + 2 edges’ pattern). The edge angles are often steeper in the distal part, but this could be due to the greater thickness of the blank in this zone (Figure 5.17: 4). Sometimes the two edges are intensively retouched, like the classic Mousterian points made on a thick blank (Figure 5.17: 3). In some cases, the intensity of the retouch seems to correspond to resharpening.

Alternatively, the point is often created by a single retouched edge, mainly distal, associated with an edge that has been left unworked: the retouch then serves only to regularise the edge in the distal part in order to obtain the point. Sometimes, on a point obtained directly from flaking, an edge is locally modified only distally by abrupt retouch; this retouched edge is then opposed to an unworked or retouched edge (acute functional angle) with or without traces of use, evoking the morphology of a backed knife (Figure 5.17: 5, 6).

These points are most often transformed by slightly invasive scalar retouch (Table 5.35); the superimposed scalar retouch, also very present, is used on thicker blanks, at least locally.

Unit	Total tools retouched on ventral face		Scrapers on ventral face		Short points on ventral face		Blades on ventral face		Elongated points on ventral face	
	N	%	N	%	N	%	N	%	N	%
Units 7-8	2	*	1	*	0	*	1	*	0	*
Unit 9	42		19	45.24	2	4.76	18	42.86	3	7.14
Unit 10	60		31	51.67	9	15.00	18	30.00	2	3.33

Table 5.38. Hayonim units 10 to 7-8 – Frequencies of the different categories of pieces retouched on ventral face. Small samples are noted by an asterisk. Percentages are of ‘total number of tools retouched on ventral face’.

Tools retouched on ventral face (Figure 5.17: 1, 7-9, 12)

One of the notable elements in the toolkits of these lower units, at least in units 10 and 9, is the significant number of blanks transformed by retouch on their ventral face (18.3% of the retouched tools in unit 10; 10.2% in unit 9; Table 5.13). They are very rare in units 7-8 and tend to disappear in the overlying levels.

This phenomenon is clearly identified for scrapers and retouched blades and less pronounced for points (short and elongated) (Table 5.38).

Location/intensity/retouch type

We observed high variability in the blank types, in the location (most often on two edges, complete or partial), as well as in the retouch type. The retouch can be scalar, marginal, not very invasive, and more or less flat (more or less parallel to the lower face). These are clearly the most frequent types (n = 27/60 in unit 10; n = 25/42 in unit 9) (Figure 5.15: 8, 9; Figure 5.17: 1). But they can also be invasive and subparallel to the lower face, thus flat and invasive (n = 22/60 in unit 10; n = 7/42 in unit 9) (Figure 5.17: 8, 12). In some cases, this invasive retouch comprises several rows (called here ‘laminated’ retouch (*retouches feuilletées*)) and the retouch scars have many small hinge or step terminations in the thickness of the piece (n = 7/60 in unit 10; n = 5/42 in unit 9) (Figure 5.17: 7, 9).

In the case of flat retouch (parallel to the ventral face), the functional edge angle is maintained during the transformation process. In contrast, non-flat retouch intersects the working edge, thus changing the functional edge angle.

In some cases (n = 4 in unit 10; n = 5 in unit 9), these transformations clearly correspond to intensive resharpening, and the blank is more intensely modified by the retouch on one edge than it is on the other; this results in a significant dissymmetry of the piece (Figure 5.17: 9).

Upper Palaeolithic-type tools (Figure 5.17: 10, 11)

There are few UP-type tools in these lower units (5.5-6.5%, and even fewer in unit 9, 2.4%; Tables 5.29, 5.30). They are mostly burins (13 in unit 10, 14 in unit 9, 10 in units 7-8), and a few end-scrapers, perforators, and truncated tools, which are very infrequent. The few end-scrapers are generally made on flake blanks, and exceptionally the end of a blade: (unit 10 = 1 on a flake, unit 9 = 1 on a Levallois flake; units 7-8 = 4, three of which are on blade fragments).

Angle burins, dihedral burins, transverse burins, and burins on the ventral face are present (Figure 5.17: 10, 11) and no doubt contributed to microblade production alongside pieces that can more easily be identified as burin-cores/lamellar and small flake cores. The latter are generally made on thicker and more diverse blanks than regular burins, often with cortex

The ‘UP-type tool’ component at Hayonim is not prevalent, in contrast to what has long been put forward for EMP assemblages (Bar-Yosef 1994; Marks 1981, 1992; Shea 2003).

5.5.3.1.5 Cores (Figure 5.18)

When introducing the cores, it is important to make a few remarks about them in general. In these units, the proportion of cores-on-flakes is high, and the numbers obtained correspond to a minimum since any remains of the lower face of the flake are often no longer visible due to frequent overshoot removals. These numerous cores-on-flakes

thus reflect the exploitation of the ventral face (26 to 40%; Table 5.39), a feature present throughout the sequence, although with variations.

The presence of these cores on the ventral face of flakes poses the problem of identifying the flaking system they represent if we do not wish to include them all in one very broad category, but rather to consider the existence of flaking systems that have been identified on blocks in these assemblages, and here carried out on flake blanks. We have thus sought criteria to determine which production systems were used to exploit these lower flake surfaces.

First, we should note that, in relation to their small size, the presence of numerous accidental longitudinal overshot or lateral edge detachments makes it difficult to identify the flaking system because the core preparation stigmata, if they existed (in the case of Levallois, for example), have probably disappeared.

Nevertheless, a careful examination of these cores-on-flakes has enabled us to identify various core types reflecting different flaking systems:

- Some of the cores-on-flakes display all of the features of the Levallois system, including traces of the flaking surface preparation; prepared striking platform; and flake removals parallel to the intersection plane between two hierarchical surfaces. They have consequently been included in the Levallois core category (in this case, we are dealing with what is called a ‘technical shortcut’: the convexities necessary to detach flakes are already present due to the convex morphology of the ventral face of the core-flake. Few or no adjustments are therefore necessary to shape the flaking surface. This option is sometimes referred to as a ‘Kombewa initiation’ (Boëda 2013).
- Other cores-on-flakes have no remains of the preparation removal but a carefully prepared striking platform is present. In addition, the flaking surface is more or less parallel to the intersection between the flaking surface and the striking platform preparation surface. Given these characteristics, it is difficult to ensure they belong to the Levallois system (absence of flaking surface preparation stigmata), even if it is probable. We have thus grouped them with cores whose attribution to the Levallois system is possible but not certain, in the category we call ‘Levallois core?’.
- Finally, many cores on the ventral flake surface display a few scars located in the same plane, parallel to the one separating the upper and lower face. The structure of these cores is thus similar to the Levallois system, but they bear no shaping stigmata and the striking platform is absent or just slightly prepared. We have grouped these cores under the term ‘summary exploitation of a preferential surface’ by few removals. We recognise a hierarchical treatment of surfaces comparable to the Levallois system but without any trace of preparation or shaping of the core. We have thus made this a separate category whose role in the assemblage deserves to be considered.

5.5.3.1.5.1 Features of the cores (Table 5.39)

Whatever the flaking system, at their discarded stage, flake-producing cores dominate (e.g., predominantly in units 10 and 9). Blade cores, present throughout the sequence, are never in the majority. Poorly represented in the upper units of the sequence, they are globally scarce even in the lower levels that concern us here (from 10 to 25.7%), whereas elongated blanks are found in remarkable proportions.

These observations would thus indicate either that the final stage of these cores is not representative of the production of elongated blanks that could have been obtained at the beginning of the sequence (= reconversion of blade cores into flake cores?), or that the elongated products were, at least in part, knapped elsewhere and then brought to the site. In the case of onsite flaking, it is possible that the previous blade cores were later used to produce small blades or elongated flakes. Lacking data on the origins of raw materials, it is difficult to discuss these two options and, in particular, to provide real arguments for the flaking of elongated products off-site, which is, nevertheless, a very probable hypothesis.

Unit	Total assemblage	Cores		On flake blank		Flake cores		Blade cores		Bladelet cores		Levallois cores		Levallois? cores		Preferential surface cores		'Semi-tournant' cores	
		N	N	%	N	%	N	%	N	%	N	%	N	%	N	%	N	%	N
Units 7-8	845	35	4.14	14	40.00	24	68.57	9	25.71	2	5.71	3	8.57	5	14.28	2	5.71	11	31.43
Unit 9	1819	60	3.29	16	26.67	48	80.00	6	10.00	3	5.00	9	15.00	21	35.00	5	8.33	6	10.00
Unit 10	1681	65	3.87	17	26.15	56	86.15	7	10.77	2	3.08	11	16.92	20	30.77	7	10.77	6	9.23

5.5.3.1.5.2 Description of the main core categories

We have identified two main core categories reflecting different volumetric flaking concepts:

- The Levallois (and related) flaking system, corresponding to an exclusive exploitation of the broad face of the core (= facial flaking).
- The Laminar system, corresponding, on the other hand, to a so-called 'volumetric' exploitation, with variants that most often display flaking of the wide face of the core in association with lateral flaking in its thickness. Exploitation only of the narrow face of the core (frontal flaking) is much less common.

Table 5.39. Hayonim units 10 to 7-8 – Main categories of cores. Percentages are of 'total number of cores', except core percentage calculated from the total assemblage.

Exclusive exploitation of the wide face

Clearly identifiable Levallois cores, as well as those that we call 'Levallois?' (less typical; see definition below), dominate the core assemblages, with the Levallois? cores being the most abundant (respectively, 8.6 to 16.9% for the Levallois cores, and 14.3 to 35% for the Levallois? cores; Table 5.39). Most of the Levallois? cores are small (average length between 4.2 and 4.5 cm) and exploited to exhaustion (low thicknesses, in particular), which sometimes makes them difficult to read. Even if cores with a typical morphology are not dominant, cores of the Levallois concept are thus in the majority.

Typical Levallois cores (*sensu stricto*)

The typical Levallois cores are most often recurrent, thus producing several Levallois blanks per prepared/ exploited surface (Table 5.40). The flaking methods identified at the final stage are more or less equally divided between unidirectional parallel, unidirectional convergent, and bidirectional. On the other hand, there is no centripetal flaking. These cores are most often made on blocks (nodules, slabs, etc.), and rarely on the ventral face of flakes.

The striking platform preparation surfaces remain largely cortical and are only slightly prepared. Installed in the proximal part of the core in the case of unidirectional flaking, the striking platforms cover about 1/3 of the core periphery (Figure 5.18: 2). In the case of bidirectional flaking, two striking platforms, generally limited in size, are created at the two ends of the core, strictly opposite each other (Figure 5.18: 1, 3).

At Hayonim, the unidirectional convergent Levallois cores often have steep lateral edges, especially in the distal part (a phenomenon described previously at Kebara [Meignen 1995, 2019]), thus giving these cores a characteristic morphology in section, different from the classic Levallois morphology. They have a thick trapezoidal section in the proximal part of the core and a very thick triangular section in the distal 1/3 of the core, indicating very thick overshoot removals in their distal part. This core type has also been identified at Misliya (Zaidner and Weinstein-Evron 2020). In many cases, the question of the limit between these unidirectional convergent cores considered as Levallois and the morphologies, at the end of their exploitation, of semi-rotating cores made on the wide face of the volume, is raised.

Core types		Unit 10		Unit 9		Units 7-8	
Levallois cores	Total	11		9		3	
including	preferential	4		0		1	
	recurrent	6		8		2	
	<i>including</i>		centr	0	0		0
			bidir	3	2		1
			unid par	1	2		1
			unid conv	2	4		0
	indeterminate	1		1		0	
Levallois ? cores	Total	20		21		5	
including	preferential	10		4		0	
	recurrent	8		15		5	
	<i>including</i>		centr	1	1		0
			bidir	1	3		1
			unid par	2	10		3
			unid conv	1	0		1
			crossed	3	1		0
	indeterminate	2		2			
Semi-tournant cores	Total	6		6		11	
			1 str pltf/unid conv	1	0		1
			1 str pltf/unid par	3	2		8
				(including 1 for bladelets)	(including 1 for bladelets)		
			2 str pltf/ bidir opp	0	0		0
			2 str pltf/ twisted	2	4		2
				(including 1 for bladelets)			
Preferential surface exploitation	7		5		2		
Upper surface exploitation (cf Nahr Ibrahim)	0		1		1		
Others	multiple str.pltf	1		0		1	
	isolated removals	19		16		11	
	discoid	0		1		0	
	fragments	1		1		1	
Total		65		60		35	

Table 5.40. Hayonim units 10 to 7-8 – Detailed counts of cores. KEY: Str pltf = striking platform; unid par = unidirectional parallel; unid conv = unidirectional convergent; bidir = bidirectional; centr = centripetal.

Atypical “Levallois?” cores

These cores are well represented, mainly in the basal levels (units 9 and 10; less clear in units 7–8; Table 5.39) where they constitute the most frequent core group. They are most often made on blocks, but also on the ventral face of flakes, in which case the Levallois flaking surface is only slightly prepared. In this latter case, the cores display the features of the Levallois structure: flaking on a wide face; two hierarchical surfaces; flaking parallel to the intersection plane of the two surfaces, and a carefully prepared striking platform, but the remains of the preparation of the Levallois surface are not (or no longer) visible.

This situation is often the consequence of either the detachment of large preferential flakes at the end of flaking or of accidental overshots/lateral edge flakes, which may have erased all or some of the traces of the flaking surface shaping phase, thus making the attribution to the Levallois uncertain. These cores are most often recurrent and exploited by parallel unidirectional removals.

Like the typical Levallois cores, these cores are quite small and thus frequently display flaking accidents in the final phase (overshots, hinge terminations, fractures).

Cores with the ‘exploitation of a preferential surface’

These are cores made on the lower face of flakes that display a small series of contiguous removals organised in the same plane, parallel to the intersection plane between the upper and lower face of the core-flake. However, we observe no evidence for the preparation of the flaking surface and only sometimes a very summary preparation of the striking platform. This is thus an organised but succinct exploitation of a preferential surface, similar to the Levallois structure, which differentiates it from the ‘isolated removals’ category (only one or two non-contiguous removals) which we have included in the ‘other cores’ category.

In units 10 to 7–8, the ‘preferential surface flaking’ cores are not very numerous (5.7 to 10.8% of the cores; Tables 5.39, 5.40) and are always lightly exploited (2 to 3 scars). They correspond to part of what some authors classify as a ‘core-on-flake’ (Hovers 2009; Malinsky-Buller 2016, for instance). Few in number, they play a secondary role in the productions of these units, in the form of small Kombewa-type flakes, whose particularity is the presence of a characteristic biconvex cross section edge from a morphofunctional point of view. This production can be considered as evidence of an expedient flaking component.

Volumetric exploitation/Laminar cores (Table 5.39) (Figures 5.11: 1–3; 5.12: 1; 5.13: 3; 5.18: 4–6)

Surprisingly, cores characteristic of the Laminar flaking system are not very numerous in these units ($n = 6$, i.e., 9 to 10% of cores in units 9 and 10; $n = 11$, i.e., more than 30% of cores, in units 7–8; Table 5.39). They show both a clear volumetric production system (very different from the Levallois previously described), as well as morphological variability in direct relationship to the exploitation concepts adopted.

These cores most often have a subquadrangular or subtriangular morphology. The flaking is organised along the longitudinal axis of the core. As previously described, in this Laminar system, there is no complete shaping of the volume, but only a modification of the part that is exploited (flaking surface, striking platform). In particular, the ‘back’ (the part opposite the flaking surface) often remains cortical or natural.

The blades are extracted in a continuous series (recurrent exploitation), according to a mostly semi-rotating pattern, from one or two striking platforms. The resulting cores are identified in the form of semi-pyramidal and semi-prismatic cores (resulting from the semi-rotating pattern) (Meignen 2000).

The unidirectional cores, the most frequent in these units ($n = 4$ in unit 10, $n = 2$ in unit 9, $n = 9$ in units 7–8; Table 5.40), display a highly convex section with their flaking surface expanding to the lateral edges around a large part of the core periphery (semi-rotating) (Figure 5.11: 1, 2; 5.18: 4–6). Their morphology is most often semi-pyramidal and their size is variable, including small, and geared toward the production of large to small blades, or even microblades (Figure 5.11: 2).

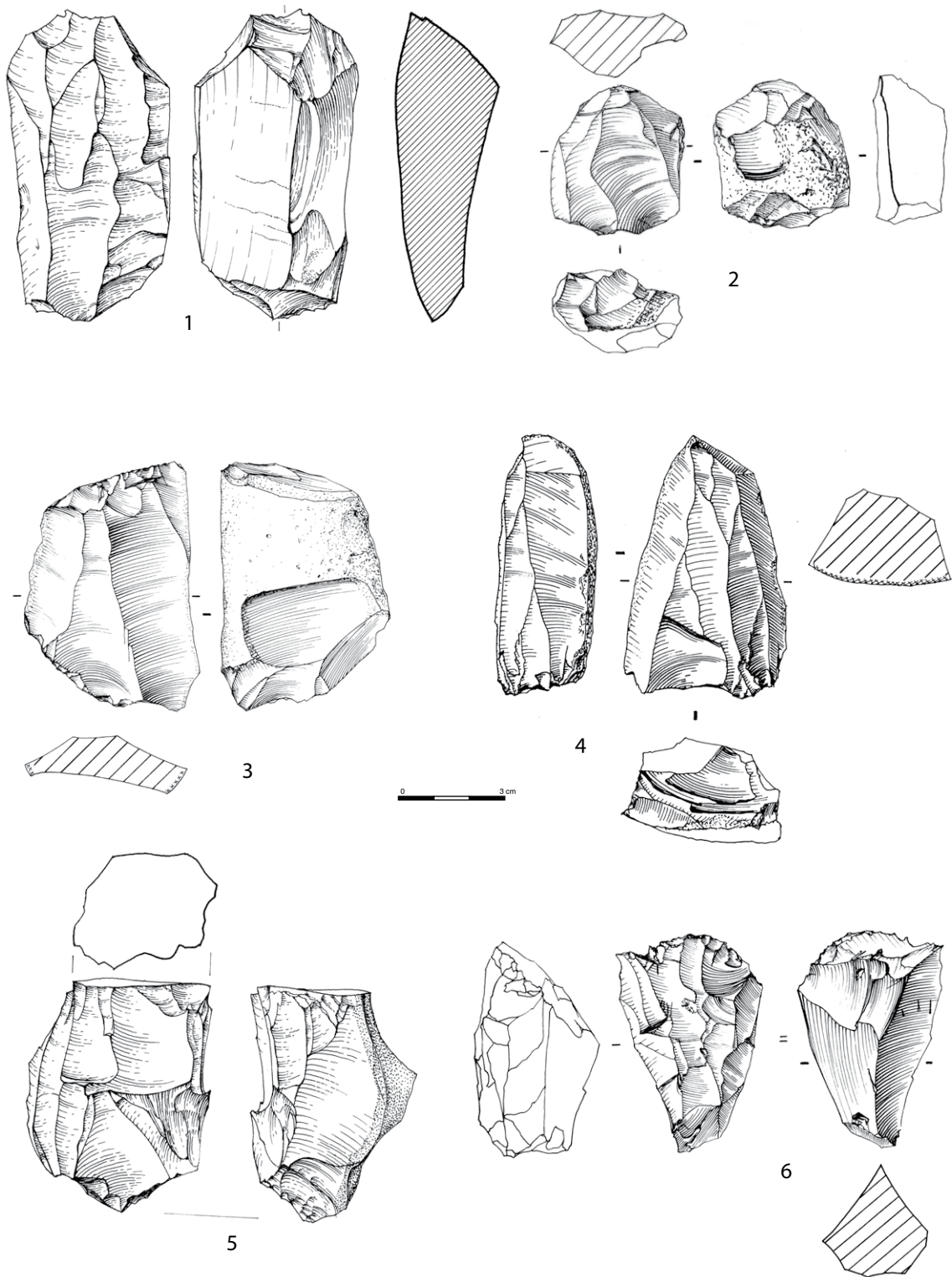


Figure 5.18. Hayonim Layer F (units 10 to 7-8), Early MP – Cores. 1, 3. *Bidirectional Levallois cores*. 2. *Unidirectional Levallois core*. 4-6 *Unidirectional Laminar cores*.

For some unidirectional cores, the exploitation is mainly organised on the wide face, which then passes laterally onto an edge for a short exploitation sequence in the thickness of the core, after a reorientation of the striking platform (Figure 5.11: 3). In these specific cases, there is a break in the flaking sequence with the juxtaposition of two intersecting flaking surfaces, one on the wide face, and the other along the narrow face of the core (more or less perpendicular). This exploitation pattern differs significantly from the semi-pyramidal cores previously described on which the transfer to a lateral face is continuous. This is clearly a volumetric concept, but the exploitation sequence of the narrow face is not very developed. The core remains globally flat and not very thick.

Mostly subquadrangular in morphology, the few cores corresponding to a bidirectional exploitation (Table 5.40) display two opposed platforms slightly or largely off-axis. In the case of clearly offset striking platforms, two intersecting flaking surfaces are exploited, one along the widest face, the other along the narrow face of the core, the intersection of which creates the convexities necessary for blade detachment. The resulting flaking surface is highly convex and the core morphology is semi-prismatic (Meignen 2011). Such bidirectional exploitation has also been identified by specific overshot blades that remove the opposite offset striking platform (Figure 5.13: 1, 2).

In the case of slightly offset striking platforms, the exploitation remains mainly on the broad face, but the removals are of a different axis, resulting in elongated products with a characteristic upper face and profile (Figure 5.12: 2, 3). These blades have on their dorsal face, mainly unidirectional parallel scars, and in opposition, one or two large scars oblique to these parallel removals. The 'broken' longitudinal profile of these blades, thus showing a break due to an operation carried out from two non-strictly opposed striking platforms, allows them to be easily distinguished from blades extracted from bidirectional Levallois cores with a continuous, straight, or slightly convex profile.

These cores often have a flat plain striking platform, or slightly faceted platform (1–3 scars).

Other cores

A fairly large proportion of cores do not fit into any of these categories. They are said to be 'informal' (Tables 5.39, 5.40), corresponding either to removals from several unorganised striking platforms or to isolated unorganised removals, partly on ventral flake face ('isolated removals' Malinsky-Buller 2016).

All the cores are generally small, especially the Levallois and Levallois? cores, whose average length is 4.2 to 4.5 cm. Laminar cores are longer and thicker, and their dimensions are very variable. Due to the very small number of cores, it is necessary to be cautious in our interpretations.

5.5.3.1.6 Core trimming elements (CTEs) (Figure 5.19)

These are products associated with core shaping and maintenance and are often technically informative. Rather than the commonly used term 'trimming (which we will also use for convenience), the terms 'core management pieces' (Hovers 2009), or 'core maintenance element' (Zaidner and Weinstein-Evron 2020) would be more accurate.

Depending on the flaking systems considered, various categories of CTEs have been identified:

- Classic *débordants* flakes (present in the Levallois system) (Beyries and Boëda 1983).
- Cortical-backed *débordants* flakes (used in both the Levallois and Laminar systems), here the most numerous.
- Crested blades
- The overshot products that are considered to be intentional. We should note, however, that it is sometimes difficult to distinguish between intentional "overshots" and those due to flaking accidents.

Unit	<i>Débordants</i> with cortical back		<i>Débordants</i> with non-cortical back		Classical <i>débordants</i> including (<i>dos limités</i>)		Crested blades		Total CTE
	N	%	N	%	N	%	N	%	
Units 7-8	32	78.05	1	2.44	2 (1)	4.88	6	14.63	41
Unit 9	68	78.16	9	10.34	3 (1)	3.45	7	8.05	87
Unit 10	71	83.53	4	4.71	4 (3)	4.71	6	7.06	85

Table 5.41. Hayonim units 10 to 7-8 – Main categories of CTEs. Among the classical *débordants*, the number of those called *à dos limité* are shown in parentheses.

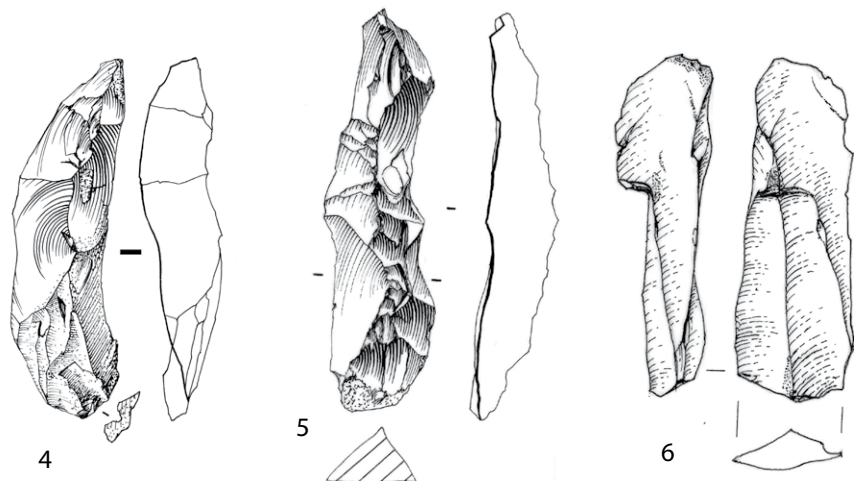
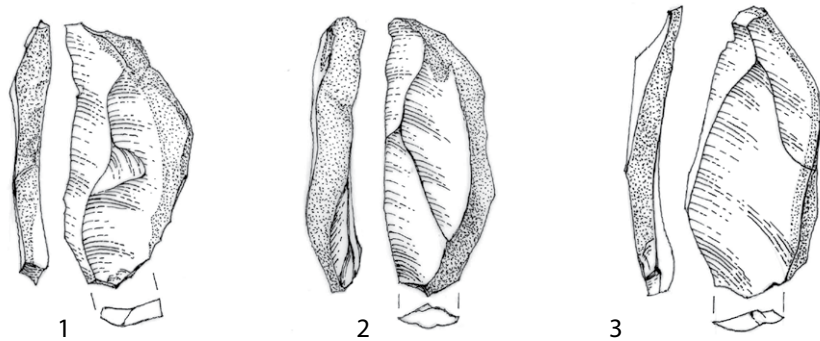


Figure 5.19. Hayonim Layer F (units 10 to 7-8), Early MP – CTEs. 1-3. Cortical-backed *débordants* products. 4, 5. Crested blades. 6. Intentional overshoot ('overshooting') blade for restoration of the flaking surface.

5.5.3.1.6.1 Classic *débordants* flakes or blades

These products are defined as flakes or blades removed along the lateral edge of a flaking surface to create or maintain lateral convexities. The classic forms of these pieces described in Beyries and Boëda (1983) are more specifically related to the Levallois flaking system and are especially present and easily identifiable when the striking platform preparation removals on the lower surface of the cores are present over more or less the entire periphery. These edge products display stigmata of these striking platform preparations, which thus constitute the back.

In units 10 to 7-8, there are very few classic *débordants* products (3.5 to 5% of CTEs; Table 5.41). Their characteristics (in particular the back) are the consequence of a centripetal preparation phase (mainly for preferential or recurrent centripetal cores), a modality that is, as we have seen, poorly developed in these units. Their low quantity is therefore directly related to the exploitation methods used.

5.5.3.1.6.2 Cortical *débordants* products

These pieces are sometimes called ‘naturally backed flakes’ (Hovers 2009) or ‘naturally backed knives’ (NBK; for instance, Centi and Zaidner 2021; Shimelmitz and Kuhn 2013).

Like the classic *débordant* products, they consist of a flake or blade removed along the lateral edge of a flaking surface to create or maintain lateral convexities. But these have a natural, most often cortical back in the case of a uni/bidirectional exploitation pattern in which the lower face of the core remains largely cortical (Meignen 1995). They thus play the same role as the *débordants* products previously described. Their role in the creation and maintenance of convexities is generally accepted, even if, surprisingly, they are sometimes not counted among the *débordants* products (for instance Zaidner and Weinstein-Evron 2020).

Cortical *débordants* products (generally in the form of elongated cortical-backed blades or flakes) are used in both the Levallois and Laminar systems. It is often difficult to attribute them to one system or other because the organisation of the removals in these units is very similar in both systems (unidirectional parallel and convergent dominant). However, given the morphology of the flaking surfaces, Levallois-related cortical-backed blades generally have wider and thinner sections (‘flat/flat right-angled triangle’ section), whereas Laminar edge blades are narrower and thicker, (‘thick/right-angled triangle’ section).

In the lower units (10 to 7–8), *débordants* products with cortical backs, sometimes overshot, largely dominate all of the CTEs (78 à 84%; Table 5.41). These features are related to the largely unidirectional (parallel or convergent) exploitation of the cores, whether in the Levallois or the Laminar system.

In the case of unidirectional parallel or bidirectional exploitations, the thickness of the cortical edge products is more or less constant along their entire length, with a slightly twisted profile (Figure 5.19: 1, 2). On the other hand, in the case of unidirectional convergent operations, they are thicker at the distal end and have a twisted profile (Figure 5.19: 3).

Since these pieces are used in both flaking systems, they cannot be considered as a specific product of the Levallois system, as is sometimes claimed in the literature.

5.5.3.1.6.3 Crested blades (Figure 5.19: 4, 5)

Crested blades are not very abundant in these levels, despite the fact that they are dominated by the blade production (n = 6, in units 10 and 7–8; n = 7, in unit 9; Table 5.41). The crested blades have either two sides (central crest) or one (lateral crests). Used to shape the core, these anterior and lateral crested blades are most often partial. Distally crested blades enable the flaking surface to be lengthened (removal of longer blanks due to the guide-ridge thus created) and the distal convexities to be maintained while facilitating the detachment of subtriangular products (creation of a guide-ridge). Lateral ridges, used to maintain the transverse convexity (*cintrage*) of the flaking surface are very rare (Figure 5.19: 5).

However, the small proportion of these crested blades confirms the minimal investment in the Laminar core preparation and maintenance, a behaviour already identified based on the cores themselves.

In addition to these products, which are typically recognised as core shaping/maintenance elements, there are overshooting/overshot blades. These pieces display either a distal cortical overshoot or the removal of part of the core, large or not, or an opposed striking platform. For these pieces, it is difficult to distinguish an intentional act (designated as ‘overshooting’) from a flaking accident (overshot). The repeated presence of such artefacts in an assemblage suggests the practice was intentional.

Among the overshooting products identified as intentional, some were used to create distal convexities, while others enabled the restoration of the flaking surface (e.g., removal of previous hinge-flake scars or irregularities in the raw material, in which case, the term ‘trimming’ is appropriate) (Figure 5.19: 6). In any case, these specific products (whether

intentional or accidental) provide ample information on the flaking systems adopted since they often remove a significant part of the cores, such as the opposed striking platform and the proximal part of the products detached from it (Figure 5.13: 1, 2).

5.5.3.1.7 Summary of the main features of units 10 to 7–8

Based on the data from these lower units, it is possible to propose an interpretation of the occupation types in the cave. Given the abundance of cores, flaking by-products and, in particular, cortical flakes and CTEs, it is clear that at least some of the blanks were made onsite. Meanwhile, the high proportion of blades compared with the low number of blade cores and/or semi-rotating cores in the cave raises the question of their origin. Were elongated products imported already knapped, and perhaps already retouched, or were numerous blade cores converted into flake cores at the final stage?

To test these hypotheses, we tentatively calculated the ratio of blade to semi-rotated cores in the different units. For these calculations, we chose to take into account the numbers of semi-rotated cores (rather than the blade cores) because they are the main producers of elongated blanks, even if they are no longer identifiable as blade cores in the final stage. This ratio, which varies according to level, still shows a large excess of elongated blanks, suggesting a clear import of elongated products (ratio of elongated products to semi-rotated cores: unit 10 = 78.7; unit 9 = 109.5; units 7–8 = 33). We are well aware that the calculation of this ratio is only an approximate criterion that must be interpreted with caution. The calculated ratio is probably overestimated since the number of cores is probably underestimated, considering that some of the cores that produced blades are no longer identifiable as such in their final stage. Nevertheless, the values here are high enough that the introduction of elongated blanks, mainly blades, is the most likely hypothesis. Our lack of precise data on the raw materials used does not allow us to confirm this hypothesis, however.

The behaviour seems to differ for Levallois production, which appears to have been mainly produced locally, even if the data in units 7–8 might show a low import of Levallois products (ratio of Levallois blanks to Levallois cores: unit 10 = 12; unit 9 = 12.5; units 7–8 = 23.8).

In the same manner, the high proportions of retouched products, especially blade tools, seem to indicate either numerous in situ tool-manufacturing activities or, more likely, the import of blanks (especially blades), possibly already retouched (personal gear). Both provisioning strategies (provisioning of individuals and provisioning of place) are thus attested in these lower units.

5.5.3.2 Lithic production from units 6 to 4

5.5.3.2.1 Preliminary techno-economic considerations

Units 6–4 show a significant increase in the debitage proportions (ordinary and cortical flakes) (Table 5.15). This is especially visible in the proportions of cortical products (units 6–4: 27.5 to 32% of the complete assemblage versus 17.5 to 23% for the lower units). This is associated with a clear proportion of cores, especially in units 5 and 6, and a significant decrease in retouched blanks.

Furthermore, the density calculations show low values for units 5 and 6, and a less clear value for unit 4, again in contrast to the values observed in units 10 to 7–8 (Table 5.8).

There are, therefore, clear changes in the composition of these assemblages compared with those of the underlying units, suggesting changes in the organisation of lithic resource production and management.

5.5.3.2.2 Elongated blank production

Units 6–4 are characterised by the production of elongated blanks (blades and points) (Figure 5.20: 1–8), which are still quite present, even if their numbers are clearly lower than in the lower units (16 to 21% compared with 29 to 49% in the lower units; Tables 5.10, 5.12).

Unit	Total elongated products					Elongated Levallois					Laminar				
	blades		elongated points		total elongated	blades		elongated points		total elongated	blades		elongated points		total elongated
	N	%	N	%	N	N	%	N	%	N	N	%	N	%	N
Unit 4	348	97.75	8	2.25	356	44	91.67	4	8.33	48	152	97.44	4	2.56	156
Unit 5	132	85.71	22	14.29	154	20	80.00	5	20.00	25	59	80.82	14	19.18	73
Unit 6	142	95.95	6	4.05	148	51	92.73	4	7.27	55	40	95.24	2	4.76	42

Table 5.42. Hayonim units 6 to 4 – Frequencies of blades versus elongated points. Excluding blanks of retouched tools.

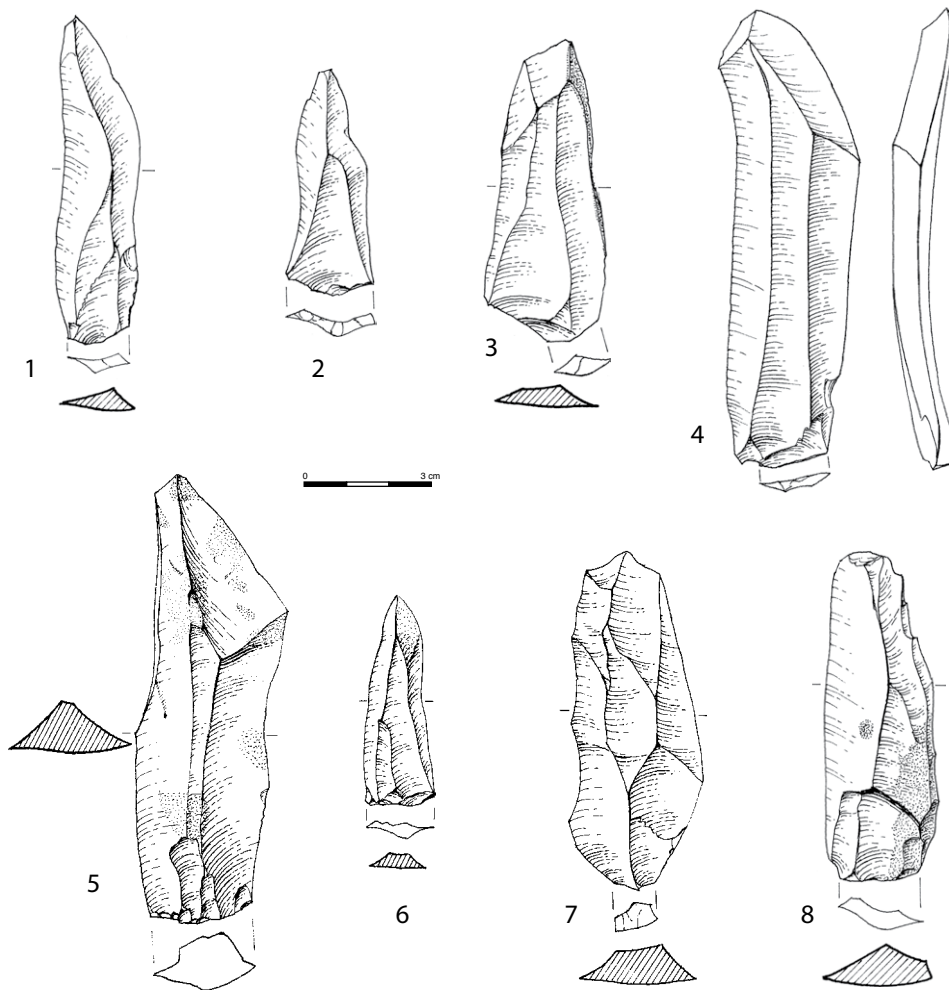


Figure 5.20. Hayonim Layer Lower E (units 6–4), Early MP – Elongated blanks. 1, 3, 4. Levallois blades. 2. Elongated Levallois point. 5, 7, 8. Laminar blades. 6. Elongated point.

This production goes hand in hand with a significant Levallois production, particularly of short blanks (flakes and points = 8 to 15% of the assemblages; between 69 and 76% of the Levallois production; Table 5.11), which is an increase compared with the lower units. These assemblages again include the whole range of Levallois products (blades, flakes, and points).

Based on the above criteria (Figure 5.10), the elongated blades and points were attributed to one of the two systems, with, however, a significant proportion of undifferentiated pieces, as in the lower units. Thick, narrow or wide blades from the Laminar system dominate the elongated products (27 to 47%: true in units 5 and 4, but not in unit 6; Table 5.12). The production linked to the Laminar system is particularly remarkable in units 4 and 5, where the blade proportions are proportionally higher

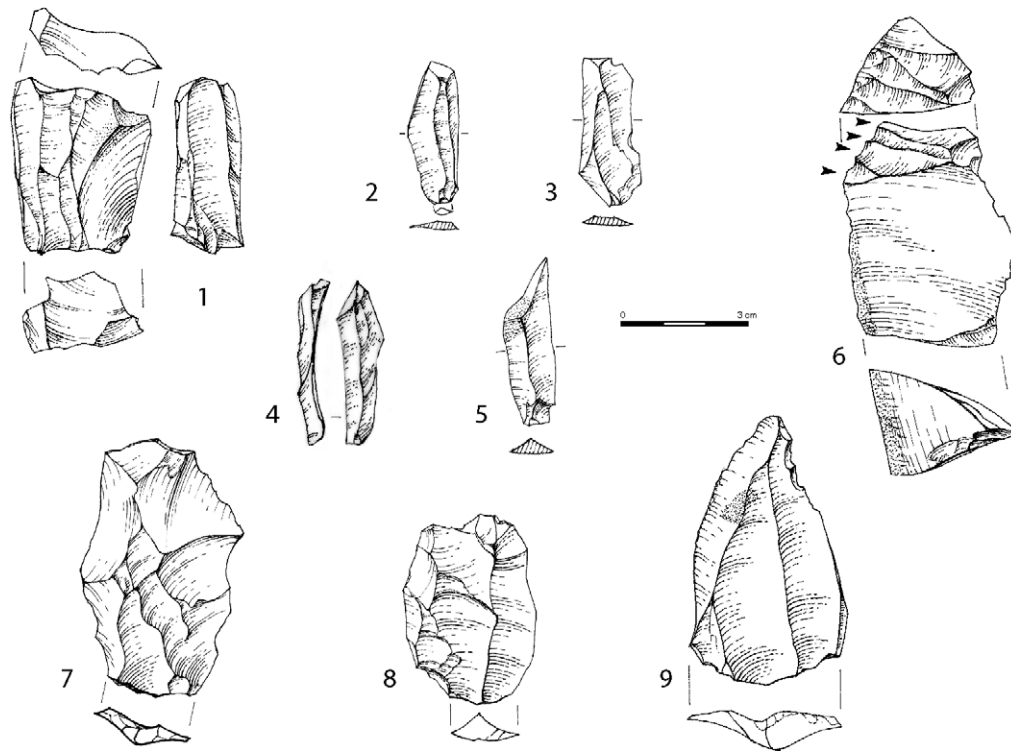


Figure 5.21. Hayonim Layer Lower E (units 6–4), Early MP. 1. Bladelet core. 2, 3, 5. Bladelets. 4. Lamellar CTE. 6. Burin-core?. 7–9. Short Levallois products.

than in the lower units. These are mainly blades, while the points obtained directly by flaking are always much less abundant (Table 5.42), regardless of the flaking system used (Levallois or Laminar).

As reported in the lower units, a production of small blades and bladelets was recognised in these intermediate units (Figure 5.21: 1–6). In general, very few (unit 5, $n = 23$; unit 6, $n = 16$), they are however a little better represented in unit 4. Some of them, often small blades, correspond to core maintenance products. It is also worth noting the presence of flakes bearing traces of previous lamellar removals (CTE or flaking accident?). The production of small, elongated blanks embedded within production systems comparable to those of the blades took therefore place onsite, as in the lower units. Again, a number of burin spalls corresponds to the probable exploitation of core-burins, or even classical burins (Figure 5.21: 6).

5.5.3.2.2.1 Morphology of the blades and elongated points

As in the lower units, there is a high degree of morphological variability in the blade production (as shown by the fairly high coefficients of variation), largely due to the flaking systems used (in particular, Laminar type D2), in which the core shaping phase is minimal and often limited to the part of the core that would be exploited.

Overall, the elongated blanks, mainly blades, have distal ends that are most often quadrangular, though subtriangular and sub-oval morphologies are also common (Table 5.43). True triangular morphologies (proximally wide blades, clearly pointed) are few. However, the blades and points obtained during the flaking process, which generally have an irregular morphology, show a strong tendency toward globally convergent edges (42 to 90%; Table 5.43), a little less clear characteristic in unit 4 where more or less parallel edges increase.

As in units 10 to 7–8, these elongated products are mainly obtained by parallel unidirectional removals followed closely by convergent unidirectional patterns for units 5 and 6, and by bidirectional patterns in unit 4 (Table 5.44).

We shall now consider the two main blades categories (Levallois and Laminar).

	Total blades/elongated points			Levallois blades/elongated points			Laminar blades/points		
	Unit 6	Unit 5	Unit 4	Unit 6	Unit 5	Unit 4	Unit 6	Unit 5	Unit 4
Edges	N = 80	N = 71	N = 212	N = 33	N = 10	N = 31	N = 21	N = 39	N = 97
	%	%	%	%	%	%	%	%	%
parallel	0.00	1.41	1.89	0.00	0.00	0.00	0.00	2.56	4.12
more or less parallel	20.00	15.49	33.96	18.18	10.00	41.94	23.81	17.95	36.08
convergent	65.00	73.24	47.64	72.73	90.00	48.39	47.62	69.23	42.27
divergent	15.00	9.86	16.51	9.09	0.00	9.68	28.57	10.26	17.53
Distal ends	N = 117	N = 119	N = 282	N = 46	N = 20	N = 40	N = 30	N = 58	N = 127
	%	%	%	%	%	%	%	%	%
subovular	32.48	21.85	26.60	39.13	20.00	22.50	30.00	15.52	21.26
subtriangular	29.06	40.34	26.24	32.61	55.00	27.50	23.33	46.55	25.20
subquadrangular	38.46	37.82	47.16	28.26	25.00	50.00	46.67	37.93	52.76

Elongated Levallois products:

These products are mostly wide thin blades (Table 5.45) with thin trapezoidal sections in their proximal part, associated with trapezoidal or triangular sections distally. Elongated points are rare, a little less so in unit 5 (Table 5.42) (Figure 5.20: 2), but once again, the blades often have convergent edges (less so in unit 4) (Table 5.43).

There is no obvious dominance in the dorsal scar patterns (Table 5.44). All three patterns (bidirectional/unidirectional, parallel and convergent) are well represented, with a slight dominance of one or the other depending on the unit. The slightly more pronounced bidirectional patterns in unit 4 are associated with an increase in more or less parallel edges, while in unit 5, subtriangular morphologies are slightly more frequent, in association with an increased number of points, which are generally prepared by unidirectional convergent removals (Tables 5.43, 5.44).

Laminar products:

The Laminar products include thick wide blades (resulting from exploitation of the broad surface of the core) (Figure 5.20: 5, 7) whose numbers are equal to those of the thick narrow blades, which are, however, less numerous than in the lower units (Table 5.18). These products most often have thick trapezoidal sections in their proximal zone, in association with thick triangular sections in the distal zone. Elongated points are very rare (Table 5.42) (Figure 5.20: 6). The blades are subquadrangular or subtriangular in morphology (Table 5.43). Again, the edges are generally convergent (42 to 70%; Table 5.43), although this tendency is slightly less marked in unit 4.

These blades were produced via diverse patterns (Table 5.44): generally unidirectional convergent flaking dominates, but not by much, whereas bidirectional flaking dominates in unit 4 (Figure 5.20: 5, 7), where the Laminar production is highly developed. In fact, the entire unit 4 production (Levallois and Laminar) is characterised by a bidirectional flaking system.

We must thus emphasise the importance in these units of a marked tendency toward converging edges, not only for the points (which are not very abundant) but also for the blades in general, a feature already noted in the assemblages of units 10 to 7–8.

5.5.3.2.2.2 Striking platforms (Table 5.46)

Faceted butts dominate the entire elongated production (always well over 55%). Faceting is clear in the case of Levallois productions, but faceted butts are also strongly represented (and superior to plain butts) in the Laminar production. Only unit 4 shows a dominant proportion of plain butts. We should note, however, as for the lower units,

Table 5.43. Hayonim units 6 to 4 – General characteristics of blades and elongated points. Percentages calculated from the number of artefacts on which the characteristics are identifiable.

Table 5.44. Hayonim units 6 to 4 – Dominant dorsal scar patterns of the elongated products. Excluding indeterminate patterns. KEY: unid par = unidirectional parallel; unid conv = unidirectional convergent; bidir = bidirectional; centr = centripetal.

Unit	Total elongated		Levallois		Laminar	
	N = 125	%	N = 122	%	N = 294	%
Unit 4	unid par	40.80	unid par	39.34	unid par	37.07
	unid conv	32.00	unid conv	31.15	bidir	33.33
Unit 5	N = 122	%	N = 21	%	N = 55	%
	unid par	39.34	unid conv	42.86	unid conv	43.64
Unit 6	unid conv	31.15	bidir	33.33	unid par	29.09
	N = 125	%	N = 48	%	N = 125	%
	unid par	40.80	unid par	39.58	unid par	40.80
	unid conv	32.00	unid conv	33.33	unid conv	32.00

	Levallois blades/elongated points						Laminar blades /elongated points						Total blades /elongated points					
	Unit 6		Unit 5		Unit 4		Unit 6		Unit 5		Unit 4		Unit 6		Unit 5		Unit 4	
	N	%	N	%	N	%	N	%	N	%	N	%	N	%	N	%	N	%
wide thin	37	67.27	20	83.33	24	50.00	0	0.00	2	2.85	0	0.00	46	31.08	36	24.16	50	13.97
wide thick	9	16.36	4	16.67	5	10.42	17	41.46	38	54.29	77	49.36	51	34.46	62	41.61	133	37.15
narrow thin	8	14.55	0	0.00	17	35.42	0	0.00	3	4.29	3	1.92	13	8.78	10	6.71	42	11.73
narrow thick	1	1.82	0	0.00	2	4.16	24	58.54	27	38.57	76	48.72	38	25.68	41	27.52	133	37.15
Total	55	100.00	24	100.00	48	100.00	41	100.00	70	100.00	156	100.00	148	100.00	149	100.00	358	100.00

Table 5.45. Hayonim units 6 to 4 – Morphologies of the elongated products. Excluding blanks of retouched tools.

Unit	Total elongated			Total elongated Levallois			total Laminar		
	identifiable butts	faceted	plain	identifiable butts	faceted	plain	identifiable butts	faceted	plain
	N	%	%	N	%	%	N	%	%
Unit 4	165	55.20	52.73	43	55.81	37.21	122	36.89	58.20
Unit 5	74	62.16	36.49	18	*		56	60.71	37.50
Unit 6	70	68.57	30.00	42	69.05	28.57	28	67.86	32.14

Table 5.46. Hayonim units 6 to 4 – Faceted versus plain butts for the elongated products. Small samples are noted by an asterisk. Percentages are of total number of identifiable butts.

that the faceted butts of the Laminar production often display only two or three, more or less well-defined facets. These observations suggest that the striking platform was less intensively prepared on the Laminar cores.

5.5.3.2.2.3 Morphometry (Tables 5.47a, b)

All the blades in the assemblage have average lengths (mean: 61–62 mm), with a L/W ratio remarkably similar from one unit to another (approx. 2.62–2.64; Table 5.47a). Laminar blades and points are overall longer but the difference is not statistically significant. On the other hand, these pieces are much thicker than their Levallois counterparts, resulting in significant differences in the W/T ratios (T-tests: significant differences for thickness and W/T; Table 5.47a).

Differences also appear in the butt thicknesses, which are greater in the Laminar system than in the Levallois one (Table 5.47b). This is an important feature that goes hand in hand with the roughly faceted butts, which are different from those of the thinner Levallois products. These features undoubtedly resulted from a different flaking gesture (internal percussion), which would be similar, on the other hand, in the case of the plain butts and the roughly faceted butts of the Laminar system. It is important to note that all of these morphometric features are remarkably similar to those observed in the lower units.

Unit	Total blades/elongated points						Levallois blades/elongated points						Laminar blades/points					
	N	Length	Width	Thickness	L/W	W/T	N	Length	Width	Thickness	L/W	W/T	N	Length	Width	Thickness	L/W	W/T
Unit 4	244	61.65 (17.25)	24.29 (7.35)	8.62 (3.74)	2.62 (0.57)	3.12 (1.11)	38	61.89 (15.58)	25.79 (7.08)	6.18 (2.15)	2.45 (0.41)	4.35 (1.00)	110	65.88 (19.08)	25.58 (7.94)	9.92 (3.48)	2.65 (0.60)	2.69 (0.65)
Unit 5	90	61.21 (14.15)	23.80 (6.33)	8.07 (2.94)	2.64 (0.54)	3.22 (1.07)	14	56.57 (10.75)	23.29 (3.73)	5.29 (1.27)	2.43 (0.29)	4.55 (0.94)	45	62.80 (14.45)	24.11 (6.34)	8.69 (2.54)	2.68 (0.53)	2.88 (0.67)
Unit 6	99	61.89 (12.79)	24.10 (5.56)	8.12 (4.30)	2.62 (0.46)	3.43 (1.21)	38	60.05 (11.93)	23.79 (5.51)	5.66 (1.66)	2.57 (0.39)	4.38 (0.96)	26	66.27 (13.72)	24.19 (4.55)	10.61 (5.48)	2.79 (0.59)	2.60 (0.79)
T-test for Laminar versus Levallois elongated products																		
p values at an alpha [significance] level of 0.05																		
	Unit 6	Unit 5	Unit 4															
Length	0.059	0.143	0.248															
Width	0.759	0.646	0.887															
Thickness	<0.0001	<0.0001	<0.0001															
L/W	0.077	0.111	0.057															
W/T	<0.0001	<0.0001	<0.0001															
Coefficient of variation for elongated products																		
	Unit 6	Unit 5	Unit 4															
Length CV	0.21	0.23	0.28															
Width CV	0.23	0.27	0.30															
Thickness CV	0.53	0.36	0.43															

Table 5.47a. Hayonim units 6 to 4 – Metrical attributes (in mm) of the elongated products. Complete artefacts only. Standard deviations are given in parentheses.

Unit	Total blades/elongated points			Levallois elongated			Laminar blades/points		
	N	Width	Thickness	N	Width	Thickness	N	Width	Thickness
Unit 4	213	15.79 (6.21)	5.95 (2.59)	34	17.41 (7.35)	5.12 (2.57)	99	16.97 (6.24)	6.52 (2.71)
Unit 5	83	16.49 (5.39)	6.01 (2.47)	*			43	18.84 (5.63)	6.77 (2.38)
Unit 6	88	16.53 (5.39)	5.66 (1.99)	34	17 (5.86)	5 (1.89)	23	18.26 (4.97)	6.09 (2.04)

Table 5.47b. Hayonim units 6 to 4 – Metrical attributes (in mm) of the elongated product butts. Small samples are noted by an asterisk. Complete artefacts only. Standard deviations are given in parentheses.

T-test for Laminar versus Levallois elongated product butts			
p values at an alpha [significance] level of 0.05			
	Unit 6	Unit 5	Unit 4
Butt width	0.402	*	0.734
Butt thickness	0.044	*	0.010
Butt W/T	0.771	*	0.001

Table 5.48. Hayonim units 6 to 4 – Cortical elongated blanks (blades and elongated points).

Unit	Total elongated blanks		Cortical elongated blanks		Including cortical back	
	N	%	N	%	N	%
Unit 4	358		147	41.06	62	17.32
Unit 5	154		57	37.01	28	18.18
Unit 6	150		62	41.33	26	17.33

5.5.3.2.2.4 Elongated cortical blanks

A sizable proportion of these elongated blanks (39–41%; Table 5.48) have cortex on their dorsal surface or in the form of a back or back + overshoot. Cortex on the upper surface is generally not prevalent, however, and the proportion of pieces with cortical backs is not very high (17–18%; Table 5.48). A substantial proportion of these cortical backs or backs + cortical overshooting can be considered as CTEs implemented to create or maintain the convexities necessary to detach blanks from the core (see *infra*).

5.5.3.2.3 Levallois production

Table 5.12 gives the total number of blades as well as those evaluated for each production system.

The Levallois production is smaller here than in the lower units (11.7 to 21%; Table 5.11), especially in units 4 and 5, which have the lowest proportion in the sequence. The full range of Levallois products is present (Figures 5.20: 1–3; 5.21: 7–9), however, with a notable decrease in blades and elongated points. Short blanks (flakes and points), more abundant than in the lower units, are now in the majority (69 to 76% of Levallois products; Table 5.11).

5.5.3.2.3.1 Composition

Among these short products, the morphology of the flakes with an elongated tendency (L/W 1.52–1.66) are most often subquadrangular (Table 5.49), followed by subtriangular (in units 6 and 5). The presence of short Levallois points (L/W between 1.5–1.6; Table 5.50) is notable, especially in unit 6 (10.8%), although they are less abundant than in the underlying units. And as in these units, they are often more numerous than the elongated points (units 6 and 4; Table 5.49).

Unit 4	Levallois flakes		Levallois short points		Levallois blades		Levallois elongated points		Total Levallois	
	N = 137		N = 17		N = 36		N = 4		N = 194	
	n	%	n	%	n	%	n	%	n	%
subcirc/ovalar	29	21.17	0	0.00	8	22.22	1	*	38	19.59
subtriangular	20	14.60	17	100.00	8	22.22	3	*	48	24.74
subquadrangular	88	64.23	0	0.00	20	55.56	0	*	108	55.67

Unit 5	Levallois flakes		Levallois short points		Levallois blades		Levallois elongated points		Total Levallois	
	N = 37		N = 5		N = 15		N = 5		N = 62	
	n	%	n	%	n	%	n	%	n	%
subcirc/ovalar	5	13.51	0	0.00	4	*	0	0.00	9	14.52
subtriangular	8	21.62	5	100.00	6	*	5	100.00	24	38.71
subquadrangular	24	64.87	0	0.00	5	*	0	0.00	29	46.77

Unit 6	Levallois flakes		Levallois short points		Levallois blades		Levallois elongated points		Total Levallois	
	N = 85		N = 19		N = 42		N = 4		N = 150	
	n	%	n	%	n	%	n	%	n	%
subcirc/ovalar	20	23.53	0	0.00	18	42.86	0	0.00	38	25.33
subtriangular	21	24.71	19	100.00	11	26.19	4	100.00	55	36.67
subquadrangular	44	51.76	0	0.00	13	30.95	0	0.00	57	38.00

Table 5.49. Hayonim units 6 to 4 – Morphologies of the Levallois blanks. Percentages are of 'total number of identifiable morphologies'.

Unit	Levallois flakes						Short Levallois points					
	N	Length	Width	Thickness	L/W	W/T	N	Length	Width	Thickness	L/W	W/T
Unit 4	117	47.07	31.74	6.53	1.52	5.15	16	45.63	30.00	5.81	1.53	5.58
		(11.70)	(7.96)	(2.1)	(0.33)	(1.44)		(11.06)	(4.66)	(1.72)	(0.34)	(1.87)
Unit 5	27	50.26	33.74	6.59	1.60	5.15	5	*	*	*	*	*
		(11.68)	(13.32)	(1.6)	(0.37)	(1.38)						
Unit 6	67	50.19	30.63	5.99	1.66	5.39	17	46.18	29.47	6.29	1.59	4.92
		(11.89)	(6.92)	(1.67)	(0.25)	(1.49)		(16.37)	(10.54)	(2.20)	(0.27)	(1.44)

Table 5.50. Hayonim units 6 to 4 – Metrical attributes (in mm) of the short Levallois blanks. Small samples are noted by an asterisk. Complete artefacts only. Standard deviations are given in parentheses.

5.5.3.2.3.2 Striking platforms

Careful preparation of the striking platforms should be noted for all of the Levallois products, reflected by a clear dominance of faceted butts, most often convex (Table 5.51). Only unit 4 has a clearer presence of plain butts, whether for flakes or blades, undoubtedly related to the importance of the Laminar production. The striking platform preparations of the short Levallois points are particularly careful (IF = 88 to 95), with a non-negligible presence of the so-called *chapeau de gendarme* butts. Short points with a broad base, a morphology that is associated with this specific striking platform preparation (Meignen 1995, 2019) are present, though not numerous (small number of short points).

5.5.3.2.3.3 Dorsal scar patterns

The organisation of the removals on the upper face (Table 5.52) shows, for the whole Levallois production (flakes, blades, points), a dominant unidirectional convergent preparation/exploitation pattern, except in unit 4, which is distinguished by a bidirectional

Unit	Levallois flakes			Levallois short points			Levallois blades			Total Levallois		
	identifiable butts	faceted	plain	identifiable butts	faceted	plain	identifiable butts	faceted	plain	identifiable butts	faceted	plain
	N	%	%	N	%	%	N	%	%	N	%	%
Unit 4	146	63.01	31.51	17	88.24	11.76	48	55.81	37.21	206	63.59	31.07
		(3.42)			(17.65)						(3.88)	
Unit 5	36	72.22	25.00	5	*	*	18	*	*	59	71.19	27.12
		(2.77)									(1.69)	
Unit 6	102	79.41	18.63	18	94.44	5.56	42	69.05	28.57	162	78.4	19.75
		(3.92)			(33.33)						(6.17)	

Table 5.51. Hayonim units 6 to 4 – Faceted versus plain butts for the Levallois blanks. Small samples are noted by an asterisk. Percentages are of ‘total number of identifiable butts’. The percentage of *chapeau de gendarme* butts is shown italicised in parentheses.

Table 5.52. Hayonim units 6 to 4 – Dominant dorsal scar patterns of the Levallois blanks. Excluding indeterminate patterns. Small samples are noted by an asterisk. KEY: unid par = unidirectional parallel; unid conv = unidirectional convergent; bidir = bidirectional; centr = centripetal.

Unit	Total Levallois		Levallois flakes		Short Levallois points		Elongated Levallois	
Unit 4	N = 211	%	N = 148	%	N = 17	%	N = 46	%
	bidir	33.65	bidir	33.78	unid conv	76.47	bidir	39.13
	unid par	23.22	unid par	23.65	bidir	17.65	unid par	30.43
	% centr	7.11	% centr	9.46	% centr	0.00	% centr	2.17
Unit 5	N = 67	%	N = 41	%	N = 5	%	N = 21	%
	unid conv	37.31	unid conv	31.71	unid conv	*	unid conv	42.86
	unid par	22.39	unid par	26.83	bidir	*	bidir	33.33
	% centr	4.48	% centr	7.32	% centr	0.00	% centr	0.00
Unit 6	N = 157	%	N = 90	%	N = 19	%	N = 48	%
	unid conv	46.50	unid conv	44.44	unid conv	89.47	unid par	39.58
	bidir	23.57	bidir	26.67	bidir	5.26	unid conv	33.33
	% centr	1.91	% centr	3.33	% centr	0.00	% centr	0.00

dominant pattern. These dominants are followed, depending on the units, by parallel unidirectional (units 5 and 4) or bidirectional (unit 6) patterns. This is the situation observed for flakes and, to a lesser extent, for blades, whereas points are mostly prepared by unidirectional convergent removals. We should thus note, in this intermediate assemblage, the development of bidirectional scars, especially in unit 4 (Table 5.52).

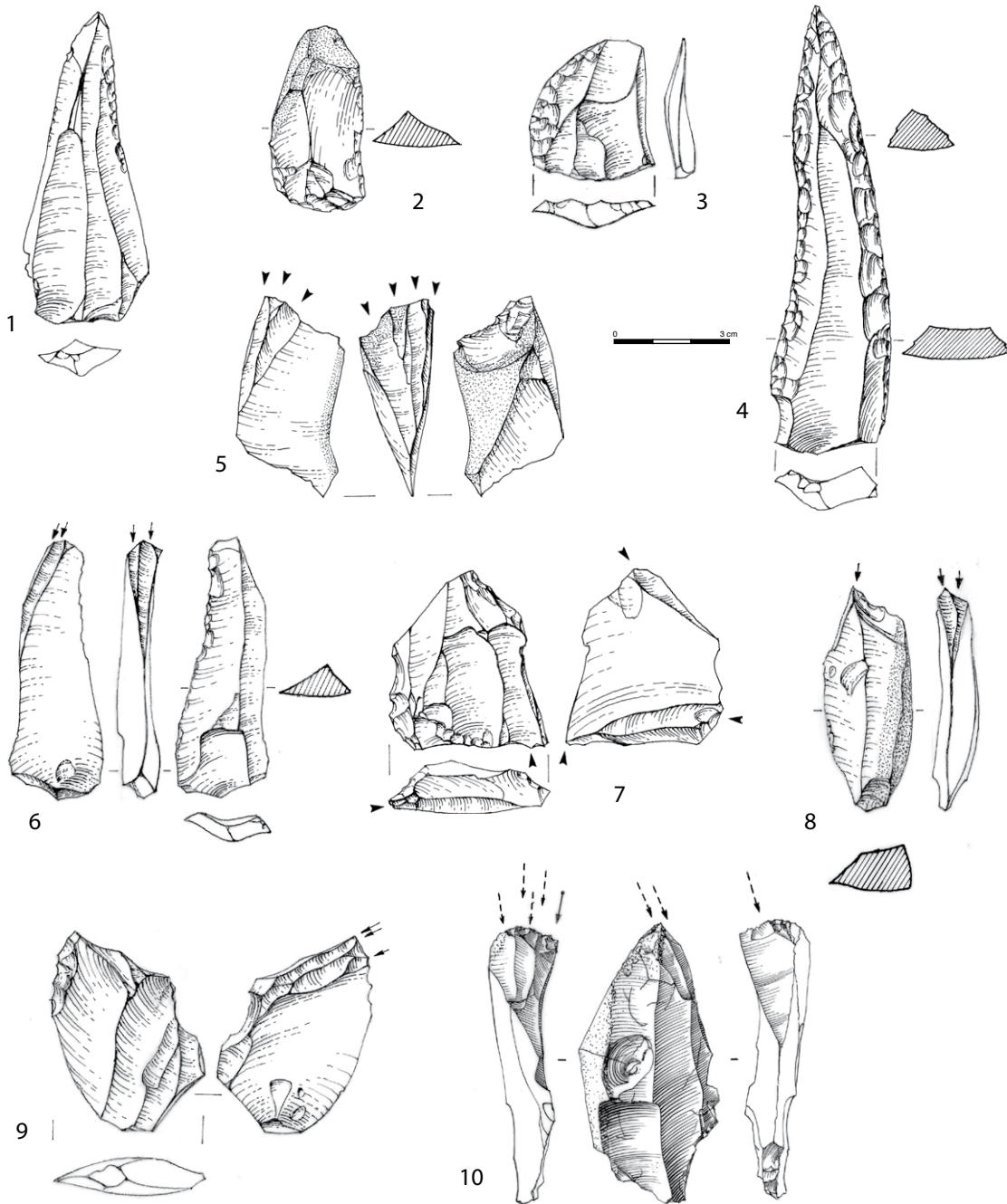
We should also note that in all of these units, as in the lower units, there are very few centripetal patterns (1.9 to 7.1% for all Levallois; Table 5.52), even if this pattern is slightly more pronounced for Levallois flakes, particularly in unit 4. These remarks, based on unworked Levallois products, remain similar when we look at unworked and retouched Levallois products (same dominant features).

5.5.3.2.4 Retouched tools (Figure 5.22)

N.B. The small number of artefacts in units 5 (n = 20) and 6 (n = 38) made it difficult to conduct a detailed statistical study of the tools. Only unit 4 (n = 130) enabled a more detailed study.

5.5.3.2.4.1 Tool assemblage composition (Tables 5.53, 5.54)

These intermediate units are characterised by a low proportion of retouched products (2.7 to 4.6%; Table 5.54), clearly less than in the lower units (Table 5.13). Side-scrapers now generally dominate the tool assemblage, (Figure 5.22: 2, 3), with a marked development of



UP-type tools in parallel (Table 5.54; Figure 5.22: 5–10). The number of retouched blades and elongated points has decreased relative to the lower units (Table 5.13), even if they are slightly more developed in unit 4 (22.3% of the tools) (Figure 5.22: 1, 4). In particular, the low numbers of retouched elongated points should be noted, whereas this was a particularly remarkable feature in the lower units.

In unit 4 (the only unit with a sufficient sample to discuss the tool assemblage composition in more detail), blades with one or two retouched edges are represented in equal proportions (Table 5.53). The retouch is most often scalar ($n = 18$ out of 24). The blanks are rarely cortical (no selection of this type of blank for retouching). Although few in number, the retouched blades from unit 4 have characteristics close to those of the lower units.

Figure 5.22. Hayonim Layer Lower E (units 6–4), Early MP – Retouched tools.

1, 4. Retouched elongated points (4 with 'superimposed scalar' retouch). 2, 3. Side-scrapers. 5–10. Burins (5, 7, 9 burin-cores?).

Tool category	Unit 6	Unit 5	Unit 4
	N	N	N
Retouched blade (one edge)	1	1	11
Retouched blade (two edges)	0	0	13
Short retouched point	2	0	1
Elongated retouched point	2	2	5
Simple scraper	9	5	25
Double scraper	2		5
<i>Déjeté</i> scraper			3
Transverse scraper			2
Scraper on ventral face			1
Abrupt ret scraper	1		1
Burin	7	6	16
Awl	1		
Truncation			4
Notch	2		7
Denticulate	3	1	9
Retouches on ventral face	2		1
Retouched flake/blade	2	2	7
Miscellaneous		1	15
Nahr Ibrahim piece	3	2	2
Notch+Nahr Ibrahim	1		2
Total	38	20	130

Table 5.53. Hayonim units 6 to 4 – Typological breakdown.

Unit	Total assemblage		without cores		Retouched products		Total retouched elongated blank		Retouched blades		Elongated retouched points		Short retouched points		Scrapers		Scrapers on ventral face		UP tools		Burins		Notches + denticulates	
	N	%	N	%	N	%	N	%	N	%	N	%	N	%	N	%	N	%	N	%	N	%	N	%
Unit 4	2383		2299		130	5.65	29	22.31	24	18.46	5	3.85	1	0.77	37	28.46	1	0.77	20	15.38	16	12.31	16	12.31
Unit 5	786		752		20	2.66	3	15.00	1	5.00	2	10.00	0	0.00	5	25.00	0	0.00	6	30.00	6	30.00	1	5.00
Unit 6	978		937		38	4.06	3	7.89	1	2.63	2	5.26	2	5.26	12	31.58	2	5.26	8	21.05	7	18.42	5	13.16

Table 5.54. Hayonim units 6 to 4 – Frequencies of retouched tool categories. Percentage of retouched products is of 'total assemblage without cores'. Percentages for each category of retouched pieces are of 'total number of retouched products'.

The retouched tools therefore mainly comprise tools on short blanks, most often non-Levallois (Table 5.55). Nearly all of the scrapers have a single retouched edge (usually lateral, sometimes transverse) (Table 5.53). Tools with convergent edges are remarkably few; in particular, short Levallois retouched points are poorly represented (Table 5.54), although they were a characteristic component of the underlying units.

In contrast to the lower levels, the almost complete disappearance of tools on ventral face should also be noted (Table 5.54).

Made most often on non-cortical blanks, most of the side-scrapers were transformed by scalar retouch (data available only for unit 4: n = 31 out of 37), and much less often by marginal retouch (n = 4).

On the other hand, UP-type tools are prominent in this assemblage (from 15 to 30%; Table 5.54). They are mainly burins, either classic burins (angle burin, dihedral burin, transverse burin) (Figure 5.22: 6, 8, 10) or multiple burins from a notch, whose removals

Unit	Identifiable blanks	On elongated blank		On short Levallois blank		On short non-Levallois blank	
	N	N	%	N	%	N	%
Unit 4	111	39	35.14	15	13.51	57	51.35
Unit 5	17	4	*	1	*	12	*
Unit 6	32	9	28.13	6	18.75	17	53.13

Table 5.55. Hayonim units 6 to 4 – Blank types of the retouched tools. Data not available are noted by an asterisk. Percentages are of 'total number of identifiable blanks'.

were made either in the thickness (narrow part) of the blank (Figure 5.22: 5) or partly on the wide face of the flake blank. In several cases, the term burin-core is more appropriate since the microblades (recognised in the products, even if they are not very numerous) were mostly detached from the thickness (narrow part) of the flakes (Figure 5.22: 5, 7, 9). This is especially true in unit 4. Some of these pieces, which were clearly very productive, were counted among the lamellar cores (Figure 5.21: 6). The burin blanks are most often flakes or blades; the burin-cores are on thicker, often cortical blanks.

Notches and denticulates are not very abundant (Table 5.54) but are a bit more numerous in unit 4. In this unit, we should also note the presence of several flakes or blade fragments that have very localised retouches and therefore, are considered as 'retouched flake' or 'miscellaneous'.

The Nahr Ibrahim technique pieces are again scarce (Table 5.13). They are generally made on thick flakes.

5.5.3.2.4.2 Tool blanks (Table 5.55)

Most of the tools are made on short, most often non-Levallois, flakes. We should note the presence of tools on blades as well, in much lower proportions, however, than in the lower units (35.1% in unit 4; 28.1% in unit 6). In unit 5, the numbers are too small to be included in this calculation.

5.5.3.2.4.3 Striking platforms

In unit 4 (the only unit with a sufficient sample), faceted butts slightly dominate plain butts. This small difference is probably related to the development of Laminar-related blanks in this unit, in which plain butts dominate (Table 5.46).

5.5.3.2.5 Cores (Tables 5.56, 5.57) (Figure 5.23)

Proportionally numerous in these intermediate units (3.6 to 4.2%), the cores are frequently made on the ventral face of flakes (24.4 to 38.2%; Table 5.56). Those producing flakes are the most abundant as in the whole sequence (71.8 to 82.9%), but blade cores are still well represented, often with a semi-prismatic morphology, especially in units 5 and 4 (15.3%, 17.7%, respectively; Table 5.56), where their numbers sometimes exceed those identified in the lower units.

Few Levallois cores were identified (8.8–14.6%), and they are generally typical (Figure 5.23: 1, 2). Atypical Levallois cores, which correspond either to cores that are structurally Levallois, but whose exploitation was poorly controlled, or to cores that are probably Levallois, but broken, are not numerous either (Levallois? cores: 2.9 to 17.1%). These two core categories, most often recurrent, are mostly exploited by uni/bidirectional removals, and rarely by centripetal ones (Table 5.57).

While elongated products are less abundant here than in the lower units (see above), semi-rotating cores remain proportionally quite numerous (Table 5.57), especially in units 5 and 4, the latter also being distinguished by a larger production of small blades and bladelets (Table 5.56). These cores, whose exploitation often ends with elongated flakes rather than true blades, are most often unidirectional (parallel or more rarely convergent) or bidirectional (with slightly (Figures 5.12: 1; 5.23: 3) or highly (Figures 5.13: 3; 5.21: 1, for bladelets; 5.23: 4) offset striking platforms, the latter being the most frequent). The

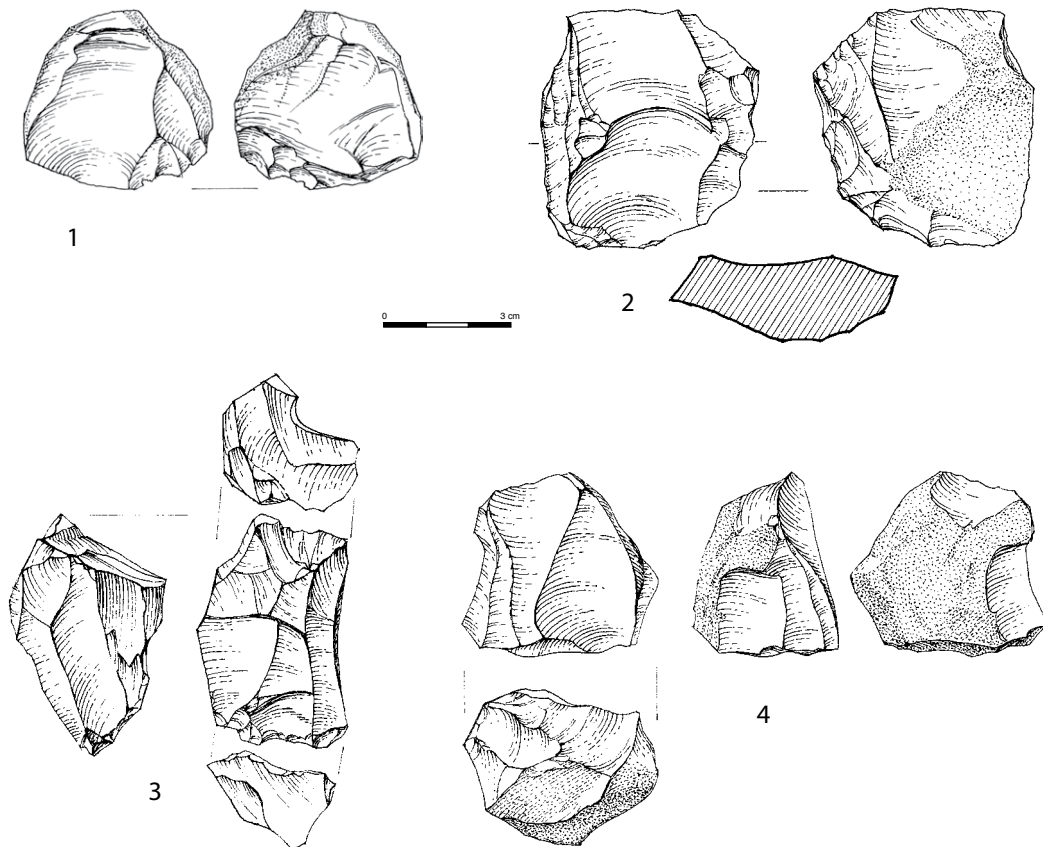


Figure 5.23. Hayonim Layer Lower E (units 6–4), Early MP – Cores. 1, 2. *Levallois cores*. 3. *Laminar bidirectional core with slightly offset striking platforms*. 4. *Laminar bidirectional core with highly offset striking platforms*.

Unit	Total assemblage	Cores		On flake blank		Flake cores		Blade cores		Bladelet cores		Levallois cores		Levallois? cores		Preferential surface cores		'Semi-tournant' cores	
		N	N	%	N	%	N	%	N	%	N	%	N	%	N	%	N	%	N
Unit 4	2392	85	3.55	27	31.76	61	71.76	13	15.29	9	10.59	9	10.59	14	16.47	11	12.94	22	25.88
Unit 5	786	34	4.33	13	38.24	25	73.53	6	17.65	3	8.82	3	8.82	1	2.94	4	11.76	13	38.24
Unit 6	978	41	4.19	10	24.39	34	82.93	4	9.76	3	7.32	6	14.63	7	17.07	9	21.98	8	19.51

Table 5.56. Hayonim units 6 to 4 – Main categories of cores. Percentages are of 'total number of cores', except core percentage calculated from the total assemblage.

broad face of the core was most often exploited, followed by the broad face + narrow face. Frontal flaking (on the narrow face) is much less common. The striking platform preparations are minimal, consisting of one to three large, very inclined removals. In a very few cases, the transverse convexity and width of the flaking surface were roughly controlled by removals from the back of the core ((Figure 5.12: 1). The variants of the semi-rotating flaking system described here based on the cores are also identified by the presence of characteristic overshoot/overshooting blades. (Figure 5.24 : 1–5).

These two main core/flaking system categories are completed by a specific production that we have called 'preferential surface exploitation', which is quite frequent here (11.8 to 22% of cores; Table 5.56). This system enables the detachment of small flakes (sometimes called 'Kombewa flakes') bearing traces of the lower face of the core-on-flake from which they originate. These small flakes thus have a working edge that is at least partially biconvex. They were not subsequently retouched into tools, however. It is thus difficult to determine whether this type of production was intentional or opportunistic.

Core types		Unit 6		Unit 5		Unit 4	
Levallois cores		Total	6		3		9
including	preferential	2			1		2
	recurrent	4			2		7
	<i>including</i>		centr	0	0		4
			bidir	0	1		0
			unid par	2	0		1
			unid conv	0	1		1
			crossed	2	0		1
Levallois ? cores		Total	7		1		14
including	preferential	0			0		1
	recurrent	7			1		10
	<i>including</i>		centr	1	0		1
			bidir	2	0		2
			unid par	2	1		4
			unid conv	2	0		2
			crossed	0	0		1
	indeterminate						3
Semi-tournant cores		Total	8		13		22
			1 str pltf/unid conv	0	2		3
			1 str pltf/unid par	5	5		5
			2 str pltf/ bidir opp	0	4		5
			2 str pltf/ twisted	3	2		8
			indeterminate/ broken				1
Preferential surface exploitation		9		4	11		
Upper surface exploitation (cf Nahr Ibrahim)		0		0	0		
Others	multiple str. pltf	3			2		7
	isolated removals	7			7		18
	discoid	1			4		4
Total		41		34	85		

Table 5.57. Hayonim units 6 to 4 – Detailed counts of cores. KEY: Str pltf = striking platform; unid par = unidirectional parallel; unid conv = unidirectional convergent; bidir = bidirectional; centr = centripetal.

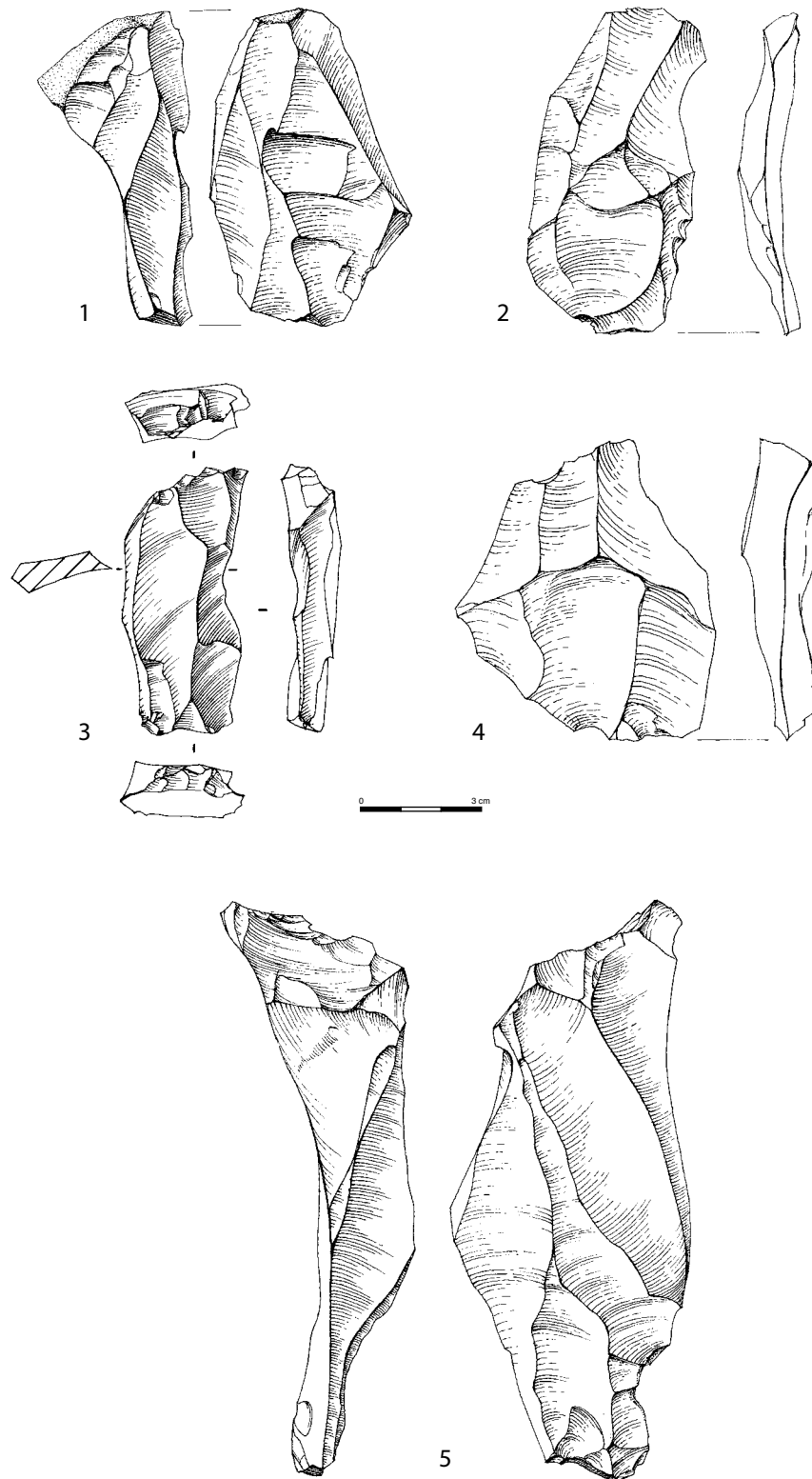


Figure 5.24. Hayonim Layer Lower E (units 6–4), Early MP – Overshot/overshooting pieces, characteristic of the Laminar reduction system. 1. From unidirectional core. 2, 4. From bidirectional core with slightly offset striking platforms. 3, 5. From bidirectional core with highly offset striking platforms.

Finally, there is a fairly large number of much less structured ‘miscellaneous’ cores corresponding either to removals from multiple platforms or to a few unorganised removals. There are also a few discoid cores (1 in unit 6, 4 in unit 5, and 4 in unit 4).

5.5.3.2.6 Core trimming elements (CTEs) (Table 5.58) (Figure 5.25)

In these intermediate units, CTEs are not very numerous, but slightly more abundant in unit 4 (unit 6: n = 35/ unit 5: n = 29/ unit 4: n = 89; Table 5. 58), while debitage is frequent.

These CTEs correspond mainly to elongated *débordants* blades or flakes whose role is to create and maintain the lateral and distal convexities of the core. Given the predominantly uni/bidirectional flaking systems (Levallois or Laminar), the *débordants* products frequently have a cortical back (Figure 5.25: 1, 2, 3). In the case of unidirectional convergent pattern, they are often both intentionally overshot and slightly skewed (*éclats débordants outrepassants*; Meignen 1995, 2019).

As previously mentioned for the lower units, it is often difficult to attribute these cortical *débordants* products to either the Levallois or the Laminar system because the organisation of the removals is similar in the two systems (unidirectional dominant). Only their more or less wide thin/wide thick morphology enables us, in some cases, to distinguish them.

There are very few classic *débordants* products linked to Levallois flaking, present only in unit 4 (n = 10) where they still show a slight increase compared with the lower units. This trend is associated with a slight increase in centripetal pattern noted among the Levallois cores and flakes of this level. But overall, the low representation of classic *débordants* products is consistent with the low representation of centripetal preparation/exploitation of Levallois cores.

Crested blades are rare (unit 6: n = 1; unit 4: n = 2) and consist only of lateral crested blades used to enlarge the flaking surface, thus reflecting the low investment in shaping and maintaining Laminar cores (Figure 5.25: 5, 6).

Moreover, in all of these units, it is important to note the more or less prevalent presence of overshoot/overshooting blades, for which it is often difficult to determine whether the overshooting is the result of an intentional gesture or a flaking accident. In units 6–4, these blades usually originate from the Laminar system. In some cases, the overshooting seems to be intentional and associated with the creation or maintenance of distal convexities (Figure 5.25: 7) and the elongation of the flaking surface (Figure 5.25: 8), thus probably reflecting an intentional operation. In other cases, numerous and easy to identify, this overshoot removes the second offset striking platform or the apical/distal part of the semi-pyramidal core, for example. These pieces then correspond either to a change in the orientation of the flaking surface (intentional?) (Figure 5.24: 3, 5), or to a flaking accident, which ‘disfigures’ the core (Figure 5.24: 1).

5.5.3.2.7 Summary of the main features of units 6–4

These intermediate units are thus characterised by:

- A significant decrease in the number of blades compared with the lower units. However, it is important to note that the characteristics of this production remain the same:
 - the Laminar system is dominant (even more so in these units);
 - the morphology of the blades (subquadrangular/subtriangular), their morphometric characteristics, the tendency to convergent edges, and the

Unit	<i>Débordants</i> with cortical back		<i>Débordants</i> with non-cortical back		Classical <i>débordants</i> including <i>dos limités</i>		Crested blades		Total CTE
	N	%	N	%	N	%	N	%	
Unit 4	76	85.39	1	1.12	10 (4)	11.24	2	2.25	89
Unit 5	29	100.00	0	0.00	0	0.00	0	0.00	29
Unit 6	31	88.57	3	8.57	0	0.00	1	2.86	35

Table 5.58. Hayonim units 6 to 4 – Main categories of CTEs. Among the classical *débordants*, the number of those called *à dos limité* are shown in parentheses.

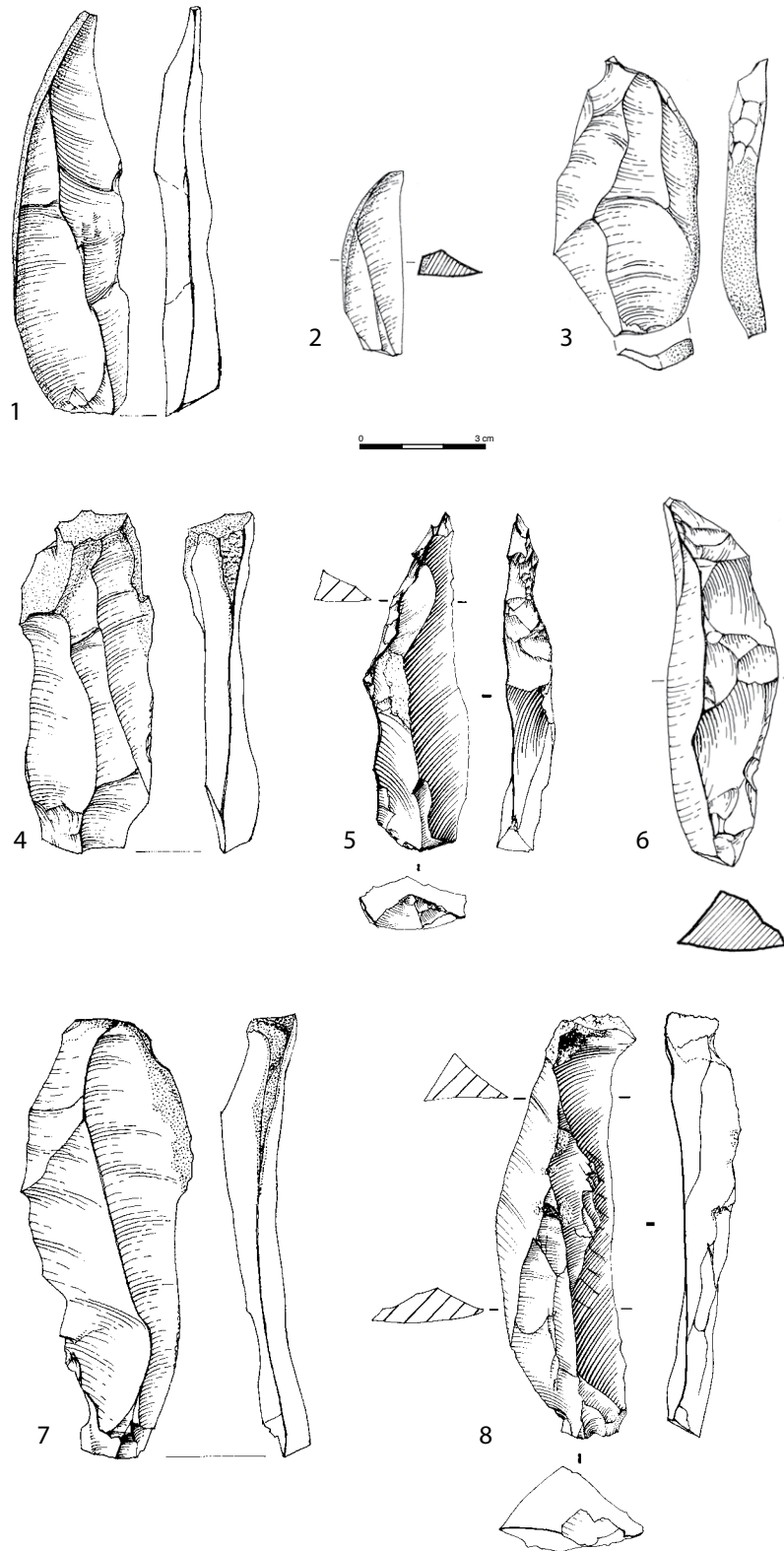


Figure 5.25. Hayonim Layer Lower E (units 6–4), Early MP – CTEs. 1–3. *Cortical-backed débordants products*. 4, 7, 8. *Overshooting blades*. 5, 6. *Crested blades*.

clearly dominant faceting of the butts, are all elements similar to those observed in units 10 to 7–8, and;

- semi-rotating cores are still abundant, although the proportion of blades decreases significantly. Unidirectional parallel and convergent flaking systems dominate, while the bidirectional system develops in unit 4.
- Overall, the Levallois production decreases. Levallois flakes are more frequent but mostly the short points decrease. The characteristics of the Levallois blanks are similar to those of the lower units even if the composition of the whole assemblage changes a bit.
- Another crucial point is that the proportions of retouched products are much lower, especially for retouched blades and points. There is also a decrease in convergent tools (few convergent side-scrapers and retouched points).
- Side-scrapers become the dominant tools, accompanied by an increase in UP tools (mainly burins, especially in unit 4).

Concerning the techno-economic composition of these assemblages, the relatively low blade proportions are surprising given the rather high number of blade cores. The ratios of blades to semi-rotating cores, although clearly lower than those of the underlying levels (unit 6 = 19.6; unit 5 = 12.2; unit 4 = 18.1), suggest that the majority of the production was done onsite, in association with a probable low import of elongated blanks produced off-site (or in another part of the cave). The Levallois products, consisting mainly of flakes, were also mostly made onsite, in association with a possible low import of Levallois products (but the numbers are low) (ratio of Levallois products to Levallois cores: unit 6 = 15; unit 5 = 21.2; unit 4 = 11.7)

Retouched tools are quite rare, especially retouched blades and elongated points. This is probably due to the smaller number of blades in the assemblage.

All this goes hand in hand with very low occupation densities. These results suggest a provisioning of place, with this time, few blade imports, most likely corresponding to short occupations.

5.5.3.3 Lithic production from units 3 and 1–2

Preliminary remarks

During our study of the artefacts from the upper units, we encountered a specific problem that must be explained to understand the slightly different approach that we took for these units (i.e., sometimes studying only a sample of artefacts).

The lithic artefacts of units 1–2 recovered during our excavations (section straightening and excavation of partial squares left by the previous Bar-Yosef excavations) were insufficient for a detailed study of these upper units. In our study, we thus decided to include at least some of the artefacts from the earlier excavations, and primarily, the plotted products, for which the provenance was well controlled. Our analysis of these plotted artefacts showed a bias toward typical objects (tools, Levallois) with a dimension limit for plotted objects above the conventional limit of our excavations (> 2.5 cm). Products such as tools and Levallois products were indeed plotted, while cortical and ordinary products were categorised as unplotted when their lengths were approximately 2.5 cm. This sorting is obvious for cortical and ordinary products (some large cortical pieces are included with the unplotted ones, for example), but does not seem to have been applied to tools, Levallois products, or blades. It was thus necessary to reintegrate into our study the products that should have been plotted so that the balances of the major technological groups would be respected (otherwise, a deficit in cortical products, which are numerous in these levels, would have distorted our results).

To correct this bias, we have thus introduced into our study the artefacts that, based on their dimensions, should have been plotted (cortical and ordinary flakes, tools, Levallois,

blades; in fact this mainly concerns cortical and ordinary flakes), in order to have a fair idea of the overall composition of these assemblages.

Unfortunately, due to a lack of time and the abundance of the artefacts, we could not conduct detailed analyses of all of the artefacts recovered. We have thus carried out, and present in this study, general counts covering the totality of the artefacts (those from our excavations + the artefacts recovered from previous excavations), thus concerning mainly the technological and techno-economic characteristics of the production. We also present more detailed studies of a large sample of tools, blades, and Levallois products, comprising artefacts from our excavations, plus plotted pieces from previous excavations. These detailed studies concern only those categories for which we were able to verify the low bias introduced into the selection. Results obtained on sample are indicated in the corresponding tables.

5.5.3.3.1 Remarks on the techno-economic composition

These assemblages are characterised by high proportions of flaking by-products (ordinary and cortical flakes) (64.5 and 59.3%), and numerous, mostly Levallois, cores (3.9 and 3.8%; Table 5.15). The proportions of retouched products are average (Table 5.10), a bit higher than in units 6–4 but much lower than in the lower units.

These upper levels are also characterised by low lithic artefact densities similar to those estimated in units 6–4 (Table 5.8), thus contrasting with the higher occupation densities in the lower units.

Within the sequence, significant changes are observed in the upper units.

5.5.3.3.2 Levallois production (Figures 5.26; 5.27: 1–2)

5.5.3.3.2.1 Assemblage composition

The changes in these units mainly concern the composition of the Levallois production. The whole range of Levallois blanks (flakes, blades, and points) is still present (Table 5.11), but there is a noticeable decrease in the number of elongated blades and points. The short blanks (especially flakes) thus become the majority (unit 3 = 85.7%; units 1–2 = 83.3%) (Figure 5.26: 1-9). However, it is important to note that in units 1–2, the presence of elongated Levallois blades and points is still substantial (total elongated Levallois = 16.7% of the Levallois blanks) (Figure 5.27: 1–2).

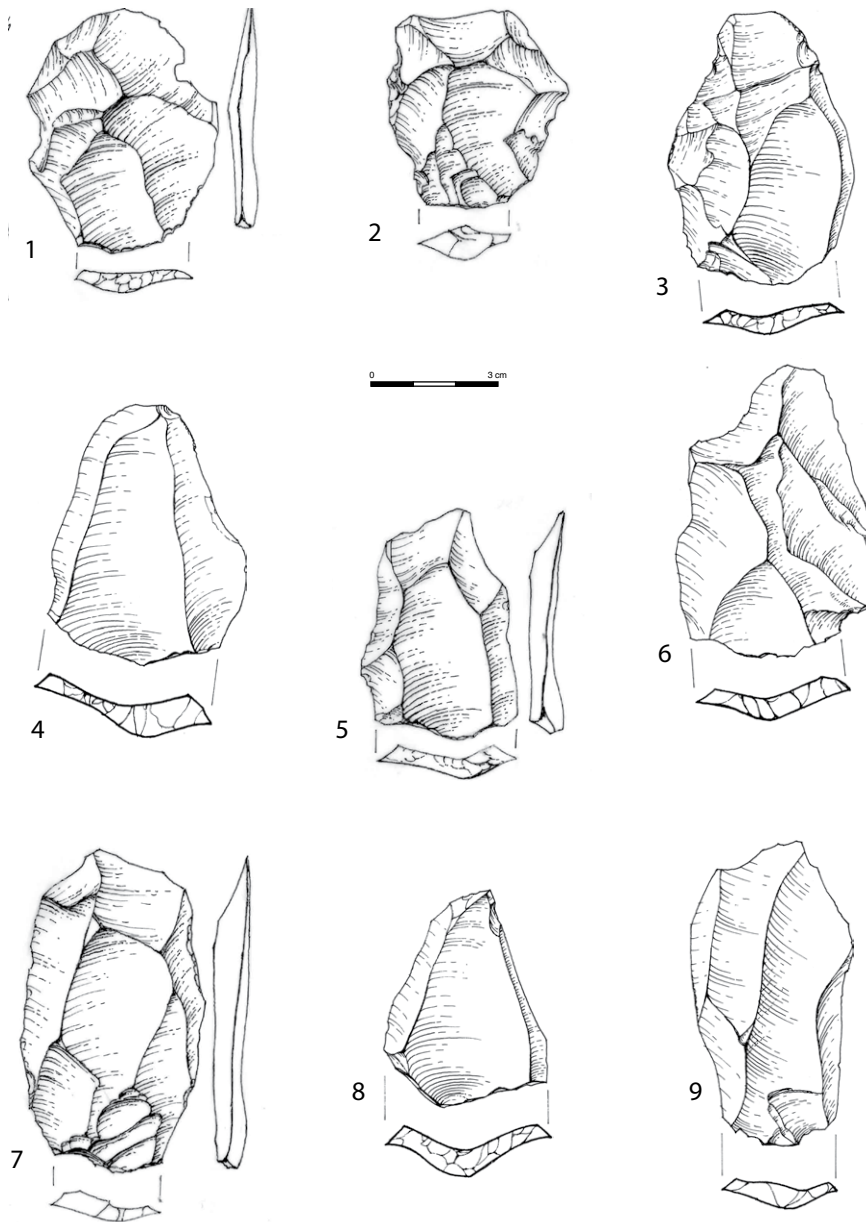


Figure 5.26. Hayonim Layer Upper E (units 3–1), onset Mid MP–. 1–9. *Short Levallois products (1, 2, 5–7. centripetal scar pattern).*

5.5.3.3.2.2 Morphology

In unit 3, the whole Levallois production is dominated by subquadrangular morphologies followed closely by triangular ones (Table 5.59). The Levallois flakes and blades are mostly subquadrangular, while the few points (short and elongated) are, of course, triangular. These characteristics remain close to those of the underlying units (units 6–4).

On the other hand, in units 1–2, we note a significant change in the morphologies of the Levallois blanks (Table 5.59), with subcircular/suboval morphologies developing. This is especially true for the flakes and, to a lesser extent, the blades, which remain mostly subquadrangular. The presence of quite a few points (short and elongated) increases the proportions of triangular morphologies.

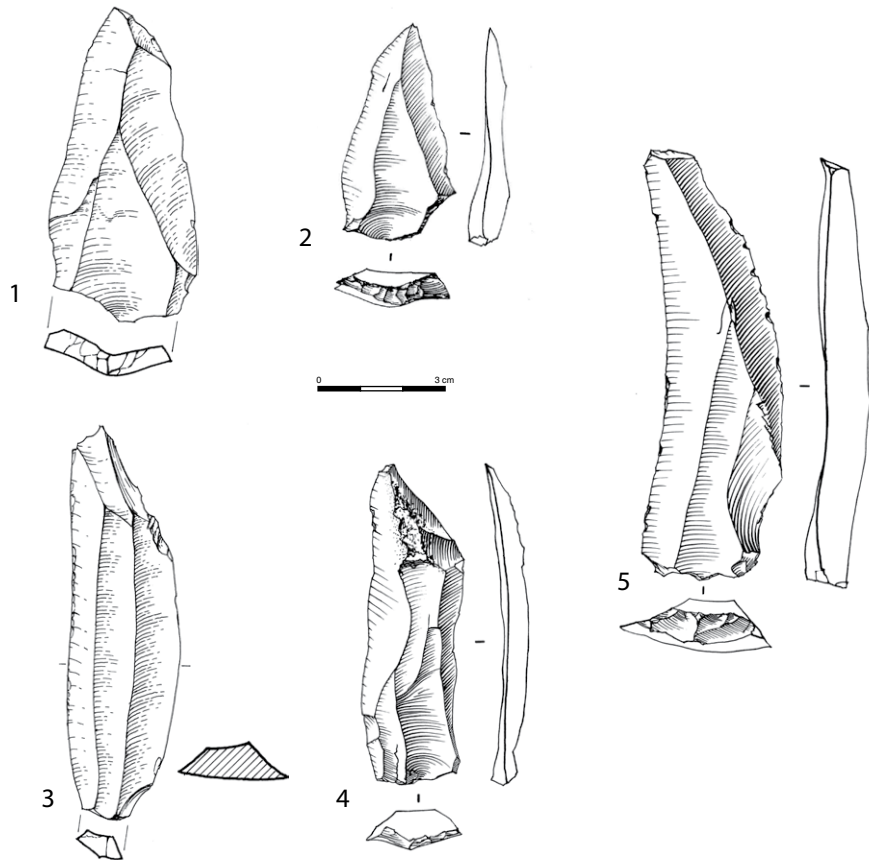


Figure 5.27. Hayonim Layer Upper E (units 3–1), onset Mid MP – Elongated products. 1. Levallois blade. 2. Elongated Levallois point. 3–5. Laminar blades.

	Levallois flakes		Levallois short points		Levallois blades		Levallois elongated points		Total Levallois	
	n	%	n	%	n	%	n	%	n	%
Units 1-2**	N = 345		N = 36		N = 76		N = 20		N = 477	
Subcirc/ovalar	144	41.74	0	0.00	28	36.84	0	0.00	172	36.06
Subtriangular	64	18.55	36	100.00	17	22.37	19	95.00	136	28.51
Subquadrangular	137	39.71	0	0.00	31	40.79	1	5.00	169	35.43
Unit 3	N = 196		N = 12		N = 34		N = 6		N = 248	
Subcirc/ovalar	53	27.04	0	0.00	6	17.65	0	0.00	59	23.79
Subtriangular	62	31.63	12	100.00	12	35.29	6	100.00	92	37.10
Subquadrangular	81	41.33	0	0.00	16	47.06	0	0.00	97	39.11

Table 5.59. Hayonim units 3 to 1-2 – Morphologies of the Levallois blanks. Percentages are of 'total number of identifiable morphologies'. **Data for units 1-2 are based on the study of the selected sample (see text).

Unit	Levallois flakes			Levallois short points			Elongated Levallois			Total Levallois		
	identifiable butts	faceted	plain	identifiable butts	faceted	plain	identifiable butts	faceted	plain	identifiable butts	faceted	plain
	N	%	%	N	%	%	N	%	%	N	%	%
Units 1-2**	368	72.83	23.37	36	100.00	0.00	100	62.00	31.00	504	72.62	23.21
		<i>(5.7)</i>			<i>(38.9)</i>			<i>(3.0)</i>			<i>(7.5)</i>	
Unit 3	202	76.73	19.31	11	*		38	73.68	13.16	251	77.29	17.53
		<i>(3.5)</i>									<i>(3.6)</i>	

Table 5.60. Hayonim units 3 to 1-2 – Faceted versus plain butts for the Levallois. Small samples are noted by an asterisk. Percentages are of 'total number of identifiable butts'. The percentage of *chapeau de gendarme* butts is shown italicised in parentheses. **Data for units 1-2 are based on the study of the selected sample (see text).

Unit	Levallois flakes						Short Levallois points					
	N	Length	Width	Thickness	L/W	W/T	N	Length	Width	Thickness	L/W	W/T
Units 1-2**	285	51.55	35.20	8.08	1.51	4.64	34	50.94	32.88	6.97	1.58	5.05
		<i>(11.36)</i>	<i>(8.69)</i>	<i>(2.71)</i>	<i>(0.33)</i>	<i>(1.29)</i>		<i>(11.41)</i>	<i>(7.49)</i>	<i>(2.24)</i>	<i>(0.29)</i>	<i>(1.65)</i>
Unit 3	170	46.75	31.81	6.75	1.51	6.55	10	43.40	26.70	5.40	1.61	5.13
		<i>(10.00)</i>	<i>(7.20)</i>	<i>(2.10)</i>	<i>(0.33)</i>	<i>(1.61)</i>		<i>(12.76)</i>	<i>(5.08)</i>	<i>(1.26)</i>	<i>(0.26)</i>	<i>(1.23)</i>

Table 5.61. Hayonim units 3 to 1-2 – Metrical attributes (in mm) of the short Levallois blanks. Complete artefacts only. Standard deviations are given in parentheses. **Data for units 1-2 are based on the study of the selected sample (see text).

5.5.3.3.2.3 Striking platforms

All these Levallois blanks are characterised by a careful striking platform preparation, resulting in a clear dominance of faceted butts (especially convex faceted) (Table 5.60). In units 1-2, this feature is more prevalent for Levallois flakes than for elongated ones. The *chapeau de gendarme* shape of the striking platform is frequently used to obtain short Levallois points (Figure 26: 8), although not in the remarkable proportions observed in some Late MP assemblages (Henry 2003; Meignen 2019).

5.5.3.3.2.4 Morphometry

The Levallois flakes, of medium size (46.7 mm in unit 3; 51.6 mm in units 1-2), still have an elongated modulus (L/W = 1.5; Table 5.61), but with much lower values than in the underlying units, probably in relation to the increased number of short flakes. These are the lowest L/W ratios of the sequence. In particular, they are significantly lower than the L/W ratios of the Levallois flakes identified in the Late MP assemblages (described as elongated by Copeland 1975; Hauck 2011a; Hovers 1998; Meignen 2019; Meignen and Bar-Yosef 1992).

The short points retain moduli similar to those of the underlying units (overall modulus between 1.58-1.61; Table 5.61), thus superior to what was identified at Kebara and Tor Faraj Late MP assemblages in which the short Levallois points often have broad bases.

5.5.3.3.2.5 Dorsal scar patterns

In these upper units, we observed notable changes in the organisation of the upper face removals (i.e., in the Levallois core exploitation modalities). Centripetal exploitation, which was previously quite rare, becomes more frequent for flake production as early as in unit 3, and then even more clearly in the upper units 1-2 (Table 5.62). In unit 3, for the whole Levallois production, the unidirectional parallel and convergent patterns still dominate, as observed in the majority of the sequence. The flakes (quantitatively the most numerous) also show unidirectional convergent and bidirectional scars.

Table 5.62. Hayonim units 3 to 1–2 – Dominant dorsal scar patterns of the Levallois blanks. Small samples are noted by an asterisk. Excluding indeterminate patterns. **Data for units 1–2 are based on the study of the selected sample (see text). KEY: unid par = unidirectional parallel; unid conv = unidirectional convergent; bidir = bidirectional; centr = centripetal.

Unit	Total Levallois		Levallois flakes		Short Levallois points		Elongated Levallois	
Units 1–2**	N = 509	%	N = 372	%	N = 35	%	N = 102	%
	centr	25.74	centr	34.95	unid conv	77.14	unid par	31.37
	bidir	22.79	bidir	23.12	croisé	11.43	unid conv	31.37
	% centr	25.74	% centr	34.95	% centr	2.86	% centr	0.00
Unit 3	N = 258	%	N = 207	%	N = 12	*	N = 39	%
	unid conv	31.78	unid conv	29.47			unid conv	33.33
	bidir	27.13	bidir	28.99			bidir	23.08
	% centr	18.22	% centr	21.74			unid par	23.08
							% centr	0.00

However, from this unit onward, there is a notable increase in centripetal patterns for the production of flakes (21.7%; Table 5.62). This tendency increases significantly in units 1–2, where the majority of flakes are obtained by centripetal exploitation, which is also the dominant element in the Levallois production as a whole. This change in exploitation modalities is reflected in a stronger development of subcircular/sub-oval morphologies in units 1–2, whereas the Levallois blanks of unit 3 still present mainly subquadrangular/subtriangular morphologies (Table 5.59), a situation comparable to that observed in the underlying levels.

To test the possibility of successive exploitation phases according to different patterns (centripetal versus unidirectional/bidirectional, a pattern that we were able to highlight in the unit XI at Kebara), we analysed the dimensions of the Levallois flakes of units 1–2 according to their production pattern. The results show that this is not the case here as the dimensions corresponding to the different patterns are equivalent (Mean length of Levallois flakes: centripetal 51.79 [10.38]; uni/bidirectional 51.78 [11.83]). The different patterns were thus produced at all stages of the reduction sequence.

Furthermore, it is worth noting the low number of scars on the upper surface of Levallois flakes in these units (units 1–2 = mean 4.7 [1.5]/ unit 3 = mean 4.4 [1.3]) where centripetal preparation/exploitation patterns tend to become more prevalent. This observation suggests that the preparation of the Levallois surface before flake detachments was not highly developed. In any case, it is less developed than for Levallois flakes from Qafzeh or Neshar Ramla, which are clearly centripetal, and for which the number of scars on the upper face of the flakes is greater (Qafzeh: from 5.6 to 7.6 according to the units [Hovers 2009: 70]; Neshar Ramla unit III: 5.4 [Prevost and Zaidner 2020]).

5.5.3.3.3 Elongated blank productions (Figure 5.27)

5.5.3.3.3.1 Morphology of the blades and elongated points

Not only do the proportions of elongated blanks decrease relative to the underlying levels as a whole (Table 5.10), but their composition also changes (Tables 5.12, 5.12bis): the elongated Levallois component increases significantly, especially in units 1–2 (unit 3 = 19.1%, units 1–2 = 40.9%) (Figure 5.27: 1–2), while Laminar productions tend to disappear (Figure 5.27: 3–4). Still present in unit 3 (about 23.3%; Table 5.12), the latter represent only 16.7% in units 1–2 (based on a sample; Table 5.12bis).

Among these elongated products, blades clearly dominate elongated points, both in the Levallois production (81.7% in units 1–2; 86.7% in unit 3) and in the Laminar production (76.6% in units 1–2; 94.7% in unit 3) (Table 5.63).

The data presented below concern the entire elongated production, with some more specific comments on the elongated Levallois production. It is important to keep in mind, in these upper units, the notable proportions of blanks whose flaking system could not be identified (so-called ‘undifferentiated’) (unit 3: 57.6%; units 1–2: 42.3%; Table 5.12),

Unit	Total elongated products					Elongated Levallois					Laminar				
	blades		elongated points		total elongated	blades		elongated points		total elongated	blades		elongated points		total elongated
	N	%	N	%	N	N	%	N	%	N	N	%	N	%	N
Units 1-2**	242	86.12	39	13.88	281	94	81.74	21	18.26	115	36	76.60	11	23.40	47
Unit 3	233	96.28	9	3.72	242	39	86.67	6	13.33	45	54	94.74	3	5.26	57

Table 5.63 Hayonim units 3 to 1-2 – Frequencies of blades versus elongated points. Excluding blanks of retouched tools. **Data for units 1-2 are based on the study of the selected sample (see text).

	Levallois blades/elongated points				Total blades /elongated points			
	Unit 3		Units 1-2**		Unit 3		Units 1-2**	
	N	%	N	%	N	%	N	%
wide thin	26	61.90	81	74.31	37	15.68	107	35.55
wide thick	8	19.05	8	7.34	92	38.98	82	27.24
narrow thin	7	16.67	20	18.35	23	9.75	47	15.61
narrow thick	1	2.38	0	0.00	84	35.59	65	21.60
Total	42	100.00	109	100.00	236	100.00	301	100.00

Table 5.64. Hayonim units 3 to 1-2 – Morphologies of the elongated products. Excluding blanks of retouched tools. **Data for units 1-2 are based on the study of the selected sample (see text).

Edges	Total blades/elongated points		Levallois blades/elongated points	
	Unit 3	Units 1-2	Unit 3	Units 1-2
	N = 175	N = 245	N = 33	N = 93
	%	%	%	%
parallel	0.57	2.86	0.00	5.38
more or less parallel	31.43	31.84	39.39	33.33
convergent	51.43	53.47	48.49	54.84
divergent	16.56	11.83	12.12	6.45
Distal ends	N = 201	N = 223	N = 40	N = 95
	%	%	%	%
subovalar	30.35	31.39	15.00	29.47
subtriangular	29.35	33.18	45.00	37.89
subquadrangular	40.30	35.43	40.00	32.64

Table 5.65. Hayonim units 3 to 1-2 – General characteristics of blades and elongated points. Percentages calculated from the number of artefacts on which the characteristics are identifiable. **Data for units 1-2 are based on the study of the selected sample (see text).

	Total elongated		Levallois elongated	
	N = 257	%	N = 102	%
Units 1-2**				
unid par	37.74		unid par	31.37
unid conv	26.07		unid conv	31.37
bidir	26.07			
Unit 3	N = 185	%	N = 39	%
unid par	35.68		unid conv	33.33
unid conv	25.41		unid par	23.08
			bidir	23.08

Table 5.66. Hayonim units 3 to 1-2 – Dominant dorsal scar patterns of the elongated products. Excluding indeterminate patterns. **Data for units 1-2 are based on the study of the selected sample (see text). KEY: unid par = unidirectional parallel; unid conv = unidirectional convergent; bidir = bidirectional; centr = centripetal.

which are always more abundant than those from the Laminar or Levallois systems. This ‘undifferentiated’ category will thus strongly influence the general characteristics of the blade assemblage. We thus take into account the data concerning all of the blades to characterise the production.

In unit 3, blades from the Laminar system are still quite frequent (Table 5.12). As in the underlying units, their morphological variability is significant. Generally, the blades and points in unit 3 are most often wide and thick or even narrow and thick relative to the still significant presence of Laminar blanks (Table 5.64). The blades are most often quadrangular, and the points are subtriangular (Table 5.65). Unidirectional parallel exploitation patterns are the most frequent (Table 5.66). On the other hand, the Levallois component (blades and points) is characterised by wide and thin blades with a subtriangular or subquadrangular morphology (Tables 5.64, 5.65), obtained mostly via unidirectional convergent organisations (Table 5.66). The striking feature is once again the dominance of convergent edges, whereas triangular morphologies are not systematically dominant.

In units 1–2, on the other hand, production linked to the Laminar system decreases sharply in favour of the Levallois system (16.7% versus 40.9%; Table 5.12 bis). In these units, thin wide blades are more numerous than thick ones, which are still substantially present (Table 5.64), and it is, of course, the abundant elongated Levallois products that determine this characteristic. The morphologies are predominantly quadrangular (Table 5.65), with a large subtriangular dominance for Levallois blanks due to the presence of elongated points (Table 5.63). Again, the flaking patterns are mainly unidirectional parallel, with a development of unidirectional convergent patterns for the Levallois product category (Table 5.66). And in all cases, the blanks frequently have convergent edges (Table 5.65), and much less often, parallel edges.

5.5.3.3.3.2 Morphometry (Tables 5.67a, b)

As in the underlying units, the Laminar blades differ from the Levallois blades mainly in their thickness (Table 5.67a; T-test: significant differences for thickness and W/T, while the small differences observed for other dimensions (length and width) are not statistically significant.

Unit	Total blades/elongated points						Levallois blades/elongated points						Laminar blades/points					
	N	Length	Width	Thickness	L/W	W/T	N	Length	Width	Thickness	L/W	W/T	N	Length	Width	Thickness	L/W	W/T
Units 1–2**	231	64.90 (14.80)	25.64 (6.73)	8.98 (3.77)	2.60 (0.52)	3.14 (0.96)	85	61.72 (14.08)	25.26 (6.58)	6.95 (2.23)	2.50 (0.46)	3.79 (0.84)	47	69.02 (15.93)	27.00 (7.87)	11.07 (3.57)	2.65 (0.59)	2.52 (0.54)
Unit 3	161	64.40 (15.50)	25.22 (6.36)	9.25 (3.60)	2.60 (0.49)	3.01 (1.05)	32	63.47 (14.27)	26.13 (7.25)	6.28 (2.02)	2.46 (0.30)	4.34 (0.98)	42	69.19 (17.91)	26.21 (6.55)	10.81 (4.34)	2.70 (0.62)	2.58 (0.63)
T-test for Laminar versus Levallois elongated products																		
p values at an alpha [significance] level of 0.05																		
	Unit 3	Units 1–2																
Length	0.153	0.010																
Width	0.956	0.191																
Thickness	<0.0001	<0.0001																
L/W	0.042	0.116																
W/T	<0.0001	<0.0001																

Table 5.67a. Hayonim units 3 to 1–2 – Metrical attributes (in mm) of the elongated products. Complete artefacts only. Standard deviations are given in parentheses. **Data for units 1–2 are based on the study of the selected sample (see text).

Unit	Total blades/elongated points			Levallois elongated			Laminar blades/points		
	N	Width	Thickness	N	Width	Thickness	N	Width	Thickness
Units 1-2**	211	16.20 (7.55)	5.58 (2.43)	77	17.52 (7.76)	4.97 (1.97)	38	16.29 (7.2)	6.63 (3.03)
Unit 3	143	15.67 (6.66)	5.28 (2.33)	28	18.21 (8.01)	4.54 (1.77)	39	17.56 (6.15)	6.03 (2.76)

T-test for Laminar versus Levallois elongated product butts

p values at an alpha [significance] level of 0.05

	Unit 3	Units 1-2
Butt width	0.708	0.415
Butt thickness	0.015	0.001
Butt W/T	0.008	<0.0001

Table 5.67b. Hayonim units 3 to 1-2 – Metrical attributes (in mm) of the elongated product butts. Complete artefacts only. Standard deviations are given in parentheses. **Data for units 1-2 are based on the study of the selected sample (see text).

Unit	Total elongated			Elongated Levallois		
	identifiable butts	faceted	plain	identifiable butts	faceted	plain
	N	%	%	N	%	%
Units 1-2	264	52.27	39.77	100	62.00	31.00
Unit 3	190	54.21	35.79	45	73.68	13.16

Table 5.68. Hayonim units 3 to 1-2 – Faceted versus plain butts for the elongated products. Percentages are of 'total number of identifiable butts'. **Data for units 1-2 are based on the study of the selected sample (see text).

Unit	Total elongated blanks	Cortical elongated blanks		Including cortical back	
	N	N	%	N	%
Units 1-2**	294	105	35.71	52	17.69
Unit 3	225	104	46.22	50	22.22

Table 5.69. Hayonim units 3 to 1-2 – Cortical elongated blanks (blades and elongated points). **Data for units 1-2 are based on the study of the selected sample (see text).

5.5.3.3.3 Striking platforms

In unit 3 and units 1-2, all of the elongated blanks have carefully faceted butts (Table 5.68). This feature is even more pronounced in the Levallois productions, in which the striking platform was particularly well prepared. Here again, the Laminar blades have thicker butts than the Levallois ones (Table 5.67b, T-tests for thickness and W/T indicate significant differences).

Furthermore, in these higher units, elongated cortical products are widely present, even though the cortical areas/surfaces are not very widely developed (Table 5.69).

5.5.3.3.4 Retouched tools (Figure 5.28)

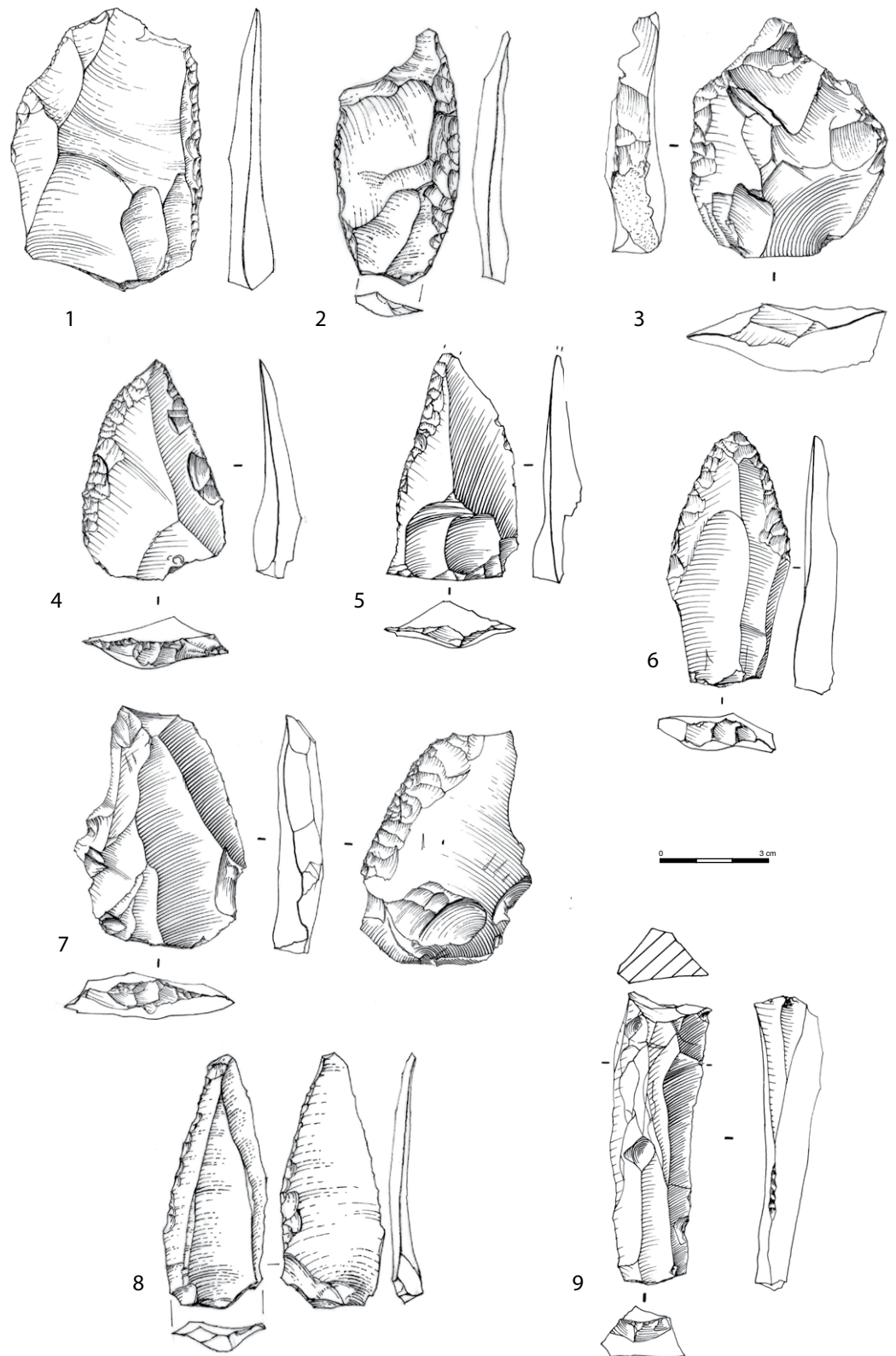


Figure 5.28. Hayonim Layer Upper E (units 3-1), onset Mid MP – Retouched tools. 1-6. Side-scrapers. 7. Scraper retouched on ventral face. 8. Retouched elongated point. 9. Burin on blade.

Tool category	Unit 3	Units 1-2**
	N	N
Retouched blade (one edge)	11	22
Retouched blade (two edges)	4	7
Short retouched point	6	5
Elongated retouched point	7	8
Simple scraper	64	108
Double scraper	14	18
Convergent scraper	8	10
Déjeté scraper	2	2
Transverse scraper	3	1
Scraper on ventral face	6	1
Abrupt ret scraper	0	0
Alternate ret scraper	1	1
Endscraper	2	6
Burin	15	8
Awl	0	0
Truncation	2	2
Notch	10	9
Denticulate	15	14
Retouches on ventral face	4	8
Retouched flake/blade	10	30
Miscellaneous	27	3
Nahr Ibrahim piece	10	10
Notch+Nahr Ibrahim	1	3
Total	222	276

Table 5.70. Hayonim units 3 to 1-2 – Typological breakdown. **Data for units 1-2 are based on the study of the selected sample (see text).

Unit	Retouched products		Total retouched elongated blanks		Retouched blades		Elongated retouched points		Short retouched points		Scrapers		Scrapers on ventral face		UP tools		Burins		Notches+denticulates	
	N	%	N	%	N	%	N	%	N	%	N	%	N	%	N	%	N	%	N	%
Units 1-2**	276		37	13.41	29	10.51	8	2.90	5	1.81	141	51.09	3	1.09	16	5.80	8	2.90	23	8.33
Unit 3	222		22	9.91	15	6.76	7	3.15	6	2.70	98	44.14	7	3.15	19	8.56	15	6.76	25	11.26

5.5.3.3.4.1 Tool assemblage composition (Tables 5.70, 5.71)

The proportions of retouched tools are quite high in these units (10.4% in unit 3; 8.8% in units 1-2), higher than in units 6-4, but significantly lower than in the lower units (Table 5.10). Side-scrapers dominate the tools (Figure 5.28: 1-7), while retouched blades and elongated points are not very abundant (Table 5.71 and Figure 5.28: 8), thus prolonging the trend of decrease already observed in units 6-4 (Table 5.13). In particular, retouched elongated points tend to disappear (3.1% in unit 3, 2.9% in units 1-2), whereas they were a characteristic element of the lower units. The blades are mostly retouched on one edge only, and often along the entire length of the edge.

Elongated products (blades and a few points) were rarely used as tool blanks (16.9% in unit 3, 20.4% in units 1-2; Table 5.72), even more so than in units 6-4. The blade component thus tends to disappear as the stratigraphy progresses. The tools are mostly on short blanks (Table 5.72), and for the first time in the sequence, Levallois blanks (flakes and a few points) were those most frequently used (50.77% in unit 3, 40.7% in units 1-2). This trend is especially prevalent for side-scrapers (61.4% in unit 3, 56.7% in units 1-2). Nearly all of the scrapers, which are very numerous, have only one retouched edge (Table 5.70). They are most often, simple scrapers, and more rarely transverse scrapers. Their retouch is most often slightly invasive scalar (69.4% in unit 3; 78% in units 1-2), and much less often, marginal retouch (17.3% in unit 3; 17.7% in units 1-2). These tools are

Table 5.71. Hayonim units 3 to 1-2 – Frequencies of retouched tool categories. Percentages are of 'total number of retouched products'. **Data for units 1-2 are based on the study of the selected sample (see text).

Table 5.72. Hayonim units 3 to 1–2 – Blank types of the retouched tools. Percentages are of ‘total number of identifiable blanks’. **Data for units 1–2 are based on the study of the selected sample (see text).

Unit	Identifiable blanks		On elongated blank		On short Levallois blank		On short non-Levallois blank	
	N	%	N	%	N	%	N	%
Units 1-2**	221		45	20.36	90	40.72	86	38.91
Unit 3	130		22	16.92	66	50.77	42	32.31

Unit	Total retouched			Tools on Levallois blank			Tools on blade			Tools on non-Levallois blade		
	identifiable butts	faceted	plain	identifiable butts	faceted	plain	identifiable butts	faceted	plain	identifiable butts	faceted	plain
	N	%	%	N	%	%	N	%	%	N	%	%
Units 1-2**	170	65.29	31.76	101	82.18	15.84	31	74.19	19.35	13	*	*
Unit 3	151	67.55	25.83	90	77.78	16.67	29	68.97	24.14	21	*	*

Table 5.73. Hayonim units 3 to 1–2 – Faceted versus plain butts for the retouched tools. Small samples are noted by an asterisk. Percentages are of ‘total number of identifiable butts’. **Data for units 1–2 are based on the study of the selected sample (see text).

frequently atypical, with retouch not covering the entire edge. The blanks are thus only slightly transformed. In addition to this unfinished aspect of the scrapers, it is important to note the presence of many blanks with partial localised retouch of different types (categorised as ‘retouched flake’ and miscellaneous’).

Convergent tools (retouched points, convergent and skewed scrapers) are comparatively scarce. Scrapers with retouch on ventral face are also rare, as in units 6–4, whereas their presence was particularly noticeable in Units 10 to 7–8.

UP-type tools are few here (8.6% in unit 3, 5.8 in units 1–2; Table 5.71), in contrast to the immediately underlying units (units 6–4). Mostly consisting of burins (on blades (Figure 5.28: 9) or flakes) in unit 3, they include some end-scrapers in units 1–2, most often transformed on the end of flakes.

Notches and denticulates are present but not widely represented (Table 5.71). The notches are most often on non-Levallois flakes, and rarely on blades.

Finally, we should emphasise the presence of a small assemblage of Nahr Ibrahim technique pieces completed by some pieces whose secondary removals were extracted not from a truncation (as in the case of the Nahr Ibrahim technique) but from a wide shallow notch that truncates the blank in the distal part (Table 5.70). The truncation in both cases (usually proximal, sometimes distal) is generally on the lower face and the secondary removals on the upper face.

5.5.3.3.4.2 Striking platforms

In these units, the tool butts are carefully prepared by faceting, and faceted butts, most often convex, are always more numerous than plain butts. This dominance is greater for tools on Levallois blanks, and a bit less for tools on blades (Table 5.73).

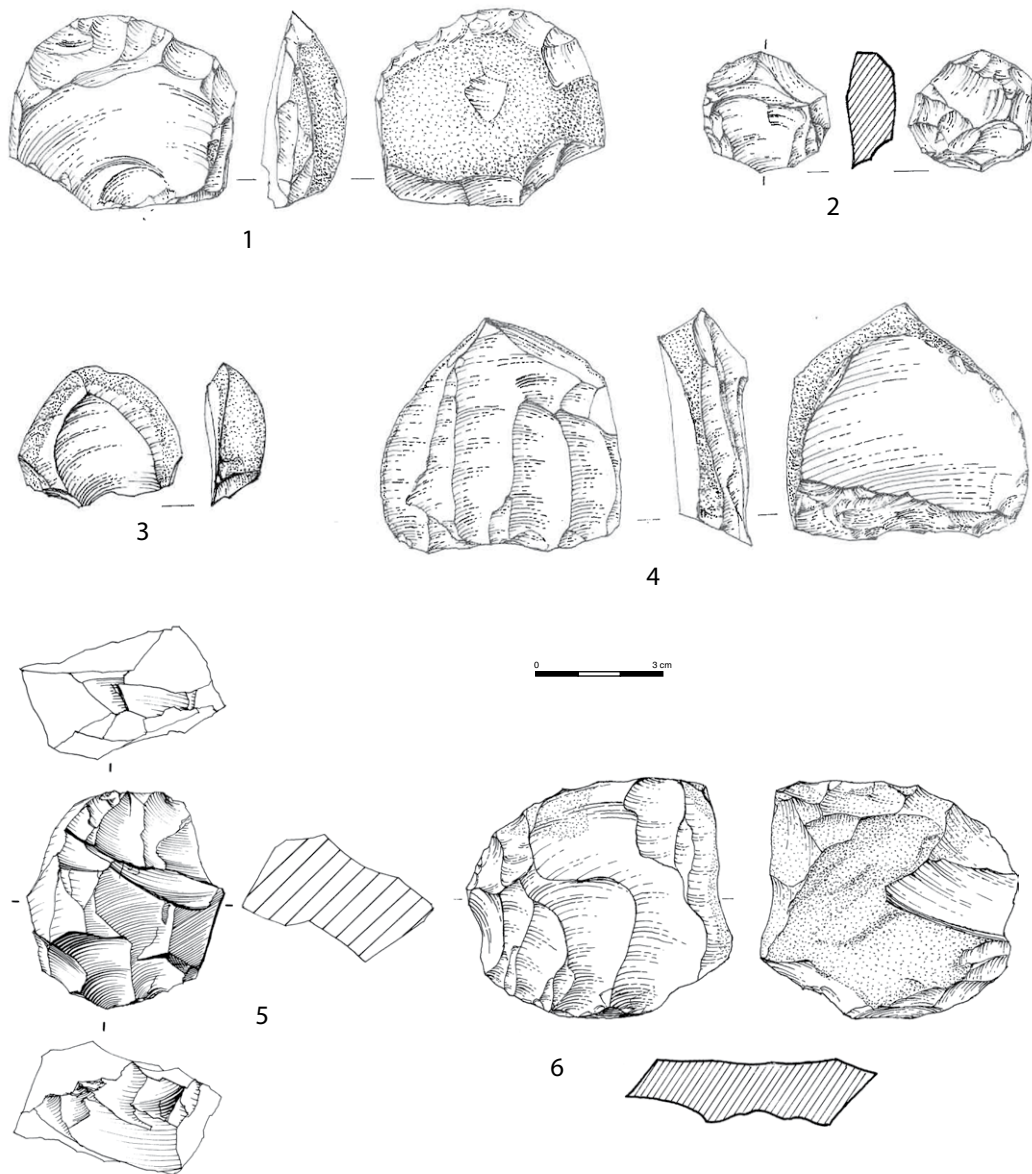


Figure 5.29. Hayonim Layer Upper E (units 3–1), onset Mid MP – Cores. 1, 2. *Levallois preferential cores*. 4, 6. *Levallois recurrent unidirectional cores*. 3. *'Preferential surface exploitation' (on flake)*. 5. *Laminar bidirectional core with slightly offset striking platforms (elongated flake production at the final stage)*.

5.5.3.3.5 Cores (Tables 5.74, 5.75) (Figure 5.29)

Proportionally still numerous in these upper units, the cores were frequently made on flakes (29.1 to 34.3%), most often via an exploitation of the ventral face of the flake blank (Table 5.74). Flake cores are clearly the most abundant, especially in units 1–2 (highest of the sequence: 90.2%), while blade cores are very rare, especially in units 1–2 (9.3% in unit 3, 2.1% in units 1–2), as are those for small blades/bladelets, which are nearly absent.

Levallois cores, the most numerous (32.9% in units 1–2; 31.4% in unit 3; Table 5.74), thus largely dominate the semi-rotating cores. This abundance is even more remarkable if we add the 'Levallois?' category, whose attribution to Levallois flaking is probable, though not certain. The typical Levallois cores that make up this latter group are often on flakes and correspond either to structurally Levallois cores whose exploitation has been poorly controlled—large removals that are distally or laterally overshot, making

Unit	Total assemblage	Cores		On flake blank		Flake cores		Blade cores		Bladelet cores		Levallois cores		Levallois? cores		Preferential surface cores		'Semi-tournant' cores	
		N	%	N	%	N	%	N	%	N	%	N	%	N	%	N	%	N	%
Units 1-2	4033	143	34.27	49	129	90.21	3	2.10	1	0.69	47	32.87	28	19.58	24	16.78	2	1.39	
Unit 3	2209	86	29.07	25	67	77.91	8	9.30	0	0.00	27	31.40	27	31.40	9	10.47	8	9.30	

Table 5.74. Hayonim units 3 to 1-2 – Main categories of cores. Excluding few cores in a bad state of preservation due to fire impact. Percentages are of 'total number of cores', except core percentage calculated from the total assemblage.

Core types		Unit 3		Units 1-2	
Levallois cores	Total	27		47	
	preferential	10		22	
	recurrent	17		25	
including	<i>including</i>	centr	4	12	
		bidir	1	2	
		unid par	6	5	
		unid conv	6	1	
		crossed	0	4	
		broken		1	
Levallois ? cores	Total	27		28	
	preferential	8		11	
	recurrent	13		12	
including	<i>including</i>	centr	0	3	
		bidir	3	2	
		unid par	2	4	
		unid conv	5	1	
		crossed	1	1	
		indet	2	1	
	indeterminate/broken	6	5		
Semi-tournant cores	Total	8		2	
	1 str pltf/unid conv	1		0	
	1 str pltf/unid par	2		1	
	2 str pltf/bidir opp	1		0	
	2 str pltf/twisted	4		1	
Preferential surface exploitation	Total	8		24	
Upper surface exploitation (cf Nahr Ibrahim)	Total	1		6	
Others	multiple str.pltf	3		4	
	isolated removals	9		25	
	discoid	1		6	
	fragments	2		1	
Total	86		143		

Table 5.75. Hayonim units 3 to 1-2 – Detailed counts of cores. KEY: Str pltf = striking platform; unid par = unidirectional parallel; unid conv = unidirectional convergent; bidir = bidirectional; centr = centripetal.

it difficult to identify the Levallois preparation—or to cores that are probably Levallois but are fractured. These upper levels are thus characterised by a remarkable presence of Levallois flaking (Figure 5.29: 1, 2, 4, 6), the highest prevalence of this flaking system in the entire sequence.

Among the Levallois methods, preferential methods narrowly dominate and are well represented (Table 5.75 and Figure 5.29: 1-2). Among the typical Levallois cores, in unit 3, unidirectional (parallel and convergent) exploitation modalities are still substantial (Figure 5.29: 4, 6), while centripetal recurrent exploitations are highly dominant in

units 1–2. The exploitation modalities of the atypical Levallois (Levallois?) cores are more diverse, with a slight dominance of the unidirectional organisation.

Together with the much less abundant blades in these assemblages, semi-rotating cores are poorly represented here, especially in units 1–2 where they have practically disappeared (9.3% in unit 3, 1.4% in units 1–2; Table 5.74). They are also rather atypical, most often having elongated flake scars rather than blade scars in the final stage (Figure 5.29: 5).

These two main categories of cores and flaking systems are completed by a specific production that we have named ‘preferential surface exploitation’ (Figure 5.29: 3) which is quite well represented here (especially in units 1–2: 16.8% of cores; Table 5.74). This flaking system is most often carried out on the ventral face of the flake blank, but some examples of preferential surface exploitation on the upper face should also be noted (Table 5.75). The limit between ‘core on the upper surface of the flake’ and Nahr Ibrahim technique pieces is not always easy to distinguish. Let us recall that we consider as a core the pieces on which the removals subsequent to the preparation of the ‘truncation’ (= striking platform) are sufficiently large and organised (contiguous).

Finally, there is a relatively large set of much less structured ‘miscellaneous’ cores corresponding either to removals from multiple platforms or to a few unorganised detachments.

There are also a few discoid cores (1 in unit 6, 4 in unit 5, and 4 in unit 4).

5.5.3.3.6 Core trimming elements (CTEs)

In the upper units, there is a notable change in the CTEs. Even if cortical *débordants* flakes (including *débordants outrepassants* flakes) remain in the majority (Table 5.76) (in association with the continuation of unidirectional/bidirectional flaking), classic *débordants* flakes also become more numerous. On the latter, the back corresponds to a series of removals to prepare the striking platforms over more or less the entire periphery of the core in the context of preferential or recurrent cores whose shaping and/or flaking is achieved by centripetal removals. Attesting to this last option (Levallois recurrent centripetal), we observed a significant proportion of these *débordants* flakes called ‘with a limited back’ (*débordant à dos limité*; Meignen 1993). These *débordants* flakes restore locally the convexities, thus removing only part of the periphery and not the whole length of the edge. They are generally offset (technological and morphological axis do not overlap) and are classically called ‘pseudo-Levallois flake’ (subrectangular) or ‘pseudo-Levallois point’ (subtriangular) in the Bordes typology. They are most frequent in the Levallois centripetal recurrent exploitation (Meignen 1993).

Crested blades practically disappear in units 1–2, in which Laminar productions are very rare. They are still present in unit 3, however (most often partial crests where blade and semi-rotating cores persist).

5.5.3.3.7 Summary of the main features of units 3–1

The upper units show clear changes within this sequence: (Tables 5.10, 5.11)

- A clear development of Levallois flakes with centripetal reduction patterns (Tables 5.10, 5.62), starting in unit 3 and becoming very clear in units 1–2, whereas these modalities were practically absent in the underlying units. The morphologies of the resulting products are sub-oval in units 1–2, while subtriangular/subquadrangular forms are still dominant in Unit 3.
- These characteristics are associated with a clear increase in preferential Levallois cores and centripetal recurrent cores in units 1–2, while unidirectional recurrent cores are still numerous in unit 3 (Table 5.75). The CTE products also attest to these changes (increase in classic *débordants* flakes including those with a limited back, characteristic of centripetal recurrent reduction systems).
- A clear decrease in elongated blanks (Table 5.12), with a Levallois component that increases at the expense of Laminar productions.

Table 5.76. Hayonim units 3 to 1–2 – Main categories of CTEs. Among the classical *débordants*, the number of those called *à dos limité* are shown in parentheses.

Unit	<i>Débordants</i> with cortical back		<i>Débordants</i> with non-cortical back		Classical <i>débordants</i> including <i>dos limités</i>		Crested blades		Total CTE
	N	%	N	%	N	%	N	%	
Units 1–2	83	70.94	9	7.69	23 (12)	19.66	2	1.71	117
Unit 3	70	72.92	5	5.21	14 (9)	14.58	7	7.29	96

- A noticeable change in the range of retouched tools, among which flake tools (mainly scrapers) become predominant (to the detriment of tools on elongated blanks).

The techno-economic composition of these upper-level assemblages is largely dominated by Levallois products, most of which were knapped in situ, as shown by the high proportions of cortical and ordinary products, the notable percentage of cores associated with this flaking system, and the presence of the corresponding CTEs. The Laminar component, which tends to disappear in units 1–2, was most likely imported given the very low number of semi-rotating cores. Blade production thus played a secondary role, Levallois being the dominant system. It is interesting to note that in unit 3 there is a slight deficit of Levallois products relative to the number of corresponding cores, which could indicate a possible import of these flakes (Levallois products = 378, Levallois cores = 54, ratio 7:1) to the site.

5.5.4 Overview of the Middle Palaeolithic sequence

5.5.4.1 Introduction

In view of the results obtained, the long MP sequence at Hayonim can be defined by a dominant production of flakes, even if the characteristic element, which is strikingly so throughout a large part of the sequence, is the marked presence of elongated blanks (blades and points), more so than in the majority of Middle Palaeolithic sites in the Near East.

The Levallois reduction system is well represented in all of the units, making it a good example of the Levantine MP, which is a specific entity (Bar-Yosef 2006) sometimes characterised by a slow pace of cultural change. Hovers and Belfer-Cohen (2013: 350) spoke of a period of stasis lasting more than 200 ka, during which simple variations around a restricted technical repertoire have been identified. These authors characterise the Levantine MP as a period of ‘retention rather than gain and loss’ in the technical repertoire.

The results of our study nuance this perception of the MP, at least in terms of the lithic productions, by insisting on the particularities of the Early MP (a period largely represented at Hayonim in units 10 to 4), which would indicate, at the beginning of the MP, elements that somewhat contradict this image of stability or even stagnation. The Hayonim archaeological sequence (as well as those of other sites, such as Misliya, Hummal, and Tabun) documents, first of all, the presence of a Laminar component that represents a technical innovation, in contrast with the immediately prior Acheulo-Yabrudian traditions. This is certainly not a total revolution in production concepts (Laminar productions are known earlier in the Amudian but they originate from radically different tool production and management systems). However, it is indeed an innovative element adopted on a sufficiently large scale (based on the present state of knowledge), for us to define a specific Early MP technical entity that is distinct from both what comes before it (Acheulo-Yabrudian), and what follows it (Middle and Late MP). The latter two entities are characterised by the supremacy of the Levallois system, specifically a loss of diversity in the technical systems in comparison to the Early MP. This technical entity develops over a fairly long period (240 ka–160 ka) and, therefore, cannot be considered as an epiphenomenon.

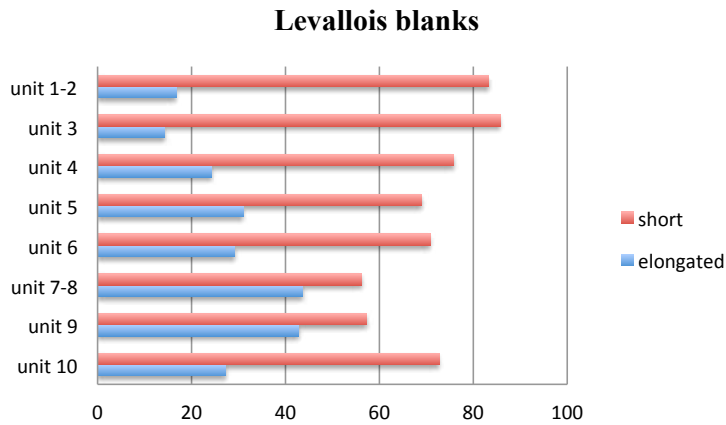


Figure 5.30. Hayonim – Frequencies of short versus elongated Levallois blanks in units 10 to 1–2.

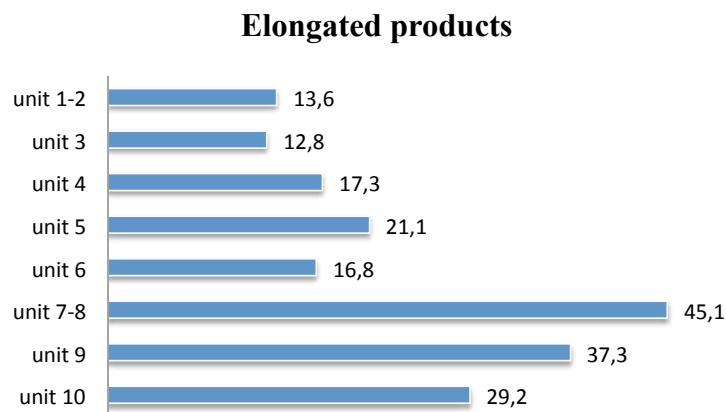


Figure 5.31. Hayonim – Frequencies of elongated products in units 10 to 1–2.

The Hayonim Layer F and E sequence is characterised by the presence of the Levallois reduction system throughout it (Table 5.11)—identified based on products, cores and CTEs. From the beginning of the Early MP, around 210 ka–220 ka, the Levallois is represented by its full range of products—thus ‘full-fledged’—with, nevertheless, a clear dominance of short blanks (especially elongated flakes), which tend to increase within the sequence (Figure 5.30).

This flake production is closely associated with a production of elongated blanks (blades and points), more or less prevalent in different levels (high in the lower levels, very low in the upper levels). These elongated products were obtained via two reduction systems: Levallois and Laminar, which are either successive on the same core, or carried out on different cores (see discussion above) (Figure 5.31).

Variations are also observed in the range of retouched tools in relation to the production systems (dominance of blade tools at the base and flake tools/scrapper later).

The question thus arises as to whether the assemblages in this sequence belong to the different facies already known in the Middle Palaeolithic of the Near East.

While the attribution to the entity classically defined under the term Early MP is not in doubt for the artefacts in units 10 to 7–8 (Meignen 2007, 2011; Meignen and Bar-Yosef 2020), the question arises for the succeeding units, especially units 6–4 (Layer Lower E). Concerning the assemblages of the upper levels (Layer Upper E), though they already seem, on first analysis, to be distinct, one can wonder about the links they retain with the underlying levels, and which processes could explain the observed changes.

In the following discussions, the chronology of these different features must be kept in mind, as well as the chronological gap of about 30 ka, corresponding to the erosive event that separates Layer F from Layer Lower E.

5.5.4.2 Main characteristics of the different unit groups

Units 10 to 7–8 (Layer F; 210 ka–220 ka)

Though not homogeneous in all of their features, the assemblages of the lower levels are distinguished by:

- Abundant elongated productions (blades and points, in the Levallois and Laminar reduction systems), clearly more prevalent in Layer F (units 10, 9, 7–8) (between 30 and 45%) than in the other units (Table 5.10) (Figure 5.31).
- The products of the Laminar system dominate over those of the Levallois system. Blades are always more abundant than elongated points (Table 5.12).
- A serial production of often quite thick blades with an irregular morphology but globally converging edges. They are most often subquadrangular, but also sub-oval and subtriangular, most often produced via unidirectional reduction systems (parallel and convergent).

In addition to this remarkable blade production, we must also mention:

- A significant Levallois production (Table 5.11) comprising the whole range of products (Figure 5.30), which are dominated by elongated flakes with a subquadrangular morphology, like the blades. Here again, the reduction systems are mostly unidirectional (parallel and convergent). Starting in these basal levels, Levallois points (short and elongated) are present, obtained mostly via a unidirectional convergent system. This is their first appearance in the Mousterian tools of the Levant. It should be noted, moreover, that there is almost no centripetal exploitation.
- A major feature of these units is the high proportion of retouched tools (Table 5.10 and Figure 5.32), especially retouched blades and elongated points, which dominate the assemblages (Table 5.13 and Figure 5.33). At Hayonim, retouched blades are more common than retouched elongated points.
- The proportions of tools on blades are remarkable (Table 5.14), breaking with the other units, thus indicating a clear selection of elongated blanks for the constitution of the toolkit. This is undoubtedly the most striking element of these assemblages. This elongated component is completed by numerous tools on short blanks, mainly scrapers (Table 5.13 and Figure 5.34), among which those transformed by retouch on ventral face are the original feature of these lower levels.
- Upper Palaeolithic tools are few (2.4 to 6.3%) and consist mainly of burins.
- Considering the production, the characteristics of the cores are surprising (Table 5.77):

Based on the cores, flake production dominates; the proportions of blade cores are not very striking, except units 7–8 (= 25.7%) (Figure 5.35).

Similarly, the proportions of semi-rotating cores are quite average (9–10%, except for units 7–8: 31.4%; Table 5.39 and Figure 5.36), although they are a priori the main source for the abundant production of blades. However, they are in some cases less numerous than the blade cores as in their final stage of exploitation, elongated flakes are removed rather than true blades.

Retouched tools

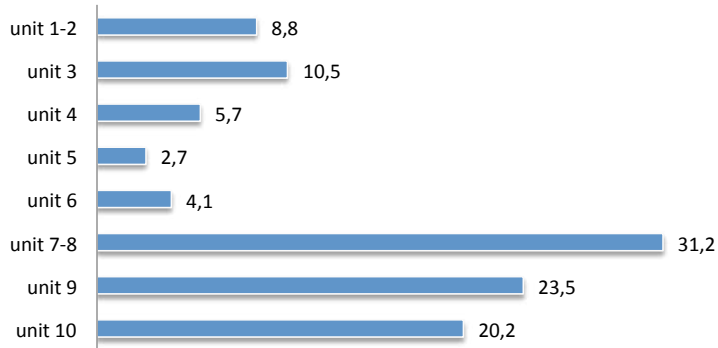


Figure 5.32. Hayonim – Frequencies of retouched tools in units 10 to 1-2.

Retouched blades/elongated points

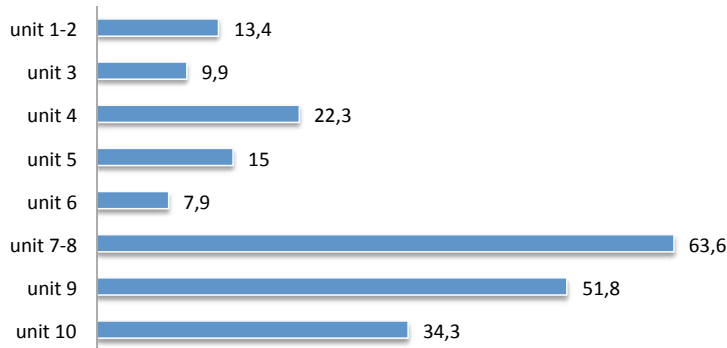


Figure 5.33. Hayonim – Frequencies of retouched blades and elongated points in units 10 to 1-2.

Scrapers

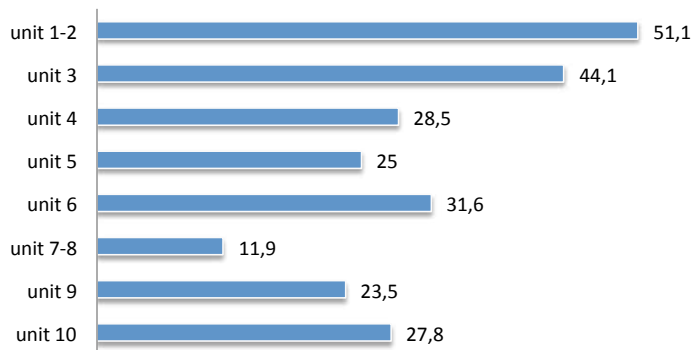


Figure 5.34. Hayonim – Frequencies of scrapers in units 10 to 1-2.

Unit	Total assemblage	Cores		On flake blank		Flake cores		Blade cores		Bladelet cores		Levallois cores		Levallois? cores		Preferential surface cores		'Semi-tournant' cores	
	N	N	N	%	N	%	N	%	N	%	N	%	N	%	N	%	N	%	
Units 1-2	4033	143	49	34.27	129	90.21	3	2.10	1	0.70	47	32.87	28	19.58	24	16.78	2	1.39	
Unit 3	2209	86	25	29.07	67	77.91	8	9.30	0	0.00	27	31.40	27	31.40	9	10.47	8	9.30	
Unit 4	2392	85	27	31.76	61	71.76	13	15.29	9	10.59	9	10.59	14	16.47	11	12.94	22	25.88	
Unit 5	786	34	13	38.24	25	73.53	6	17.65	3	8.82	3	8.82	1	2.94	4	11.76	13	38.24	
Unit 6	978	41	10	24.39	34	82.93	4	9.76	3	7.32	6	14.63	7	17.07	9	21.98	8	19.51	
Units 7-8	845	35	14	40.00	24	68.57	9	25.71	2	5.71	3	8.57	5	14.28	2	5.71	11	31.43	
Unit 9	1819	60	16	26.67	48	80.00	6	10.00	3	5.00	9	15.00	21	35.00	5	8.33	6	10.00	
Unit 10	1681	65	17	26.15	56	86.15	7	10.77	2	3.08	11	16.92	20	30.77	7	10.77	6	9.23	

Table 5.77. Hayonim units 10 to 1-2 – Main categories of cores. Percentages are of 'total number of cores', except core percentage calculated from the total assemblage.

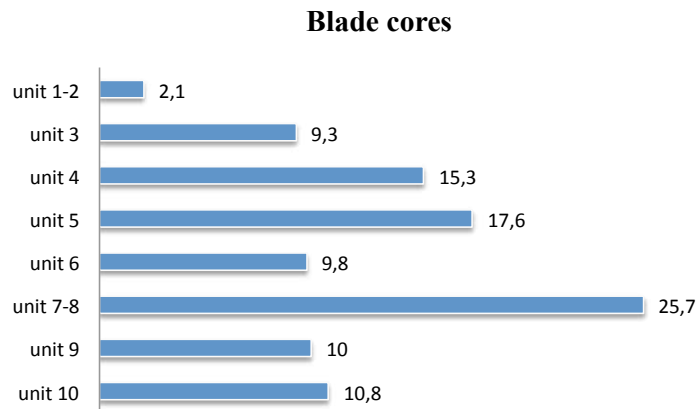


Figure 5.35. Hayonim – Frequencies of blade cores in units 10 to 1-2.

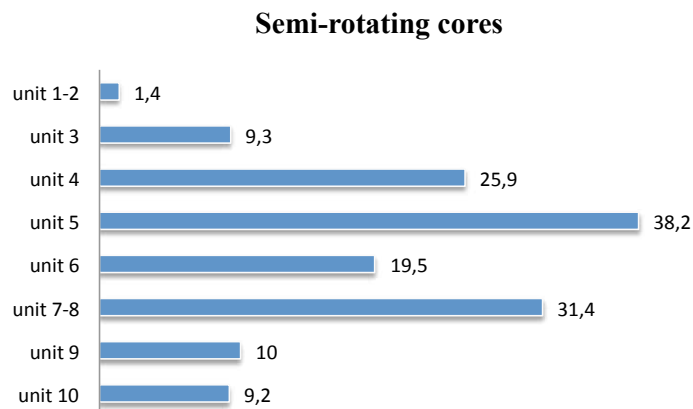


Figure 5.36. Hayonim – Frequencies of semi-rotating cores in units 10 to 1-2.

Lithic densities

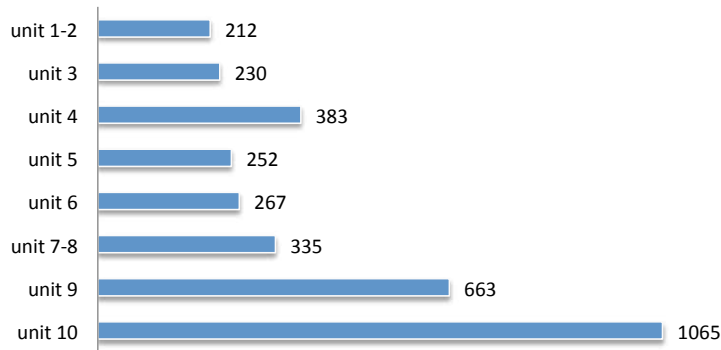


Figure 5.37. Hayonim – Lithic densities in units 10 to 1–2.

From a techno-economic perspective

The widespread presence of all of the elements of the reduction sequences (Levallois as well as Laminar) indicates substantial blade and flake production activities onsite, in cave entrance area, near the porch.

On the other hand, as we described earlier, the high blade proportions seem to correspond to the import of a large part of these blanks, already prepared off-site, or at least in another part of the cave. These elongated pieces were introduced in the form of unworked blanks, or possibly in the form of retouched tools, given the high proportions of retouched blades and points. The Levallois production is largely organised within the cave.

The high proportions of retouched products, especially those on blades, attest to the frequency of tool maintenance activities, some of which show an intensive use (some of the retouched blades/some tools on ventral face).

These data go hand in hand with the artefact densities, which are certainly the highest of the entire sequence (Figure 5.37), but which remain relatively low compared with other sites (e.g., Late MP at Kebara [Bar-Yosef 1998] and the Early MP at Misliya [Weinstein-Evron and Zaidner 2017]), indicating relatively short occupations during which production activities and tool use occurred. The absence of preserved bones hinders further interpretation of the activities performed in the cave.

The procurement strategies at this site are thus based on a ‘provisioning of place’ strategy (import of raw material subsequently knapped onsite) accompanied by a ‘provisioning of individuals’ strategy (import of personal gear, mainly in the form of blades [unworked and/or retouched]).

Units 6 to 4 (Layer Lower E; 185 ka–160 ka)

In these intermediate units:

- While the proportion of elongated blanks (blades/points) substantially decreases (Table 5.10 and Figure 5.31), the general characteristics of this production remain similar to those of the lower levels.
- In these assemblages, semi-rotating cores are still numerous (Table 5.77 and Figure 5.36).
- Among the elongated blanks, the Laminar products are dominant in units 5 and 4 (Table 5.12). The blade morphologies (subquadrangular and subtriangular), as well as the reduction systems, are very similar to those of the lower levels (unidirectional parallel and convergent dominant with, however, the development of bidirectional in unit 4; Table 5.52).

Table 5.78. Hayonim units 10 to 1–2 – Dominant dorsal scar patterns of the Levallois blanks. Excluding indeterminate patterns. **Data for units 1–2 are based on the study of the selected sample (see text). KEY: unid par = unidirectional parallel; unid conv = unidirectional convergent; bidir = bidirectional; centr = centripetal.

Unit	Total Levallois					Levallois flakes				
	pattern 1	%	pattern 2	%	% centr	pattern 1	%	pattern 2	%	% centr
Units 1-2**	centr	25.74	bidir	22.79	25.74	centr	34.95	bidir	23.12	34.95
Unit 3	unid conv	31.78	bidir	27.13	18.22	unid conv	29.47	bidir	28.99	21.74
Unit 4	bidir	33.65	unid par	23.22	7.11	bidir	33.78	unid par	23.65	9.46
Unit 5	unid conv	37.31	unid par	22.39	4.48	unid conv	31.71	unid par	26.83	7.32
Unit 6	unid conv	46.50	bidir	23.57	1.91	unid conv	44.44	bidir	26.67	3.33
Units 7-8	unid conv	35.24	unid par	27.62	2.86	unid par	29.63	bidir	29.63	5.56
Unit 9	unid conv	43.98	unid par	34.72	1.85	unid conv	39.67	unid par	35.54	3.31
Unit 10	unid conv	38.99	unid par	38.99	1.83	unid par	45.45	unid conv	30.30	2.27

- The Levallois production is still dominated by short blanks (elongated flakes) (Table 5.11 and Figure 5.30) with subquadrangular and subtriangular morphologies, obtained via unidirectional exploitation systems (convergent and parallel), similar, therefore, to the patterns identified in the lower units, but also more exceptionally bidirectional, particularly in unit 4 (Table 5.78). Elongated Levallois products (blades and points) regress (Figure 5.30), as do the short points.

We also observe:

- A sharp decrease in the proportion of retouched tools (Table 5.10 and Figure 5.32), especially retouched blades and elongated points (Figure 5.33). Blade tools are no longer the major component of the toolkit (Table 5.13). This is one of the most striking points of these levels.
- On the contrary, short blanks now dominate; scrapers are the most frequent tools (Table 5.13 and Figure 5.34), among which those on ventral faces, abundant in the lower levels, are now present in insignificant proportions (Table 5.54). On the other hand, UP tools are well represented (Table 5.13), especially burins, raising the question of their role in the production of bladelets.

From a techno-economic point of view:

Characterised by very low lithic artefact densities (Figure 5.37), especially in units 6-5, these assemblages show high proportions of debitage products (especially cortical products) (Table 5.15 and Figure 5.38)—much higher than observed in the lower levels—and a slight increase in cores (especially blade cores; Table 5.77), while the percentages of retouched pieces drop considerably (2.7 to 5.7%; Figure 5.32).

The Laminar and Levallois reduction sequences were mostly conducted onsite (provisioning of place) while the proportion of imported products in the assemblages (introduction of personal gear) is much lower.

Units 3 to 1–2 (Layer Upper E; 145 ka–130 ka)

Clear changes occur in the upper part of the sequence:

- A low representation of elongated blank production (blades and points, Levallois and Laminar) (Table 5.10 and Figure 5.31). In these units, the elongated Levallois component increases while the Laminar production decreases (Table 5.12). The Laminar component (wide/narrow thick blades), still quite abundant in unit 3, decreases while wide Levallois blades increase in units 1–2 (Table 5.12). Together with the considerable decrease of thick elongated blanks, the semi-rotating cores, still present in unit 3, tend to disappear in units 1–2 (Table 5.77 and Figure 5.36).

Debitage products

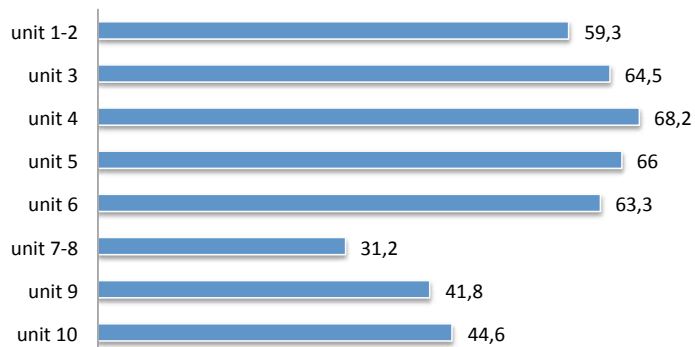


Figure 5.38. Hayonim – Frequencies ofdebitage products (ordinary and cortical blanks) in units 10 to 1-2.

Centripetal Levallois flakes

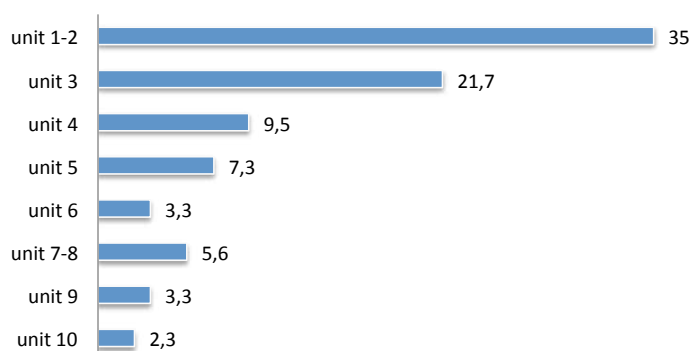


Figure 5.39. Hayonim – Frequencies of centripetal Levallois flakes in units 10 to 1-2.

Levallois flake morphologies

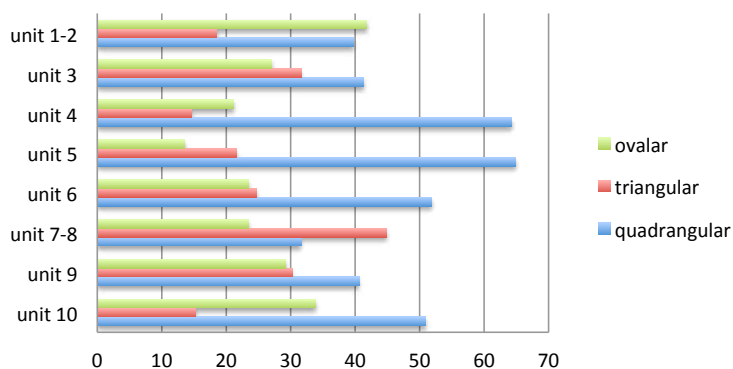


Figure 5.40. Hayonim – Frequencies of the different Levallois flake morphologies in units 10 to 1-2.

- Levallois flakes dominate the production. While the Levallois production remains in proportions similar to those of the underlying units, with however a marked increase in units 1-2 (unit 3 = 17.8; units 1-2 = 24.38; Table 5.11), its composition differs: we observe a clear development of short blanks, especially Levallois flakes (unit 3 = 85.72, units 1-2 = 83.30; Table 5.11 and Figure 5.30). The most striking element, however, is the development of centripetal preparation/exploitation patterns which started in unit 3 and became very clear in units 1-2 (Table 5.62 and Figure 5.39), whereas

Levallois cores

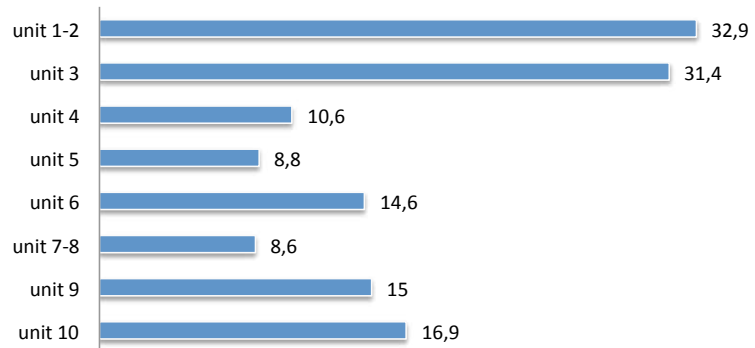


Figure 5.41. Hayonim – Frequencies of Levallois cores in units 10 to 1–2.

Scrapers vs elongated retouched products

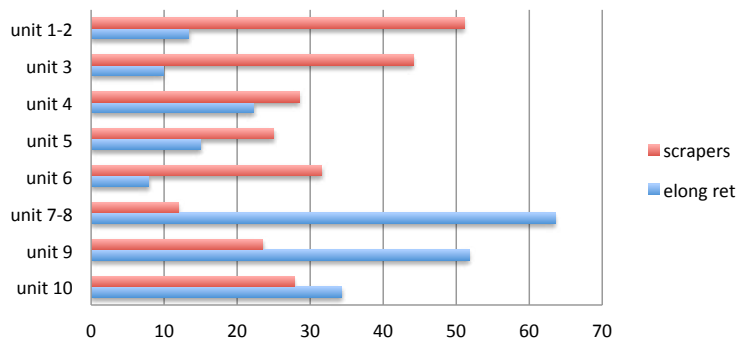


Figure 5.42. Hayonim – Frequencies of scrapers versus elongated retouched products in units 10 to 1–2.

they were poorly represented in the underlying levels. This change is reflected in the increase of flakes with a sub-oval morphology in units 1–2, while subtriangular/sub-quadrangular shapes are still dominant in unit 3 (Table 5.59 and Figure 5.40), as in the underlying units. There is also a clear increase in Levallois cores (Figure 5.41), especially preferential (centripetal preparation phase) and centripetal recurrent Levallois cores in units 1–2, while many unidirectional recurrent cores are still present in unit 3 (Table 5.75), as observed in the underlying units (Tables 5.40, 5.57).

- A notable change occurs in the retouched tools, among which the flake tools (mainly scrapers) become preponderant, to the detriment of tools on elongated blanks, which decrease considerably, confirming the trend already observed in the units 6–4 (Table 5.13 and Figure 5.42).

We thus observe a development of the Levallois system for flake production via preparation/exploitation modalities by centripetal removals, with a dominance of scrapers. According to the TL dates, this change would have occurred around 145 ka/130 ka.

Clearly these assemblages no longer correspond to the Early MP (loss of all characteristic elements) but are more similar to the Mid-Middle Palaeolithic assemblages (Qafzeh, Skhul, Neshar Ramla, etc., see discussions below) which develop during the MIS 5.

From a techno-economic point of view:

Although the production systems implemented in these upper levels change markedly (development of the centripetal Levallois), the occupation patterns in the cave remain similar to those identified in the immediately underlying units.

Oriented toward the Levallois system, blank production was mostly conducted onsite in the Central Area of the cave, attested by the numerous by-products, including cores and CTEs characteristic of this flaking system. The ratios of Levallois products to Levallois cores confirm a strategy of provisioning of place, with the possibility of Levallois blanks being exported in unit 3 when the Palaeolithic people left the cave (ratio in unit 3 = 7; in units 1–2 = 12.6).

The Laminar component is quite secondary, practically disappearing in units 1–2. It likely corresponds to an introduction of these products in their finished state (personal gear), as suggested by the very low presence of cores corresponding to this production.

Given the low densities of lithic artefacts (Figure 5.37), these data suggest short-term occupations during which tool production, use, and maintenance were the main activities.

5.5.5. Discussion of the Hayonim MP sequence in the context of the Levantine MP

What do these results tell us?

Units 10 to 7–8 (Layer F; 210 ka–220 ka)

With their specific characteristics—elongated blanks (blades and points) selected for retouching, a majority of retouched blades and points among the tools, a coexistence of Laminar and Levallois blade production systems, and the emergence of the full-fledged Levallois—the lithic assemblages of units 10 to 7–8 (Layer F) are an integral part of the Early MP (Meignen and Bar-Yosef 2020). These assemblages were also largely implicated in the research that defined the particularities of this technical entity.

A comparison of the results obtained for the Hayonim sequence with the data of the few recently published sites associated with this period (Hummal 6b [Wojtczak 2014, 2015]; Misliya 5–6c [Zaidner and Weinstein-Evron 2020]; Tabun unit IX [Shimelmitz and Kuhn 2013]; Abou Sif [Wojtczak and Malinsky-Buller 2022; Table 5.79]) enables us not only to define the main characteristics of the Early MP entity but also to evaluate its variability, which is rarely mentioned:

- An indisputable feature of these Early MP tools, which is systematically highlighted, is that the proportions of elongated blanks always constitute a high proportion of these assemblages. These proportions vary, however, from 30 to 50%, and are thus not always largely dominant (Table 5.79). It is probable that the variations observed in these percentages are related to behaviours of lithic resources management (variable proportions of imported blades), at least in some assemblages (behaviour observed in the Hayonim 10 to 7–8 levels (see above), described at Tabun IX, most probably also present at Misliya and Hummal, even if this is not always clearly stated by the authors).
- The blades were obtained from Laminar and Levallois flaking systems, both of which are still present but in highly variable proportions depending on the assemblage (Meignen 2007, 2011 and references therein).
- The most specific point is undoubtedly the high proportion of tools made on blades, but here again in variable proportions (Table 5.79). Points and especially retouched blades are the most frequent forms. This feature is particularly striking at Hummal, where retouched blades dominate the assemblage. The retouched points, often considered as the marker element of this entity, are dominant only in the Misliya assemblage. In view of these observations, it seems that the selection of elongated blanks to make tools is the characteristic element, more than the frequency of retouched elongated points, tools that are certainly remarkable but whose predominance is not the general rule.
- The Levallois production is always well represented, including the significant presence of short blanks with, in particular, the first appearance of Levallois points in the PM of Levant (Table 5.79). On these last two points, we should note, however, that the Hummal assemblage seems to be an exception. In effect, the Hummal assemblages are

	Tabun unit IX	Hummal 6b	Hayonim unit 10	Hayonim unit 9	Hayonim units 7-8	Misliya 5-6c	Abou Sif B	Abou Sif C
	<i>(Shimelmitz and Kuhn 2013)</i>	<i>(Wojtczak 2014)</i>	<i>(Meignen this volume)</i>	<i>(Meignen this volume)</i>	<i>(Meignen this volume)</i>	<i>(Zaidner and Weinstein-Evron 2020)</i>	<i>(Wojtczak and Malinsky-Buller 2022)</i>	<i>(Wojtczak and Malinsky-Buller 2022)</i>
Blady component	50.1%	50.3%	29.2%	37.3%	45.1%	36.2%	44.7%	54.6%
Retouched tools made on blades	*	78.7%	44.2%	64.5%	78.5%	59.1%	62.0%	77.9%
Ret blades and elongated points	*	70.4%	34.2%	51.8%	63.6%	55.9%	*	*
<i>including</i>								
retouched blades		44.8%	21.4%	36.6%	39.1%	15.0%		
retouched elongated points		25.6%	12.8%	15.2%	24.5%	40.9%		
Levallois component	51.4%	7.0%	23.1%	21.4%	23.5%	> 21.6%	23.5%	18.0%
Proportion Lev points/tot Lev	18.8%	5.5%	26.8%	13.6%	28.9%	*	*	*
<i>including</i>								
short Levallois points	11.0%	4.1%	16.6%	7.7%	14.7%			
elongated Levallois points	7.8%	1.4%	10.2%	5.9%	14.2%			

Table 5.79. Main characteristics of selected Levantine Early Middle Palaeolithic assemblages. Data not available are noted by an asterisk.

distinguished by the low frequency of Levallois products (Wojtczak 2014, and personal communication) and, above all, the predominance of blade production, mostly associated with the Laminar system (Table 5.79). This is undoubtedly one of the elements that led the first authors (Bergman and Ohnuma 1983; Copeland 1983; Copeland 1985; Meignen 1994; Monigal 2001) to define it as a separate, original and independent entity, stratigraphically situated between Acheulo-Yabrudian and the Mousterian. It was then considered chronologically earlier than the Early Levantine Mousterian (Monigal 2001), which was then defined based on the Tabun unit IX assemblages, largely dominated by Levallois methods for blade production. Subsequent discoveries and studies (assemblages from Hayonim [Meignen 2011], Tabun IX [Shimelmitz and Kuhn 2013], Misliya [Zaidner and Weinstein-Evron 2014; Zaidner and Weinstein-Evron 2020], Emanuel [Goder-Goldberger et al. 2012], as well as the radiometric dating now available (Mercier et al. 2007; Mercier et al. 1995; Valladas et al. 2013), have clarified the overall picture of this Early MP entity in its different variants and chronology. The radiochronological data available for the Hummal levels, although widely discussed (Richter et al. 2011), suggest that these assemblages do not significantly predate other Early MP assemblages, such as Tabun IX or Hayonim F, as previously assumed, but are part of the internal variability of this entity (Meignen 2007, 2011).

In the literature, Early MP assemblages are often characterised by higher proportions of retouched products than in the other MPs that follow them, thus making exception to the often described image of a Levantine MP usually slightly retouched. These notable proportions of retouched tools are undoubtedly related to site use pattern (import and curation of personal gear; Hovers 2001; Meignen this chapter; Meignen et al. 2006, and references therein). But it is very likely that, due to the low standardisation of the production, especially in the Laminar system, additional transformation (retouching the active part or the prehensile area of the tool) was often necessary to obtain the desired functional characteristics.

Units 6–4 (Layer Lower E; 185 ka–160 ka)

The question of whether these assemblages belong to Early MP deserves to be discussed. As we have seen, they are characterised by significant changes in their composition compared with previous assemblages.

Elongated blanks (blades and points) are less well represented but the technical production methods are quite similar to those identified in the lower units. Semi-rotating

cores, which produce blades, are still largely present. The percentage of retouched products, still often on blades, clearly decreases (Table 5.10), especially retouched blades and points, emblematic of the Early MP (Table 5.13).

If we consider these various elements (and especially blade production), we can, however, consider that the assemblages of units 6–4 conform to the variability of the Early MP. The cores and CTEs collected in unit 4 (the most significant assemblage of these intermediate units) are highly representative of the Laminar production, as we previously identified it (Figures 5.13: 3; 5.24: 1, 5). The differences observed with the lower units are mainly quantitative and are probably due to the different modalities of raw material management in the region.

In effect, a comparison of the data obtained for the assemblages of the lower units (Early MP) with those of units 6–4 shows the same blade production modalities, only the proportions of these products in the assemblages are different (they are much less numerous in units 6–4). The cores are also of the same type, and the semi-rotating cores are particularly well represented, being more numerous even in unit 5 (Figure 5.36), while the corresponding production (blades) is greatly decreased.

Given the low lithic artefact densities in units 6–4, the characteristics described above are most likely the consequence of short-term occupations, during which elongated blank production activities took place. On the other hand, the ratios of blades to semi-rotating cores are much lower than those observed in the lower units. This would indicate little import into the cave, in contrast to the remarkable import of blades (unworked or retouched) evident in units 10 to 7/8. These results indicate a somewhat different strategy for provisioning the site, based here mainly on a ‘provisioning of place’ behaviour.

It is clear that the relatively low proportions of elongated blanks observed here do not fit with the range variability that we have highlighted for the Early MPs (see above). However, the notable representation of cores linked to the production of elongated blanks, and the presence of elongated CTEs displaying the characteristic offset opposed striking platforms (Figures 5.13: 3; 5.23: 3; 5.24: 2-5), are sufficiently diagnostic to attribute these assemblages to the Early MP.

The low representation of retouched blanks (especially retouched blades and points) could be both a consequence of the much lower proportions of imported elongated blanks and short occupation periods during which less preparation/recycling of retouched tools was necessary.

These data would then support the arguments previously advanced in favour of the intermediate levels (units 6–4) belonging to the Early MP entity—the variations observed being rather ‘economic’ while the technical repertoire would remain similar to that of the lower units.

However, it is difficult to demonstrate the strength of the links between these two groups of units given the large chronological gap of about 30 ka, corresponding to the erosion highlighted in the field between Layer F (units 10 to 7–8) and Layer Lower E (units 6–4). However, we should remind that chronologically these units, dated to 185 ka–160 ka, are still within the margins recognised for the Early MP in the region (Early MP dating at Misliya: 212+/- 27 to 166 ka +/- 27 ka; Valladas et al. 2013).

If we now consider the assemblages of the upper units:

Units 3–1 (Layer Upper E; 145 ka–130 ka)

The significant changes between the assemblages of units 6–4 and those of the higher units start in unit 3 (they still show characteristics in continuity with units 6–4) and become very clear in units 1–2.

From unit 3 onward, there is a high proportion of Levallois cores and related products (which become even more numerous in units 1–2) (Table 5.77), as well as high percentages of short Levallois blanks (mainly flakes) (Table 5.10). The classic *débordant*

Table 5.80. Hayonim units 10 to 1–2 – Main categories of CTEs. Among the classical *débordants*, the number of those called *à dos limité* are shown in parentheses.

Unit	<i>Débordants</i> with cortical back		<i>Débordants</i> with non-cortical back		Classical <i>débordants</i> including <i>dos limités</i>		Crested blades		Total CTE
	N	%	N	%	N	%	N	%	
Units 1–2	83	70.94	9	7.69	23 (12)	19.66	2	1.71	117
Unit 3	70	72.92	5	5.21	14 (9)	14.58	7	7.29	96
Unit 4	76	85.39	1	1.12	10 (4)	11.24	2	2.25	89
Unit 5	29	100.00	0	0.00	0	0.00	0	0.00	29
Unit 6	31	88.57	3	8.57	0	0.00	1	2.86	35
Units 7–8	32	78.05	1	2.44	2 (1)	4.88	6	14.63	41
Unit 9	68	78.16	9	10.34	3 (1)	3.45	7	8.05	87
Unit 10	71	83.53	4	4.71	4 (3)	4.71	6	7.06	85

Total Levallois

	Unit 10		Unit 9		Units 7–8		Unit 6		Unit 5		Unit 4		Unit 3		Units 1–2**	
	N = 197		N = 194		N = 98		N = 150		N = 62		N = 194		N = 248		N = 477	
	n	%	n	%	n	%	n	%	n	%	n	%	n	%	n	%
subcirc/ovalar	46	23.35	50	25.77	23	23.47	38	25.33	9	14.52	38	19.59	59	23.79	172	36.06
subtriangular	72	36.55	73	37.63	44	44.90	55	36.67	24	38.71	48	24.74	92	37.10	136	28.51
subquadrangular	79	40.10	71	36.60	31	31.63	57	38.00	29	46.77	108	55.67	97	39.11	169	35.43

Levallois flakes																
	Unit 10		Unit 9		Units 7–8		Unit 6		Unit 5		Unit 4		Unit 3		Units 1–2**	
	N = 112		N = 106		N = 49		N = 85		N = 37		N = 137		N = 196		N = 345	
	n	%	n	%	n	%	n	%	n	%	n	%	n	%	n	%
subcirc/ovalar	38	33.93	31	29.24	16	32.65	20	23.53	5	13.51	29	21.17	53	27.04	144	41.74
subtriangular	17	15.18	32	30.19	12	24.49	21	24.71	8	21.62	20	14.60	62	31.63	64	18.55
subquadrangular	57	50.89	43	40.57	21	42.86	44	51.76	24	64.87	88	64.23	81	41.33	137	39.71

Table 5.81. Hayonim units 10 to 1–2 – Morphologies of the Levallois blanks. Percentages are of 'total number of identifiable morphologies'. **Data for units 1–2 are based on the study of the selected sample (see text).

products, linked to the shaping/maintenance of the centripetal Levallois cores, increase (Table 5.80). The production of elongated blanks decreases.

On the other hand, certain characteristics of the tools in unit 3 still show affinities with those of the underlying units 6–4, characteristics that disappear (or diminish) in units 1–2.

Among the blades, the Laminar component is still prominent in unit 3 (thick blades from Laminar flaking dominate) (Table 5.12), in association with the semi-rotating cores still present, whereas they practically disappear in units 1–2 (Table 5.77).

The scar patterns of Levallois flakes are still dominated by unidirectional convergent and bidirectional organisations in unit 3, even though centripetal patterns are present (Table 5.78); these only become dominant in units 1–2 (Figure 5.39). Correlatively, the morphologies of the Levallois products are still predominantly subtriangular/subquadrangular in unit 3; sub-oval morphologies dominate only in units 1–2 (Table 5.81, Figure 5.40).

In unit 3, recurrent Levallois cores are predominantly uni/bidirectional (as in the underlying units), whereas centripetal recurrent Levallois cores, along with flake cores with preferential centripetal preparation, dominate in units 1–2 (Table 5.75).

We thus observe progressive changes in the production methods and products sought: loss of certain characteristics (blade production, especially Laminar) in favour of new ones (centripetal Levallois production), which are progressively established. It is only in units 1–2 that the dominant centripetal Levallois flakes, mainly of sub-oval morphology, are solidly established (i.e., around 129 ka +/- 13 ka [unit 2 in Mercier et al. 2007]).

The characteristics of the assemblages of units 1–2 show clear affinities with the more or less contemporary (Nesher Ramla unit VI; Skhul) or slightly later (MIS 5; Qafzeh, Nesher Ramla I-III) centripetal-dominant assemblages, even if the development of centripetal modalities is still much less marked than in these sites. Comparisons with these more or less contemporary or slightly later assemblages should give us keys to understanding the processes involved.

Therefore, as we have seen, the Hayonim sequence documents the Late LP to Early MP transition and, more specifically, the onset of the Early MP, its development, and finally its gradual disappearance to give way to the beginnings of what are classically called Mid-MP assemblages, which reach their peak during MIS 5.

This sequence therefore contributes to our understanding of the main changes observed in the Levant from MIS 7 to the beginning of MIS 5.

Acknowledgements

Numerous people and some granting agencies were responsible for making this research on lithic collections possible under very good conditions.

First of all, I would like to thank the late Ofer Bar-Yosef and Bernard Vandermeersch for inviting me in such a challenging research project.

I am deeply indebted to Ofer in many ways: for his many invitations to Harvard and Jerusalem of course, but even more for all of the scientific exchanges and lively debates we had in the field and at home on many topics about the early human capabilities and knowledge.

I am also grateful to the different Directors and the staff from the Centre de Recherche Français de Jérusalem (CNRS) who gave me their technical and friendly support during this project: especially Daniel Ladiray who drew all of the lithic artefacts presented in this chapter, and Marjolaine for her support in photography.

Several grants from the French Ministry of Foreign Affairs and from the Irene Levi Sala CARE Archaeological Foundation assisted my lithic studies during long stays in Jerusalem, without which this research would not have been possible.

All along this research, I have benefited from the friendly help of the Hayonim team during the fieldwork, and from many other colleagues, especially in the Institute of Archaeology (Hebrew University of Jerusalem), a place where I have been always, and still now, very warmly welcomed by scholars from all generations who became very good friends. Many thanks to all of them for making me feel at home there in Jerusalem.

Technological, cultural and behavioural changes in the Levant from the Late Lower Palaeolithic to the Mid-Middle Palaeolithic: Contribution from the Hayonim sequence

Liliane Meignen

The long archaeological sequence at Hayonim is more than 7 m deep and covers a period including the Late Lower Palaeolithic (Acheulo-Yabrudian/Layer G, unit 11—undated but earlier than 220ka—) and a large part of the Middle Palaeolithic.

During this period, previously recognised major behavioural and cultural changes can be identified in the Hayonim sequence based on the interdisciplinary studies we have conducted.

These major changes concern, first of all, the domain of lithic technology, whose production systems change, either radically during the Late Lower Palaeolithic (Late LP)/Early Middle Palaeolithic (Early MP) transition, or more gradually during the ‘disappearance’ of the Early MP. The processes underlying these changes are the subject of numerous debates, to which Hayonim contributes essential elements.

The second domain in which significant transformations are observed is the settlement patterns within the region. The Hayonim data have already contributed to the identification of long-term trends in this field during the transition from the early to later Levantine Mousterian (Hovers 2001; Hovers and Belfer-Cohen 2013; Meignen, Speth, and Stiner 2006).

In this concluding section, we summarise the information and discussions that our recent research contributes to these two broad research questions.

6.1 Changes in lithic production

In the long Hayonim sequence, extending from the Late MIS 8 to the Late MIS 6, the results of our research highlight, in addition to the importance of the Early MP levels identified through 3.5 m of deep deposits, two major periods of change in the technical repertoires:

- Onset and development of the Early MP during the ‘Late LP to MP Transition’, with a shift from Acheulo-Yabrudian (Layer G, unit 11) to the Early MP (Layers F and Lower E, units 10 to 4) (Meignen and Bar-Yosef 2020);
- Disappearance of the Early MP, with technological changes observed between the Early MP (Layers F and Lower E, units 10 to 4) and the appearance of Levallois MP assemblages quite similar to those of the Mid-MP (Layer Upper E, units 3 and 1–2).

While among recent studies, some sites, such as Misliya (Zaidner and Weinstein-Evron 2016; Zaidner and Weinstein-Evron 2020), Hummal and El Kowm Basin (Hauck 2011a; Le Tensorer et al. 2011; Wojtczak 2014), Tabun (Shimelmitz et al. 2014b; Shimelmitz and Kuhn 2013; Shimelmitz et al. 2021; Shimelmitz et al. 2016) and Dederiyeh (Nishiaki, Kanjou, and Akazawa 2017, 2022; Nishiaki et al. 2011), contribute information on the transition between the Late LP and Early MP, only the Hayonim sequence documents, within the same stratigraphic sequence, the disappearance of the Early MP and the development of the subsequent tool assemblages.

For example, research conducted on the Hummal sequence (Syria), where the Early MP (Hummalian) and later MP are also present, did not enable this type of study because the stratigraphic relations between the levels containing the Levallois-Mousterian (Level 5; Hauck 2011a) and those containing the Hummalian (Level 6; Le Tensorer et al. 2011) lack stratigraphic continuity (Hauck et al. 2010: 156) in a site where the stratigraphy is very complex. In the long Tabun sequence, the depositional context of units VIII-II, intermediate between unit IX (Early MP) and unit I: 18-26 (‘Levallois-Mousterian’ Layer C), also does not allow this question to be addressed due to disturbed deposits (Jelinek 1982a). Finally, at the Neshar Ramla site, while units V-VI do cover the period of interest, they do not contain any Early MP assemblages (Zaidner et al. 2021).

The results obtained from the Hayonim sequence thus contribute new elements to the debates concerning the processes of change in the technical repertoires of the groups occupying the Levant at the end of the Middle Pleistocene to the beginning of the Late Pleistocene, a crucial period in the development of *Homo sapiens* and Neanderthals between Africa and Eurasia.

Integrated with the data corpus that has been updated by recent discoveries and research programs in the region, and concerning more or less contemporary levels, our research enables us to propose the following ideas.

6.1.1 Transition from the Lower to Middle Palaeolithic: technological break between the Acheulo-Yabrudian and Early MP

In the Levant, the Late Lower Palaeolithic is characterised by flake tools and a *chaîne opératoire* producing thick, often cortical blanks that were generally transformed into scrapers, frequently via Quina retouching (Yabrudian). This production shares many features with the European Quina Mousterian (Bordes 1955; Dibble 1991; Jelinek 1982a, b), as underlined by Kuhn’s definition of a ‘Quina/Yabrudian pattern’ (Kuhn 2013b) that concerns not only blank production but also tool management. This lithic production system, previously unknown in the Levant and elsewhere, clearly represents a post-Acheulean technical innovation.

In the various Late LP assemblages, this production of thick blanks is frequently associated with a more or less substantial bifacial component. These Late LP assemblages include a significant number of bifaces in the so-called ‘Acheulean’ facies *sensu* Jelinek (1982a, b), as described in unit 11 at Hayonim and unit X at Tabun (Shimelmitz et al. 2021); or most frequently include a few bifaces (‘Acheulo-Yabrudian’ facies) (identified at Misliya [Zaidner and Weinstein-Evron 2016] and at Tabun Beds J82BS, J83B1 [Shimelmitz et al. 2014b]); or sometimes lack bifaces (‘Yabrudian’ facies) (described for instance at Dederiyeh [Nishiaki, Kanjou, and Akazawa 2017]). Neither of these lithic production systems (bifacial shaping and the Quina-like reduction strategy) is observed in any of the succeeding Levantine Middle Palaeolithic assemblages.

Conversely, as previously described at Hayonim, the Early MP is globally characterised by the total disappearance of bifacial shaping and Quina-like productions, as well as by the coexistence of Levallois and Laminar reduction systems, including a significant blade component in the same assemblages. The high proportions of retouched tools shaped on elongated products (blades and points) are also noteworthy. Moreover, from the onset of the Early MP, around 250 ka–230 ka (as evidenced at Misliya [Valladas et al. 2013]), the Levallois flaking system appears in its fully-fledged form, with the whole range of end-products: flakes, blades, and, even more importantly, Levallois points. The latter constitutes a new component in this toolkit (Hovers and Belfer-Cohen 2013; Malinsky-Buller 2016; Meignen and Bar-Yosef 2020; Shimelmitz et al. 2016; Weinstein-Evron and Zaidner 2017; Zaidner and Weinstein-Evron 2020), still present later in the Mid-MP (at Neshar Ramla, Skhul, Qafzeh XV [Zaidner et al. 2021, and references therein]) and which largely expanded later in the Late Levantine Middle Palaeolithic (Bar-Yosef and Meignen 1992; Meignen 2019; Meignen and Bar-Yosef 1992).

In the Levant, between the end of the Late LP and the Early MP, a technological package (Acheulo-Yabrudian in Hayonim) was replaced by a new one corresponding to a rapid cultural turnover process. A marked technological break is observed in the lithic technological sphere that might be linked to social and/or biological changes (Hershkovitz et al. 2018; Hovers and Belfer-Cohen 2013; Malinsky-Buller 2016; Malinsky-Buller and Hovers 2019; Zaidner et al. 2021; Zaidner and Weinstein-Evron 2016) (see discussion below).

However, some authors argue for a form of continuity between the Acheulo-Yabrudian and Early MP (Jelinek 1982b; Klein 1999; Nishiaki 1989; and more recently, Shimelmitz et al. 2021; Shimelmitz et al. 2016), based specifically on blade production. Some authors have suggested that the blade manufacturing identified in the Early MP may represent a regional development of the that already seen in the Late LP Amudian industries (thus serving as evidence for cultural continuity based on this component [Bar-Yosef 1982; Copeland 1985; Copeland 1995; Jelinek 1982a, b; Shimelmitz et al. 2016; Wojtczak 2015]). However, careful observation of the currently available data shows that these two blade-producing industries are qualitatively different in their overall technological organisation (Meignen and Bar-Yosef 2020), which is seen differences in the production methods and morphofunctional characteristics of the end-products, as well as in differences in the tool manufacturing and management. In the Amudian, the main technical investment was devoted to raw material selection and core exploitation, as well as to the well-controlled production of blanks that did not need further shaping, and could thus be directly used as tools. This contrasts with the greater technical investment in blank retouching in the Early MP (see Meignen and Bar-Yosef 2020 for more details).

Shimelmitz et al. (2016, 2021), based on a detailed analysis of the Late Lower Palaeolithic upper levels at Tabun, underline ‘particular technological choices within the reduction sequences of the Acheulo-Yabrudian that suggest some continuity in technological tradition’. The elements of continuity recognised by these authors mainly concern the degree of predetermination of scraper-blank production, control of the convexities of the flaking surface, and the recycling of handaxes for blade production. These analyses enable them to conclude ‘the knowledge and control of many technological procedures already manifest in the Late LP may have facilitated the rapid shift toward a more intensive use of the Levallois method in the Levant’ (Shimelmitz et al. 2016). The processes at play during the Acheulo-Yabrudian to Early MP transition would thus correspond, for these authors, to the combination of previously used debitage concepts with new ones, a phenomenon that could be related to the arrival of new human groups in the region. While this latter interpretation is possible (see discussion below), we should emphasise that the elements of continuity evoked in the arguments presented by these authors are very small in scale compared with the major technological changes described above, and are even questionable at times: the degree of predetermination evoked for the Amudian and Yabrudian productions is much weaker than that identified in the Levallois conceptions

(i.e., less control of the morphology of the products, especially in the Yabrudian). The production of blanks from bifaces has, of course, been recognised in various assemblages (DeBono and Goren-Inbar 2001; Shimelmitz et al. 2016, and references therein), but the productivity of this method is very low compared with that of the Levallois system. It must be emphasised, as previously stated, that the Lower Palaeolithic/Middle Palaeolithic transition resulted in a radical change in the technical repertoire, consisting of the total loss of the two previously known lithic production systems (bifacial shaping and Quina-like reduction system: thick blanks, retouching), and their replacement by a new gain: the explosion of the Levallois production system. The technical repertoire known in the Acheulo-Yabrudian may have facilitated the adoption of new production systems, but few traces of them remain. While it is probably fair to say that the previous repertoire in the Acheulo-Yabrudian was not totally eradicated, the impact of the arrival of new technologies is very strong indeed.

Based on the available data, it therefore seems clear that the hypothesis of a break in the technical repertoire is the most likely option (Malinsky-Buller 2016; Meignen and Bar-Yosef 2020; Zaidner and Weinstein-Evron 2016; Zaidner and Weinstein-Evron 2020). However, we must stress that, as many authors have already done (Blasco et al. 2014; Kuhn and Stiner 2019; Rolland 2000; Shimelmitz and Kuhn 2017a, and references therein; Stiner, Gopher, and Barkai 2011) a certain number of behaviours in domains other than lithic production, clearly established since the Acheulo-Yabrudian, continued without major changes during Early MP.

The increase in burning remains in the middle of the Acheulo-Yabrudian sequence (Shimelmitz et al. 2014b; Stiner, Gopher, and Barkai 2011, and references therein) suggests a shift to mastered fire production and its habitual use at around 325 ka–350 ka. During the Acheulo-Yabrudian, the systematic repetitive cave occupations and the changes in land-use patterns with a differentiation between food acquisition locations (kill site) and food consumption locations (deferred consumption in a habitation site) clearly illustrate fundamental behavioural changes in subsistence strategies—consisting of the organisation of hominin societies around base camps (Kuhn and Stiner 2019a, and references therein)—and most likely in the social systems of resource distribution (Stiner, Barkai, and Gopher 2009). These significant changes continued without significant modification in the occupations of the Early MP.

The implementation of all of these innovations during the Acheulo-Yabrudian (generally considered as the end of the Lower Palaeolithic) is thus not synchronous with the main abrupt technological shift that we have just described. This lag between changes in some behavioural domains (arrhythmia) is a phenomenon already described for other periods (see Kuhn [2013a] for the Initial UP-UP transition and Perlès [2013] for the Neolithic), with the factors of change operating at different temporal scales. This highlights the difficulties encountered in choosing the criteria we should use to define the major entities such as Lower Palaeolithic, Middle Palaeolithic and Upper Palaeolithic (see also Shimelmitz and Kuhn 2017a).

What does this ‘abrupt’ change in technical repertoires mean?

How can we interpret the widespread development of the Levallois system?

The meaning of these striking changes in lithic technology is still largely debated. The most significant element is the large-scale adoption of the Levallois system in all its complexity, a production method whose main feature consists of a greater control of the morphology of the products obtained. The adoption of a new technique to the detriment of another formerly used one is a significant event. A new flaking system becomes generalised either because the technique adopted is easier and/or more productive, or because it is better adapted to new needs (Pelegrin 1995).

The spread of the Levallois system observed at the beginning of the Early MP could be related to another aspect of lithic technical organisation: the hafting and composite tools (Boëda 1997, 2013; Bonilauri 2010, 2015; Kuhn 2013b; Shimelmitz et al. 2016). Hafted tools

are largely documented as part of the Middle Palaeolithic technical repertoire (Anderson-Gerfaud and Helmer 1987; Boëda et al. 1996; Bonilauri 2015; Rots 2015), even in the Early MP (Groman-Yaroslavski, Zaidner, and Weinstein-Evron 2016; Rots 2013).

One of the key aspects of Levallois technology, in tandem with the increased control over core configuration and maintenance, is its capacity to systematically produce a series of recurrent morphotypes; that is, relatively thin blanks with long regular cutting edges and acute edge angles (Boëda 1997; Delagnes and Meignen 2006). Significant variability in the overall contour and size of the intended products is observed as a consequence of the numerous modes of initialisation and production. At the same time, a high degree of standardisation of their proximal part (similar narrow butts) is recognised as a result of the carefully prepared striking platform. Faceting increases the precision of the percussion gesture and the control of the blank detachment, resulting in a greater regularity of the morphofunctional characteristics of the proximal part of the blank (Boëda 1997, 2013; Bonilauri 2010, 2015). This, in turn, facilitates different types of hafting (axial, lateral; Bonilauri 2010, 2015).

This option contrasts, for example, with the broad thick flakes/scrapers of the Acheulo-Yabrudian (at Hayonim unit 11 and other sites, such as Tabun, Qesem, Misliya, Dederiyeh), whose cutting edges opposite their cortical 'back' probably facilitated manual prehension, thus suggesting they were handheld tools (Boëda 2013; Shimelmitz et al. 2014b; Shimelmitz et al. 2016; Zupancich et al. 2016). The same hypothesis can be proposed for the Acheulo-Yabrudian bifaces previously described in Hayonim unit 11, Misliya, Jamal, and Tabun, for instance (Shimelmitz et al. 2016, and references therein), with their thick cortical or roughly prepared butt that is well adapted for gripping, as well as for the Amudian blades with their often cortical back opposite the cutting edge (Lemorini et al. 2006; Shimelmitz et al. 2016). The widespread development of Levallois technology may thus reflect a significant innovation in terms of tool ergonomics, with a shift from handheld tools during the Late LP to the commonly hafted tools in the Early MP (Boëda 1997, 2013; Groman-Yaroslavski, Zaidner, and Weinstein-Evron 2016; Hovers and Belfer-Cohen 2013; Kuhn 2013b; Shimelmitz et al. 2014b; Shimelmitz et al. 2016).

The expansion and diversification of the Levallois system at the onset of the Middle Palaeolithic raise the issue of its origin. The hypothesis of a possible arrival of exogenous populations or new ideas has often been proposed (Bar-Yosef 2017; Foley and Lahr 1997; Hershkovitz et al. 2018; Lahr and Foley 2003; Malinsky-Buller 2016; Malinsky-Buller and Hovers 2019; Weinstein-Evron and Zaidner 2017; Zaidner and Weinstein-Evron 2020). Although human fossil remains directly associated with the Early MP are rare, the recently published maxilla from Misliya unit 6, associated with Early MP artefacts dated to ca. 185 ka, suggests that early modern humans were probably the producers of the Levantine Early MP (Hershkovitz et al. 2018; Weinstein-Evron and Zaidner 2017). These results attest to the first appearance of early *Homo sapiens* in the Levant and suggest an out of Africa expansion of *Homo sapiens* earlier than the generally accepted younger wave (90 ka–120 ka) of the Qafzeh/Skhul hominins (Bar-Yosef 1998a; Hovers 2009; Vandermeersch 1982). These new data have been used to lend weight to a dispersal scenario explaining the 'appearance' of the Levallois technology in the Levant (Hershkovitz et al. 2018).

However, the presently available archaeological information does not show an unquestionable link with African lithic productions developed earlier than 250 ka, specifically before the onset of the Levantine Early MP. Even if Levallois technology is documented in eastern African sites at around 300 ka, most of these early Levallois productions appear to be oriented toward the production of Levallois flakes through preferential or recurrent centripetal methods (Shea 2008; Tryon and Faith 2013; Tryon, McBrearty, and Texier 2005). Tryon et al. (2005) did note some diversification of the Levallois reduction strategies during the Early Middle Stone Age (Early MSA), around 200 ka–250 ka, marked by the sporadic development of Levallois point production in the sequences of the Kaphthurin Formation (Koimilot 2; Tryon 2006) and more extensively in the Gademotta/Kulkuletti site complex (Douze 2013; Douze and Delagnes 2016; Sahle et al. 2014; Wendorf

and Schild 1974). Moreover, the Early MSA assemblages from ETH-72-1, a site dated to between 280 ka and 184 ka display an increase in Levallois points slightly modified by localised retouch. However, in these assemblages, unifacial/bifacial shaping was still the dominant process used to produce convergent tools. Elongated Levallois and Laminar items are described (blade production) but in low frequencies (Douze 2013; Sahle et al. 2014). Therefore, even if we acknowledge the presence of the Levallois point component and the tendency toward convergent tools shared by the early MSA in this area and the Levantine Early MP, the main characteristics of the Levantine Early MP are not observed in these African sites. The Early MSA convergent tools differ from the Levantine Early MP points, which were often manufactured on elongated blanks and never bifacially transformed. Moreover, the characteristic intensive production of retouched blades and elongated retouched points that we described previously for the Early MP is unknown in eastern Africa. Therefore, although the fossil evidence supports a scenario of an African origin of the Early MP hominins (Hershkovitz et al. 2018), this assumption does not seem to be unequivocally supported by the archaeological data.

These statements should, however, be tempered as it is unlikely that specific lithic assemblages can be equated with human populations. As the archaeological record generally reflects adaptations to social and physical environments, it seems unlikely that the technical repertoire of dispersing populations would have remained strictly identical to that of the parent populations (Goder-Goldberger, Gubenko, and Hovers 2016; Groucutt et al. 2015b). Such remark must warn against the over interpretation of similarities between assemblages from different regions. We must keep in mind that the observed differences could also result from the long geographical distances between northeastern Africa and the Levant, as well as the unknown period of time between the Early MSA of Gademotta and the Levantine Early MP, due to the low degree of resolution of our dating methods (Zaidner and Weinstein-Evron 2020).

But, in sum, in the absence of any potential ‘ancestral’ industries in the region, the clear discontinuity in the technological repertoire between the Late LP and Early MP should be taken into consideration, and the most likely hypothesis is that it resulted from the influx into the Levant of new populations bearing a new technological package (Hershkovitz et al. 2018; Malinsky-Buller 2016; Meignen and Bar-Yosef 2020; Weinstein-Evron and Zaidner 2017).

6.1.2 Variations within the Early Middle Palaeolithic (Hayonim Layers F and Lower E: units 10 to 4)

One of the important contributions of the Hayonim MP sequence is the superposition, through more than 3.50 m, of levels that we consider as Early MP. Integrated with the recently acquired data on the assemblages corresponding to this same entity, the Hayonim data thus enable us to assess this entity and attempt to define it more precisely.

First of all, as we have seen in chapter 5, based on a set of criteria among which we observe a certain variability, it can indeed be considered as a distinct entity within the Levantine Middle Pleistocene record, distinguished from the other Middle Palaeolithics that follow, based on the presence of specific products or characteristics. The hallmarks of the Early MP entity in the Levant would thus be:

- elongated blank production in various proportions, but generally higher than in the later MP;
- coexisting Laminar and Levallois flaking methods, also in various proportions;
- the selection of these elongated pieces as blanks for retouched tool production (mainly retouched blades and elongated retouched points), and;
- the emergence of the Levallois technology in its full-fledged form, which is generally prominent in these assemblages (with the exception of Hummal) from the beginning of the Early MP, including the earliest appearance of Levallois points (elongated and short ones).

However, concerning this definition, which is generally agreed upon, it is important to make some additional remarks resulting from comparisons made with the most widely described emblematic assemblages (see chapter 5, Table 5.79) and which highlight the variations within this entity.

This production of elongated blanks is indeed the hallmark of this entity but, in most cases, it coexists with a well-structured production of short blanks (Levallois). It is therefore not always quantitatively largely dominant.

The coexistence of the Laminar and Levallois production systems to obtain these elongated blanks (blades and points) is also a fundamental element, but sometimes one of the two systems is poorly represented (Meignen 2007, 2011): for example, the Levallois system is infrequent at Hummal (Malinsky-Buller 2016; Shimelmitz and Kuhn 2013; Wojtczak 2014), while the Laminar system is uncommon at Tabun unit IX (Malinsky-Buller 2016; Shimelmitz and Kuhn 2013) or Dederiyeh (Nishiaki, Kanjou, and Akazawa 2022).

Since Garrod acknowledged the industry of Layer D in Tabun as a separate facies within the MP, the elongated points were considered as the characteristic element of the Early MP assemblages then called the Mousterian type Tabun D (Bar-Yosef 1998a; Copeland 1975; Garrod and Bate 1937). The results of detailed technological analyses show, however, that short points are just as abundant, and sometimes even more abundant (Table 5.79.).

The high proportion of retouched blades and points is well known. But while the general view of the Early MP is that it is frequently characterised by the presence of retouched elongated points, which are admittedly not very common in later MP assemblages, recent analyses show that retouched blades are most often dominant in the toolkit (Misliya is the only exception). The most significant feature seems to be the selection of elongated products as tool blanks.

However, if, as we have just explained, the most recent detailed studies lead us to qualify somewhat the diagnostic characteristics of this Early MP entity, it remains true that this production of elongated blanks, with all of the characteristics previously stated (see chapter 5), remains the emblematic element that differentiates this entity from the MP assemblages that succeed it. It is important to emphasise, however, that it is only the association of these diagnostic features in an assemblage that allows it to be defined as belonging to this Early MP entity, and not the mere presence of one or a few of these criteria (as, for instance, the tendency to attribute any blady assemblage to the Tabun D type).

This deeper knowledge of the internal variability of the Early MP has led some authors to reconsider the cultural affinities of some assemblages proposed earlier when data were more limited and technological criteria less precise (see for instance, the new evaluation of Rosh Ein Mor by Goder-Goldberger and Bar-Matthews 2019). It should be noted, however, that the technological variability observed in the Late MP assemblages, which are very diverse and in some ways close to Early MP ones, sometimes makes their attribution difficult (see discussions in Goder-Goldberger and Bar-Matthews 2019; Hauck 2013; Sharon and Oron 2014).

In our discussion of the relationship between the Early MP and the other MP entities that follows, it is important not to underestimate the significant component of short Levallois blanks and, in particular, the frequent presence of short points. These pieces are present from the beginning of the Early MP and are often more abundant than the elongated points (Table 5.79) whose presence is often overemphasised in the definition of the Early MP (Shimelmitz and Kuhn 2013). Though these short Levallois points became a marker of Late MP assemblages (Meignen 2019; Meignen and Bar-Yosef 1992), they are, in fact, also present in significant proportions in some Mid-MP assemblages (Qafzeh Layer XIV-XV [Hovers 2009]; Neshar Ramla units V-VI [Zaidner et al. 2021], units I-II [Centi and Zaidner 2021] and Skhul [Ekshtain and Tryon 2019; Groucutt et al. 2017]). Present throughout the MP in the Levant, they belong to the Levallois technical background from the beginning of the Early MP.

Furthermore, based on the results and interpretations we have presented for the units 6–4 assemblages, we can expect high variability in the technological composition of tool assemblages within the Early MP in relation to the status of the site (site use). It is clear that the function of the site in the organisation of the territory, the type of occupation, and, therefore, the mobility of the artefacts can strongly influence the proportions of the products sought (here blades), and in particular decrease their number (lower import), whereas it is these products that most often allow the identification of Early MP. In such cases, as we have seen in units 6–4, it is the knapping by-products or ‘waste’ (cores, CTEs) left over from the production of the characteristic blanks that allow an Early MP attribution. It is always important to keep this possibility in mind. In fact, the more or less marked intensity of these phenomena of blade import and curation undoubtedly explains in part the variations observed in the proportions of elongated blanks (unworked or retouched) of the different assemblages mentioned (Table 5.79).

In our present state of knowledge, radiometric data, when available, place the assemblages considered as Early MP within a relatively well-defined period (250 ka/150 ka; Mercier and Valladas 2003; Mercier et al. 2007; Richter et al. 2011; Valladas et al. 2013), based on recent studies. But the presence in an assemblage of the emblematic characteristics of the Early MP cannot in any case be used as a dating criterion (contra the notion of the ‘Tabun D phase’ as defined by Copeland [1975]). Only their stratigraphic position and, even more so, their chronological attribution are the determining criteria to establish their age. Even if the majority of researchers working on the MP of the region agree with this remark in principle, there is great temptation to go as far as this chronological interpretation. In the absence of chronological data, the only interpretation that can be made is that they belong to the same technical entity, provided there is sufficient data on the assemblages. The problem arises, for example, for the Abu Sif and Douara IV assemblages, which are frequently cited as examples of the Early MP. While it is highly probable that they belong to Early MP technical entity, this in no way presages their chronology. It must be acknowledged that the use of the term ‘Early MP’ is rather ambiguous (Meignen 2011).

6.1.3 The end of the Early Middle Palaeolithic and the start of the Mid-Middle Palaeolithic (Hayonim Layer Upper E: units 3 and 1–2)

As described above, the assemblages of the upper units at Hayonim clearly differ from those of the underlying levels and no longer belong to the Early MP. Our study (chapter 5, this volume) has highlighted the loss of elements considered characteristic of the Early MP (Figures 5.31, 5.33, 5.36), in parallel with the emergence and development of Levallois flake productions via centripetal preparation/exploitation modalities (Figure 5.39), in conjunction with that of the corresponding Levallois cores (Figure 5.41). Flake tools (mostly scrapers) become predominant (Figure 5.34). All of these elements recall the lithic assemblages classically identified in the MIS 5 sites in the Levant (often called ‘Mid-MP’).

The available data show that this phenomenon does not occur abruptly as the main elements seem to develop in a differentiated manner, staggered in time and implying an incremental pattern of change. A number of Early MP elements are still present in unit 3 (continuation of blade production and associated products—cores and tools on blade—) but they are clearly diminishing. On the other hand, the characteristic elements of the Mid-MP assemblages become progressively more numerous: the Levallois flakes, cores and CTEs linked to the Levallois centripetal exploitation modalities, well represented from unit 3, but only become dominant in units 1–2 (Figures 6.1–6.4).

A discontinuity in the technical repertoires is thus perceptible between the Early MP assemblages (units 10–4) and those of the upper levels (units 3–1) as generally observed in the Levant (Hovers 2001; Hovers and Belfer-Cohen 2013; Kuhn et al. 2021; Meignen et al. 2006; Shea 2003). But it is important to emphasise that the main changes are within a previously known technical repertoire, the Levallois system. In effect, the newly developed production modalities (centripetal) are part of the Levallois repertoire.

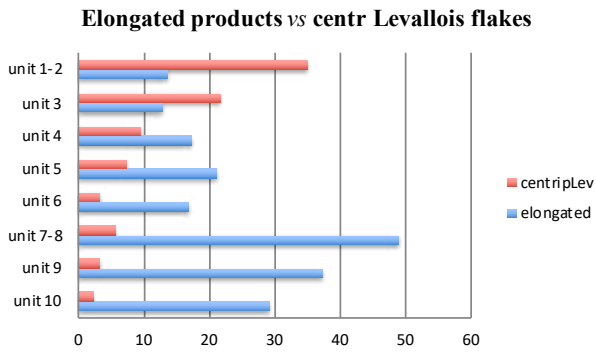


Figure 6.1. Comparison between frequencies of elongated products and centripetal Levallois flakes in units 10 to 1–2.

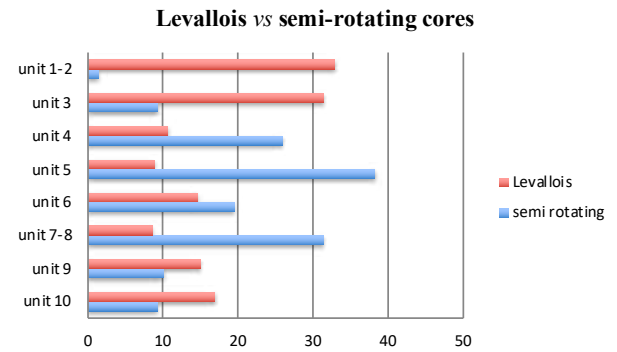


Figure 6.2. Comparison between frequencies of Levallois and semi-rotating cores in units 10 to 1–2.

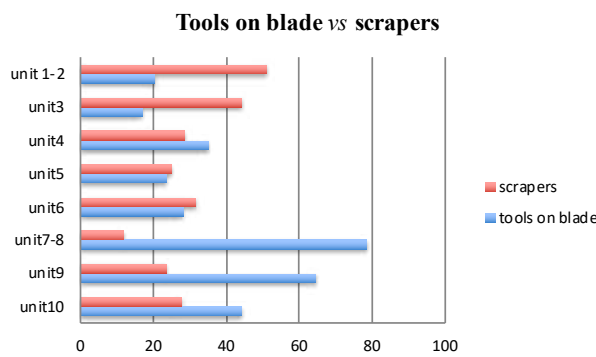


Figure 6.3. Comparison between frequencies of tools on blade and scrapers in units 10 to 1–2.

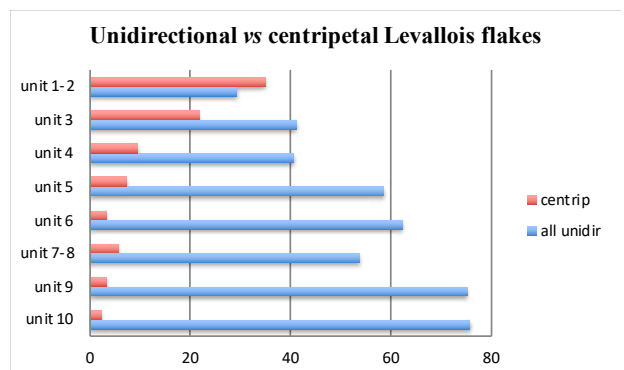


Figure 6.4. Comparison between frequencies of unidirectional and centripetal Levallois flakes in units 10 to 1–2.

However, they were rarely adopted before, during the Early MP. There is thus no real break in the technical traditions between the Early MP and Mid-MP, but simply the loss of a previous technical repertoire (blade production, especially in the Laminar system) and the adoption of new options within the already known Levallois repertoire.

These data contradict a ‘sudden’ arrival of human groups with radically different technical knowledge (as we described for the beginning of the Early MP) (‘replacement scenario’). Rather, they suggest:

- Either a transformation of their technical repertoire within the local populations. These changes would result in the disappearance of the Laminar production system in favour of Levallois flake production according to a modality intrinsically present in the Levallois repertoire (centripetal), which had not been used much until then, and which would now become predominant;
- Or the progressive integration—based on a local repertoire (comprising Laminar and Levallois, mainly unidirectional)—of a new variant/modality within the Levallois; this would be brought about by (successive?) contributions from populations of a different tradition (centripetal Levallois). We would thus be observing the transformation of the local technical repertoire under the effect of external stimuli. These changes would be accompanied by the loss of a significant part of the previous repertoire, namely blade production.

What information is available at the regional level to discuss these hypotheses?

In the Hayonim sequence, these phenomena of change take place in units 3 to 1, between 145–130 ka; the entire upper sequence thus predates the MIS 5, during which Levallois industries with a centripetal dominance see their full development.

If we take stock of the data currently available from relatively well-dated sites related to this period in the Levant, we observe, in a synthetic way, changes that appear to be globally organised chronologically, from 130 ka/145 ka to 90 ka/115 ka (second half of the MIS 6 to first half of the MIS 5). Currently available data show the following:

Hayonim units 3–1 (130 ka–145 ka):

- During this period, loss of the Laminar system still slightly present in unit 3 (Figure 6.2);
- Emergence of a centripetal Levallois production that is still not largely represented (around 35% for Levallois flakes in units 1–2) and persistence of the unidirectional Levallois (with a continuing convergent unidirectional modality in unit 3) (Figure 6.4).

Neshar Ramla unit VI (120 ka–140 ka) (broadly contemporary with units 3–1 of Hayonim) (Zaidner et al. 2021):

- Lack of blade production, especially of the Laminar flaking system;
- Dominant Levallois centripetal production (short broad flakes) (approx. 45.7% for flakes, Zaidner et al. 2021: tabl S9) coexisting with Levallois unidirectional convergent modalities for point production.

Skhul (110 ka–130 ka) (Ekshtain and Tryon 2019; Groucutt et al. 2017; Mercier et al. 1993):

- Dominant production of Levallois centripetal flakes (Ekshtain and Tryon 2019),
- coexisting with the production of Levallois points often via the unidirectional convergent modality (no quantified data available/biased collections).

Qafzeh (90 ka–115 ka) (Hovers 2009; Valladas et al. 1988):

- Clear dominance of centripetal Levallois flake production (from 36 to 78% for flakes),
- coexisting with a bidirectional modality. Incursion of unidirectional convergent modalities (point production) in Layer XV (but even in this level, the products obtained via the centripetal modality dominate [Hovers 2009]).

Neshar Ramla unit III (later than 120 ka) (Zaidner et al. 2021):

- Clear dominance of Levallois centripetal production (recurrent and preferential) for oval and rectangular flakes (67%).

Neshar Ramla units II-I (later than 120 ka) (Centi and Zaidner 2021; Varoner et al. 2022):

- Coexistence of centripetal Levallois methods for the production of oval and rectilinear flakes, with triangular flake production often obtained by convergent unidirectional detachments (the convergent unidirectional modalities are clearly more frequent in the higher levels (unit I (Pelvis Horizon) and between IIa and IIB (Stones Horizon) (Varoner et al. 2022).

Based on these data, several remarks can be made:

- The cultural and chronological data from Neshar Ramla unit VI (Zaidner et al. 2021) and Hayonim units 3–1 (chapter 5, this volume), document an earlier onset (during the later part of MIS 6) of the technological traits classically regarded as characterising MIS 5 in the Levant (Levallois centripetal technology);
- The Mid-MP industries (mainly dated to MIS 5) are not as homogeneous as they were long assumed to be as is implied by the identification of a ‘Tabun C phase’ (Bar-Yosef 2000; Copeland 1975; Shea 2003; but see also Groucutt et al. 2017);
- It is only in MIS 5 (assemblages from Qafzeh, Neshar Ramla unit III) that the ‘centripetal Levallois flake’ component largely dominates the production, even if unidirectional convergent mode again becomes important in assemblages from units I–II onward (Centi Zaidner 2021; Varoner et al. 2021)
- In assemblages chronologically earlier than MIS5 (Neshar Ramla unit VI, Skhul, Hayonim units 3–1), a unidirectional (often convergent) Levallois component known earlier in Early MP assemblages persists, as we described at Hayonim;
- In this context, the assemblages of units 3–1 at Hayonim, the oldest of the ensemble considered, are those in which the proportion of centripetal flake production is the lowest. In effect, although the development of centripetal modalities in units 1–2 undoubtedly represents a notable change in the archaeological sequence of Hayonim, these centripetal flake productions are still much less frequent than what is observed in the MIS 5 sites (Qafzeh [Hovers 2009]; Neshar Ramla unit III [Prévost and Zaidner 2020], and even units I–II [Centi and Zaidner 2021]).

How can we interpret these data?

First, these data confirm, and thus allow us to generalise on a regional scale, the gradual development of the centripetal Levallois that the results obtained in the Hayonim sequence suggested. They also enable us to discuss the processes involved in the changes observed between the Early MP and Mid-MP. The question of whether the shift from the Early MP to the Mid-MP was an autochthonous process or was triggered by demic dispersals needed to be tested.

The gradual establishment of the predominance of centripetal Levallois technology in the assemblages, which seems to follow an overall chronological evolution, makes it possible to eliminate the hypothesis of a massive arrival of human groups carrying this tradition (centripetal Levallois), which would be indicative of a large diffusion phenomenon. The changes in the technical repertoire are not abrupt, and therefore do not imply a complete replacement of the technical repertoire/culture or population, and the ‘replacement scenario’ can, therefore, be ruled out.

On the other hand, it seems that the data presented above concerning the changes observed in the Levant, and in particular in the Hayonim sequence, at the end of MIS 6–beginning of MIS 5, are consistent with what can be expected from an indigenous, regional development based on the Levallois traditions already present in the region.

Following the definition proposed by Malinsky-Buller and Hovers (2019) for autochthonous (regional) developments, we see in the Levant from the late MIS 6 to MIS 5: a ‘gradual accumulation of technological modifications (*in our case, the gradual development of Levallois centripetal modalities and the gradual loss of blade production*) until a novel technological repertoire becomes stabilised (*in our case, the predominance of Levallois centripetal reduction in Mid-MP assemblages, as observed in Qafzeh and Neshar Ramla unit III, for instance*)’. The presence of short Levallois points alongside centripetal Levallois products in the oldest assemblages (Skhul, Neshar Ramla unit VI) could then correspond to the persistence of the Levallois point production already present in the Early MP at Hayonim, Tabun IX, and Misliya (Table 5.79).

Therefore, the new technical option (centripetal modality) was superimposed onto a background of technical knowledge (Levallois technology) that was receptive due to its similar ways of doing things.

Regardless whether this incremental pattern of change was triggered by discontinuous or sporadic contacts with an incoming population (from Africa? the Arabian Peninsula?), it is not easy to control archaeologically, especially since the local populations already had technical knowledge similar to the succeeding technologies. We should recall that the changes observed are made within the same tradition (Levallois technology) by the development of one of the modalities (centripetal) at the expense of the others.

The absence of a major break in the lithic repertoires from the Early MP to the onset of the Mid-MP does not mean that no population contact occurred. It is not impossible, for instance, that exterior influences, such as periodic contact with incoming populations or a diffusion of ideas and tool-making fashions through cultural interactions stimulated the formation of a new toolkit by a limited fusion of local and non-local technical repertoire. This process of technical change employed pre-existing knowledge and facilitated what can be defined mainly as a local development.

As frequently mentioned, Africa, and especially East Africa, constitutes one of the possible sources of these influences, as does North-East Africa, which has more limited documentation, however (Groucutt et al. 2015a, b, and references therein). Based on the currently available data in East Africa, whose limitations (small number of sites, few technological studies, lack of chronological resolution) are rightly pointed out by some authors (Groucutt et al. 2015b; Tryon and Faith 2013; Tryon, McBrearty, and Texier 2005), the Levallois centripetal technology is considered as the key feature in the Early MSA assemblages from MIS 8 to MIS 5 (Shea 2008; Tryon 2006; Tryon, McBrearty, and Texier 2005; Yellen et al. 2005). In some assemblages, this centripetal method occurs together with Levallois point production by the unidirectional convergent method (Gademotta/Kulkuletti complex [Douze 2013; Douze and Delagnes 2016]; Koimilot locus 2 [Tryon et al. 2005]). The diversification of Levallois methods is thus identified from the beginning of Early MSA. Among the range of retouched tools, convergent tools (unifacially or bifacially retouched points made on Levallois and other flake blanks) play a key role (Clark 1988; Douze 2013; Douze and Delagnes 2016; McBrearty and Brooks 2000; Tryon and Faith 2013). However, it should be noted that the production of unidirectional convergent Levallois points becomes rare in Africa during the MIS 5 (Zaidner et al. 2021), contrary to what is observed in the Levant. This would support the hypothesis of a local origin of the Levallois points identified in the oldest sites (Nesher Ramla unit VI, Skhul, for instance).

The development of a centripetal Levallois production, identified mainly in East Africa, but also in Northeast Africa and the Arabian Peninsula (e.g., Groucutt et al. 2015a, b; Petraglia et al. 2011; Shea 2008; Tryon, McBrearty, and Texier 2005), is of course reminiscent of lithic production methods identified in the Levant in MIS 5 assemblages (Qafzeh, Skhul), although with clear differences, particularly in the tools used (unidirectional convergent Levallois points are rare in the MIS 5 in Africa; the frequent bifacial points of the Early MSA are absent in the Levant assemblages). These predominantly centripetal Levallois production methods have, however, often been considered as evidence of a diffusion of *Homo sapiens* from Africa (and/or through part of the Arabian Peninsula) during MIS 5 (Bar-Yosef 2000; Groucutt et al. 2018; Groucutt et al. 2015a, b; Petraglia et al. 2012).

Insofar as recent data now indicate an earlier presence of centripetal Levallois (Nesher Ramla VI [Zaidner et al. 2021], Hayonim units 1-3 [chapter 5, this volume]), the hypothesis of an African influence is now conceivable from the end of MIS 6. On the other hand, recent fossil data show that these centripetal Levallois productions, associated in unit VI of Nesher Ramla with a taxonomically different human type (*Nesher Ramla Homo*; Hershkovitz et al. 2021), are therefore not specific to *Homo sapiens*. These results made it clear that there is no direct correlation between morphotype/taxonomic groups and lithic technology. The presence of Levallois centripetal productions can no longer be used as a criterion to trace the presence and dispersal of *Homo sapiens* out of Africa.

At the end of MIS 6 in the Levant, the gradual development of centripetal Levallois modalities described above suggests—according to the hypothesis that exchanges between dispersing Early MSA groups and the Levantine MP did indeed take place—sporadic, discontinuous contacts, which functioned as repeated stimuli.

The variability shown by the human remains from Neshar Ramla unit VI, Qafzeh, Skhul (Arensburg and Belfer-Cohen 1998; Hershkovitz et al. 2021; Tillier 2006a, b; Tillier and Arensburg 2017, and references therein) and the radiometric dates suggest repeated pulses of hominin movements over a fairly long period of time (end of MIS 6–MIS 5). These may have played a role in the processes of technological change previously described (changes in the aim of the production and the reduction strategies, without the phenomenon being abrupt).

The data recently published by Zaidner et al. (2021) show that the strong technological affinities observed between the assemblages of Neshar Ramla, Qafzeh, Skhul are undoubtedly the result of frequent interactions between Hominid populations of different types (Late Middle Pleistocene *Homo* in Neshar Ramla, *Homo sapiens* in Skhul and Qafzeh). Moreover, palaeogenetic studies suggest gene flow between archaic *Homo* populations and *Homo sapiens* during the late Middle and early Late Pleistocene (Hajdinjak et al. 2018; Posth et al. 2017). Thus, anthropological and archaeological data highlight interactions between different human lineages as early as the end of the MIS 6/early MIS 5, which could explain the changes in the technical repertoires observed and their implementation modalities.

6.1.4 Conclusion

Therefore, as in many other regions, the archaeological data from the Levant suggest a complex history involving population movements at different scales and in different directions.

The arrival of the MP in the Levant is thus the result of a long history, from MIS 7 to MIS 5, based on significant changes before leading, around 120 ka–130 ka, to a technical entity largely dominated by the Levallois, which was then more or less stable over several millennia. These transformations of the technical repertoires were carried out according to different implementation processes, which we have been able to highlight in the Hayonim sequence, and more widely in the Levant.

The emergence of the Early MP (Late LP/Early MP transition) is marked by major changes in the technical repertoires—complete loss of two production systems (bifacial and Quina-like), replacement by, and wide development of new lithic production systems (Levallois and Laminar), thus breaking with the previous technological repertoire.

This indicates a fast tempo of the cultural changes expected to occur among effective ‘semi-connected’ groups faced with the influx of new populations with a new cultural package (Malinsky-Buller and Hovers 2019: 122). It should be remembered, however, that these ‘abrupt’ changes in the field of lithic production are superimposed on behaviours in other domains that have remained unchanged since the Late Lower Palaeolithic (extensive and habitual use of fire, repetitive cave occupations, new land-use patterns (Kuhn and Stiner 2019, and references therein).

On the contrary, the disappearance of the Early MP and the shift to Mid-MP industries dominated by the Levallois centripetal system, lead to, at the regional scale, smaller and more gradual changes entailing the abandonment of part of the production systems implemented during 50 ka and the adoption of new flaking modalities in a production system already known and established.

The end of the Early MP entity is not marked by a strong break in the technical repertoire. The gradual changes are expressed by the objectives of production (e.g., flakes became dominant, while elongated blank production ceased) and the methods of obtaining these products. The latter change progressively with the disappearance of the unidirectional Levallois (still present in Hayonim unit 3; Neshar Ramla VI; Skhul) in favour of the centripetal modality, which becomes largely dominant (Neshar Ramla unit III; Qafzeh) but never exclusive (cf. Neshar Ramla I-II).

It is possible that the changes observed in this case correspond to the impact of external influences on the already existing Levallois foundation, which served as a stimulus for the development of the centripetal option (always present in the Levallois repertoire but more or less adopted). However, it is difficult to support this interpretation more broadly and definitively as the Hayonim sequence is the only one currently available to precisely document this phenomenon (end of the Early MP and emergence of Mid-MP assemblages) in stratigraphic continuity. However, as recent discoveries show, in an area with active ongoing research, the factual data is changeable, which can disrupt established patterns.

6.2 Changes in settlement patterns in the Levantine Middle Palaeolithic

6.2.1 Introduction

In a previous publication that broadly explored the nature of long-term trends in settlement patterns over the roughly 200,000 years of the Levantine Middle Palaeolithic (Meignen et al. 2006), the data from Hayonim Cave were considered as representative of the Early Middle Palaeolithic. At this time, we were well aware of the need for additional, more detailed information, especially through the MP sequence from Hayonim. The different contributions presented in this volume aim to meet this objective.

In synthesising the information we had at that time, we identified what we consider as major contrasts between the Early Middle Palaeolithic and late Middle Palaeolithic in provisioning strategies and land-use patterns.

Based on the limited evidence then published, the Early MP sites were schematically characterised by low occupation intensity (low densities of lithic and faunal remains), coupled with evidence of complete onsite core reductions that suggested short-term residential camps and a high mobility strategy (circulating mobility). As then observed at Tabun unit IX (Jelinek 1982a), Hummal Ia (Copeland 1985), and Hayonim Layer F, relatively high proportions of retouched tools indicative of heavy blank curation, suggest that in the context of this high mobility, people carried at least a limited toolkit across the landscape (Meignen et al. 2006).

Conversely, the Late MP sites, more numerous than those of the Early MP and more densely occupied, often occur in multilayered sequences. They show a range of more diverse site functions. The Late MP sites then considered (Kebara, Amud, Umm el Tlel, Quneitra, Farah II) mostly pointed to patterns of low residential mobility with some occupations resembling task-specific activity loci, and others much longer-term repetitive occupations (base camps). In the long stratigraphic sequences (Umm el Tlel, Kebara), these strategies vary over time.

This vision was undoubtedly a bit of a caricature, given the small amount of data available at the time, but it is still generally true for a certain number of sites, even if it must now be qualified based on the documentation that has been considerably expanded. During the past two decades, new excavation and research programs focused on these periods have considerably increased the available data. This is the case of the research on the Early MP sites at Hummal Levels 5–6 (Wojtczak 2011, 2014, 2015), Tabun unit IX (Shimelmitz and Kuhn 2013; Shimelmitz et al. 2014b; Shimelmitz et al. 2016), Misliya (Weinstein-Evron and Zaidner 2017; Yeshurun, Bar-Oz, and Weinstein-Evron 2007; Zaidner and Weinstein-Evron 2014, 2016, 2020), Emanuel Cave (Goder-Goldberger et al. 2012), Dederiyeh Cave (Nishiaki et al. 2022) and Hayonim units 10 to 1 (Meignen 2011; Meignen and Bar-Yosef 2020; Meignen et al. 2010; Meignen et al. 2009; Stiner 2005). New studies on Mid and Late MP sites are even more numerous: Amud (Ekshtain et al. 2017), Kebara (Meignen 2019; Meignen et al. 2009; Meignen, Speth, and Bar-Yosef 2017; Meignen et al. 2019; Speth et al. 2012), Neshar Ramla (Centi and Zaidner 2021, 2022; Ekshtain and Zaidner 2022; Prevost and Zaidner 2020; Zaidner et al. 2021; Zaidner et al. 2018; Zaidner et al. 2016; Zaidner et al. 2014), Qafzeh (Hovers 2009), Ein Qashish (Ekshtain et al. 2019; Ekshtain et al. 2014; Hovers et al. 2014; Hovers et al. 2008; Malinsky-Buller, Ekshtain and

Hovers 2014; Mitki et al. 2021), Nahal Mahanayem Outlet/NMO (Sharon 2018; Sharon and Oron 2014).

In this context, the interdisciplinary studies conducted on the Hayonim sequence, now analysed at a finer scale based on the unit groups we have defined from the lithic productions (chapter 5, this volume), will serve as a basis to nuance the mobility patterns identified among the Mousterian occupations of the cave. These data will then be integrated into the broader context of recently published results from the Levant for the period under consideration.

In the framework of the interdisciplinary studies conducted on the Hayonim MP sequence, we used a combination of proxies to address changes in mobility aspects of land-use strategies, the lithic artefacts being the most informative as they are the most ubiquitous archaeological remains available for study. They are probably also the most adequate material to discuss provisioning strategies (curation versus expediency in production, provisioning of the individual versus provisioning of place), which, in turn, are generally considered as the results of different mobility patterns (Binford 1973, 1980; Kuhn 1992, 1995). Lithic reduction is most often a spatially fragmented process (Gamble 1999; Geneste 1985; Kuhn 1992, 2013b; Roebroeks, Kolen, and Rensink 1988; Turq et al. 2013), the lithic assemblage composition reflecting not only the activities of production and tool use carried out on the spot within the habitat but also the products brought ready for use or taken away during movements within the region. We have largely relied on the concepts of provisioning of individual versus provisioning of place defined by Kuhn (1992), notions often closer to the archaeological reality (because descriptive) than the mobility patterns we deduce from them (interpretative).

In the same way, the procurement, processing, and consumption of animal resources were organised and carried out in different places and times as people moved across the landscape (Binford 1978; Rabinovich and Tchernov 1995; Rabinovitch and Hovers 2004; Speth 2012; Speth and Tchernov 1998a; Stiner 1991; Stiner 2005; Yeshurun 2013; Yeshurun, Bar-Oz, and Weinstein-Evron 2007). Faunal studies thus provide useful information on the selective transport of carcass elements and the onsite carcass processing activities. At Hayonim, mineralogical studies (FTIR) show marked variations in bone distributions, which have been interpreted as resulting from advanced diagenesis and decomposition in limited zones, alongside other zones whose chemistry clearly favoured the preservation of bones and wood ash (Stiner et al. 2001b; chapter 4, this volume). The Layer F occupations, for example, constitute an extreme case: the bones are very poorly preserved, thus limiting interpretations of the lower levels.

On the other hand, even if diagenetic phenomena seem to be important in the entirety of these deposits, the abundance of combustion structures has made it possible to deduce information on behaviours, which, even if they cannot be interpreted with the same resolution as the behaviours in the management of lithics, give precious information on the important role played by fire in human installations.

The degrees of precision of our information thus vary according to the domains considered. Nevertheless, all of these results allow us to characterise the behaviours of human groups from the Early MP to the beginnings of Mid-MP.

6.2.2 Hayonim in the Levantine context: Early Middle Palaeolithic versus Late Middle Palaeolithic settlement patterns ?

In the Hayonim sequence, the new information provided by the lithic productions confirms the main characteristics defined earlier, while also qualifying them. The numerous successive occupations of the long MP sequence (units 10 to 1) show, as a whole, low occupation intensity, which is reflected in all units by low artefact densities (lithics and bones). The densities of lithic artefacts greater than 2 cm long at Hayonim were estimated to average 300 artefacts/m³ throughout the entire MP sequence over 10,000–15,000 years (Bar-Yosef 1998a: 51). These densities, now calculated more precisely by unit groups, show significant variations (chapter 5, Table 5.8), with higher densities in the basal units (Layer

F, units 10 to 7–8: from 1065 to 335 artefacts/m³) than in the succeeding units (Layer Lower E, units 6–4: from 383 to 252 pieces/m³; Layer Upper E, units 3–1: from 230 to 212 pieces/m³). However, these densities remain well below those estimated for Late MP occupations at Kebara, at 1000–1200 pieces/m³ in 3000 TL years (Bar-Yosef 1998a), and at Amud, over 1000–1500 pieces/m³ in sub-units B1–B2 (Hovers 2001).

We thus observe a low artefact density throughout the sequence, which probably reflects the low intensity and low repetitiveness of the occupations. The information obtained in our study based on the lithic artefact and density calculations nevertheless shows some nuances in the occupation intensity and tool management strategies in the territories.

In all of the Hayonim MP assemblages (Table 6.1), although they represent successive but ephemeral short-term occupations, all stages of stone tool production (Levallois and Laminar reduction strategies) and their maintenance appear to have been carried out in the cave. This strategy is clearly reflected by the presence of the typical by-products of the different stages of core reduction (cortical flakes, ordinary flakes, CTEs, and cores). Raw material logistics mainly involved complete flint nodules or roughly prepared cores brought to the cave (provisioning of place), alongside varying numbers of blanks produced off-site (provisioning of individuals), depending on the units. The range of raw material procurement goes from a largely dominant focus on onsite core reduction to, in some units, a quite significant reliance on imported blanks alongside this onsite production.

The latter is observed in units 10 to 7–8, levels in which the occupation densities are the highest. In these units, strategies of provisioning of place (bringing raw or more or less prepared nodules into the cave), dominant in particular for Levallois productions, are accompanied by a clear import of blades, sometimes retouched. The latter correspond to a provisioning of individuals strategy, as defined by Kuhn (1995) in reference to tools that probably belonged to the personal gear of individuals. The high ratios of retouched tools can be interpreted as off-site produced curated artefacts brought to the site for further use and maintenance. The high visibility of the personal toolkit component suggests short-term occupations.

Most of the flint raw materials were collected in the vicinity of the cave, but in unit 10 (the only unit for which information is available), a few artefacts in exotic raw materials were imported from a distance of 30–40 km (Delage, Meignen, and Bar-Yosef 2000; Meignen et al. 2006). These exotic blanks were not exclusively imported in the form of finished products; Levallois and Laminar blanks were imported along with debitage by-products. This non-local flint component reflects the exploitation of a large territory but does not appear to be the result of a specific curation strategy (Meignen et al. 2006). The transport of stone artefacts in a wide variety of forms is a frequent behaviour recognised during the MP (see Turq et al. 2013, and references therein).

In an identical context (same cave and groups belonging to the same Early MP technical tradition), the assemblages of units 6–4 show somewhat different provisioning strategies: the knapping was largely conducted at the site. For Laminar and Levallois productions, blades, in particular, were produced onsite and less frequently imported. In these units, therefore, some products (blades or Levallois products) were introduced into the cave, but the proportion of personal gear is smaller than in the lower units.

The low proportions of retouched products (between 2.7 and 5.7%; chapter 5, Table 5.10) (especially retouched blades) are probably partly the result of this low import of blades, but they are also probably linked to the very short-term occupations during which a lower demand for processed and recycled tools is likely. The low lithic artefact densities support this interpretation.

Hayonim Cave would thus have been occupied over a long period (units 10 to 4; from 220 ka to 160 ka), with a gap of circa 30 ka (deposits not preserved due to erosion) by groups with the same technical traditions (Early MP). The cave occupation modalities remained globally the same (low occupation intensity, short-term residential camps in association with a high mobility strategy). However, within this sequence, changes in

Layer	Lithic assemblages	Fireplaces	Fauna	Phytoliths	Interpretation
Upper E (units 3–1) <i>Onset of Mid-MP</i>	<ul style="list-style-type: none"> • Low artefact densities • Onsite knapping activities (Levallois) • Low frequency of retouched tools 	<i>Poorly preserved</i>	<ul style="list-style-type: none"> • Exploitation of ungulates and tortoises, never in great quantities • Transport of nearly complete carcasses of gazelles and fallow-deer for processing/ consumption in the cave 	<ul style="list-style-type: none"> • Mainly phytoliths of dicotyledonous leaves and wood-bark suggesting the non-selective use of bushes and branches as the main fuel 	<ul style="list-style-type: none"> • Low occupation intensity • Short-term residential camps • Provisioning of place strategy
Lower E (units 6–4) <i>Early MP</i>	<ul style="list-style-type: none"> • Low artefact densities • Mostly onsite knapping activities (Levallois and Laminar) • Low proportion of retouched tools • Low proportion of imported blades 	<ul style="list-style-type: none"> • Superposition of successive, often thin, hearths (short-duration combustion episodes) • Stacking on top of each other in unit 6, resulting in large and thick hearths 	<ul style="list-style-type: none"> • Same strategies as in Upper E 	<ul style="list-style-type: none"> • Same strategies as in Upper E 	<ul style="list-style-type: none"> • Low occupation intensity, but repetitive returns to the same area in the cave • Short-term residential camps • Provisioning of place strategy
Layer F (units 10–7/8) <i>Early MP</i>	<ul style="list-style-type: none"> • Low artefact densities but higher than in Layer E • Onsite knapping (Levallois, Laminar) • High proportions of retouched tools, especially elongated tools • Import of blades/highly curated 	<i>Poorly preserved</i>	<i>Poorly preserved</i>		<ul style="list-style-type: none"> • Low occupation intensity • Short-term residential camps • Mixed strategy of provisioning of individuals and provisioning of place

Table 6.1. Hayonim Middle Palaeolithic sequence: synthesis of the main results obtained in the different fields of research.

the way tools were managed across the territory are observed (more or less emphasis on ‘personal gear’ in the strategies adopted), which may be interpreted in terms of occupation duration and intensity. The higher densities of lithic artefacts and the more intensive tool maintenance activities (higher proportions of retouched/resharpened tools, especially imported ones?) in the basal levels (Layer F) could reflect slightly longer and more intensive occupations (larger groups?).

The differences observed between the basal units (Layer F) and those that followed (Layer Lower E) would thus be due to a diachronic change in the provisioning of activities in the cave (remembering that about 30 ka separate these occupations). But we must also keep in mind that the different positioning of the samples in the cave (Layer F at the entrance of the cave/Layer Lower E in the Central Area inside the cave) could explain these differences, reflecting a spatial organisation of activities between the entrance area of the cave, near the porch (where retouched tools would be more numerous), and the Central Area (where the production of blanks and debitage would be more intensive). This hypothesis is impossible to test, however, because no level has been excavated in continuity in these two areas (see chapter 1).

As for the upper-level assemblages (units 3–1; Layer Upper E), we must remember that they no longer belong to the Early MP technical tradition, which tends to disappear at this time and is replaced by the dominant production of short Levallois blanks. However, the data acquired during our study show that the cave occupation modalities remain essentially the same.

The lithic artefact densities are always low (chapter 5, Table 5.8), indicating low occupation intensities. In situ debitage is attested by high proportions of cortical and ordinary products, high percentages of cores, and the presence of the corresponding CTEs (core-edge flakes). Blade production plays a secondary role, with Levallois being the dominant product. If we refer to the few experimental references available (Bourguignon, Brenet, and Folgado 2006; Brenet et al. 2009; Geneste 1985) the overall composition of these assemblages, and, in particular, the proportions of Levallois products relative to the corresponding cores, suggest a majority provisioning of place strategy. It is interesting to note, however, that in unit 3, a slight deficit of Levallois products relative to the number of corresponding cores, which could indicate that some of the flakes were exported away from the site (Levallois products = 378, Levallois core = 54, ratio 7:1). The low retouched tool frequency shows that the majority of Levallois blanks were used directly, without any further modification.

However it should be born in mind that, while the segmented nature of the core reduction sequences during the MP is now an established fact (Shimelmitz et al. 2021; Turq et al. 2013, and references therein), it is often difficult to precisely evaluate the actual circulation of the artefact categories concerned since the assemblages available to us usually correspond to a palimpsest of successive occupations that systematically include import/export phenomena superimposed on the production activities carried out in situ (Turq et al. 2013). These lithic transport phenomena have been clearly demonstrated in assemblages where refitting studies have been performed (see references in Turq et al. 2013), but they are more difficult to demonstrate in classic technological studies, especially when experimental references that would enable an estimation of expected ratios do not exist (for the Laminar debitage system, for example). Studies involving the identification of raw materials are one of the surest ways to highlight these transports but, unfortunately, none have been conducted on the Hayonim assemblages. In this case, therefore, only the very visible import/export behaviour could be identified (e.g., in the Hayonim units 10 to 7–8).

These initial interpretations proposed based on the lithic technological organisation at Hayonim have, moreover, been largely documented and confirmed by zooarchaeological studies (Stiner 2005; chapter 4, this volume), which concern only artefacts from Layer E (units 6-1) (Table 6.1).

The faunal analyses indicate the exploitation of ungulates and tortoises but never in great quantities, pointing to low human population densities in all of the Layer E units, as well as narrow diets that were rich in high-yield game types. The total number of individual ungulates (MNI) is small despite the long periods represented. The lack of gnawing damage by carnivores may simply be another indication that the accumulation of refuse in the site was minimal and widely scattered through time, and perhaps insufficient to attract large carnivores with any regularity.

The ungulate mortality patterns and body-part profiles indicate systematic hunting of gazelle, fallow deer, and, to a lesser extent, aurochs. The hunters transported complete or nearly complete carcasses of gazelles and fallow deer to the cave for processing, focusing their attention on meat and marrow-rich body parts. The carcasses of aurochs, a much larger species are somewhat less complete. Carcass processing and consumption took place in the cave. The impact damage on bones shows a combination of through-bone dismemberment techniques and the extraction of medullary marrow from the larger limbs. Tortoises, frequently found near or within hearth areas, were roasted, often on their backs, and then cracked open with the aid of a hammer and anvil.

The high frequencies of post-depositional burning traces on bones (also observed on the lithic artefacts; see chapter 5, this volume) indicate that surface debris was often charred before being deeply buried by sediments, an observation suggesting that many fires were built and maintained inside the cave. But the hearths must have been relatively short-lived since the bones rarely reached the stage of calcination.

This abundance of burning activities is also confirmed by field observations and micromorphological studies of the deposits (see chapter 3, this volume). The evidence of burning activities is striking. The superposition and imbrication of the fire structures convey the intensity of the activities related to the use of fire. The core importance of fire facilities in MP daily social and economic life is first reflected in the composition of the cave deposits, most often derived from combustion activities (ashes/mixed ashy sediments and combustion features). A spectacular accumulation over several metres thick—also identified in other MP sites in the Levant (e.g., Kebara, Amud)—suggests they were predominantly installed on these ashy sediments. It is clear the human groups lived consistently in an ‘ashy environment’, which was associated with intensive fire-related activities.

Within these ash deposits, depending on the level, there are also numerous, more or less well-preserved combustion features, often identifiable despite the significant trampling that testifies to the repetitive occupations in the central area of the cave.

In all of Layer Lower E (units 6 to 4), the combustion features observed generally result from the superposition of successive, often thin, hearths corresponding to short-duration combustion episodes.

In the basal levels (unit 6), in particular, the hearths identified in the field, often very large (diameters from 100 to 150 cm) and thick (generally 10–20 cm, up to 30 cm), were created by the stacking of numerous, probably short-duration combustion episodes on top of each other.

This situation was recorded in detail by Karkanas (2021) in the framework of a long experimental project on open fires, supplemented by compression, mineralogical and chemical analyses. Numerous reconstructions of experimental fires allowed him to specify the conditions under which archaeological fires are formed and preserved, even if they are not very thick. He concludes that they always consist of superimposed short combustion episodes, which are often difficult to identify in the field.

The large and thick hearths in unit 6 thus indicate, not long-term occupations as one might think, but repetitive occupations with a systematic return to a specific area of the cave as well as the probable maintenance, through these successive (and fairly close in time?) occupations, of the same organisation of the inhabited space.

The situation is different in the subsequent levels (units 5–4), where the numerous, thinner combustion features, not corresponding to a systematic stacking of successive hearths, are frequently more intensively disturbed by the succeeding occupations (trampling). They then take the form of large ashen areas with only partially identifiable hearth remains. The slight superposition and dispersion of these combustion features suggest that the spatial organisation observed in the underlying levels was not maintained in these levels. These observations suggest fairly short-term occupations, probably more widely spaced in time.

In all cases, the observed combustion features clearly indicate brief and repetitive burning episodes, thus corresponding to the idea of short-term occupations. Overall, all of the observations (in the field and via micromorphological analyses, in particular) indicate considerable reuse of certain locations in the cave, albeit as visits that were sometimes probably separated by extended periods of absence.

Because charcoal is lacking, only the study of the phytoliths gives us information on the fuels used for the fireplaces (Table 6.1). This analysis reveals the use of bushes and branches as the main fuel (Albert et al. 2003) that would correspond to a non-selective collection of any available woody plants in close proximity to the cave.

This hypothesis is supported by the presence of red baked clay pellets whose general systematic presence in the hearths could be explained by the collection of bushes growing on the terra rossa ground present all around the cave. This non-selective behaviour would translate flexible requirements in terms of the quality and efficiency of the fuels collected, in association with short-term occupations.

In sum, based on this large amount of data, Hayonim Cave appears to have been a residential camp at which production and consumption activities took place (manufacture, use and maintenance of lithic tools, deferred consumption of prey carcasses, food processing, food sharing with the other members of the group, cooperative fire maintenance); however, it was visited only for short episodes of time. Complete core reductions onsite, together with a diverse toolkit and the faunal composition rule out the possibility of a task-specific location.

These repetitive occupations were probably separated by long periods of absence, as shown by the abundance of rodent remains in part of the infill.

Early MP settlement patterns

The settlement patterns identified in the few other Early MP sites in the Levant are often similar to this scenario: short-term occupations, low artefact density, low occupation intensity, as well as a mixed strategy of provisioning of place, completed by the introduction of variable quantities of personal gear.

This is the case, for example, for unit IX in Tabun Cave, Mount Carmel (Jelinek 1977, 1982a, b; Shimelmitz and Kuhn 2013). Jelinek (1982a) argued that the assemblage from this unit shows evidence for a selective transport of artefacts made elsewhere, either inside or outside the cave. In particular, the blades are numerous (Iflam: 50.1; Shimelmitz and Kuhn 2013), while the corresponding cores are rare. However, considering the debitage elements present in the assemblage (cortical products, in particular, CTEs and cores), Shimelmitz and Kuhn (2013) consider that at least some blank production took place at or very close to the cave. With its low densities of lithic artefacts (bed 39 = 170 artefacts/m³; Jelinek 1977), Tabun unit IX should be considered as a short-term residential camp, partly provisioned by the introduction of personal gear in the form of Levallois blades and flakes.

In the lower levels of Emanuel Cave (Goder-Goldberger et al. 2012), short successive occupations are characterised by low numbers of lithic artefacts resulting in low densities more or less similar to those observed at Hayonim. While initial core trimming elements are few, all stages of the local flint reduction sequence are represented, but in small numbers, thus suggesting that part of core reduction took place onsite. At the same time, however, some blanks and a few cores seem to have been brought to the cave. The authors consider that, even if the occupations were ephemeral, residential activities were performed at the site.

At the same time, however, some Early MP settlements indicate the same lithic production and consumption activities described in the Hayonim sequence, but the occupations are more intensive and sequential, and contain higher lithic artefact densities.

The assemblages from the Misliya Upper Terrace (Weinstein-Evron and Zaidner 2017; Yeshurun, Bar-Oz, and Weinstein-Evron 2007; Zaidner and Weinstein-Evron 2020) and Hummal 6b (Wojtczak 2015), for instance, are illustrative of this pattern.

At Misliya, the high lithic artefact densities (around 3000 lithic artefacts/m³; Weinstein-Evron and Zaidner 2017) and faunal remains (Yeshurun, Bar-Oz, and Weinstein-Evron 2007) suggest an intensive occupation throughout the Upper Terrace sequence. The knapping was largely done onsite, as evidenced by the presence of artefacts from the different stages of the lithic reduction sequences (cortical flakes and blades, CTEs, cores, blanks, Levallois and Laminar products), indicating a provisioning of place strategy. But at the same time, we notice that blades and elongated points are present in high proportions (Zaidner and Weinstein-Evron 2020: Table 3) while the corresponding cores are rare. This pattern suggests that part of the elongated products (retouched or non-retouched) were imported to the cave as personal gear (provisioning of individuals), in addition to the onsite production (provisioning of place strategy). These products were then heavily curated, as evidenced by the high proportion of elongated retouched points.

In the Hummal 6b level, intensive occupations are attested by lithic artefact densities (Wojtczak 2015, Table 1: 2682 artefacts/m³), but it should be kept in mind that such concentrations could also partially result from palimpsests caused by a slow sedimentation rate (Wojtczak 2015: 645). Nearly all stages of lithic reduction are present at the site (numerous cores, including the semi-rotating ones for blade production; high blade proportions, including heavily retouched specimens suggesting onsite curation, or perhaps recycling strategies). While the provisioning of place strategy is evident (Wojtczak 2014, 2015), the high proportion of blades (often heavily retouched) relative to the number of blade cores suggests the introduction of personal gear (i.e., transporting curated, prepared artefacts across the landscape) in the form of blades and retouched blades, subsequently maintained onsite.

Whether these higher intensities are the result of settlement duration (longer duration of individual occupations), more returns to the site, and/or larger groups inhabiting the site, is an open question. Given the difficulties involved in isolating individual occupations, it is difficult to decide. These features could be thus indicative of more extended occupations or denser groups. As observed at Hayonim, they suggest a dominant provisioning of place strategy, while at the same time, the presence of heavily

retouched lithic tools suggests a curation strategy, which we previously reported for the lower units at Hayonim (Layer F).

The interpretation of the assemblages from Abu Sif (Neuville 1951), a rock shelter located in the Judean desert, is more problematic because the collections, dispersed in different locations, are probably altered by biased collection strategies during the excavations (Wojtczak and Malinsky-Buller 2022). Nevertheless, some characteristics are sufficiently clear to allow us to draw conclusions about this site. The low lithic artefact densities, low proportion of debitage by-products (especially for cores), and the introduction of finished tools (retouched and non-retouched) suggest short-term occupations (Meignen et al. 2006; Neuville 1951; Wojtczak and Malinsky-Buller 2022). The conditions under which the material was excavated could of course be the cause of the low proportions of debitage products. However, many of the characteristics of the Abu Sif tools correspond perfectly with the recently studied Early MP assemblages. The selection made during the excavation, which is obvious for the small elements that are absent and possible/probable for some of the knapping by-products, does not seem drastic. For example, the proportions of elongated blanks (Abu Sif B: 44.7%; Abu Sif C: 54.6%), and the abundant retouched tools (Abu Sif B: 31.4%; Abu Sif C: 22%) (Wojtczak and Malinsky-Buller 2022), are found in proportions similar to those at other Early MP sites (chapter 5, Table 5.79). The heavily retouched pieces from Abu Sif may, therefore, result from a maintenance strategy often identified in the other Early MP assemblages.

We should also note that the low representation of knapping products was sufficiently obvious during the excavation (thus before selection) for Neuville to point out that ‘most of the knapping activities were conducted away from the site’ (1951: 54).

The characteristics described are consistent with an assemblage that would correspond to frequent provisioning of individuals by the inhabitants of the site (Hovers 2001; Meignen et al. 2006). On the other hand, the role played by provisioning of place is more difficult to assess, although, as we have just suggested, it does not seem to be very important.

Therefore, both levels at Abu Sif rock shelter could be considered as short-term campsites (Meignen et al. 2006; Wojtczak and Malinsky-Buller 2022). The hypothesis of a task-specific location suggested by the impressive homogeneity of the toolkit (elongated retouched points and shorter triangular tools) (Meignen et al. 2006) is difficult to argue in the absence of data on animal resources.

In 2006, Meignen et al. reported that the Rosh Ein Mor site in the Negev Desert, considered by Marks and colleagues (Marks and Friedel 1977; Munday 1979) as belonging to a radiating mobility system, was an exception among the Early MP sites known at the time. A recent re-evaluation and new dating of these assemblages led Goder-Goldberger and Bar-Matthews (2019) to attribute them to the Late MP, with dates from 70 ka–35 ka. The mobility patterns identified by Marks and colleagues (radiating mobility pattern, classically identified in Late MP sites) are therefore consistent with this new attribution.

The currently available data based now on more numerous sites thus broadly confirm the land-use and mobility patterns identified in Hayonim’s Early MP levels, which are generally considered to be representative of Early MP. Evidence of both strategies (provisioning of place and provisioning of individuals) is found in every assemblage, even if the proportion attributed to the provisioning of individuals, sometimes more difficult to evaluate, has not always been reported.

The coexistence of different provisioning strategies in each assemblage is not surprising. Ethnographic data show that among modern hunter-gatherers, mobility patterns vary over the course of a year and spatially within their territory (Bamforth 1991; Binford 1978; Kelly 1995); foragers often practice a mixture of technological/provisioning strategies (Henry 1998; Kuhn 1992, 1995). The transport of a mobile toolkit (‘personal gear’; Binford 1977, 1979) appears to be universal among mobile societies. Mobile hunters-gatherers carry at least a minimal toolkit to fulfill the needs encountered (Kuhn 1995).

Archaeologically, in short-term occupation sites at which onsite knapping activities are not prevalent, the imported toolkits, composed of versatile items (large blanks, retouched tools, cores), that can be prepared, maintained, re-used, recycled (personal gear), are easily identified. Inversely, as the duration of site occupation and onsite knapping increase, the large quantities of tool manufacturing debris rapidly swamp the transported toolkit (Kuhn 1995), making its identification difficult and requiring detailed and systematic technological and petrographic studies. The variations observed in the Early MP assemblages described above (especially the proportions of blades and tools on elongated blanks) are most likely linked to this phenomenon. Since the duration of Early MP occupations is generally short, the existence of an imported component (personal gear), later curated onsite, could often be identified, suggesting high residential mobility patterns based on frequent residential movements of the human groups. The procurement strategies implemented at the Early MP sites are probably one of the main factors determining the varied proportions of this imported and then curated component (unworked blades, retouched blades, and elongated points).

Late MP settlement patterns

In the early 2000s, based on the then published studies, several researchers highlighted a diachronic shift in the nature of settlement and mobility patterns between the two major MP periods (Early MP and Late MP) (Hovers 2001; Meignen et al. 2006). The data then available (mainly from Kebara, Amud, Umm el Tlel, Quneitra, and Farah II) suggested the existence, in the Late MP, of more numerous sites with differentiated and complementary functions (base camps/habitation sites and task-specific locations, such as hunting stations, quarries, and workshops) characterised by different raw material provisioning strategies and tool availability. These data seemed to indicate a lower residential mobility of the groups.

The data acquired since then show a more complex situation. In the last two decades, numerous discoveries and studies of sites chronologically later than the Early MP (Mid and Late MP) have considerably expanded the record of this period. This is especially true of numerous open-air sites, more abundant during this second part of the MP (Umm El Tlel [Griggo et al. 2011], Hummal [Hauck et al. 2010], Neshar Ramla [Zaidner et al. 2018], Ein Qashish [Ekshtain et al. 2019; Malinsky-Buller, Ekshtain, and Hovers 2014], NMO [Sharon 2018]) for which recent techno-economic studies (procurement and management of raw materials and animal resources) have highlighted diverse behaviours in terms of settlement patterns, and the important role these sites play in our understanding of this period (Ekshtain et al. 2019; Hovers 2017; Malinsky-Buller, Ekshtain, and Hovers 2014; Sharon, Zaidner, and Hovers 2014).

In contrast to Levantine MP caves, often perceived as habitation sites (Hovers and Belfer-Cohen 2013), Levantine open-air sites have been historically identified as task-specific short-term sites dedicated to hunting and butchering activities or lithic raw material quarries and workshops (Hovers 2017). More recent research—reported in the workshop publication ‘Opportunities, problems and future directions in the studies of MP open-air sites’ (Sharon, Zaidner, and Hovers 2014), followed by numerous other publications—has clearly highlighted the important role these sites play in the regional settlement patterns (Ekshtain et al. 2019; Hovers 2017; Malinsky-Buller, Ekshtain, and Hovers 2014; Sharon, Zaidner, and Hovers 2014; Zaidner et al. 2014).

While long-term repetitive occupations (base camps) are indeed most often located in caves (e.g., Kebara, Amud, and Dederiyeh), the abundant data collected in the last decade show that open-air sites exhibit a range of functions, from ephemeral task-specific sites (Griggo et al. 2011; Sharon and Oron 2014; Varoner et al. 2022) including repeatedly visited workshops (Ekshtain et al. 2012; Gopher and Barkai 2014) to temporary habitation sites (Crater Gershtein, Zaidner, and Yeshurun 2022; Ekshtain et al. 2019; Goren-Inbar 1990; Hovers et al. 2014; Malinsky-Buller, Ekshtain, and Hovers 2014; Oron and Goren-Inbar 2014; Zaidner et al. 2018). The observed characteristics of open-air sites,

therefore, represent a continuum of roles from task-specific to more generalised 'home bases' (Ekshtain et al. 2019; Hovers 2017).

Ephemeral task-specific sites are relatively rare in the late Middle Palaeolithic Levantine record (but see Umm El Tlel Level VI1a0 [Griggo et al. 2011], NMO [Sharon and Oron 2014], Neshar Ramla 'pelvis horizon' unit I lower part [Varoner et al. 2022] as best examples), partially due to taphonomic factors. Most of the open-air sites at this period correspond to short-term residential camps (temporary habitation site), a type of occupation also identified in some cave levels (e.g., Kebara units VII–VI [Meignen, Speth, and Bar-Yosef 2017; Meignen et al. 2019]; Shovakh Cave [Malinsky-Buller et al. 2021] [see below]).

Detailed lithic and faunal studies have shown that diverse activities (lithic knapping and use; animal/vegetal resource processing and consumption) were carried out at all of these short-term camps all over variable occupation durations. The strategies of raw material procurement are most often mixed (provisioning of place alongside the introduction of personal gear).

Among these sites, some open-air or caves sites that were occupied for a fairly short duration seem to have been more oriented toward specific tasks, such as hunting and animal consumption and processing. This is the case, for example, in the open-air site of Neshar Ramla IIB lower (Centi and Zaidner 2022), but also at Kebara Cave units VII–VI (Meignen, Speth, and Bar-Yosef 2017; Meignen et al. 2019), where, following the intensive long-term occupations during lower units (XI–VIII), the cave was used as an intermediate staging point where limited initial carcass processing took place, after which higher-utility marrow bones were transported elsewhere.

Other sites and levels, on the other hand, were used repeatedly as generalised residential sites ('home base'), even if the occupations were ephemeral. This situation was already described at Quneitra (Goren-Inbar 1990), and more recently at Ein Qashish (Ekshtain et al. 2019; Ekshtain et al. 2014; Hovers et al. 2014; Malinsky-Buller, Ekshtain, and Hovers 2014), an open-air site located in the Yizra'el Valley.

Variations within this type of occupation, corresponding to slightly different occupation durations have been observed, for example, in the long MP sequence of the open-air site of Neshar Ramla (Zaidner et al. 2014). But also in a cave context, in the different levels of Shovakh cave, which Malinsky-Buller et al. (2021) propose to identify as 'transient camps', a term coined by Binford to describe these intermediate settlements (Binford and Binford 1966).

In some open-air sites, the different occupation types described above alternately succeed one another over long sequences, corresponding to the accumulation in the same location place of numerous remains of repetitive occupations for different uses.

This is the situation seen in the arid/semi-arid zone of the eastern Levant, where the environment must have shifted frequently from arid steppe to open grassland. At Umm el Tlel (Boëda, Griggo, and Noël-Soriano 2001; Griggo et al. 2011) and Hummal (Hauck 2011b), for instance, long sequences of repetitive Middle Palaeolithic occupations, often short-term and to a large extent dependent on more or less permanent water sources (springs, water-holes, lake margins), show a succession of task-specific locations (butchering/hunting camps) and more generalised short-term occupations/habitations.

This is also the case in the Mediterranean area, in the long sequence of Neshar Ramla (eight metres thick), which has yielded numerous successive occupations in a deep karst sinkhole and thus in a physically constrained space (Zaidner et al. 2014). Shifts in the lithic and faunal assemblage composition and densities throughout this long sequence suggest changes in the site occupation mode. These consist of alternating episodes of short-term occupations (focused on hunting and carcass processing; unit IIB Lower) of varying lengths, and more generalised prolonged occupation episodes (unit III, unit IIA/IIB) (Centi and Zaidner 2022; Crater Gershtein, Zaidner, and Yeshurun 2022; Varoner et al. 2022; Zaidner et al. 2018; Zaidner et al. 2016; Zaidner et al. 2014).

Conversely, the successive human occupations throughout the 4.5 m thick sequence of Ein Qashish do not show drastic changes in site function or activities, indicating a stable settlement system in this part of the Levant during the Late MP (Ekshtain et al. 2019).

6.2.3 Discussion and conclusion

This short review clearly highlights the diversity of habitat types in varied landscapes occupied during the Middle Palaeolithic; it moderates, in particular, the classic dichotomy often claimed between long-term ‘home base’ sites, in sheltered locations, and short-term locations in open-air sites (Ekshtain et al. 2019; Hovers 2017; Malinsky-Buller, Ekshtain, and Hovers 2014; Sharon, Zaidner, and Hovers 2014).

The augmented data corpus now available highlights significant internal variability among the site functions identified during the two major periods of the MP. However, the opposition between the short-term, low-density, repetitive occupations observed in the long Early MP sequences (Hayonim, Tabun IX—even if a few examples of more intense occupations exist (Misliya, Hummal 6b)—) and the longer-term repetitive occupations identified over long sequences in the Late MP caves, remains globally valid.

The image of Late MP settlement patterns is now more nuanced with the identification—most often in open-air sites but also in some sheltered sites/caves—of fairly short-term occupations that correspond either to rare ungulate hunting and processing episodes (task-specific locations) or, more frequently, to occupations showing a greater range of activities, alongside often very intensive animal resource processing activities. In these sites, the activities necessary for the life of the group would have taken place over a short period alongside carcass processing activities near the slaughter site. Depending on the occupation durations, the tasks diversify, and the behaviours appear to be similar to those seen in ‘habitation sites’ (Ekshtain et al. 2019).

Based on these findings, apart from the rare ephemeral task-specific locations, it seems that most of the MP occupations in both sheltered and open-air sites correspond to residential camps/habitats at which diverse activities (in situ flintknapping, tool use and maintenance, animal resource processing and consumption) were always performed. The differences in the composition of the lithic and bone assemblages would thus be related to more or less frequent occupations that were more or less close in time (Malinsky-Buller et al. 2021, and references therein).

The lithic and faunal data converge to show that the occupants of Levantine MP sites in the Mediterranean zone, in both open-air and cave contexts, usually practiced mixed lithic procurement strategies, with the proportion of place provisioning strategies increasing in parallel with occupation durations. In terms of animal resources, similar hunting strategies, selective transport of ungulate carcasses and meat-processing behaviours have been identified in the Early and later Middle Palaeolithic assemblages (Rabinovitch and Hovers 2004; Rabinovich and Tchernov 1995; Speth 2012, 2019; Speth and Clark 2006; Stiner 2005; Yeshurun, Bar-Oz, and Weinstein-Evron 2007).

The differences observed between the high residential mobility sites in the Early MP (e.g., Hayonim units 10 to 7–8) and those of the Late MP (e.g., Kebara, Amud) concern, above all, the identification in the latter of high occupation densities that are probably linked to repeated occupations of the same place (frequent and close in time) with, for example, multiseasonal use of the cave at Kebara (Meignen, Speth, and Bar-Yosef 2017; Rendu and Speth 2019; Speth 2019). These frequent returns over long periods (long stratigraphic sequences) often result in a continual structuring of inhabited space that is repeated in successive levels with a high degree of redundancy of spatial patterning through the successive occupation levels (e.g., bone waste disposal corresponding to cleaning activities at Kebara; Meignen et al. 2019; Speth et al. 2012).

This suggests small human groups with a low residential mobility within restricted annual home ranges (Hovers 2001, 2009; Hovers and Belfer-Cohen 2013) in a region in which vegetal and animal resources (and water) were probably available nearly all year-round.

The situation was different in the arid/semi-arid zone of the eastern Levant, where food and water resources were probably more seasonal and dispersed. For the long sequences of Umm el Tlel and Yabrud 1, located in the steppic zone, Pagli (2013) described successive replacements of culturally different groups moving over large territories and, therefore, without frequent returns to the same place/locale. The late Middle Palaeolithic period in the arid steppe areas would be thus characterised by higher group mobility over large, comparatively resource-poor territories that were needed to maintain the population; whereas during the same period the richer Mediterranean coastal plain could support human groups in smaller, more spatially stable territories on a year-round basis (Bar-Yosef 2000; Hovers 2001).

The data on Early MP mobility systems are more limited due to the smaller number of sites. However, they are present in the Mediterranean area as well as in arid and semi-arid zones. It is also worth noting that the occupation of caves and shelters is quite systematic and repetitive over reasonably long sequences, often in continuity with the Acheulo-Yabrudian occupations they follow (Hayonim, Tabun, Misliya, Abu Sif, Yabrud). Though this type of succession is less often observed in open-air sites, the Hummal sequence should be mentioned. At this site, the presence of water resources (artesian well) undoubtedly served as a point of attraction.

The data available at the regional scale suggest low population densities with the circulation of small, highly mobile human groups within a fairly large territory (Hovers 2001; Hovers and Belfer-Cohen 2013; Meignen et al. 2006). The Hayonim/Tabun/Misliya sequences show, however, that human groups with the same technical traditions return regularly for long periods to the same location and habitat, where they know the locally available resources (most often local raw materials, plant and animal resources that determine the mobility of the groups). However, the low lithic and bone artefact densities suggest small groups that returned for fairly short-term occupations and, especially, for visits that were probably rather spaced out in time.

These sites functioned as base camps, however, as shown by the evidence for diverse activities, most often including a complete *chaîne opératoire* for the manufacture and maintenance of tools, including imported ones, alongside food transport to the habitat. The deposits attest to the frequent use and maintenance of fire (even if the combustion features are more or less well preserved). The tool provisioning strategies most often show both the import of tools (mostly retouched or unworked blades) (Hayonim 10 to 7/8; Misliya; Tabun IX; Emanuel; Hummal 6b, Hummal 6b-2) and/or prepared cores (Emanuel), subsequently highly curated onsite. However, this imported toolkit was systematically completed by the preparation of new blanks onsite (provisioning of place). The proportion of onsite knapping is usually quite significant but does not overshadow the array of imported tools, which suggests rather short-term occupations.

Based on many criteria, these appear to be short-term occupations, and in some levels they can be frequent enough, and close enough in time, for some spatial organisation to persist. This is true, for example, in unit 6 at Hayonim (see chapter 3), in which many small, rather shallow, successive hearths, were systematically installed in the same place and accumulated to create deep combustion features, representing a significant duration of the same spatial organisation. This was an organisation of activities that, moreover, did not continue into the later occupation levels. The research of Yeshurun et al. (2020) at Misliya also showed a repetition of the activity organisation (clear around-the-fire patterns and differential use of space) around a deep hearth also made up of numerous successive combustion episodes.

But the situation is very different from what is observed in the Late MP sequences in which the same general spatial arrangement of the habitat persists over much longer periods, reflecting frequent, closely-spaced visits to the habitat, and camp maintenance behaviours that persist over long periods (e.g., activity zones and combustion features versus waste zones in units XI to IX at Kebara [Meignen et al. 2019; Speth et al. 2012]).

At the same time, the majority of contextual data points to relatively short-term occupations: low lithic and faunal artefact densities; few hunted animals (Goder-Goldberger et al. 2012; Stiner 2005); and a slow rate of anthropogenic ashy sediment accumulation in the case of Hayonim, for example (1 m³ in 10 ka–15 ka [Bar-Yosef et al. 2005]). These features would thus correspond to low occupation intensities; short burning episodes, even if sometimes repetitive in the same location, and a non-selective collection of fuels reflecting low requirements for their quality and efficiency (Albert et al. 2003; Meignen et al. 2009). The occupations described in the site of Misliya could represent a greater concentration of activities associated with a larger group, the concomitant presence of several groups (aggregation site? Hovers 2017; Weinstein-Evron and Zaidner 2017), slightly longer occupation durations, or more frequent returns to the site with less time between them.

Interestingly, and as we have already mentioned, it seems that the characteristics of the Early MP lithic assemblages (substantial presence of elongated blanks, especially tools, mainly on blades) are linked to their involvement in settlement patterns in which the import of elongated blanks produced elsewhere, and then highly curated, is the rule, specifically at sites where the provisioning of individuals (personal gear) played an important role. In these sites with relatively short-term occupations, this imported toolkit is still detectable because the debitage activities carried out onsite were not sufficiently numerous to ‘drown’ out the tool import contributions (e.g., in the Hayonim lower units, Misliya, Emanuel, Abu Sif, Tabun IX). In these assemblages, the personal gear seems to be mostly composed of elongated blanks and, at Hayonim, at least, it does not appear that Levallois blanks were widely introduced. These elongated blanks are also the ones that are most often retouched, sometimes intensively (high proportions of blade tools found at Hayonim, Hummal, Misliya, and Abu Sif (chapter 5, Table 5.79).

These land-use patterns based on ephemeral site use and mobility over large territories have been interpreted in terms of a decrease in regional population densities (Malinsky-Buller and Hovers 2019) and, more recently in other words— as the result of a ‘demographic network tightly connected through stabilised mechanisms of social learning’ (Wojtczak and Malinsky-Buller 2022).

Bibliography

- Albert, R. M., O. Bar-Yosef, L. Meignen, and S. Weiner. 2003. Quantitative phytolith study of hearths from the Natufian and Middle Palaeolithic levels of Hayonim Cave (Galilee, Israel). *Journal of Archaeological Science* 30 (4):461-480.
- Albert, R. M., F. Berna, and P. Goldberg. 2012. Insights on Neanderthal fire use at Kebara Cave (Israel) through high resolution study of prehistoric combustion features: Evidence from phytoliths and thin sections. *Quaternary International* 247:278-293.
- Albert, R. M., and D. Cabanes. 2007. Fire in prehistory: An experimental approach to combustion processes and phytolith remains. *Israel Journal of earth sciences* 56 (2-4):175-189.
- Albert, R. M., O. Lavi, L. Estroff, S. Weiner, A. Tsatskin, A. Ronen, and S. Lev-Yadun. 1999. Mode of occupation of Tabun Cave, Mt Carmel, Israel, during the Mousterian Period: A study of the sediments and phytoliths. *Journal of Archaeological Science* 26 (10):1249-1260.
- Albert, R. M., S. Weiner, O. Bar-Yosef, and L. Meignen. 2000. Phytoliths in the Middle Palaeolithic deposits of Kebara Cave, Mt Carmel, Israel: study of the plant materials used for fuel and other purposes. *Journal of Archaeological Science* 27 (10):931-947.
- Aldeias, V., H. L. Dibble, D. Sandgathe, P. Goldberg, and S. J. P. McPherron. 2016. How heat alters underlying deposits and implications for archaeological fire features: A controlled experiment. *Journal of Archaeological Science* 67:64-79.
- Aldeias, V., P. Goldberg, D. Sandgathe, F. Berna, H. L. Dibble, S. J. P. McPherron, A. Turq, and Z. Rezek. 2012. Evidence for Neandertal use of fire at Roc de Marsal (France). *Journal of Archaeological Science* 39 (7):2414-2423.
- Alpers-Afil, N. 2008. Continual fire-making by Hominins at Gesher Benot Ya'aqov, Israel. *Quaternary Science Reviews* 27 (17-18):1733-1739.
- Alpers-Afil, N., and E. Hovers. 2005. Differential use of space in the Neandertal site of Amud Cave, Israel. *Eurasian Prehistory* 3 (1):3-22.
- Alpers-Afil, N., D. Richter, and N. Goren-Inbar. 2007. Phantom hearths and the use of fire at Gesher Benot Ya'aqov, Israel. *PaleoAnthropology* 2007:1-15.
- Altemüller, H. J., and B. Van Vliet-Lanoe. 1990. Soil thin section fluorescence microscopy. In *Soil Micromorphology: A Basic and Applied Science*, ed. L. A. Douglas, 565-579. Amsterdam: Elsevier.
- Anderson-Gerfaud, P., and D. Helmer. 1987. L'emmanchement au Moustérien. In *La main et l'outil. Manches et emmanchements préhistoriques.*, ed. D. Stordeur, 37-54. Lyon: Maison de l'Orient.
- Arensburg, B., O. Bar-Yosef, A. Belfer-Cohen, and Y. Rak. 1990. Mousterian and Aurignacian Human remains from Hayonim Cave, Israel. *Paléorient* 16 (1):107-109.
- Arensburg, B., and A. Belfer-Cohen. 1998. Sapiens and Neandertals: Rethinking the Levantine Middle Paleolithic Hominids. In *Neandertals and Modern Humans in Western Asia*, eds. T. Akazawa, K. Aoki and O. B. Yosef, 311-322. New York/London: Plenum Press.

- Arpin, T. L., C. Mallol, and P. Goldberg. 2002. A new method of analyzing and documenting micromorphological thin sections using flatbed scanners: applications in geoarchaeological studies. *Geoarchaeology: An International Journal* 17:305-313.
- Assaf, E., Y. Parush, A. Gopher, and R. Barkai. 2015. Intra-site recycling variability at Qesem Cave, Israel: new evidence from Amudian and Yabrudian assemblages. *Quaternary International* 361:88-102.
- Balfet, H. 1991. *Observer l'action technique : des chaînes opératoires, pour quoi faire ?* Paris: Eds. du C.N.R.S.
- Bamforth, D. 1991. Technological organization and hunter-gatherer land-use : a California example. *American Antiquity* 56:216-234.
- Bar-Yosef, O. 1982. Some remarks on the nature of transitions in prehistory. In *The transition from lower to middle Paleolithic and the origin of modern Man*, ed. A. Ronen, 28-39. Oxford: BAR International Series 151.
- Bar-Yosef, O. 1991a. The Archaeology of the Natufian Layer at Hayonim Cave. In *The Natufian Culture in the Levant*, eds. O. Bar-Yosef and F. Valla, 81-92. Ann Arbor: International Monographs in Prehistory.
- Bar-Yosef, O. 1991b. The history of excavations at Kebara Cave. In *Le Squelette Moustérien de Kébara 2*, eds. O. Bar-Yosef and B. Vandermeersch, 17-27. Paris: (Cahiers de Paléanthropologie), Éditions du C.N.R.S.
- Bar-Yosef, O. 1994. The contribution of Southwest Asia to the study of the origin of Modern Humans. In *Origins of Anatomically Modern Humans*, eds. M. H. Nitecki and D. V. Nitecki, 23-66. New York: Plenum Press.
- Bar-Yosef, O. 1998a. Chronology of the Middle Paleolithic of the Levant. In *Neandertals and Modern Humans in Western Asia*, eds. T. Akazawa, K. Aoki and O. Bar-Yosef, 39-56. New York and London: Plenum Press.
- Bar-Yosef, O. 1998b. On the Nature of Transitions: the Middle to Upper Palaeolithic and the Neolithic Revolution. *Cambridge Archaeological Journal* 8 (2):141-163.
- Bar-Yosef, O. 2000. The Middle and Upper Paleolithic in Southwest Asia and Neighboring Regions. In *The Geography of Neandertals and Modern Humans in Europe and the Greater Mediterranean*, eds. O. Bar-Yosef and D. Pilbeam, 107-156. Cambridge (US): Peabody Museum of Archaeology and Ethnology, Harvard University.
- Bar-Yosef, O. 2006. Between observations and models. An eclectic view of Middle Paleolithic Archeology. In *Transitions before the Transition: Evolution and stability in the Middle Paleolithic and Middle Stone Age*, eds. E. Hovers and S. Kuhn, 305-325. New York, Boston, Dordrecht, London, Moscow: Springer.
- Bar-Yosef, O. 2017. Locals and Foreigners in the Levant during the Pleistocene. In *Vocation Préhistoire. Hommage à J.-M. Le Tensorer*, eds. D. Wojtczak, M. Al Najjar, R. Jagher, H. Elsuede, F. Wegmüller and M. Otte, 25-41. Liège: ERAUL.
- Bar-Yosef, O., and A. Belfer-Cohen. 1988. The early Upper Paleolithic in Levantine caves. In *The early Upper Paleolithic-Evidence from Europe and the Near East*, eds. J. F. Hoffecker and C. A. Wolf, 23-41. Oxford: BAR International Series 437.
- Bar-Yosef, O., A. Belfer-Cohen, P. Goldberg, S. Kuhn, L. Meignen, S. Weiner, and B. Vandermeersch. 2005. Archaeological background: Hayonim Cave and Meged Rockshelter. In *The Faunas of Hayonim Cave (Israel). A 200,000-Year Record of Paleolithic Diet, Demography and Society*, ed. M. Stiner, 17-38. Cambridge (US): American School of Prehistoric Research Bulletin 48, Peabody Museum of Archaeology and Ethnology, Harvard University.
- Bar-Yosef, O., and N. Goren-Inbar. 1993. *The Lithic Assemblages of Ubeidiya- A Lower Palaeolithic site in the Jordan valley*. Jerusalem: The Hebrew University of Jerusalem.
- Bar-Yosef, O., and N. Goren. 1973. Natufian remains in Hayonim Cave. *Paléorient* 1 (1):49-68.
- Bar-Yosef, O., and L. Meignen. 1992. Insights into Levantine Middle Paleolithic Cultural Variability. In *The Middle Palaeolithic : Adaptation, Behavior and Variability*, eds.

- H.L. Dibble and P. Mellars, 163-182. Philadelphia: University Museum, University of Pennsylvania.
- Bar-Yosef, O., and L. Meignen. eds. 2007. *Kebara Cave, Mt Carmel, Israel: The Middle and Upper Paleolithic Archaeology, Part I*. Cambridge (US): American School of Prehistoric Research Bulletin 49, Peabody Museum of Archaeology and Ethnology, Harvard University.
- Bar-Yosef, O., and P. Van Peer. 2009. The Chaîne Opératoire Approach in Middle Paleolithic Archaeology. *Current Anthropology* 50 (1):123-131.
- Bar-Yosef, O., and B. Vandermeersch. 1981. Note concerning the possible age of the mousterian layers in Qafzeh cave. In *Préhistoire du Levant, chronologie et organisation de l'espace depuis les origines jusqu'au VIème millénaire*, eds. J. Cauvin and P. Sanlaville, 281-285. Paris: Editions du CNRS.
- Bar-Yosef, O. , and B. Vandermeersch, eds. 1989. *Investigations in South Levantine Prehistory*. Oxford: BAR International Series 497.
- Bar-Yosef, O., and B. Vandermeersch. 1991. *Le squelette moustérien de Kebara 2, Cahiers de Paléoanthropologie*. Paris: Editions du CNRS.
- Bar-Yosef, O., and B. Vandermeersch. 2007. Introduction: The framework of the project. In *Kebara Cave, Mt Carmel, Israel- The Middle and Upper Paleolithic Archaeology, Part I*, eds. O. Bar-Yosef and L. Meignen, 1-22. Cambridge (US): American School of Prehistoric Research Bulletin 49, Peabody Museum of Archaeology and Ethnology, Harvard University.
- Bar-Yosef, O., B. Vandermeersch, B. Arensburg, A. Belfer-Cohen, P. Goldberg, H. Laville, L. Meignen, Y. Rak, J. D. Speth, E. Tchernov, A.-M. Tillier, and S. Weiner. 1992. The Excavations in Kebara Cave, Mt. Carmel. *Current Anthropology* 33 (5):497-550.
- Barkai, R., and A. Gopher. 2011. Innovative human behavior between Acheulian and Mousterian: a view from Qesem Cave, Israel. In *The Lower and Middle Palaeolithic in the Middle East and neighbouring regions*, eds. J. M. Le Tensorer, R. Ragher and M. Otte. Liège: ERAUL.
- Barkai, R., and A. Gopher. 2013. Cultural and Biological Transformations in the Middle Pleistocene Levant: A View from Qesem Cave, Israel. In *Dynamics of Learning in Neanderthals and Modern Humans – Cultural Perspectives*, eds. T. Akazawa, Y. Nishiaki and K. Aoki, 115-137: Springer Japan.
- Barkai, R., A. Gopher, S. Lauritzen, and A. Frumkin. 2003. Uranium series dates from Qesem Cave, Israel, and the end of the Lower Palaeolithic. *Nature* 423:977-979.
- Barkai, R., C. Lemorini, R. Shimelmitz, Z. Lev, M. Stiner, and A. Gopher. 2009. A blade for all seasons? Making and using Amudian blades at Qesem Cave, Israel. *Human Evolution* 24:57-75.
- Bate, D. M. A. 1937. Palaeontology: the fossil fauna of the Wady el-Mughara caves. In *The Stone Age of Mount Carmel, Part 2*, eds. D. E. E. Garrod and D. M. A. Bate, 137-240. Oxford: Clarendon Press.
- Belfer-Cohen, A. 1988. The Natufian graveyard in Hayonim Cave. *Paléorient* 14 (2):297-308.
- Belfer-Cohen, A., and O. Bar-Yosef. 1981. The Aurignacian at Hayonim Cave. *Paléorient* 7 (2):19-42.
- Bellomo, R. V. 1993. A methodological approach for identifying archaeological evidence of fire resulting from human activities. *Journal of Archaeological Science* 20 (5):525-553.
- Bergman, C. A., and K. Ohnuma. 1983. Technological notes on some blades from Hummal Ia, El-Kowm, Syria. *Quartär* 33/34:171-180.
- Berna, F., and P. Goldberg. 2008. Assessing Paleolithic pyrotechnology and associated hominin behavior in Israel. *Israel Journal of earth sciences* 56:107-121.
- Berner, R. A. 1971. *Principles of Chemical Sedimentology*: McGraw-Hill New York.
- Beyries, S., and E. Boëda. 1983. Etude technologique et traces d'utilisation des "éclats débordants" de Corbehem (Pas-de-Calais). *Bulletin de Société Préhistorique française* 80 (9):275-279.

- Binford, L. R. 1973. Interassemblage variability- the Mousterian and the “functional” argument. In *Explanation of Cultural Change- Models in Prehistory*, ed. C. Renfrew, 227-254. London: Duckworth.
- Binford, L. R. 1977. Forty-seven trips: A case study in the character of archaeological formation processes. In *Stone tools as cultural markers*, ed. R. V. S. Wright, 24-36. Canberra: Australian Institute of Aboriginal Studies.
- Binford, L. R. 1978. *Nunamiut Ethnoarchaeology*. New York: Academic Press.
- Binford, L. R. 1979. Organization and formation processes : Looking at curated technologies. *Journal of Anthropological Research* 35 (3):255-273.
- Binford, L. R. 1980. Willow smoke and dogs’ tails : hunter-gatherer settlement systems and archaeological site formation. *American Antiquity* 45 (1):4-20.
- Binford, L. R. 1981. *Bones: ancient men and modern myths*. New York: Academic press.
- Binford, L. R., and S. R. Binford. 1966. A preliminary analysis of functional variability in the Mousterian of the Levallois Facies. *American Anthropologist* 68 (2):238-296.
- Blasco, R., J. Rosell, A. Gopher, and R. Barkai. 2014. Subsistence economy and social life: A zooarchaeological view from the 300 kya central hearth at Qesem Cave, Israel. *Journal of Anthropological Archaeology* 35:248-268.
- Blasco, R., J. Rosell, P. Sañudo, A. Gopher, and R. Barkai. 2016. What happens around a fire: Faunal processing sequences and spatial distribution at Qesem Cave (300 ka), Israel. *Quaternary International* 398:190-209.
- Boëda, E. 1986. Approche technologique du concept Levallois et évaluation de son champ d’application. Thèse Doctorat, Université Paris X- Nanterre.
- Boëda, E. 1994. *Le concept Levallois : variabilité des méthodes*. Paris: CNRS Editions.
- Boëda, E. 1995. Levallois : A Volumetric Construction, Methods, a Technique. In *The Definition and Interpretation of Levallois Technology*, eds. H.L. Dibble and O. Bar-Yosef, 41-68. Madison: Prehistory Press.
- Boëda, E. 1997. Technogenèse de systèmes de production lithique au Paléolithique inférieur et moyen en Europe occidentale et au Proche Orient. Thèse Habilitation, Université Nanterre-Paris X.
- Boëda, E. 2013. *Techno-logique et Technologie. Une Paléo-histoire des objets lithiques*: Archéo-éditions.com.
- Boëda, E., J. Connant, D. Dessort, S. Muhesen, N. Mercier, H. Valladas, and N. Tisnerat. 1996. Bitumen as a hafting material on Middle Palaeolithic artefacts. *Nature* 380:336-338.
- Boëda, E., J.-M. Geneste, and L. Meignen. 1990. Identification de chaînes opératoires lithiques du Paléolithique ancien et moyen. *Paleo* 2:43-80.
- Boëda, E., C. Griggo, and S. Noël-Soriano. 2001. Différents modes d’occupation du site d’Umm el Tlell au cours du Paléolithique moyen (El Kowm, Syrie centrale). *Paléorient* 27 (2):13-28.
- Bonilauri, S. 2010. Les outils du Paléolithique moyen: une mémoire technique oubliée ? Approche techno-fonctionnelle appliquée à un assemblage lithique de conception Levallois provenant du site d’Umm el Tlel (Syrie centrale). Thèse Doctorat, Université Paris Ouest Nanterre, Nanterre.
- Bonilauri, S. 2015. Le débitage Levallois : un concept de préhension normalisé et varié ? Exemples de productions issues du site d’Umm El Tlel (Syrie Centrale). *Paléorient* 41 (1):83-115.
- Bordes, F. 1955. Le Paléolithique inférieur et moyen de Jabrud (Syrie) et la question du Pré-Aurignacien. *L’Anthropologie* 59:486-507.
- Bourguignon, L. 1996. La conception de débitage Quina. *Quaternaria Nova* VI:149-166.
- Bourguignon, L. 1997. Le Moustérien de type Quina: nouvelle définition d’une entité technique, Laboratoire d’ethnologie et de sociologie comparative, option Sociétés préhistoriques, Thèse Doctorat, Université Paris X-Nanterre.

- Bourguignon, L. 1998. Le débitage Quina de la couche 5 de Sclayn: éléments d'interprétation. In *Recherches aux grottes de Sclayn*, eds. M. Otte, M. Patou-Mathis and D. Bonjean, 249-276. Liège: ERAUL.
- Bourguignon, L. 2001. Apports de l'expérimentation et de l'analyse techno-morpho-fonctionnelle à la reconnaissance du processus d'aménagement de la retouche Quina. In *Préhistoire et Approche expérimentale*, eds. L. Bourguignon, I. Ortega and M. C. Frère-Sautot, 35-66. Montagnac: M.Mergoil.
- Bourguignon, L., M. Brenet, and M. Folgado. 2006. Le Paléolithique moyen (35-350 ka) d'Aquitaine septentrionale : émergence, développement et variabilité: le projet expérimental, atelier 3 In *Rapport final d'activité d'ACR (culture/cnrs/inrap), sous direction de J.P. Texier et J. Jaubert*, 68-81. Bordeaux: CNRS/ PACEA.
- Breeze, P. S., H. S. Groucutt, N. A. Drake, T. S. White, R. P. Jennings, and M. D. Petraglia. 2016. Palaeohydrological corridors for hominin dispersals in the Middle East 250–70,000 years ago. *Quaternary Science Review* 144:155-185.
- Brenet, M., L. Bourguignon, M. Folgado, and I. Ortega. 2009. Elaboration d'un protocole d'expérimentation lithique pour la compréhension des comportements techniques et techno-économiques au Paléolithique moyen. L'apport de nouvelles données. *Les Nouvelles de l'Archéologie* 118:61-64.
- Buisson-Catil, J. 1994. *Le Paléolithique moyen en Vaucluse*. Avignon: Service d'Archéologie du Vaucluse.
- Bullock, P., N. Fedoroff, A. Jongerius, G. Stoops, T. Tursina, and U. Babel. 1985. *Handbook for Soil Thin Section Description*. Wolverhampton: Waine Research.
- Centi, L., and Y. Zaidner. 2021. The Levallois Flaking System in Nesher Ramla Upper Sequence. *Journal of Paleolithic Archaeology* 4. DOI:10.1007/s41982-021-00088-3
- Centi, L., and Y. Zaidner. 2022. Variations in lithic artefact density as a tool for better understanding Middle Palaeolithic human behavior: the case of Nesher Ramla (Israel). *Quaternary International* 624:4-18.
- Chazan, M., and L. Kolska-Horwitz eds. 2001. *Holon: A Lower Paleolithic Site in Israel*. Cambridge (US): Peabody Museum Press, Harvard University.
- Clark-Howell, F. 1959. Upper Pleistocene stratigraphy and early Man in the Levant. *Proceedings of the American Philosophical Society* 103 (1):1-65.
- Clark, J. D. 1988. The middle stone age of east Africa and the beginnings of regional identity. *Journal of World Prehistory* 2 (3):235-305.
- Coon, C. S. 1962. *The Origin of Races*. New York: Knopf.
- Copeland, L. 1975. The Middle and Upper Paleolithic of Lebanon and Syria, in the light of recent research. In *Problems in Prehistory of North-Africa and Levant*, eds. F. Wendorf and A. Marks, 317-350. Dallas: SMU Press.
- Copeland, L. 1983. The Paleolithic industries at Adlun. In *Adlun the Stone Age. The Excavations of D.A.E. Garrod in the Lebanon. 1958-1963*, ed. D. Roe, 89-364. Oxford: BAR International Series 159.
- Copeland, L. 1985. The pointed tools of Hummal Ia (El Kowm, Syria). *Cahiers de l'Euphrate* 4:177-189.
- Copeland, L. 1995. Are Levallois flakes in the Levantine Acheulian the results of biface preparation? . In *The Definition and Interpretation of Levallois Technology*, eds. H. L. Dibble and O. Bar-Yosef, 171-183. Madison: Prehistory Press.
- Copeland, L. 2000. Yabrudian and related industries: The state of research in 1996. In *Toward Modern Humans: Yabrudian and Micoquian, 400-50 ky ago*, eds. A. Ronen and M. Weinstein-Evron, 97-117. Oxford: BAR International Series 850.
- Copeland, L., and F. Hours. 1983. Le Yabroudien d'El Kowm (Syrie) et sa place dans le Paléolithique du Levant. *Paléorient* 9 (1):21-37.
- Courty, M.-A. 2017. Fuel origin and firing product preservation in archaeological occupation contexts. *Quaternary International* 431 (Part A):116-130.

- Courty, M.-A., E. Allue, and A. Henry. 2020. Forming mechanisms of vitrified charcoals in archaeological firing-assemblages. *Journal of Archaeological Science: Reports* 30:102215.
- Courty, M.-A., E. Carbonell, J. V. Poch, and R. Banerjee. 2012. Microstratigraphic and multi-analytical evidence for advanced Neanderthal pyrotechnology at Abric Romani (Capellades, Spain). *Quaternary International* 247:294-313.
- Courty, M.-A., P. Goldberg, and R. I. Macphail. 1989. *Soils and Micromorphology in Archaeology*. Cambridge: Cambridge University Press.
- Crater Gershtein, K. M., Y. Zaidner, and R. Yeshurun. 2022. A campsite on the open plain: zooarchaeology of unit III at the Middle Paleolithic site of Neshar Ramla, Israel. *Quaternary International* 624:49-66.
- Cresswell, R. 1976. Techniques et culture, les bases d'un programme de travail. *Techniques et Culture* 1:7-59.
- DeBono, H., and N. Goren-Inbar. 2001. Note on a link between Acheulian handaxes and Levallois method. *Journal of the Israel Prehistoric Society* 31:9-23.
- Delage, C. 2001. Les ressources lithiques dans le nord d'Israël: la question des territoires d'approvisionnement natoufiens confrontés à l'hypothèse de leur sédentarité. Thèse Doctorat, Université Paris I-Sorbonne, Paris.
- Delage, C., L. Meignen, and O. Bar -Yosef. 2000. Chert procurement and the organization of lithic production in the Mousterian of Hayonim cave (Israel). *Journal of Human Evolution* 38 (3):A10-A11.
- Delagnes, A., and L. Meignen. 2006. Diversity of lithic production systems during the Middle Paleolithic in France : are there any chronological trends ? In *Transitions before the Transition: evolution and stability in the Middle Paleolithic and Middle Stone Age*, eds. E. Hovers and S. Kuhn, 85-108. New York, Boston, Dordrecht, London, Moscow: Springer.
- Dibble, H. L. 1991. Mousterian assemblage variability on an interregional scale. *Anthropological Research* 47(2):239-257.
- Dibble, H. L., S. J. P. McPherron, P. Goldberg, and D. Sandgathe eds. 2018. *The Middle Paleolithic Site of Pech de l'Azé IV*. Basel: Springer International.
- Douze, K. 2013. *Le Early Middle Stone Age d'Ethiopie: Les changements techno-économiques à la période de l'émergence des premiers Homo sapiens*. Sarrebruck: Presses Académiques Francophones.
- Douze, K., and A. Delagnes. 2016. The pattern of emergence of a Middle Stone Age tradition at Gademotta and Kulkuletti (Ethiopia) through convergent tool and point technologies. *Journal of Human Evolution* 91:93-121.
- Ekshtain, R., O. Barzilai, M. Inbar, I. Milevski, and M. Ullman. 2012. Giv'at Rabi East: a new Middle Paleolithic knapping site in the Lower Galilee, Israel. *Paléorient* 37 (2):107-122.
- Ekshtain, R., S. Ilani, I. Segal, and E. Hovers. 2017. Local and nonlocal procurement of raw material in Amud Cave, Israel: the complex mobility of Late Middle Paleolithic groups. *Geoarchaeology* 32:189-214.
- Ekshtain, R., A. Malinsky-Buller, N. Greenbaum, N. Mitki, M. C. Stahlschmidt, R. Shahack-Gross, N. Nir, N. Porat, D. E. Bar-Yosef Mayer, R. Yeshurun, E. Been, Y. Rak, N. Agha, L. Brailovsky, M. Krakovsky, P. Spivak, M. Ullman, A. Vered, O. Barzilai, and E. Hovers. 2019. Persistent Neanderthal occupation of the open-air site of 'Ein Qashish, Israel. *PLoS One* 14:1-34.
- Ekshtain, R., A. Malinsky-Buller, S. Ilani, I. Segal, and E. Hovers. 2014. Raw material exploitation around the Middle Paleolithic site of 'Ein Qashish. *Quaternary International* 331:248-266.
- Ekshtain, R., and C. A. Tryon. 2019. Lithic raw material acquisition and use by Early Homo sapiens at Skhul, Israel. *Journal of Human Evolution* 127:149-170.
- Ekshtain, R., and Y. Zaidner. 2022. Raw material exploitation at the Middle Paleolithic site of Neshar Ramla, Israel. *Quaternary International* 624:34-48.

- Farrand, W. R. 1979. Chronology and palaeoenvironment of Levantine prehistoric sites as seen from sediment studies. *Journal of Archaeological Science* 6:369-392.
- Foley, R., and M. M. Lahr. 1997. Mode 3 technologies and the evolution of Modern Humans. *Cambridge Archaeological Journal* 7 (1):3-36.
- Freund, R. 1978. Geology. In *The Lower Galilee and the Kinneret*, ed. A. Itzhaki, 9-14. Jerusalem: Keter/ Ministry of Defense.
- Frumkin, A., O. Bar-Yosef, and H. P. Schwarcz. 2011. Possible paleohydrologic and paleoclimatic effects on hominin migration and occupation of the Levantine Middle Paleolithic. *Journal of Human Evolution* 60 (4):437-451.
- Gamble, C. 1999. *The Palaeolithic societies of Europe*. Cambridge: Cambridge University Press.
- Garrod, D. A. E. 1956. Acheuléo-Jabroudien et "Pré-Aurignacien" de la grotte du Taboun (Mont Carmel); étude stratigraphique et chronologique. *Quaternaria* 3:39-59.
- Garrod, D. A. E., and D. M. A. Bate. 1937. *The Stone Age of Mount Carmel: Excavations at the Wady el-Mughara*. Oxford: Clarendon Press.
- Geneste, J.-M. 1991. Systèmes techniques de production lithique : variations techno-économiques dans les processus de réalisation des outillages paléolithiques. *Techniques et Culture* 17-18:1-35.
- Geneste, J.-M. 1985. Analyse lithique d'industries moustériennes du Périgord : une approche technologique du comportement des groupes humains au Paléolithique moyen. Thèse Doctorat, Université Bordeaux I.
- Geneste, J.-M. 1988. Systèmes d'approvisionnement en matières premières au Paléolithique moyen et au Paléolithique supérieur en Aquitaine. In *L'Homme de Néandertal. La mutation*, ed. M. Otte, 61-70. Liège: ERAUL.
- Goder-Goldberger, M., and M. Bar-Matthews. 2019. Novel chrono-cultural constraints for the Middle Paleolithic site of Rosh Ein Mor (D15), Israel. *Journal of Archaeological Science: Reports* 24:102-114.
- Goder-Goldberger, M., H. Cheng, R. L. Edwards, O. Marder, Y. Peleg, R. Yeshurun, and A. Frumkin. 2012. Emanuel Cave: The site and its bearing on early Middle Paleolithic technological variability. *Paléorient* 38:203-225.
- Goder-Goldberger, M., N. Gubenko, and E. Hovers. 2016. "Diffusion with modifications": Nubian assemblages in the central Negev highlands of Israel and their implications for Middle Paleolithic inter-regional interactions. *Quaternary International* 408:121-139.
- Goldberg, P. 1973. Sedimentology, Stratigraphy and Paleoclimatology of et-Tabun Cave, Mount Carmel, Israel. Doctoral dissertation, Geology, The University of Michigan, Ann Arbor, MI.
- Goldberg, P. 1978. Granulométrie des sédiments de la grotte de Taboun, Mont-Carmel, Israël. *Géologie Méditerranéenne* V (4):371-383.
- Goldberg, P. 1979. Micromorphology of sediments from Hayonim Cave, Israel. *Catena* 6 (2):167-181.
- Goldberg, P. 2003. Some observations on Middle and Upper Palaeolithic ashy cave and rockshelter deposits in the Near East. In *More than Meets the Eye: Studies on Upper Palaeolithic Diversity in the Near East*, eds. A. N. Goring-Morris and A. Belfer-Cohen, 19-32. Oxford: Oxbow Books.
- Goldberg, P., and O. Bar-Yosef. 1998. Site formation processes in Kebara and Hayonim Caves and their significance in Levantine Prehistoric Caves. In *Neandertals and Modern humans in Western Asia*, eds. T. Akazawa, K. Aoki and O. Bar-Yosef, 107-125. New York: Plenum Press.
- Goldberg, P., and F. Berna. 2010. Micromorphology and context. *Quaternary International* 214 (1-2):56-62.
- Goldberg, P., H. L. Dibble, F. Berna, D. Sandgathe, S. J. P. McPherron, and A. Turq. 2012. New evidence on Neandertal use of fire: Examples from Roc de Marsal and Pech de l'Azé IV. *Quaternary International* 247 (1):325-340.

- Goldberg, P., and H. Laville. 1988. Le contexte stratigraphique des occupations paléolithiques de la grotte de Kébara (Israël). *Paléorient* 14 (2):117-123.
- Goldberg, P., H. Laville, L. Meignen, and O. Bar-Yosef. 2007. Stratigraphy and geoarchaeological history of Kebara Cave, Mount Carmel. In *Kebara Cave Mt. Carmel, Israel: The Middle and Upper Paleolithic Archaeology*, eds. O. Bar-Yosef and L. Meignen, 49-89. Cambridge (US): American School of Prehistoric Research Bulletin 49. Peabody Museum of Archaeology and Ethnology, Harvard University.
- Goldberg, P., and R. I. Macphail. 2006. *Practical and Theoretical Geoarchaeology*. Oxford: Blackwell Publishing.
- Goldberg, P., S. J. P. McPherron, H. L. Dibble, and D. M. Sandgathe. 2018. Stratigraphy, Deposits, and Site Formation. In *The Middle Paleolithic Site of Pech de l'Azé IV*, eds. H. L. Dibble, S. J. P. McPherron, P. Goldberg and D. M. Sandgathe, 21-74: Springer International Publishing.
- Goldberg, P., C. E. Miller, and S. M. Mentzer. 2017. Recognizing Fire in the Paleolithic Archaeological Record. *Current Anthropology* 58, Supplement 16 (August 2017):S175-S190.
- Goldberg, P., C. E. Miller, S. Schiegl, F. Berna, B. Ligouis, N. J. Conard, and L. Wadley. 2009. Bedding, hearths, and site maintenance in the Middle Stone Age of Sibudu Cave, KwaZulu-Natal, South Africa. *Archaeological and Anthropological Sciences* 1:95-122.
- Gopher, A., A. Ayalon, M. Bar-Matthews, R. Barkai, A. Frumkin, P. Karkanas, and R. Shahack-Gross. 2010. The chronology of the late Lower Paleolithic in the Levant based on U-Th ages of speleothems from Qesem Cave, Israel. *Quaternary Geochronology* 5 (6):644-656.
- Gopher, A., and R. Barkai. 2014. Middle Paleolithic open-air industrial areas in the Galilee, Israel: The challenging study of flint extraction and reduction complexes. *Quaternary International* 331:95-102.
- Gopher, A., R. Barkai, R. Shimelmitz, M. Khalaily, C. Lemorini, I. Heshkovitz, and M. Stiner. 2005. Qesem Cave: an Amudian site in Central Israel. *Journal of The Israel Prehistoric Society* 35:69-92.
- Gopher, A., Y. Parush, E. Assaf, and R. Barkai. 2016. Spatial aspects as seen from a density analysis of lithics at Middle Pleistocene Qesem Cave: Preliminary results and observations. *Quaternary International* 398:103-117.
- Goren-Inbar, N. 1988. Too small to be true? Reevaluation of cores on flakes in Levantine Mousterian assemblages. *Lithic Technology* 17 (1):37-44.
- Goren-Inbar, N. 1990. *Quneitra: a Mousterian Site on the Golan Heights*. Jerusalem: The Hebrew University of Jerusalem.
- Goren-Inbar, N., N. Alpers, M. E. Kislev, O. Simchoni, Y. Melamed, A. Ben-Nun, and E. Werker. 2004. Evidence of Hominin control of fire at Geshert Benot Ya'aqov, Israel. *Science* 304:725-727.
- Gowlett, J. A., J. Hallos, S. Hounsell, V. Brant, and N. C. Debenham. 2005. Beeches Pit – archaeology, assemblage dynamics and early fire history of a Middle Pleistocene site in East Anglia, UK. *Eurasian Prehistory* 3 (2):3-38.
- Gowlett, J. A. J. 2006. The early settlement of northern Europe: fire history in the context of climate change and the social brain. *Comptes Rendus Palevol* 5:299-310.
- Griggo, C., E. Boëda, S. Bonilauri, H. Al Sakhel, and A. Emery-Barbier. 2011. A mousterian dromedary hunting camp: level VI1a at Umm el Tlel (el Kowm, central Syria). In *Hunting camps in Prehistory: Current Archaeological Approaches*, eds. F. Bon, S. Costamagno and N. Valdeyron, 103-129. University Toulouse II: Palethnology.
- Groman-Yaroslavski, I., Y. Zaidner, and M. Weinstein-Evron. 2016. Mousterian Abu Sif points: Foraging tools of the Early Middle Paleolithic site of Misliya Cave, Mount Carmel, Israel. *Journal of Archaeological Science: Reports* 7:312-323.
- Groucutt, H. S., R. Grün, I. A. S. Zalmout, N. A. Drake, S. J. Armitage, I. Candy, et al. 2018. *Homo sapiens* in Arabia by 85,000 years ago. *Nature Ecology and Evolution* 2:800-809.

- Groucutt, H. S., M. D. Petraglia, G. Bailey, E. M. L. Scerri, A. Parton, L. Clark-Balzan, R.P. Jennings, L. Lewis, J. Blinkhorn, N. A. Drake, P. S. Breeze, R. H. Inglis, M. H. Devès, M. Meredith-Williams, N. Boivin, M. G. Thomas, and A. Scally. 2015a. Rethinking the dispersal of *Homo sapiens* out of Africa. *Evolutionary Anthropology* 24 (4):149-164.
- Groucutt, H. S., E. M. L. Scerri, L. Lewis, L. Clark-Balzan, J. Blinkhorn, R. P. Jennings, A. Parton, and M. D. Petraglia. 2015b. Stone tool assemblages and models for the dispersal of *Homo sapiens* out of Africa. *Quaternary International* 382:8-30.
- Groucutt, H. S., E. M. L. Scerri, C. B. Stringer, and M. D. Petraglia. 2017. Skhul lithic technology and the dispersal of *Homo sapiens* into Southwest Asia. *Quaternary International* 515:30-52.
- Grün, R., and C. B. Stringer. 1991. Electron spin resonance dating and the evolution of modern humans. *Archaeometry* 33 (2):153-199.
- Hajdinjak, M., Q. Fu, A. Hübner, M. Petr, et al. 2018. Reconstructing the genetic history of late Neanderthals. *Nature* 555:652-656.
- Hauck, T. 2011a. The Mousterian sequence of Hummal and its tentative placement in the Levantine Middle Paleolithic. In *The Lower and Middle Palaeolithic in the Middle East and Neighbouring Regions*, eds. J. M. Le Tensorer, R. Jagher and M. Otte, 309-323. Liège: ERAUL.
- Hauck, T. 2011b. Mousterian technology and settlement dynamics in the site of Hummal (Syria). *Journal of Human Evolution* 61:519-537.
- Hauck, T. 2013. *The Mousterian sequence of Hummal (Syria)*. Rahden/Westfalia: Verlag Marie Leidorf GmbH.
- Hauck, T., D. Wojtczak, F. Wegmüller, and J.-M. Le Tensorer. 2010. Variation in lower and middle Paleolithic land use strategies in the Syrian Desert steppe: the example of Hummal (El Kowm area). In *Settlement Dynamics of the Middle Paleolithic and Middle Stone Age*, eds. N. J. Conard and A. Delagnes, 145-162. Tübingen: Kerns Verlag.
- Hedges, R. E., and A. R. Millard. 1995. Bones and groundwater: towards the modelling of diagenetic processes. *Journal of Archaeological Science* 22 (2):155-164.
- Hedges, R. E., A. R. Millard, and A. W. Pike. 1995. Measurements and relationships of diagenetic alteration of bone from three archaeological sites. *Journal of Archaeological Science* 22 (2):201-209.
- Henry, A. G. 2017. Neanderthal Cooking and the Costs of Fire. *Current Anthropology* 58 (S16):S329-S336.
- Henry, D. O. 1998. Intrasite spatial patterns and behavioral modernity: Indications from the Late Levantine Mousterian Rockshelter of Tor Faraj, Southern Jordan. In *Neandertals and Modern Humans in Western Asia*, eds. T. Akazawa, K. Aoki and O. Bar-Yosef, 127-142. New York/London: Plenum Press.
- Henry, D. O. 2003. *Neandertals in the Levant. Behavioral Organization and the Beginnings of Human Modernity*. London-New York: Continuum.
- Henry, D. O. 2012. The palimpsest problem, hearth pattern analysis, and Middle Paleolithic site structure. *Quaternary International* 247:246-266.
- Henry, D. O., A. Leroi-Gourhan, and S. Davis. 1981. The excavation of Hayonim Terrace: An examination of terminal Pleistocene climatic and adaptative changes. *Journal of Archaeological Science* 8:33-58.
- Hershkovitz, I., H. May, R. Sarig, A. Pokhojaev, D. Grimaud-Herve, E. Bruner, C. Fornai, R. Quam, J. L. Arsuaga, V. A. Krenn, M. Martinon-Torres, J. M. Bermúdez de Castro, L. Martín-Frances, V. Slon, L. Albessard-Ball, A. Vialet, T. Schüller, G. Manzi, A. Profico, F. Di Vincenzo, G. W. Weber, and Y. Zaidner. 2021. A middle Pleistocene *Homo* from Neshar Ramla, Israel. *Science* 372:1424-1428.
- Hershkovitz, I., G. W. Weber, R. Quam, M. Duval, R. Grün, L. Kinsley, A. Ayalon, M. Bar-Matthews, H. Valladas, N. Mercier, J. L. Arsuaga, M. Martín-Torres, J. M. Bermúdez de Castro, C. Fornai, L. Martín-Frances, R. Sarig, H. May, V. A. Krenn, V. Slon, L. Rodríguez, R. García, C. Lorenzo, J. M. Carretero, A. Frumkin, R. Shahack-Gross, D. E. Bar-Yosef Mayer, Y. Cui, X. Wu, N. Peled, I. Groman-Yaroslavski, L. Weissbrod,

- R. Yeshurun, A. Tsatskin, Y. Zaidner, and M. Weinstein-Evron. 2018. The earliest modern humans outside Africa. *Science* 359:456-459.
- Hoggard, C. S. 2017. Considering the function of Middle Palaeolithic blade technologies through an examination of experimental blade edge angles. *Journal of Archaeological Science: Reports* 16:233-239.
- Hovers, E. 1998. The Lithic assemblages of Amud Cave: Implications for understanding the end of the Mousterian in the Levant. In *Neandertals and Modern Humans in Western Asia*, eds. T. Akazawa, K. Aoki and O. Bar-Yosef, 143-163. New York: Plenum Press.
- Hovers, E. 2001. Territorial behavior in the Middle Paleolithic of the Southern Levant. In *Settlement Dynamics of the Middle Paleolithic and Middle Stone Age*, ed. N. Conard, 123-152. Tübingen: Kerns Verlag.
- Hovers, E. 2007. The Many Faces of Cores-on-flakes: A Perspective from the Levantine Mousterian. In *Tools versus Cores: Alternative Approaches to Stone Tool Analysis*, ed. S. J. P. McPherron, 42-74. Newcastle: Cambridge Scholars Publishing.
- Hovers, E. 2009. *The Lithic Assemblages of Qafzeh Cave*. Oxford: Oxford University Press.
- Hovers, E. 2017. Middle Paleolithic open-air sites. In *Quaternary of the Levant: Environments, Climate Change, and Humans*, eds. Y. Enzel and O. Bar-Yosef, 593-600. Cambridge: Cambridge University Press.
- Hovers, E., and A. Belfer-Cohen. 2013. On variability and complexity: lessons from the Levantine Middle Paleolithic record. *Current Anthropology* 54 (8):S337-S357.
- Hovers, E., R. Ekshtain, N. Greenbaum, A. Malinsky-Buller, N. Nir, and R. Yeshurun. 2014. Islands in a stream? Reconstructing site formation processes in the late Middle Paleolithic site of 'Ein Qashish, northern Israel. *Quaternary International* 331:216-233.
- Hovers, E., A. Malinsky-Buller, R. Ekshtain, M. Oron, and R. Yeshurun. 2008. Ein Qashish—a new Middle Paleolithic open-air site in Northern Israel. *Journal of The Israel Prehistoric Society* 38:7-40.
- Howells, W. W. 1970. Mount Carmel Men: Morphological relationships. Paper read at VIIIth International Congress of Anthropological and Ethnological Sciences, at Tokyo/Kyoto.
- Howells, W. W. 1976. Explaining Modern Man : Evolutionists Versus Migrationists. *Journal of Human Evolution* 5:477-495.
- Inizan, M.-L., H. Roche, and J. Tixier. 1992. *Technology of Knapped Stone*. Meudon: CREP.
- Isaac, G. L. 1982. Early hominids and fire at Chesowanja, Kenya. *Nature* 296:870.
- Jagher, R., D. Wojtczak, J.-M. Le Tensorer, M. Al-Nahar, K. Abu Ghaneimeh, F. Hourani, A. Sanson, F. Follmann, S. Lo Russo, S. Al Shoubaki, and H. Le Tensorer. 2016. The first human settlements on the Left Bank of the Jordan Valley. In *SLSA Annual Report*, 239-266: Swiss-Liechtenstein Foundation for Archaeological Research Abroad
- Jelinek, A. J. 1977. A preliminary study of flakes from the Tabun Cave, Mount Carmel. In *Eretz-Israel, Memorial Volume for Moshe Stekelis*, 13, 87-96.
- Jelinek, A. J. 1981a. The Middle Paleolithic in the Southern Levant from the Perspective of the Tabun Cave. In *Préhistoire du Levant, chronologie et organisation de l'espace depuis les origines jusqu'au VIème millénaire*, eds. J. Cauvin and P. Sanlaville, 265-280. Paris: Editions du CNRS.
- Jelinek, A. J. 1981b. The Middle Paleolithic of the Levant. Synthesis. In *Préhistoire du Levant, chronologie et organisation de l'espace depuis les origines jusqu'au VIème millénaire*, eds. J. Cauvin and P. Sanlaville, 299-302. Paris: Editions du CNRS.
- Jelinek, A. J. 1982a. The Middle Paleolithic in the Southern Levant, with comments on the appearance of modern *Homo sapiens*. In *The transition from Lower to Middle Paleolithic and the origin of modern man*, ed. A. Ronen, 57-104. Oxford: BAR Int. Series 151.
- Jelinek, A. J. 1982b. The Tabun Cave and Paleolithic man in the Levant. *Science* 216:1369 -1375.
- Jelinek, A. J. 1990. The Amudian in the Context of the Mugharan Tradition at the Tabun Cave (Mount Carmel), Israel. In *The Emergence of Modern Humans. An Archaeological Perspective*, ed. P. Mellars, 81-90. Edinburgh: Edinburgh Univ. Press.

- Jelinek, A. J., W. R. Farrand, G. Haas, A. Horowitz, and P. Goldberg. 1973. New excavations at the Tabun Cave, Mount Carmel, Israel, 1967-1972: a preliminary report. *Paléorient* 1(2):151-183.
- Karkanas, P. 2021. All about wood ash: Long term fire experiments reveal unknown aspects of the formation and preservation of ash with critical implications on the emergence and use of fire in the past. *Journal of Archaeological Science* 135:105476.
- Karkanas, P., O. Bar-Yosef, P. Goldberg, and S. Weiner. 2000. Diagenesis in prehistoric caves: the use of minerals that form in situ to assess the completeness of the archaeological record. *Journal of Archaeological Science* 27 (10):915-929.
- Karkanas, P., R. Shahack-Gross, A. Ayalon, M. Bar-Matthews, R. Barkai, A. Frumkin, A. Gopher, and M. C. Stiner. 2007. Evidence for habitual use of fire at the end of the Lower Paleolithic: Site-formation processes at Qesem Cave, Israel. *Journal of Human Evolution* 53 (2):197-212.
- Karlin, C., P. Bodu, and J. Pelegrin. 1991. Processus techniques et chaînes opératoires. Comment les préhistoriens s'approprient un concept élaboré par les ethnologues. In *Observer l'action technique : des chaînes opératoires, pour quoi faire ?*, ed. H. Balfet, 101-117. Paris: Editions du CNRS.
- Kelly, R. L. 1995. *The Foraging Spectrum : Diversity in Hunter-gatherer Lifeways*. Washington: The Smithsonian Institute Press.
- Khalaily, H., Y. Goren, and F. R. Valla. 1993. A late Pottery Neolithic assemblage from Hayonim Terrace, Western Galilee. *Mitekufat Haeven, Journal of the Israel Prehistoric Society* 25:132-144.
- Klein, R. G. 1999. *The Human Career*. Chicago: University of Chicago Press.
- Kuhn, S. L. 1992. On planning and curated technologies in the Middle Paleolithic. *Journal of Anthropological Research* 48 (3):185-213.
- Kuhn, S. L. 1995. *Mousterian Lithic technology. An ecological perspective*. Princeton: Princeton University Press.
- Kuhn, S. L. 2013a. Questions of Complexity and Scale in Explanations for Cultural Transitions in the Pleistocene : A Case Study from the Early Upper Paleolithic. *Journal of Archaeological Method and Theory* 20:194-211.
- Kuhn, S. L. 2013b. Roots of the Middle Paleolithic in Eurasia. *Current Anthropology* 54 (S8):S255-S268.
- Kuhn, S. L., and A. E. Clark. 2015. Artifact densities and assemblage formation: evidence from Tabun Cave. *Journal of Anthropological Archaeology* 38:8-16.
- Kuhn, S. L., M. H. Moncel, M. Weinstein-Evron, and Y. Zaidner. 2021. Introduction to special issue "The Lower to Middle Paleolithic boundaries: Evolutionary threshold or continuum?". *Journal of Human Evolution* 159. DOI:10.1016/j.jhevol.2021.103054
- Kuhn, S. L., and M. C. Stiner. 2019. Hearth and home in the Middle Pleistocene. *Journal of Anthropological Research* 75 (3):305-327.
- Lahr, M. M., and R. A. Foley. 2003. Demography, dispersal and human evolution in the last glacial period. In *Neanderthals and modern humans in the European landscape during the last glaciation: archaeological results of the Stage 3 project.*, eds. T. H. van Andel and W. Davies, 241-256. Cambridge: McDonald Institute for Archaeological Research.
- Le Tensorer, J.-M. 2005/2006. Le Yabroudien et la transition du Paléolithique ancien au Paléolithique moyen en Syrie: l'exemple d'El Kowm. *Munibe (Antropologia-Arkeologia) Homenaje a Jesus Altuna* 57 (2):71-82.
- Le Tensorer, J.-M., V. Von Falkenstein, H. Le Tensorer, and S. Muhesen. 2011. Hummal : a very long paleolithic sequence in the steppe of Central Syria- considerations on Lower Paleolithic and the beginning of Middle Paleolithic. In *The Lower and Middle Palaeolithic in the Middle East and the Neighbouring Regions*, eds. J.-M. Le Tensorer, R. Jagher and M. Otte, 235-248. Liège: ERAUL.
- Leierer, L., M. Jambrina-Enríquez, A. V. Herrera-Herrera, R. Connolly, C. M. Hernández, B. Galvan, and C. Mallol. 2019. Insights into the timing, intensity and natural

- setting of Neanderthal occupation from the geoarchaeological study of combustion structures: A micromorphological and biomarker investigation of El Salt, unit Xb, Alcoy, Spain. *PLoS ONE* 14 (4).
- Lemonnier, P. 1976. La description des chaînes opératoires : contribution à l'analyse des systèmes techniques. *Techniques et Culture* 1:100-151.
- Lemonnier, P. 1983. L'étude des systèmes techniques, une urgence en technologie culturelle. *Techniques et Culture (nouvelle série)* 1:11-34.
- Lemonnier, P. 1992. *Elements for an Anthropology of Technology*. Ann Arbor: Museum of Anthropology, University of Michigan.
- Lemorini, C., L. Bourguignon, A. Zupancich, A. Gopher, and R. Barkai. 2015. A scraper's life history: Morpho-techno-functional and use-wear analysis of Quina and demi-Quina scrapers from Qesem Cave, Israel. *Quaternary International* 398:86-93.
- Lemorini, C., M. C. Stiner, A. Gopher, R. Shimelmitz, and R. Barkai. 2006. Use-wear analysis of an Amudian laminar assemblage from the Acheuleo-Yabrudian of Qesem Cave, Israel. *Journal of Archaeological Science* 33:921-934.
- Leroi-Gourhan, A. 1964. *Le geste et la parole : I, technique et langage*. Paris: Albin Michel.
- Lyman, R. L. 1994. *Vertebrate Taphonomy*. Cambridge: Cambridge University Press.
- Macphail, R. I., and P. Goldberg. 2018. *Applied Soils and Micromorphology in Archaeology*. Cambridge: Cambridge University Press.
- Madella, M., M. K. Jones, P. Goldberg, Y. Goren, and E. Hovers. 2002. Exploitation of plant resources by Neanderthals in Amud Cave (Israel): the evidence from phytolith studies. *Journal of Archaeological Science* 29 (7):703-719.
- Malinsky-Buller, A. 2016. The Muddle in the Middle Pleistocene: The Lower-Middle Paleolithic Transition from the Levantine Perspective. *Journal of World Prehistory* 29:1-78.
- Malinsky-Buller, A., R. Ekshtain, and E. Hovers. 2014. Organization of lithic technology at 'Ein Qashish, a late Middle Paleolithic open-air site in Israel. *Quaternary International* 331:234-247.
- Malinsky-Buller, A., R. Ekshtain, N. Munro, and E. Hovers. 2021. Back to base: re-thinking variations in settlement and mobility behaviors in the Levantine Late Middle Paleolithic as seen from Shovakh Cave. *Archaeological and Anthropological Sciences*. DOI: 10.1007/s12520-021-01313-4.
- Malinsky-Buller, A., and E. Hovers. 2019. One size does not fit all: Group size and the late middle Pleistocene prehistoric archive. *Journal of Human Evolution* 127:118-132.
- Mallol, C., D. Cabanes, and J. Baena. 2010. Microstratigraphy and diagenesis at the upper Pleistocene site of Esquilieu Cave (Cantabria, Spain). *Quaternary International* 214 (1-2):70-81.
- Mallol, C., and A. Henry. 2017. Ethnoarchaeology of Paleolithic fire: methodological considerations. *Current Anthropology* 58 (S16):S217-S229.
- Mallol, C., C. M. Hernández, D. Cabanes, A. Sistiaga, J. Machado, Á. Rodríguez, L. Pérez, and B. Galván. 2013. The black layer of Middle Palaeolithic combustion structures. Interpretation and archaeostratigraphic implications. *Journal of Archaeological Science* 40 (5):2515-2537.
- Mallol, C., F. W. Marlowe, B. M. Wood, and C. C. Porter. 2007. Earth, wind, and fire: ethnoarchaeological signals of Hadza fires. *Journal of Archaeological Science* 34 (12):2035-2052.
- Mallol, C. M., S. M. Mentzer, and C. E. Miller. 2017. Combustion Features. In *Encyclopedia of Archaeological Soil and Sediment Micromorphology*, eds. C. Nicosia and G. Stoops, 299-330. Oxford: Wiley-Blackwell.
- Marder, O., G. Gvirtzman, H. Ron, H. Khalaily, M. Wieder, R. Bankirer, R. Rabinovich, N. Porat, and I. Saragusti. 1999. The Lower Paleolithic site of Revadim Quarry, preliminary finds. *Journal of The Israel Prehistoric Society* 28:21-53.

- Marks, A. E. 1981. The Middle Paleolithic of the Negev (Israël). In *Préhistoire du Levant- Chronologie et organisation de l'espace depuis les origines jusqu'au VI^e mill.*, eds. J. Cauvin and P. Sanlaville, 287-298. Paris: Editions du CNRS.
- Marks, A. E. 1992. Typological Variability in the Levantine Middle Paleolithic. In *The Middle Paleolithic: Adaptation, Behavior and Variability*, eds. H. L. Dibble and P. Mellars, 127-142. Philadelphia: The University Museum/Univ. of Pennsylvania.
- Marks, A. E., and D. A. Friedel. 1977. Prehistoric settlement patterns in the Avdat/Agev area. In *Prehistory and Paleoenvironments in the Central Negev, Israel.*, ed. A. E. Marks, 131-158. Dallas: SMU Press.
- Mauss, M. 1947. *Manuel d'ethnographie*. Paris: Payot.
- McBrearty, S., and A. Brooks. 2000. The Revolution that wasn't: a new interpretation of the origin of modern human behavior. *Journal of Human Evolution* 39:453-563.
- McConnell, D. 1952. The crystal chemistry of carbonate apatites and their relationship to the composition of calcified tissues. *Journal of Dental Research* 31 (1):53-63.
- McCown, T., and A. Keith. 1939. *The Stone Age of Mount Carmel: The Fossil Human Remains from the Levalloiso-Mousterian*. Oxford: Clarendon.
- McPherron, S. J. P. ed. 2007. *Tools versus Cores: Alternative Approaches to Stone Tool Analysis*. Newcastle: Cambridge Scholars Publishing.
- Meignen, L. ed. 1993. *L'abri des Canalettes. Un habitat moustérien sur les grands Causses (Nant, Aveyron)*. Paris: CNRS Editions.
- Meignen, L. 1994. Paléolithique moyen au Proche-Orient : le phénomène laminaire. In *Les industries laminaires au Paléolithique moyen*, eds. S. Révillion and A. Tuffreau, 125-159. Paris: CNRS Editions.
- Meignen, L. 1995. Levallois lithic production systems in the Middle Palaeolithic of the Near East : The case of the unidirectional method. In *The Definition and Interpretation of Levallois Technology*, eds. H.L. Dibble and O. Bar-Yosef, 361-380. Madison: Prehistory Press.
- Meignen, L. 1998. Hayonim cave lithic assemblages in the context of the Near-Eastern Middle Palaeolithic : a preliminary report. In *Neandertals and Modern Humans in Western Asia*, eds. T. Akazawa, K. Aoki and O. Bar-Yosef, 165-180. New York: Plenum Press.
- Meignen, L. 2000. Early Middle Palaeolithic Blade Technology in Southwestern Asia. *Acta Anthropologica Sinica* suppl. 19:158-168.
- Meignen, L. 2007. Middle Paleolithic blade assemblages in the Near East : a reassessment. In *Caucasus and the initial dispersals in the Old World*, 133-148. St Petersburg: Russian Academy of Sciences, Institute of the History of material culture.
- Meignen, L. 2011. Contribution of Hayonim cave assemblages to the understanding of the so-called "Early Levantine Mousterian". In *The Lower and Middle Paleolithic in the Middle East and neighbouring regions*, eds. J. M. Le Tensorer, R. Ragher and M. Otte, 85-100. Liège: ERAUL.
- Meignen, L. 2019. The Mousterian lithic assemblages from Kebara cave. In *Kebara Cave, Mt Carmel, Israel- The Middle and Upper Paleolithic Archaeology, Part II*, eds. L. Meignen and O. Bar-Yosef, 1-147. Cambridge (US): American School of Prehistoric Research Bulletin 51, Peabody Museum Press, Harvard University.
- Meignen, L., and O. Bar-Yosef. 1992. Middle Palaeolithic Variability in Kebara Cave (Mount Carmel, Israël). In *The Evolution and Dispersal of Modern Humans in Asia*, eds. T. Akazawa, K. Aoki and T. Kimura, 129-148. Tokyo: Hokusen-Sha.
- Meignen, L., and O. Bar-Yosef eds. 2019. *Kebara Cave, Mt. Carmel, Israel. The Middle and Upper Paleolithic Archaeology. Part II*. Cambridge (US): American School of Prehistoric Research Bulletin 51, Peabody Museum of Archaeology and Ethnology, Harvard University.
- Meignen, L., and O. Bar-Yosef. 2020. Acheulo-Yabrudian and Early Middle Paleolithic at Hayonim Cave (Western Galilee, Israel): Continuity or break? *Journal of Human Evolution* 139. DOI:10.1016/j.jhevol.2019.102733

- Meignen, L., O. Bar-Yosef, J. Speth, and M. Stiner. 2006. Middle Paleolithic settlement patterns in the Levant. In *Transitions before the Transition: Evolution and stability in the Middle Paleolithic and Middle Stone Age*, eds. E. Hovers and S. Kuhn, 149-170. New York, Boston, Dordrecht, London, Moscow: Springer.
- Meignen, L., O. Bar-Yosef, M. Stiner, S. Kuhn, P. Goldberg, and S. Weiner. 2010. Apport des analyses minéralogiques (en spectrométrie infra-rouge Transformation de Fourier) à l'interprétation des structures anthropiques : les concentrations osseuses dans les niveaux moustériens des grottes de Kébara et Hayonim (Israël). In *Mise en commun des approches en taphonomie/ Sharing taphonomic approaches*, eds. M. P. Coumont, C. Thiebaut and A. Averbough, 93-108: Paleo Special Issue.
- Meignen, L., A. Delagnes, and L. Bourguignon. 2009. Patterns of lithic material procurement and transformation during the Middle Paleolithic in Western Europe. In *Lithic Materials and Paleolithic Societies*, eds. B. Adams and B. Blades, 15-24. Oxford: Blackwell Publishing.
- Meignen, L., P. Goldberg, R. M. Albert, and O. Bar-Yosef. 2009. Structures de combustion, choix des combustibles et degré de mobilité des groupes dans le Paléolithique moyen du Proche-Orient : exemples des grottes de Kébara et d'Hayonim (Israël). In *Gestion des combustibles au Paléolithique et Mésolithique: nouveaux outils, nouvelles interprétations/Fuel management during the Paleolithic and Mesolithic period: new tools, new interpretations*, eds. I. Théry-Parisot, S. Costamagno and A. Henry, 111-118. Oxford: Archeopress.
- Meignen, L., P. Goldberg, and O. Bar-Yosef. 2007. The Hearths at Kebara Cave and Their Role in Site Formation Processes. In *Kebara Cave Mt. Carmel, Israel. The Middle and Upper Paleolithic Archaeology. Part I*, eds. O. Bar-Yosef and L. Meignen, 91-122. Cambridge (US): American School of Prehistoric Research Bulletin 49, Peabody Museum of Archaeology and Ethnology, Harvard University.
- Meignen, L., P. Goldberg, and O. Bar-Yosef. 2017. Together in the field: interdisciplinary work in Kebara and Hayonim caves (Israel). *Archaeological and Anthropological Sciences* 9 (8):1603-1612.
- Meignen, L., J. D. Speth, and O. Bar-Yosef. 2017. Stratégies de subsistance et fonction de site au Paléolithique moyen récent : apports de la séquence de Kebara (Mt Carmel, Israël). *Paléorient* 43 (1):9-47.
- Meignen, L., J. D. Speth, O. Bar-Yosef, and A. Belfer-Cohen. 2019. Changes in the use of Kebara cave during the Middle Paleolithic and Upper Paleolithic times. In *Kebara Cave, Mt Carmel, Israel- The Middle and Upper Paleolithic Archaeology, Part II*, eds. L. Meignen and O. Bar-Yosef, 413-440. Cambridge (US): American School of Prehistoric Research Bulletin 51, Peabody Museum Press, Harvard University.
- Meignen, L., J. D. Speth, and M. C. Stiner. 2006. Middle Paleolithic settlement patterns in the Levant. In *Transitions Before the Transition: Evolution and Stability in the Middle Paleolithic and Middle Stone Age*, eds. E. Hovers and S. L. Kuhn, 149-169. New York: Kluwer.
- Mentzer, S. M. 2002. Micromorphological and geochemical analyses of the hearth deposits from Pech de l'Azé IV, France. Senior Thesis, Archaeology, Boston University, Boston.
- Mentzer, S. M. 2011. Macro- and Micro-Scale Geoarchaeology of Ucagizli Caves I and II, Hatay, Turkey, PhD Thesis, Anthropology, The University of Arizona.
- Mentzer, S. M. 2014. Microarchaeological approaches to the identification and interpretation of combustion features in prehistoric archaeological sites. *Journal of Archaeological Method and Theory* 21 (3):616-668.
- Mentzer, S. M. 2016. Hearths and Combustion Features. In *Encyclopedia of Geoarchaeology*, ed. A. S. Gilbert, 411-424. Dordrecht: Springer.
- Mentzer, S. M., and J. Quade. 2013. Compositional and isotopic analytical methods in archaeological micromorphology. *Geoarchaeology* 28:87-97.

- Mercier, N., and H. Valladas. 2003. Reassessment of TL age estimates of burnt flints from the Paleolithic site of Tabun Cave, Israel. *Journal of Human Evolution* 45:401-409.
- Mercier, N., H. Valladas, O. Bar-Yosef, B. Vandermeersch, C. Stringer, and J. L. Joron. 1993. Thermoluminescence date for the Mousterian burial site of Es-Skhul, Mt. Carmel. *Journal of Archaeological Science* 20 (2):169-174.
- Mercier, N., H. Valladas, L. Froget, J. L. Joron, J. L. Reyss, S. Weiner, P. Goldberg, L. Meignen, O. Bar-Yosef, S. Kuhn, M. Stiner, A. Belfer-Cohen, A.-M. Tillier, B. Arensburg, and B. Vandermeersch. 2007. Hayonim Cave: a TL-based chronology of a Levantine Mousterian sequence. *Journal of Archeological Science* 34 (7):1064-1077.
- Mercier, N., H. Valladas, J. L. Joron, S. Schiegl, O. Bar-Yosef, and S. Weiner. 1995a. Thermoluminescence dating and the problem of geochemical evolution of sediments- A case study : the Mousterian Levels at Hayonim. *Israel Journal of Chemistry* 35:137-141.
- Mercier, N., H. Valladas, and G. Valladas. 1995b. Flint thermoluminescence dates from the CFR Laboratory at Gif : contribution to the study of the chronology of the Middle Palaeolithic. *Quaternary Science Reviews (Quaternary Geochronology)* 14:351-364.
- Mitki, N., R. Yeshurun, R. Ekshtain, A. Malinsky-Buller, and E. Hovers. 2021. A multi-proxy approach to Middle Paleolithic mobility : A case study from the open-air site of Ein Qashish (Israel). *Journal of Archaeological Science : Reports* 38: 103088.
- Monchot, H., and L. K. Horwitz. 2007. Taxon representation and age and sex distribution. In *Holon: A Lower Paleolithic site in Israel*. eds. M. Chazan and L. Kolska-Horwitz, 85-88. Cambridge (US): American School of Prehistoric Research, Peabody Museum Press, Harvard University.
- Monigal, K. 2001. Lower and Middle Paleolithic blade industries and the Dawn of the Upper Paleolithic in the Levant. *Archaeology, Ethnology and Anthropology of Eurasia* 1 (5):11-24.
- Monigal, K. 2002. The Levantine Leptolithic: Blade production from the Lower Paleolithic to the dawn of the Upper Paleolithic. PhD, Southern Methodist University, Dallas.
- Movius, H. L. 1966. The hearths of the Upper Perigordian and Aurignacian horizons at the Abri Pataud, Les Eyzies (Dordogne), and their possible significance. *American Anthropologist* 68 (2):296-325.
- Munday, F. C. 1979. Levantine Mousterian technological variability : a perspective from the Negev. *Paléorient* 5:87-104.
- Murphree, W. C., and V. Aldeias. 2022. The evolution of pyrotechnology in the Upper Palaeolithic of Europe. *Archaeological and Anthropological Sciences* 14 (10):202.
- Neuville, R. 1951. *Le Paléolithique et le Mésolithique du désert de Judée*. Paris: Masson et Cie.
- Nicosia, C., and G. Stoops. 2017. *Archaeological Soil and Sediment Micromorphology*. Oxford: John Wiley & Sons.
- Nielsen-Marsh, C. M., and R. E. M. Hedges. 2000a. Patterns of diagenesis in bone I: the effects of site environments. *Journal of Archaeological Science* 27 (12):1139-1150.
- Nielsen-Marsh, C. M., and R. E. M. Hedges. 2000b. Patterns of diagenesis in bone II: effects of acetic acid treatment and the removal of diagenetic CO²⁻³. *Journal of Archaeological Science* 27 (12):1151-1159.
- Nishiaki, Y. 1989. Early blade industries in the Levant : the placement of Douara IV industry in the context of the Levantine Early Middle Paleolithic. *Paléorient* 15(1):215-229.
- Nishiaki, Y., T. Akazawa, and Y. Kanjou. 2022. The Early Middle Palaeolithic industry of Dederiyeh Cave, Northwest Syria. *L'Anthropologie*. DOI:10.1016/j.anthro.2022.103028
- Nishiaki, Y., Y. Kanjou, and T. Akazawa. 2017. The Yabrudian industry of Dederiyeh Cave, Northwest Syria. In *Vocation Préhistoire. Hommage à J.-M. Le Tensorer*, eds. D. Wojtczak, M. Al Najjar, R. Jagher, H. Elsuede, F. Wegmüller and M. Otte, 67-76. Liège: ERAUL.

- Nishiaki, Y., Y. Kanjou, S. Muhesen, and T. Akazawa. 2011. Recent progress in Lower and Middle Palaeolithic research at Dederiyeh Cave, Northwest Syria. In *The Lower and Middle Palaeolithic in the Middle East and Neighbouring regions*, eds. J.-M. Le Tensorer, R. Jagher and M. Otte, 67-76. Liège: ERAUL.
- Oron, M., and N. Goren-Inbar. 2014. Mousterian intra-site spatial patterning at Quneitra, Golan Heights. *Quaternary International* 331:186-202.
- Pagli, M. 2013. Variabilité du Moustérien au Proche-Orient. Approche géographique des dynamiques de changement en milieu méditerranéen et en milieu steppique. Thèse Doctorat, Préhistoire, université Paris Ouest Nanterre La Défense.
- Parush, Y., E. Assaf, V. Slon, A. Gopher, and R. Barkai. 2015. Looking for sharp edges: Modes of flint recycling at Middle Pleistocene Qesem Cave, Israel. *Quaternary International* 361:61-87.
- Parush, Y., A. Gopher, and R. Barkai. 2016. Amudian versus Yabrudian under the rock shelf: A study of two lithic assemblages from Qesem Cave, Israel. *Quaternary International* 398:13-36.
- Pelegrin, J. 1990. Prehistoric lithic technology : some aspects of research. *Archaeological Review from Cambridge* 9 (1):116-125.
- Pelegrin, J. 1995. *Technologie lithique : le Chatelperronien de Roc-de-Combe (Lot) et de La Côte (Dordogne)*. Paris: CNRS Editions.
- Pelegrin, J., C. Karlin, and P. Bodu. 1988. "Chaînes opératoires" : un outil pour le préhistorien. In *Technologie préhistorique : journée d'études technologiques en préhistoire*, ed. J. Tixier, 55-62. Paris: Editions du C.N.R.S.
- Perlès, C. 2013. Tempi of Change: When Soloists Don't Play Together. Arrhythmia in 'Continuous' Change. *Journal of Archaeological Method and Theory* 20 (2):281-299.
- Petraglia, M. D., A. Alsharekh, P. Breeze, C. Clarkson, R. Crassard, N. A. Drake, H. S. Groucutt, R. Jennings, A. G. Parker, A. Parton, R. G. Roberts, C. Shipton, C. Matheson, A. al-Omari, and M.-A. Veall. 2012. Hominin dispersal into the Nefud desert and Middle Palaeolithic settlement along the Jubbah palaeolake, northern Arabia. *PLoS ONE* 7 (11): 49840.
- Petraglia, M. D., A. M. Alsharekh, R. Crassard, N. A. Drake, H. S. Groucutt, A. G. Parker, and R. G. Roberts. 2011. Middle Paleolithic occupation on a Marine Isotope Stage 5 lakeshore in the Nefud Desert, Saudi Arabia. *Quaternary Science Reviews* 30:1555-1559.
- Petraglia, M. D., M. Haslam, D. Q. Fuller, N. Boivin, and C. Clarkson. 2010. Out of Africa: New hypotheses and evidence for the dispersal of Homo sapiens along the Indian Ocean rim. *Annals of Human Biology* 37 (3):288-311.
- Ploux, S. 1991. Technologie, technicité, techniciens : méthode de détermination d'auteurs et comportements techniques individuels. In *25 ans d'études technologiques en préhistoire : bilan et perspectives*, 201-214. Juan-les-Pins: Ed. A.P.D.C.A.
- Posth, C., C. Wißing, K. Kitagawa, L. Pagani, L. Van Holstein, F. Racimo, K. Wehrberger, N. J. Conard, C. J. Kind, H. Bocherens, and J. Krause. 2017. Deeply divergent archaic mitochondrial genome provides lower time boundary for African gene flow into Neanderthals. *Nature Communications* 8. DOI:10.1038/ncomms16046.
- Preece, R. C., J. A. Gowlett, S. A. Parfitt, D. R. Bridgland, and S. Lewis. 2006. Humans in the Hoxnian: habitat, context and fire use at Beeches Pit, West Stow, Suffolk, UK. *Journal of Quaternary Science* 21 (5):485-496.
- Prevost, M., and Y. Zaidner. 2020. New insights into early MIS 5 lithic technological behavior in the Levant: Neshar Ramla, Israel as a case study. *PLoS ONE* 15 (4). DOI:10.1371/journal.pone.0231109.
- Rabinovich, R., and E. Tchernov. 1995. Chronological, paleoecological and taphonomical aspects of the Middle Paleolithic site of Qafzeh, Israel. In *Archaeozoology of the Near East*, eds. H. Buitenhuis and H. P. Uerpmann, 5-43. Leiden: Backhuys.
- Rabinovitch, R., and E. Hovers. 2004. Faunal Analysis from Amud Cave: Preliminary results and Interpretations. *International Journal of Osteoarchaeology* 14:287-306.

- Rendu, W., and J. D. Speth. 2019. Seasonality of Kebara's Middle Paleolithic Occupations: A Cementum Increment Analysis. In *Kebara Cave, Mt Carmel, Israel- The Middle and Upper Paleolithic Archaeology, Part II*, eds. L. Meignen and O. Bar-Yosef, 237-255. Cambridge (US): American School of Prehistoric Research Bulletin 51, Peabody Museum of Archaeology and Ethnology, Harvard University.
- Richter, D., T. Hauck, D. B. Wojtczak, and J.-M. Le Tensorer. 2011. Chronometric age estimates for the site of Hummal (El Kowm, Syria). In *The Lower and Middle Palaeolithic in the Middle East and Neighboring Regions*, eds. J.-M. Le Tensorer, R. Jagher and M. Otte, 197-208. Liège: Presses Universitaires de Liege.
- Rink, W., H. Schwarcz, S. Weiner, P. Goldberg, L. Meignen, and O. Bar -Yosef. 2004. Age of the Mousterian industry at Hayonim Cave, Northern Israel, using electron spin resonance and $^{230}\text{Th}/^{234}\text{U}$ methods. *Journal of Archaeological Science* 31:953-964.
- Roebroeks, W., J. Kolen, and E. Rensink. 1988. Planning depth, anticipation and the organization of middle palaeolithic technology : the "archaic natives" meet Eve's descendants. *Helinium* XXVIII:17-34.
- Roebroeks, W., and P. Villa. 2011. On the earliest evidence for habitual use of fire in Europe. *Proceedings of the National Academy of Sciences of the United States of America* 108 (13):5209-5214.
- Rolland, N. 2000. Cave occupation, fire-making, hominid/carnivore coevolution, and Middle Pleistocene emergence of home-base settlement systems. *Acta Anthropologica Sinica* 19 (suppl):209-217.
- Rolland, N. 2004. Was the emergence of home bases and domestic fire a punctuated event? A review of the Middle Pleistocene record in Eurasia. *Asian Perspectives: the Journal of Archaeology for Asia and the Pacific* 43:248-281.
- Rollefson, G. O., L. A. Quintero, and P. J. Wilke. 2006. Late Acheulian variability in the Southern Levant: a contrast of the Western and Eastern margins of the Levantine corridor. *Near Eastern Archaeology* 69 (2):61-72.
- Rosell, J., and R. Blasco. 2019. The early use of fire among Neanderthals from a zooarchaeological perspective. *Quaternary Science Reviews* 217:268-283.
- Rots, V. 2013. Insights into early Middle Palaeolithic tool use and hafting in Western Europe. The functional analysis of level IIa of the early Middle Palaeolithic site of Biache-Saint-Vaast (France). *Journal of Archaeological Science* 40:497-506.
- Rots, V. 2015. Hafting and Site Function in the European Middle Paleolithic. In *Settlement Dynamics of the Middle Paleolithic and Middle Stone Age*, eds. N. Conard and A. Delagnes, 383-410. Tübingen: Kerns Verlag.
- Roux, V. 2007. Ethnoarchaeology: A Non Historical Science of Reference Necessary for Interpreting the Past. *Journal of Archaeological Method and Theory* 14 (2):153-178.
- Rowlett, R. M. 2000. Fire control by Homo erectus in East Africa and Asia. *Acta Anthropologica Sinica* 19 (Suppl):198-208.
- Rust, A. 1950. *Die Höhlenfunfe von Jabrud (Syrien)*. Neumünster: Karl Wachholz Verlag.
- Sahle, Y., L. E. Morgan, D. R. Braun, B. Atnafu, and W. K. Hutchings. 2014. Chronological and behavioral contexts of the earliest Middle Stone Age in the Gademotta Formation, Main Ethiopian Rift. *Quaternary International* 331:6-19.
- Sandgathe, D. M., H. L. Dibble, P. Goldberg, S. J. P. McPherron, A. Turq, L. Niven, and J. Hodgkins. 2011. On the Role of Fire in Neandertal Adaptations in Western Europe: Evidence from Pech de l'Azé and Roc de Marsal, France. *PaleoAnthropology* 216-242.
- Schiegl, S., P. Goldberg, O. Bar-Yosef, and S. Weiner. 1996. Ash Deposits in Hayonim and Kebara Caves, Israel: macroscopic, microscopic and mineralogical observations, and their archaeological implications. *Journal of Archaeological Science* 23:763-781.
- Schiegl, S., S. Lev-Yadun, O. Bar-Yosef, A. El Goresy, and S. Weiner. 1994. Siliceous aggregates from prehistoric wood ash: a major component of sediments in Kebara and Hayonim Caves (Israel). *Israel Journal of Earth Sciences* 43:267-278.

- Schwarcz, H. P., W. M. Buhay, R. Grün, H. Valladas, E. Tchernov, O. Bar-Yosef, and B. Vandermeersch. 1989. ESR dating of the Neanderthal site, Kebara Cave, Israel. *Journal of Archaeological Science* 16 (6):653-659.
- Schwarcz, H. P., R. Grün, B. Vandermeersch, O. Bar-Yosef, H. Valladas, and E. Tchernov. 1988. ESR dates for the hominid burial site of Qafzeh in Israël. *Journal of Human Evolution* 17:733-737.
- Sellet, F. 1993. Chaîne opératoire; the concept and its application. *Lithic Technology* 18 (1-2):106-112.
- Shahack-Gross, R., O. Bar-Yosef, and S. Weiner. 1997. Black-coloured bones in Hayonim Cave, Israel: Differentiating between burning and oxide staining. *Journal of Archaeological Science* 24 (5):439-446.
- Shahack-Gross, R., F. Berna, P. Karkanas, C. Lemorini, A. Gopher, and R. Barkai. 2014. Evidence for the repeated use of a central hearth at Middle Pleistocene (300 ky ago) Qesem Cave, Israel. *Journal of Archaeological Science* 44:12-21.
- Shahack-Gross, R., F. Berna, P. Karkanas, and S. Weiner. 2004. Bat guano and preservation of archaeological remains in cave sites. *Journal of Archaeological Science* 31 (9):1259-1272.
- Sharon, G. 2018. A Week in the Life of the Mousterian Hunter. In *The Middle and Upper Paleolithic Archeology of the Levant and Beyond*, eds. Y. Nishiaki, Akazawa, T., 35-47. Singapore: Springer.
- Sharon, G., and M. Oron. 2014. The lithic tool arsenal of a Mousterian hunter. *Quaternary International* 331:167-185.
- Sharon, G., Y. Zaidner, and E. Hovers. 2014. Opportunities, problems and future directions in the study of open-air Middle Paleolithic sites. *Quaternary International* 331:1-5.
- Shea, J. J. 2003. The Middle Paleolithic of the Eastern Mediterranean Levant. *Journal of World Prehistory* 17 (4):313-394.
- Shea, J. J. 2008. The Middle Stone Age archaeology of the Lower Omo Valley Kibish Formation: Excavations, lithic assemblages, and inferred patterns of early Homo sapiens behavior. *Journal of Human Evolution* 55:448-485.
- Shimelmitz, R. 2009. Lithic blade production in the Middle Pleistocene of the Levant. PhD Thesis, Tel Aviv University.
- Shimelmitz, R. 2015. The recycling of flint throughout the Lower and Middle Paleolithic sequence of Tabun Cave, Israel. *Quaternary International* 361:34-45.
- Shimelmitz, R., R. Barkai, and A. Gopher. 2011. Systematic blade production at late Lower Paleolithic (400–200 ka) Qesem Cave, Israel. *Journal of Human Evolution* 61 (4):458-479.
- Shimelmitz, R., M. Bisson, M. Weinstein-Evron, and S. L. Kuhn. 2017. Handaxe manufacture and re-sharpening throughout the Lower Paleolithic sequence of Tabun Cave. *Quaternary International* 428:118-131.
- Shimelmitz, R., and S. L. Kuhn. 2013. Early Mousterian Levallois Technology in Unit IX of Tabun Cave. *PaleoAnthropology*:1-27.
- Shimelmitz, R., and S. L. Kuhn. 2017a. Shifting understandings of the Acheulo-Yabrudian complex and the Lower to Middle Paleolithic transition at Tabun Cave. In *Vocation Préhistoire. Hommage à J.-M. Le Tensorer*, 343-353. Liège: ERAUL.
- Shimelmitz, R., and S. L. Kuhn. 2017b. The toolkit in the core: There is more to Levallois production than predetermination. *Quaternary International* 464:81-91.
- Shimelmitz, R., S. L. Kuhn, M. Bisson, and M. Weinstein-Evron. 2021. The end of the Acheulo-Yabrudian and the Lower Paleolithic in the Levant: A view from the “transitional” unit X of Tabun Cave, Israel. *Archaeological and Anthropological Sciences* 13, 66. DOI:10.1007/s12520-021-01304-5
- Shimelmitz, R., S. L. Kuhn, A. J. Jelinek, A. Ronen, A. E. Clark, and M. Weinstein-Evron. 2014a. ‘Fire at will’: The emergence of habitual fire use 350,000 years ago. *Journal of Human Evolution* 77:196-203.

- Shimelmitz, R., S. L. Kuhn, A. Ronen, and M. Weinstein-Evron. 2014b. Predetermined Flake Production at the Lower/Middle Paleolithic Boundary: Yabrudian Scraper-Blank Technology. *PLoS ONE* 9 (9):e106293. .
- Shimelmitz, R., S. L. Kuhn, and M. Weinstein-Evron. 2020. The evolution of raw procurement strategies: A view from the deep sequence of Tabun Cave, Israel. *Journal of Human Evolution* 143. DOI: 10.1016/j.jhevol.2020.102787
- Shimelmitz, R., M. Weinstein-Evron, A. Ronen, and S. L. Kuhn. 2016. The Lower to Middle Paleolithic transition and the diversification of Levallois technology in the Southern Levant: Evidence from Tabun Cave, Israel. *Quaternary International* 409:23-40.
- Shipman, P., G. Foster, and M. Schoeninger. 1984. Burnt bones and teeth: an experimental study of color, morphology, crystal structure and shrinkage. *Journal of Archaeological Science* 11 (4):307-325.
- Skinner, J. 1970. El Masloukh: A Yabroudian site in Lebanon. *Bulletin du Musée de Beyrouth* 23:143-172.
- Sorensen, A. C., and F. Scherjon. 2018. fiReproxies: A computational model providing insight into heat-affected archaeological lithic assemblages. *PLoS ONE* 13 (5). DOI: 10.1371/journal.pone.0196777.
- Soressi, M., and J.-M. Geneste. 2011. The history and efficacy of the Chaîne Opératoire approach to lithic analysis: Studying techniques to reveal past societies in an evolutionary perspective. *PaleoAnthropology*:334-350.
- Speth, J. D. 2007. Housekeeping, Neandertal-Style: Hearth placement and midden formation in Kebara Cave (Israel). In *Transitions before the transition: evolution and stability in the Middle Paleolithic and Middle Stone Age*, eds. E. Hovers and S. L. Kuhn, 171-188. New York: Springer Science.
- Speth, J. D. 2012. Middle Paleolithic Subsistence in the Near East: Zooarchaeological Perspectives—Past, Present, and Future. *Before Farming* 2 (1):1-45.
- Speth, J. D. 2019. Kebara as a Late Pleistocene settlement: insights from the ungulate remains. In *Kebara Cave, Mt Carmel, Israel- The Middle and Upper Paleolithic Archaeology, Part II*, eds. L. Meignen and O. Bar-Yosef, 169-236. Cambridge (US): American School of Prehistoric Research Bulletin 51, Peabody Museum of Archaeology and Ethnology, Harvard University.
- Speth, J. D., and J. L. Clark. 2006. Hunting and overhunting in the Levantine Late Middle Palaeolithic. *Before Farming* 3:1-42.
- Speth, J. D., L. Meignen, O. Bar-Yosef, and P. Goldberg. 2012. Spatial organization of Middle Paleolithic occupation X in Kebara Cave (Israel): Concentrations of animal bones. *Quaternary International* 247:85-102.
- Speth, J. D., and E. Tchernov. 1998. The Role of Hunting and Scavenging in Neandertal Procurement Strategies : New Evidence from Kebara Cave (Israel). In *Neanderthals and Modern Humans in West Asia*, eds. O. Bar-Yosef and T. Akazawa, 223-240. New York: Plenum Press.
- Speth, J. D., and E. Tchernov. 2001. Neandertals hunting and meat-processing in the Near East. In *Meat-Eating and Human Evolution*, eds. C. B. Stanford and H. T. Bunn, 52-72. Oxford: Oxford University Press.
- Stahlschmidt, M. C., C. E. Miller, B. Ligouis, U. Hambach, P. Goldberg, F. Berna, D. Richter, B. Urban, J. Serangeli, and N. J. Conard. 2015. On the evidence for human use and control of fire at Schöningen. *Journal of Human Evolution* 89:181-201.
- Stiner, M. C. 1991. Food procurement and transport by human and non-human predators. *Journal of Archaeological Science* 18:455-482.
- Stiner, M. C. 1994. *Honor among Thieves: A Zooarchaeological Study of Neandertal Ecology*. Princeton, New Jersey: Princeton University Press.
- Stiner, M. C. 2002. On in situ attrition and vertebrate body part profiles. *Journal of Archaeological Science* 29 (9):979-991.

- Stiner, M. C. 2004. A comparison of photon densitometry and computed tomography parameters of bone density in ungulate body part profiles. *Journal of Taphonomy* 2 (3):117-145.
- Stiner, M. C. 2005. *The Faunas of Hayonim Cave (Israel). A 200,000-Year Record of Paleolithic Diet, Demography and Society*. Cambridge (US): American School of Prehistoric Research Bulletin 48, Peabody Museum of Archaeology and Ethnology, Harvard University.
- Stiner, M. C. 2018. On the co-evolution of hearth and home-making during the Middle Pleistocene in the Levant. In *Crossing the Human Threshold: Dynamic Transformation and Persistent Places during the Middle Pleistocene*, eds. M. Pope, J. McNabb and C. Gamble, 83-105. London and New York: Routledge.
- Stiner, M. C. 2021. The challenges of documenting coevolution and niche construction: The example of domestic spaces. *Evolutionary Anthropology: Issues, News, and Reviews* 30 (1):63-70.
- Stiner, M. C., R. Barkai, and A. Gopher. 2009. Cooperative hunting and meat sharing 400-200 kya at Qesem Cave, Israel. *Proceedings of National Academy of Science (USA)* 106 (32):13207-13212.
- Stiner, M. C., A. Gopher, and R. Barkai. 2011. Hearth-side socioeconomics, hunting and paleoecology during the late Lower Paleolithic at Qesem Cave, Israel. *Journal of Human Evolution* 60 (2):213-233.
- Stiner, M. C., F. C. Howell, B. Martínez-Navarro, E. Tchernov, and O. Bar-Yosef. 2001a. Outside Africa: Middle Pleistocene *Lycaon* from Hayonim Cave, Israel. *Bolletino della Società Paleontologica Italiana* 40 (2):293-302.
- Stiner, M. C., S.L. Kuhn, T. Surovell, P. Goldberg, A. Margaris, L. Meignen, S. Weiner, and O. Bar-Yosef. 2005. Bone, ash, and shell preservation in Hayonim Cave. In *The Faunas of Hayonim Cave (Israel). A 200,000-Year Record of Paleolithic Diet, Demography and Society*, ed. M. C. Stiner, 59-79. Cambridge (US): American School of Prehistoric Research Bulletin 48, Peabody Museum of Archaeology and Ethnology, Harvard University.
- Stiner, M. C., S. L. Kuhn, T. A. Surovell, P. Goldberg, L. Meignen, S. Weiner, and O. Bar-Yosef. 2001b. Bone Preservation in Hayonim Cave (Israel): a Macroscopic and Mineralogical Study. *Journal of Archaeological Science* 28 (6):643-659.
- Stiner, M. C., S. L. Kuhn, S. Weiner, and O. Bar-Yosef. 1995. Differential burning, recrystallization, and fragmentation of archaeological bone. *Journal of Archaeological Science* 22:223-237.
- Stoops, G. 2021. *Guidelines for Analysis and Description of Soil and Regolith Thin Sections, 2nd Edition*. Hoboken, NJ: John Wiley & Sons.
- Stoops, G., V. Marcelino, and F. Mees eds. 2018. *Interpretation of Micromorphological Features of Soils and Regoliths, 2nd Edition*. Amsterdam: Elsevier.
- Surovell, T. A., and M. C. Stiner. 2001. Standardizing infra-red measures of bone mineral crystallinity: an experimental approach. *Journal of Archaeological Science* 28:633-642.
- Tchernov, E. 1981. The Biostratigraphy of the Middle East. In *Préhistoire du Levant*, 67-97. Paris: Editions du CNRS.
- Tchernov, E. 1988. Biochronology of the Middle Palaeolithic and dispersal events of Hominids in the Levant. In *L'Homme de Néandertal. L'environnement*, ed. M. Otte, 153-168. Liège: ERAUL.
- Tchernov, E. 1989. The Middle Palaeolithic mammalian sequence and its bearing on the origin of *Homo sapiens*. In *Investigations in South Levantine Prehistory*, ed. O. Bar-Yosef and B. Vandermeersch, 25-42. Oxford: BAR International Series 497.
- Tchernov, E. 1992a. The Afro-Arabian component in the Levantine mammalian fauna: a short biogeographical review. *Israel Journal of Zoology* 38:155-192.
- Tchernov, E. 1992b. Biochronology, paleoecology, and dispersal events of Hominids in the southern Levant. In *The Evolution and Dispersal of Modern Humans in Asia*, eds. T. Akazawa, K. Aoki and T. Kimura, 149-188. Tokyo: Hokusen-sha.

- Tchernov, E. 1994. New comments on the biostratigraphy of the Middle and Upper Pleistocene of the southern Levant. In *Late Quaternary Chronology and Paleoclimates of the Eastern Mediterranean, Radiocarbon*, eds. O. Bar-Yosef and R. S. Kra, 333-350. Tucson: University of Arizona.
- Tchernov, E. 1998a. Are late Pleistocene environmental factors, faunal changes and cultural transformations causally connected? The case of the southern Levant. *Paléorient* 23 (2):209-228.
- Tchernov, E. 1998b. The faunal sequence of the Southwest Asian Middle Paleolithic in relation to hominid dispersal events. In *Neanderthals and Modern Humans in Western Asia*, eds. Akazawa T., Aoki K. and O. Bar-Yosef, 77-90. New York: Plenum Press.
- Théry-Parisot, I., and S. Costamagno. 2005. Propriétés combustibles des ossements: données expérimentales et réflexions archéologiques sur leur emploi dans les sites paléolithiques. *Gallia préhistoire* 47:235-254.
- Tillier, A.-M. 2006a. Les plus anciens *Homo sapiens (sapiens)*. Perspectives biologiques, chronologique et taxinomique. *Diogenes* 214:132-146.
- Tillier, A.-M. 2006b. Earliest Modern Humans in Eurasia: Evidence from the Near East. *Biennial Books of EAA* 4:99-115.
- Tillier, A.-M., and B. Arensburg. 2017. Le Levant méditerranéen et les nomades moustériens : un territoire de confluence. *Bulletins et Mémoires de la Société d'Anthropologie de Paris* 29:195-201.
- Tillier, A.-M., B. Arensburg, A. Belfer-Cohen, and B. Vandermeersch. 2011. Early Hominid remains from Hayonim Cave (Israel) in the context of the Late Middle and Upper Pleistocene record from the Near East. *Paléorient* 37 (2):47-63.
- Tostevin, G. B. 2000. Behavioral change and regional variation across the Middle to Upper Paleolithic transition in Central Europe, Eastern Europe and the Levant, PhD thesis, Department of Anthropology, Harvard University, Cambridge.
- Tostevin, G. B. 2011. Special Issue: Reduction Sequence, Chaîne Opératoire, and Other Methods: The Epistemologies of Different Approaches to Lithic Analysis. Introduction. *PaleoAnthropology*:293-389.
- Trinkaus, E. 1983. *The Shanidar Neanderthals*. New York: Academic press.
- Tryon, C. A. 2006. "Early" Middle Stone Age lithic technology of the Kapthurin Formation (Kenya). *Current Anthropology* 47 (2):367-375.
- Tryon, C. A., and J. T. Faith. 2013. Variability in the Middle Stone Age of eastern Africa. *Current Anthropology* 54 (Suppl.8):S234-S254.
- Tryon, C. A., S. McBrearty, and P.-J. Texier. 2005. Levallois lithic technology from the Kapthurin formation, Kenya: Acheulian origin and Middle Stone Age diversity. *African Archaeological review* 22(4):199-229.
- Turq, A., W. Roebroeks, L. Bourguignon, and J. P. Faivre. 2013. The fragmented character of Middle Palaeolithic stone tool technology. *Journal of Human Evolution* 65:641-655.
- Valla, F. R., F. Le Mort, and H. Plisson. 1991. Les fouilles en cours sur la Terrasse d'Hayonim. In *The Natufian Culture in the Levant*, eds. O. Bar-Yosef and F. R. Valla. Ann Arbor, Michigan: International Monographs in Prehistory.
- Valladas, H., J. L. Joron, G. Valladas, B. Arensburg, O. Bar-Yosef, A. Belfer-Cohen, P. Goldberg, H. Laville, L. Meignen, Y. Rak, E. Tchernov, A.-M. Tillier, and B. Vandermeersch. 1987. Thermoluminescence dates for the Neanderthal burial site at Kebara in Israel. *Nature* 330:159-160.
- Valladas, H., N. Mercier, I. Hershkovitz, Y. Zaidner, A. Tsatskin, R. Yeshurun, L. Vialettes, J. L. Joron, J. L. Reyss, and M. Weinstein-Evron. 2013. Dating the Lower to Middle Paleolithic transition in the Levant: a view from Misliya Cave, Mount Carmel, Israel. *Journal of Human Evolution* 65:585-593.
- Valladas, H., J. L. Reyss, J. L. Joron, G. Valladas, O. Bar-Yosef, and B. Vandermeersch. 1988. Thermoluminescence dates for the Mousterian Proto-Cro-Magnons from Qafzeh Cave (Israel). *Nature* 331:614-616.

- Vallverdú-Poch, J., and M.-A. Courty. 2012. Microstratigraphic analysis of level J deposits: a dual Paleoenvironmental-Paleoethnographic contribution to Paleolithic archeology at the Abric Romaní. In *High Resolution Archaeology and Neanderthal Behavior*, 77-133: Springer International Publishing.
- Vallverdú, J., S. Alonso, A. Bargalló, R. Bartrolí, G. Campeny, Á. Carrancho, I. Expósito, M. Fontanals, J. Gabucio, and B. Gómez. 2012. Combustion structures of archaeological level O and Mousterian activity areas with use of fire at the Abric Romaní rockshelter (NE Iberian Peninsula). *Quaternary International* 247:313-324.
- Vandermeersch, B. 1981. *Les hommes fossiles de Qafzeh (Israël)*. Paris: Editions du CNRS.
- Vandermeersch, B. 1982. The first Homo sapiens sapiens in the Near East. In *The Transition from the Lower to the Middle Palaeolithic and the Origin of Modern Man*, ed. A. Ronen, 297-300. Oxford: BAR International Series 151.
- Vandermeersch, B. 1995. Le rôle du Levant dans l'évolution de l'humanité au Pléistocène supérieur. *Paléorient* 21 (2):25-34.
- Varoner, O., O. Marder, M. Orbach, R. Yeshurun, and Y. Zaidner. 2022. Lithic provisioning strategies at the Middle Paleolithic open-air site of Nesher Ramla, Israel: a case study from the upper sequence. *Quaternary International* 624:19-33.
- Weiner, S. 2010. *Microarchaeology: Beyond the Visible Archaeological Record*. New York: Cambridge University Press.
- Weiner, S., and O. Bar-Yosef. 1990. States of Preservation of Bones from Prehistoric Sites in the Near East: A Survey. *Journal of Archaeological Science* 17:187-196.
- Weiner, S., F. Berna, I. Cohen-Ofri, R. Shahack-Gross, R. M. Albert, P. Karkanas, L. Meignen, and O. Bar-Yosef. 2007. Mineral distributions in Kebara Cave: diagenesis and its effect on the archaeological record. In *Kebara Cave, Mt. Carmel, Israel: The Middle and Upper Paleolithic Archaeology*, eds. O. Bar-Yosef and L. Meignen, 131-146. Cambridge (US): American School of Prehistoric Research Bulletin 49, Peabody Museum of Archaeology and Ethnology, Harvard University.
- Weiner, S., and P. Goldberg. 1990. On-site Fourier Transform Infrared Spectrometry at an archaeological excavation. *Spectroscopy* 5:46-50.
- Weiner, S., P. Goldberg, and O. Bar-Yosef. 1993. Bone preservation in Kebara Cave, Israel using on-site Fourier transform infrared spectrometry. *Journal of Archaeological Science* 20:613-627.
- Weiner, S., P. Goldberg, and O. Bar-Yosef. 2000. Overview of ash studies in two prehistoric caves in Israel: implications to field archaeology. In *The Practical Impact of Science on Field Archaeology*, eds. S. Gitin and S. Pike, 85-90. London: Archetype Publications Ltd.
- Weiner, S., P. Goldberg, and O. Bar-Yosef. 2002. Three-dimensional distribution of minerals in the sediments of Hayonim Cave, Israel: Diagenetic processes and archaeological implications. *Journal of Archaeological Science* 29:1289-1308.
- Weiner, S., and P. A. Price. 1986. Disaggregation of bone into crystals. *Calcified Tissue International* 39 (6):365-375.
- Weiner, S., S. Schiegl, and O. Bar-Yosef. 1995. Recognizing ash deposits in the archaeological record: a mineralogical study at Kebara and Hayonim Caves, Israel. *Acta Anthropologica Sinica* 14:340-351.
- Weiner, S., S. Schiegl, P. Goldberg, and O. Bar-Yosef. 1995. Mineral assemblages in Kebara and Hayonim, Israel: excavation strategies, bone preservation and wood ash remnants. *Israel Journal of Chemistry* 35:143-154.
- Weinstein-Evron, M., G. Bar-Oz, Y. Zaidner, A. Tsatskin, D. Druck, N. Porat, and I. Hershkovitz. 2003. Introducing Misliya cave, Mount Carmel, Israel: a new continuous Lower/Middle Paleolithic sequence in the Levant. *Eurasian Prehistory* 1 (1):31-55.
- Weinstein-Evron, M., and Y. Zaidner. 2017. The Acheulo-Yabrudian- Early Middle Paleolithic Sequence of Misliya Cave, Mount Carmel, Israel. In *Human Paleontology and Prehistory. Contributions in Honor of Yoel Rak*, eds. E. Hovers and A. Marom, 187-201: Springer International Publishing.

- Wendorf, F., and R. Schild. 1974. *Middle Stone Age Sequence from the Central Rift Valley, Ethiopia*. Wrocław: Polska Akademia Nauk Instytut Historii Kultury Materialnej.
- Wojtczak, D. 2011. Hummal (Central Syria) and its eponymous industry. In *The Lower and Middle Palaeolithic in the Middle East and the Neighbouring Regions*, eds. J.-M. Le Tensorer, R. Jagher and M. Otte, 289-307. Liège: ERAUL.
- Wojtczak, D. 2014. The Early Middle Palaeolithic blade industry from Hummal (Central Syria). PhD thesis, Basel University.
- Wojtczak, D. 2015. Rethinking the Hummalian industry/ Repenser l'industrie hummalienne. *L'Anthropologie* 119:610-658.
- Wojtczak, D., J. M. Le Tensorer, and Y. E. Demidenko. 2014. Hummalian industry (El Kowm, Central Syria): Core reduction variability in the Levantine Early Middle Palaeolithic. *Quartär* 61:23-48.
- Wojtczak, D., and A. Malinsky-Buller. 2022. The Levantine Early Middle Palaeolithic in retrospect -Reassessing the contribution of Abou-Sif to the understanding of Palaeolithic record. *Archaeological Research in Asia* 30. DOI:10.1016/j.ara.2022.100366.
- Wolpoff, M. H., C. B. Stringer, R. G. Kruszynski, R. M. Jacobi, and A. Apsimon. 1981. Allez Neanderthal. *Nature* 289:823-824.
- Wrangham, R. W., and R. N. Carmody. 2010. Human adaptation to the control of fire. *Evolutionary Anthropology* 19 (5):187-199.
- Yellen, J., A. Brooks, D. Helgren, M. Tappen, S. Ambrose, R. Bonnefille, J. G. Feathers, G. Goodfriend, K. Ludwig, P. Renne, and K. Stewart. 2005. The Archaeology of Aduma Middle Stone Age Sites in the Awash Valley, Ethiopia. *PaleoAnthropology* 10:25-100.
- Yeshurun, R. 2013. Middle Paleolithic prey choice inferred from a natural pitfall trap: Rantis Cave, Israel. In *Zooarchaeology and Modern Human Origins: Human Hunting Behavior during the Later Pleistocene*, eds. J. L. Clark and J. D. Speth, 45-58. Dordrecht: Springer.
- Yeshurun, R. 2016. Paleolithic animal remains in the Mount Carmel caves: A review of the historical and modern research. In *Bones and Identity: Zooarchaeological Approaches to Reconstructing Social and Cultural Landscapes in Southwest Asia* eds. N. Marom, R. Yeshurun, L. Weissbrod and G. Bar-Oz, 1-24. Oxford and Philadelphia: Oxbow Books.
- Yeshurun, R., G. Bar-Oz, and M. Weinstein-Evron. 2007. Modern hunting behavior in the early Middle Paleolithic: faunal remains from Misliya Cave, Mount Carmel, Israel. *Journal of Human Evolution* 53:656-677.
- Yeshurun, R., D. Malkinson, K. M. Crater Gershtein, Y. Zaidner, and M. Weinstein-Evron. 2020. Site occupation dynamics of early modern humans at Misliya Cave (Mount Carmel, Israel): Evidence from the spatial taphonomy of faunal remains. *Journal of Human Evolution* 143. DOI:10.1016/j.jhevol.2020.102797.
- Zaidner, Y., L. Centi, M. Prévost, N. Mercier, C. Falguières, O. Tombret, E. Pons-branchu, N. Porat, R. Shahack-gross, D. E. Friesem, R. Yeshurun, Z. Turgeman-Yaffe, A. Frumkin, G. Herzlinger, R. Ekshtain, M. Shemer, O. Varoner, R. Sarig, H. May, and I. Hershkovitz. 2021. Middle Pleistocene Homo behavior and culture at 140,000 to 120,000 years ago and interactions with Homo sapiens. *Science* 372:1429-1433.
- Zaidner, Y., L. Centi, M. Prévost, M. Shemer, and O. Varoner. 2018. An open-air site at Neshar Ramla, Israel, and new insights into Levantine Middle Paleolithic technology and site use. In *The Middle and Upper Paleolithic Archeology of the Levant and beyond*, eds. Y. Nishiaki and T. Akazawa, 11-33. Singapore: Springer.
- Zaidner, Y., D. Druck, and M. Weinstein-Evron. 2006. Acheulo-Yabrudian handaxes from Misliya Cave, Mount Carmel, Israel. In *Axe Age, Acheulian Tool-Making from Quarry to Discard*, eds. N. Goren-Inbar and G. Sharon, 243-266. London: Equinox.
- Zaidner, Y., A. Frumkin, D. E. Friesem, A. Tsatskin, and R. Shahack-Gross. 2016. Landscapes, depositional environments and human occupation at Middle Paleolithic

- open-air sites in the southern Levant, with new insights from Neshar Ramla, Israel. *Quaternary Science Review* 138:76-86.
- Zaidner, Y., A. Frumkin, N. Porat, A. Tsatskin, R. Yeshurun, and L. Weissbrod. 2014. A series of Mousterian occupations in a new type of site: The Neshar Ramla karst depression, Israel. *Journal of Human Evolution* 66:1-17.
- Zaidner, Y., and M. Weinstein-Evron. 2014. Making a point: the Early Middle Palaeolithic tool assemblage of Misliya Cave, Mount Carmel, Israel. *Before Farming* 4:1-23.
- Zaidner, Y., and M. Weinstein-Evron. 2016. The end of the Lower Paleolithic in the Levant: The Acheulo-Yabrudian lithic technology at Misliya Cave, Israel. *Quaternary International* 409:9-22.
- Zaidner, Y., and M. Weinstein-Evron. 2020. The emergence of the Levallois technology in the Levant: A view from the Early Middle Paleolithic site of Misliya Cave, Israel. *Journal of Human Evolution* 144:102785.
- Zupancich, A., C. Lemorini, A. Gopher, and R. Barkai. 2016. On Quina and demi-Quina scraper handling: Preliminary results from the late Lower Paleolithic site of Qesem Cave, Israel. *Quaternary International* 398:94-102.



Hayonim Cave

The research presented in this book results from an international interdisciplinary research program in Hayonim cave (Israel) from 1992 to 2000, directed by Prof O. Bar-Yosef (Harvard University) and L. Meignen (CNRS, France), and focusing on a long archaeological sequence dated to circa 300-140 000 years ago. The intensive fieldwork and research following it allowed us to document an essential period of human history in the Levant: the end of the Lower Palaeolithic and Early Middle Palaeolithic, during which recent discoveries showed that the early H. sapiens, expanding out of Africa, reached SW Asia around 180-190 000 y ago.

This book brings together the impressive findings of nine years of excavations and analysis by an interdisciplinary team of well-known scholars from US universities (Harvard, Boston, University of Arizona), Weizmann Institute (Israel) as well as from the French CNRS.

Several complementary approaches are implemented to understand early human economic, cultural and behavioral changes observed at this crucial period. It is based on detailed studies of lithic artifact technology, the remains of systematic fire use and cave occupation by early humans, and foraging strategies that include the early development of human adaptations for hunting large prey. In the context of the highly debated cultural break observed at the end of the Lower Palaeolithic, we propose new interpretations based on these innovative results.

This volume will provide a cornerstone for the history of humankind in a critical geographic region, at the crossroads between Africa and Eurasia.

sidestonepress

ISBN: 978-94-6426-185-1



9 789464 261851 >

